

**Proposal for Gamnom Ni, Cr and PGE Block, Kamjong District, Manipur
for Preliminary Survey (G3 Stage) under NMET**

**(Basemetals/ Ferrous/ Non-Ferrous/ Industrial/
Strategic & Critical/ Precious metals etc.)**

Prepared by



United Exploration India Pvt. Ltd.

**Axis mall C Block New town
4th Floor, Rajarhat, New Town
Kolkata-700156**

Place: Kolkata, West Bengal

Date: 16/10/2024

CONTENT

Content No.	SUBJECTS	Page no.
1	General Information of Gamnom Ni, Cr, Co and PGE Block	1 - 4
2	Detailed Description of Proposal:	5 - 19
2.1	Block Summery	5-12
2.1.1	Physiography	4-5
2.1.1.1	Drainage	5
2.1.2	Background Geology (Regional Geology & Local Geology of the block)	6-12
2.1.2.1	Regional Geology	6-11
2.1.2.2	Local Geology	12
2.1.3	Mineral Potentiality Based on Geology, Geophysics, Ground Geochemistry	12-15
2.1.4	Scope for The Exploration:	15-16
2.1.5	Observation and Recommendation of Previous Work	16
2.2	Previous Work	16-17
2.3	Block Boundary	17
2.4	Planned Methodology	17-18
2.5	Nature Quantum and Target	19
2.6	Project Schedule	20
2.7	Project Cost	21-23
2.8	Reference Literature	24

LIST OF FIGURES

Figure No.	SUBJECTS	Page no.
Figure 1	Physiographic map of proposed block	5
Figure 2	Map showing drainage pattern of the proposed block	5
Figure 3	Geological map of the area around Ukhrul, Naga-Manipur Hills, Manipur covering T.S. Nos. 83K/7,8,11 & 12.	11
Figure 4	Serpentinized Peridotite	12
Figure 5	Sheared Peridotite	12
Figure 6	Sample location within the block	13
Figure 7	Geological map of the proposed block	15

LIST OF TABELS

Table No.	SUBJECTS	Page no.
Table 1	Generalized Litho-Stratigraphy of Manipur	7-8
Table 2	Analysis of Bedrock Sediment Samples	13-14
Table 3	Analysis of Petrochemical Samples	14
Table 4	Analysis of Pit Samples	14
Table 5	Block Boundary Coordinates	17

PLATE LIST

Plate No	Description
Plate-1	Geological map with location index
Plate-2	Geological map (1:50000 SCALE)
Plate-3	Proposed block boundary over Geological map
Plate-4	Proposed block boundary over topographic map

ANNEXURE LIST

Annexure No	Description
Annexure-1	Reference Literature
	<ol style="list-style-type: none"> 1. Reconnaissance survey for chromium, nickel and base metal mineralization in Gamnom-Yentem area in part of Ophiolite belt, Ukhrul District, Manipur (G-4) by Imomeren Ao (Senior Geologist) and Vales Savio Peter (Senior Geologist). 2. Interim report on geochemical mapping in the Ophiolite belt in parts of ukhrul district, Manipur (Field Seaso:2018-19) By

**NMET Proposal (For G₃ exploration)
Gamnom Ni, Cr and PGE Block
Kamjong, Manipur**

	A.Elou (Senior Geologist) L. Somorjit Singh (Senior Geologist), Geological Survey of India.
Annexure-2	Gazette Notification of Accreditation
Annexure-3	Details of Project Members and Associates

1 GENERAL INFORMATION OF GAMNOM NI, CR, CO AND PGE BLOCK:

Features	Details
Block ID	Gamnom Ni, Cr and PGE Block
Exploration Agency	United Exploration India Pvt. Ltd. (UEIPL)
Commodity	Nickel, Chromium, Cobalt and PGE
Mineral Belt	Manipur Ophiolite Belt
Completion period with entire time schedule to complete the project	12 months
Objectives	<p>Exploration for Nickel, Chromium, Cobalt and PGE is governed by the industrial demand of the mineral. Demand of the above-mentioned minerals is increasing day by day for various industrial uses.</p> <p>Based on the evaluation of geological and geochemical data available, the present exploration program has been formulated to fulfill the following objectives.</p> <ol style="list-style-type: none">To carry out Geological & Structural mapping on 1:5000 scale for identification of Nickel, chromium, cobalt and PGE bearing formation (host rock) with the structural features to identify the surface manifestation and lateral disposition of the mineralized zones.To collect surface (Bedrock/stream sediment) samples & analyse for Nickel, chromium, cobalt and PGE and decide further course of Exploration program.Geomagnetic and Self potential survey will be conducted to identify the potential area for drilling.

**NMET Proposal (For G₃ exploration)
Gamnom Ni, Cr and PGE Block
Kamjong, Manipur**

	Features	Details
		<p>iv. To know the subsurface extension of ore body boreholes will be drilled based on analytical results of surface samples and geophysical anomaly data.</p> <p>v. To estimate reconnaissance resources as per UNFC norms and Minerals (Evidence of Mineral Contents) Rule-2015 at G-3 level mineral exploration.</p>
	Whether the work will be carried out by the proposed agency or through outsourcing and details thereof Components to be outsourced and name of the outsourced agency	UEIPL and its associates
	Name / number of the geoscientists	5 geoscientists will involve (2 geologist, 1 geophysicist, 1 resource geologist, 1 GIS specialists)
	Expected field days	8 months
1	Location	
	Latitude	25° 0' 31.928" N to 25° 1' 33.416" N
	Longitude	94° 26' 36.298" E to 94° 27' 34.830" E
	Village	Gamnom
	Tehsil/Taluk	-
	Districts	Kamjong
	State	Manipur
2	Area (hectares/square Kilometers)	
	Block Area	1.50 Sq. Km.
	Forest Area	Data Not Available
	Govt Land Area	Data Not Available
	Private Land Area	Data Not Available
3	Accessibility (Aerial Distance)	
	Nearest Rail Head	Silchar

**NMET Proposal (For G₃ exploration)
Gannom Ni, Cr and PGE Block
Kamjong, Manipur**

	Features	Details
	Road	A metaled road is passing through the proposed block boundary and connect with NH-102 A.
	Airport	Imphal International Airport (90 km).
4	Hydrography	
	Local/Surface Drainage Pattern	The overall drainage pattern shows dendritic to sub-parallel drainage.
	Rivers/Streams	Some 1 st and 2 nd order streams are running through the block boundary.
5	Climate	
	Mean Annual Rainfall	124 mm.
	Temperature (December)(Minimum) Temperatures (June)(Maximum)	The weather conditions in this area is characterized by a mild and moderate climate. In winter, there is much less rainfall here than in summer. The Köppen-Geiger climate classification identifies this particular weather pattern as belonging to the category of Cwb. The average temperature is 16.5 °C. The annual precipitation in this location is approximately 1489 mm.
6	Topography	
	Toposheet Number	83K/8
	Morphology of the area	The area consists of highly rugged topography with hills running along the NW-SE direction.
7	Availability of baseline geoscience data	
	Geological Map (1:50k/25k)	1:50000
	Geochemical Map	1:50000
	Geophysical Map (Aero-physical, Ground geophysical, regional as well as local scale GP maps)	Not Available
8	Justification for taking up Reconnaissance	This block has been identified based on analytical results of the Geochemical data carried out by GSI in the proposed block. There are 15 BRS points noted

	Features	Details
	Survey/ Regional exploration	<p>within the proposed block, where values of Cr vary from 2229 to 328416 ppm (Average: 24682 ppm) and Ni varies from 500 to 4167 ppm (average value: 2326 ppm). Therefore, the proposed block is very much potential for Ni, Cr and associated Co deposits and required for detail exploration.</p> <p>The depth persistence of the podiform chromite within the transitional-cumulate peridotite is to be investigated along with depth persistence of the deposit. The limonitic and saprolitic soil capping developed above the mafic/ultramafic rocks is a target zone for mineralization of Ni, Co, PGE.</p> <p>Field study carried out by UEIPL geologists also recorded the presence of chromite pods within transitional peridotite. Lateritic soil capping observed in and around sheared Peridotite is also important target zone for Nickel and PGE prospecting.</p>

2 DETAILED DESCRIPTION OF THE PROPOSAL:

2.1 Block Summary:

2.1.1 PHYSIOGRAPHY:

The area is characterized by a rugged hilly terrain with N-S to NNW-SSE trending parallel ridges intervened by deep and wide valley. In the proposed block, elevation is varied from 1360 m to 2221 m. The inherent lithology exposed in the area controls the physiography, the ridges within the project area are made up of mafic and ultramafic rocks (Figure 1).

**NMET Proposal (For G₃ exploration)
Gamnom Ni, Cr and PGE Block
Kamjong, Manipur**

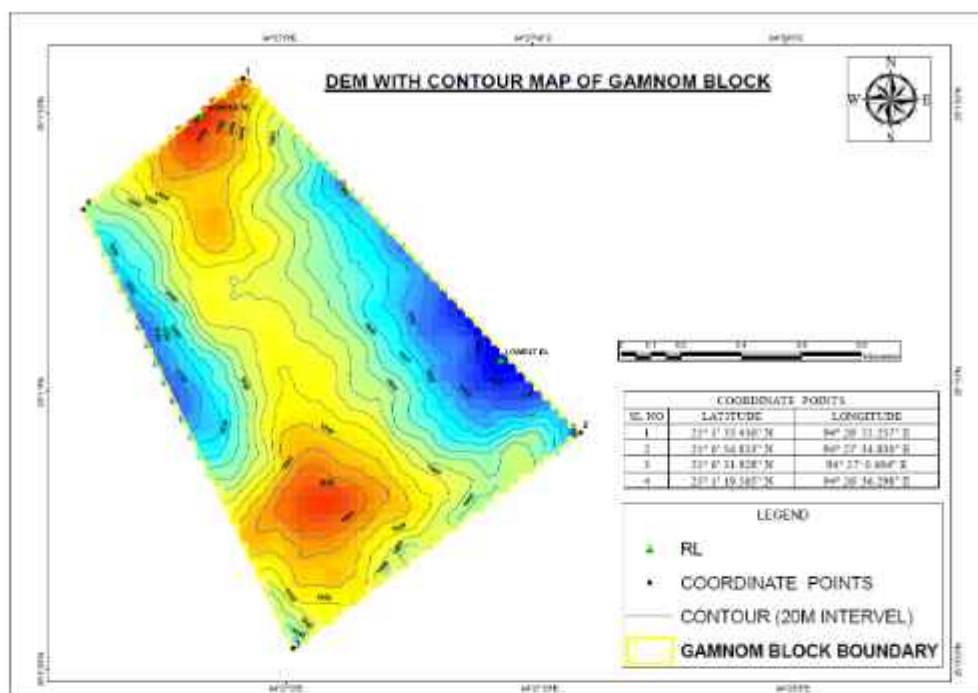


Figure 1: Physiographic map of proposed block

2.1.1.1 Drainage:

The overall drainage pattern shows dendritic to sub-parallel drainage.

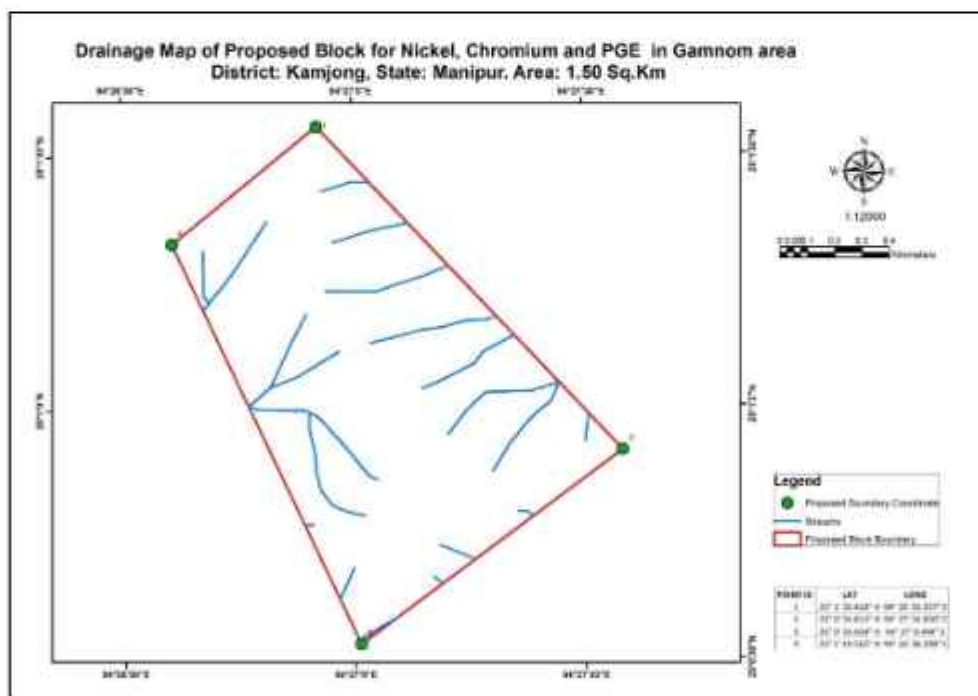


Figure 2: Map showing drainage pattern of proposed block

2.1.2 BACKGROUND GEOLOGY (REGIONAL GEOLOGY & GEOLOGY OF THE BLOCK):

2.1.2.1 Regional Geology

The eastern part of the Indian subcontinent reveals the presence of oceanic lithosphere that was emplaced during the Late Jurassic period, over the continent. This fragment denotes an accretionary wedge in the supra-subduction zone, as the Indian plate is subducted below the Myanmar plate. It is known as the Naga Hills Ophiolite Belt (NHO). The NHO ophiolite belt trends NNE-SSW and spans about 200 km in length and 15 km in width. It is surrounded on the east by Cenozoic sedimentary rocks of the central lowland of Myanmar and on the west by Paleogene Disang sediments (Chattopadhyay et al., 1983).

The stratigraphic succession of Manipur shows the younging direction towards west to east. The tectonic stratigraphic domain of Manipur geology can be classified into four units -1) Low-grade meta-sedimentary unit in the easternmost part represented by slate and phyllite 2) Linear NNE-SSW trending dismembered tectonic slices of Ophiolite Belt, 3) Thick Palaeogene folded sedimentary sequences revealed by the Disang and Barail groups and 4) Neogene sediments of Surma Basin which constitutes sedimentary units of Surma, Tipam, and Dupitilla Groups.

The first detailed geological investigation in Manipur was carried out by D.R. Oldham in 1883. Pascoe conducted further investigations in 1912 and 1950 and reported the presence of serpentinite along the contacts of the Disang and Makware beds of Burma. The Geological Survey of India conducted a series of mineral investigations and systematic geological mapping programs in different parts of Manipur in the late 1950s. The preliminary investigations of various workers, including Chakraborty and Raina (1985), Dutta (1959), Alwar et al. (1960-61), and Ghosal (1972), focused on areas around Nungou, Ningthi, Kwatha, Nampisha, Humine Moreh, and Ukhrul for limestone. Chattopadhyay and Roy (1975) mapped parts of Toposheet no. 83K/8 and classified the geological succession into two groups: Chingai Formation and Kongai Formation. The Chingai formation was correlated with the Disang (Eocene Age).

Systematic geological mapping in the eastern parts of the Ukhrul district carried out by Shukla et al. (1985) records lherzolite and amphibolites in the ophiolite belt. Das et. al., (1987) carried out an interdisciplinary study in ophiolites of Manipur and evaluation of potential mineralization.

Table 1: Generalized Litho-Stratigraphy of Manipur State. (Modified After Ibotombi & Singh, 2006 And Kesari, 2011)

AGE	GROUP	FORMATION	LITHOLOGICAL DESCRIPTION
Recent	Quaternary		Alluvium and terrace deposits, sand, silt, clay, gravel, pebbles and boulders, etc.
-----Unconformity-----			
Oligocene	Barail	Laisong	Thin to medium-bedded grey sandstone with trace fossils, cross-bedded sandstone, ripple marks, coal streaks and plant fossils
-----Gradational Contact-----			
Eocene	Disung	Upper Disung	Thinly bedded shale with thin intercalations of siltstone and sandstone containing exotic blocks of limestone, polymictic conglomerate, and quartzite. Ophiolite-derived lithic clast of basalt, peridotite, and volcanic. Large-scale cross-bedded sandstone with trace fossils and coal streaks.
-----Gradational Contact-----			
			Thin to medium bedded shale and Sandstone rhythmite, thinly bedded shale with large scale trough cross-bedded sandstone at places. Contains exotic blocks of Quartzite and limestone
-----Gradational Contact-----			
		Lower Disung	Thinly bedded shale with thin intercalations of siltstone and sandstone. Thin chert interbedded with shale at places. Slate phyllite at the base
-----Tectonic Contact-----			
Cretaceous to	Oceanic Pelagic	Lushat	Thinly bedded shale with siltstone intercalations, thinly bedded intercalations of

**NMET Proposal (For G₃ exploration)
Gamnom Ni, Cr and PGE Block
Kamjong, Manipur**

Lower Eocene	Sediments		volcano tuffaceous green, whitish and purplish ash beds with marl, chert bearing radiolarians and diatoms
-----Gradational Contact-----			
Cretaceous to Early Eocene		Ophiolite Suite	Volcanic rocks with flow breccias, gabbro plagiogranite/pyroxenite/ilherzolite/hurzburgite/dunite/peridotite exhibiting high degree of serpentinization with disseminated nodular, massive podiform chromite and layered chromite.
-----Base not exposed-----			

Ophiolite belt

The Ophiolite Belt is the southern continuation of the Naga Hills Ophiolite Belt showing a general NNE-SSW trend. Lithologically the Ophiolite Suite is characterized by tectonised mantle peridotite (lherzolite), transitional peridotite (mostly hurzburgite), cumulate mafic/ultramafic sequence (peridotite, layered gabbro, anorthosite, and plagiogranite), volcanic (pillow basalt and andesite) and volcano-clastics.

Tectonite mantle Peridotite

Tectonised mantle peridotite is partly exposed along the Shirui-Phangrai road section and Gamnom-Singcha village road section as detached blocks and lenses embedded within a strongly deformed and serpentinised matrix.

Transitional Peridotite

Transitional peridotite is mainly exposed at Shirui, Phangrai, and Gamnom villages, characterized by harzburgite with minor lherzolite occurring as detached blocks and lenses embedded within a strongly deformed and serpentinised matrix, with thick limonitic soil capping developed above the rock. The transitional peridotite occurs as a lensoidal outcrop within the ocean pelagic sediments having varying dimensions in linear arrangement following the NNE-SSW strike of these bodies having thrust contact. Chromite pods of varying dimensions are also found to occur within transitional peridotite units.

Cumulate

Above the transitional peridotite, there is a layered mafic-ultramafic cumulate. This is well exposed in the higher topographic reaches, such as the hilltops of Gamnom, Shirui, Phangrai, and east of Kalhang Khunou village. The cumulate is represented by

the peridotite and gabbro as major lithounits. The sparse vegetation cover in these areas also makes the cumulate more visible.

Gabbro

The mafic cumulates are characterized by the gabbro and its anorthositic variants exposed east of Shirui peak and Gamnom village.

Volcanics

Volcanic rocks at the east of Phangrai zero point are represented by vesicular/amygdular flow basalt, Andesite, and volcanic agglomerate. These rocks interbed with chert and cherty limestone from Flinch Corner to the Gamnom village section.

Ocean Pelagic Sediments

The ocean pelagic sediments are well exposed in the eastern part of the east of Kalhang Khunou, Phangrai, and Gamnom-Singhcha villages, where the mafic-ultramafic Ophiolite-thrusted slice sheets lie above the Ocean Pelagic Sediments (OPS).

Olistostrome

The olistostromal lithounit occurs in close association with the Disang shale. The major Olistostrome unit occurs in between the Disang Group of rocks and the Ophiolite Belt. This lithofacies is characterized by the chaotic distribution of exotic olistholit blocks of limestone, sandstone, and siltstone within shale along the Thoubal River section east of Kalhang Khunou village.

Disung Group

The Paleogene Disang sediments are well exposed along the western part of Ukhrul town, Kachai, Lamlang, Tuinem, Tallui, and Phadang villages. Geomorphologically the Paleogene sedimentary topography has attained second-order matured topography. The Paleogene Disang sediments are dissected by the series of almost NNE-SSW trending east-dipping thrust slices.

Lower Disang Formation: The lithofacies assemblage of this formation is defined by the predominance of argillite lithofacies, which is well exposed in and around the west of Ukhrul town, Choithor, Kachai, and Tulloi village sections.

Upper Disang Formation: This lithofacies overlies the Lower Disang Formation having a gradational litho-contact. The area around Ukhrul town, Hundung, and Shangshak Khunou villages is characterized by dark grey shale, siltstone, and sandstone rhythmite sequences. The sedimentary structures have various proportions of thin to thick horizontal laminations, large-scale trough cross-bedding, small-scale

current ripple cross laminations, and ripple marks. Additionally, there have been findings of *Cruziana* (*Thalassinoid horizontalis* isp. and *Helminthopsis albelii* sp.) and *Skolithos* (*Ophiomorpha* isp. and *Ophiomorpha nodosa* isp.) ichnofossil assemblages, as well as gastropod faunal assemblages like *Turritella* sp. and bivalvia.

Barail Group

The Barail Group, represented by the Laisong Formation is well exposed in the western part of and around Lamlang, Lamlang Shikor, Somdal Khullen, and Kachai, Hokhorim villages. The Laisong Formation is characterized by the predominance of arenaceous over argillaceous proportion. The presence of well-preserved plant leaves impressions and wood fossils with coal streak located north of Shirui village support a shallow marine deltaic depositional environment for the Laisong Formation.

Recent Alluvium

The recent alluvium consists of sandy soil, silt, and clay which can be categorized as residual or transported soils. These sediments are visible along the Thoubal River and its tributaries. This geological formation is characterized by large-scale cross-bedded sand, which is a result of meandering fluvial deposits.

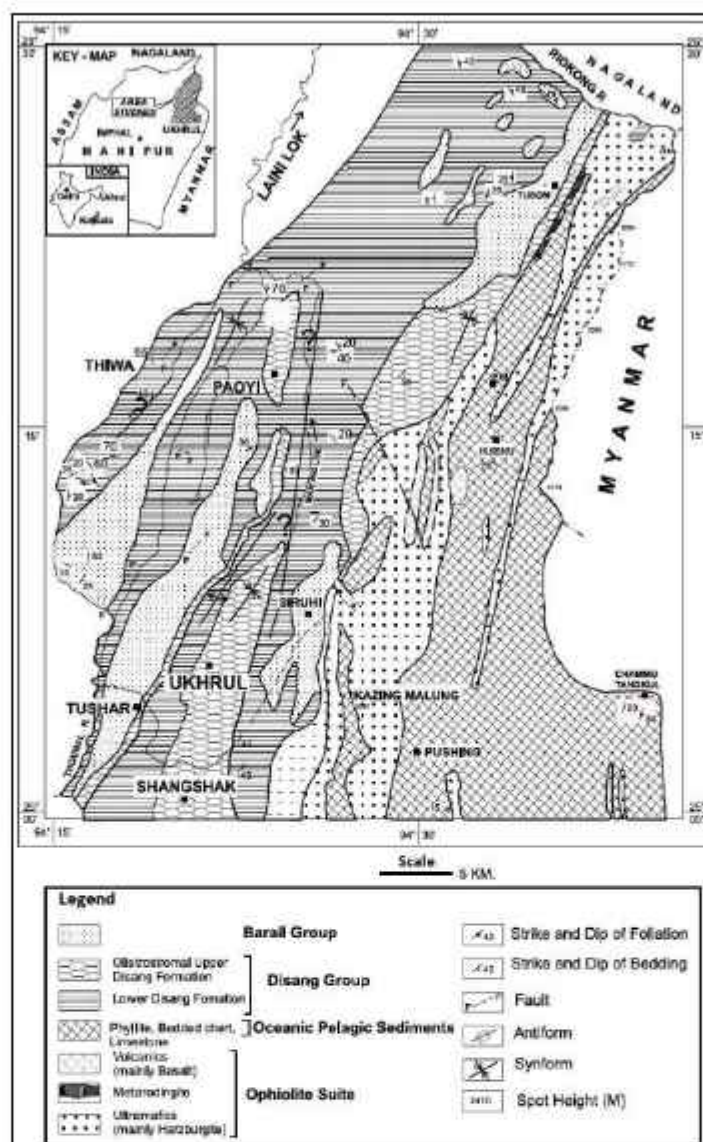


Fig No 3: Geological map of the area around Ukhrul, Naga-Manipur Hills, Manipur covering T.S. Nos. 83K/7,8,11 & 12.
(Modified after Joshi and Vidyadharan, 2008)

Structure

The intensity of deformation in the Ophiolite suite increases from west to east. The tectonic contact between the Ophiolite and sedimentary succession can be clearly seen along the Gamnom-Singhcha village section. The strike of the bed is NNE-SSW, with a sub-vertical eastward dip ranging from 78° to 88°. Within the mafic/ultramafic sequence, the contact zone shows extensive development of mylonite, serpentinization, and talcose alteration. The OPS in this zone are slightly metamorphosed to slate and phyllite, which are easily identified by the slaty cleavage and sweat quartz veins aligned along the S1 planes.

2.1.2.2 Local Geology

The proposed block occupies 1.50 sq. km and part of the Manipur ophiolite belt. During the field visit by UEIPL geologists Peridotite, Sandstone, Shale have been found. Peridotites are serpentinized at places and sheared also. Laterite soil profile has been found over the peridotites at some places. The detail stratigraphic succession will be confirmed after detail geological mapping. However, considering the regional geology, Ophiolite unit represented by peridotite is older and probably the Sandstone and Shale belongs to Upper Lushat formation.



Fig No 4: Serpentinized Peridotite



Fig No 5: Sheared Peridotite

2.1.3 MINERAL POTENTIALITY BASED ON GEOLOGY, GEOPHYSICS, GROUND GEOCHEMISTRY:

Reconnaissance survey for chromium, nickel and base metal mineralization in Gamnom-Yentem area in part of Ophiolite belt, Ukhrul District, Manipur (G-4) was carried out by Imomeren Ao (Senior Geologist) and Vales Savio Peter (Senior Geologist) in 2019-20.

This block has been identified based on their analytical results of the Geochemical data. There are 15 BRS points noted within the proposed block, where values of Cr vary from 2229 to 328416 ppm (Average: 24682 ppm) and Ni varies from 500 to 4167 ppm (average value: 2326 ppm).

**NMET Proposal (For G3 exploration)
Gamnom Ni, Cr and PGE Block
Kamjong, Manipur**

Further, the petrochemical samples in the form of fresh grab samples were analyzed and the values of Cr ranges between 2872 to 302143 ppm (Only 4 samples within the proposed block). Ni values ranges between 2516 to 11254 ppm (Only 4 samples within the block).

Therefore, the proposed block is very much potential for Ni, Cr and associated Co deposits and required for detail exploration.

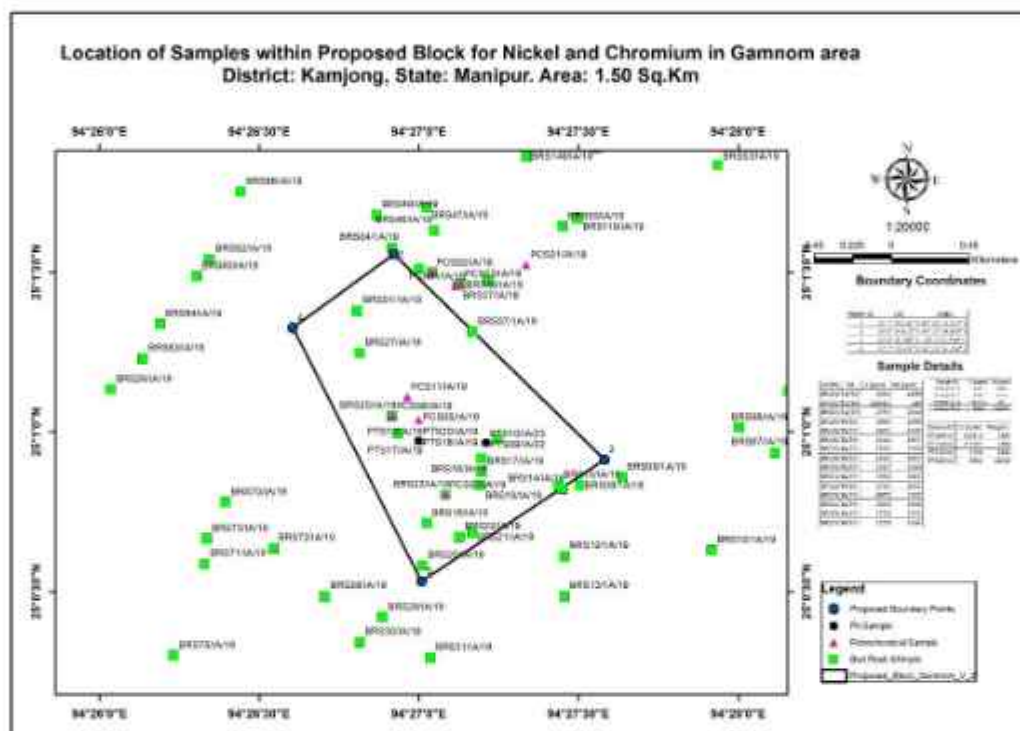


Fig No 6: Sample Location within the Block

Table 2: Analysis of Bed Rock Samples

SAMPLE NO.	Cr (ppm)	Ni (ppm)
BRS01/1A/19	2813	2300
BRS05/1A/19	328416	500
BRS07/1A/19	2797	2350
BRS14/1A/19	3864	2498

BRS15/IA/19	3621	4167
BRS16/IA/19	2524	2971
BRS17/IA/19	2332	1920
BRS19/IA/19	2411	2027
BRS20/IA/19	2517	2340
BRS21/IA/19	2930	2045
BRS22/IA/19	2724	2031
BRS23/IA/19	6879	1937
BRS24/IA/19	2628	2368
BRS25/IA/19	2753	3371
BRS27/IA/19	2229	2264

Table 3: Analysis of Petrochemical Samples

Sample ID	Cr (ppm)	Ni (ppm)
PCSo5/IA/19	2872	8048
PCSo7/IA/19	3251	2516
PCSo8/IA/19	302143	NA
PCSo11/IA/19	4839	11254

Table 4: Analysis of Pit Samples

Sample ID	Cr (ppm)	Ni (ppm)
PTS09/IA/22	233312	1296
PTS10/IA/23	277101	1484
PTS18/IA/19	3120	5430

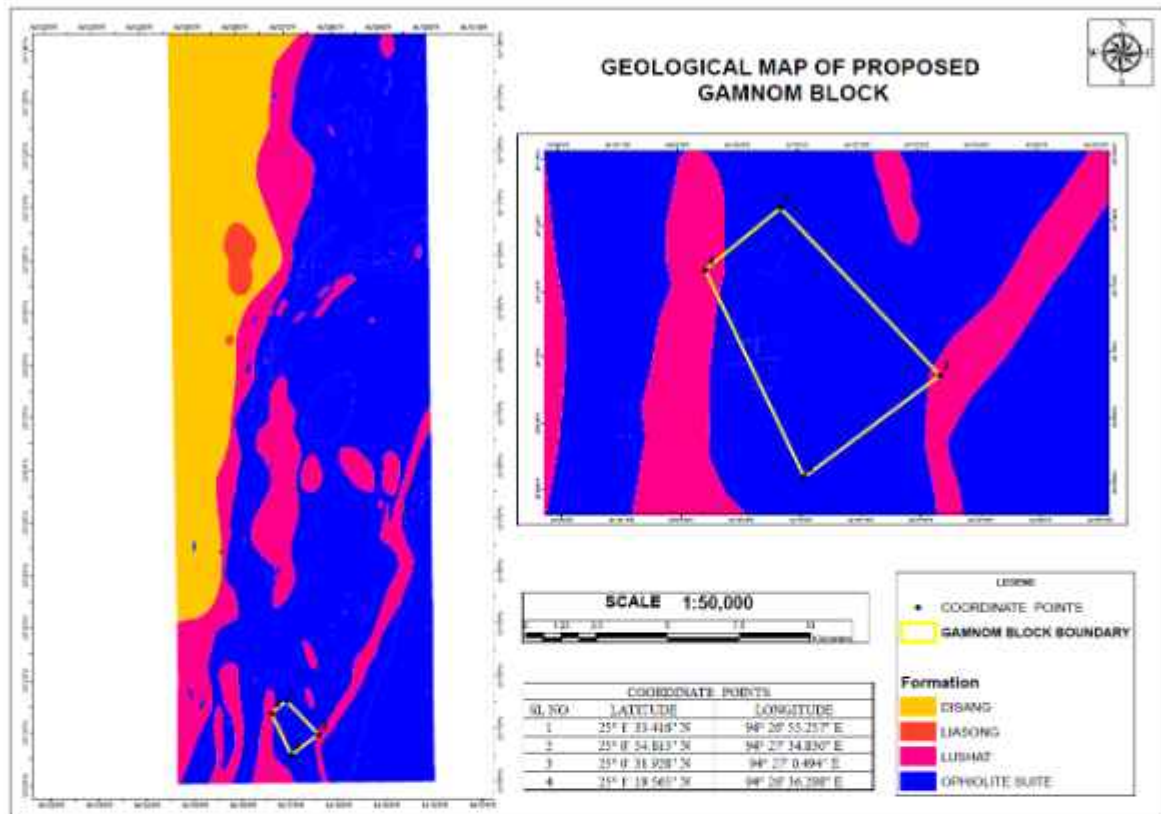


Figure 7: Geological map of the proposed block

(Source: Geological Survey of India)

2.1.4 SCOPE FOR THE EXPLORATION:

- Geological mapping in 1:4000 scale
- Bed Rock Sampling
- Stream Sediment Sampling
- Soil Sampling
- Pitting and trenching
- Scout Drilling
- Petrographic study
- Geophysical investigation (Magnetic survey)
- Petrographic study
- Chemical analysis and ICPMS of the samples for PGE and AAS for Ni, Cr.

- k. Geological report preparation.

2.1.5 OBSERVATION AND RECOMMENDATIONS OF PREVIOUS WORK:

Reconnaissance survey for chromium, nickel and base metal mineralization in Gamnom-Yentem area in part of Ophiolite belt, Ukhrul District, Manipur (G-4) was carried out by Imomeren Ao (Senior Geologist) and Vales Savio Peter (Senior Geologist) in 2019-20.

This block has been identified based on their analytical results of the Geochemical data. There are 15 BRS points noted within the proposed block, where values of Cr vary from 2229 to 328416 ppm (Average: 24682 ppm) and Ni varies from 500 to 4167 ppm (average value: 2326 ppm).

Further, the petrochemical samples in the form of fresh grab samples were analyzed and the values of Cr ranges between 2872 to 302143 ppm (Only 4 samples within the proposed block). Ni values ranges between 2516 to 11254 ppm (Only 4 samples within the block).

Therefore, the proposed block is very much potential for Ni, Cr and associated Co deposits and required for detail exploration.

Based on the evaluation of previous work, the present Preliminary Survey program at G-3 level has been prepared. The Geological Mapping combined with surface, stream and soil sampling, pitting, trenching followed by geophysical investigation scout drilling will be helpful in assessing the disposition of the mineralized zones, structural features like shears and faults if any.

2.2 Previous Work:

2.2.1 GSI EXPLORATION:

Reconnaissance survey for chromium, nickel and base metal mineralization in Gamnom-Yentem area in part of Ophiolite belt, Ukhrul District, Manipur (G-4) was carried out by Imomeren Ao (Senior Geologist) and Vales Savio Peter (Senior Geologist) in 2019-20.

This block has been identified based on analytical results of the Geochemical data carried out by GSI in the proposed block. There are 15 BRS points noted within the proposed block, where values of Cr vary from 2229 to 328416 ppm (Average: 24682 ppm) and Ni varies from 500 to 4167 ppm (average value: 2326 ppm). Therefore, the

proposed block is very much potential for Ni, Cr and associated Co deposits and required for detail exploration.

The depth persistence of the podiform chromite from the transitional-cumulate peridotite is to be investigated along with depth persistence of the supergene enrichment of Cr, Ni and Co from the limonitic and saprolitic soil capping developed above the mafic/ultramafic rocks.

Further, Geochemical Mapping was also carried out within Toposheet area 83K/8 which also includes our proposed block (in Field Seaso:2018-19) By A.Elou (Senior Geologist) L. Somorjit Singh (Senior Geologist), Geological Survey of India.

2.3 Block Boundary:

The block falls in survey of India toposheet no 83K/8 of Manipur and covers 1.50 Sq. Km area in and around villages named Gamnom of Kamjong district. The Co-ordinates of the corner points of the proposed block area are given below.

Table 5: Block Boundary Coordinates

Point ID	LAT	LONG
1	25° 1' 33.416" N	94° 26' 55.257" E
2	25° 0' 54.813" N	94° 27' 34.830" E
3	25° 0' 31.928" N	94° 27' 0.494" E
4	25° 1' 19.565" N	94° 26' 36.298" E

2.4 Planned Methodology

The exploration program is proposed in accordance to the objective set for preliminary survey (G-3) of the block. The Exploration shall be carried out as per Minerals (Evidence of Mineral Contents) Rule-2015. Accordingly, the following scheme of exploration is formulated in order to achieve the objectives. The details of different activities to be carried out are presented in subsequent paragraphs.

- i) **Geological Mapping:** Geological mapping will be done in the entire area on 1:4000 scale. Rock types, their contact, structural features will be mapped. Surface manifestations of the mineralization available along with their surface disposition will be marked on map.

- ii) **Geochemical Survey:** Regional grab/ chip/ stream sediment/ soil sampling to be carried out at regular interval.
 - a. Grab Sampling: During the course of Geological mapping, bed rock samples shall be collected for identifying various litho units.
 - b. Soil Sampling: Soil samples will be carried out in entire area to delineate mineralized zone.
- iii) **Ground Geophysical Survey:** Based on the geology of the area, Magnetic survey will be conducted.
- iv) **Pitting:** Shallow trenching/Pits (Excavation) shall be carried out in the potential zones identified based on the results of geological mapping and geochemical sampling. A provision of shallow pitting on mineralized zones (if any) (1m X 1m X 1m) with 100 cubic meters is kept.
- v) **Scout Drilling:** Based on Geological Mapping, Geochemical Sampling, the extension of the mineralized zones (ore bodies) will be marked. To find out the potentiality of mineralized zones in strike & dip direction, 4 no scout boreholes involving 500m of drilling will be carried out for upper (first) level of intersection of mineralized zones.
- vi) **Chemical Analysis:** All samples need to analyzed for Cr, Ni, Co and PGE (Bed Rock Sample).
- vii) **Petrographic study:** XRF studies have mostly been performed on samples to determine the grain size morphology and crystallinity.
- viii) **Data verification and Quality Check:** Standard reporting of resources are classified and estimated by using two types of data. Data acquired from previous exploration and data generated by exploring the block. Data verification and Gap analysis is the interpretive or indirect methods. Interpretive Data may include results from mapping, seismic, magnetic, gravity and other geophysical and geological surveys. An Interpretive Data, may be used in conjunction with Explored Data to improve confidence levels.

QA/QC will be strictly followed during the collection, recording and storage of any of the data ultimately used in the geological report preparation. This programme should be concerned with, but not limited to, data verification, drill sample recovery, sample size, sample preparation, analytical methods, the use of duplicates/blanks/standards, effects of multiple periods of data acquisition and consistency of interpretation in three dimensions.

2.5 Nature Quantum and target

Components	G3	Quantum of Work
Geological Mapping	i) 1:4000 Scale	Geological mapping 1.50 sq.km
	ii) Assessment of lithology, structure, surface mineralization and analysis of old history of mining if any	
Geochemical Survey	i) Regional grab/ chip/ stream sediment/ soil sampling	BRS: 75 Soil Sample: 100
Geophysical Survey	Magnetic Survey	Ground Magnetic Survey over 550 station point
Pit Sampling		100 Cub m
Scout Drilling	Few boreholes if required along the positive profiles delineated by surface sampling/ pitting/ trenching	200 m
Core sample	Sample from mineralize zones as well as hanging wall/ footwall side to be collected.	200 nos. drill core samples and 100 no Pit samples.
Geochemical Analysis	To understand the chemical analysis data for searching the required mineral	ICPMS: 100 ICPMS PGE: 50
Petrographic and mineralogical studies	Principal rock types, mineral assemblage, identification of minerals of interest	XRF: 100
Synthesis of all available data	i. Integration of regional geophysical, geological and geochemical data, if not done earlier	3 Hard copies
Not required in the quantum of the work	ii. Synthesis of all available data and report writing	

NMET Proposal (For G3 exploration)
Gamnong Ni, Cr and PGE Block
Kamjong, Manipur

2.6 Project schedule

Item of work in monthly time frame	Month-1	Month-2	Month-3	Month-4	Month-5	Month-6	Month-7	Month-8	Month-9	Month-10	Month-11	Month-12
Ground Geophysical Survey												
Magnetic Survey												
Geological Survey												
Large Scale mapping in 1:4000 Scale												
Geochemical Survey												
Bedrock and Soil sampling												
Pitting												
Pitting												
Chemical Analysis												
Sample analysis												
Scout Drilling (if required)												
Drilling												
Core Logging/sampling												
Petrographic and Mineral graphic studies												
Petrographic study												
XRD/ XRF study												
Geological report												

2.7 Project cost

S. No.	Item of Work *	Unit *	Rates as per NMET SoC 2020-21		Estimated Cost of the Proposal		Remarks
			SoC-Item No. *	Rates as per SoC * (a)	Qty. (b)	Total Amount (Rs) (a*b)	
A	Geological Mapping Other Geological Work & Surveying						
	Geological mapping, (1:4000 scale) & Trenching, drilling work						
i	a. Charges for Geologist per day (Field) for geological mapping & trenching work, drilling work	day	1.2b	11,000	180	19,80,000	
ii	b. Labours Charges; Base rate	day		522	360	1,87,920	
	d. Charges for one Sampler per day (1 Party)	one sampler per day	1.5.2	5,100	35	1,78,500	
	e. Labours (4 Nos)	day		522	140	73,080	
	Sub Total- A					24,19,500	
B	Ground Geophysical Survey						
1	Magnetic (30 Lkm)	Point	3.2a	1,800	2,000	36,00,000	
3	Geophysicist party days (Field)	per day	3.18a	11,000	30	3,30,000	

NMET Proposal (For G3 exploration)
Gannom Ni, Cr and PGE Block
Kamjong, Manipur

4	c. Labours Charges	day		522	60	31,320	
5							
	Sub Total- B					39,61,320	
	TOTAL FIELD EXPLORATION COST					63,80,820	
	EXPLORATION COST FOR NORTH EAST STATES AND HILLY TERRAIN		Section 5 of SoC			2,13,75,747	Exploration rates shall be 3.35 times higher than the normal SoC rate for carrying out exploration work in North Eastern States and hilly terrain of Himalaya region.
C	Charges for Geologist per day (HQ)	day		9,000	90	8,10,000	
	Geophysicist party days (HQ)	per day	3.18b	9,000	30	2,70,000	
D	LABORATORY STUDIES						
1	Chemical Analysis						
i)	Geochemical Sampling-Surface samples (Bedrock/Channel /Soil/Stream sediment)						
	a. ICPMS	Nos	4.1.14	7,731	100	7,73,100	
	b. ICPMS-PGE	Nos	4.1.5d	11,800	50	5,90,000	
	c. XRF	Nos	4.1.15a	4,200	100	4,20,000	
2	<u>Physical & Petrological Studies</u>						

**NMET Proposal (For G3 exploration)
Gamnom Ni, Cr and PGE Block
Kamjong, Manipur**

i	Preparation of thin section	Nos	4.3.1	2,353	50	1,17,650	
ii	Study of thin section	Nos	4.3.4	4,232	50	2,11,600	
v	Digital Photographs	Nos	4.3.7	280	50	14,000	
	Sub-Total					32,06,350	
E	Total A to G					2,45,82,097	
F	Geological Report Preparation	5 Hard copies with a soft copy	5.2	5.2 (iii)		19,04,821	Reimbursement will be made after submission of the final Geological Report in Hard Copies (5 Nos) and the soft copy to NMET.
G	Peer review Charges		As per EC decision			30,000	
H	Preparation of Exploration Proposal (5 Hard copies with a soft copy)	5 Hard copies with a soft copy	5.1	2% of the Cost or Rs. 5.0 Lakhs whichever is less		3,80,000	EA will be reimbursed after submission of the Hard Copies and the soft copy of the final proposal along with Maps and Plan as suggested by the TCC-NMET in its meeting while clearing the proposal.
I	Total Estimated Cost without GST					2,68,96,918	
J	Provision for GST (18% of J)					48,41,445	GST will be reimbursed as per actual and as per notified prescribed rate
K	Total Estimated Cost with GST					3,17,38,364	
	or Say Rs. In Lakhs					317.38	

2.8 Reference

3. Reconnaissance survey for chromium, nickel and base metal mineralization in Gamnom-Yentem area in part of Ophiolite belt, Ukhul District, Manipur (G-4) by Imomeren Ao (Senior Geologist) and Vales Savio Peter (Senior Geologist).
4. Interim report on geochemical mapping in the Ophiolite belt in parts of Ukhul district, Manipur (Field Season: 2018-19) By A. Elow (Senior Geologist) L. Somorjit Singh (Senior Geologist), Geological Survey of India.



भारत सरकार
Government of India
भारतीय भूवैज्ञानिक सर्वेक्षण
Geological Survey of India

मणिपुर के उखरूल जिला के हिस्सों, टी.एस. सं. ८३के/८ के अंदर
ओफीयोलाइट क्षेत्र में भूरासायनिक मानचित्रण पर अंतरिम प्रतिवेदन

INTERIM REPORT ON GEOCHEMICAL MAPPING IN THE
OPHIOLITE BELT IN PARTS OF UKHRUL DISTRICT, MANIPUR
IN T.S. NO. 83K/8

टोपोशीट सं: ८३के/८ / Toposheet No.: 83K/8
मद सं: एम १ ए जि सि एस - जि सि एम / एन सि / एन इ आर/ एस यु/ एम एन/ २०१८/ १७५३१
Item No: M1AGCS-GCM/NC/NER/SU-MAN/2018/17531

कार्य सत्र २०१८-२०१९ का अंतरिम प्रतिवेदन
Interim report for field season 2018-2019

ए. ईलो, वरिष्ठ भूवैज्ञानिक
एल. सोमोरजित सिंह, वरिष्ठ भूवैज्ञानिक

A. Elow, Senior Geologist
L. Somorjit Singh, Senior Geologist

मिशन - १
MISSION - I

राज्य इकाई: मणिपुर - नगालैंड / State Unit: Manipur - Nagaland
उत्तर पूर्वी क्षेत्र / North Eastern Region
इम्फाल / Imphal

दिसम्बर, २०१९
December, 2019

**INTERIM REPORT ON GEOCHEMICAL MAPPING IN THE OPHIOLITE BELT IN
PARTS OF UKHRUL DISTRICT, MANIPUR IN T.S. NO. 83K/8**

(Code No.: M1AGCS-GCM/NC/NER/SU-MAN/2018/17531)

(Field Season: 2018-19)

By

**A. Elow, Senior Geologist
L. Somorjit Singh, Senior Geologist**

Contents

	Page No.
<i>Abstract</i>	<i>i-vi</i>
Chapter 1 Introduction	1-10
1.1 General	1
1.2. Location and accessibility	1
1.3. Physiography, Drainage, Land use and Land cover	2
1.4. Water supply	6
1.5. Soil erosion	7
1.6. Climate	7
1.7. Flora and Fauna	8
1.8. Present work	9
1.10 Acknowledgement	10
Chapter 2 Geology	11-43
2.1 Regional Geology	11
2.2 Previous Work	14
2.3 Geology of the study area	16
2.4 Structures	34
2.5 Petrographical Study	36
2.6 Economic Geology	41
Chapter 3 Sampling Methodology and Procedure	44-56
3.1 Equipment used in sampling	44
3.2 Sampling media	45
3.2.1 Stream sediment/slope wash samples	45
3.2.2 Soil samples- Regolith and C- horizon soil	49
3.2.3 Stream water samples	51
3.2.4 Duplicate samples	53
3.2.5 Rock sampling	54
3.3 Field data sheet	55
3.4 Processing and storage of samples	55
3.5 Sample contamination	56
Chapter 4 Statistical Analysis of Chemical Data	57-59
4.1 Statistical analysis	57
4.1.1 Check for error and outliers	58
4.1.2 Statistical treatment of data in MS Excel	58
Chapter 5 Geochemical Anomaly	60-160
5.1. Normal Background Values	60

5.2 Preparation of Geochemical Maps	61
5.2.1 Correlation Matrix	63
5.3 Distribution of Major Elements in the Stream Sediments	66-87
5.4 Distribution of Trace Elements in the Stream Sediments	87-132
5.5 Distribution of Rare Earth Elements in the Stream Sediments	132-160
Chapter 6 Study of Water, Soil and Duplicate Samples	161-172
6.1 Water sample analysis	161
6.2 Soil samples	162
6.2.1: Interpretation of soil samples	166
6.3. Duplicate Samples	172
Chapter 7 Summary, Conclusion and Recommendation	173-176
7.1 Summary	173
7.2 Conclusion	173
7.3 Recommendation	175
References	177-179
Locality Index	180
List of Plate	
Plate No.1: Geological map of Toposheet No. 83K/8	181
Plate No.2: Sample collection point superimposed on drainage map of Toposheet No. 83K/8.	182
Plate No.3: Geomorphological map of Toposheet No. 83K/8.	183
Plate No.4: Land Use and Land Cover map of Toposheet No. 83K/8.	184
Plate No.5: Drainage Map showing sample locations in different media of T.S. Nos. 83K/08 on 1:50000 scale.	
Annexure-I Analytical data of Major and Minor Oxides of stream sediment/Slope Wash Samples	185-190
Annexure-II Analytical Data of Trace Elements of stream sediment/Slope Wash Samples	191-197
Annexure-III Analytical Data of Rare Earth Elements of stream sediment/Slope Wash Samples	198-204
Annexure-IV Analytical Data of Oxides of Soil Samples	205
Annexure-V Analytical Data of Trace Elements of Soil Samples	206
Annexure-VI Analytical Data of Rare Earth Elements of Soil Samples	207
Annexure-VII Analytical data of Stream Water Samples: Trace Elements	208-209
Annexure-VIII Analytical data of Oxides of Duplicate Stream Sediment/Slope wash Samples with Original Samples	210
Annexure-IX Analytical data of REEs of Duplicate Stream Sediment/Slope wash Samples with Original Samples	211
Annexure-X Analytical data of Trace Elements of Duplicate Stream Sediment/Slope wash Samples with Original Samples	212
Annexure-XI Status of analytical chemical data received	213
List of Figures	
Fig.1.1: Location map of the study area.	2
Fig.1.2: Drainage map of the study area	3
Fig.1.3: DEM map for the study area (Toposheet No.83K/8).	4
Fig.1.4: Geomorphological map of the study area (Toposheet No.83K/8)	5
Fig.1.5: Land Use and Land Cover map of the study area (Toposheet No.83K/8)	6
Fig.2.1: Geological map of the area around Ukhrul, Naga-Manipur Hills, Manipur	12
Fig.2.2: Geological map of the study area (Toposheet No.83K/8)	16
Fig.2.3: Tectonised peridotite.	27
Fig.2.4: Tectonised peridotite embedded within foliated serpentinised groundmass.	27
Fig.2.5: Tectonised peridotite with sparse anhedral pyroxene grains embedded with serpentinised groundmass.	27

Fig 2.6: Serpentinite vein dissecting across with peridotite.	27
Fig 2.7: Thin limonitic soil profile developed above Transitional-Cumulate peridotite rock.	17
Fig 2.8: Two sets of asbestos vein dissection the tectonised peridotite.	27
Fig 2.9: Transitional peridotite pyroxene grains embedded with serpentinised groundmass	28
Fig 2.10: Tectonised peridotite showing olivine neo-blast around the margin of resolved opx grain.	28
Fig 2.11: Crude layered banding of cumulate peridotite showing hob-nail texture.	28
Fig 2.12: Cumulate peridotite showing euhedral opx (Bronzite mineral embedded with serpentinised peridotite groundmass.	28
Fig 2.13: Pods of massive chromite within cumulate peridotite.	28
Fig 2.14: Thick limonitic soil profile developed above cumulate peridotite.	28
Fig 2.15: Grabbro.	29
Fig 2.16: Anorthosite.	29
Fig 2.17: Pillow basalt.	29
Fig 2.18: Vesicular pillow basalt.	29
Fig 2.19: Amygdular volcanic bomb within limestone.	29
Fig 2.20: Volcanic ash bed inter-bedded with shale.	29
Fig 2.21: Disseminated pyrite within chert nodules.	30
Fig 2.22: Thinly inter-bedded bedded Marl with volcanic ash bed.	30
Fig 2.23: Olistoliths of sandstone/siltstone and limestone within shale.	30
Fig 2.24: Pyrite crystals within exotic olistolith block of limestone.	30
Fig 2.25: Exotic block of sandstone with juvenile quartzs.	30
Fig 2.26: Olistolith block of variegated colour banded chert.	30
Fig 2.27: Exotic olistolith block of red radiolarian chert.	31
Fig 2.28: Graphia sp. within exotic limestone block.	31
Fig 2.29: Thin intercalations of shale and siltstone.	31
Fig 2.30: Chert nodules within shale.	31
Fig 2.31: Thickly bedded sandstone with thin shale intercalations.	31
Fig 2.32: Cruziana ichnofacies (Trail marks) within shale and siltstone intercalations.	31
Fig 2.33: Ophiomorpha Nodosa isp. (Domichnia) within sandstone.	32
Fig 2.34: Skolithos ichnofacies (Domichnia) within thinly laminated siltstone.	32
Fig 2.35: Shell fragments of bivalves within sandstone.	32
Fig 2.36: Turetelia within sandstone.	32
Fig 2.37: Medium to thickly bedded sandstone with thin shale intercalations.	32
Fig 2.38: Trough cross-bedded sandstone with pebbly basal lags.	32
Fig 2.39: Rose diagram depicting NW (321.7°) paleo-current flow direction.	33
Fig 2.40: Plant leaf impression within sandstone.	33
Fig 2.41: Wood fossil marked by cellulose fiber striations and coal streak within sandstone	33
Fig 2.42: Large scale cross bedded sand along the Thoubal River bank.	33
Fig 2.43: Clayey silt along the Thoubal River tributary river bank.	33
Fig 2.44: Boulders along the Thoubal River course.	34
Fig 2.45: Pebbles and cobbles along the Thoubal River bank.	34
Fig 2.3.1: Tectonic contact between Ophiolite and Paleogene sediments.	35
Fig 2.3.2: Highly sheared and mylonitised contact zone.	35
Fig 2.3.3: Quartz vein align parallel to the slaty cleavage.	35
Fig 2.3.4: Brecciated zone within ophiolite body.	35
Fig 2.3.5: Quartz vein dissecting across the body of sandstone.	36
Fig 2.3.6: Highly sheared and mylonitised serpentinised mafic/ ultramafic rock.	36
Fig 2.3.7: Highly sheared and mylonitised carbonaceous shale at the base of the clippe.	36
Fig 2.3.8: Highly sheared and mylonitised serpentinised mafic/ ultramafic rock.	36
Fig.2.4.1 to 2.4.4: Photomicrograph of transitional peridotite	38
Fig: 2.4.5 and 2.4.6: Photomicrograph of Spinel harzburgite	39
Fig: 2.4.7 and 2.4.8: Photomicrograph of Iherzolite	39
Fig: 2.4.9 to 2.4.12: Photomicrograph of pillow basalt	40
Fig: 2.4.13: Photomicrograph of chromite	41
Fig: 2.4.14: Photomicrograph of chert	41

Fig. 2.4.15: Photomicrograph of lithic quartz arenite	41
Fig. 2.5.1: Chromite boulders exposed above weathered mafic/ultramafic reddish soil.	43
Fig. 2.5.2: Thick limonitic reddish soil developed above mafic/ultramafic rock.	43
Fig. 2.5.3: Thin lateritic bed developed above mafic/ultramafic rock.	43
Fig. 2.5.4: Medium to thickly bedded limestone with thin shale intercalation (Cretaceous age).	43
Fig. 2.5.5: Limestone containing volcanic bombs.	43
Fig. 2.5.6: Thin intercalations of limestone and volcanic ash beds (Upper Cretaceous-Lower Eocene age).	43
Fig.3.1: Sample numbering scheme	46
Fig.3.2 & 3.3: Collection of Stream Sediments	47
Fig.3.4: Stream Sediment/Slope Wash Sample Location Map (Toposheet No.83K/8)	48
Fig.3.5: Soil sampling profile from Ophiolite Belt	49
Fig.3.6: Soil sampling profile from Disang Group	49
Fig.3.7: Soil sample profile from Barail Group	49
Fig.3.8: Soil sampling profile from Olistostrome	49
Fig.3.9: Soil (Regolith & C-Horizon) Sample Location Map (Toposheet No.83K/8)	50
Fig.3.10: Water sample collection	51
Fig.3.11: Stream Water Sample Location Map (Toposheet No.83K/8)	53
Fig.3.12: Field data Sheet	54
Fig.3.13: Sun drying of the stream sediment/slope wash samples at camp.	55
Fig.3.14: Delumping of the stream sediment/slope wash samples at camp	55
Fig.3.15: Sieving of the samples at camp.	56
Fig.3.16: Packing of samples at Camp.	56
Fig. 5.1 to 5.310 Spatial distribution of major oxides in the stream sediments	66-86
Fig. 5.11 to 5.32 Spatial distribution of trace elements in the stream sediments	88-131
Fig. 5.33 to 5.46 Spatial distribution of REEs in the stream sediments	133-160
Fig.6.1 Major and trace element concentration spider diagram for soil (regolith and C-horizon soil sample for Olistostrome and Barial Group)	167
Fig.6.2 Major and trace element concentration spider diagram for soil (regolith and C-horizon soil sample from Ophiolite Belt, OPS and Disang Group)	168
Fig.6.3 Major and trace element concentration spider diagram for soil (regolith and C-horizon soil sample from Ophiolite Belt, OPS and Disang Group)	169
Fig.6.4 Rare earth element (REE) concentration spider diagram for soil (regolith and C-horizon soil)	169
Fig.7.1 Mineral prospect block A and B for chromium, nickel and cobalt as a NGCM spin off project.	176
List of Tables:	
Table 1.1: Nature and quantum of work and time schedule	9
Table 1.2: Field stays details of Officers.	10
Table No. 2. 1: Generalised litho-stratigraphy of Manipur state	13
Table No. 2.2: Litho-stratigraphy of the study area.	18
Table 4.1: Methodologies employed for analysis of samples	57
Table 4.2: Univariate statistical summary of the major oxides from the stream sediment/slope wash samples	58
Table 4.3: Univariate statistical summary of Trace elements and REE's from the stream sediment/slope wash samples	59
Table 5.1: Table showing background value, anomalous value and significantly anomalous values of Oxides and Trace elements from the stream sediment/slope wash samples along with their % of no. of observations	62-63
Table: 5.2. Correlation matrix of Oxides	64
Table: 5.3. Correlation Matrix of Rare Earth Elements	64
Table: 5.4. Correlation Matrix of Trace Elements	65
Table 6.1: Water Samples with location	161
Table 6.2: Statistical summary of some of trace elements and REEs in water samples.	162
Table 6.3: Soil Samples with Location	163
Table 6.4: Statistical summary of major oxides in soil samples (Regolith)	163
Table 6.5: Statistical summary of major oxides in soil samples (C-Horizon)	164

Table 6.6: Statistical summary of Trace elements in soil samples (Regolith)	164
Table 6.7: Statistical summary of Trace elements in soil samples (C-horizon)	165
Table 6.8: Statistical summary of REE elements in soil samples (Regolith)	165
Table 6.9: Statistical summary of REE elements in soil samples (C-horizon)	166
Table :6.10 U.S. Recommended Daily Allowances (USRDA) and biological roles of elements that the National Research Council (1989) lists as essential to health	170
Table:6.11 Micronutrient levels (ppm) in Soil (Compiled from WHO data and others)	171
Table :6.12 Environmental and human health soil quality guidelines (CCME 1996, updated 2004) All values in ppm	171



**GEOCHEMICAL MAPPING IN THE OPHIOLITE BELT IN PARTS OF UKHRUL
DISTRICT, MANIPUR IN T.S. NO. 83K/8
(Field Season: 2018-19)**

Code No.: MLAGCS-GCM/NC/NER/SU-MAN/2018/17531

by

A. Elow, Senior Geologist and Laishram Somorjit Singh, Senior Geologist

सारांश

F.S. 2018-19 के दौरान नेशनल जियोकेमिकल मैपिंग प्रोग्राम के एक भाग के रूप में जियोकेमिकल मैपिंग (GCM) के लिए टोपोशीट संख्या 83K/8 में 671 वर्ग किमी का क्षेत्र 1: 50,000 पैमाने पर लिया गया था जो अक्षांश $25^{\circ} 00' 24''$ to $24^{\circ} 15' N$ और देशांतर $94^{\circ} 15'$ से $92^{\circ} 30' E$ के द्वारा बंधे हैं और उखरूल जिले, मणिपुर राज्य का हिस्सा शामिल है। एन.जी.सी.एम का मुख्य उद्देश्य पूरे देश के लिए विभिन्न तत्वों का सहज भू-रासायनिक मानचित्र बनाना है, जिसका उपयोग प्राकृतिक संसाधनों और कृषि, पर्यावरण, सार्वजनिक स्वास्थ्य और सामाजिक क्षेत्र के अन्य क्षेत्रों में अनुप्रयोगों के प्रबंधन / विकास के लिए भू-रासायनिक आधार रेखा डेटाबेस के रूप में किया जा सकता है।

अध्ययन क्षेत्र मणिपुर राज्य के पूर्वी भाग में स्थित है। अध्ययन क्षेत्र के प्रमुख भूवैज्ञानिक सेट अप को तीन डोमेन में वर्गीकृत किया जा सकता है। क) ओफियोलाइट्स बेल्ट पूर्वी हिस्से में फैलता है, अध्ययन क्षेत्र के लगभग 27% हिस्से पर कब्जा कर लेता है। लिथोलॉजिकल रूप से, यह टेक्टोनाइज्ड मेटल पेरिडोटाइट (Iherzolite), संक्रमणकालीन पेरिडोटाइट (ज्यादातर हर्जबर्ग), कम्प्लेक्स माफिक / अल्ट्रामैफिक सीक्वेंस (हर्जोइट, लेयर्ड गैब्रो, एनरथोसाइट और प्लैगीओबैसाइट), ज्वालामुखी (तकिया बेसाल्ट (तकिया बेसाल्ट) की विशेषता है। पेट्रोग्राफिक अध्ययन से पता चलता है कि संक्रमणकालीन और संचयी पेरिडोटाइट प्रकृति में प्रमुख रूप से हर्जबर्ग है। ख) पेलियोसीन टू ऑलिगोसेंस तलछटी उत्तराधिकार मध्य और पश्चिमी भाग पर

कब्जा करता है जो अध्ययन क्षेत्र के लगभग 70% क्षेत्र को कवर करता है। इस इकाई को चट्टानों के डिसैंग और बरैल समूह द्वारा दर्शाया गया है जो रंग चूना पत्थर को सफेद करने के लिए पर्पलिश के विदेशी ब्लॉक हैं जो ग्रेफाइट का उत्पादन करते हैं। जो एक सृजनात्मक समुद्री जीव है, विदेशी चूना पत्थर ब्लॉक की आयु को दर्शाता है। ग) हाल के एलुवियम समूह के लिए होलोसीन सबसे कम समतापिक उत्तराधिकार का प्रतिनिधित्व करता है, जो रेतीली से लेकर मृण्मय मिट्टी, कंकड़, बटिया और बोल्टर तक होता है, जो ज्यादातर निकटवर्ती ओफियोलाइट बेल्ट और पैलोजेन तलछटी इलाके से प्राप्त होता है। प्राकृतिक भूगोल रूप से, क्षेत्र एक बीहड़ स्थलाकृति का प्रतिनिधित्व करता है जो संरचना और इसके निहित लिथोलॉजी द्वारा नियंत्रित होता है। समग्र जल निकासी पैटर्न वृक्षवत् पैटर्न से उप-समानांतर पैटर्न के समान दिखाता है। ओफियोलाइट बेल्ट पर उच्च लकीरें विरल वनस्पति कवर दिखाती हैं, मध्य ढलानों को मामूली घने देवदार के जंगल द्वारा कवर किया जाता है।

कुल 168 नग धारा तलछट के नमूनों (एसएस) को 2'x 2, बिड से, 09 नग मिट्टी (C-Horizon) और रेजोलिथ (R), 09 ड्रिलिकेट स्ट्रीम / स्लोप वॉश, 09 स्ट्रीम पानी के नमूने 5 'x 5' बिड अंतराल से रासायनिक विश्लेषण के लिए एकत्र किए गए थे और पेट्रोग्राफी अध्ययन के लिए 16 रॉक नमूने एकत्र किए गए थे।

पैकेज ए (प्रमुख ऑक्साइड) और एच (आर.ई.ई और ट्रेस तत्व) के विश्लेषणात्मक परिणाम प्राप्त हुए हैं। सामान्य तौर पर, क्षेत्र के प्रवाह तलछट में तत्वों का मौलिक वितरण पैटर्न अंतर्निहित और आसपास के लिथोलॉजी के साथ सुसंगत है।

ओफियोलाइट बेल्ट से इसकी सिद्धता वाले खलहंग खुल्लेन, फंगराई, शिरुई और गमनोम गाँवों के पूर्व से एकत्र की गई धारा तलछट Cr (958 से 4810 पी.पी.एम), Ni (917 से 5681 पी.पी.एम) Co (88 से 678 पीपीएम) और Fe_2O_3 (16.23 से 29.13%) के विषम मूल्यों को दर्शाती है। Cr, Ni, Co, Cu और Fe_2O_3 के बीच मजबूत सकारात्मक सहसंबंध देखा जाता है। सर्पिलीनकृत माफिक / अल्ट्रामैफिक चट्टानों के ऊपर

पाँडिफॉर्म क्रोमाइट, फेरिक क्रोमाइट, लेटरिटिक / लिमोनाइटिक मिट्टी कैपिंग के क्षेत्र सबूतों से इन मौलिक विसंगतियों की उपस्थिति की पुष्टि होती है। पेट्रोग्राफिक अध्ययन भी जियोकेमिकल विसंगति की पुष्टि करते हैं। प्राथमिक ओलिविन और पाइरोक्सेन की उच्च स्तर की सर्पिलीनकरण का उल्लेख किया गया है; मैग्नेटाइट और क्रोमियम स्पिनल आमतौर पर ओलिविन खनिजों और ऑर्थोपाक्सिन के साथ जुड़ा हुआ है जो कि सर्पेटाइन में बदल जाता है।

मिट्टी के नमूने (Regolith & C-Horizon) SiO_2 , K_2O , MgO , Al_2O_3 , Fe_2O_3 , Ba, Cr, Ni और V जैसे तत्वों से समृद्ध हैं और TiO_2 , MoO , CaO और K_2O नष्ट हो जाते हैं। मिट्टी के नमूनों में सी-होरिजन, रेजोलिथ मिट्टी की तुलना में थोड़ा अधिक मूल्यों को दर्शाता है। ओफियोलाइट बेल्ट से एकत्र किए गए दो मिट्टी के नमूने क्रमशः Fe_2O_3 , Cr और Ni के विषम मूल्यों को दिखाते हैं जिसमें Fe_2O_3 : 45.91%, Cr: 11388 ppm और Ni: 4888 ppm है। मिट्टी के पैटर्न के आर.ई.ई. पैटर्न के समान एकाग्रता को दर्शाता है, उजागर रॉक मिट्टी प्रोफाइल से बरियल मिट्टी का नमूना सबसे कम एकाग्रता दिखाता है, मामूली नकारात्मक Eu विसंगति आमतौर पर सभी मिट्टी के नमूनों में देखी जाती है।

Cr, Ni और Co के खनिज वस्तुओं के जांच के लिए लिए ब्लॉक-ए और बी के रूप में दो ब्लॉकों की पहचान की गई और सीमांकित किया गया है, तथा संक्रमणकालीन-संचयी पेरिडोटाइट से उजागर पाँडिफॉर्म क्रोमाइट और सुपरगीन संवर्धन से Cr, Ni और Co अल्ट्रामाफिक चट्टानों के ऊपर विकसित लिमोनीटिक और सैप्रोलिटिक मिट्टी कैपिंग।

**GEOCHEMICAL MAPPING IN THE OPHIOLITE BELT IN PARTS OF UKHRUL
DISTRICT, MANIPUR IN T.S. NO. 83K/8
(Field Season: 2018-19)**

Code No.: MLAGCS-GCM/NC/NER/SU-MAN/2018/17531

By

A. Elow, Senior Geologist and Laishram Somorjit Singh, Senior Geologist

ABSTRACT

An area of 671 sq. km. was taken up for Geochemical Mapping (GCM) as a part of National Geochemical Mapping Programme during F.S. 2018-19 in Toposheet number 83K/8 bounded by latitudes 25°00' to 24°15' N and longitudes 94°15' to 92°30' E on 1:50,000 scale covering part of Ukhrul district, Manipur State. The main objective of the NGCM is to create seamless geochemical maps of different elements for the entire country, which can be used as a geochemical baseline database for managing/developing natural resources and applications in agricultural, environmental, public health and other spheres of societal concern.

The study area lies in the eastern part of the Manipur state. Prominent Geological set of the study area can be classified into three domains viz. a). Ophiolites Belt exposes in the eastern side, occupying about 27% of the study area. Lithologically, it is characterized by tectonised mantle peridotite (lherzolite), transitional peridotite (mostly hartzburgite), cumulate mafic/ultramafic sequence (hartzburgite, layered gabbro, anorthosite and plagiogranite), volcanic (pillow basalt and andesite) and volcano-clastics. Petrographic studies show that transitional and cumulate peridotite is dominantly hartzburgite in nature. b). Paleocene to Oligocene sedimentary succession occupying the central and western part that covers an area of about 70% of the study area. This unit is represented by the Disang and Barail Group of rocks Exotic blocks of purplish to whitish colour limestone which yields Graphia sp. which is a Cretaceous marine fauna, indicates the age of the exotic limestone block. c) Holocene to Recent Alluvium Group represents the youngest stratigraphic succession, characterised by the sandy to clayey soil, pebbles, cobbles and boulders, mostly derived

from the adjacent Ophiolite Belt and Paleogene sedimentary terrain. Physiographically, the area represents a rugged topography which is controlled by the structure and its inherent lithology. The overall drainage pattern shows dendritic to sub-parallel pattern. The higher ridges on the Ophiolite Belt show sparse vegetation cover, mid slopes are covered by moderately thick pine forest.

A total of 168 nos. of stream sediment samples (SS) were collected from 2'x 2' grid, 09 Nos. each of soil (C –Horizon) and regolith (R), 09 duplicate Stream/Slope wash, 09 stream water samples from 5' x 5' grid interval were collected for chemical analysis and 16 rock samples were collected for petrography study.

The analytical results of package A (major oxides) and H (REE's and Trace elements) have been received. In general, the elemental distribution pattern of elements in stream sediment of the area is coherent with the underlying and surrounding lithology.

The stream sediments collected from in around east of Khalhang Khullen, Phangrai, Shirui and Gamnom villages having its provenance from the Ophiolite Belt shows anomalous values of Cr (958 to 4810 ppm), Ni (917 to 5681 ppm) Co (88 to 678 ppm) and Fe_2O_3 (16.23 to 29.13%). Strong positive correlation is observed between Cr, Ni, Co, Cu and Fe_2O_3 . The presence of these elemental anomalous values is substantiated by the field evidences of podiform chromite, ferric chromite, lateritic/limonitic soil capping above the serpentinised mafic/ultramafic rocks. Petrographic studies also corroborate the geochemical anomaly. High degree of serpentinisation of primary olivine and pyroxene is noted; magnetite and Cr spinel is commonly associated with olivine minerals and orthopyroxene which is highly altered to serpentinite.

The soil samples (Regolith & C-Horizon) show enrichment of elements like SiO_2 , K_2O , MgO , Al_2O_3 , Fe_2O_3 , Ba, Cr, Ni and V, and depleted in TiO_2 , MnO, CaO and K_2O . The C-horizon soil sample shows slightly higher values as compared with the overlying regolith soil sample. Two soil samples collected from Ophiolite Belt show anomalous values of Fe_2O_3 , Cr and Ni, with Fe_2O_3 : 45.91%, Cr: 11388 ppm and Ni: 4888 ppm respectively. The REE pattern for the soil pattern shows similar concentration, the soil sample from the exposed Barial rock soil profile shows lowest concentration and slight negative Eu anomaly is commonly observed in all the soil samples.

Two blocks has been identified and demarcated as block-A and B for the mineral commodities of Cr, Ni and Co to take up for mineral investigation, the exposed podiform chromite from the transitional-cumulate peridotite and supergene enrichment of Cr, Ni and Co from the limonitic and saprolitic soil capping developed above the mafic/ultramafic rocks.



GEOCHEMICAL MAPPING IN THE OPHIOLITE BELT IN PARTS OF UKHRUL DISTRICT, MANIPUR IN T.S. NO. 83K/8

(Field Season: 2018-19)

Code No.: M1AGCS-GCM/NC/NER/SU-MAN/2018/17531

CHAPTER 1

1. Introduction

1.1 General:

The National Geochemical Mapping (NGCM) was launched by the Geological Survey of India during the annual Field Season, 2001-02. The NGCM work in Manipur state was initiated during Field Season 2010-2012, giving priority in the Obvious Geological Potential (OGP) areas represented by the mafic/ultramafic rocks of Manipur-Nagaland Ophiolite Belt. The main objective of the programme is to generate seamless geochemical baseline database which will be helpful in identification of target areas for mineral exploration, managing and development of natural resources, applications in environment, soil fertility, human and animal health, agriculture, forestry, waste disposal, natural hazards and other societal concerns. Ophiolite suite of rocks are exposed about 24% of the study area, which can be categorized as Semi Obvious Geological Potential area.

1.2 Location and accessibility:

The present study area falls under Survey of India Toposheet No. 83K/8 that comes under the jurisdiction of Ukhrul and Kamjong districts, Manipur State. The study area is well connected with Imphal (State Capital) by NH-150 with a distance of around 80 km, and also connected with Kohima via Mao and Kamjong via Gamnom by state highways. The district headquarter, Ukhrul town, is connected to the rest of the villages within the study area viz. Furing, Phungcham, Paorei, Lamlong, Tuinem, Kachai, Shangshak Khullen, Mapum, Gamnom, Shirui, Phangrai, Lungkar, Sihai Khunou, Khamason, Kalhang Khullen and Kalhang Khunou by non-metalled motorable roads or foot tracks.

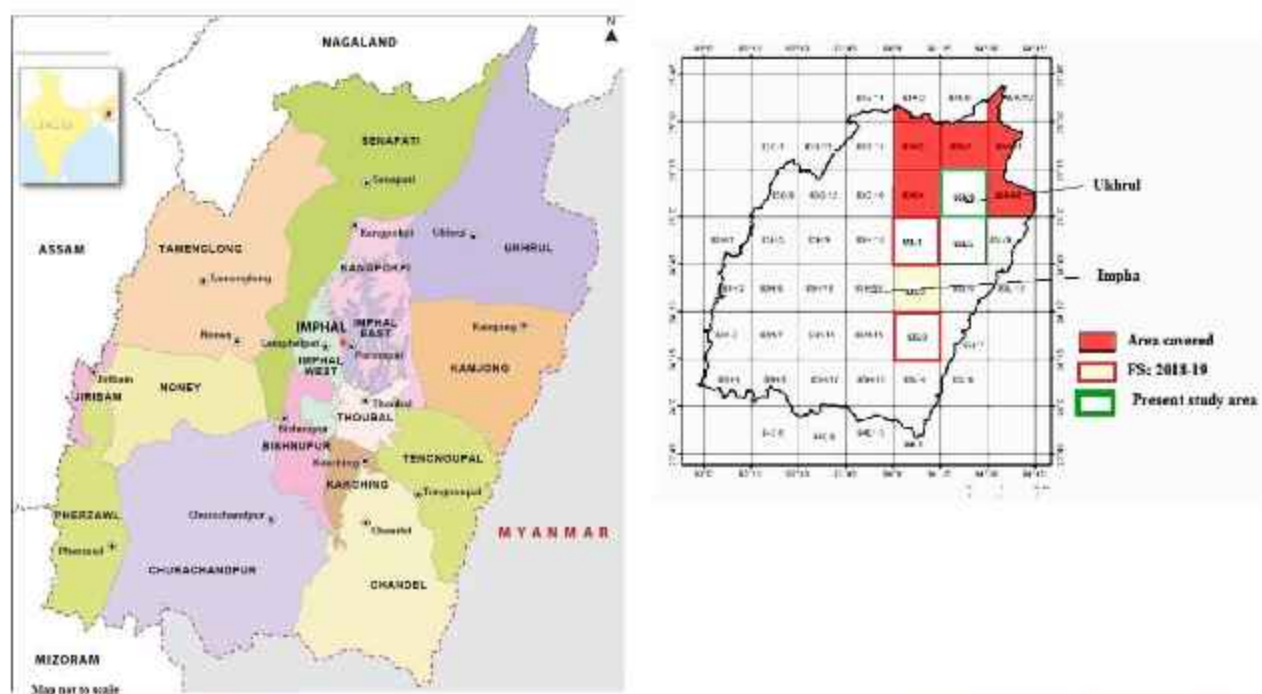


Fig.1.1: NGCM status map showing location of the study area.

1.3 Physiography, Drainage, Land use and Land cover:

The area is characterized by a rugged hilly terrain with N-S to NNE-SSW trending parallel ridges intervened by deep and wide valley. The drainage system in the western part of the study area represented by the Paleogene sediments is drained by the Thoubal River, which is joined by many tributaries; amongst them the name of Asui and Khanai Khong can be mentioned. Towards the eastern part of the study area, tributaries originating from the Ophiolite Belt flows either westerly or easterly. The Yangui and Ri rivers originate from the eastern Ophiolite Belt and flows westerly across Disang rocks joining southerly flowing Thoubal River. The overall drainage pattern shows dendritic to sub-parallel drainage. The drainage density is high with a wide network of perennial rivers and streams.

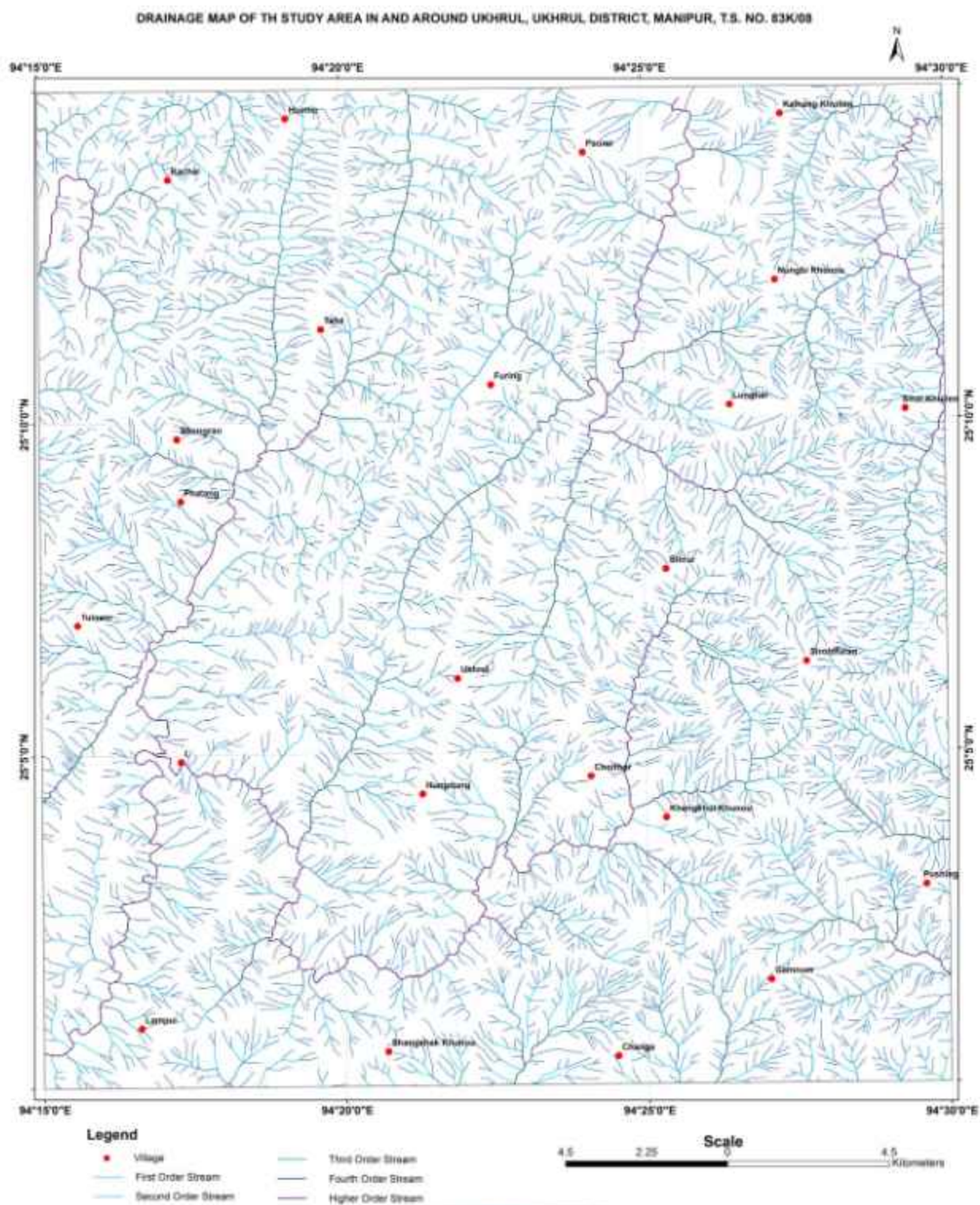


Fig.1.2: Drainage map of the study area (Toposheet No.83K/8)

The highest elevation of the area is Shirui (Sirohi) peak with 2568m above MSL lying in the eastern part and the lowest elevation is 840 m above msl located in the southwestern part of the area along the Thoubal river course. The inherent lithology exposed in the area controls the physiography, the ridges on the eastern part of the area are made up of mafic and ultramafic rocks and characterised by the sparse vegetation cover. The mid slopes are covered by moderately thick pine forests. The western part is covered with thick vegetation and the low-lying wide valley areas found on either side along the streams are mostly cultivable land.

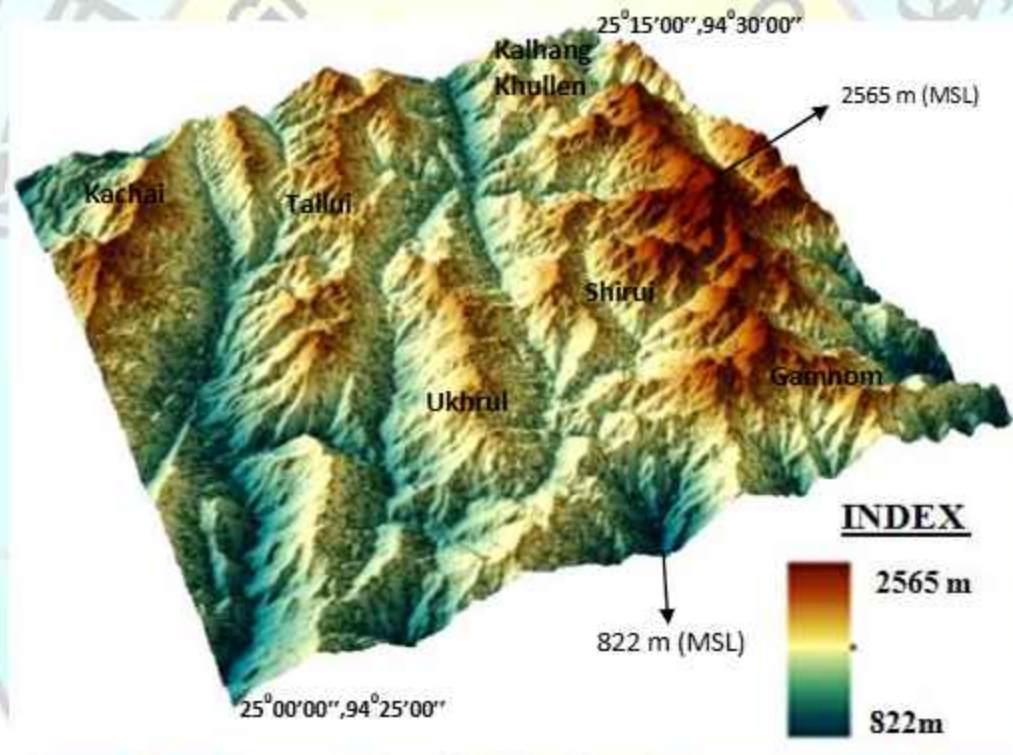


Fig.1.3: DEM map for the study area (Toposheet No.83K/8)

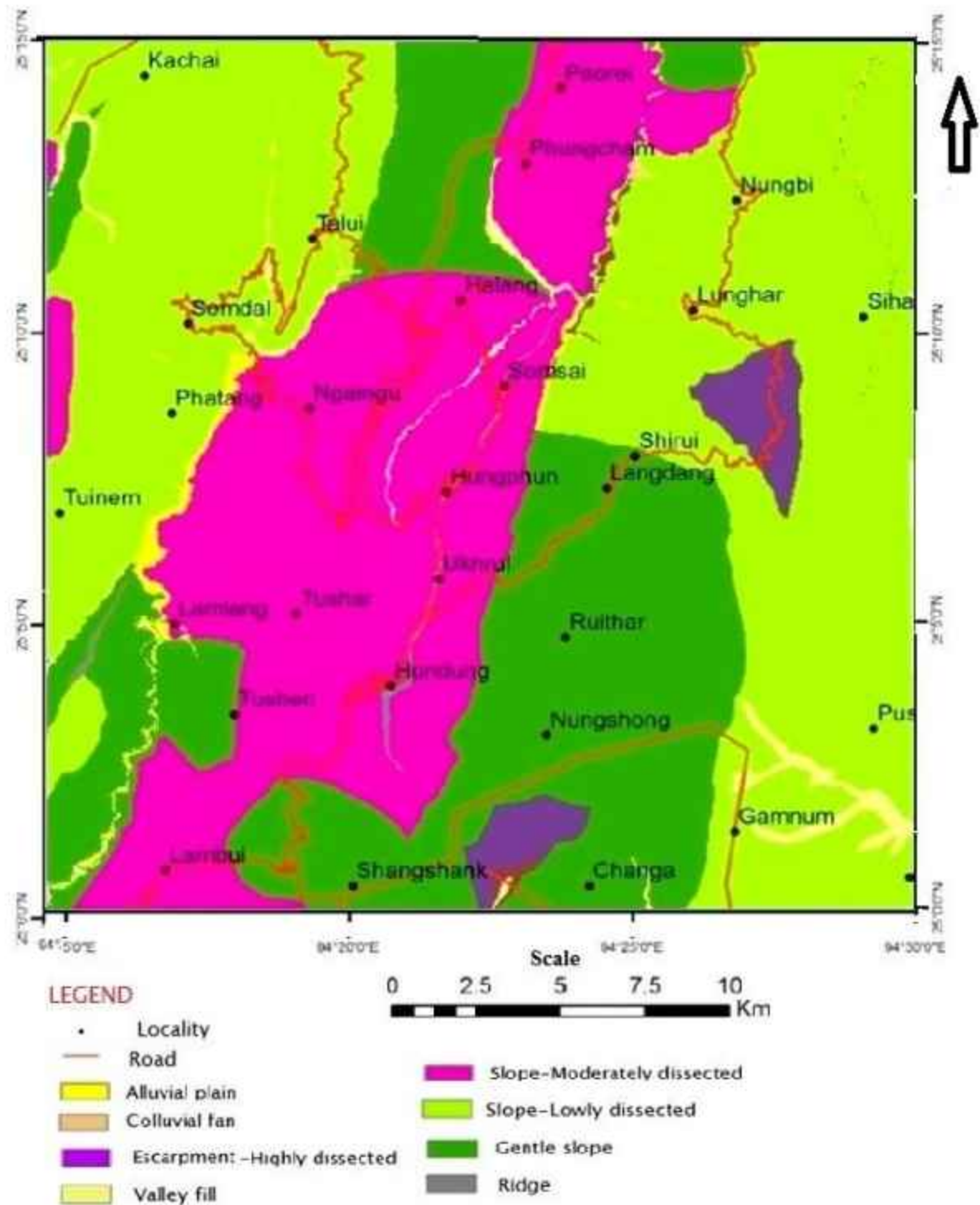


Fig.1.4: Geomorphological map of the study area (Toposheet No.83K/8)

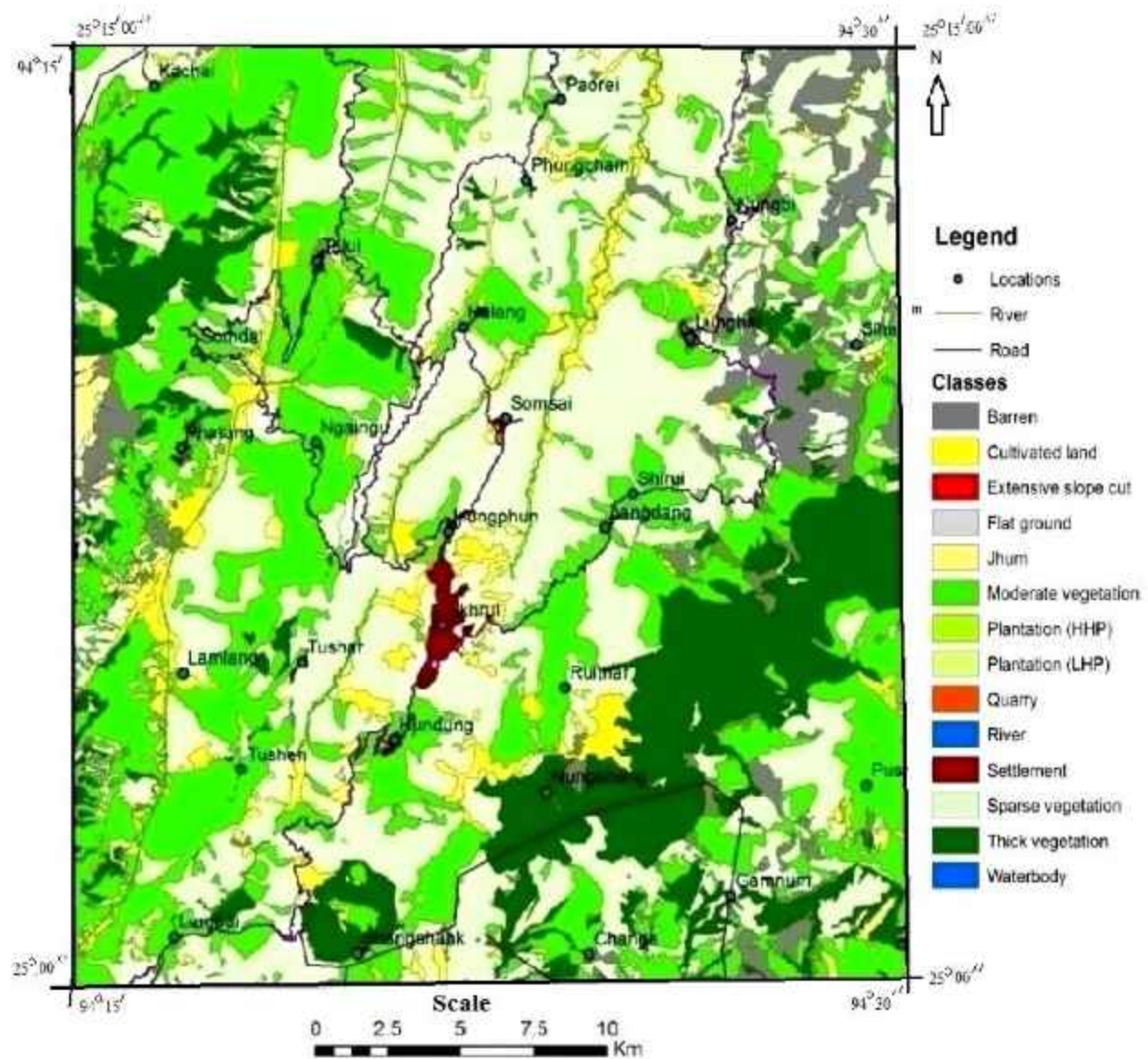


Fig.1.5: Land Use and Land Cover map of the study area (Toposheet No.83K/8)

1.4 Water supply

In the study area, villages are mostly situated along the top of the ridges and wholly depend on the accumulated water collected from streams and springs. Traditionally, villagers

carefully managed the low lying areas and water bodies for irrigation, power generation and drinking purposes etc. These age old water management practices are not reliable for all seasons leading serious water scarcity during peak winter. PHED Ukhul has come up with a free mobile water supply scheme for the people as an alternative arrangement to ease the hardship of water scarcity due to acute depletion of water at Shirui hills during this lean season.

1.5 Soil erosion

Towards the eastern part of the study area, moderate to high degree of soil erosion is observed along the mid-slope of reddish brown to black limonitic soil developed on brecciated and highly serpentinised mafic-ultramafic rocks. Such erosion can be seen at Phangrai, Shirui, Huishu and Gamnom areas.

Soil erosion within the Paleogene sedimentary terrain is mainly anthropogenic induced by the fresh slope cutting for road construction and rampant deforestation for wooden logs as well as to extend Jhum cultivation along the slope. Rain water acts as a triggering factor for soil erosion in these deforested parts. During rainy season, rain water promotes sheet as well as gully erosion which is well contributed by the exposed steep slopes in scantily vegetated/cleared forest area.

The alluvium terrace on the either side of the river bank of Thoubal river and other major river system, which is extensively used for paddy cultivation, suffers high erosion destroying the paddy during monsoonal high water discharge along the river meandering course.

1.6 Climate:

The area enjoys tropical to sub-tropical climate with brief summer and monsoon, and a long winter season. Summer is the shortest season which lasts from May to June. The temperature during the summer season varies between 20⁰C to 38⁰C. With the onset of summer season the southwest monsoon wind starts blowing from the early days of May and continues upto the months of August and September. Heavy rainfall and thunder storms are experienced

during the rainy season, which makes favorable condition for the cultivation of rice, a major crop of the state. Winter usually sets in October and lasts till upto March. During the month of December and January, the area experiences severe cold with the drop of temperature below 10°C. Strong wind blows from the northeasterly direction during the the month of February and March. The average maximum temperature varies from 25 to 30°C (between July and September) and the average rainfall of the area is of about 2000- 2300 mm Statistical booklet of Manipur Forest, 2005).

1.7 Flora & fauna:

The state of Manipur is picturesquely adorned with diverse species of flora and fauna. Some species which are unique to this particular region are being endangered. Considering the biodiversity and to ensure conservation of the flora and fauna, most of the parts of South-East Asia including Manipur and its adjoining regions of the Indo-Myanmar Hill Ranges have been declared as a bio-diversity hot spot by World Wildlife Fund. The Shirui (Sirohi) Hill National Park falls in the present study area and is the only home of the state flower Shirui (Sirohi) Lily (*Lilium mackliniae*) and is also claimed that the state bird Nongyeen (*Syrmaticus humiae humia*) is also found in the area. The present day forests in the area consists of Oaks (*Quercus*), chestnuts in high altitude areas, Pines (*Pinus longifolia*), Kokiliwon (a species of *Rhododendron*), Cane (*Arundo donax*), Bamboo (*Bambusoideae*), and bamboo (*Acacia nilotica*), palm (*Arecaceae*), ferns (*Cycas species*), canes (*Arundinaria*), orchids (*Orchis*), and varieties of thorny bushes (*Erica*), creepers and also wild oranges (*Citrus aurantium*), papaya (*Carica*), banana (*Musa paradisiaca*), gooseberry (*Phyllanthus emblica*), lemon trees (*Citrus limon*) etc. The local people generally produces wood charcoal by burning Pine and Sal from forests in open dug out pits.

The state forest is the home to many wild animals like wild cat (*Felis silvestris*), bears (*Ursus maritimus*), deers (*Odocoileus Virginianus*), wild boars (*Sus Scrofa*), monkeys (*Macaca fascicularis*), Mithun (*Bos frontalis*), wild buffalo (*Bubalus arnee*), wild-boars (*Sus scrofa*), jungle cats (*Felis chaus*), porcupine (*Erethizon Dorsaum*), squirrel (*Sciuridae*), flying squirrel (*Pteromyini*), snakes (*Chilomeniscus cinctus*), lizards (*Coleonyx variegatus*), gibbon (*Hoolock*

hoolock)etc. Besides, several types of birds are also present including Tragopan (*Tragopan blythii*) in the area. In Manipur, four varieties of hornbills are also found here. The most unique member of the fauna of Manipur is the dancing deer, also known as Sangai. Indiscriminate hunting, deforestation for Jhum cultivation, for logs by the inhabitant plays a major role in depleting the rich and rare fauna and flora in the area.

1.8 Present work:

To fulfill the objectives of generating the geochemical database of Degree sheet 83K as part of the NGCM programme for the F.S. 2018-19, Geochemical Mapping was carried out in T.S. Nos. 83K/8 on 1:50,000 scale by using multi elemental analyses. The field work was initiated on 13th June, 2018 and closed on 21th March, 2019 after achieving the targets. The NQT of the item along with the achievements are given in Table 1.1, the personnel and their field stays details in Table 1.2.

Table 1.1: Nature and quantum of work and time schedule:

Nature of work	Total workload envisaged for FS: 2018-19	Total Achievement since commencement (April, 2018)
1.GCM (1:50,000 scale)	671 sq.km	672 Sq.km
2.Sampling		
a.) Stream sediment samples (SSS) (2 km X 2 km)	168 nos.	168 Nos
b.) Soil sample (C- horizon)	09 nos.	09
c.) Regolith samples (R)	09 nos.	09
d.) Stream water samples (SW)	09 nos.	09
e.) 5% Duplicate Samples	09 nos.	09
3. Chemical analysis of samples (As per NGCM package)	(168+18+9+9)=204 nos.)	168 SSS, 9 each Regolith and Soil, 9 water samples, 9 duplicate and 18 PS samples are submitted.
4. Petrography	Two slides per major lithounit& other lithounit of interest	18 Nos.
5. Value addition and updation of existing geological map	As necessary	** value addition are highlighted below

**

- Pockets of Ophiolite body are mapped along Ukhrul-Halang road section and Kalhang Khunou. Village.
- Three types of limestone facies in the studied area viz. (i) Exotic whitish limestone blocks- *Graphia* sp. (ii) Purplish colour limestone having lithic clast of volcanic bombs and (iii) Whitish limestone (Marl) interbedded with volcanic ash beds and purplish colour volcano sedimentary shale facies

Table 1.2: Field stays details of Officers:

Field days of officers and Supervisory officers		
Name of the officers	Total field days	Remarks (if any officer/supervisory officer is changed after initiation of the project)
A. Elow, Sr. Geologist	124 days	
L. Somorjit Singh, Sr. Geologist	121 days	
C. Debojit Singh, Director	07 days	

1.9 Acknowledgement:

The authors express sincere gratitude and thanks to Dr. C. Debojit Singh, Director, State Unit: Manipur - Nagaland, Imphal Office under whose guidance the study was carried out. The author extends special acknowledge Shri. Mulkh Raj Jarngal, Addl. D.G & HoD, NER, GSI and Shri P.V. Ramanamurthy, Dy.D.G, SU: Manipur-Nagaland for the administrative support. Sincere thanks are extended to the Officer In-Charge, 54RCC, BRTF Ukhrul for extending the logistic support in executing smooth field work. The support received from the Ukhrul district village chiefs, village heads and people are highly acknowledged for their help cooperation throughout the field work. Chemical Laboratory, GSI, NER, Shillong, and ICP-MS Laboratory, GSI, Kolkata are acknowledged for providing analytical data. Last but not the least, the unstinted support of all the Officers and supporting staffs of State Unit: Manipur-Nagaland, Imphal office is highly acknowledged.

CHAPTER 2

2. GEOLOGY

2.1 Regional Geology:

The eastern part of the Indian sub-continent exposes a segment of the Late Jurassic period Neotethys oceanic lithosphere emplaced above the continent as accretionary wedge being in the supra-subduction zone where the Indian plate subducted below the Myanmar (Burmese) microplate. The fragment of ocean lithosphere designated as Naga Hills Ophiolite (NHO) belt exhibits a linear NNE–SSW trending tract with a length of about 200 km and has an average width of about 15 km. The Ophiolite Belt is bounded on the east by the Cenozoic sedimentary rocks of central lowland of Myanmar and to the west by Paleogene Disang sediments (Chattopadhyay et al., 1983).

In general the stratigraphic succession of Manipur shows younging towards west from east (Fig.2.1). The tectono stratigraphic unit of Manipur geology can be broadly classified into four domains viz. (i) Low grade meta-sedimentary unit in the easternmost part represented by slate and phyllite (ii) Linear NNE-SSW trending dismembered tectonic slices of Ophiolite Belt (iii) Thick Palaeogene folded sedimentary sequences represented by the Disang and Barail groups and (iv) Neogene sediments of Surma Basin which constitutes sedimentary units of Surma, Tipam and Dupitilla Groups.

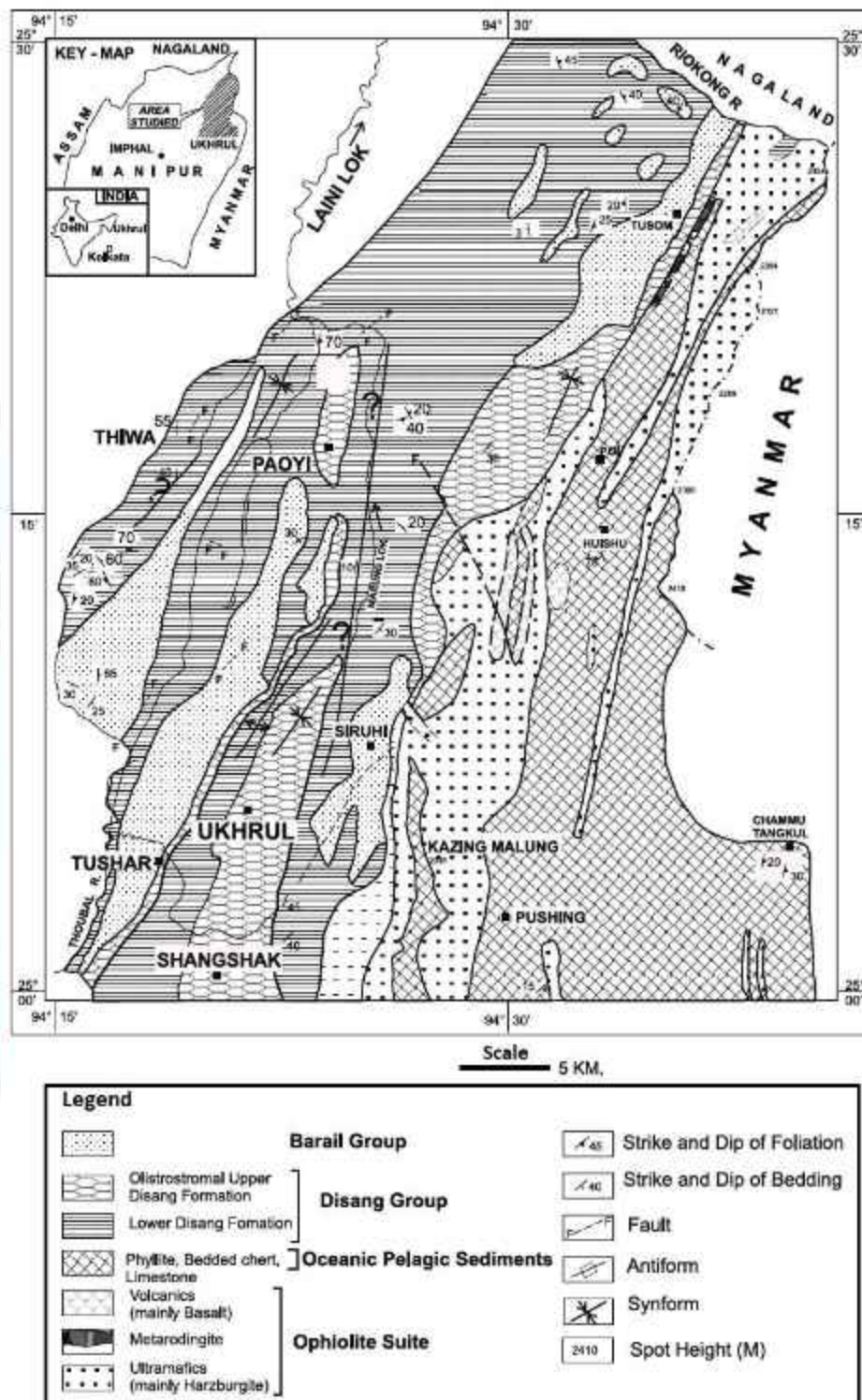


Fig.2.1: Geological map of the area around Ukhrul, Naga-Manipur Hills, Manipur covering T.S. Nos. 83K/7,8,11 & 12. (Modified after Joshi and Vidyadharan, 2008)

Table No. 2: 1: Generalised litho-stratigraphy of Manipur state.

Age	Group	Formation	Lithological description
Recent	Quaternary		Sand, silt, gravel, boulder, clay etc
-----Unconformity-----			
Mio-Pliocene	Tipam		Sandstone, clay
-----Gradational Contact-----			
Miocene	Surma	Bokabil	Shale, siltstone alteration with minor sandstone
		Bhuban	
-----Unconformity-----			
Oligocene	Barail	Renji	Coarse, gritty, massive and well bedded sandstone with current bedding and ripple marks with plant remains and coal streaks and conglomerates
		Jenam	
		Laisong	
-----Gradational Contact-----			
Eocene	Disang	Upper Disang	Shale, siltstone, greywacke with rhythmite, olistostrome with fossils and tectonic slices of ophiolite rocks.
		Lower Disang	Shale, wacke with rhythmite and minor sandstone bands
-----Tectonic Contact-----			
Creataceous to Lower Eocene	Oceanic Pelagic Sediments	Lushat	Shale interbedded with cherts (red, green and grey colour chert) bearing radiolarian and diatoms, wacke and volcano sediments.
Creataceous to Early Eocene		Ophiolite Suite	Volcanic rocks with flow breccias, gabbro/Plagiogranite/pyroxenite/ ilherzolite/ harzburgite/dunite/peridotite exhibiting hing degree of serpentinisation with disseminated nodular and massive podifrom chromite.
-----Base not exposed-----			

(Source: Modified after Ibotombi & Singh, 2006 and Kesari, 2011)

2.2 Previous work:

The first broad geological account of Manipur was recorded by D.R Oldham, when he led an expedition in 1883. Subsequently, Pascoe (1912) gave a classical account of the various mafic and ultramafic suites, later recognised as ophiolite, during his traverse to Saramati Peak. Pascoe, (1950) reported intrusive occurrence of serpentinite along the contacts of Disang and Makware beds of Burma.

The Geological Survey of India has carried out mineral investigation and systematic geological mapping programs in different parts of Manipur since late 50's. Preliminary studies for copper and nickel mineralization around Nungou, Ningthi, Konkan-Thana were carried out by Chakraborty and Raina (1985). Dutta (1959) carried out preliminary investigation for Nickel at Kwatha, Nampisha, Humine area and reported nickel concentration on serpentinitised dunite. Anand Alwar et al., (1960-61) also carried out investigation for nickel and copper mineralization in Moreh area. Ghosal (1972) carried out detailed investigation for limestone in Ukhrul, and was of the opinion that the contact of cretaceous beds with rootless ultramafic serpentinite overlying the Disang shale is tectonic and allochthonous in nature.

Mazumdar and Rapa (1972-73) carried out systematic geological mapping and mineral investigation in the serpentinite belts in parts of eastern Manipur districts. The high values of nickel (74000 ppm) and cobalt (425 ppm) in soil were reported. Ghosh et al. (1980) carried out integrated survey in parts of ultramafic belt of Manipur and located several small pockets of chromite in Gamnom area. They opined that the sedimentary rocks occurring on both sides of the ultramafic body are of the same origin. Vidyadharan and Joshi (1984) carried out systematic geological mapping in parts of Ukhrul district (Ophiolite Belt) and differentiated sedimentary rocks occurring on both sides of the ophiolite belts. They designated the sedimentary unit occurring in the western part of ophiolite as "wild flysh" and sediments towards east of the ophiolite belt as epimetamorphic sediments equivalent to Nimi Formation of Nagaland. In the course of mapping they have found a number of pockets of limestones in both the sedimentary units.

Chattopadhyay and Roy (1975) mapped in parts of Toposheet no. 83K/8 and classified the geological succession into two groups viz., Chingai Formation and Kongai Formation. The

Chingai formation was correlated with the Disang (Eocene Age) and dismembered Ophiolitic suite of rocks associated with chert, graywacke, shale, claystone mudstone. Whereas Kongai Formation is separable from the former by an unconformity and consists of conglomerate, arkosic sandstone etc. and was assigned Mio- Pliocene age. The upper unit of arenaceous beds has been correlated with Barail Group on the basis of fossil evidence and presence of streaks and lenses of coal.

Gaur and Khan (1984) reported the occurrences of exotic limestone blocks and boulders of variable size and shape within the shale/siltstone at New Paoyi, Paorei, Phungcham and Huining villages. Occurrences of salt spring of about 0.5 m in diameter was reported along the side of Vonlakunga Lok located about 3.0 km NNE of Thiwa village, and the brine from the well is processed for common salt by the locals. Shukla et al. (1985) carried out systematic geological mapping in the eastern parts of Ukhrul district and recorded lherzolite and amphibolites in the ophiolite belt. They have carried out systematic geological mapping around Kudengthabi, Chandel district and reported chromite and Rodingites within the ultramafics. Das et. al., (1987) carried out an interdisciplinary study in ophiolites of Manipur and evaluation of potential mineralization. Based on their field observation they suggested tectonic contact between sedimentary rocks and ophiolite suite of rocks and the dismembered ophiolite suite of rocks do not preserve any stratigraphic control.

The NGCM project carried in the adjacent proposed areas (T.S. No. 83L/7) of Toposheets No. 83K/6, 7, 10, 11 & 12 reported by Chubala et al., 2015 has high values of Cr and Ni of about 3231ppm and 2988ppm was reported from the grid nos. 83K/11/058/15 and 83K/11/098/15 respectively which corresponds to the ultramafics of Ophiolite suite of rocks in parts of T.S 83K/11 and water samples analysis from the Olistostromal lithounit in parts of T.S nos. 83K/6, 10 & 11, the CaCO_3 values ranges from 270ppm to 420ppm. Kevilhoutuo Theunuo et al., 2015 carried out Specialized Thematic Mapping and reported the occurrences of isolated lensoidal bodies of chromitite at Nungbi, Phangrai-Shirui, Gamnon, Pushing and East of Apong villages, where Chromitites occurs as pods, lenses, dissemination and stringers within the dunite and harzburgite rocks of transitional peridotite unit. Malachite stains in pillow basalt and alteration zone characterized by pseudogossan and boxwork structures.

2.3 Geology of the study area:

The present study area is bounded by Latitude $25^{\circ} 0'$ to $25^{\circ} 15'$ and Longitude $94^{\circ} 15'$ to $94^{\circ} 30'$ covering an area of 671 sq km including both Obvious Geological Potential and Non-Obvious Geological Potential (Non-OGP) areas. The OGP area is represented by the Ophiolite Belt, which is dismembered tectonic slices comprising predominantly of mafic-ultramafic rocks with less volcanics and pelagic sediments. The Ophiolite occupy about 27% of the study area and exposed in the eastern part of the study area in and around Shirui, Phangrai, Gamnon, Nungbi Khunou, Huishu, Sihai Khullen, Mapum and Singhcha villages.

The non-OGP area occupies the western margin with respect to the Ophiolite Belt, characterised by the thick folded Palaeogene sedimentary succession (Disang and Barail groups of rock) occupying about 70%. Litho-facies assemblages of Paleogene sediments is characterised by shales, phyllites, slates, siltstones and well bedded compact flaggy sandstone and subordinate shale, thin bedded hard sandstone and inter-bedded shale. The Recent Alluvium sediments represented by clayey soil and lithified pebbles, cobbles and boulders of sandstones, siltstones and chert occupies about 3% of the study area. The lithostratigraphy of the study area is given below in Table No.2.2.

Table No. 2.2: Litho-stratigraphy of the study area.

Age	Group	Formation	Lithological description
Recent	Quaternary		Alluvium and terrace deposits, sand, silt, clay, gravel, pebbles and boulder etc.
-----Unconformity-----			
Oligocene	Barail	Laisong	Thin to medium bedded bluish grey sandstone with trace fossils, cross bedded sandstone, ripple marks, coal streaks and plant fossils
-----Gradational Contact-----			
Eocene	Disang	Upper Disang	Thinly bedded shale with thin intercalations of siltstone and sandstone containing exotic blocks of limestone, polymictic conglomerate and quartzite. Ophiolite derived lithic clast of basalt, peridotite and volcanic. Large scale cross bedded sandstone with trace fossils and coal streaks.
			-----Gradational Contact----- Thin to medium bedded shale and sandstone rhythmite, thinly bedded shale with large scale trough cross bedded sandstone at places. Contains exotic blocks of quartzite and limestone.
			-----Gradational Contact-----
		Lower Disang	Thinly bedded shale with thin intercalations of siltstone and sandstone. Thin chert interbedded with shale at places. Slate and phyllite at the base.
-----Tectonic Contact-----			
Creataceous to Lower Eocene	Oceanic Pelagic Sediments	Lushat	Thinly bedded shale with siltstone intercalations, thinly bedded intercalations of volcano tuffaceous green, whitish and purplish ash beds with marl, chert bearing radiolarian and diatoms.
			-----Gradational Contact-----
Creataceous to Early Eocene		Ophiolite Suite	Volcanic rocks with flow breccias, gabbro/plagiogranite/pyroxenite/ilherzolite/harzburgite/dunite/peridotite exhibiting high degree of serpentinisation with disseminated nodular, massive podifrom chromite and layered chromite.
-----Base not exposed-----			

2.3.1 Ophiolite Belt

The Ophiolite Belt in the study area is the southern continuation of the Naga Hills Ophiolite Belt showing general NNE-SSW trend. The study area is devoid of complete continuous Ophiolite sequence owing to its complex SZZ tectonic setting. The Ophiolite body occurs as dismembered tectonic slices of variable dimensions sandwiched within the Paleogene sedimentary successions. In general, the width of exposed outcrop is wider in the northern side and gradually decreases in size southerly.

Lithologically the Ophiolite Suite is characterized by tectonised mantle peridotite (hercynite), transitional peridotite (mostly hartzburgite), cumulate mafic/ultramafic sequence (peridotite, layered gabbro, anorthosite and plagiogranite), volcanic (pillow basalt and andesite) and volcano-clastics. The sporadically exposed volcanics (pillow basalt and andesite) interbedded with chert are uncommonly observed. Peridotite rock represents the largest Ophiolite rock type in the study area and constitute about 70–80% of the dismembered complex. Varying degree of serpentinisation within the mafic/ultramafic rocks is commonly observed. The mafic/ultramafic rocks are overlain by the thin Ocean Pelagic Sediments (OPS).

The mafic/ultramafic rocks exposed proximal to the contact zone, shows shearing, brecciation and fracturing with well developed multiple slickensides surfaces. The reddish to orange colour in-situ limonitic soil profiles of varying thickness 0.5 to 3.5m are well developed above the ultra-mafic bodies. Few localised lateritic soil profiles are also developed above the mafic/ultramafic rocks.

2.3.1.1 Tectonised mantle peridotite

Tectonised mantle peridotite is partly exposed along Shirui-Phangrai road section and Gamnom-Singcha village road section as detached blocks and lenses embedded within a strongly deformed and serpentinised matrix (Fig: 2.3). The high degree of serpentinisation of the parent ultramafic peridotite coupled with pervasive shear foliation has overprinted over its original igneous structure (Fig: 2.4). Few relict orthopyroxene grains are observed giving resolved mineral grain texture embedded within the light green to greenish brown colour serpentinised

groundmass (Fig: 2.5). The peridotites are characterized by presence of fibrous or bladed variety of serpentines giving a scaly appearance to the rock with slickensides in all possible orientation. Within the tectonised peridotite pronounced thin to thick (1mm to 3cm) serpentinite veins dissect irregularly across the rock body (Fig: 2.6).

2.3.1.2 Transitional peridotite

Transitional peridotite is mainly exposed at Shirui, Phangrai and Gamnom villages, characterised by harzburgite with minor lherzolite occurring as detached blocks and lenses embedded within a strongly deformed and serpentinitised matrix, with thick limonitic soil capping developed above the rock (Fig:2.7). The high degree of serpentinitisation with talcose veins intruding parent ultramafic peridotite coupled with pervasive shear foliation has overprinted over its original igneous structure (Fig: 2.8). The transitional peridotite occurs as lensoidal outcrop within the ocean pelagic sediments having varying dimensions in linear arrangement following the NNE-SSW strike of these bodies having thrust contact. At field harzburgite rocks are identified based on the presence of relict orthopyroxene (~40%) grains which exhibits bronze luster and hob-nail texture within a highly serpentinitised ground mass (Fig:2.9). The rock is light to dark green in colour with medium specific gravity. The harzburgite peridotite is discernible only in less altered parts which apparently occur as lensoidal pods and angular clasts of different sizes within serpentinitised foliated/schistose rocks. In lherzolite, relict orthopyroxene grains are less and hob-nail texture is uncommon. They are light green to greenish brown in color and more serpentinitised than harzburgite rocks. Both the peridotites are characterized by presence of fibrous or bladed variety of serpentines giving a scaly appearance to the rock with slickensides in all possible orientation. Some resolved irregular bronzite mineral grains are observed with olivine neo-blast indicating early crystallised bronzite crystal mingling with the new batch of melt that has been introduced into the system, whereas the early formed olivine crystals are mostly altered to serpentinite minerals (Fig:2.10).

Chromitite pods of varying dimensions are also found to occur within transitional peridotite unit. Chromitites are dark grey to black, massive, hard and resistant unit with high specific gravity. It occurs as pods and lenses of varying dimensions. They occur as massive

podiform type or as stringers and disseminated type. These pods are generally associated in the locales where serpentinites are dominant. However, pods of chromitite bodies associated with harzburgite rocks are also observed.

2.3.1.3 Cumulate:

Layered mafic-ultramafic cumulate lies above the transitional peridotite, which is well exposed at the higher topographic reaches, characterised by the sparse vegetation cover which are well exposed at the hilltop of Gamnom, Shirui, Phangrai and east of Kalhang Khunou village in the study area.

Cumulate are represented by the peridotite and gabbro as major lithounit. Cumulate peridotitic rocks are represented by the medium to very coarse grained, melanocratic, hard and massive, which exhibit crude layering (Fig: 2.11). At places the rolled boulders of cumulate peridotite, mostly harzburgite are also commonly observed along the river section. The rock is coarse to very coarse grained melanocratic. It is characterized by large grains of orthopyroxene (1mm – 1.5 cm) embedded within the dark serpentinised groundmass and it is the most abundant mineral in harzburgite based on outcrop modal analysis (Fig:2.12). The orthopyroxene is brown to green colour. The resistant orthopyroxene minerals protrude out in a weathered surface and give a typical 'Hob-nail' texture. The crude layering observed in the rock is marked by grain size differences.

Lherzolite variety is rare and the isolated bouldery out crop is dark green to black in colour. They are hard, massive, and compact and the relict prism of orthopyroxene grains are sparsely distributed in dark crystalline serpentine matrix. Dunite is mostly altered to serpentinite and often eroded. However at places, light dull matty green color dunite rocks occur as minor patches and lenticular bodies are observed at places in Phangrai, Shirui and Gamnom village as isolated pods within cumulate peridotite. It shows mesh texture of serpentine and asbestos and occurs as pockets within the peridotite. It also hosts pods and lenses of chromite (Fig: 2.13) or as disseminated euhedral specks of chromite. The limonitic soil profiles of varying thickness (4m to 10m) characterised by the colour layering of reddish to orange colour in-situ are well developed

above the ultra-mafic bodies (Fig:2.14). Few localised lateritic soil profiles are also developed above the mafic/ultramafic rocks.

2.3.1.4 Gabbro

The mafic cumulates are characterised by the gabbro (Fig: 2.15) and it's anorthositic (Fig: 2.16) variants exposed east of Shirui peak and Gamnom village. They occur often in close association with ultramafic cumulate sequence of dunite, harzburgite and pyroxenite. Layered gabbros are mesocratic medium to coarse grained, with highly weathered outcrop look. Mineral assemblage includes feldspar along with pyroxene minerals. Crude layering can be observed at the outcrop scale. It occurs as intrusive within the lowermost transitional peridotite unit.

2.3.1.5 Volcanics

Volcanic rocks in the study area are represented by a) vesicular/amygdular flow basalt b) Andesite and d) volcanic agglomerate. These rocks occur at east of Phangrai zero point interbedded with chert and cherty limestone, Flinch corner to Gamnom village section. Vesicular/amygdular basalts (Fig: 2.17 & 2.19) are identified in the field outcrop by the typical triple point junction of the pillow lobes, which is highly weathered to reddish brown look, the chilled outer margin are highly weathered and altered spilitic groundmass as matrix are observed. However, the radial cracks are well observed with vesicles vugs-filled with amygdules of zeolites and calcite. Spheroidal weathering is common in this rock. The pillow basalts are characterized by stackings of round to elliptical pillows of various sizes (50-95 cm in diameter) (Fig: 2.17).

Volcanic andesite occurs above the basalt in the ophiolite sequence, characterised by the light green, violet and grey coloured and amygdoidal volcanics, which are well exposed along east of Phangrai zero point and Shirui peak foot-track, which is inter-bedded with volcano sedimentary purplish shale facies and chert. Volcanic agglomerate units is characterised by the angular to sub-rounded volcanic clasts of different sizes ranging from 3 to 80 cm. Larger volcanic fragments have vesicles and amygdules filled by secondary quartz, calcite and zeolites, the sub-rounded clasts identified as lapillis and bombs. Sub-rounded volcanic bombs are

observed within the purplish limestone (Fig: 2.19), which indicates volcanic eruption coeval with the deposition of limestone. The outcrop exhibits a typical weathering pattern with dark reddish grey to maroon soil colour and whitish volcanic ash beds interbedded with shale are commonly observed (Fig:2.20).

2.3.2 Ocean Pelagic Sediments

The ocean pelagic sediments is well exposed in the eastern part of the study area along east of Kalhang Khunou, Phangrai and Gamnom-Singhcha villages, where the mafic-ultramafic Ophiolite thrust slice sheets lies above the OPS. The ocean pelagic sediments is broadly characterised by the thick unit of grey to khaki green shale with dark grey chert nodules and thin interbeds of chert, pelagic limestone and siltstone. Chert occurs at the lower stratigraphic lithounits characterised by the grey and green colour inter-bedded with volcanic basalt and andesite. Disseminated pyrites are commonly observed within the chert (Fig 2.21). Thin to medium bedded, greyish to light greenish colour pelagic limestone beds are inter-bedded with greyish shale and variegated colour volcano sedimentary facies (red to purplish shale, green to buff-whitish volcanic ash beds) (Fig.2.22). The limestone is mostly composed of micritic and sparitic calcites.

The OPS exposed along the eastern side of the Gamnom village has a well defined tectonic litho-contact with the ophiolite. The OPS exposed at the contact are slightly metamorphosed to dark to greenish grey colour slaty-shale and phyllite. The slaty-shale and phyllite are defined by the thin N-S trending foliations with sub-vertical dips, the sweat quartz veins are aligned along the N-S trending foliation plane and fractures.

2.3.3 Olistostrome

The olistostromal lithounit in the present study area occurs in close association with the Disang shale. The major Olistostrome unit occurs in between Disang Group of rocks and the Ophiolite Belt. This lithofacies is characterized by chaotic distribution of exotic olistholit blocks of limestone, sandstone and siltstone within shale along the Thoubal River section east of Kalhang Khunou village (Fig: 2.23). The exotic limestone contains cubic crystals/disseminated

grains of pyrite (Fig: 2.24) indicating reducing peled depositional environment. The olistoliths of exotic sandstone blocks is characterised by sugary texture with quartz veins dissecting across the rock (Fig: 2.25). Variegated colour banded chert (Fig: 2.26) and Ophiolite derived lithic fragments are observed within the shale at places.

The exotic blocks of red radiolarian chert observed within shale unit correspond to the Upper Jurassic age (Alan T. Baxter et al., 2011) which occurs adjacent to the exotic limestone blocks (Fig: 2.27). The olistoliths of exotic limestone blocks observed in and around Ukhrul town and Flinch corner yields mega fauna like *Graphia* sp. (Fig: 2.28), which is one of the index fossil of Cretaceous age. The limestone has pyrite crystals, which indicates reducing depositional environment prevailing during the time (Cavalazzi, B. et al., 2011) (Fig: 2.24).

2.3.4 Disang Group

The Paleogene Disang sediments are well exposed along the western part of the studied area along Ukhrul town, Kachai, Lamlang, Tuinem, Tallui and Phadang villages. Geomorphologically the Paleogene sedimentary topography has attained second order matured topography. The Paleogene Disang sediments are dissected by the series of almost NNE-SSW trending east dipping thrust slices. The Disang-Ophiolite tectonic contact exposed at the foothill of Shirui peak is characterised by the tectonic boudinage of sandstone within Disang shale and silicified hard compact sandstone. Large exotic blocks of whitish colour limestone, which are dissected by a series of calcitic veins with pyrite bearing Cretaceous fauna *Graphia* sp. (Khangkhui and Mova cave), hard indurated sandstone dissected by series of cross quartz veins (Nungshang village) and polymictic conglomeratic blocks (North and East of Hundung village) are juxtaposed above the Disang sediments as thrust clippage, marked by a highly crushed mylonitic carbonised shale with slickenside surfaces at the basal litho-contact. On the basis of lithofacies assemblages and structural disposition of the strata, the Paleogene Disang Group has been divided into two formations as Lower Disang and Upper Disang formations.

(a) **Lower Disang Formation:** The lithofacies assemblage of this formation is defined by the predominance of argillite lithofacies, which is well exposed in and around west of Ukhrul town, Choithor, Kachai and Tulloi village sections (Fig: 2.29). Lithologically the Disang

sediments are represented by the thick dark grey to khaki green splintery shale with 4-6cm diameter dark grey chert nodules at places elucidating the deposition below the Carbonate Compensation Depth (Fig: 2.30). At places minor thinly bedded rhythmic sequences of sandstone/siltstone and shale are observed within the argillite dominated sedimentary facies. Associated sedimentary structures include thin horizontal laminations, thin lenticular beddings with small scale ripple cross lamination. The devoid of mega-faunal and trace fossil assemblages which supports the distal continental shelf facies.

(b) Upper Disang Formation: This lithofacies overlies the Lower Disang Formation having a gradational litho-contact. Lithologically, characterised by the predominance of rhythmic sequences of dark grey shale, siltstone and sandstone in varying proportions, which is well exposed in and around Ukhrul town, Hundung and Shangshak Khunou villages. The lithofacies assemblages in the upper stratigraphic horizons indicates more arenaceous proportion in the stratigraphic successions (Fig: 2.31), some turbidite sedimentary facies are noted at Shirui village. Associated sedimentary structures includes thin to thick horizontal laminations, large scale trough cross bedding, small scale current ripple cross laminations and ripple marks. Ichnofossil assemblages of *Cruziana* (*Thalassinoid horizontalis* isp. and *Helminthopsis albeli* isp.) (Fig: 2.32) and *Skolithos* (*Ophiomorpha* isp. and *Ophiomorpha nodosa* isp.) (Fig: 2.33 & 34) and ichnofossils and gastropod faunal assemblages (*Turritella* sp. and bivalvia) (Fig: 2.35 & 36) along with coal streaks having well defined cellulose fibrous striations of wood indicates shallow marine to brackish water depositional environment.

2.3.5 Barail Group

The Barail Group, represented by the Laisang Formation are well exposed in the western part of the study area in and around Lamlang, Lamlang Shikor, Somdal Khullen and Kachai Hokhorim villages. Barail Group of rocks has limited outcrop distribution as it rarely occurs in the study area. Few outcrops are exposed around Lunghar and Shirui village. The Laisang Formation is characterised by the predominance of arenaceous over argillaceous proportion, represented by the coarsening upward parasequences (Fig: 2.37). Isolated channel filled are observed along Shirui-Paorei village section, characterized by medium to very thickly bedded

buff to bluish grey, fine to medium grained, moderately hard and compact large scale trough cross bedded sandstone with quartzite basal pebbly lag deposit(Fig: 2.38). The Paleogeographic slope deduced from the paleo-current tilt correction analysis (Fig: 2.39) indicates the north-westerly paleo-geographic slope direction during the Late Eocene to Early Oligocene time. The presence of well preserved plant leave impressions (Fig: 2.40) and wood fossils with coal streak (Fig: 2.41) located north of Shirui village supports shallow marine deltaic depositional environment for the Laisong Formation.

2.3.6 Recent alluvium

The recent alluvium is represented by the sandy soil, silt and clay. The soils are both of residual and transported types. These sediments are exposed along Thoubal River and their tributaries. This lithofacies is characterised by the large scale cross bedded sand of meandering fluvial deposits (Fig: 2.42). Clayey soil (Fig: 2.43), pebbles, cobbles (Fig: 2.44) and boulders (Fig: 2.45) that are mostly derived from the adjacent Ophiolite Belt and Paleogene sedimentary terrain are also observed.



Fig 2.3: Tectonised peridotite. **Location:** West of Shangshak village near Assam Rifle outpost



Fig 2.4: Tectonised peridotite embedded within foliated serpentinised groundmass. **Location:** Shirui peak.



Fig 2.5: Tectonised peridotite with sparse anhedral pyroxene grains embedded with serpentinised groundmass. **Location:** East of Shangshak village



Fig 2.6: Serpentinite vein dissecting across with peridotite. **Location:** Shirui peak.



Fig 2.7: Thin limonitic soil profile developed above Transitional-Cumulate peridotite rock. **Location:** Shirui-Phangrai road section.



Fig 2.8: Two sets of asbestos vein dissection the tectonised peridotite. **Location:** West of Shirui peak.



Fig 2.9: Transitional peridotite pyroxene grains embedded with serpentinised groundmass.
Location: East of Shangshak village.



Fig 2.10: Tectonised peridotite showing olivine neo-blast around the margin of resolved opx grain.
Location: East of Shangshak village.



Fig 2.11: Crude layered banding of Cumulate peridotite showing hob-nail texture. Location: Shirui peak



Fig 2.12: Cumulate peridotite showing euhedral OPX (Bronzite mineral embedded with serpentinised peridotite groundmass. Location: Shirui peak



Fig 2.13: Pods of massive chromite within Cumulate peridotite.
Location: Shirui-Phangrai village road section.



Fig 2.14: Thick limonitic soil profile developed above cumulate peridotite. Location: Phangrai village.



Fig 2.15: Grabbro. **Location:** East of Gannom village.



Fig 2.16: Anorthosite. **Location:** Northeast of Shirui peak.



Fig 2.17: Pillow basalt. **Location:** East of Paorei village.



Fig 2.18: Vesicular pillow basalt. **Location:** East of Phangrai village.



Fig 2.19: Amygdular volcanic bomb within limestone.
Location: East of Phangrai village.



Fig 2.20: Volcanic ash bed inter-bedded with shale.
Location: East of Phangrai village.



Fig 2.21: Disseminated pyrite within chert nodules.
Location: East of Paorei village.



Fig 2.22: Thinly inter-bedded bedded Marl with volcanic ash bed. Location: East of Phangrai village.



Fig 2.23: Olistoliths of sandstone/siltstone and limestone within shale. Location: East of Paorei village.



Fig 2.24: Pyrite crystals within exotic olistolith block of limestone. Location: Near 54 BRTF camp, Ukhurul



Fig 2.25: Exotic block of sandstone with juvenile quartzs.
Location: Near Khanghui cave.



Fig 2.26: Olistolith block of variegated colour banded chert.
Location: East of Nungbi village.



Fig 2.27: Exotic olistolith block of red radiolarian chert.
Location: SE of Choithar village.



Fig 2.28: *Graphia* sp. within exotic limestone block.
Location: East of Hundung village.



Fig 2.29: Thin intercalations of shale and siltstone.
Location: East of Kalhang Khullen village along Thoubal River.



Fig 2.30: Chert nodules within shale.
Location: East of Kalhang Khullen village.



Fig 2.31: Thickly bedded sandstone with thin shale intercalations.
Location: North of Kalhang Khullen village



Fig 2.32: *Cruziana* ichnofacies (Trail marks) within shale and siltstone intercalations.
Location: South of 54BRTF camp



Fig 2.33: *Ophiomorpha nodosa* isp. (Domichnia) within sandstone.
Location: Southeast of Ukhul town.



Fig 2.34: *Skolithos* ichnofacies (Domichnia) within thinly laminated siltstone. Location: East of Kachai village.



Fig 2.35: Shell fragments of bivalves within sandstone.
Location: Southeast of Ukhul town.



Fig 2.36: *Turretella* within sandstone.
Location: Southeast of Ukhul town.



Fig 2.37: Medium to thickly bedded sandstone with thin shale intercalations.
Location: West of Flinch corner along Thoubal River.



Fig 2.38: Trough cross-bedded sandstone with pebbly basal lag.
Location: North of Phungcham village.

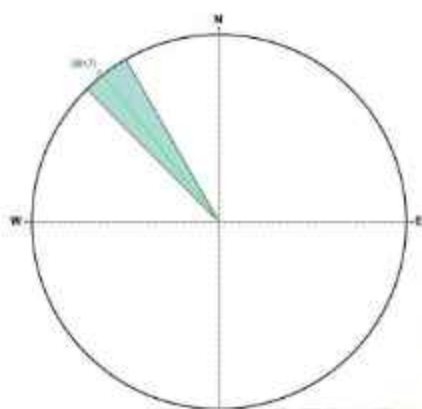


Fig 2.39: Rose diagram depicting NW (321.7°) paleo-current flow direction.



Fig 2.40: Plant leaf impression within sandstone.
Location: Southeast of Ukhul town.



Fig 2.41: Wood fossil marked by cellulose fiber striations and coal streak within sandstone. **Location:** Southeast of Ukhul town.



Fig 2.42: Large scale cross bedded sand along the Thoubal River bank.
Location: Thoubal River bank, East of Phatang village



Fig 2.43: Clayey silt along the Thoubal River tributary river bank.
Location: North of Furing village



Fig 2.44: Boulders along the Thoubal River course.
Location: Along Thoubal River bed



Fig 2.45: Pebbles and cobbles along the Thoubal River bank.
Location: Thoubal River, west of Ukhrul

2. 3. STRUCTURE

The Ophiolite suit represented by the mafic-ultramafic sequence in the present study area occurs as rootless tectonic slices delimited in east and west by ocean pelagic sediments and Paleogene sedimentary successions (Fig.2.3.1). The intensity of deformation increases from west to east, the tectonic contact between the Ophiolite and sedimentary succession is well observed along Gamnom-Singhcha village section, where the strike of the bed is NNE-SSW sub-vertical dipping easterly (78° – 88°). The extensive development of mylonite (Fig.2.3.2), serpentinitization, talcose alteration are observed at the contact zone within the mafic/ultramafic sequence. The OPS are slightly metamorphosed to slate and phyllite which are well defined by the slaty cleavage and sweat quartz veins aligned along the S1 planes (Fig.2.3.3). Away from the contact zone, the ophiolite rocks mostly represented by the peridotite which are highly brecciated with well developed slickenside surfaces of more than two sets with high degree of serpentinitisation, indicating floor rock crushing due to thrusting movement. Zone of brecciation are observed at the Shirui peak having general strike NNE-SSW within the cumulate peridotite, characterised by the angular fragments of ultramafic rocks embedded with the highly foliated serpentinite groundmass, indicating that the large ophiolite exposed along Shirui-Phangrai hill ranges are not single tectonic slice body but series of tectonic slice that are juxtaposed upon each other (Fig.2.3.4).

A hillock of hard indurated sandstone, which is dissected by the series of quartzs veins (Fig.2.3.5) was observed along the Shangshak village road section (BRTF quarry point) and classified as a tectonic klippe. The basal contact is characterised by the highly sheared and mylonitised ultramafics and shale (Fig.2.3.6) indicating the sole surface over which the sandstone hillock has moved over.

Strata bound thick polymictic conglomerate unit within Disang sediments having limited lateral facies continuity was observed along NE of Ukhrul town. The lithic clast assemblages consist of red radiolarian chert, grey chert, quartzite and sandstone. This unit is underlain by highly sheared and mylonitised carbonaceous shale (Fig.2.3.7). Well developed slickenside surface and sweat quartzs veins are also observed at the contact zone (Fig.2.3.8). This Polymictic conglomeratic unit was redefined as a klippe. Small scale mesoscopic fault and joints are commonly observed within the Paleogene sandstone and shale intercalations.



Fig 2.3.1: Tectonic contact between Ophiolite and Paleogene sediments. **Location:** East of Gamnom village.



Fig 2.3.2: Highly sheared and mylonitised contact zone. **Location:** East of Gamnom village.



Fig 2.3.3: Quartz vein align parallel to the slaty cleavage. **Location:** Gamnom-Shingcha village road section.



Fig 2.3.4: Brecciated zone within ophiolite body. **Location:** Shirui peak.



Fig 2.3.5: Quartz vein dissecting across the body of sandstone. **Location:** East of Khanghui village.



Fig 2.3.6: Highly sheared and mylonitised serpentinitised mafic/ultramafic rock. **Location:** East of Shangshak village.



Fig 2.3.7: Highly sheared and mylonitised carbonaceous shale at the base of the clippe. **Location:** Southeast of Ukhul town.



Fig 2.3.8: Highly sheared and mylonitised serpentinitised mafic/ultramafic rock. **Location:** Southeast of 54 BRIF camp.

2.4 Petrographical Study

(a). Transitional peridotite

Harzburgite is the most common peridotite found in the study area. Mineralogically, characterised by predominance of olivine, orthopyroxene with minor amount of clinopyroxene and chrome spinel. High degree of serpentinisation of primary olivine and pyroxene is observed, which show mesh texture. Serpentinization of olivine releases fine opaques as magnetite (Fig.2.4.1, Fig.2.4.2). Clinopyroxene also occur as exsolved phase within orthopyroxene (Fig. 2.4.2). Secondary olivine occurs as neoblast along the resolved grain boundary of primary orthopyroxene grain and fractures planes (Fig.2.4.3 and 2.4.4).

(b). Cumulate

Harzburgite is the dominant rock of ultramafic cumulates with minor ilherzolite in the study area. Mineralogically, characterised by predominance of olivine, orthopyroxene and clinopyroxene. The rock is characterized by interlocking grains showing hypidiomorphic granular texture. Orthopyroxene is coarse grained, feebly pleochroic and show slight pinkish colour. Small olivine grain occurs as inclusion within orthopyroxene and serpentine veinlets traverse across both the minerals (Fig.4.10, Fig.4.11, and Fig 4.12). Spinel harzburgite consisting of serpentinised olivine, non-pleochroic orthopyroxene and partially reabsorbed Cr-spinel with inclusions of serpentine. Cr-spinel with enveloped by magnetite and magnetite veins cut across vermicular spinel and exhibits xenomorphic texture.

Ilherzolite is characterized by the predominant of olivine, opx with minor amount of cpx, Cr-spinel and magnetite. Primary olivine shows high degree of serpentinisation exhibiting strong mesh texture. The Cr-spinel occurs as reddish brown to yellowish brown in colour and commonly associated with olivine minerals and orthopyroxene. Magnetite occurring as exsolved phase of spinel shows anhedral grain boundary. Olivine neoblast are seen along the grain boundaries of orthopyroxene and clinopyroxene grain boundary and fractures.

(c). Volcanics

Basalts are the predominant volcanic rock comprising of plagioclase, clinopyroxene, quartz, k-feldspar, opaques and glass. The centre portion of the pillow basalt shows the predominance of plagioclase feldspar phenocryst, which shows ophitic, sub-ophitic. Clinopyroxene with glass matrix groundmass between inter phenocryst grain boundary. Plagioclase occurs as coarse laths of phenocryst grains. Chloritization of clinopyroxene and sausrutization of plagioclase is commonly observed (Fig.2.4.9 and 2.4.10). The outer chilled margin of the pillow basalt shows few phenocryst of subhedral to anhedral plagioclase feldspar, showing sub-ophitic texture embedded within the fine ground matrix of glass and pyroxene (Fig. 2.4.11 and 2.4.12).

(d) Chromite:

Chromite mineralisation occurs within transitional and cumulate peridotite as orbicular and massive podiform chromite. The individual chromite grains shows subhedral grain boundary, high relief and highly fractured. The inter chromite grain boundary and brecciated fracture are filled by the serpentinised ground matrix (Fig: 2.4.13).

(e). Sedimentary rocks

(i) Chert

The chert shows the mono-mineral composition of crypto-crystalline silica. The recrystallised quartz veins dissect across the body, which shows micro faulting which indicates deformation pressure solution secondary recrystallisation along the weak plane (Fig.2.4.14)

(ii) Sandstone

The modal analysis of the sandstone shows lithic quartz arenite composition, characterised by the predominance of undulose quartz with lithic fragment of shale. Bimodal grain size distribution is observed, the larger quartz grain shows sub-angular to sub rounded grain boundary and the smaller grain shows sub-rounded to rounded grain boundary, elucidating two provenance area. The inter-mineral grain contact is most line contact with little point and sutured contact. The undulose extinction of quartz grain is common, indicating the deformational stress that the rock has undergone. (Fig.2.4.14)



Fig.2.4.1 (PPL)

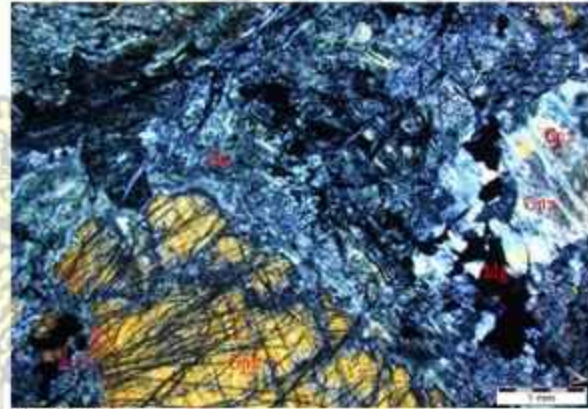


Fig.2.4.2 (CPL)

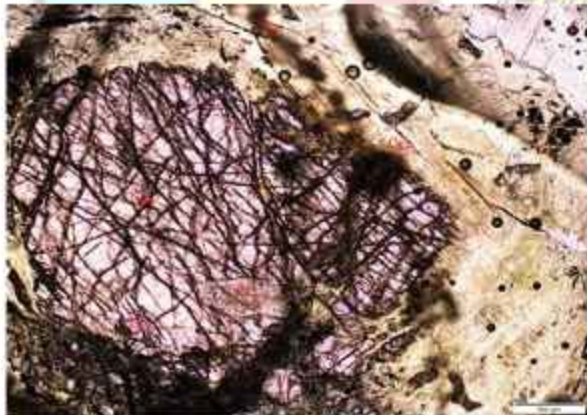


Fig.2.4.3 (PPL)



Fig.2.4.4 (CPL)

Fig: 2.4.1 and 2.4.2: Photomicrograph of transitional peridotite showing highly fractured olivine and highly altered to serpentine forming mesh or sieve texture with vermicular magnetite bodies along the margin. Exsolution of clinopyroxene in orthopyroxene is commonly observed Chrome spinel

Fig: 2.4.3 and 2.4.4: Photomicrograph of transitional peridotite showing mesh texture of primary orthopyroxene and corroded resolved grain boundary surrounded by the serpentinised ground matrix with olivine neoblast along the orthopyroxene grain boundary and fractures.



Fig:2.4.5 (PPL)

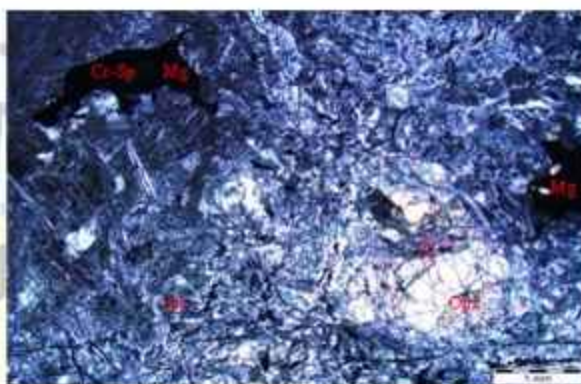


Fig:2.4.6 (CPL)



Fig:2.4.7(PPL)



Fig:2.4.8(CPL)

Fig: 2.4.5 and 2.4.6: Photomicrograph of Spinel harzburgite showing serpentinised olivine, non-pleochroic orthopyroxene and partially reabsorbed Cr-spinel with inclusions of serpentine. Cr-spinel with enveloped by magnetite and magnetite veins dissects the Cr-spinel.

Fig: 2.4.7 and 2.4.8: Photomicrograph of Ilherzolite showing serpentinised olivine exhibiting strong mesh texture, Cr-spinel and magnetite veins are seen within serpentinised primary olivine and orthopyroxene. Olivine neoblast are seen along the grain boundaries of orthopyroxene and clinopyroxene grain boundary and fractures.



Fig:2.4.9 (CPL)



Fig:2.4.10(CPL)



Fig:2.4.11 (PPL)



Fig:2.4.12 (CPL)

Fig: 2.4.9 and 2.4.10: Photomicrograph of pillow basalt shows the predominance of plagioclase feldspar phenocryst, which shows ophitic, sub-ophitic. Clinopyroxene with glass matrix groundmass between inter phenocryst grain boundary.

Fig: 2.4.11 and 2.4.12: Photomicrograph of outer chilled margin of the pillow basalt shows few phenocryst of subhedral to anhedral plagioclase feldspar, showing sub-ophitic texture embedded within the fine ground matrix of glass

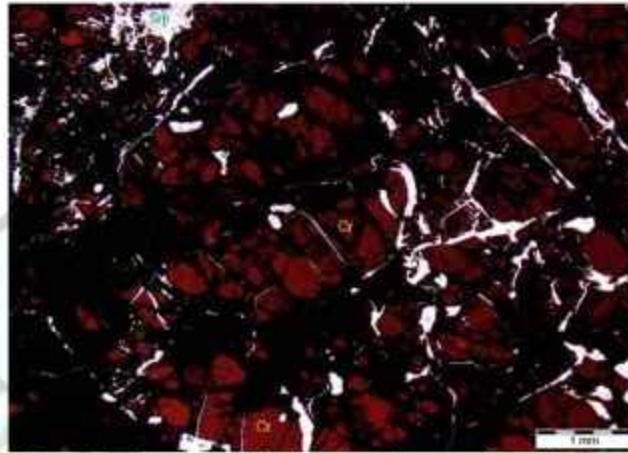


Fig: 2.4.13: Photomicrograph of chromite showing highly brecciated nature, where the inter-cumulate grain pore spaces and fractures are filled with serpentinised groundmass.

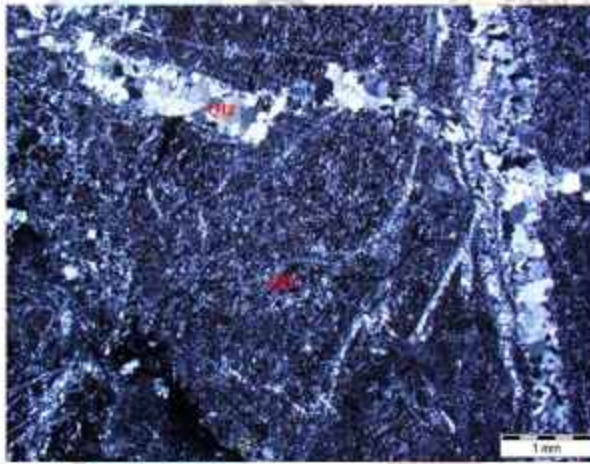


Fig:2.4.14 (CPL)



Fig:2.4.15(CPL)

Fig: 2.4.14: Photomicrograph of chert showing the dominant mono-mineral silica with recrystallised quartz vein dissecting across the rock showing micro faulting.

Fig: 2.4.15: Photomicrograph of lithic quartz arenite having lithic fragment of shale. The quartz grain shows bimodal grain size distribution.

2.5 Economic Geology

The chromitite and limestone bodies' broadly represents the important economic mineral resources in the present study area, which is located along the central and the eastern margin of the studied T.S. No. 83K/8. The minor minerals in the study area are represented by the medium

to thickly bedded sandstone of Laisong Formation and exotic sandstone blocks which is extensively used for dimensional sandstone for road construction, building material and sand mining.

a). Chromitite

Chromite as identified in the field by the dark grey to black colour, high specific gravity and occurs as massive, orbicular, pods, lenses, dissemination and stringers within the transitional and cumulate peridotite (dunitic and harzburgite rocks). The occurrences of several chromitite bodies were located along the NNE-SSW trending hill ridges at Phangrai, Shirui and Gamnom villages (Fig.2.5.1). Several chromitite bodies occurring as pods and boulders are observed along the streams originating from the higher Ophiolite ridges.

Thin limonitic reddish soil capping is observed along the NNE-SSW trending flat undulating topographic higher ridges of Phangrai-Shirui and Gamnom villages. The thickness of this limonitic soil increases towards mid-slope area, where distinct layering of reddish to yellowish colour is observed (Fig.2.5.2). Thin locals of lateritic bed developed above the mafic/ultramafic rocks are observed at Phangrai ridge (Fig.2.5.3). This limonitic soil capping and lateritic beds can be a good prospect for mineral commodities like Cr, Ni and Co.

b). Limestone

The limestone occurs mostly as exotic blocks within Paleogene sediments. Limestone also occurs as bedded deposit in minor amount in the eastern part of the study area. Broadly limestone occurrences in the study area can be categorized into three facies viz.

(i) Exotic whitish colour limestone blocks dissected by calcitic veins across the body yielding Cretaceous faunas (*Globotruncana* Sp. and *Graphia* Sp.) are observed in and around Ukhrul town, Shangshak Khullen, Hundung, Choithor, Khangkhui and Mova villages. (Fig.2.5.4)

(ii) Exotic purplish colour limestone blocks containing volcanic bombs. This limestone facies shows distinct whitish to grey colour bands. The occurrences of this facies is localised in nature within Paleogene sediments and is exposed east of Phangrai village. (Fig.2.5.5)

(iii) Rhythmic sequence of thin marl and volcano-sedimentary sequences interbeds within the OPS (Fig.2.5.6). This facies is laterally persistent along the strike length and limited in stratigraphic thickness and is well exposed along Phangrai-Sihai village section and Kalhang Khunou-Huishu villages section.

Comparing the three limestone facies observed in the study area, the exotic whitish colour limestone blocks of Cretaceous limestone is the most prospecting limestone deposit in the study area.



Fig. 2.5.1: Chromite boulders exposed above weathered mafic/ultramafic reddish soil. **Location:** Phangrai hill top.



Fig. 2.5.2: Thick limonitic reddish soil developed above mafic/ultramafic rock. **Location:** Flinch corner-Gamnom village section



Fig. 2.5.3: Thin lateritic bed developed above mafic/ultramafic rock. **Location:** South of 54BRTF camp.



Fig. 2.5.4: Medium to thickly bedded limestone with thin shale intercalation (Cretaceous age). **Location:** Ukhrul town.



Fig. 2.5.5: Limestone containing volcanic bombs. **Location:** East of Phangrai village.

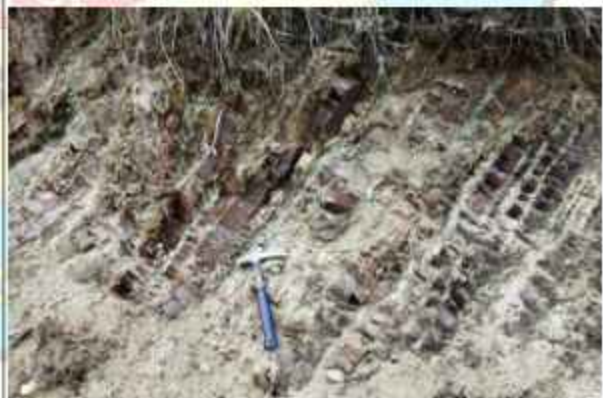


Fig. 2.5.6: Thin intercalations of limestone and volcanic ash beds (Upper Cretaceous-Lower Eocene age). **Location:** East of Phangrai village.

CHAPTER 3

3. SAMPLING METHODOLOGY AND PROCEDURE

GSI has adopted the first and second GCM guidelines of the Forum of European Geological Surveys (FOREGS), a forum of geochemists and geologists of 26 European countries and the GCM work carried out by China and few other countries. Sampling was carried out on toposheet basis. Sampling was done as per the methods and procedures of Standard Operating Procedure (SOP) for National Geochemical Mapping (NGCM) provided by GSI (Year 2014). Different features and parameters have been taken into consideration while carrying out geochemical mapping. Some of the important features are the sampling equipment, sampling media, processing and storage of samples and sample contamination. Due care was taken and constant vigil was kept during the entire process of sampling right from sample collection up to sample storage. Two thematic maps of the study area have been prepared viz. Landuse & Landcover map and Geomorphological map (fig.1.4 & 1.5). These two maps have been prepared with the help of google maps, google earth, toposheets as well as field observations.

3.1 Equipment used in sampling:

- a) Toposheet of the area as a base map for controlling locations.
- b) Geological map on 1:50,000 scale for the target area in order to understand geological setup and determining spatial limitations of sampling.
- c) Drainage maps (1:50,000 scale) of the sampling area for planning and executing the stream sediment sampling which forms base for preparing contour maps of various elements analysed(Fig. 1.2).
- d) Implements/tools required for stream sediment sampling like field data sheets, GPS, digital camera, hand scoops, polythene sample bag, stickers for numbering, permanent marker pen of various colour and weighing machine etc.; for processing the samples like - 120 nylon sieve, plastic tub, brush for cleaning the sieves, wooden pestles for powdering lumps, cloth duster, plastic sheet for covering the samples in drying (if required), PET jars of

500 gm & 250 gm capacity etc. For water sampling, water sampling kit which includes disposable syringes, disposable filters, funnel, Jerry can, plastic bottles of 500 ml, 200 ml & 100 ml size, nitric acid (HNO_3) and potassium dichromate ($\text{K}_2\text{Cr}_2\text{O}_7$), distilled water is required.

3.2 Sampling media

The sampling media as listed below have been selected on consideration of their most representative nature of the surface environment, and therefore are the most commonly used media in the geological investigations.

- Stream sediment/slope wash (S): reflects the average geogenic composition of a catchment basin.
- Soil: Regolith (R): upper horizon/top soil (0-25cm) without the top organic layer (<2mm). It reflects variations in geogenic compositions of the uppermost layers of the earth's crust. C-horizon: a 25 cm layer within a depth range of 50 cm to 200 cm. Comparison of soil and regolith would give information about environmental changes affecting anthropogenic contamination of the top layer (R).
- Stream water (filtered and unfiltered) (W): reflecting interplay in the geo-sphere. At the same time it is the main source of drinking water.
- Rock sample: Microscopic study of rock.

3.2.1 Stream sediment/slope wash samples (S)

Stream sediment sampling was taken up on 2 km x 2 km. The origin of the grid was kept at the SW corner of the toposheet (1:50,000), this leads the extreme northern row and the eastern columns to be little larger or smaller than the standard 2 km x 2 km ones. If it is more than 50% of the size, it has been considered as an independent and if it less than 50%, it has been merged with the adjacent grid. The stream sediment samples collected from the 1st, 2nd or 3rd order streams. In case drainage is absent, slope wash materials and materials generated by small scale gully erosion have been collected from the lowest elevation within that 2km x 2km grid

considering it to be '0' order stream from 3 to 5 places of the slope to make a representative sample of the cell. Each stream sediment sample comprises materials taken from 3 to 5 places from both sides of the stream bank over a stream stretch of 50 to 200 m length. Materials collected are of finer grain size (natural fraction) available at the center of the stream. Due care has been taken not to collect the material fallen from the banks of the stream while collecting samples from narrow channels. Similarly, contamination has been avoided while sampling. The field datasheet containing of 17 components has been filled properly. The data of latitude, longitude and elevation have been taken with the help of GPS.

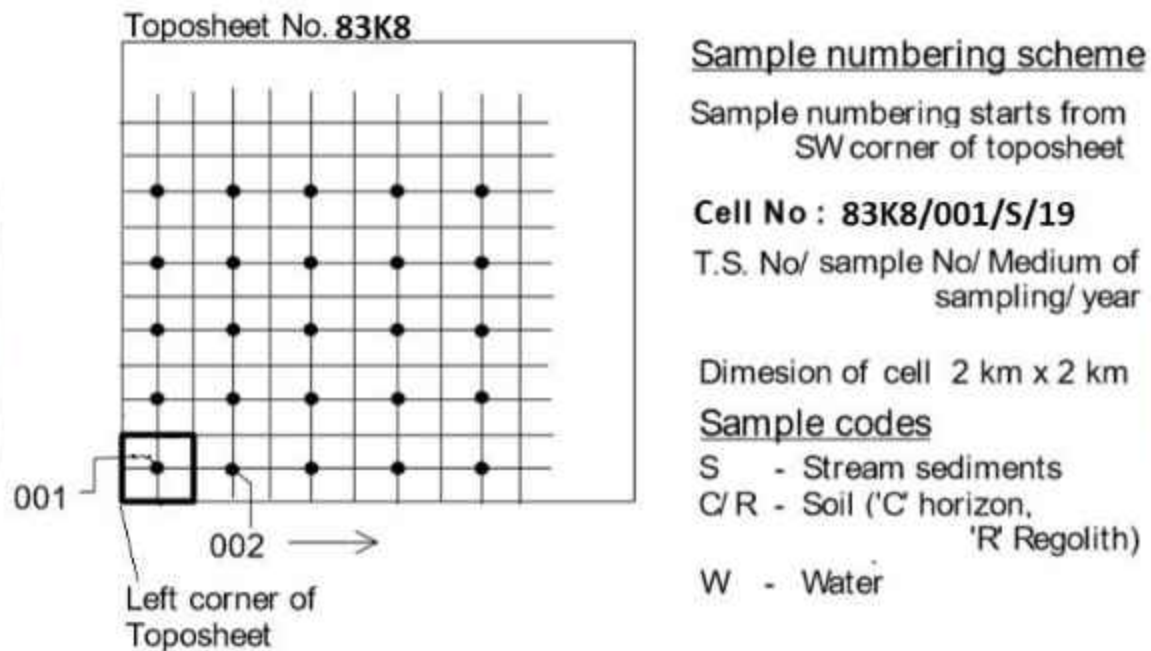


Fig.3.1: Sample numbering scheme

In Ukhurul district, the areas are covered with thick vegetation and show steep ridges and narrow gorges topography. Many sample collection points are located in rugged and inaccessible terrain. Due to non-availability of dry stream sediment in this region, wet samples weighing about 5 to 7 kg each were collected in thick polythene bags with proper labeling.



Fig.3.2: Collection of Stream Sediments



Fig.3.3: Collection of Stream Sediments.



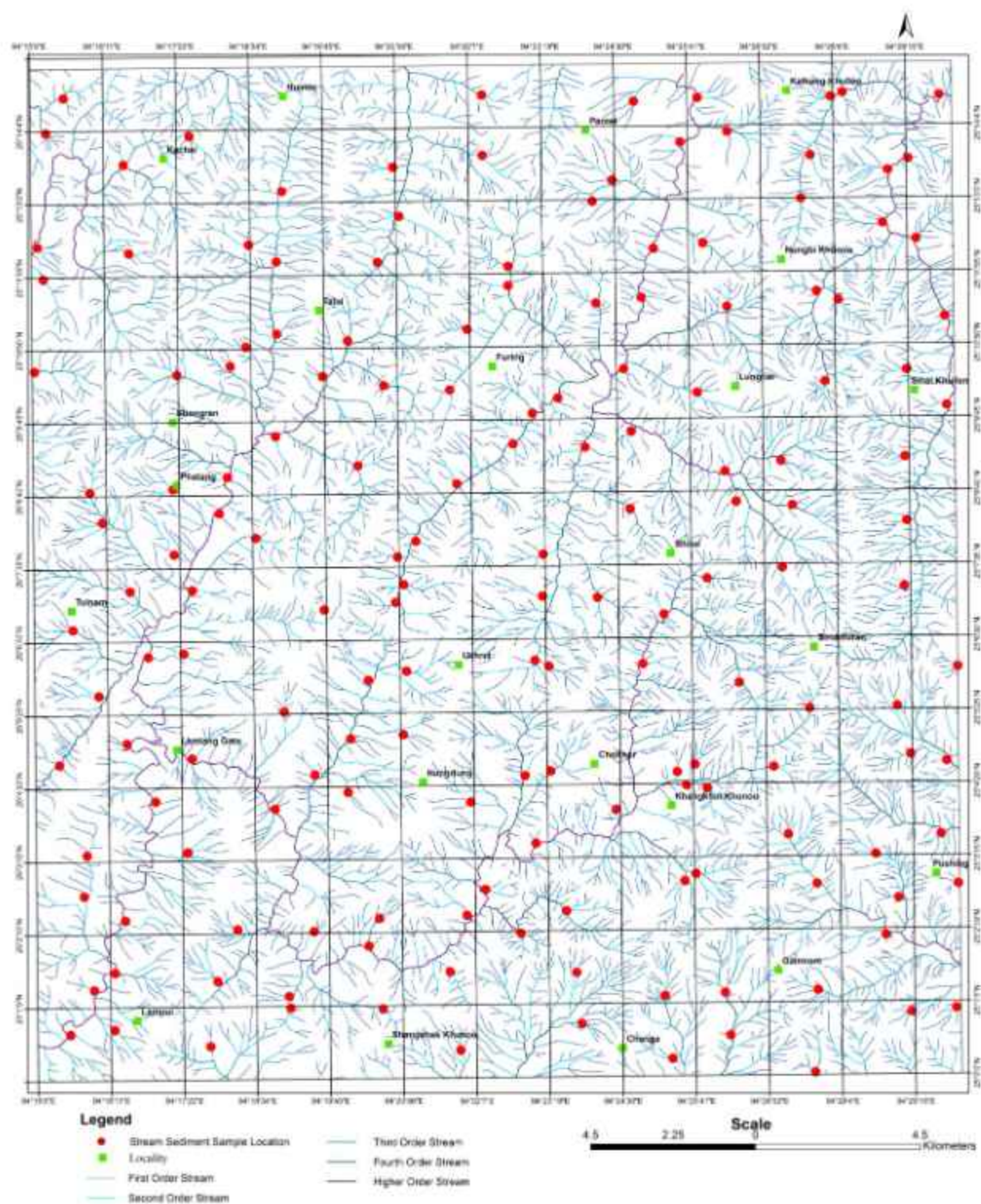


Fig.3.4: Stream Sediment/Slope Wash Sample Location Map (Toposheet No.83K/8)

3.2.2 Soil samples: Regolith (R) and C- horizon (R & C):

Soil samples have been collected from a suitable site where soil profile is well developed within the 5' x 5' grid where one Toposheet is divided into 9 quadrants (1, 2, 3, 4, 5, 6, 7, 8 & 9) starting from the SW corner of the toposheet. The soil sample collection site was decided after a careful study of the residual soil developed in the area. While sampling, care has been taken not to collect transported material such as alluvium or colluvium and emphasis has been given on collecting residual soil. Soil samples were not taken from the agricultural lands as far as possible since the contamination of topsoil due to human activity may be there. Samples from two different depths were collected from each sampling site i.e. topsoil/regolith (R) from 0-25 cm (excluding materials from the organic layer wherever present) and a sub soil sample (C) from a 25 cm thick section within a depth range of 50 to 200 cm (the C soil horizon). Where soil profile does not reach a depth of 75 cm, then lower samples were taken after undoubtedly identifying the soil profile as 'B' or 'C' horizon.



Fig:3.5: Soil sampling profile from Ophiolite Belt



Fig:3.6: Soil sampling profile from Disang Group



Fig:3.7: Soil sample profile from Barail Group



Fig:3.8: Soil sampling profile from Olistostrome

3.2.3 Stream water samples (W):

Stream water sampling was done in 5' x 5' grids from flowing streams which represents that particular grid i.e. the water basin should originate within the grid and covering maximum area. The water samples were collected in transparent white prescribes bottles for the following analysis.

- 1 x 1000 ml bottle unfiltered water for major IC ion and mercury analysis.
- 1 x 100 ml bottle filtered water ICP-MS and ICP-AES analysis.
- 1 x 60 ml bottle for (Dissolved Organic Carbon) analysis.

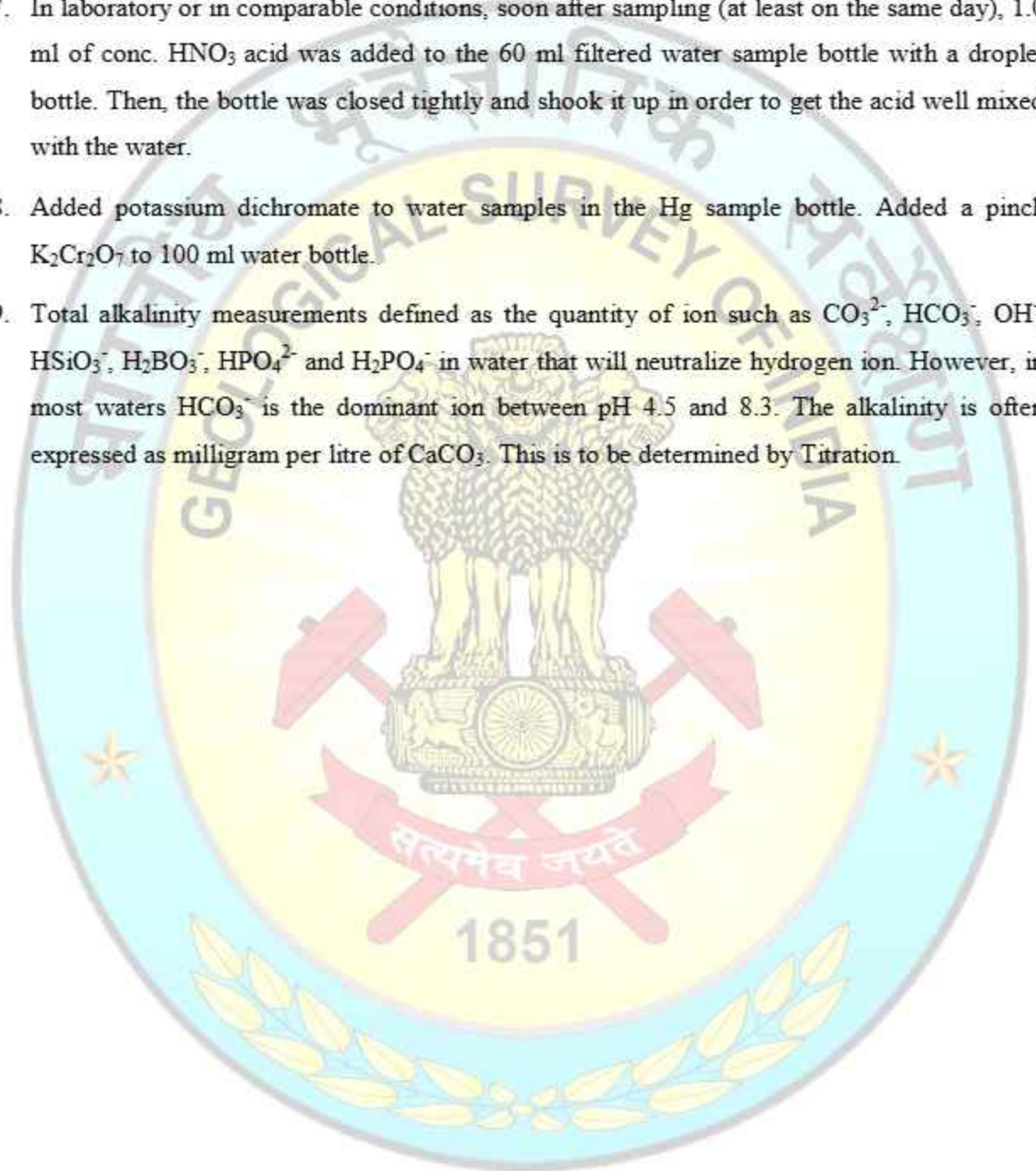


Fig.3.10: Water sample collection

The following procedure was followed during collection of the stream water samples:

1. Label all the bottles as per the guidelines.
2. Marked sample location in the map and data sheet.
3. Rinsed the polythene decanter twice and filling with stream water.
4. Filled 100 ml sample bottle with filtered water, after rinsing it twice with filtered sample water.
5. Filled the 100 ml bottle with filtered water in the same way as above.

6. Rinsed the 500 ml sample bottle with sample water twice and filled it up so that bottle is completely filled with water and no air bubbles are left in the bottle.
7. In laboratory or in comparable conditions, soon after sampling (at least on the same day), 1.0 ml of conc. HNO_3 acid was added to the 60 ml filtered water sample bottle with a droplet bottle. Then, the bottle was closed tightly and shook it up in order to get the acid well mixed with the water.
8. Added potassium dichromate to water samples in the Hg sample bottle. Added a pinch $\text{K}_2\text{Cr}_2\text{O}_7$ to 100 ml water bottle.
9. Total alkalinity measurements defined as the quantity of ion such as CO_3^{2-} , HCO_3^- , OH^- , HSiO_3^- , H_2BO_3^- , HPO_4^{2-} and H_2PO_4^- in water that will neutralize hydrogen ion. However, in most waters HCO_3^- is the dominant ion between pH 4.5 and 8.3. The alkalinity is often expressed as milligram per litre of CaCO_3 . This is to be determined by Titration.



stream sediment samples are collected for comparative studies in between the analytical data of duplicate sample with original stream sediment sample to confirm the precision of equipments and methodologies followed during sampling and chemical analysis. Permissible variation in between the analytical results indicates the accurateness in the methodologies.

3.2.5 Rock sampling:

Rock samples have been collected from the well exposed fresh rock surfaces of different lithounits of the area to study the petrography and geochemistry of the rocks in the area. The samples were collected for preparation of thin section for microscopic study. Due care has been taken to avoid the collection of weathered rock while sampling.

3.3 Field Data Sheet:

The collection of stream sediment samples was recorded in the 27 column field data sheet. The field data sheets have been appended to the report. The details of the columns and abbreviations used are given below:-

NATIONAL GEOCHEMICAL MAPPING

Name of the Sampler: A. Elow
Designation: Senior Geologist
Operation: SU-M&N
District: Ukhrul

Region: North Eastern
State: Manipur
Site Description:

Date: 05/11/2018
Sample Media: Stream sediment/Soil
Toposheet No.: 83K/8
Composite No.:

Sl. No.	Grid No.	Longitude	Latitude	Elevation	Sample Type	Stream Order	Upstream Length (in m)	Basin area (km ²)	Stream Condition
1	89	94°27'9.57"	25°7'31.9"	1920	SS	2nd	2100 m	>1	Wet (Perennial)
	Channel Character	Stream Bed Material	Rock type	Rock	Formation	Group	Structure	Structural Measurement	Metamorphic minerals
	Natural	Pebbly Sand	Igneous	Harzburgite	Ophiolite Suit	Mafic Ultramafic	Foliation	N10E/76 easterly	
	Land use	Landscape type	Mineralization	Contamination	Soil horizon	Soil depth	Slope	Remarks on geological set-up	
	Forest	Undulating	Chromite, Latent soil				Steely sloping > 20° (4)		

Foot Note: Sample Type: Stream sediment (SSS), Tank sediment (TS), Soil (S); Water: Stream water (SW), Spring water (SP), Well (WW); Stream order: 1,2,3,4,5 etc.; Stream condition: Wet (W), Dry (D); Channel character: Natural (N), Reinforced (R), Man made (M) etc.; Stream bed predominant material: Gravel (G), Sand (Sd), Silt (St), Clay (C), Rocky (Rk); Rock type: Igneous basic (IgB), Igneous metamorphic (IgM), Metamorphic (M), Metamorphic high grade (Mhg), Sedimentary (S); Rock: Four latter code may be used eg. Granite (GRAN), Amphibolite (AMPH), Quartzite (QUAR), Formation: Bskabil, Dupitila etc.; Group: Sumra, Tipam etc.; Structure: Course grained etc.; Structural measurement: Strike & Dip etc.; Landscape: Plain (P), Undulating (U), Rugged (R); Land use: Agriculture (A), Pasture land (P), Forest (F), Barren (B), Others: Specify; Contamination: Old working (OW), Mine dump (MD), Others Specify; Soil horizon: Weathered bed rock R & C horizons with calcareous concentrations (Cact), C-horizon without calcareous concentration (C), Transported soil (A)

Human Health

Fig.3.12: Field data Sheet

3.4 Processing and storage of samples:

Mostly the samples collected from the field are wet or with high moisture content due to prolong monsoon, thick vegetation and humid climate of the area. The wet stream sediment samples collected from the field were spread out on transparent plastic sheets at field camp to dry the samples naturally. After drying, the samples were de-lumped using wooden-mortar and pestle, and sieved through -120 mesh. At least 1000 gm sample was collected for each 2 x 2km grid sample and divided into two parts of 500 gm each by coning and quartering. One part was stored at GCM repository as original sample for each grid sample and the other 500g will be sent to the Chemical Lab for analysis.

For soil samples, the samples were de-lumped and sieved with -120 mesh after drying by spreading over transparent plastic sheets. Two sets of samples weighing 500 gm each were collected from the processed Regolith and C-horizons of each soil sample. One set of samples was sent for chemical analysis and the other set was stored at GCM repository for future reference.

For petrographic studies, the collected rock samples were sent to the petrology lab for the preparation of thin section for microscopic studies.



Fig 3.13: Sun drying of the stream sediment/slope wash samples at camp.



Fig 3.14: Delumping of the stream sediment/slope wash samples at camp



Fig.3.15: Sieving of the samples at camp.



Fig.3.16: Packing of samples at Camp.

Proper numbering of samples and recording of data were done in the 17 column standard field data sheets which were further entered in the NGCM Excel data sheet of GSI. So, the numbering of a unit sample was recorded as Toposheet No./Unit or Cell Grid No./Name of media/Year of collection. Where 83K8/1/S/14 represents a cell samples (2 km x 2 km) in which 'S' stands for stream sediment. Similarly, 'R' for regolith or topsoil, 'C' for soil from C-horizon, 'W' for water sample, 'HM' for heavy mineral, 'BR' for bed rock samples of XRD analysis and 'PS' for petrographic study samples stand for other media.

3.5 Sample contamination:

Contamination during the course of the sampling process has been taken due care. In the agricultural and cultivated areas where possible pesticides / insecticides contamination is expected, samples were collected during dry season. Settlements/inhabitation areas may also contribute to sample contamination. So, samples were collected keeping these factors in mind to avoid contamination.

CHAPTER 4

4. STATISTICAL ANALYSIS AND CHEMICAL DATA

Geochemical mapping require handling of various analytical data base on stream sediment, soil and water samples collected from given specified area. High quality and consistency of the obtained data are ensured by using standardized sampling methods and by treating and analyzing of all the data statistically.

4.1 Statistical analysis:

A total of 168 stream sediment/slope wash samples, 18 soil samples, 9 duplicate samples and 9 stream water samples have been collected and sent to Chemical Laboratory for analysis. Package A (Major & Minor Oxides and some Trace Elements) and Package H (Trace and RE Elements) analysis result of the total 168 stream sediment/slope wash samples, 18 soil samples and 9 duplicate samples have been received (Annexure I, II, III, IV, V, VI, VIII, IX and X). For stream water sample analysis, Package B and C analysis results have been received (Annexure VII). Results of the remaining samples are yet to be received from Chemical Division. Analytical result status along with the packages index is given in annexure XI.

Table 4.1: Methodologies employed for analysis of samples

Packages	Methods	Elements
Package A	XRF	Major, Minor oxides and some trace elements
Package B	GF-AAS	Au
Package C	F-AAS	Li and Ce
Package D	HG-AAS	As, Sb, Se and Te
Package E	SIE	F
Package F	GF-AAS	Cd and Ag
Package G	GF-AAS	Hg
Package H	ICP-MS	REE & HREE and some trace elements
Package I	AAS/ICP	Platinum and Palladium
Package W(A) +W(B)+W(C) Major, Minor and trace elements in water samples, Bicarbonates, salinity, PH etc.		

4.1.1 Check for errors and outliers

The count function was used to find out number of numerical entries in each column and checking was done for counts less than the actual number of samples. The number of entries showing values below detection limit were recorded, then the auto filter option was used to check for the errors due to comma, blank space, 'O' in place of '0', etc. and necessary corrections were made.

4.1.2 Statistical treatment of data in MS Excel

The elemental data received were treated statistically. The analytical data of some elements contains values below the detection limit and required data validation was done.

A. Basic and univariate statistics

The descriptive statistics function of MS Excel was used to find the univariate statistics containing the number of samples or count (n), minimum value, maximum value, mean, median, variance, standard deviation, skewness and kurtosis for stream sediment samples and soil samples (Table 4.2 & 4.3). The mean, median and mode values were compared to have a theoretical assessment of the normality in the distribution of element. Threshold and anomaly values were calculated using the following formula:

$$\text{Threshold} = \text{Mean} + 2 \times \text{Standard Deviation (SD)}; \text{Anomaly} = 2 \times \text{Threshold value (TV)}$$

Table 4.2: Univariate statistical summary of the major oxides from the stream sediment/slope wash samples (values are in % and n=168)

Oxides	Mean	Median	Minimum	Maximum	Variance	Std.Dev.	Skewness	Kurtosis
SiO ₂ (%)	59.26	60.34	36.61	80.02	52.4	7.24	-0.93	1.41
Al ₂ O ₃ (%)	14.57	15.06	3.08	20.02	7.4	2.71	-1.38	3.05
Fe ₂ O ₃ (%)	7.49	6.48	2.36	29.13	17.3	4.16	2.90	9.49
TiO ₂ (%)	0.88	0.87	0.22	1.97	0.1	0.23	1.20	5.85
CaO (%)	0.49	0.40	0.06	2.09	0.1	0.33	1.80	4.24
MgO (%)	2.37	1.44	0.59	24.92	11.0	3.31	4.37	21.22
MnO (%)	0.17	0.12	0.03	1.68	0.0	0.18	5.11	33.73
Na ₂ O (%)	0.46	0.45	0.07	1.42	0.1	0.23	0.80	1.34
K ₂ O (%)	1.72	1.77	0.18	3.37	0.3	0.53	-0.12	1.74
P ₂ O ₅ (%)	0.15	0.13	0.06	0.46	0.0	0.06	1.71	3.78

Table 4.3: Univariate statistical summary of Trace elements from the stream sediment/slope wash samples (values are in ppm & ppb and n=168)

Elements	Mean	Median	Minimum	Maximum	Variance	S.D	Skewness	Kurtosis
Ba (ppm)	279.35	237.00	25.00	844.00	18456.5	135.85	1.52	3.02
Co (ppm)	43.17	23.00	2.00	678.00	5151.2	71.77	5.26	37.99
Cr (ppm)	565.68	229.50	52.00	4810.00	866273.4	930.73	2.95	7.89
Cu (ppm)	32.08	32.00	9.00	71.00	98.6	9.93	0.70	1.35
Ga (ppm)	15.56	16.00	5.00	24.00	11.2	3.35	-0.24	0.22
Nb (ppm)	12.94	12.00	0.25	39.00	19.0	4.35	2.28	10.88
Ni (ppm)	363.69	96.50	17.00	5681.00	659954.7	812.37	3.65	15.08
Pb (ppm)	17.36	17.00	1.00	38.00	32.57995	5.71	0.35	1.02
Rb (ppm)	86.04	87.01	18.29	164.66	534.8	23.12	0.08	1.66
Se (ppm)	16.69	16.00	5.00	36.00	23.3	4.82	1.510	4.79
Sr (ppm)	67.78	69.50	14.00	210.00	603.5	24.57	1.00	6.14
Th (ppm)	10.48	10.14	2.72	19.27	8.0	2.83	0.26	0.94
V (ppm)	123.92	121.50	54.00	375.00	1209.3	34.77	3.26	19.78
Y (ppm)	22.80	23.00	5.00	53.00	34.2	5.85	0.69	4.50
Zn (ppm)	89.73	91.00	36.00	157.00	389.8	19.74	0.53	1.15
Zr (ppm)	224.40	224.50	31.00	575.00	5608.9	74.89	0.81	4.64
La (ppb)	32.27	31.01	10.48	58.16	73.6	8.58	0.24	0.75
Ce (ppb)	60.90	58.51	19.02	119.17	282.4	16.80	0.66	1.45
Pr (ppb)	7.44	7.11	2.07	14.65	4.1	2.03	0.53	1.56
Nd (ppb)	27.41	26.20	7.537	58.79	57.7	7.59	0.78	2.50
Eu (ppb)	1.24	1.19	0.250	2.97	0.2	0.40	1.00	3.23
Sm (ppb)	5.48	5.33	1.49	12.73	2.6	1.61	1.25	4.41
Gd (ppb)	5.29	5.12	1.50	12.64	2.4	1.53	1.26	4.29
Tb (ppb)	0.79	0.76	0.22	1.89	0.1	0.23	0.88	3.68
Dy (ppb)	4.66	4.53	1.30	10.55	1.5	1.21	0.98	3.55
Ho (ppb)	0.89	0.88	0.25	1.94	0.05	0.22	0.42	3.79
Er (ppb)	2.65	2.62	0.75	5.14	0.3	0.57	0.39	2.79
Tm (ppb)	0.33	0.25	0.13	0.79	0.0	0.13	1.26	0.32
Yb (ppb)	2.78	2.76	0.79	4.62	0.3	0.54	-0.16	2.13
Lu (ppb)	0.34	0.25	0.13	0.74	0.0	0.13	0.92	-0.71
Sn (ppm)	3.58	3.49	0.48	11.12	2.3	1.52	1.80	6.06
Hf (ppm)	8.78	8.69	1.79	26.93	12.1	3.48	1.52	6.64
Ta (ppm)	1.15	1.10	0.12	4.15	0.3	0.52	1.60	6.96
Ge (ppm)	1.49	1.33	0.66	5.41	0.4	0.64	3.16	12.98
Be (ppm)	1.51	1.51	0.44	2.75	0.2	0.41	0.34	0.82
U (ppm)	2.15	2.16	0.66	3.53	0.2	0.49	-0.28	1.36

CHAPTER 5

5. GEOCHEMICAL ANOMALY

Applied geochemical surveys essentially serve two basic purposes:

1. Detection of geochemical anomalies both natural, e.g., related to mineral occurrences, and anthropogenic, e.g., related to industrial releases; and
2. Mapping and establishing natural background levels or baselines.

Present work aims to depict the elemental distribution in the study area using the contour maps. The spatial distribution maps of different elements produced here are a prerequisite for mineral investigation, as also helpful in environmental assessment, agriculture, health and for any rural or urban development planning. The stream sediment/slope wash samples in general do not represent a single litho unit but rather represents a combined lithology of the area. Broadly the surface geology and geochemical signature are complimentary of each other. But there could be discrepancies owing to the unavailability of exposures. These areas require further detailed study.

5.1. NORMAL BACKGROUND VALUES

The Background is defined as the normal abundance of an element in barren earth's material. For a specific element the normal background values differs in different types of earth materials/media under different chemical conditions. For example, the standard normal background value for Pb, Co, etc, are different in soil, stream sediment/slope wash samples, bed rock, stream water sample media, and also varies in different conditions depending on the chemical environment, which is controlled by the latitude and longitude. Certain environmental conditions can either enrich or deplete the elemental concentrations. Thus the distribution of an element in a specific media is not uniform and is expressed as a range of values. In the present study the dispersion of the values about the mean, i.e. dispersion by one standard deviation (between $M+1SD$ and $M-1SD$) is considered as the background value for a specific element.

Values about the mean, i.e. dispersion by two standard deviations (between $M+2SD$ and $M-2SD$) are high or low values.

The univariate statistical parameters of major and trace elements of the stream sediment/slope wash samples are given in Table 4.1 and 4.2 respectively. The frequency table and cumulative percentage for major elements and trace elements are given along with the spatial elemental distribution maps.

5.2 Preparation of Geochemical Maps

Mere observation of the tabulated analytical data does not give any impression about the nature of distributions of the elements, nor does this tabulated data help much in understanding the relation between element dispersion pattern with the geology of the area. Therefore, preparation of element distribution maps is one of the main objectives for any geochemical mapping project to understand the distribution of the elements and their relation with the geology of the area. Apart from giving clues for potential area of mineralization, these maps can be used for the purposes of environmental assessment, agricultural best practices, health, etc. The composition of the sediments which are the product of weathering and erosion of soil and rocks in the upstream catchments area closely approximates with the natural sample (Howarth and Thorton, 1983).

The spatial distribution maps or the geochemical maps of the 10 major and 36 trace elements were prepared (Fig 5.1 to 5.46) to study the influence of surface lithology on sediment geochemistry. Surfer-8 software was used for preparation of geochemical maps by ordinary kriging method. The geochemical distributions of the elements were then compared with the geology of the area by overlaying geochemical maps of the elements on the geological map of the study area. The high values ($>M+2SD$) in the overlay map are shown as blue hatch while significant values ($>M+3SD$) are shown as blue colour. The $M+2SD$ and $M+3SD$ values of each element were calculated along with their percentage of observed values above and given in Table 5.1.

Table 5.1: Table showing background value, anomalous value and significantly anomalous values of Oxides and Trace elements from the stream sediment/slope wash samples along with their % of no. of observations (values are in ppm & ppb and n=168)

	M+SD (Background Value)	M+2SD (Anomalous Value)	M+3SD (Sig. Anomalous Value)	Samples > M+2SD (%)	Samples > M+3SD (%)
SiO ₂ (%)	66.5024	73.74449	80.98656	0.60	0.00
Al ₂ O ₃ (%)	17.2910	20.00538	22.71974	0.60	0.00
Fe ₂ O ₃ (%)	11.6553	15.81531	19.97531	6.55	2.98
TiO ₂ (%)	1.1177	1.349509	1.581288	3.57	2.38
CaO (%)	0.8242	1.155779	1.487359	6.55	1.79
MgO (%)	5.6884	9.003526	12.31865	4.76	2.98
MnO (%)	0.3644	0.554258	0.744095	2.98	1.19
Na ₂ O (%)	0.6880	0.918162	1.148315	2.38	0.00
K ₂ O (%)	2.2491	2.781448	3.313779	3.57	0.60
P ₂ O ₅ (%)	0.2100	0.273642	0.337279	5.36	2.38
Ba (ppm)	415.1998	551.0544	686.909	4.76	1.79
Co (ppm)	114.9444	186.7161	258.4879	4.76	1.79
Cr (ppm)	1496.4167	2427.155	3357.893	8.33	4.17
Cu (ppm)	42.0089	51.94038	61.87188	4.17	1.19
Ga (ppm)	18.9124	22.26533	25.61823	1.79	0.00
Nb (ppm)	17.2995	21.65701	26.01453	4.17	1.79
Ni (ppm)	1176.0665	1988.442	2800.818	5.95	3.57
Pb (ppm)	23.0710	28.77886	34.48675	4.17	0.60
Rb (ppm)	109.1757	132.3025	155.4293	3.57	1.19
Se (ppm)	21.5143	26.33804	31.16183	4.17	3.57
Sr (ppm)	92.3465	116.9133	141.4801	1.79	0.00
Th (ppm)	13.3178	16.15077	18.9837	2.98	0.60
V (ppm)	158.6915	193.4663	228.2411	2.38	1.19
Y (ppm)	28.6496	34.50167	40.3537	3.57	0.60
Zn (ppm)	109.4691	129.2119	148.9548	3.57	1.19
Zr (ppm)	299.2971	374.1895	449.0818	2.38	1.79
La (ppb)	40.8530	49.43145	58.00993	4.76	0.60
Ce (ppb)	77.7049	94.50969	111.3145	4.76	1.19
Pr (ppb)	9.4753	11.50683	13.53834	4.17	1.19
Nd (ppb)	35.0108	42.60997	50.20916	4.76	1.19
Eu (ppb)	1.6458	2.051491	2.457214	3.57	1.79
Sm (ppb)	7.0892	8.695238	10.30123	2.98	1.19
Gd (ppb)	6.8326	8.365959	9.899293	2.98	1.79
Tb (ppb)	1.0188	1.251227	1.483645	4.17	1.19
Dy (ppb)	5.8672	7.076808	8.286464	4.76	0.60

Ho (ppb)	1.1172	1.339984	1.562817	4.76	0.60
Er (ppb)	3.2263	3.800198	4.374048	3.57	0.60
Tm (ppb)	0.4666	0.600919	0.735266	4.76	0.60
Yb (ppb)	3.3237	3.866343	4.408968	3.57	0.60
Lu (ppb)	0.4829	0.621478	0.76001	3.57	0.00
Sn (ppm)	5.1057	6.630857	8.155974	4.76	2.98
Hf (ppm)	12.2626	15.74367	19.22474	2.38	1.79
Ta (ppm)	1.6695	2.188095	2.706651	4.17	1.19
Ge (ppm)	2.1376	2.781436	3.42524	4.76	2.98
Be (ppm)	1.9178	2.32555	2.733298	4.76	0.60
U (ppm)	2.6450	3.137956	3.630947	2.98	0.00

5.2.1 Correlation Matrix:

From bivariate statistical analysis, correlation among the elements was determined. A correlation matrix is a table showing correlation coefficients between variables. Correlation coefficient is a measure of strength and direction of the linear relationship between two variables. The values of the correlation coefficient can range from -1 to +1. A high positive correlation (Value close to +1) between a pair of oxides/elements indicates high degree of geochemical affinity between the pair. A high negative correlation (Value close to -1) between a pair of oxides/elements indicates high negative geochemical affinity between the pair. Arbitrarily more than 0.85 correlation values between two variables assume to be very strongly correlated. The correlation value between 0.65 and 0.85 is considered as strong correlation while value in between 0.5 to 0.65 as moderate. Moderate correlation, strong correlation and very strong correlations are represented by red, blue and green colors respectively in the correlation tables (Table nos. 5.2, 5.3 and 5.4).

Table: 5.2. Correlation matrix of Oxides

	SiO ₂	Al ₂ O ₃	Fe ₂ O ₃	TiO ₂	CaO	MgO	MnO	Na ₂ O	K ₂ O	P ₂ O ₅
SiO ₂	1.00									
Al ₂ O ₃	0.25	1.00								
Fe ₂ O ₃	-0.81	-0.40	1.00							
TiO ₂	0.18	0.44	-0.28	1.00						
CaO	-0.60	-0.35	0.36	-0.12	1.00					
MgO	-0.62	-0.68	0.47	-0.50	0.54	1.00				
MnO	-0.54	-0.34	0.69	-0.18	0.23	0.23	1.00			
Na ₂ O	0.12	0.40	-0.26	0.33	0.06	-0.20	-0.27	1.00		
K ₂ O	0.31	0.76	-0.51	0.30	-0.22	-0.54	-0.34	0.37	1.00	
P ₂ O ₅	-0.36	-0.03	0.14	0.26	0.39	-0.01	0.27	-0.12	-0.01	1.00

Table: 5.3. Correlation Matrix of Rare Earth Elements

	La	Ce	Pr	Nd	Sm	Eu	Gd	Tb	Dy	Ho	Er	Tm	Yb	Lu
La	1.00													
Ce	0.93	1.00												
Pr	0.97	0.94	1.00											
Nd	0.94	0.92	0.99	1.00										
Sm	0.82	0.83	0.92	0.96	1.00									
Eu	0.67	0.68	0.78	0.85	0.95	1.00								
Gd	0.79	0.81	0.89	0.93	0.99	0.95	1.00							
Tb	0.74	0.75	0.84	0.89	0.97	0.96	0.98	1.00						
Dy	0.72	0.74	0.82	0.87	0.95	0.93	0.97	0.99	1.00					
Ho	0.74	0.75	0.82	0.87	0.92	0.90	0.94	0.97	0.98	1.00				
Er	0.75	0.75	0.83	0.86	0.90	0.87	0.92	0.95	0.97	0.99	1.00			
Tm	0.53	0.55	0.59	0.62	0.67	0.63	0.70	0.71	0.75	0.73	0.74	1.00		
Yb	0.74	0.73	0.80	0.82	0.83	0.78	0.84	0.88	0.91	0.95	0.98	0.72	1.00	
Lu	0.48	0.47	0.53	0.55	0.58	0.53	0.61	0.64	0.68	0.68	0.70	0.89	0.73	1.00

Table: 5.4. Correlation Matrix of Trace Elements

	Ba	Co	Cr	Cu	Ga	Nb	Ni	Pb	Rb	Sc	Sr	Th	V	Y	Zn	Zr	Sn	Hf	Ta	Ge	Be	U
Ba	1.00																					
Co	0.15	1.00																				
Cr	0.06	0.87	1.00																			
Cu	0.35	0.37	0.23	1.00																		
Ga	0.34	-0.33	-0.45	0.39	1.00																	
Nb	0.24	-0.23	-0.29	0.09	0.38	1.00																
Ni	0.00	0.83	0.88	0.27	-0.43	-0.31	1.00															
Pb	0.34	-0.09	-0.19	0.13	0.53	0.21	-0.26	1.00														
Rb	0.39	-0.32	-0.38	0.09	0.69	0.30	-0.40	0.59	1.00													
Sc	0.26	0.44	0.43	0.56	0.27	-0.07	0.47	0.11	0.00	1.00												
Sr	0.24	-0.49	-0.57	0.04	0.48	0.28	-0.54	0.24	0.30	-0.14	1.00											
Th	0.41	-0.21	-0.26	0.02	0.59	0.40	-0.31	0.64	0.83	0.05	0.16	1.00										
V	0.25	0.26	0.15	0.54	0.49	0.11	0.13	0.15	0.03	0.63	0.11	0.05	1.00									
Y	0.33	-0.42	-0.56	0.23	0.73	0.46	-0.49	0.52	0.59	0.05	0.50	0.52	0.26	1.00								
Zn	0.47	0.30	0.28	0.60	0.49	0.18	0.24	0.27	0.33	0.55	0.11	0.28	0.53	0.29	1.00							
Zr	0.00	-0.53	-0.50	-0.43	0.14	0.27	-0.59	0.30	0.22	-0.31	0.29	0.33	-0.26	0.32	-0.32	1.00						
Sn	-0.03	-0.02	-0.02	-0.02	-0.06	-0.01	-0.02	0.04	-0.02	-0.01	0.03	-0.03	-0.02	0.01	-0.07	0.00	1.00					
Hf	-0.05	-0.43	-0.38	-0.42	0.05	0.14	-0.45	0.22	0.13	-0.33	0.20	0.23	-0.27	0.19	-0.35	0.87	-0.02	1.00				
Ta	0.14	-0.31	-0.35	-0.07	0.20	0.75	-0.36	0.07	0.25	-0.28	0.25	0.33	-0.15	0.41	-0.03	0.32	-0.02	0.21	1.00			
Ge	0.21	0.80	0.77	0.49	0.00	-0.09	0.73	0.04	-0.11	0.74	-0.39	0.00	0.46	-0.18	0.59	-0.48	0.05	-0.46	-0.23	1.00		
Be	0.43	-0.10	-0.23	0.32	0.74	0.40	-0.23	0.63	0.83	0.20	0.29	0.79	0.23	0.67	0.47	0.17	0.01	0.09	0.30	0.15	1.00	
U	0.38	-0.22	-0.24	-0.12	0.42	0.33	-0.35	0.57	0.69	-0.04	0.14	0.88	-0.04	0.41	0.10	0.50	-0.04	0.42	0.32	-0.10	0.60	1.00

5.3. Distribution of Major Elements in the Stream Sediments

The major oxides represented by the 10 elements (i.e., SiO_2 , Al_2O_3 , Fe_2O_3 , TiO_2 , CaO , MgO , MnO , Na_2O , K_2O and P_2O_5) forms the basic building block of all major rock forming minerals. This major oxide plays a vital role in understanding the petrogenesis of igneous, metamorphic and sedimentary rocks. The SiO_2 is used as an important index mineral for petrogenetic studies of igneous rock as an index of magmatic differentiation. The higher values of SiO_2 in the study area are confined within the Paleogene Disang and Barial sediments are exposed. The Fe_2O_3 and MgO shows higher values in the eastern part, where mafic/ultramafic rocks are well exposed with varying thickness of lateritic soil capping is developed above the protolith rock. The CaO shows higher values along the eastern part of the study area where exotic limestone blocks and thinly interbedded marl and shale of the Ocean Pelagic Sediments are exposed.

5.3.1 Silicon (Si):

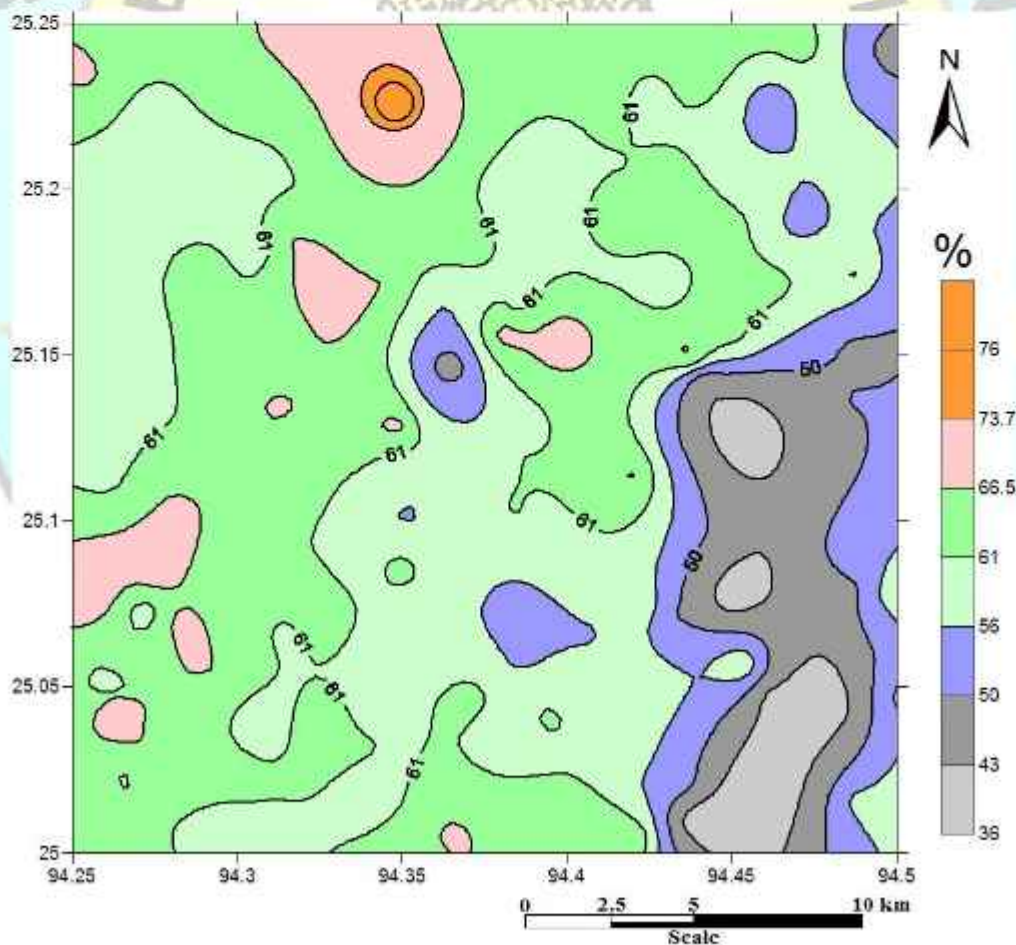


Fig. 5.1a. Spatial distribution of SiO_2 in the Stream sediments.

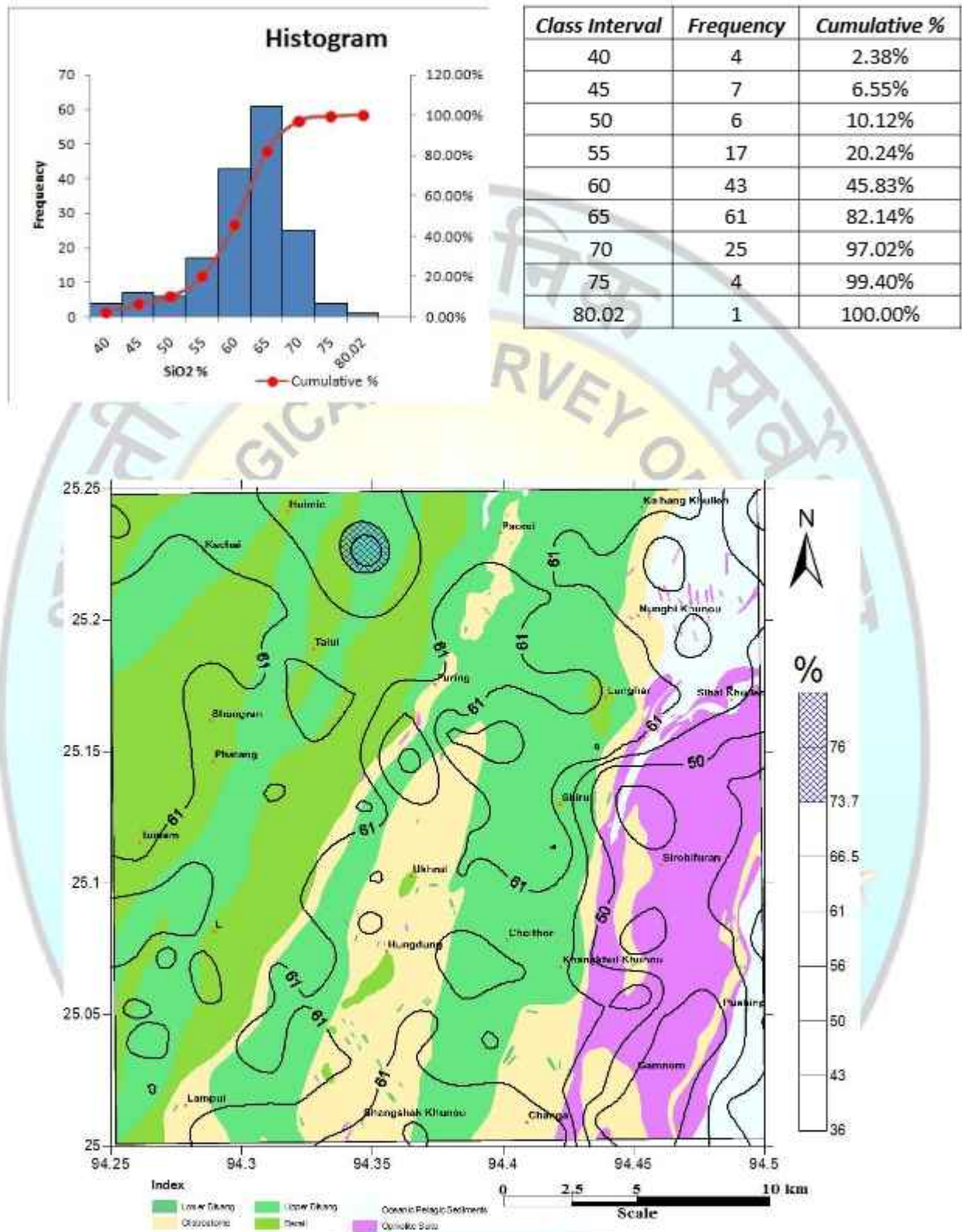


Fig. 5.1b. Spatial distribution of SiO_2 in the stream sediment/slope wash samples overlaid on geology of the study area.

SiO₂ in stream sediment

The median value of SiO₂ in stream sediments is 59.26 % with values varies from 36.61 to 80.02 % (Annexure-I). The maximum concentration is observed from Paleogene Barail sediments (Grid No. 161 of T.S. No. 83K/8). The minimum concentration is recorded from the eastern part of the study area, where the Ophiolite suite of rocks are exposed (Grid No.24 of T.S. No. 83K/8).

The distribution of SiO₂ in the area as evidenced from the contour map (Fig 5.1a) is mainly controlled by the underlying inherent lithology that contributes sediments to the stream/river system. The western part of the area shows higher SiO₂ concentration, which corresponds to Paleogene sediments as compared with the eastern part of the area where Ophiolite Belt is exposed (Fig.5.1b). The very fine grained quartz/feldspar/clay might have contributed SiO₂ to the adjoining streams.

In the eastern part of the study area, the weathering of the silicate mineral phases in the ultramafic suite of rocks like olivine, pyroxene and feldspar could have contributed SiO₂ in the adjoining streams.

In stream sediment, SiO₂ shows positive correlation with Al₂O₃, TiO₂, K₂O Na₂O and Zr but shows negative correlation with Fe₂O₃, CaO, MgO and MnO. The strong positive correlation between SiO and Zr and TiO₂ suggest the presence of rutile and zircon as heavy mineral in the stream sediments in the western part of the area, where the Paleogene sediments are exposed.

5.3.2. Aluminium (Al):

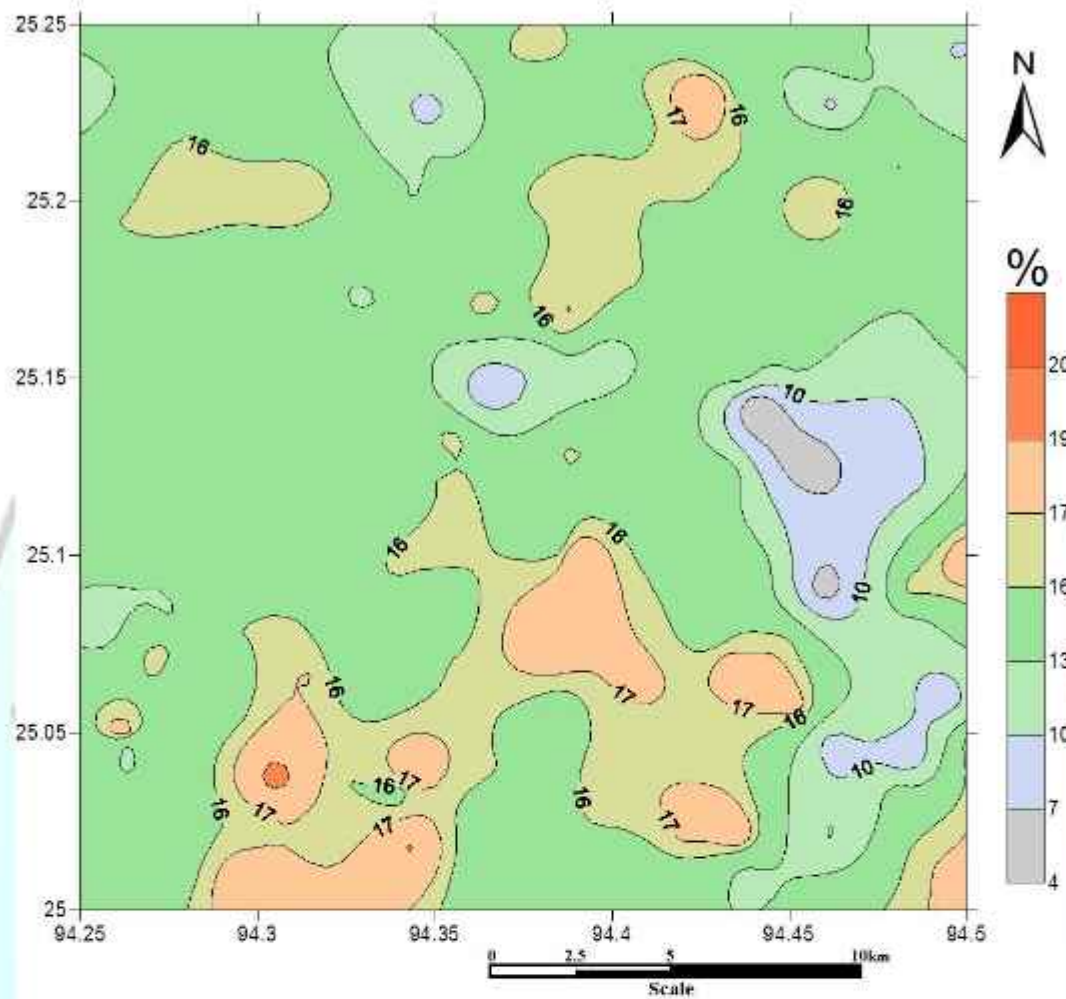
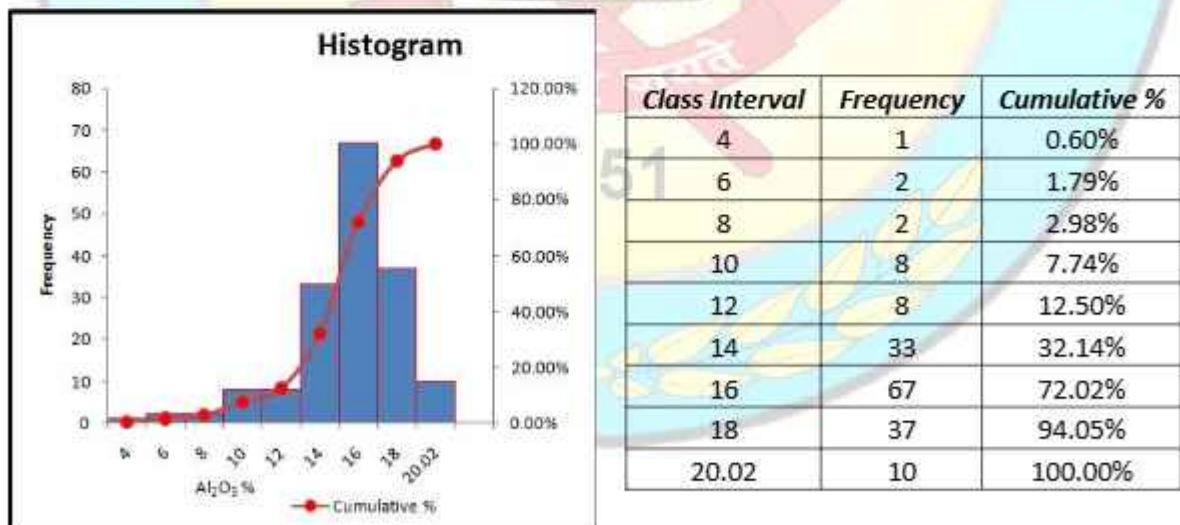


Fig. 5.2a. Spatial distribution of Al_2O_3 in the stream sediment/slope wash samples



5.3.3. Iron (Fe):

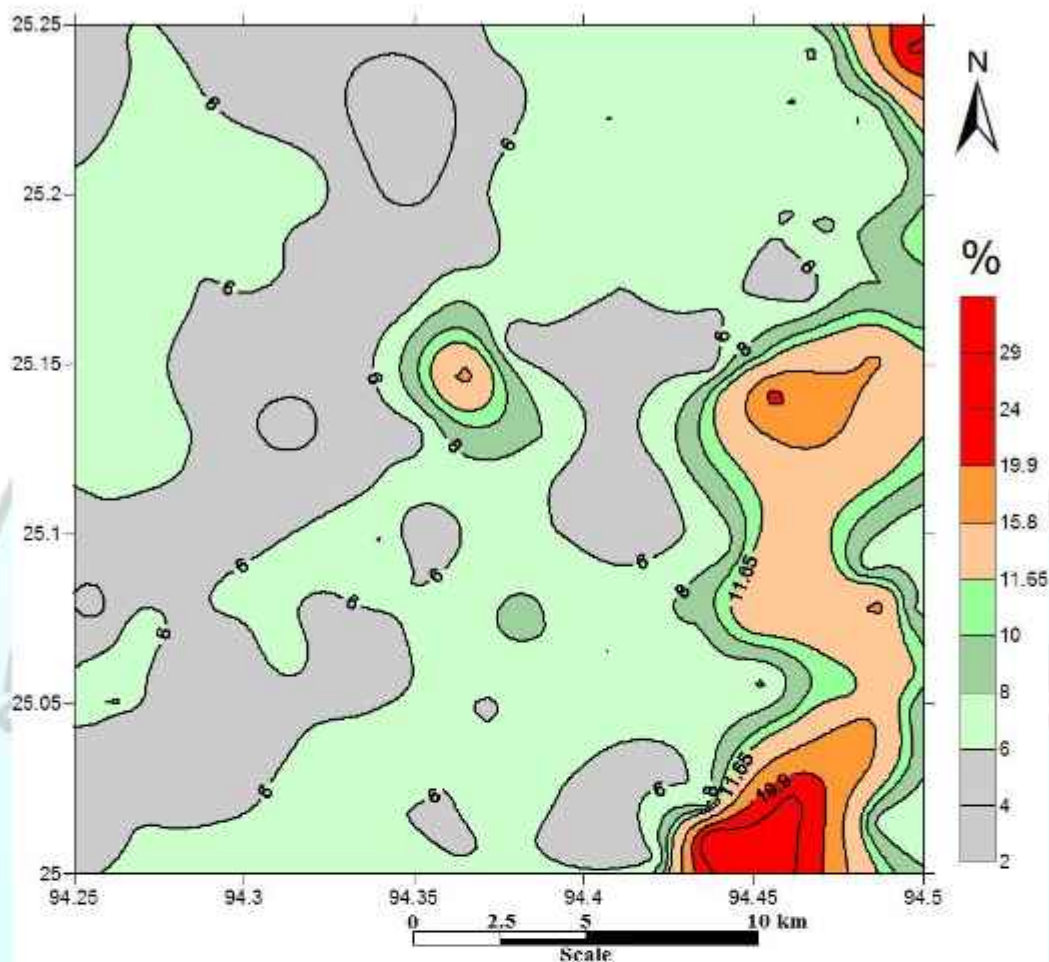
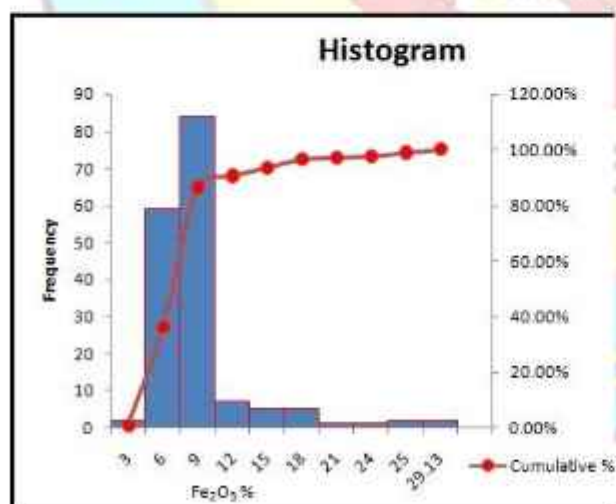


Fig. 5.3a. Spatial distribution of Fe_2O_3 in the stream sediment/slope wash samples



Class Interval	Frequency	Cumulative %
3	2	1.19%
6	59	36.31%
9	84	86.31%
12	7	90.48%
15	5	93.45%
18	5	96.43%
21	1	97.02%
24	1	97.62%
25	2	98.81%
29.13	2	100.00%

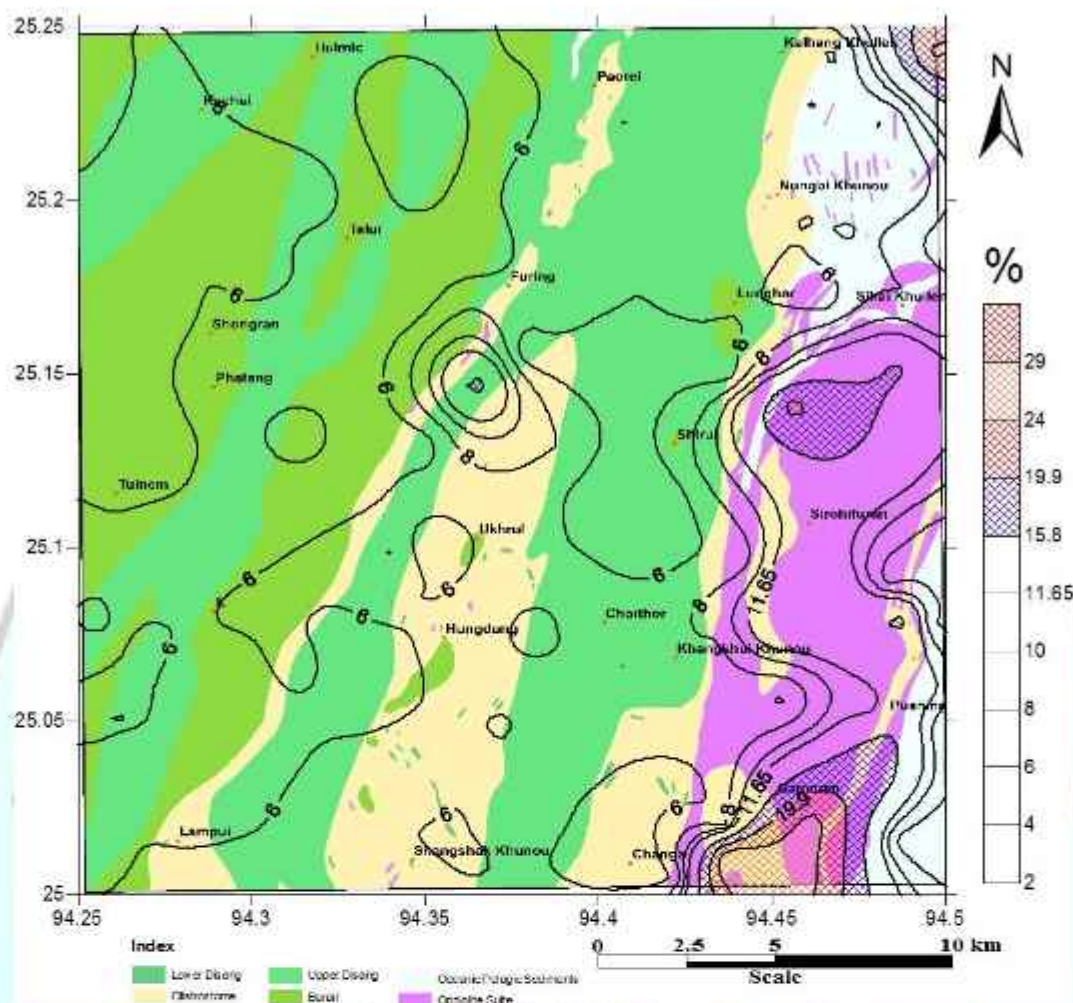


Fig. 5.3b. Spatial distribution of Fe_2O_3 in the stream sediment/slope wash samples overlaid on geology of the study area.

Fe_2O_3 in stream sediment

The median value of Fe_2O_3 in stream sediments is 6.48% and the values varies from 2.36 to 29.13%(Annexure-I) showing maximum value in the south western corner of the study area (Grid No.10) where transitional peridotite (hurlburgite) is exposed. The distribution is positive skewed with a value 2.90 of and positive kurtosis of 9.49.

In general stream sediment samples having its provenance from the Ophiolite Belt shows higher value of Fe_2O_3 (Fig. 5.3b). The high degree of serpentinisation of the mafic/ultramafic rock in the Ophiolite Belt may contribute the Fe_2O_3 in stream sediments as supported by the good positive correlation with CaO , MgO , MnO , Co , Cr and Ni .

5.3.4. Manganese (Mn):

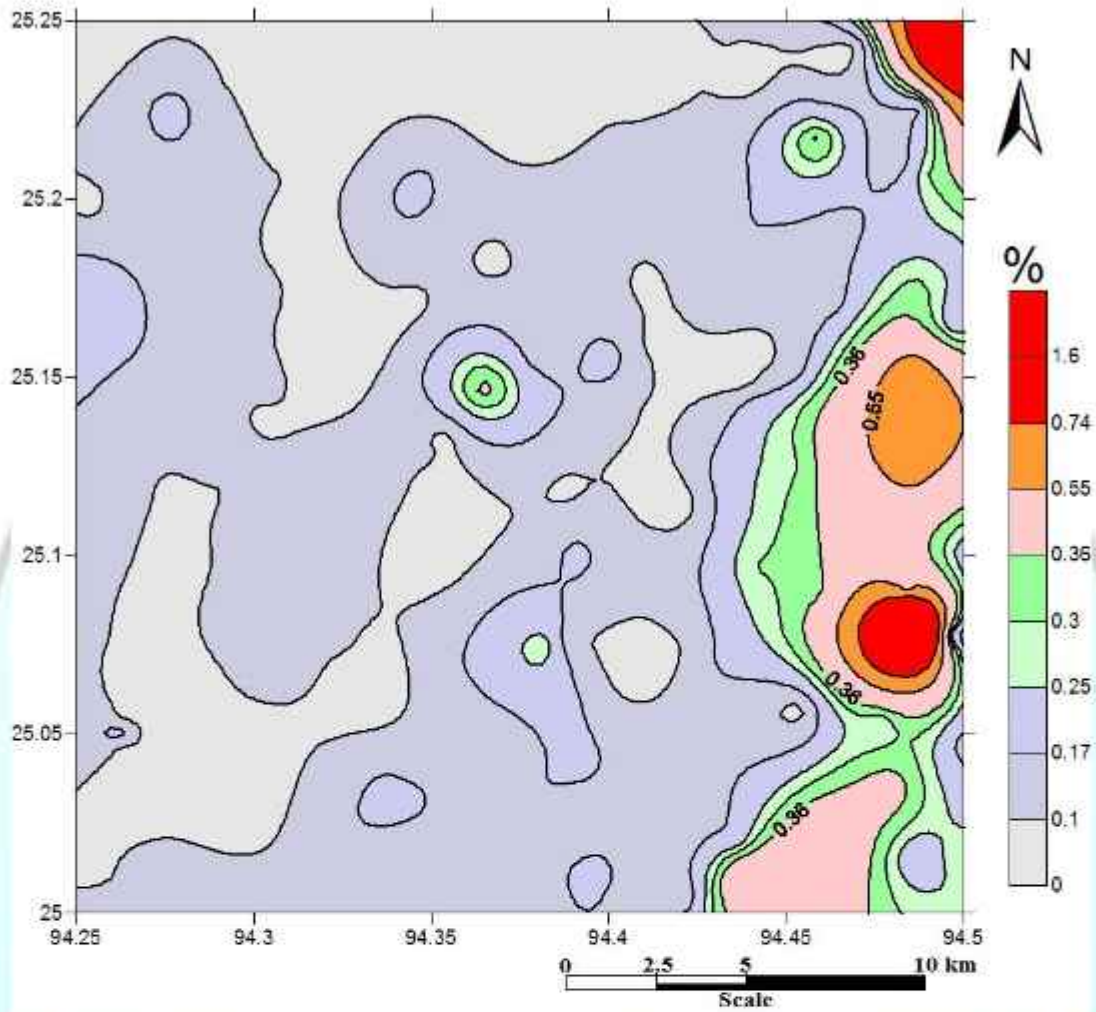
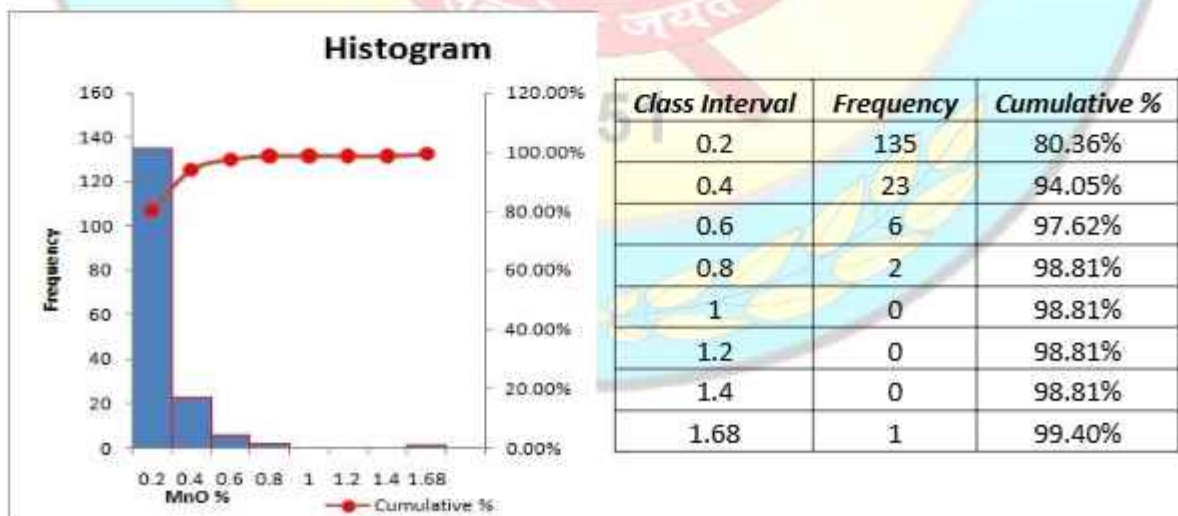
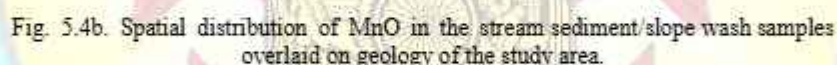


Fig. 5.4a. Spatial distribution of MnO in the stream sediment/slope wash samples





The median value of MnO in stream sediments is 0.05%, and the values vary from 0.03 to 1.68% (Annexure-I) showing maximum value in the south eastern part of the study area (Grid No. 64) where Ophiolite body is exposed. The distribution is positively skewed with a value of 5.11 and positive kurtosis of 33.73.

74

5.3.5. Magnesium (Mg):

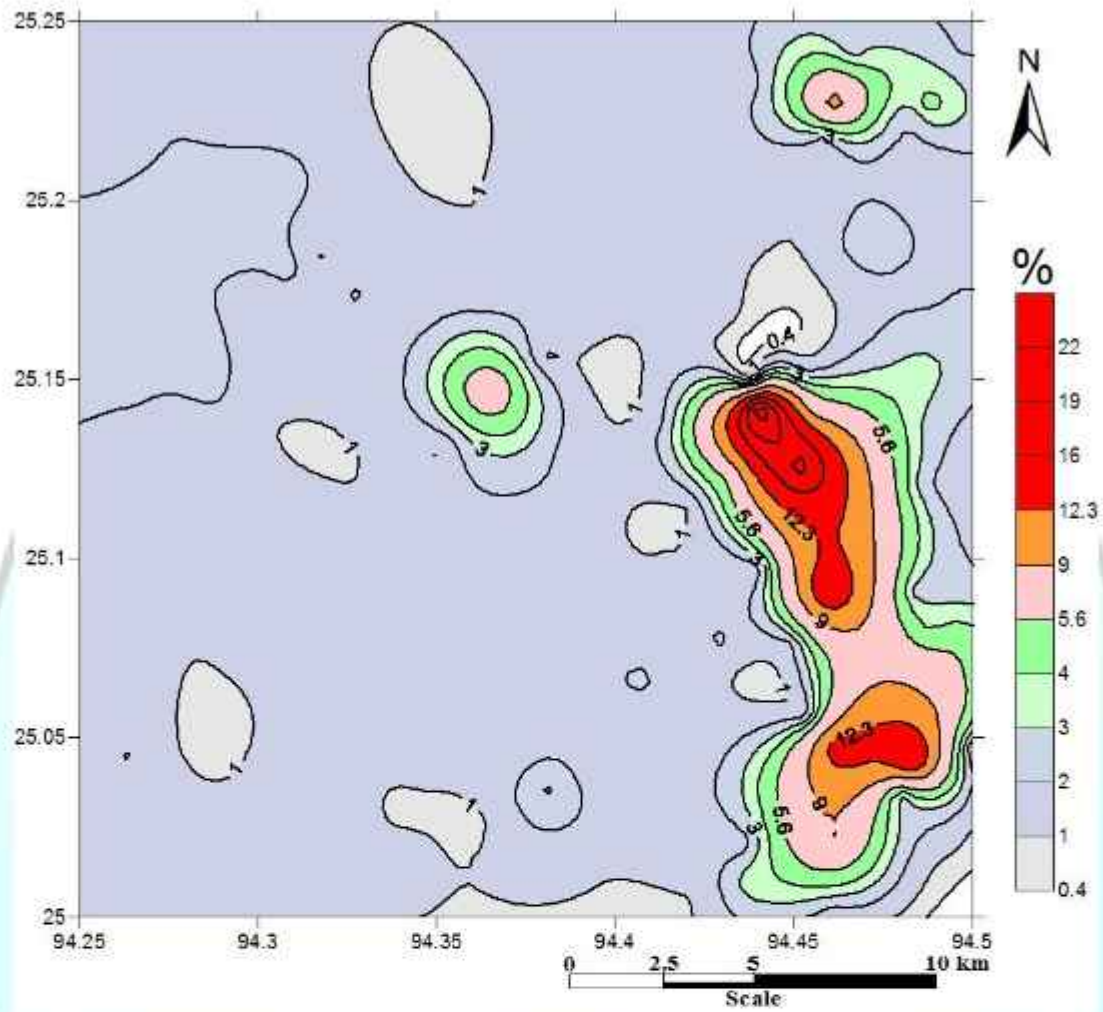
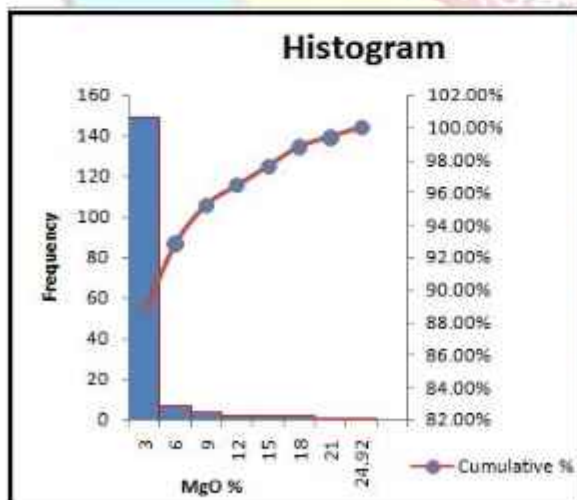


Fig. 5.5a. Spatial distribution of MgO in the stream sediment/slope wash samples.



Class Interval	Frequency	Cumulative %
3	149	88.69%
6	7	92.86%
9	4	95.24%
12	2	96.43%
15	2	97.62%
18	2	98.81%
21	1	99.40%
24.92	1	100.00%

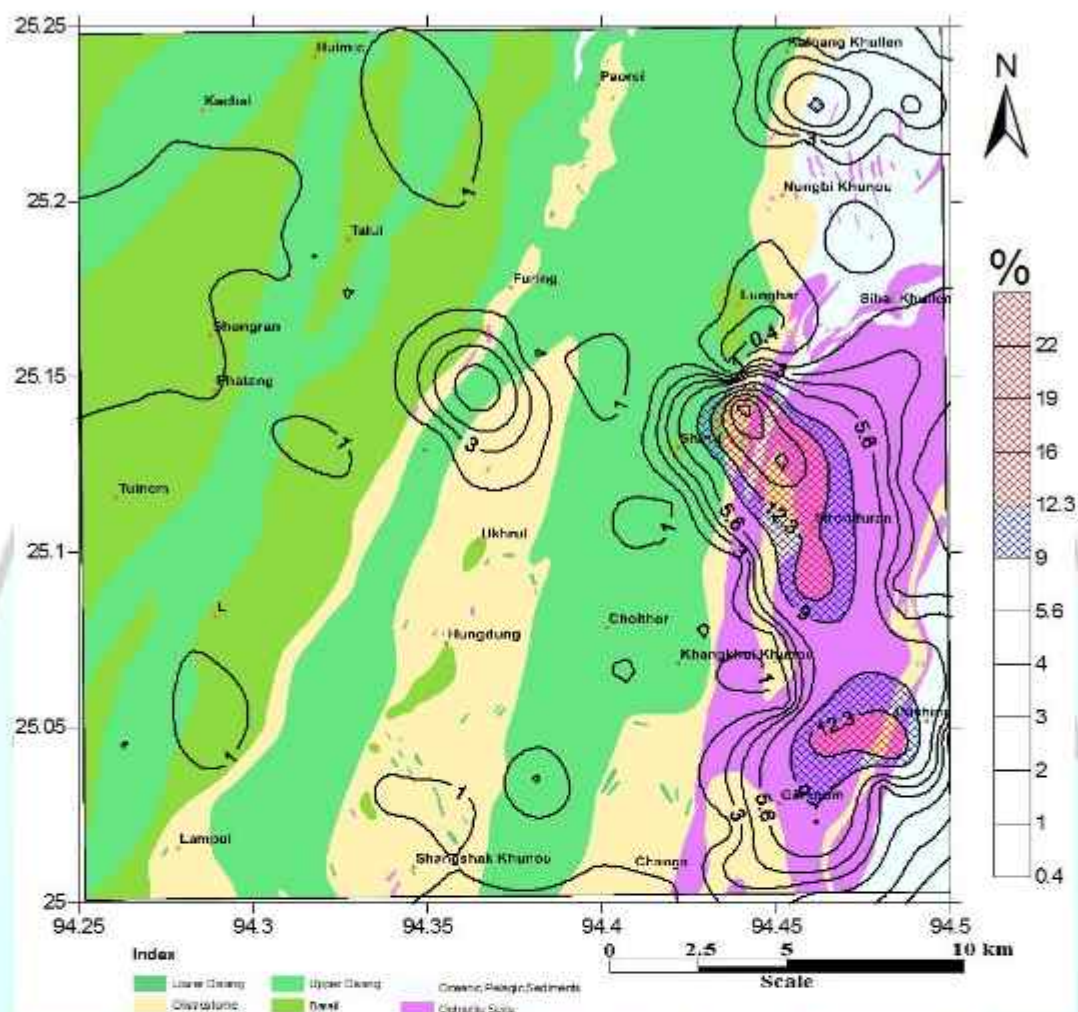


Fig. 5.5b. Spatial distribution of MgO in the stream sediment/slope wash samples overlaid on geology of the study area.

MgO in stream sediment

The median value of MgO in stream sediments is 1.44% with values varies from 0.59 to 24.92% (Annexture-I) showing maximum value in the eastern part of the study area (Grid No. 101) where the Ophiolite suite of rocks are exposed. The distribution pattern show a positive skewness of 4.38 and positive kurtosis value of 21.22.

The distribution of MgO is comparatively higher in the eastern part of the study area where Ophiolite bodies are exposed (Fig.5.5b). MgO has a strong positive correlation with Fe_2O_3 , CaO, MnO, Cr, Ni and Cu. which suggest the presence of mafic/ultramafic peridotite rock minerals that has undergone serpentinisation and subsequent weathering of Mg bearing mineral phase like olivine, pyroxene, amphibole, spinel, serpentine and talc.

5.3.6. Calcium (Ca):

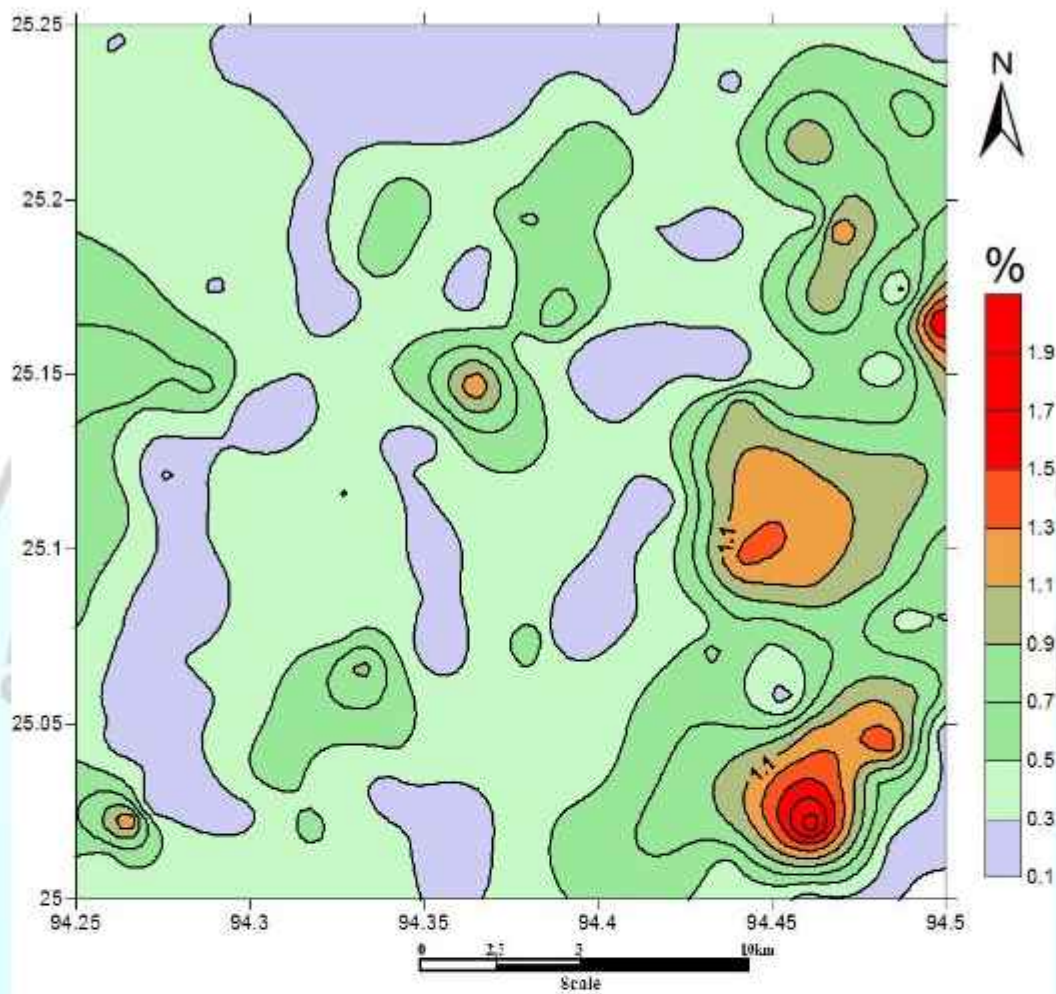
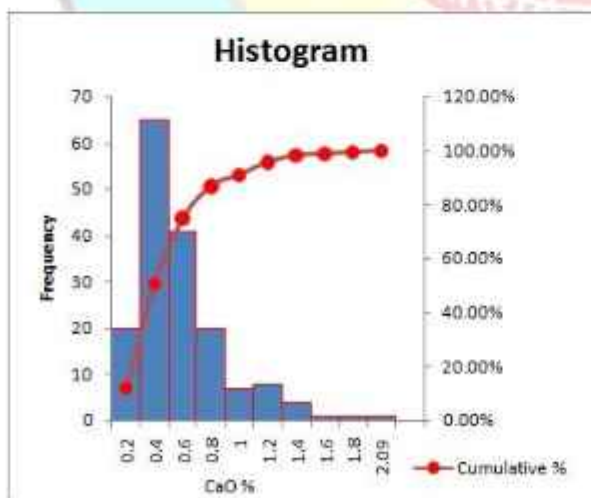


Fig. 5.6a. Spatial distribution of CaO in the stream sediment/slope wash samples



Class Interval	Frequency	Cumulative %
0.2	20	11.90%
0.4	65	50.60%
0.6	41	75.00%
0.8	20	86.90%
1	7	91.07%
1.2	8	95.83%
1.4	4	98.21%
1.6	1	98.81%
1.8	1	99.40%
2.09	1	100.00%

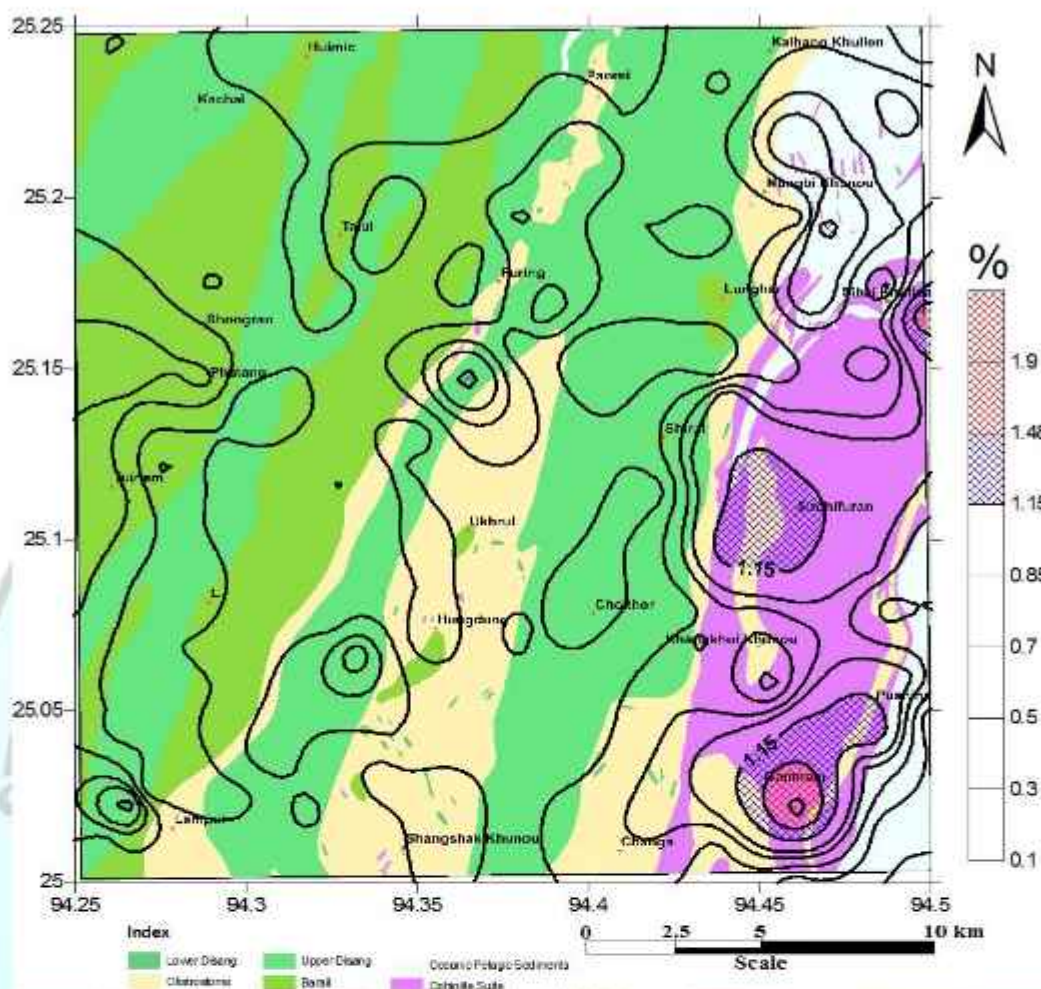


Fig. 5.6b. Spatial distribution of CaO in the stream sediment/slope wash samples overlaid on geology of the study area.

CaO in stream sediment

The median value of CaO in stream sediments is 0.40% with values varying from 0.06 to 2.09% (Annexure-I) showing maximum value in Grid No.24 where mafic and ultramafic rocks are exposed. The distribution is highly positive skewed and kurtosis with values of 1.81 and 4.24 respectively.

CaO distribution map shows higher concentration is slightly higher in the eastern part of the area, where the exotic limestone blocks and thinly bedded chert are exposed at the outcrop (Fig. 5.6b). CaO in stream sediment has a strong positive correlation with MgO, Fe₂O₃, Na₂O & Sr suggest the presence of limestone which is supported by the field evidence of exotic limestone blocks and thinly bedded marl with Olistostrome and Ocean Pelagic Sediments.

5.3.7. Sodium (Na):

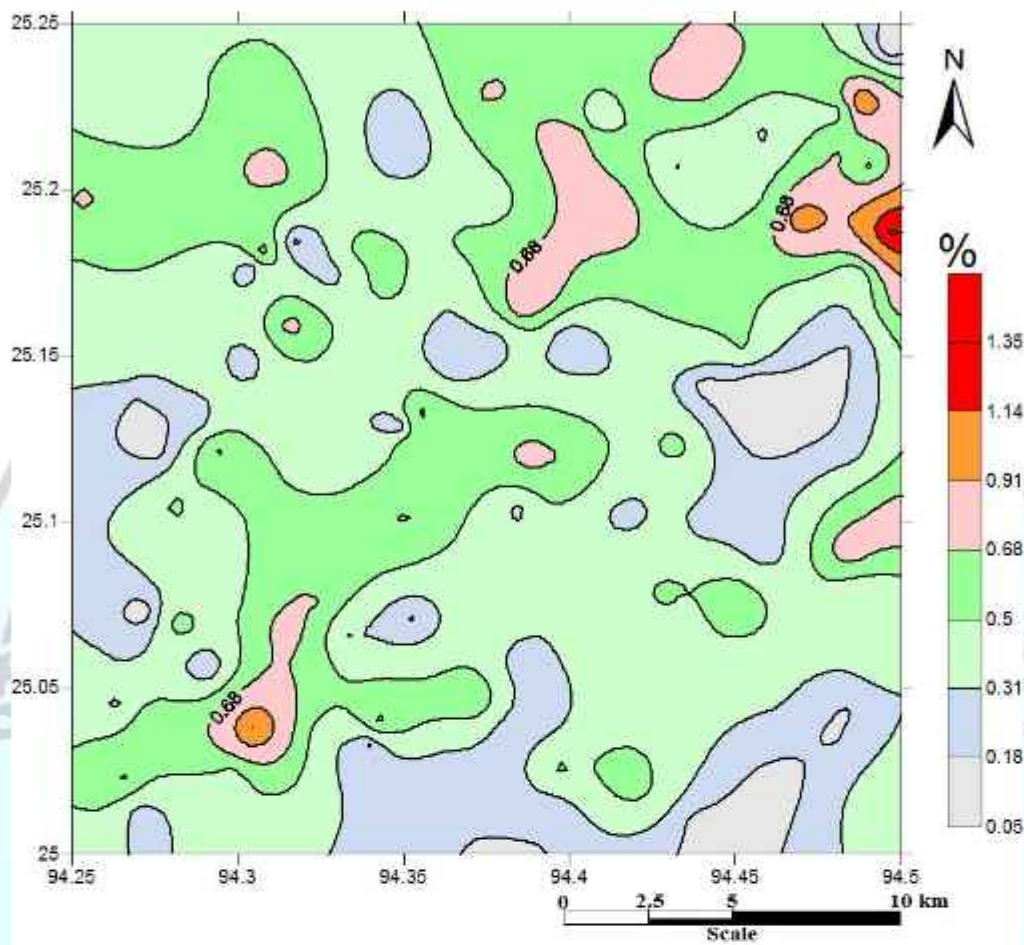
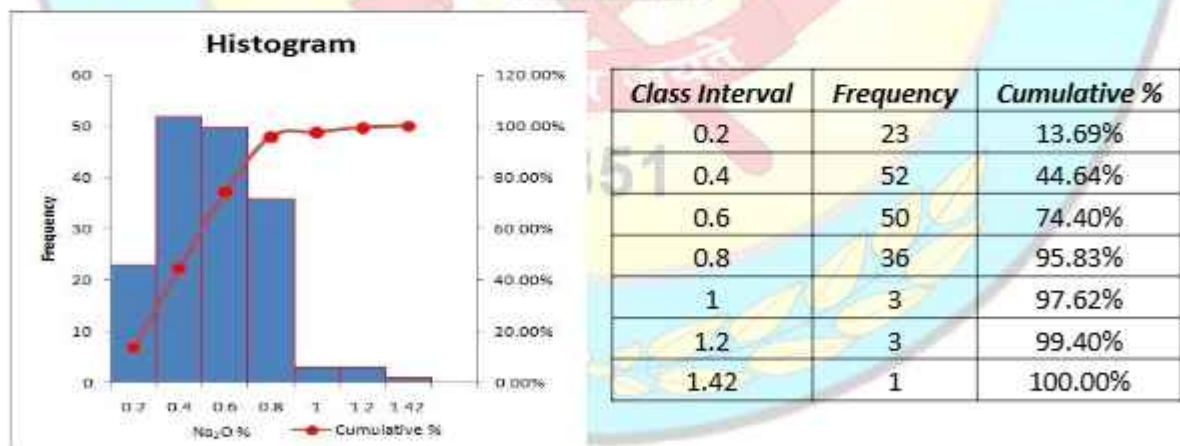


Fig. 5.7a. Spatial distribution of Na_2O in the stream sediment/slope wash samples.



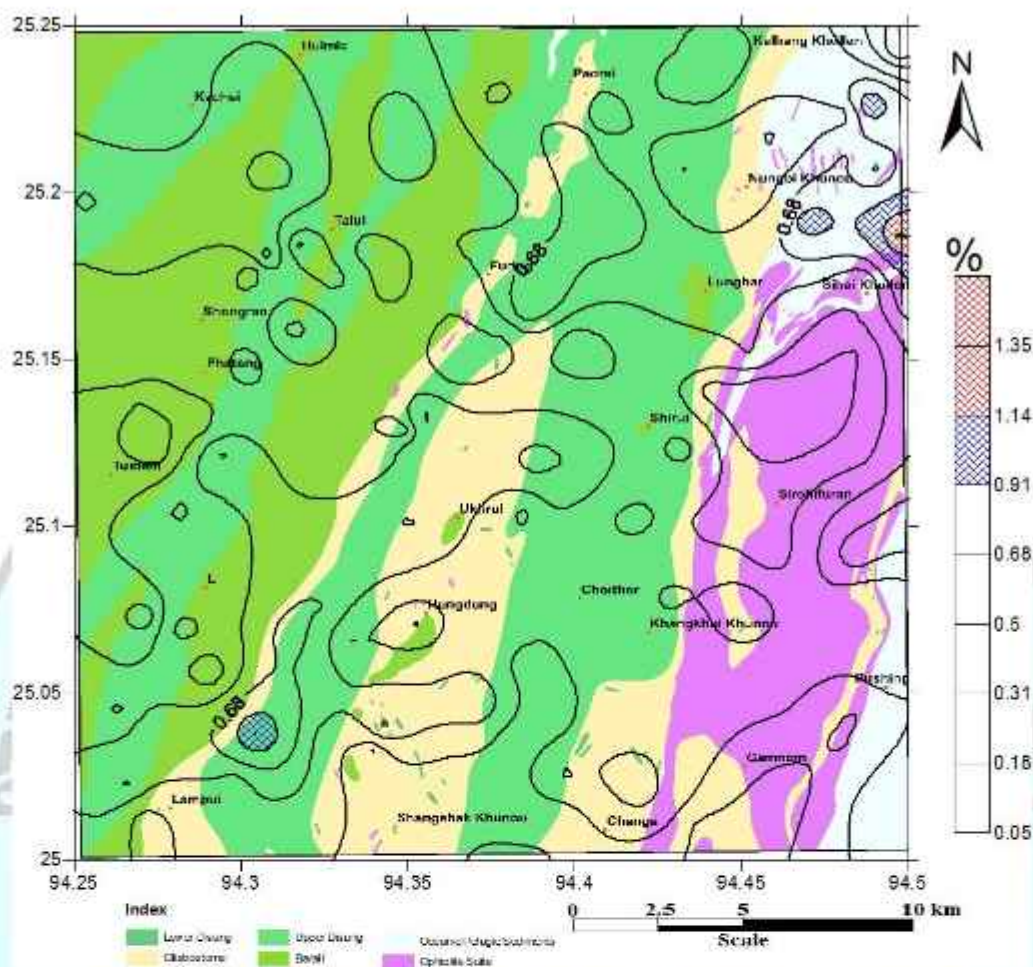


Fig. 5.7b. Spatial distribution of Na_2O in the stream sediment/slope wash samples overlaid on geology of the study area.

Na_2O in stream sediment

The median value of Na_2O in stream sediments is 0.45% with values varying from 0.07 to 1.42% (Annexure-I) showing maximum value in the south western corner of the study area, Grid No.43 of T.S. No. 83K/8 where rocks of Ocean Pelagic Sediments are exposed. The lower values of Na_2O are observed all along the geological terrain (Fig. 5.7a & b) and shows both positively skewed and kurtosis having values of 0.81 and 1.34 distribution is respectively.

The Na_2O is alkali metal and associated mainly with silicate mineral phases like feldspar in shale, siltstone and sandstone of Disang and Barail rock. In the Ophiolite rock Na_2O is associated with feldspar mineral phase in basalt, plagiogranite and gabbro. The lower values of Na_2O suggest that the Na_2O released by the weathering of feldspar mineral into clay is strongly depressed and dissolved in the water media and leached out of the

system. The positive correlation of Na_2O with other mobile elements like CaO , K_2O and Sr supports the same.

5.3.8. Potassium (K):

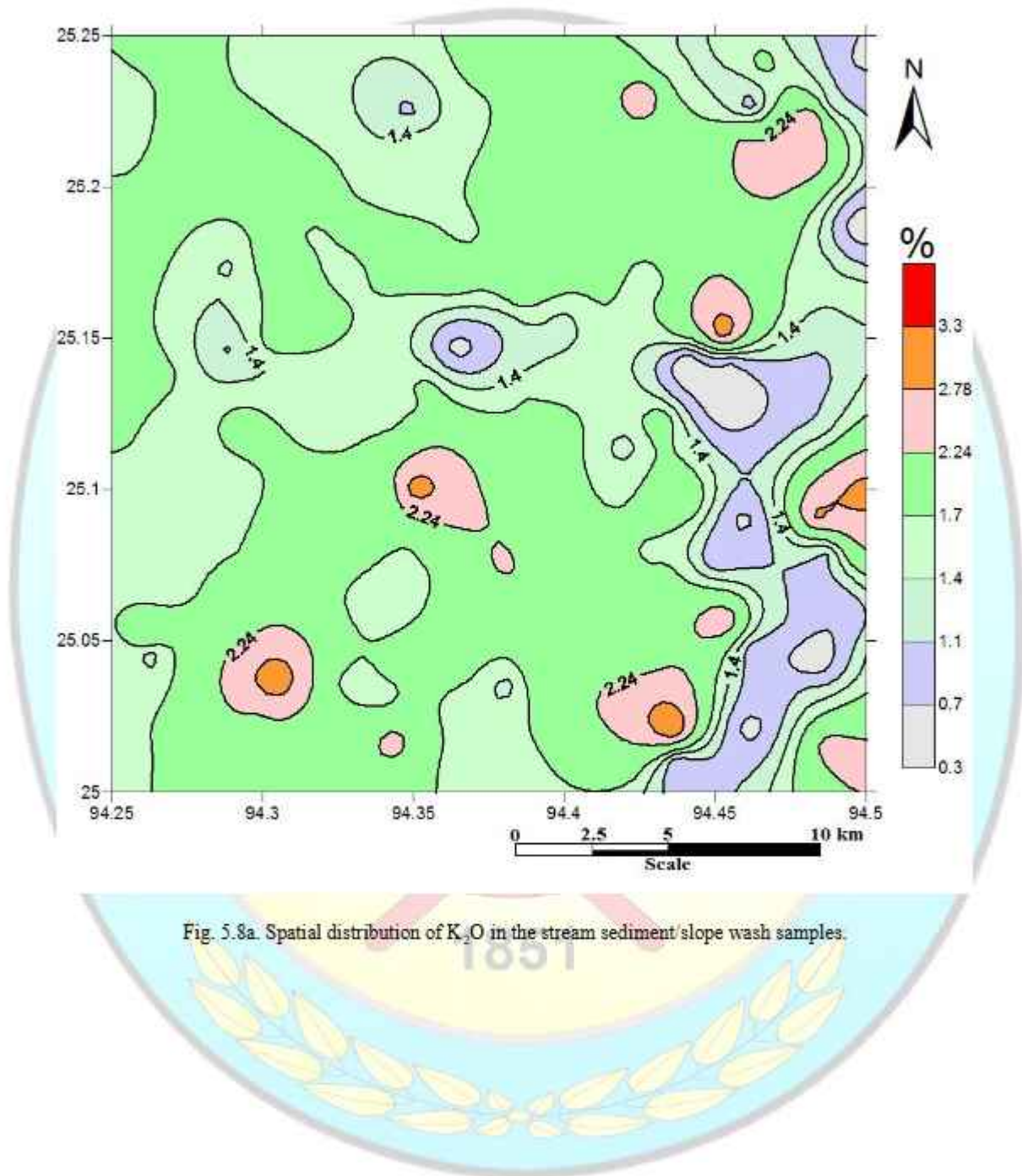


Fig. 5.8a. Spatial distribution of K_2O in the stream sediment/slope wash samples.

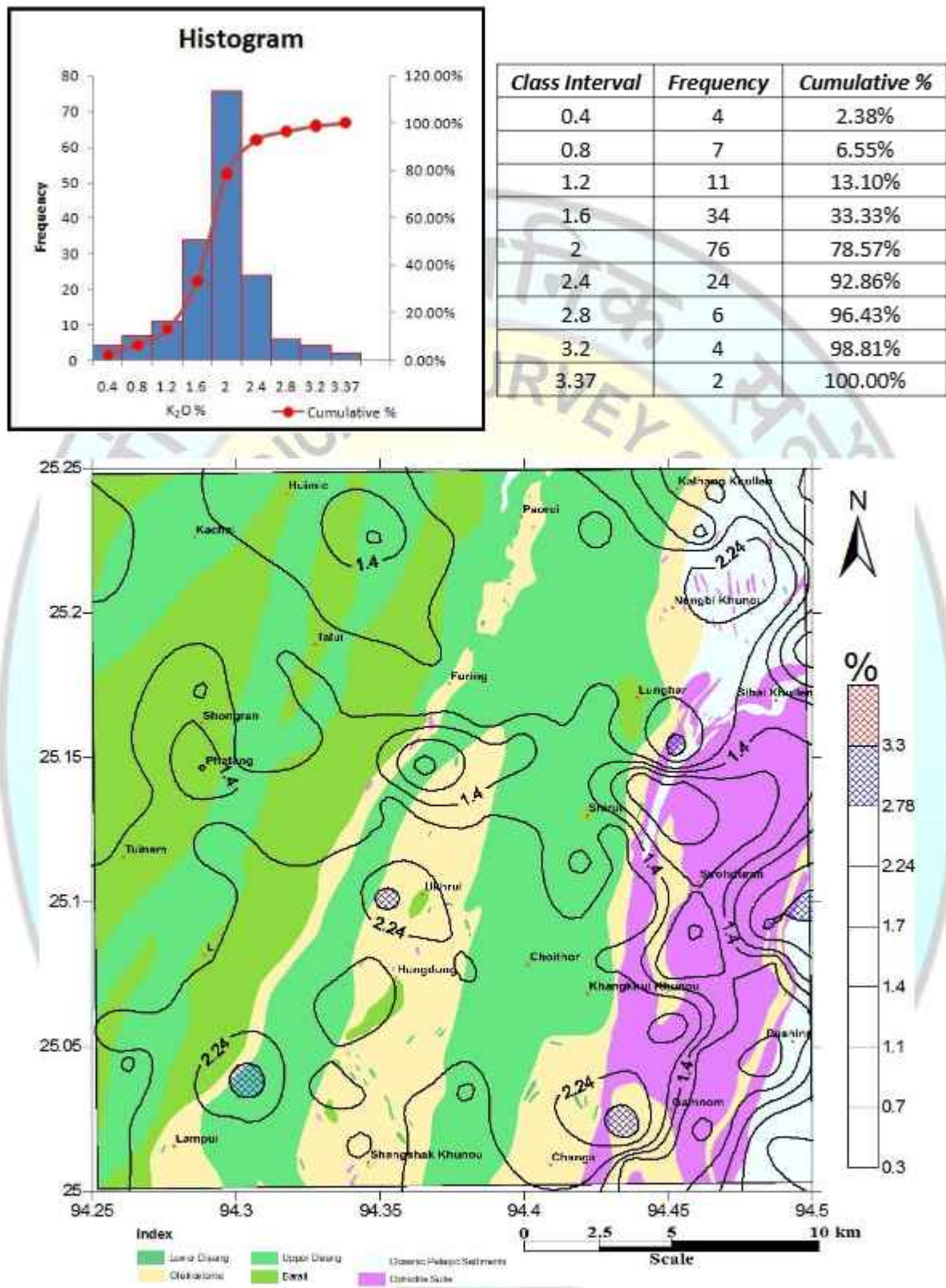


Fig. 5.8b. Spatial distribution of K₂O in the stream sediment/slope wash samples overlaid on geology of the study area.

K₂O in stream sediment

The median value of K₂O in stream sediments is 1.77% with values varying 0.18 to 3.37% (Annexure-I) showing maximum value in the south eastern corner of the study area, Grid No.23 of T.S. No. 83K/8 where Olistostromal lithounit are exposed. The distribution is represented by a negative skewness of -0.12 and positive kurtosis of 1.74.

Potassium is very soluble and occurs as simple cation K⁺ over the entire stability field of natural water (Brookins 1988). But its mobility is limited by its incorporation into clay minerals, adsorption into surface of the clay minerals and organic matter, and consumption by growing plants and thus does not get flushed out of the provenance. Hence, K₂O content in stream sediments is inversely proportional with grain size; SiO₂ decreases and K₂O increases in fine grained samples. K₂O shows positive correlation with Al₂O₃, SiO₂, TiO₂ and Sr.

5.3.9. Titanium (Ti):

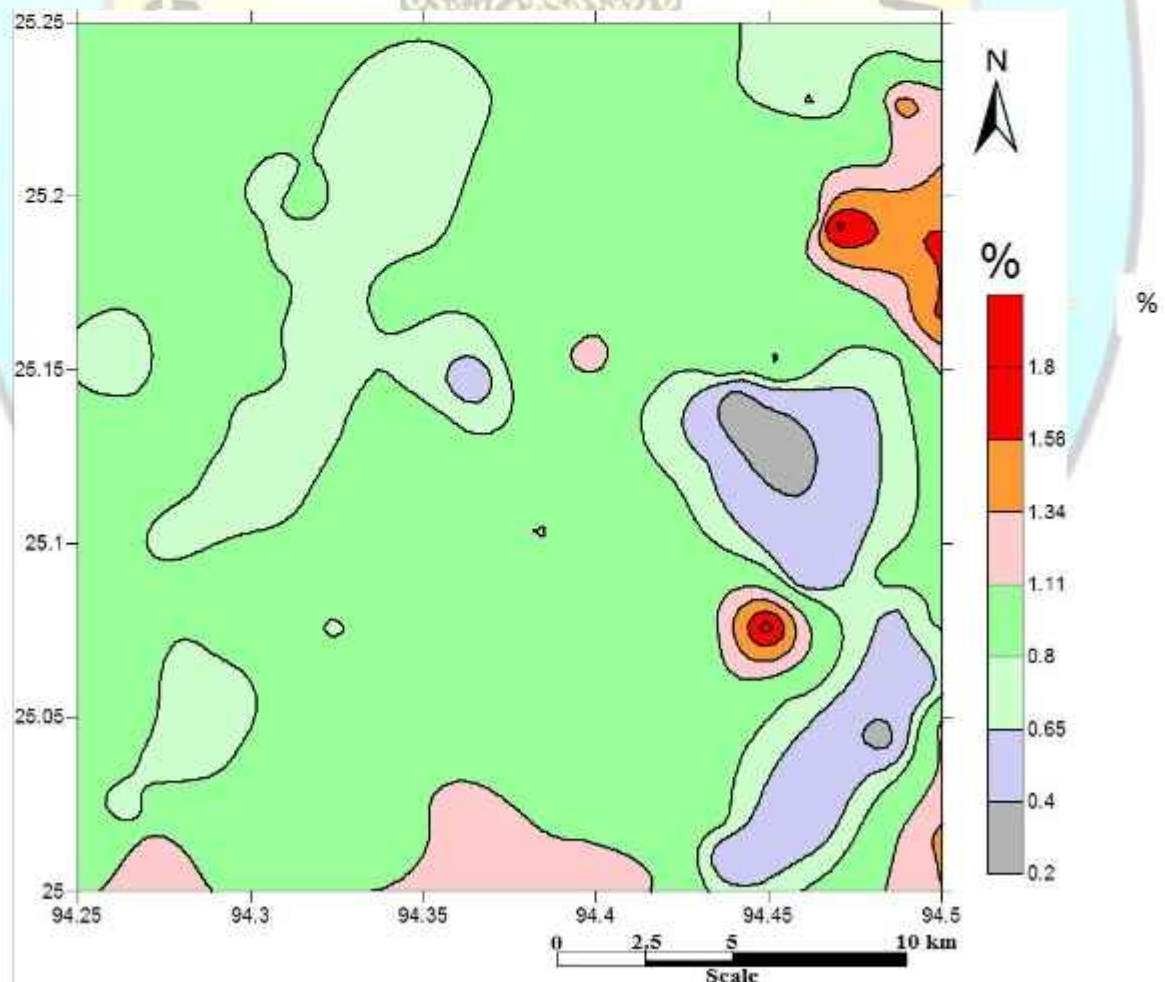


Fig. 5.9a. Spatial distribution of TiO_2 in the stream sediment/slope wash samples

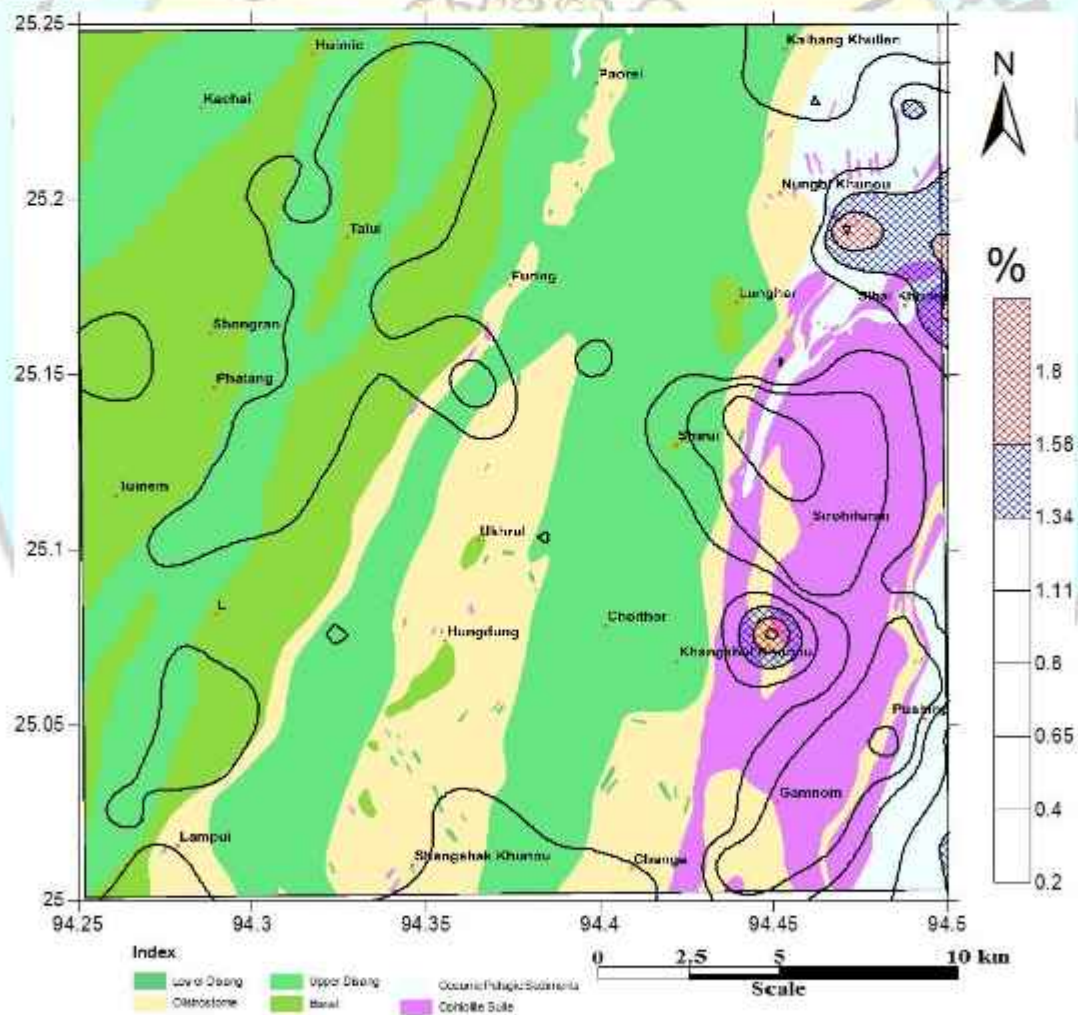
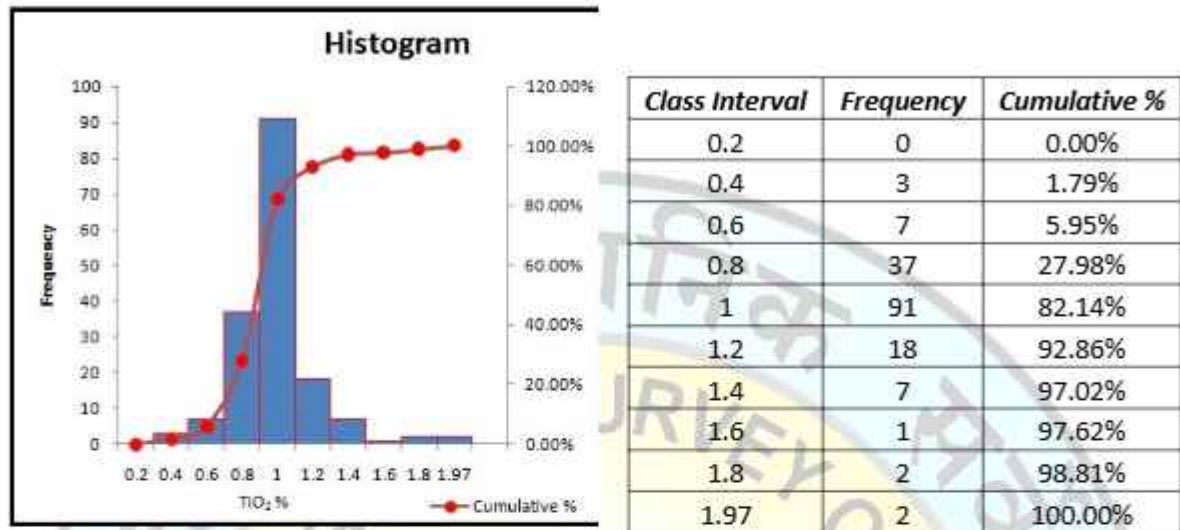


Fig. 5.9b. Spatial distribution of TiO_2 in the stream sediment/slope wash samples overlaid on geology of the study area.

TiO₂ in stream sediment

The median value of TiO₂ in stream sediments is 0.87% with values varying from 0.22 to 1.97% (Annexure-I) showing maximum value in Grid No. 63 of 83K/ where the Ophiolite suite of rocks are exposed. The distribution of TiO₂ is almost uniform throughout the area (Fig.5.9a & b). The stream sediments show close to normal distribution with positive skewness value of 1.21 and positive kurtosis of 5.85 and doesn't show good positive/negative correlation with other oxides/elements. This may be due to the absent of may be due to absence of TiO₂ bearing mineral phases like rutile, which is commonly associated with felsic igneous rock and the study area in the eastern part is dominated by the mafic/ultramafic rocks of Ophiolite Belt.

5.3.10. Phosphorous (P):

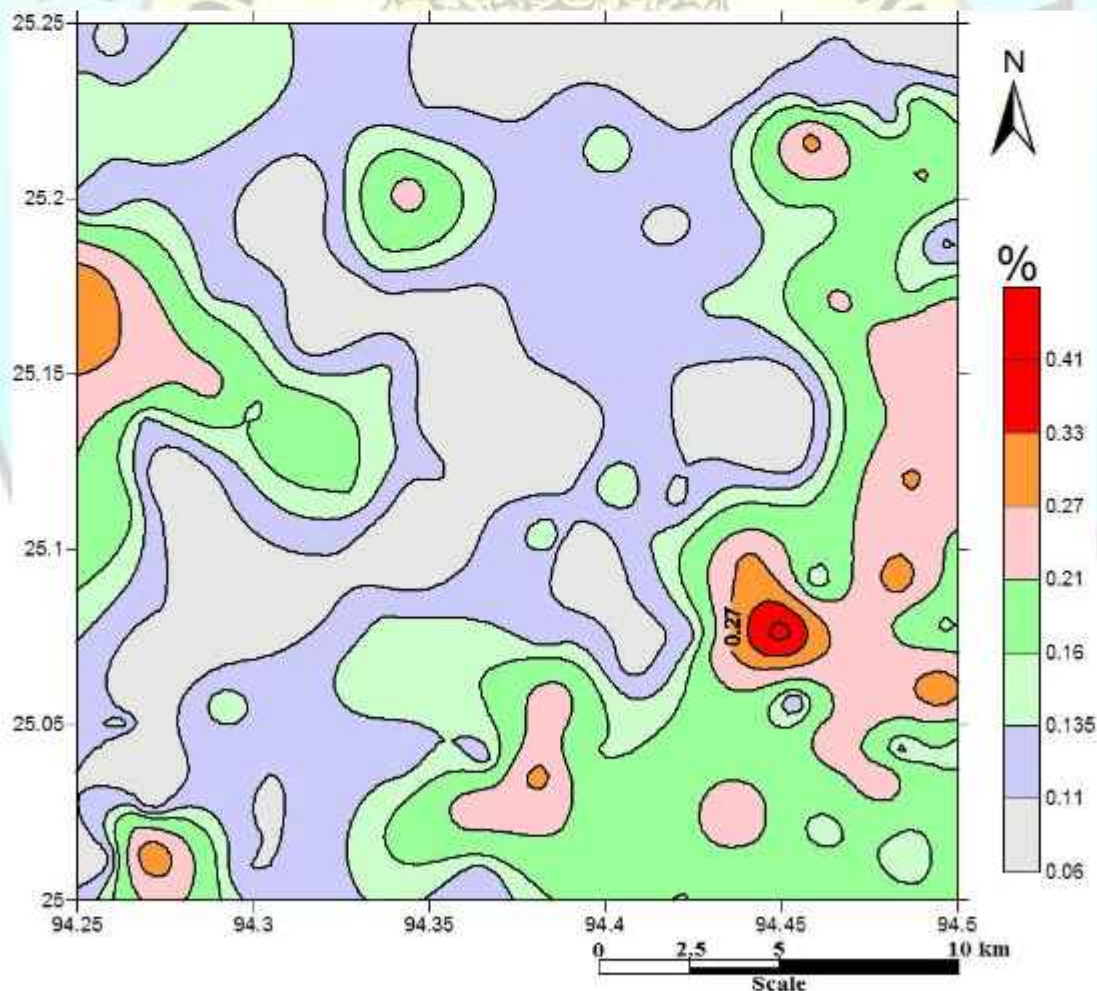


Fig. 5.10a. Spatial distribution of P₂O₅ in the stream sediment/slope wash samples.

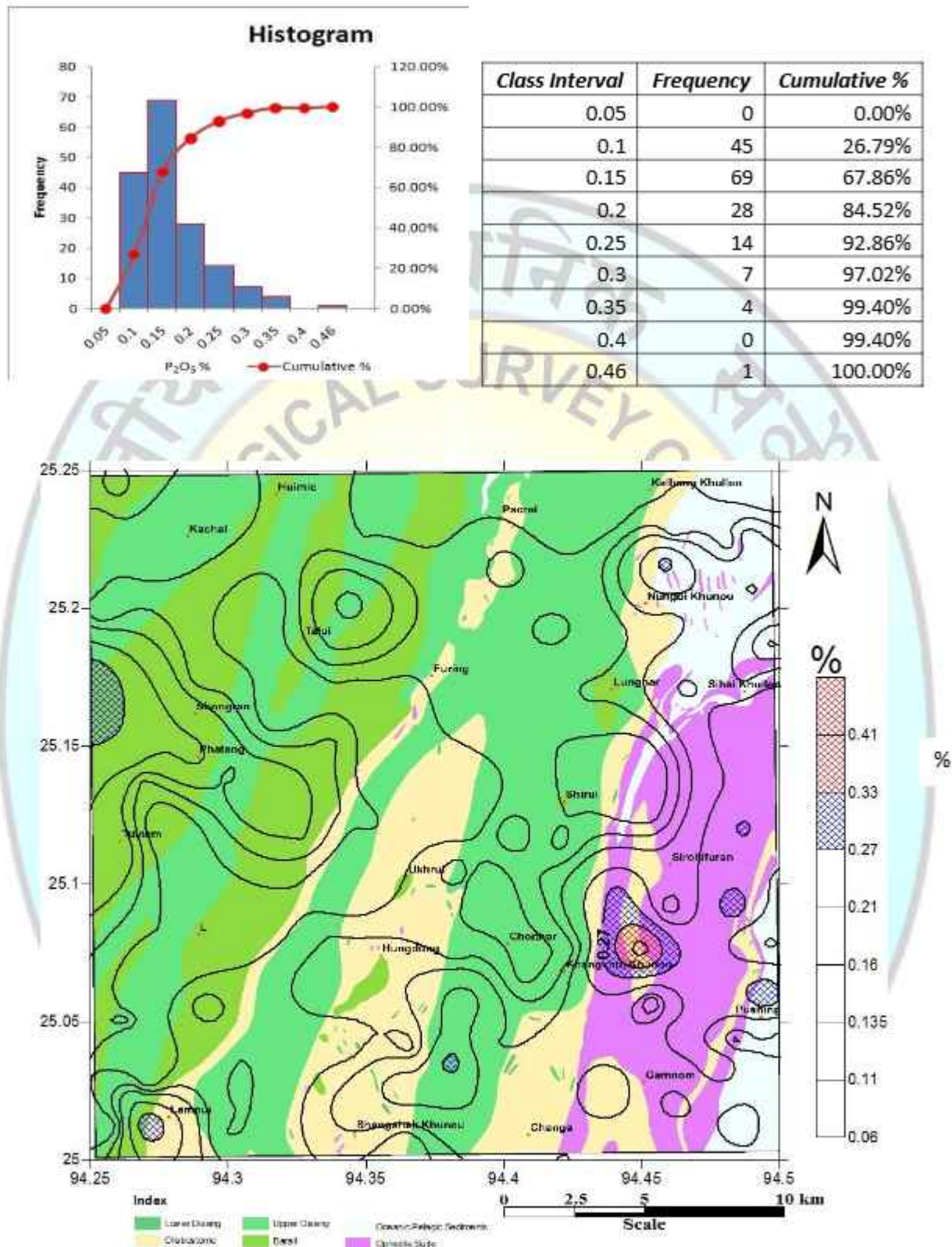


Fig. 5.10b. Spatial distribution of P_2O_5 in the stream sediment/slope wash samples overlaid on geology of the study area

P₂O₅ in stream sediment

The median value of P₂O₅ in stream sediments is 0.13% with values varying from 0.06 to 0.46% (Annexure-I) showing maximum values in the south eastern part of the study area, Grid No. 63 of T.S. No. 83K/8 where the Ophiolite rocks are exposed. The distribution is positively skewed with a value of 1.71 and positively kurtosis of 3.78. The overall P₂O₅ values are low in the area (Fig. 5.10a & b). Slightly higher values are observed in hilly areas, where terrace agriculture farming is practice by the locals. The positive correlation with MnO, Fe₂O₃, TiO₂ and CaO not much geogenic control. The slightly high values of P₂O₅ may be due to anthropogenic factor of using fertilizer in the agriculture farm.

5.4. Distribution of Trace Elements in the Stream Sediments

The trace element plays a vital role in understanding the petrogenesis of igneous, metamorphic and sedimentary rocks. The 22 trace elements (Ba, Co, Cr, Cu, Ga, Nb, Ni, Pb, Rb, Sc, Sr, Th, V, Y, Zn, Zr, Sn, Hf, Ta, Ge, Be and U) were analysed in the present study. The trace elements like Y, Th, Zr, Nb, Ti and Sc are most suited trace elements for provenance and tectonic setting because of their relatively low mobility during sedimentary processes and low residence time in sea water (Holland., 1978). In general the incompatible trace elements like K, Rb, Sr, Ba, Zr and Th are more concentrated in the sediments represented by the Paleogene Disang and Ocean Pelagic Sediments. The trace elements like Ni, Co and Cr are compatible with mantle phase minerals like olivine, pyroxene, spinel and garnet. The higher values of Ni, Co and Cr are observed from the eastern part of the study area where mafic/ultramafic rocks are well exposed. Cr being a trace element plays the major role in chromitite rock, which is well exposed in the Ophiolite Belt of the study area. The high amount of Cr and Ni are stongly dispersed into stream sediments derived from the mafic/ultramafic provenance.

5.4.1. Barium (Ba):

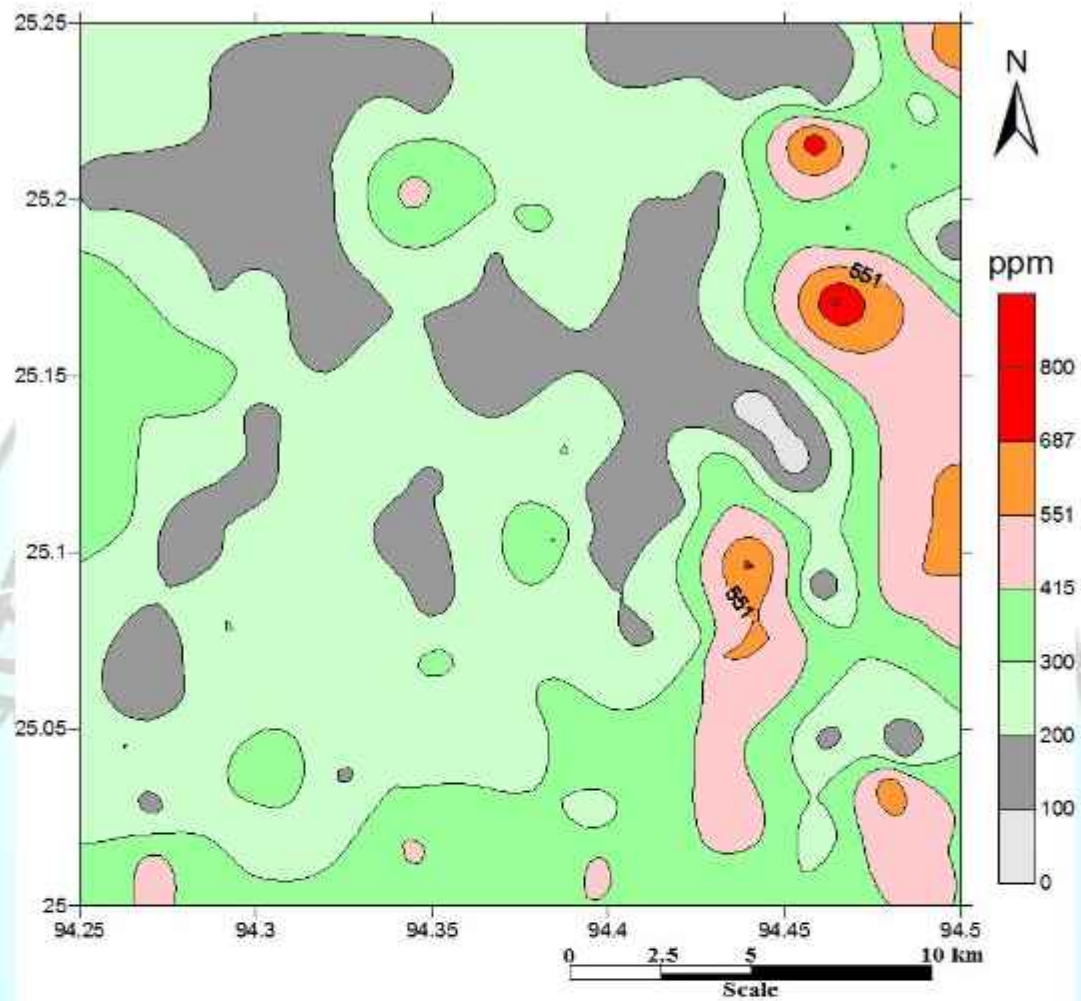
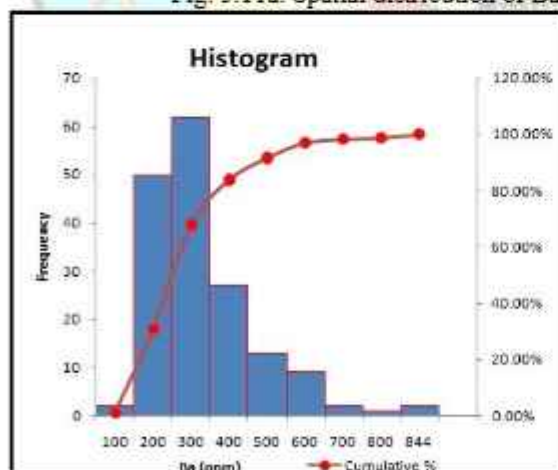


Fig. 5.11a. Spatial distribution of Ba in the stream sediment/slope wash samples.



Class Interval	Frequency	Cumulative %
100	2	1.19%
200	50	30.95%
300	62	67.86%
400	27	83.93%
500	13	91.67%
600	9	97.02%
700	2	98.21%
800	1	98.81%
844	2	100.00%

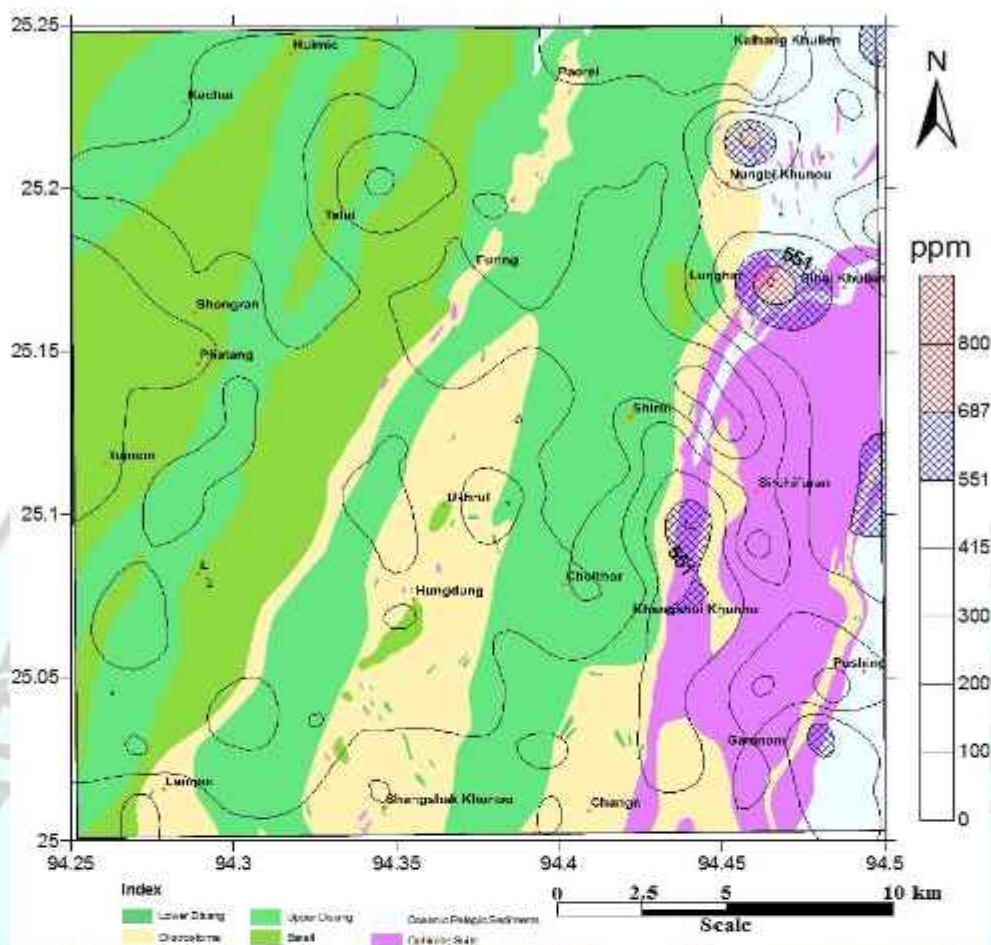


Fig. 5.11b. Spatial distribution of Ba in the stream sediment/slope wash samples overlaid on geology of the study area

Ba in stream sediment

The median value of Ba in stream sediments is 237ppm with values varying from 25 to 844ppm (Annexure-II) showing maximum value in the north eastern part of the study area, Grid No. 128 of T.S. No. 83K/8 where the exotic limestone blocks and thinly intercalated marl with volcanosedimentary facies of Ocean Pelagic Sediments (OPS) are exposed. The stream sediments show positive skewness and kurtosis with values of 1.52 and 3.03 respectively.

The distribution of Ba in the area is higher in the OPS but slightly lower in the Paleogene sediments (Fig. 5.11a & b). Ba has good positive correlation with most of the major oxides except SiO_2 , MgO and Na_2O . The higher values of Ba in the OPS and areas where exotic limestone blocks having caverns are exosed may be due to meteoric water leaching of some barite veins within limestone and marl and subsequently concentrated within the stream sediments.

5.4.2. Gallium (Ga):

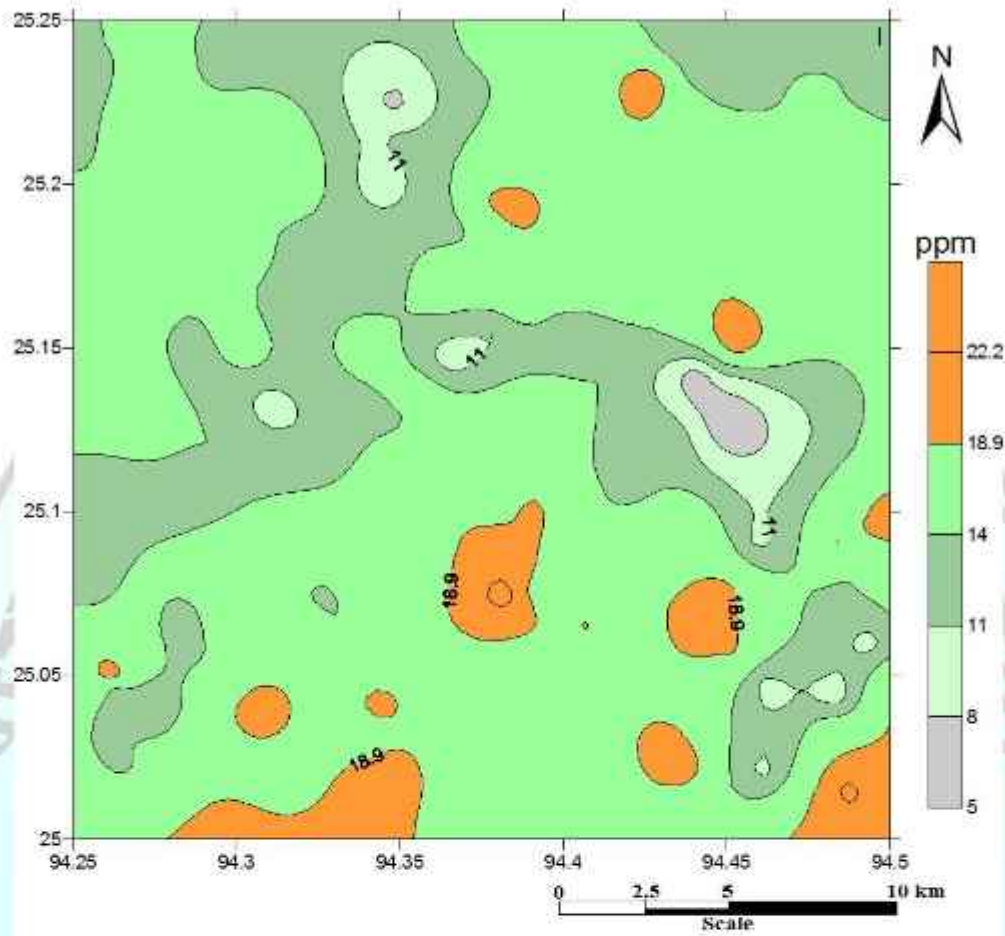
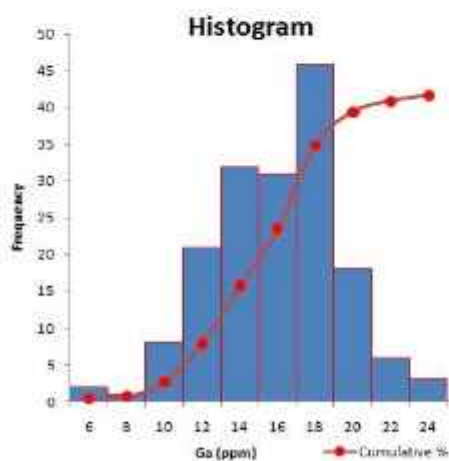


Fig. 5.12a. Spatial distribution of Ga in the stream sediment/slope wash samples.



Class Interval	Frequency	Cumulative %
6	2	1.19%
8	1	1.79%
10	8	6.55%
12	21	19.05%
14	32	38.10%
16	31	56.55%
18	46	83.93%
20	18	94.64%
22	6	98.21%
24	3	100.00%

5.4.3. Scandium (Sc):

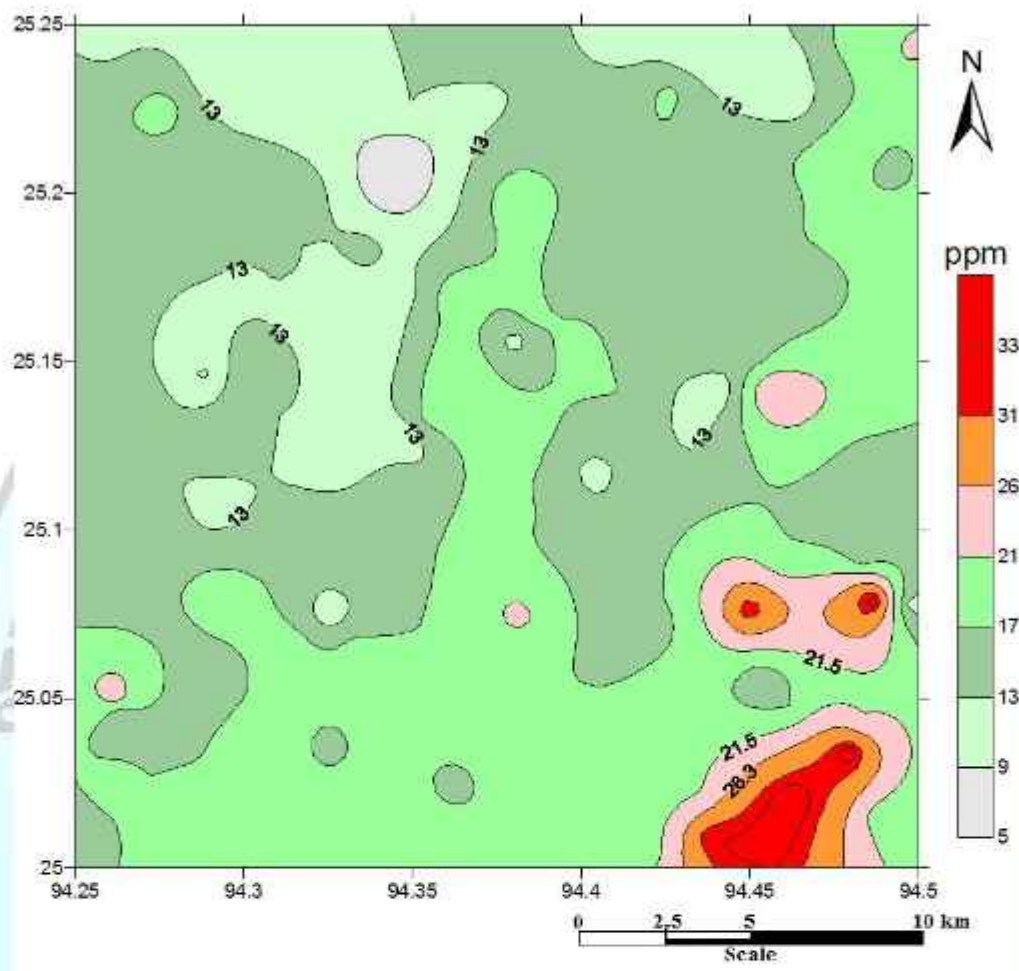
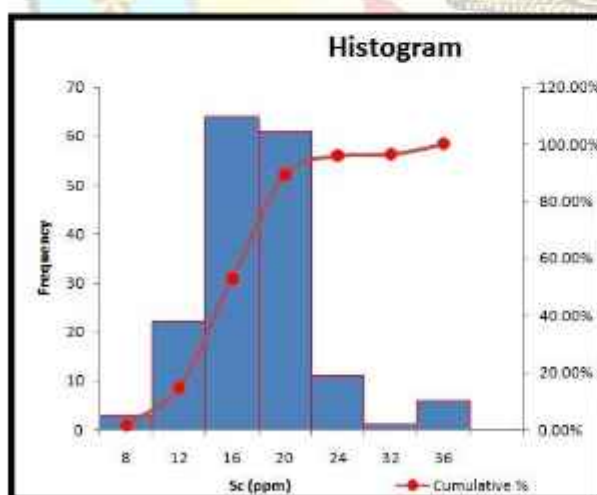


Fig. 5.13a. Spatial distribution of Sc in the stream sediment/slope wash samples



Class Interval	Frequency	Cumulative %
8	3	1.79%
12	22	14.88%
16	64	52.98%
20	61	89.29%
24	11	95.83%
32	1	96.43%
36	6	100.00%

5.4.4. Vanadium (V):

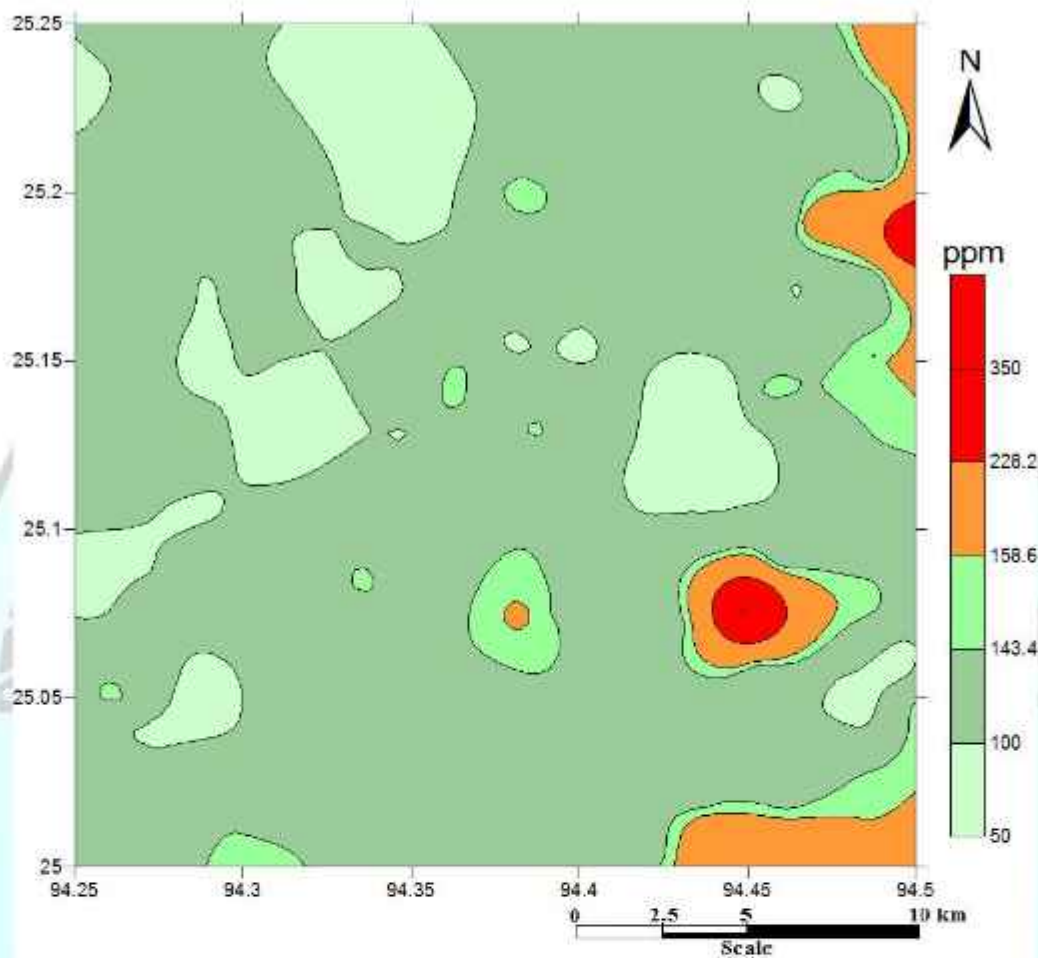
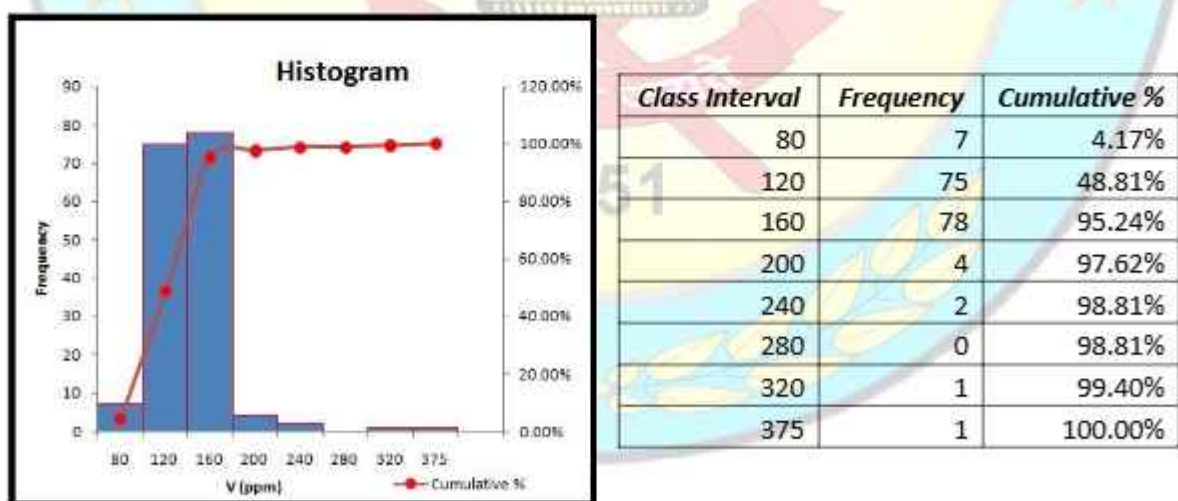


Fig.5.14a. Spatial distribution of V in the stream sediment/slope wash samples.



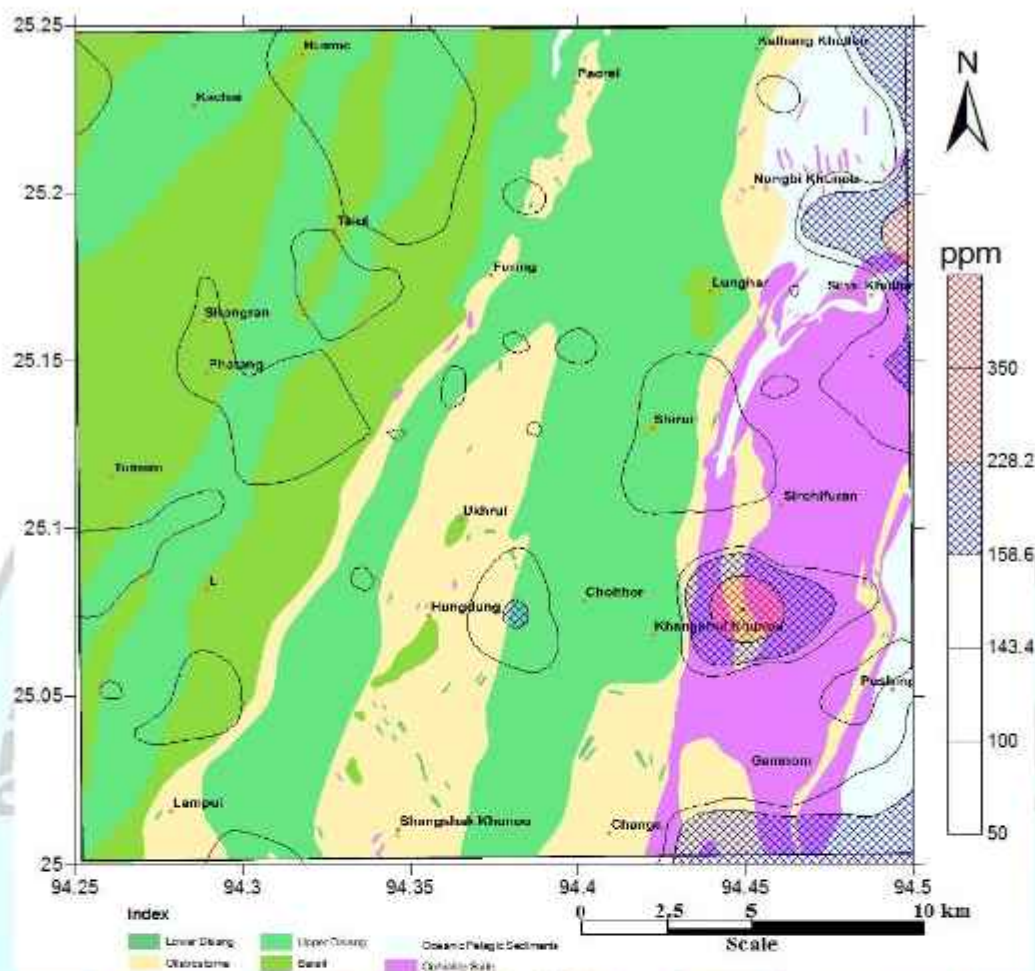


Fig.5.14b. Spatial distribution of V in the stream sediment/slope wash samples overlaid on geology of the study area.

V in stream sediment

Vanadium in stream sediments has a median value of 121.5 ppm with values varying from 54 to 375 ppm (Annexure-II) showing maximum value in the south eastern part of the study area, Grid No.63 of T.S. No. 83K/8 (Fig.5.14a & b) where cumulate peridotite host podiform massive ferric chromite. Petrographic studies of harzburgite rock shows chrome spinel and magnetite mineralisation within harzburgite. The V may be associated with mantle mineral phases like ferric chromite and magnetite and the subsequent serpentinisation and weathering of the rock may have contributed to the stream sediments.

5.4.5. Thorium (Th):

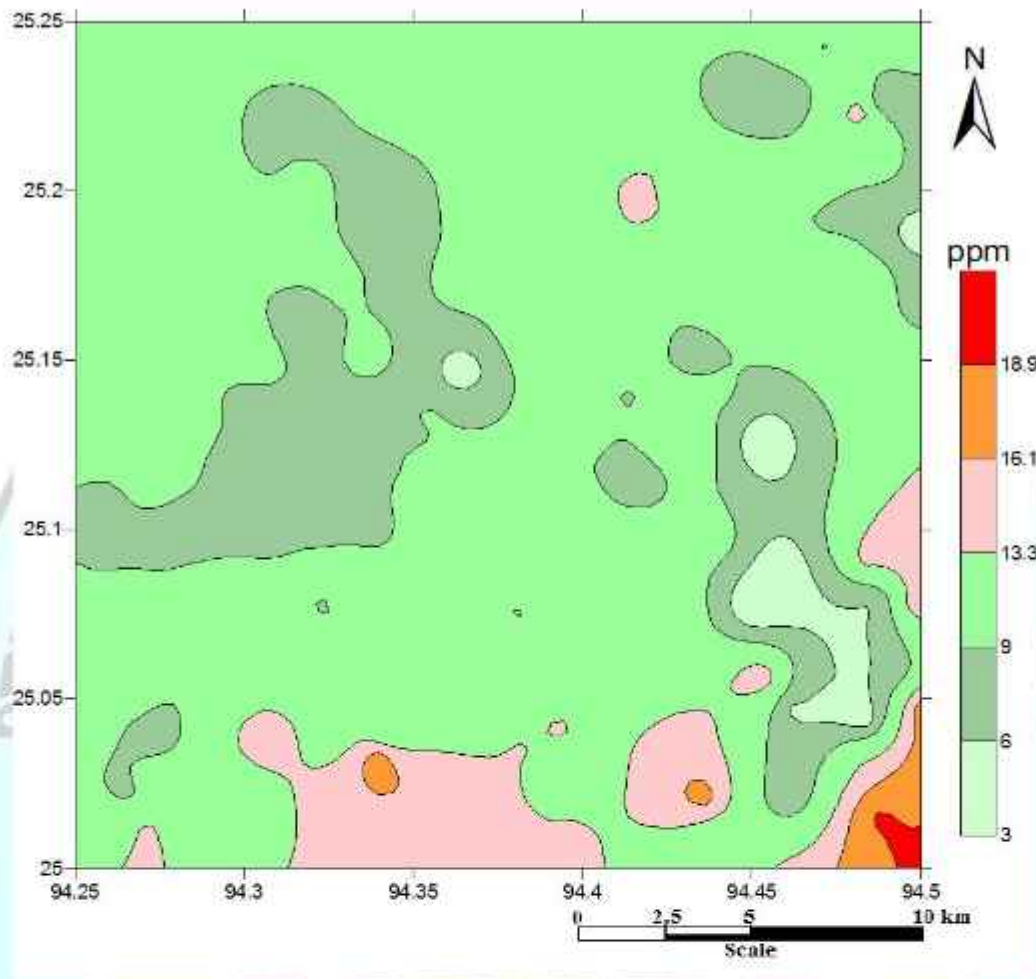
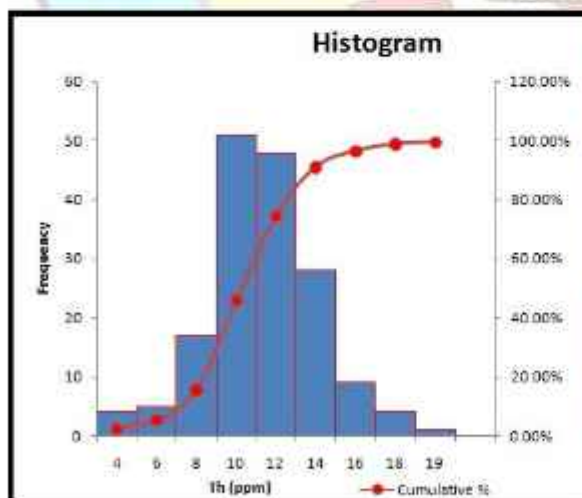


Fig.5.15a. Spatial distribution of Th in the stream sediment/slope wash samples.



Class Interval	Frequency	Cumulative %
4	4	2.38%
6	5	5.36%
8	17	15.48%
10	51	45.83%
12	48	74.40%
14	28	91.07%
16	9	96.43%
18	4	98.81%
19	1	99.40%

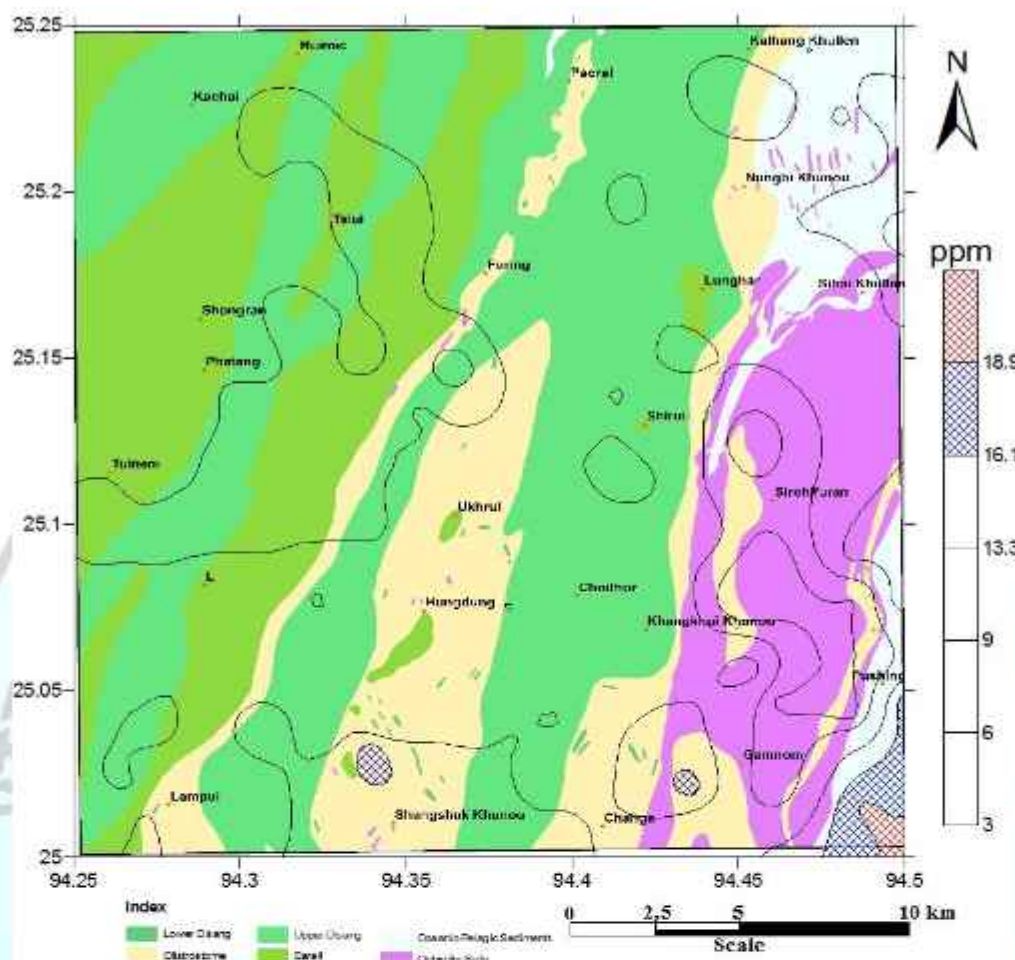


Fig.5.15b. Spatial distribution of Th in the stream sediment/slope wash samples overlaid on geology of the study area.

Th in stream sediment

The median value of Th in stream sediments is 10.14 ppm with values varying from 2.72 to 19.27 ppm (Annexure-II). The slightly high values are observed in Disang and OPS sediments, the maximum values in the south eastern part of the study area, Grid No. 12 of T.S. No. 83K/8 where OPS shale are well exposed (Fig. 5.15a & b). The distribution is positive skewed with a value of 0.27 and positive kurtosis of 0.94. Th being a robust relative immobile radioactive element and is mostly associated with fine grain sediments, which can have both proximal and distal provenance and shows good positive correlation with radioactive.

5.4.6. Lead (Pb):

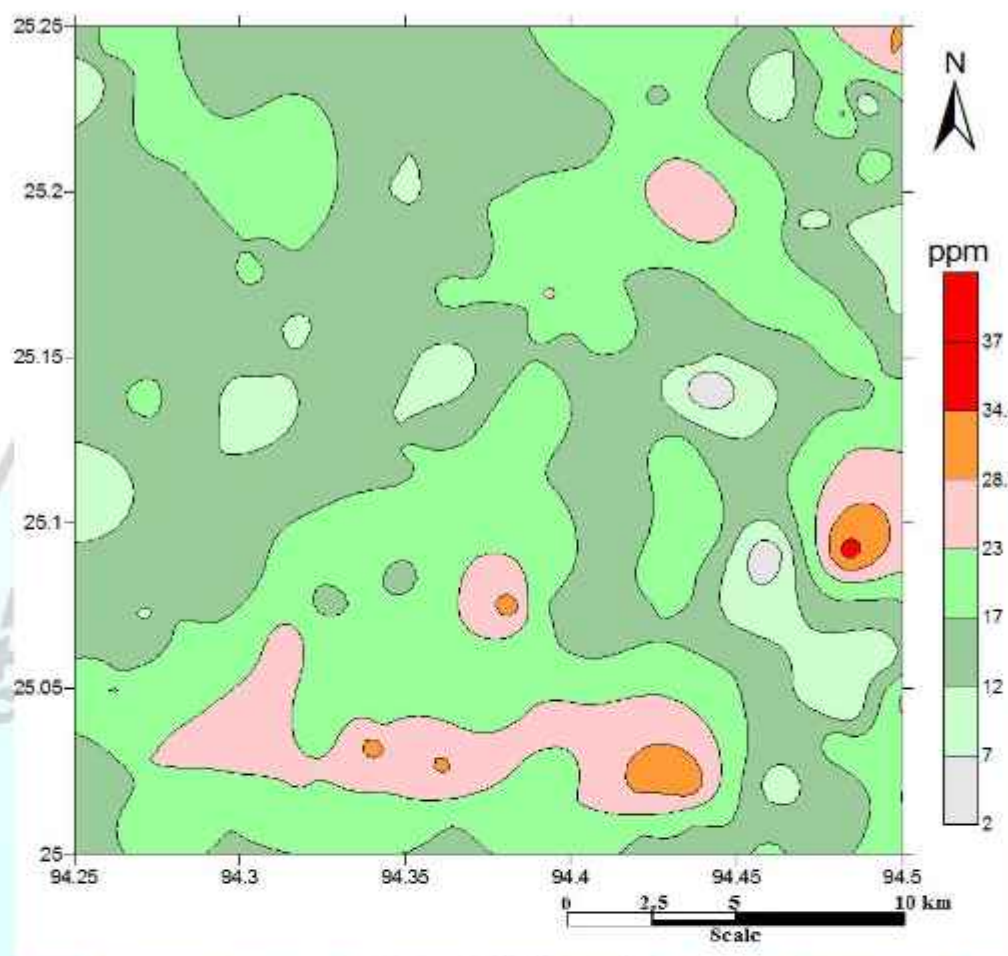
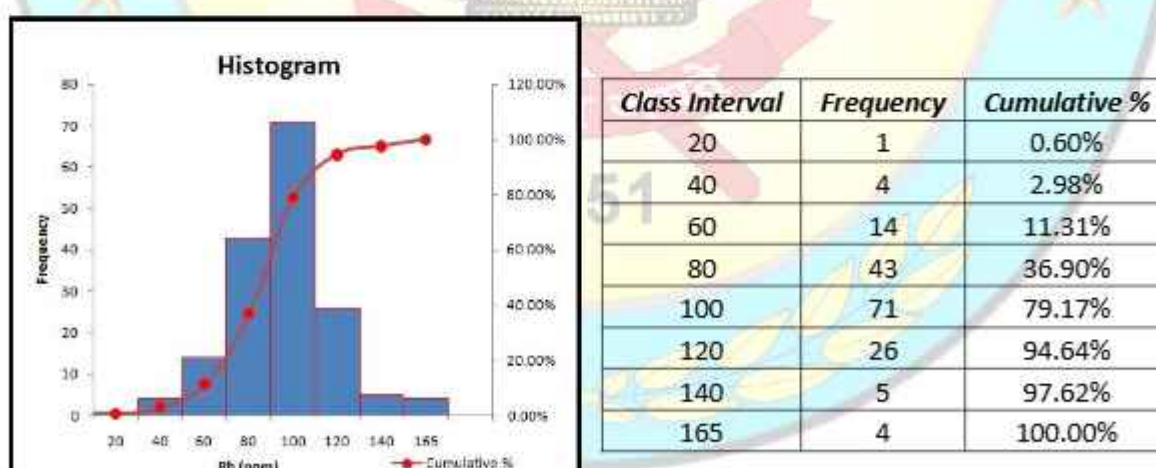


Fig.5.16a Spatial distribution of Pb in the stream sediment/slope wash samples.



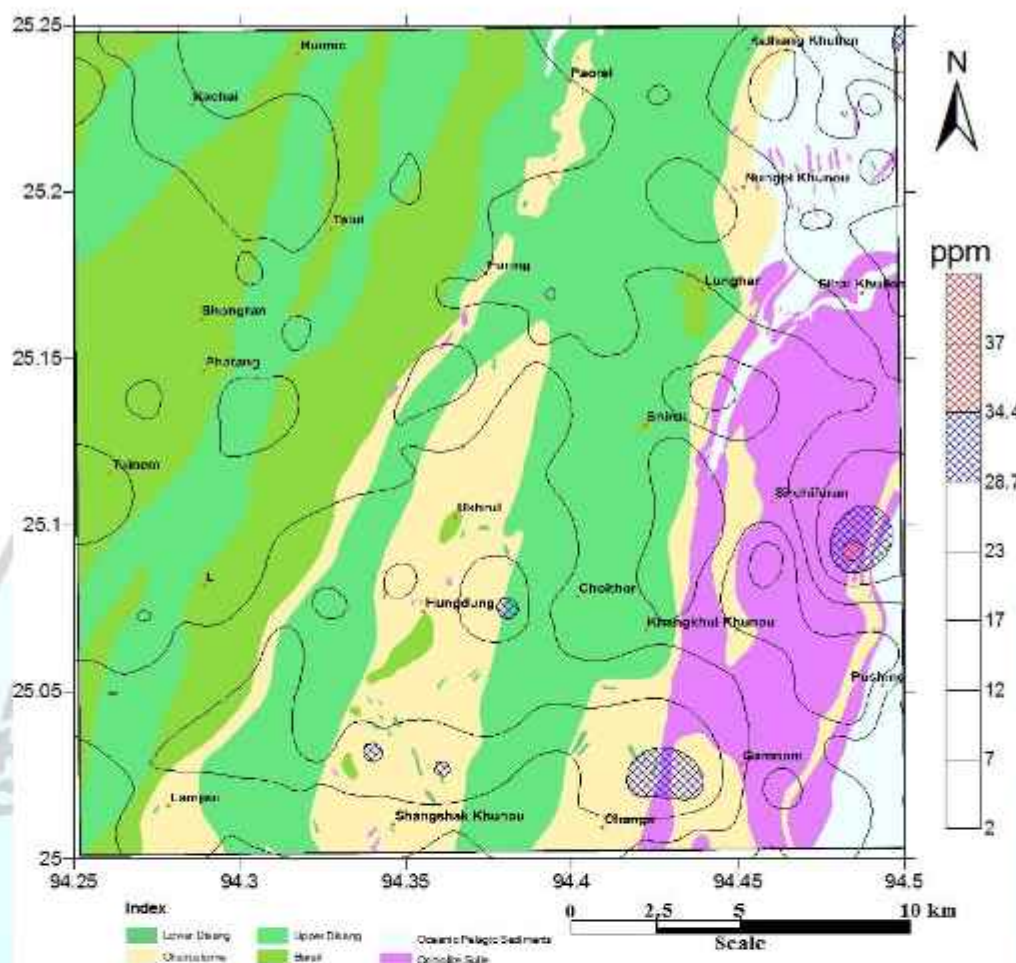


Fig.5.16b. Spatial distribution of Pb in the stream sediment/slope wash samples overlaid on geology of the study area.

Pb in stream sediment

The median value of Pb in stream sediments is 17 ppm with values varying from 2 to 38 ppm (Annexure-II). The higher values of Pb are observed where Ophiolite rocks are exposed. The higher values are observed in near tectonic contact zone between Ophiolite and OPS (mostly marl thinly interbedded with shale) with maximum value observed in Grid No.23 of T.S. No. 83K/8 (Fig.5.16a & b). The distribution is very near to normal distribution with positive skewness and kurtosis values of 5.68 and 53.80 respectively. The higher values of Pb may be due to the presence of some Pb bearing metamorphic mineral phases at the tectonic contact zone.

5.4.7. Nickel (Ni):

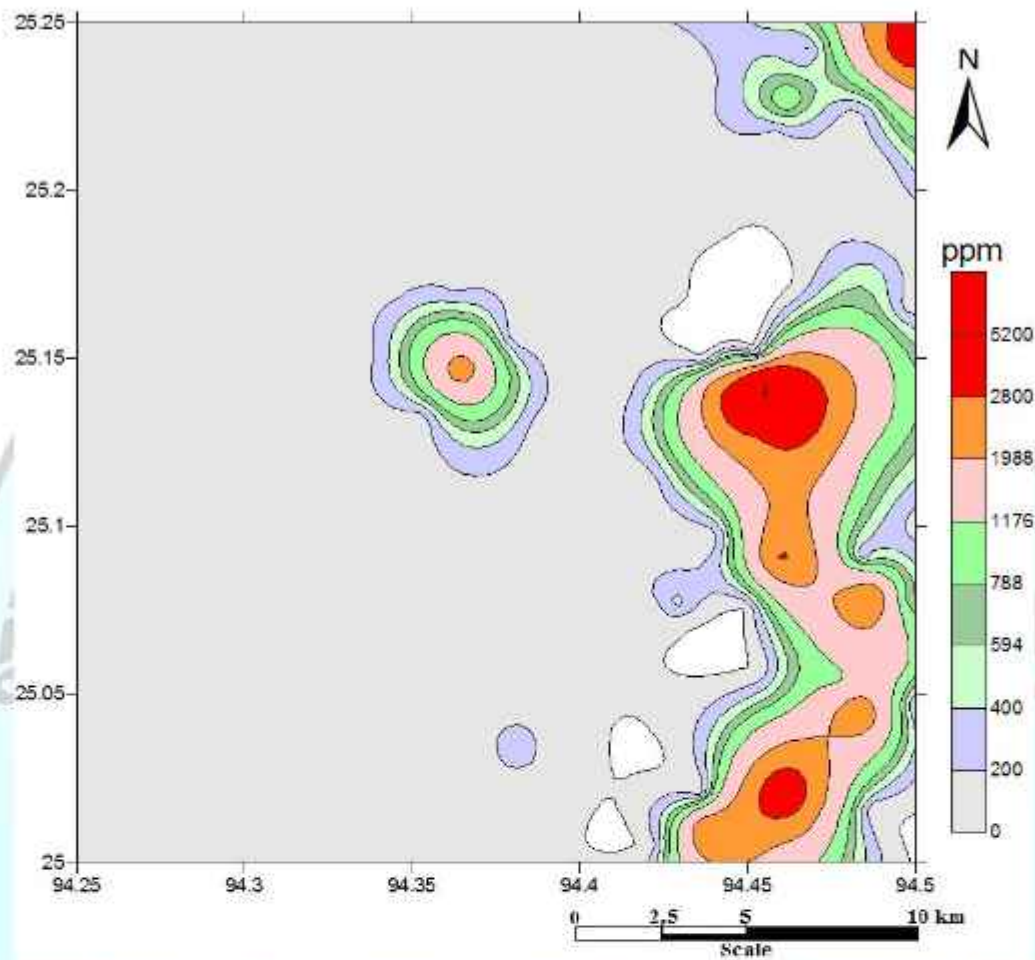
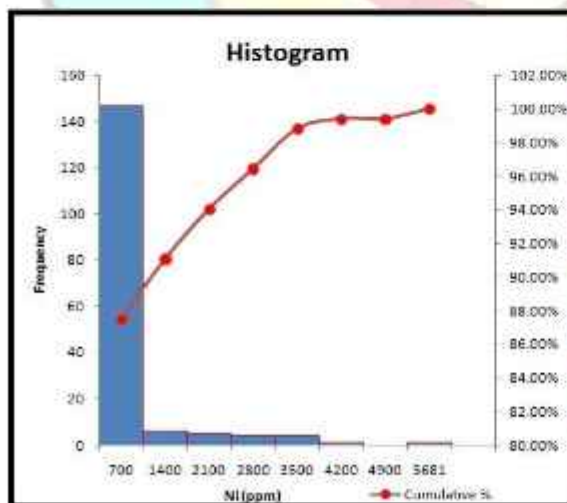


Fig.5.17a.Spatial distribution of Ni in the stream sediment/slope wash samples.



Class Interval	Frequency	Cumulative %
700	147	87.50%
1400	6	91.07%
2100	5	94.05%
2800	4	96.43%
3500	4	98.81%
4200	1	99.40%
4900	0	99.40%
5681	1	100.00%

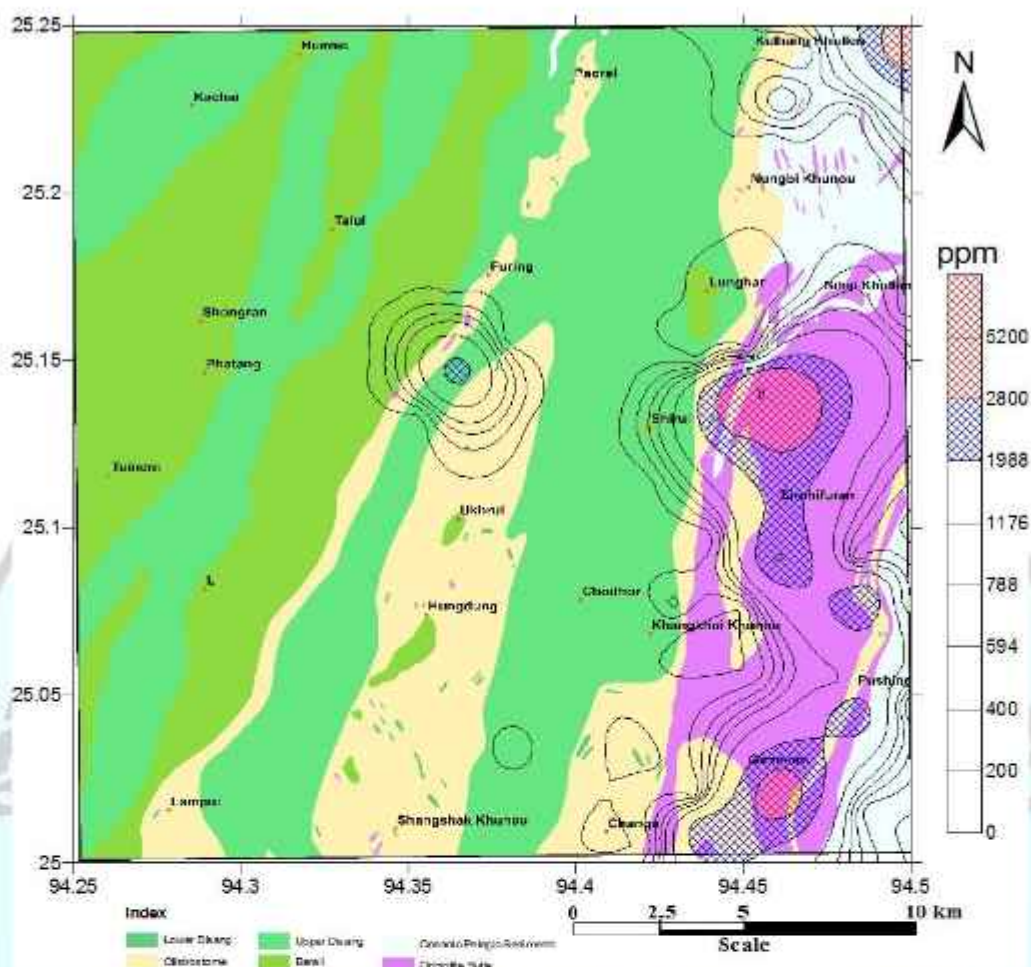


Fig.5.17b. Spatial distribution of Ni in the stream sediment/slope wash samples overlaid on geology of the study area.

Ni in stream sediment

The median value of Ni in stream sediments is 96.5ppm with values varying from 17 to 5681 ppm (Annexure-II) showing maximum value in the eastern part of the study, where the mafic/ultramafic rock hosting podiform chromite are well exposed. The maximum value is observed in Grid No. 102 of T.S. No. 83K/8, where, varying thickness of lateritic soil capping is above the mafic/ultramafic rock (Fig.5.17a & b). The distribution is positively skewed and kurtosis with values of 3.65 and 15.08 respectively.

Ni shows strong positive correlations with Fe_2O_3 , MgO , Cr and Co, which may be due to the presence of Ni bearing mineral phases within the lateritic soil profile are mainly goethite, garnierite and ulmannite. The high Ni values in the eastern part of the study area can be accounted due to the weathering of the lateritic soil (duricrust, plasmic and saprolite soil) that has contributed Ni in the stream sediments.

5.4.8. Cobalt (Co):

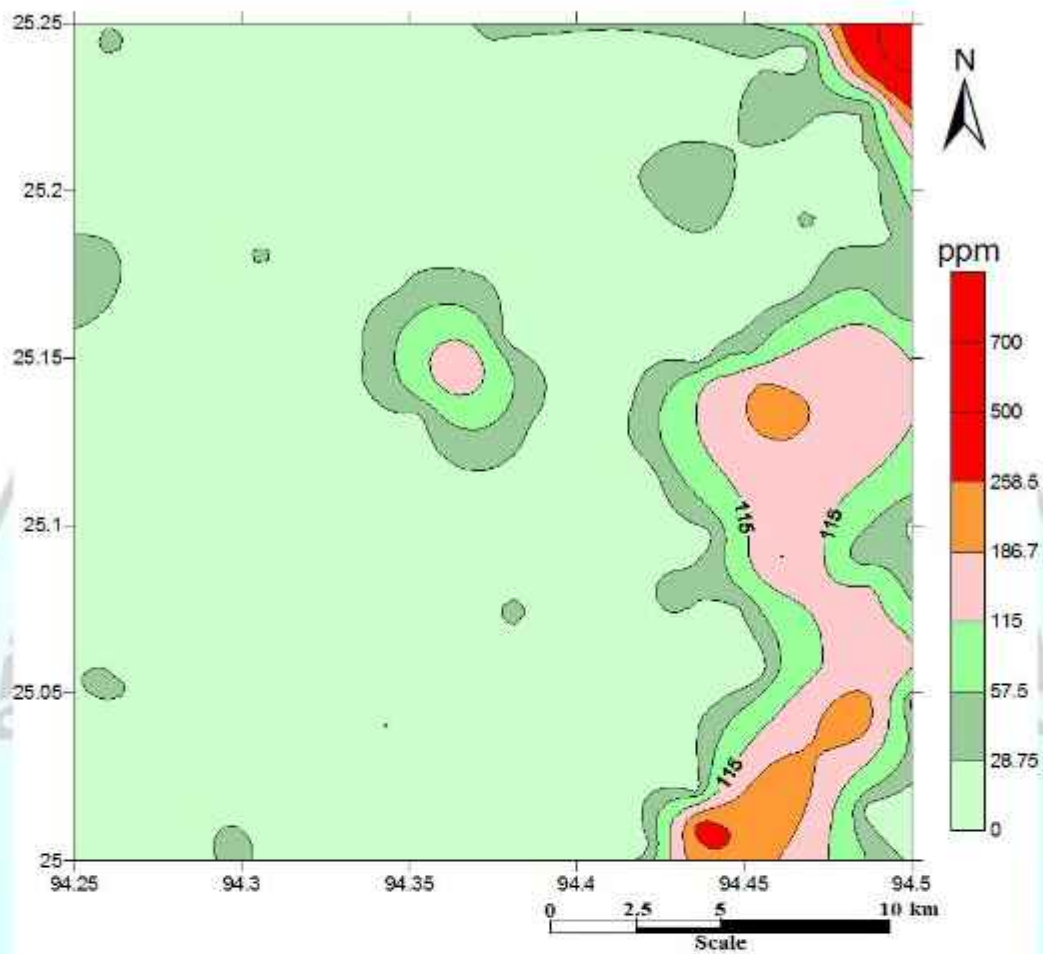
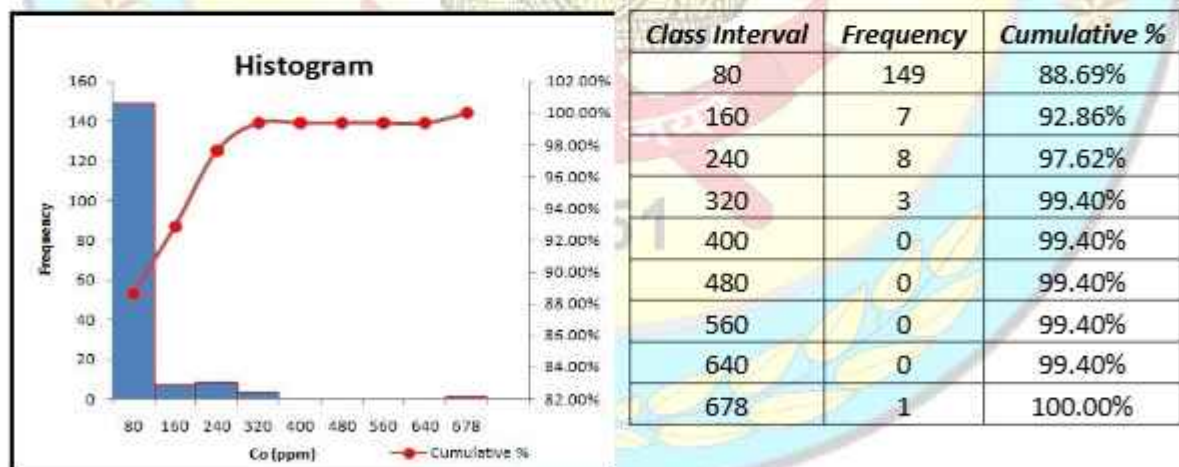


Fig.5.18a. Spatial distribution of Co in the stream sediment/slope wash samples



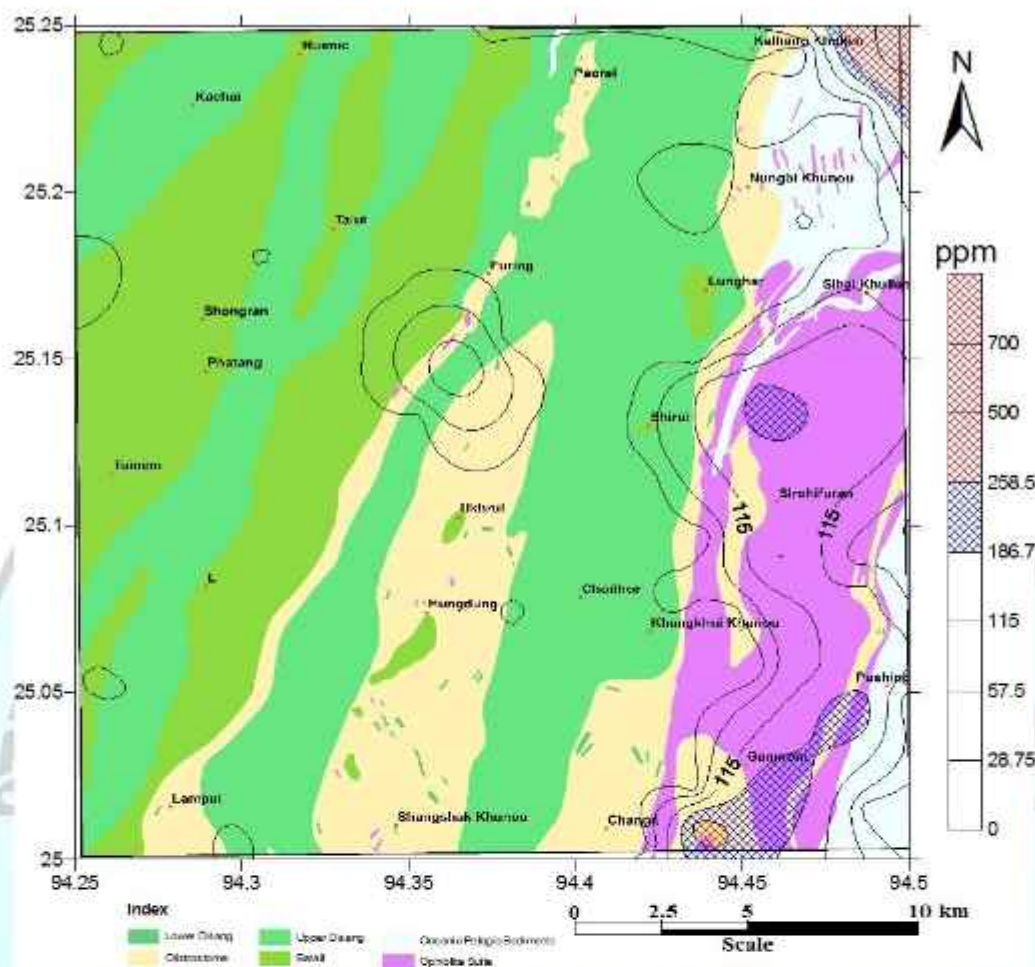


Fig.5.18b. Spatial distribution of Co in the stream sediment/slope wash samples overlaid on geology of the study area

Co in stream sediment

The median value of Co in stream sediment is 23 ppm with values varying from 2 to 678 ppm (Annexure-II) showing maximum value in Grid No. 182 of T.S. No. 83K/8 where Ophiolite suite of rocks are exposed. The stream sediments show very near to normal distribution with positive skewness of 5.26 and positive kurtosis of 37.99.

The distribution map shows a high concentration in the eastern part of the area, where the Ophiolite rocks are well exposed (Fig. 5.18a & b). However, relatively low Co concentration is noted within the Paleogene sediments. The Co from the stream sediments derived from the Ophiolite Belt in the eastern part shows very strong positive correlation with Fe_2O_3 , Ni and Cr, suggesting the association of Co in mineral phases like garnierite and cobaltite within the lateritic soil. The subsequent weathering may have contributed Co in the stream sediments.

5.4.9. Rubidium (Rb):

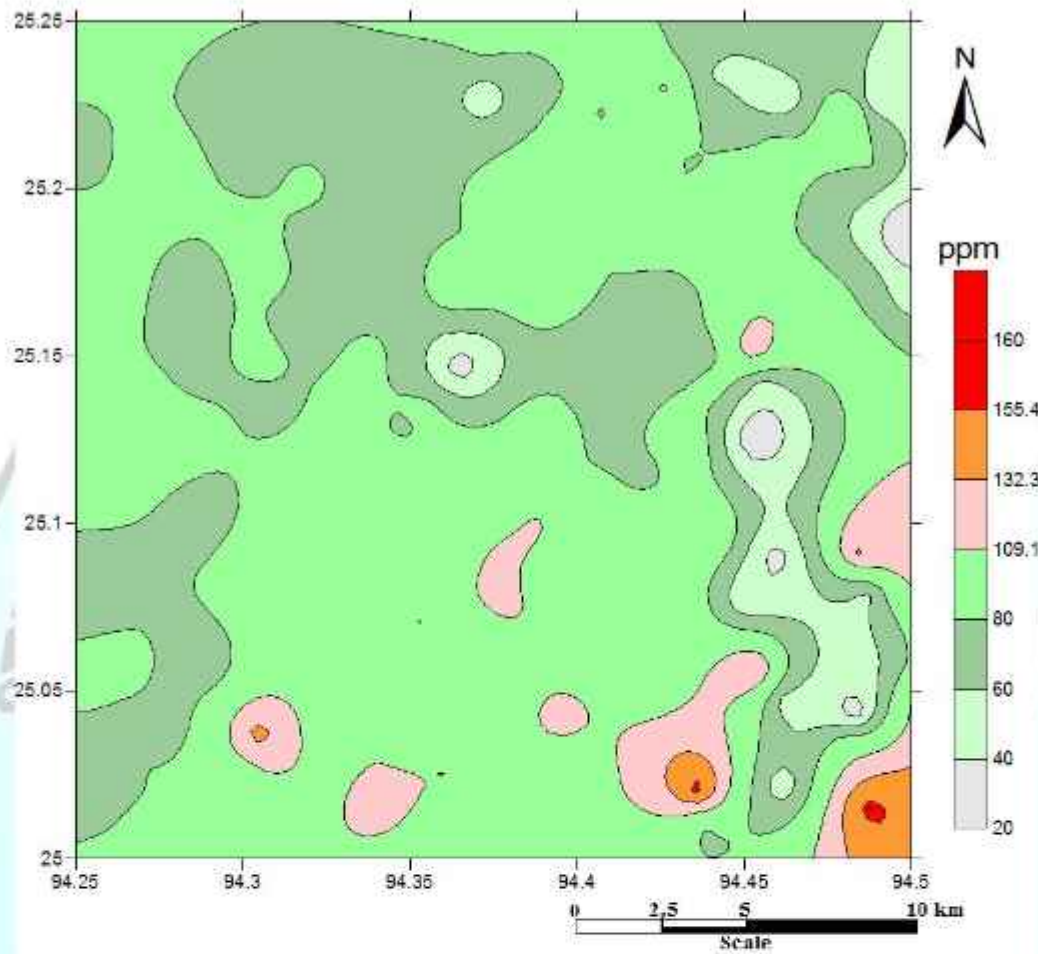
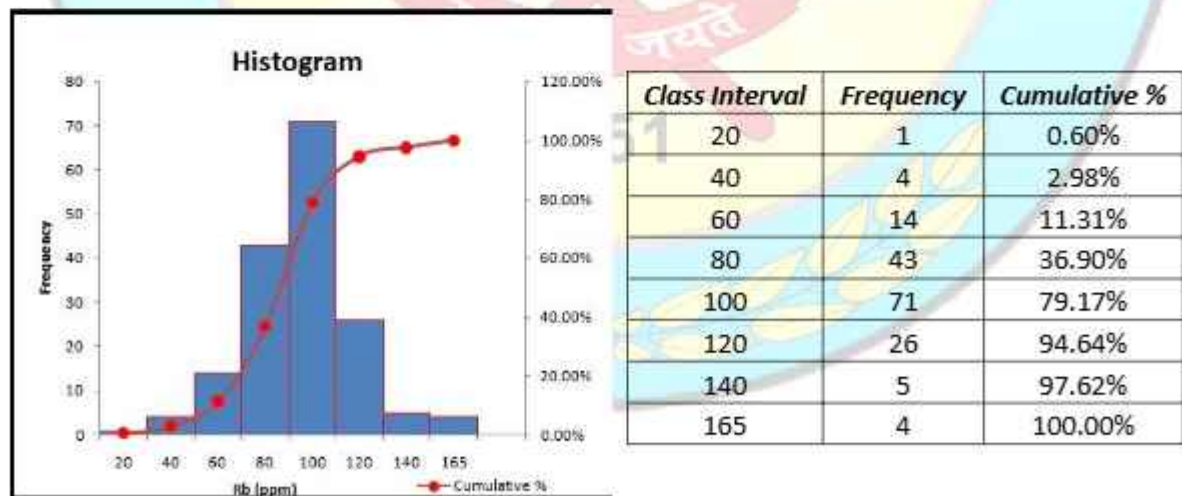


Fig 5.19a. Spatial distribution of Rb in the stream sediment/slope wash samples



5.4.10. Strontium (Sr):

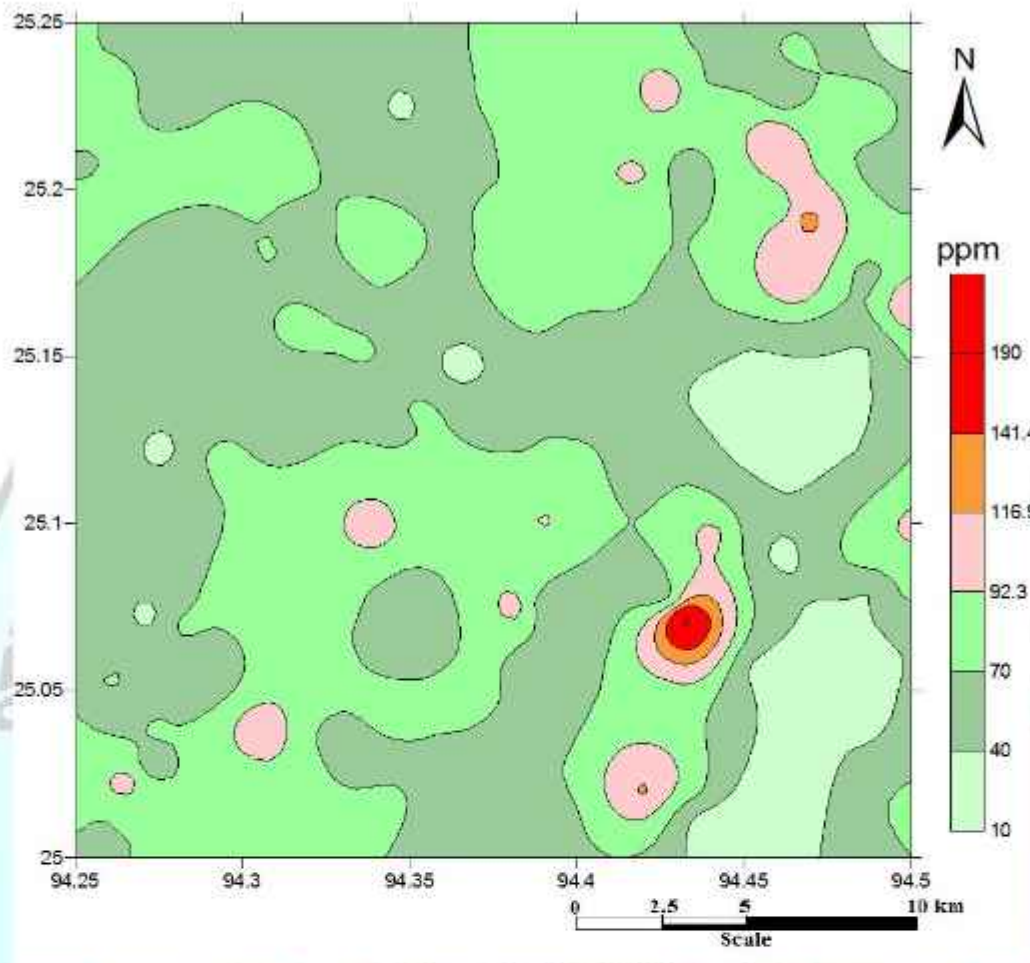
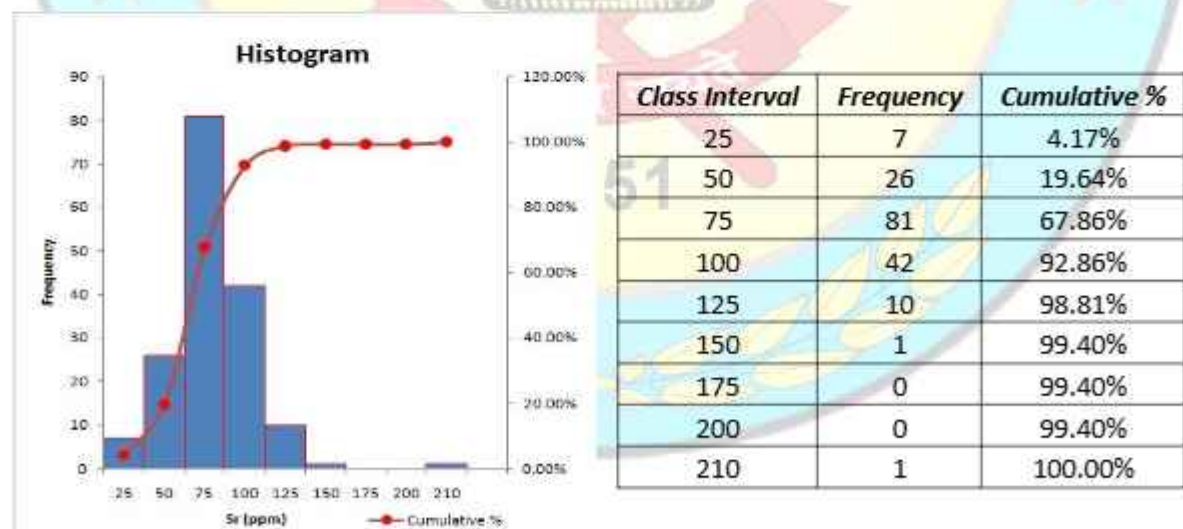


Fig.5.20a. Spatial distribution of Sr in the stream sediment/slope wash samples.



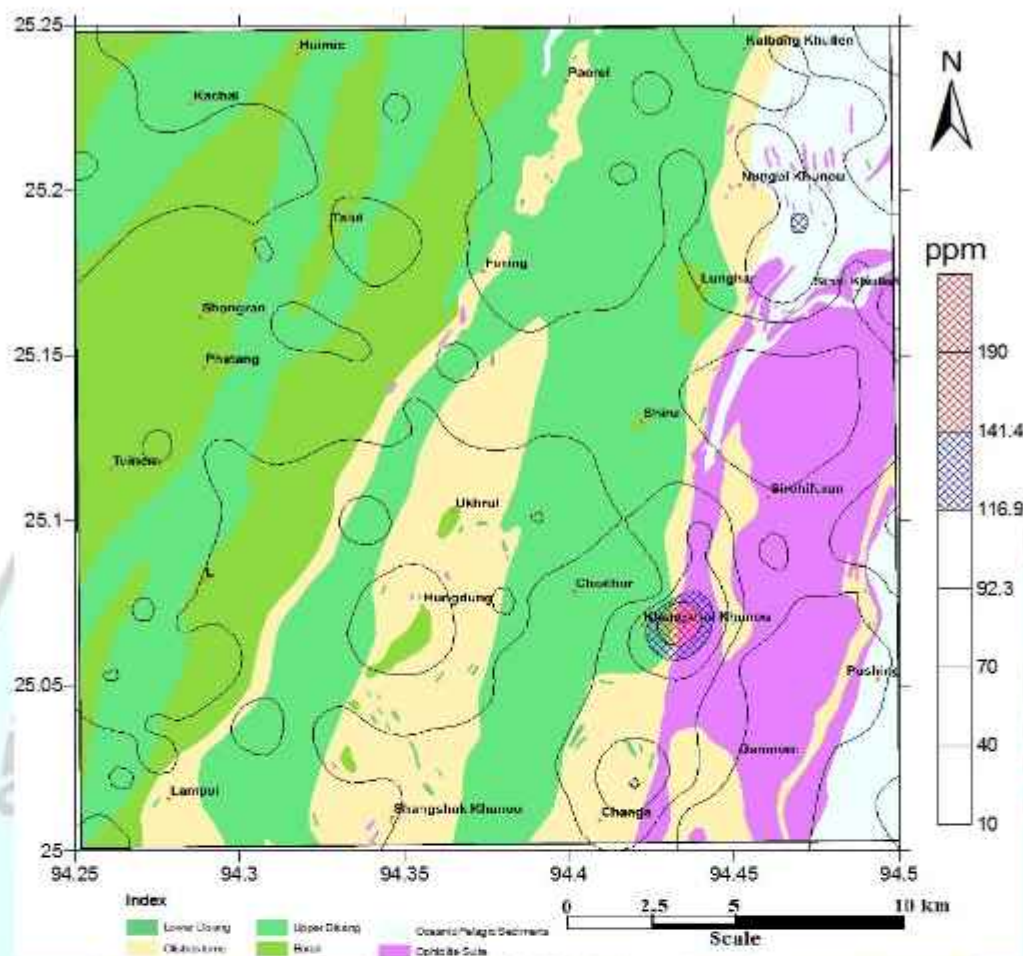


Fig.5.20b. Spatial distribution of Sr in the stream sediment/slope wash samples overlaid on geology of the study area.

Sr in stream sediment

The median value of Sr in stream sediments is 69.50ppm with values varying from 14 to 210ppm (Annexure-II). The high values of Sr in the study area correspond to the eastern part of the study area, where carbonate sedimentary facies are exposed. The highest value is observed in Grid No. 49 of T.S. No. 83K/8 where a hillock of exotic limestone block with interconnected cave is exposed (Fig.5.20a & b). The distribution is positive skewed and kurtosis with values of 1.00 and 6.14 respectively.

The Sr does not occur in free state in nature and occur mostly in association with other minerals dominantly carbonate. Sr similar atomic radii with Ca can have mutual substitution with each other (Marorie Wilson., 1989). The extensive dissolution of limestone by the meteoric water as evident by the interconnected caves within limestone block may have contributed Sr in the sediments.

5.4.11. Yttrium (Y):

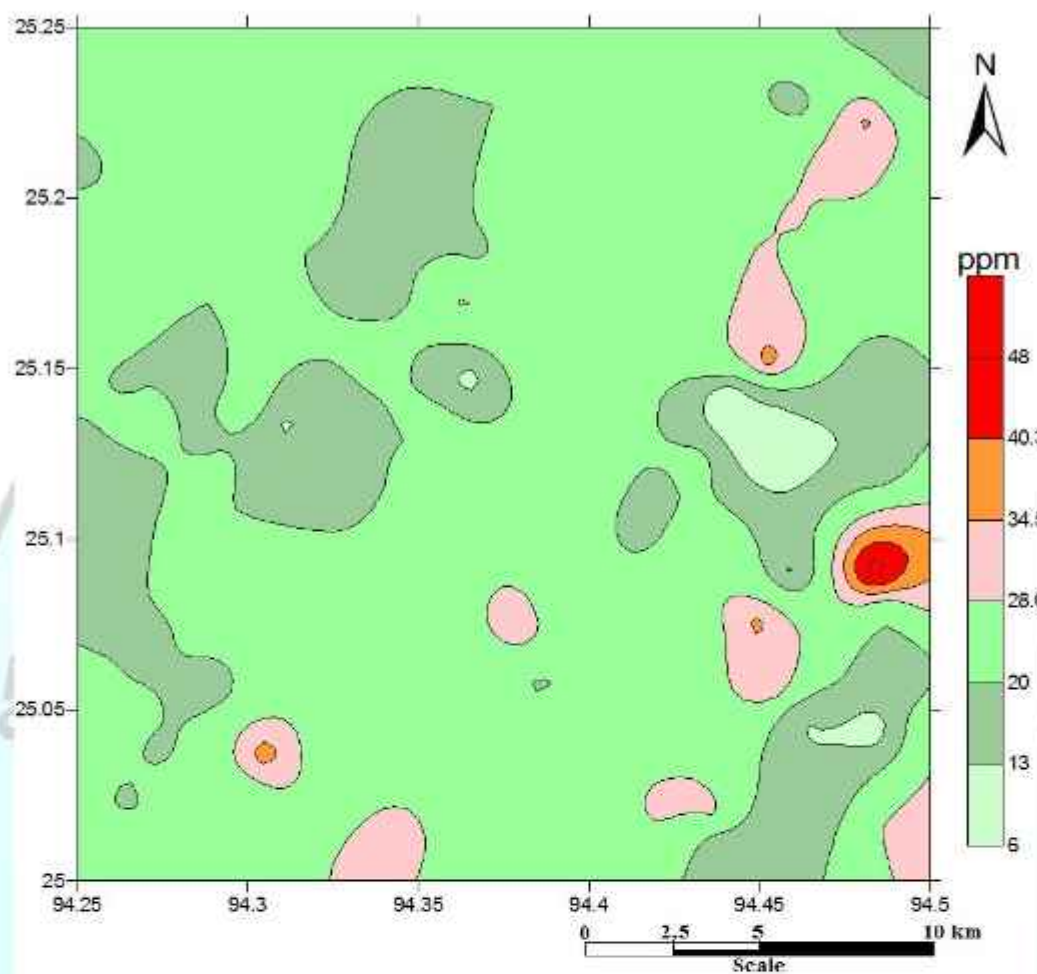
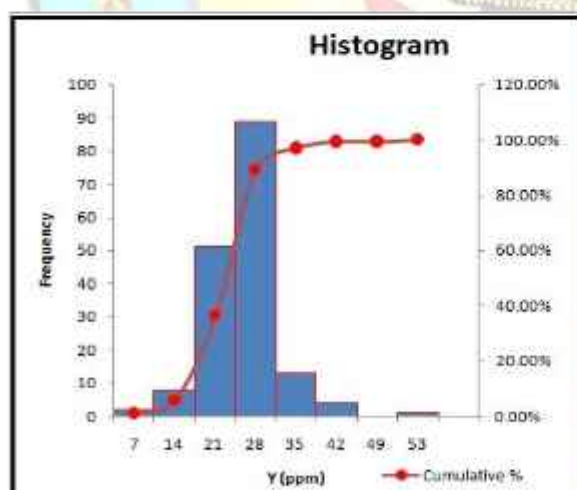


Fig. 5.21a Spatial distribution of Y in the stream sediment/slope wash samples.



<i>Class Interval</i>	<i>Frequency</i>	<i>Cumulative %</i>
7	2	1.19%
14	8	5.95%
21	51	36.31%
28	89	89.29%
35	13	97.02%
42	4	99.40%
49	0	99.40%
53	1	100.00%

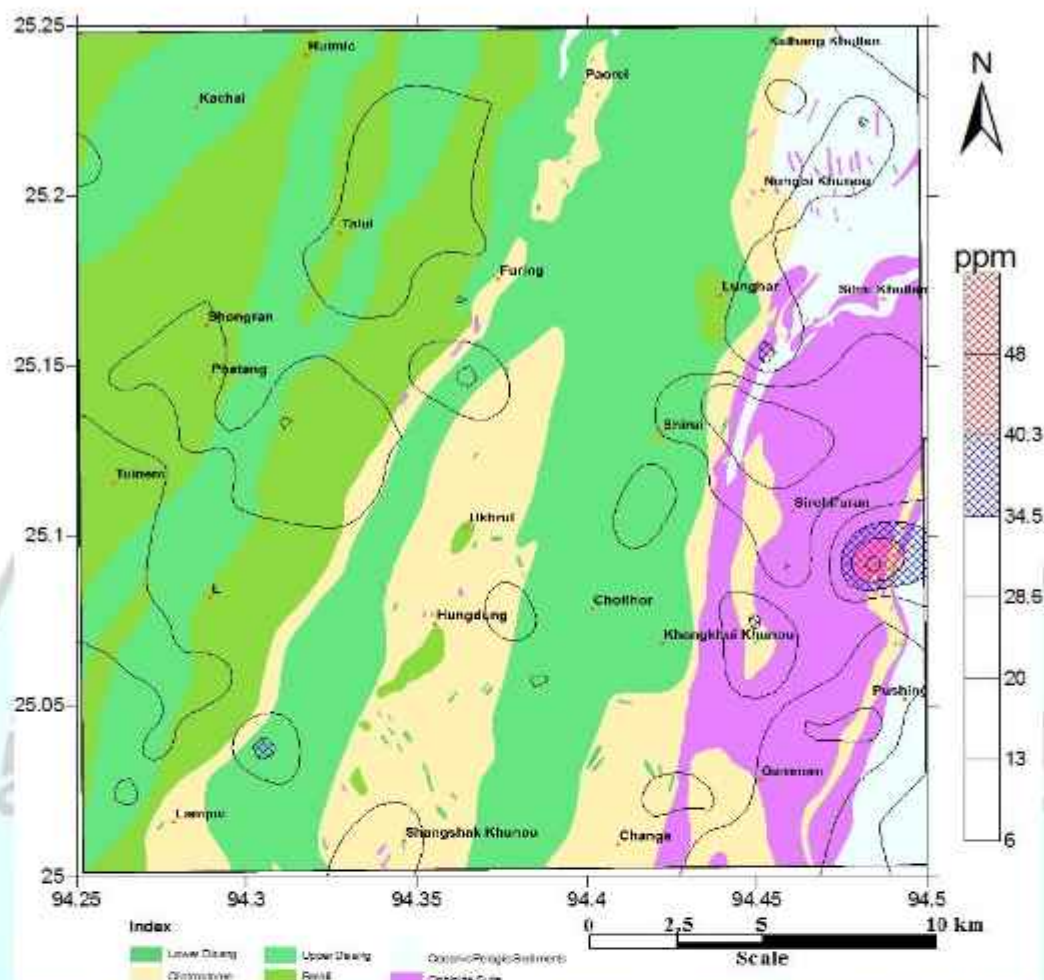


Fig. 5.21b. Spatial distribution of Y in the stream sediment/slope wash samples overlaid on geology of the study area.

Y in stream sediment

The median value of Y in stream sediments is 27 ppm with values varying from 5 to 53 ppm (Annexure-II). The higher values of Y are observed from the eastern part of the study area, with maximum value in Grid No. 77 of T.S. No. 83K/8 where rocks of Ophiolite and OPS are exposed (Fig. 5.21a & b). The distribution is positive skewed and kurtosis with values of 0.70 and 4.50 respectively. Y behaves as an incompatible element resembling HREE. The high values of Y in the ophiolite belt may be due to the presence mineral phase like garnet and amphibole in the stream sediments derieved from the mafic/ultramafic rocks.

5.4.12. Zirconium (Zr):

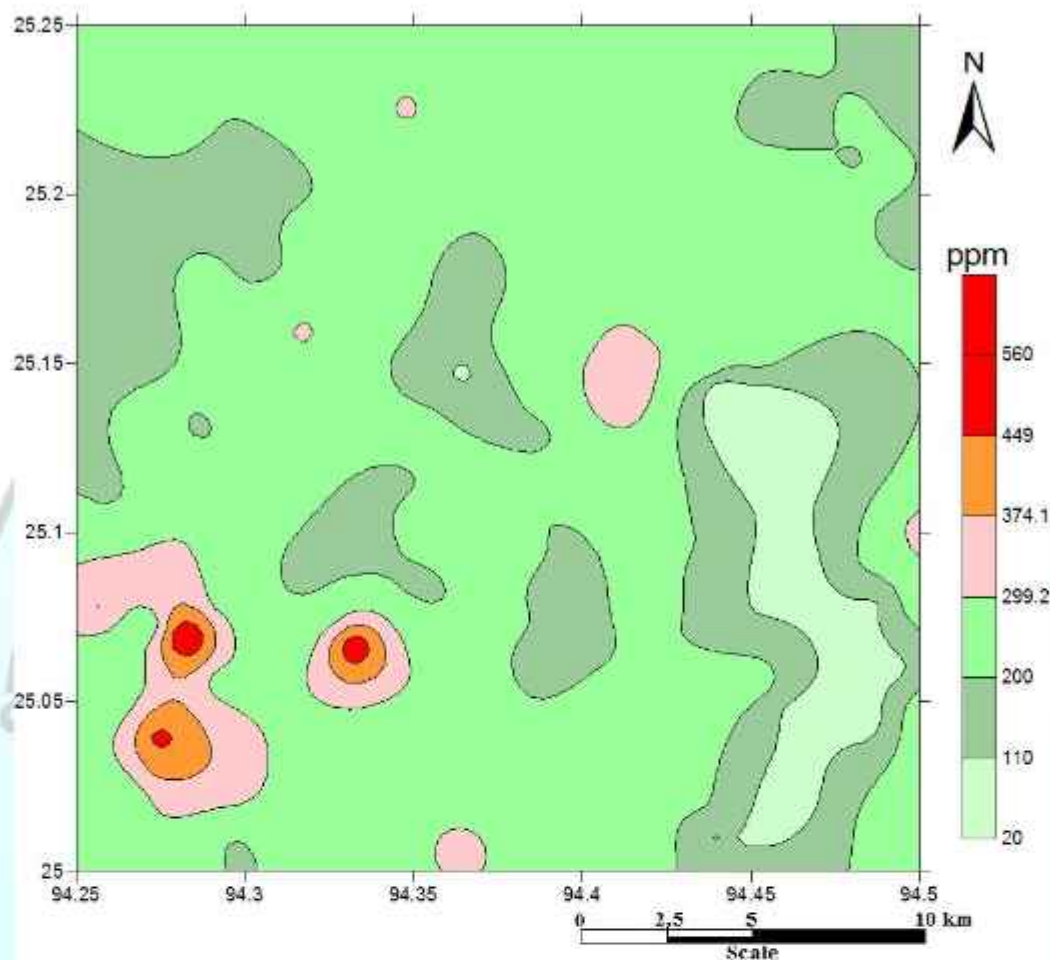
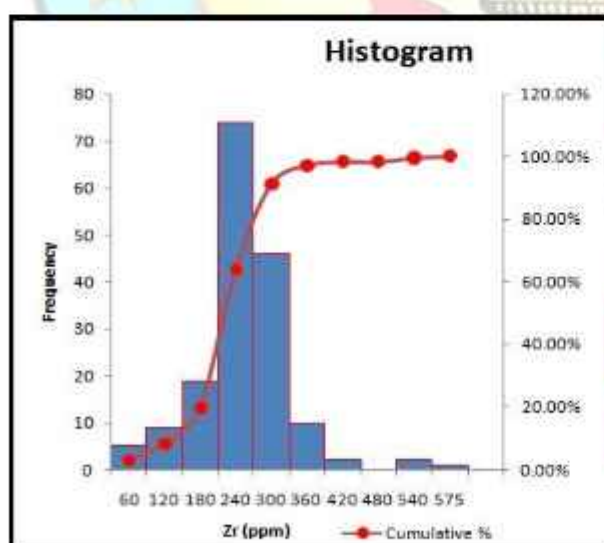


Fig. 5.22a Spatial distribution of Zr in the stream sediment/slope wash samples.



Class Interval	Frequency	Cumulative %
60	5	2.98%
120	9	8.33%
180	19	19.64%
240	74	63.69%
300	46	91.07%
360	10	97.02%
420	2	98.21%
480	0	98.21%
540	2	99.40%
575	1	100.00%

5.4.13. Niobium (Nb):

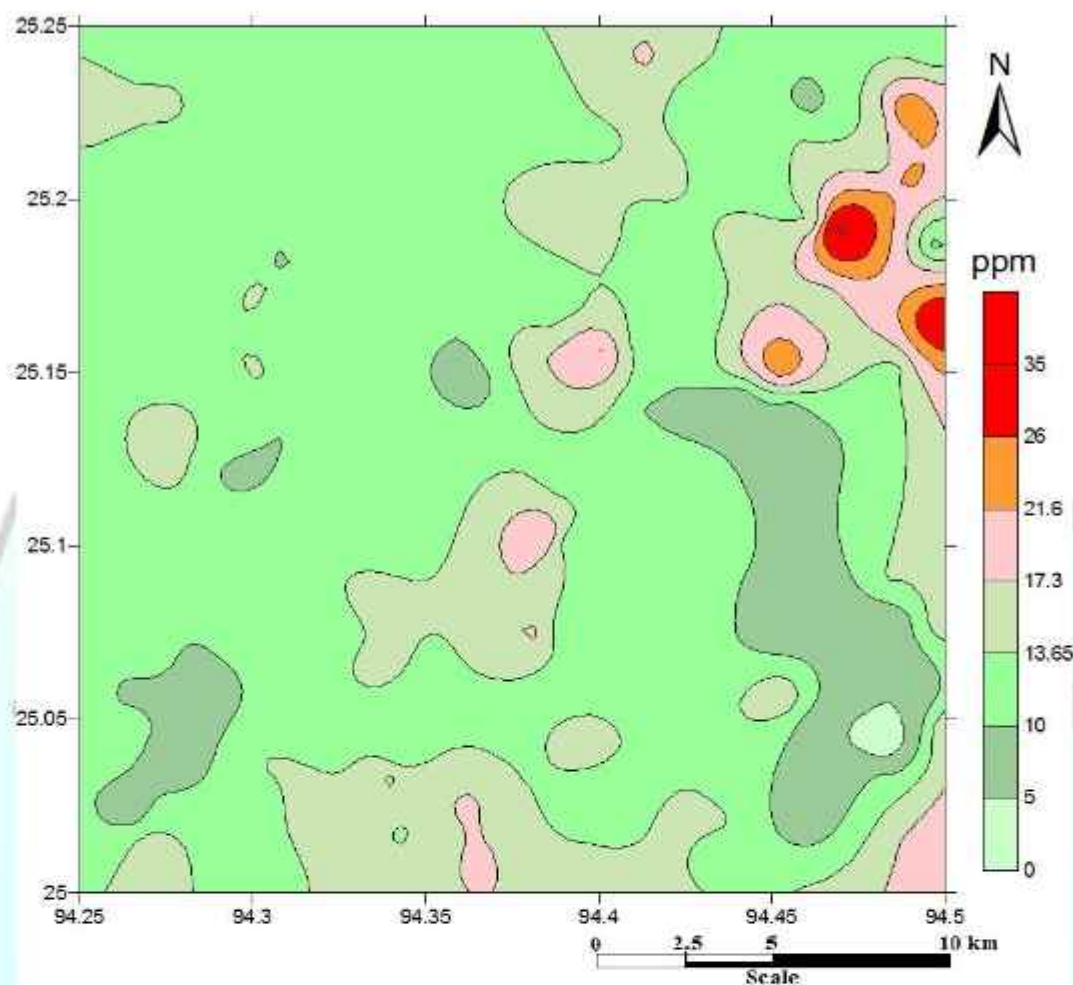
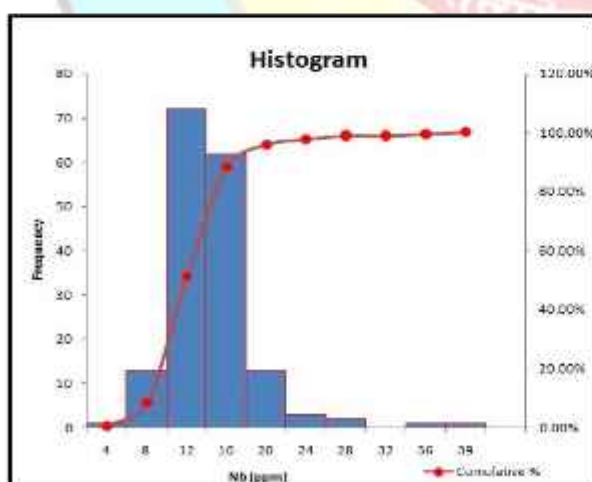


Fig 5.23a. Spatial distribution of Nb in the stream sediment/slope wash samples



Class Interval	Frequency	Cumulative %
4	1	0.60%
8	13	8.33%
12	72	51.19%
16	62	88.10%
20	13	95.83%
24	3	97.62%
28	2	98.81%
32	0	98.81%
36	1	99.40%
39	1	100.00%

5.4.14. Chromium (Cr):

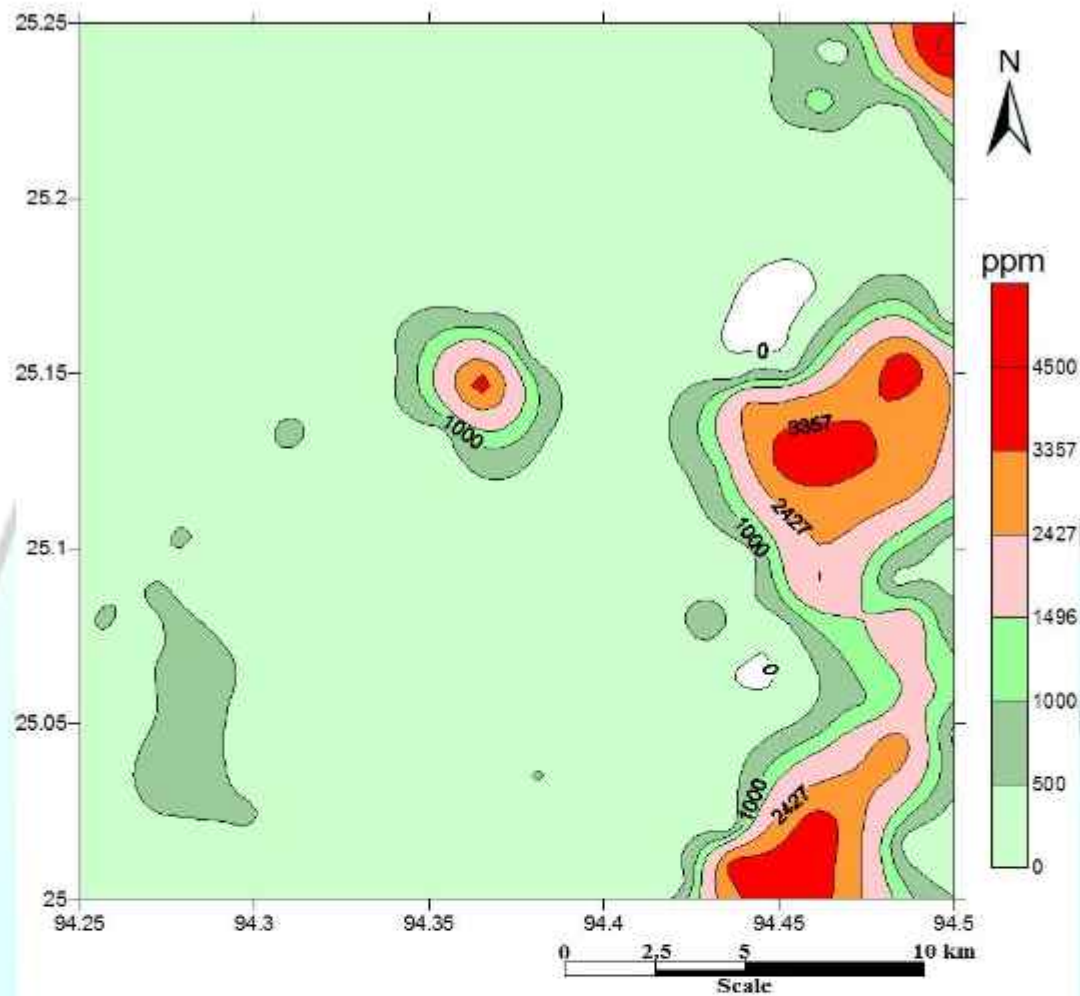
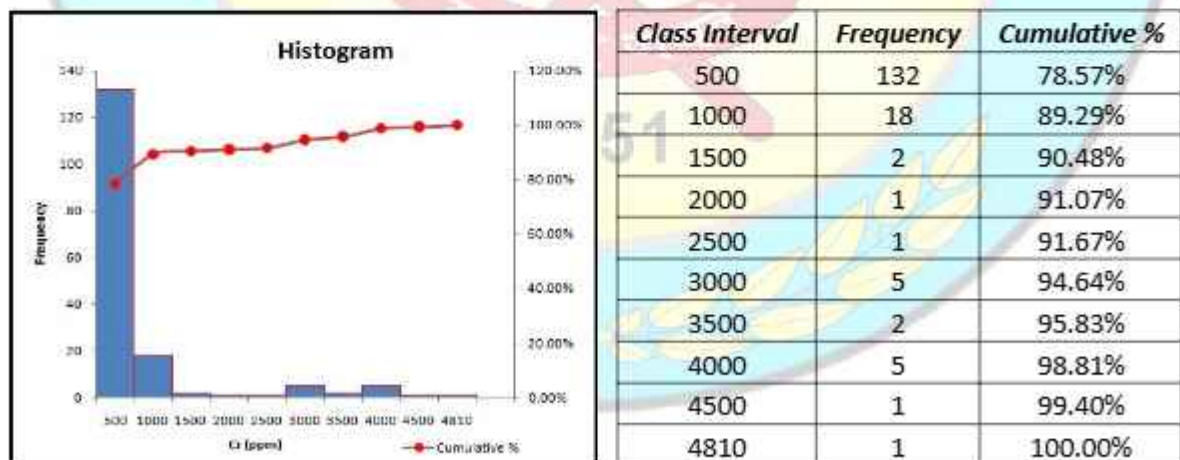


Fig 5.24a. Spatial distribution of Cr in the stream sediment/slope wash samples.



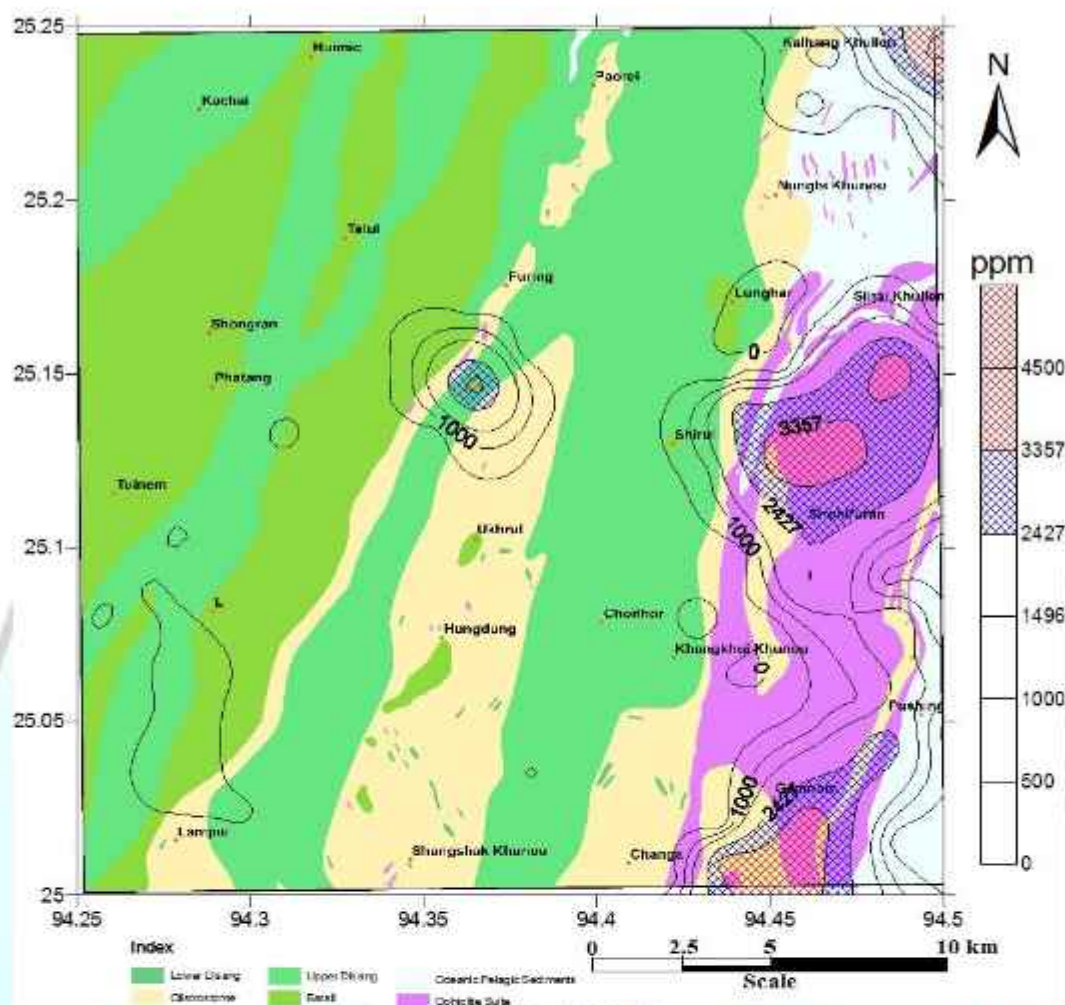


Fig.5.24b. Spatial distribution of Cr in the stream sediment/slope wash samples overlaid on geology of the study area.

Cr in stream sediment

The median value of Cr in stream sediments is 229.5ppm with a range of values from 52 to 4810ppm (Annexure-II) showing maximum value in the north eastern corner of the study area, Grid No. 182 of T.S. No. 83K/8 where rocks of Ophiolite suite are well exposed. The distribution is highly positive skewed with a value of 2.95 and positive kurtosis of 7.9.

Cr content of the whole area is almost high. However, the maximum concentration of Cr is confined along the eastern part of the area, where Ophiolite rocks are well exposed (Fig.5.24a & b). Cr shows strong positive correlation with Fe_2O_3 , Ni, Co and Cu suggest good prospect of chromium mineralisation which is collaborated by the field evidence of podiform chromitite within the transitional and cumulate peridotite. Chromium occurs in

the environment primarily in two valence states, trivalent chromium Cr (III) and hexavalent Cr (VI). Cr (III) is much less toxic than Cr (VI). Toxicity of Cr in soils and stream sediments is less compared to that of water (Das & Mishra 2007).

5.4.15. Copper (Cu):

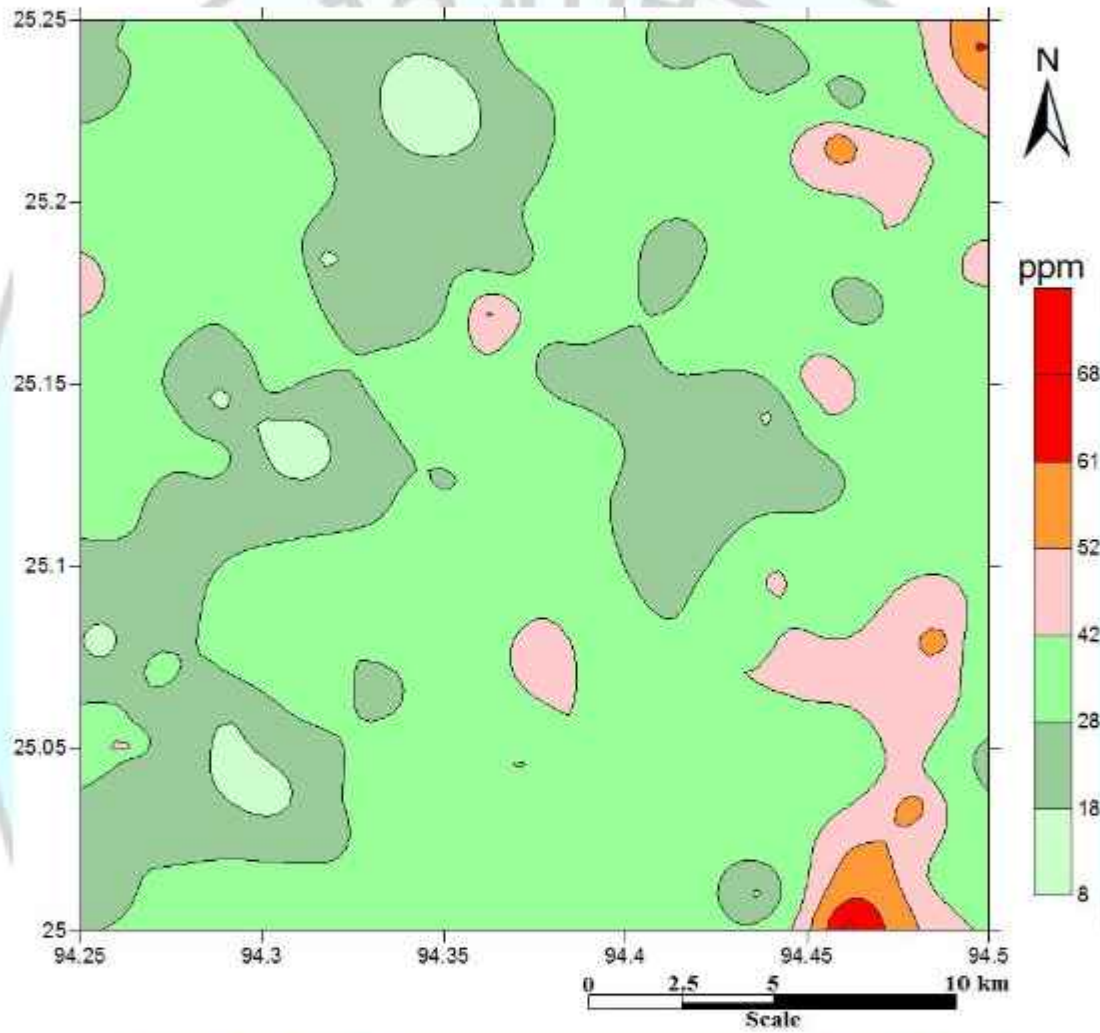


Fig.5.25a.Spatial distribution of Cu in the stream sediment/slope wash samples.

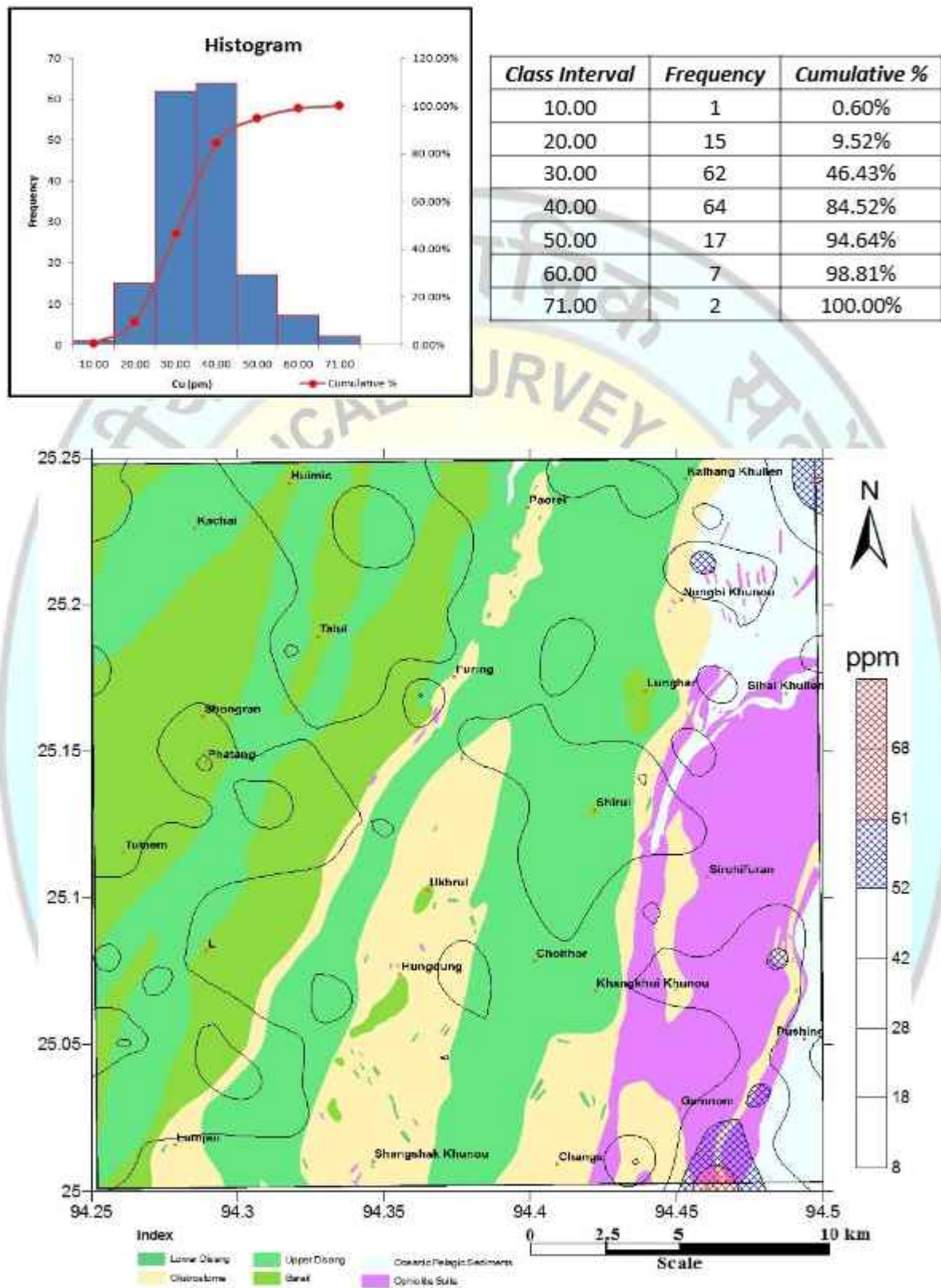


Fig.5.25b.Spatial distribution of Cu in the stream sediment/slope wash samples overlaid on geology of the study area.

Cu in stream sediment

The median value of Cu in the stream sediments of the study area is 32ppm with values varying from 9 to 71ppm (Annexure-II). The high values of Cu are observed in the eastern part of the study area, where mafic/ultramafic rocks are exposed. The highest value is observed in the south eastern corner of the study area in Grid No. 11 of T.S. No. 83K/8. The distribution is positive skewed and kurtosis with values of 0.7 and 1.35 respectively.

The distribution pattern of Cu is more in the sheared zone of Ophiolite body (Fig. 5.25a & b), which is evident by the presence of malachite stain within serpentinised peridotite. Cu shows a strong good positive correlation with Ni, Cr and Fe_2O_3 .

5.4.16. Zinc (Zn):

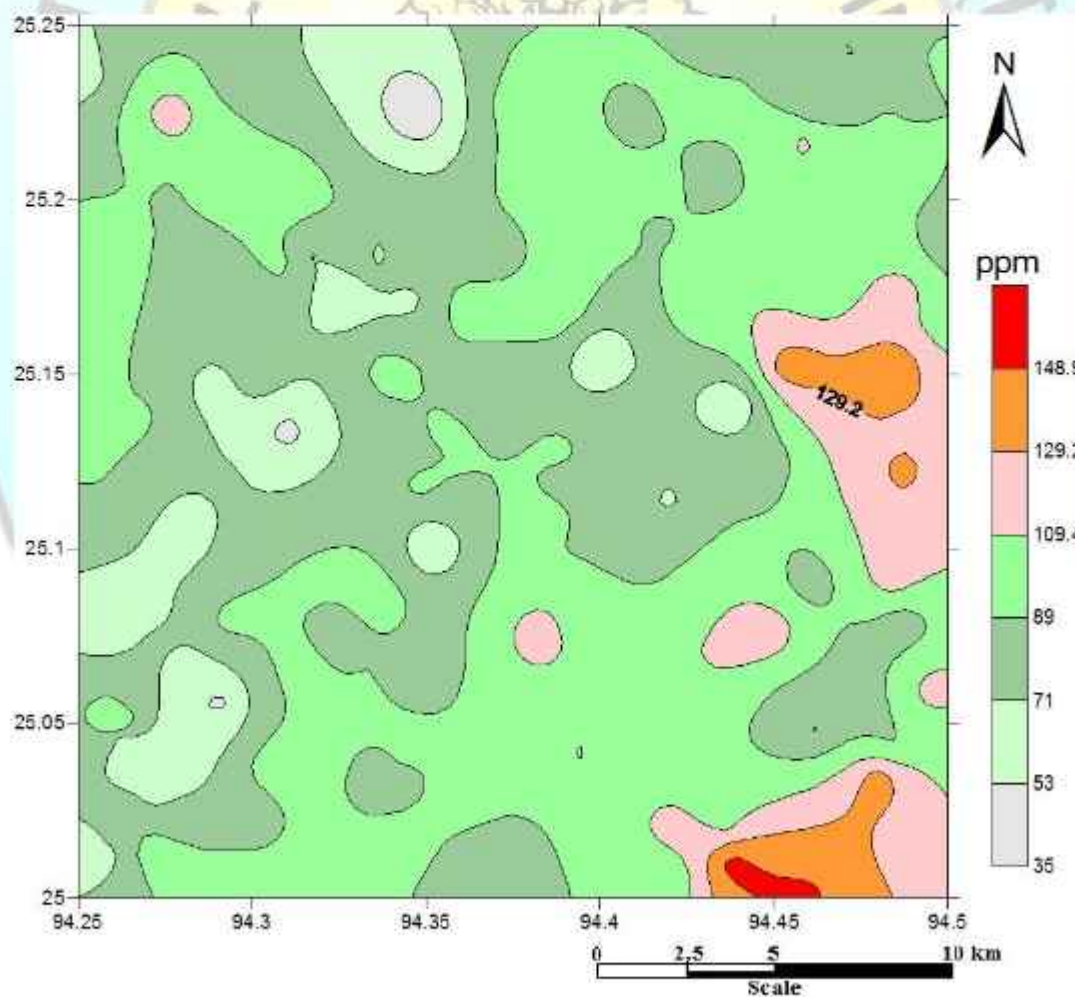
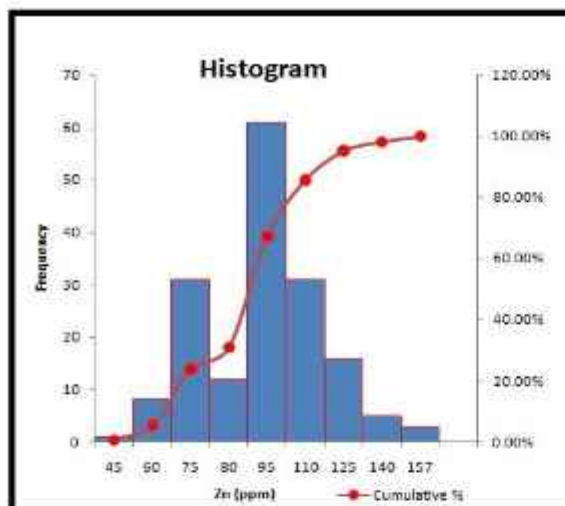


Fig.5.26a.Spatial distribution of Zn in the stream sediment/slope wash samples.



Class Interval	Frequency	Cumulative %
45	1	0.60%
60	8	5.36%
75	31	23.81%
80	12	30.95%
95	61	67.26%
110	31	85.71%
125	16	95.24%
140	5	98.21%
157	3	100.00%

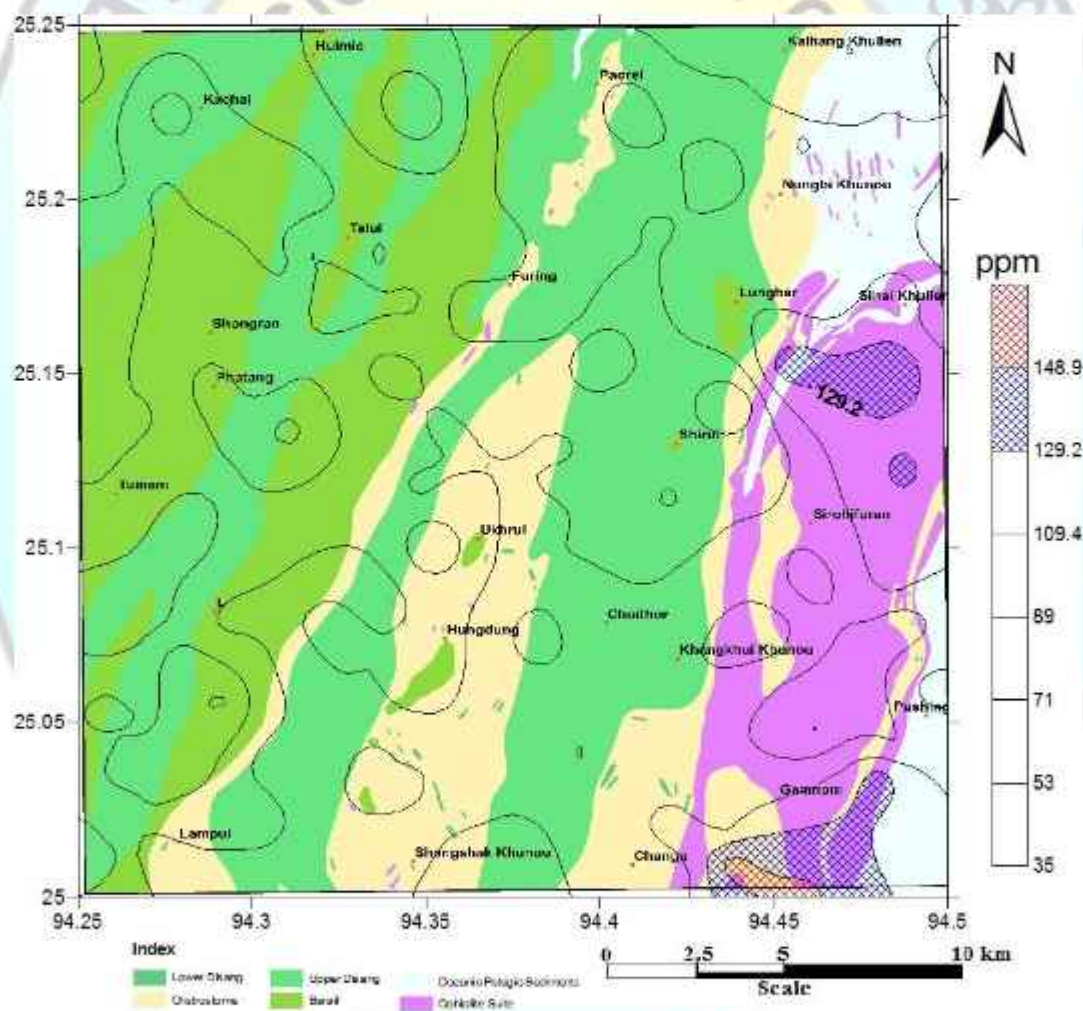


Fig.5.26b.Spatial distribution of Zn in the stream sediment/slope wash samples overlaid on geology of the study area.

Zn in stream sediment

The median value of Zn in stream sediments is 91 ppm with values varying from 36 ppm to 157 ppm (Annexure-II) showing maximum value in the southern part of the study area, Grid No. 10 of T.S. No. 83K/8 where Ophiolite rocks are exposed (Fig.5.26a & b). It shows positive skewness and kurtosis with values of 0.53 and 1.15 respectively.

The Zn distribution map shows moderate concentration throughout the area.

5.4.17. Beryllium (Be):

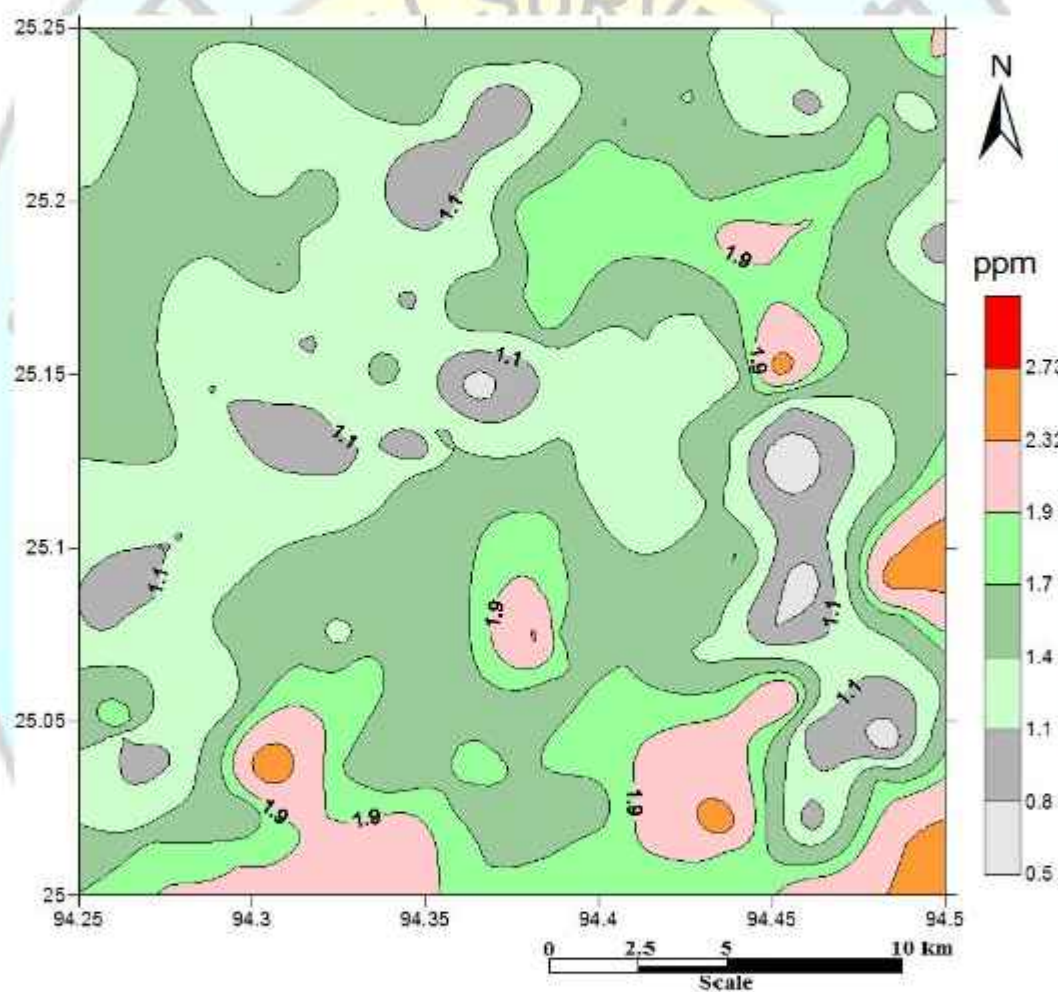


Fig.5.27a. Spatial distribution of Be in the stream sediment /slope wash samples

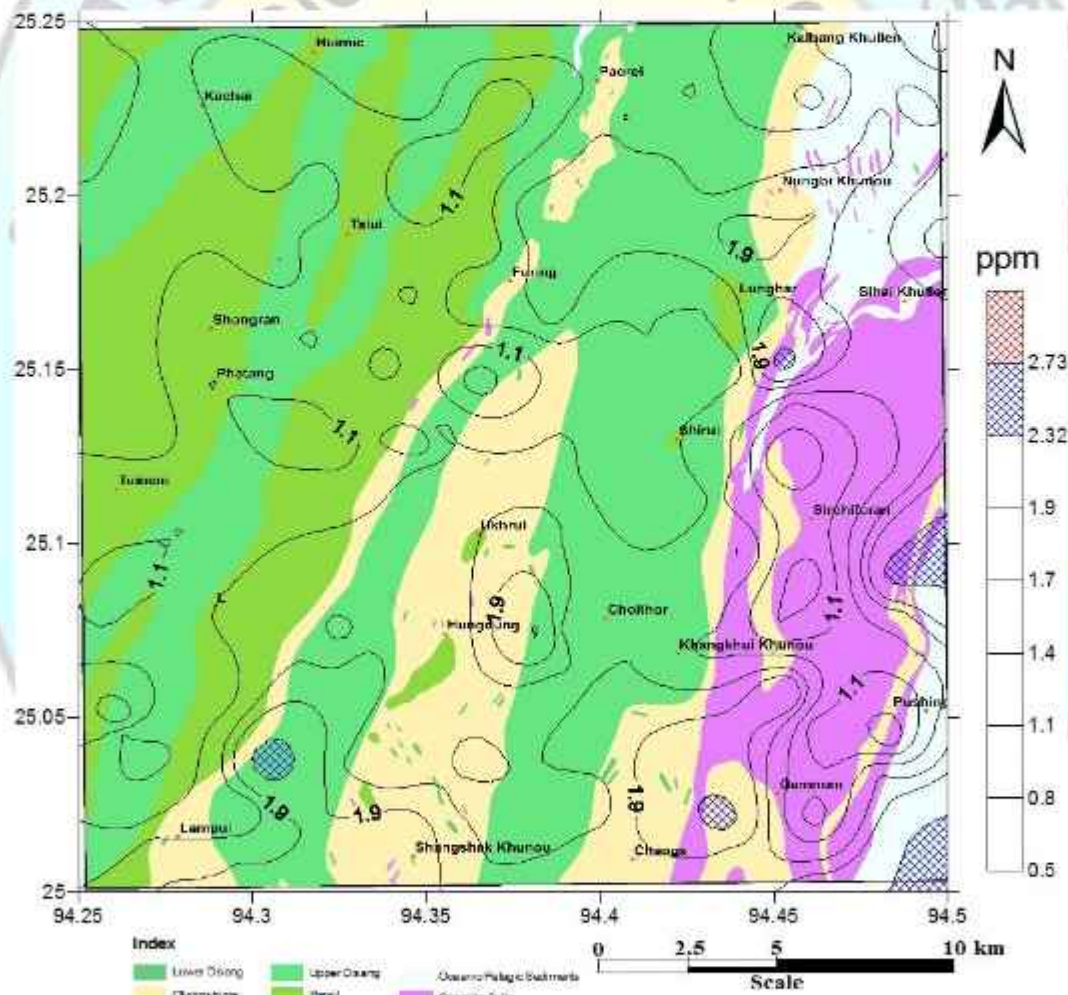
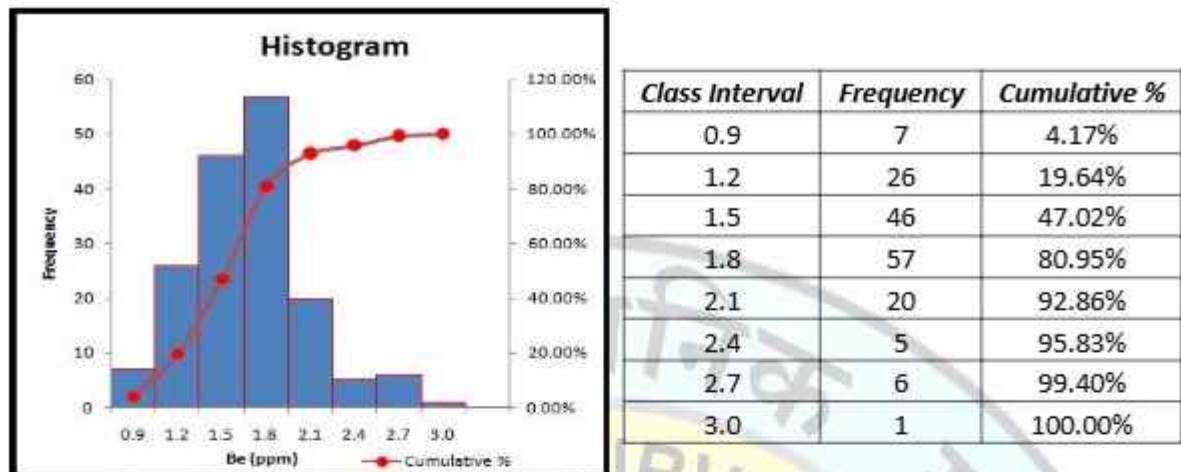


Fig.5.27b. Spatial distribution of Be in the stream sediment /slope wash samples overlaid on geology of the study area.

Be in stream sediment

The median value of Be in stream sediments is 1.51 ppb with values varying from 0.44 to 2.75 ppm (Annexure-II). The high values of Be are observed in the eastern part of the study area, where the Ocean Pelagic Sediments are exposed (Fig. 5.27a & b). The highest value in the south western part of the study area in Grid No. 29 of T.S. No. 83K/8 where the Olistostrome, Paleogene sediments are exposed. The distribution is positive skewness and kurtosis with values of 0.34 and 0.81 respectively. The Be showing high values eastern part of the area may be due to the presence of Be bearing mineral phase beryl within the calcitic veins of metamorphosed calcitic vein dissection across the limestone body within OPS.

5.4.18. Germanium (Ge):

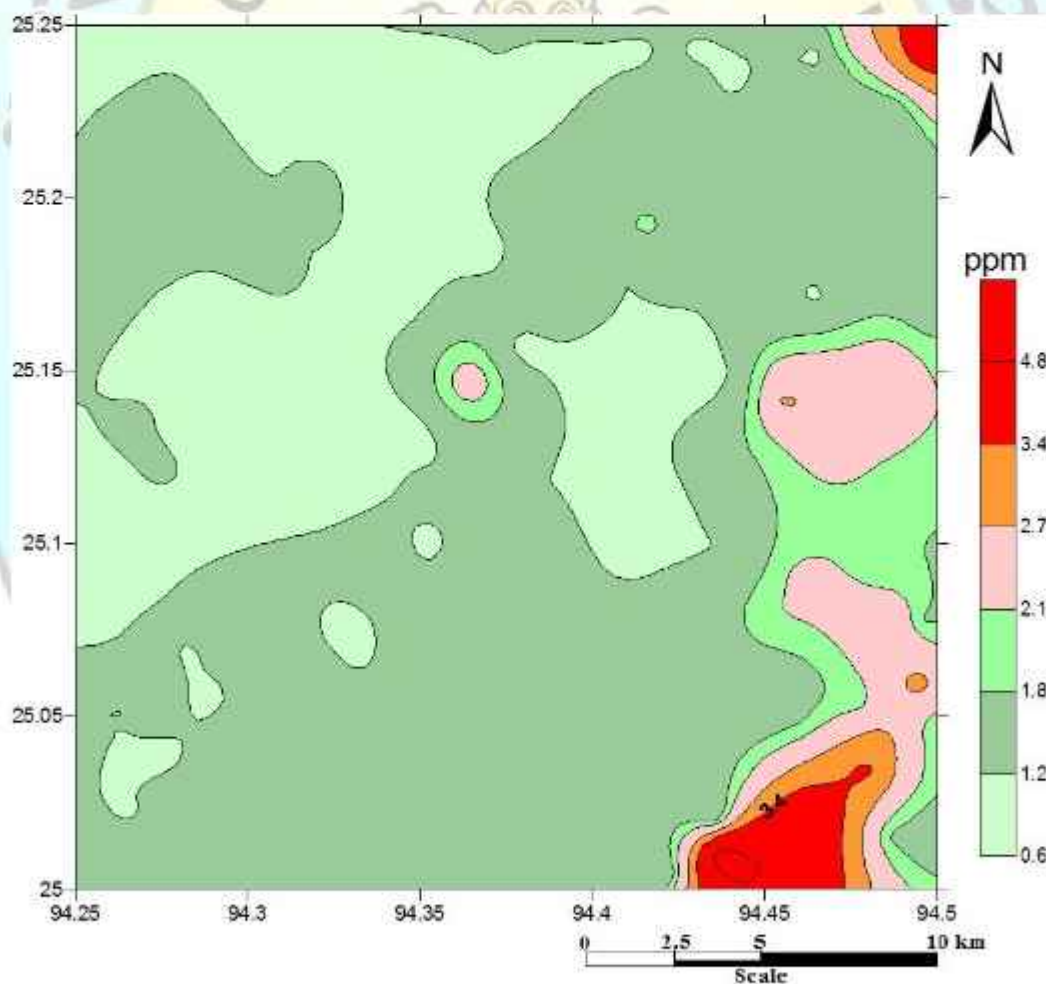


Fig.5.28a. Spatial distribution of Ge in the stream sediment/slope wash samples

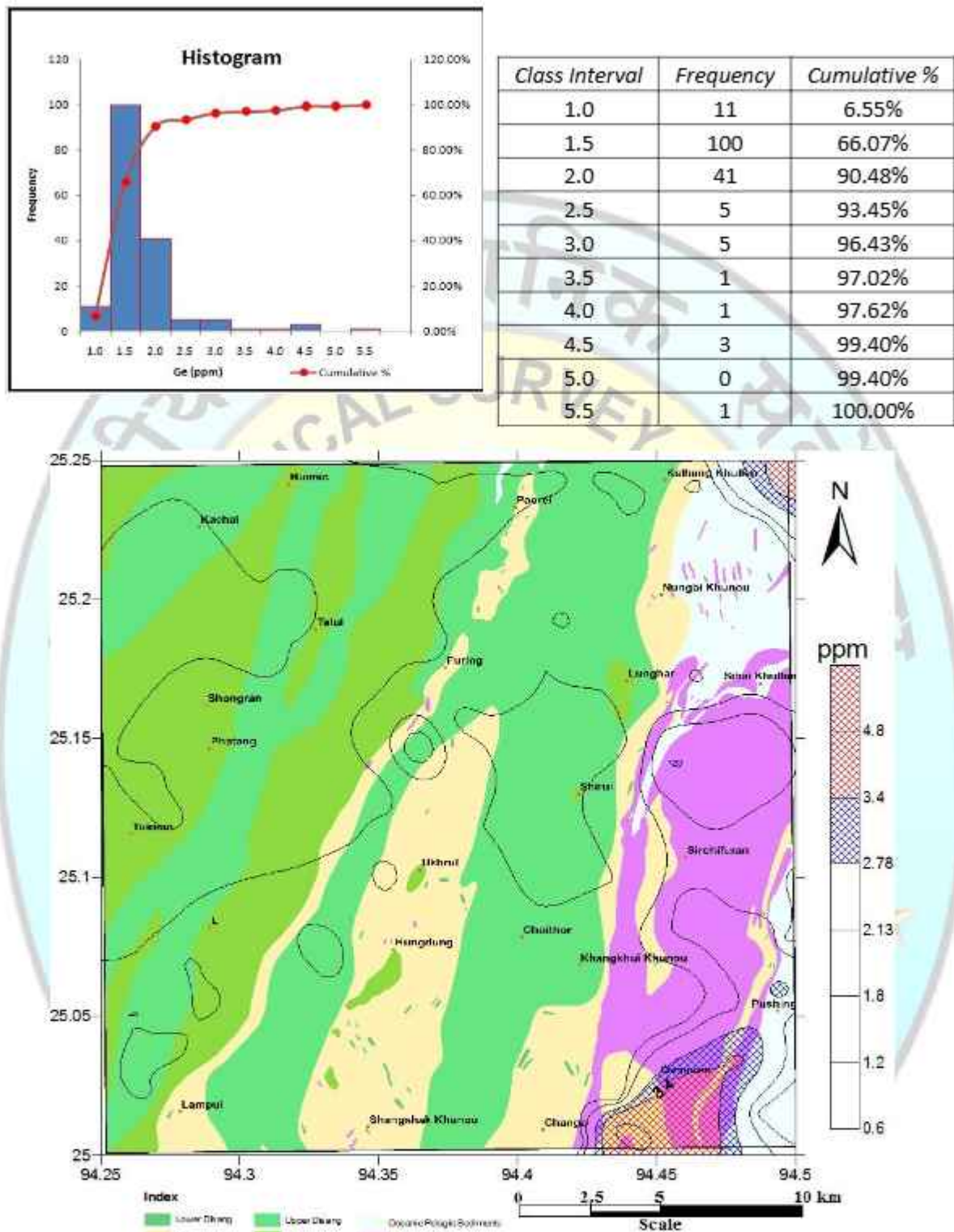


Fig.5.28b. Spatial distribution of Ge in the stream sediment/slope wash samples overlaid on geology of the study area.

Ge in stream sediment

The median value of Ge in stream sediments is 1.33 ppb with values varying from 0.66 to 5.42 ppb (Annexure-II) showing maximum value in southern part of the study area, Grid No. 10 of T.S. No. 83K/8 where rocks of ophiolite and olistostrome are exposed. The distribution is positive skewed and kurtosis with a value of 3.16 and 12.98 respectively. The distribution of Ge is uniformly low in the study area (Fig. 5.28a & b).

5.4.19. Tin (Sn):

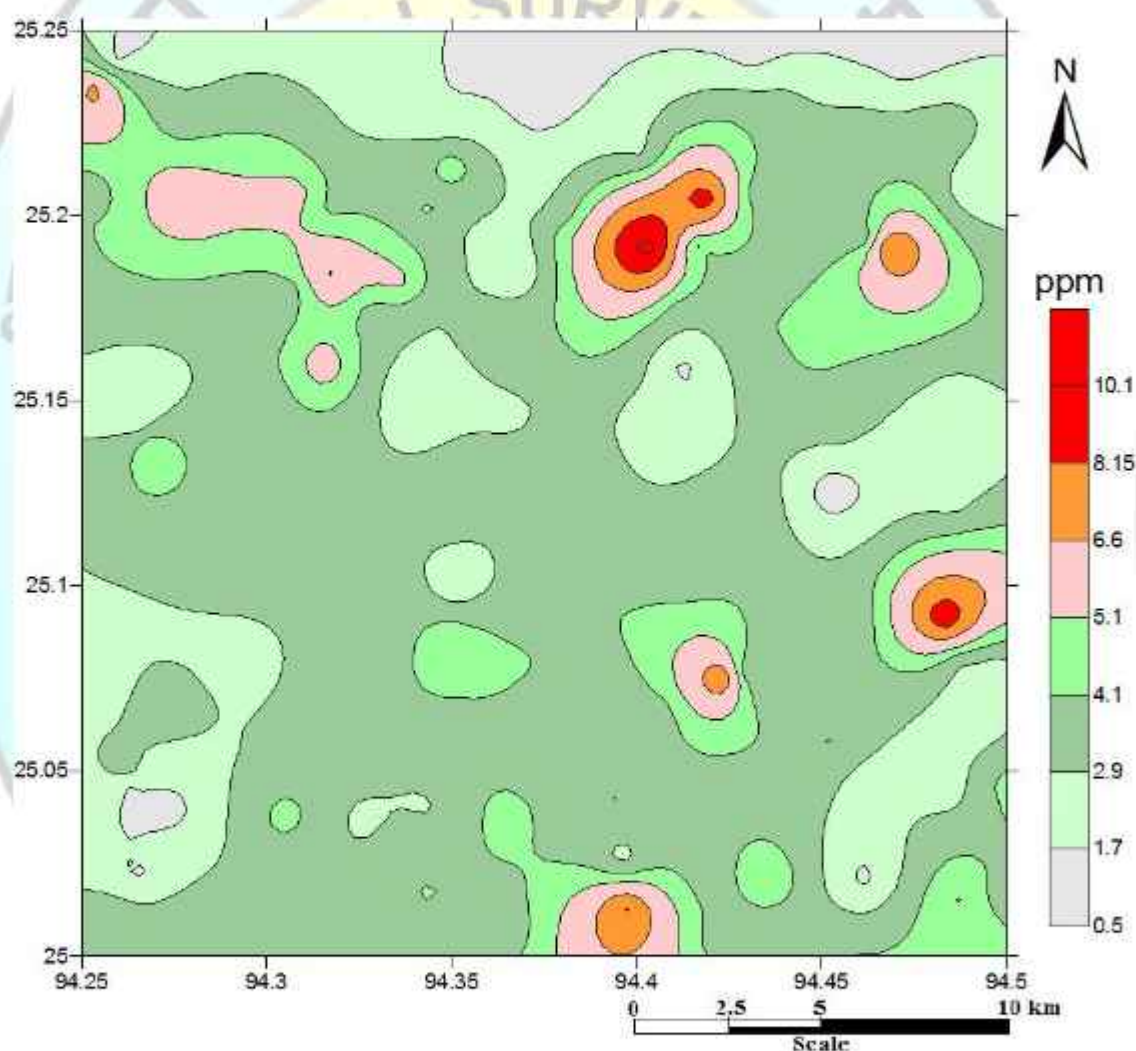
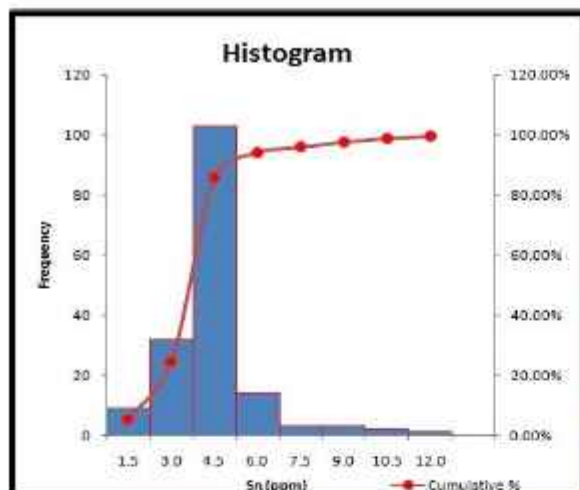


Fig 5.29a Spatial distribution of Sn in the stream sediment/slope wash samples.



Class Interval	Frequency	Cumulative %
1.5	9	5.36%
3.0	32	24.40%
4.5	103	85.71%
6.0	14	94.05%
7.5	3	95.83%
9.0	3	97.62%
10.5	2	98.81%
12.0	1	99.40%

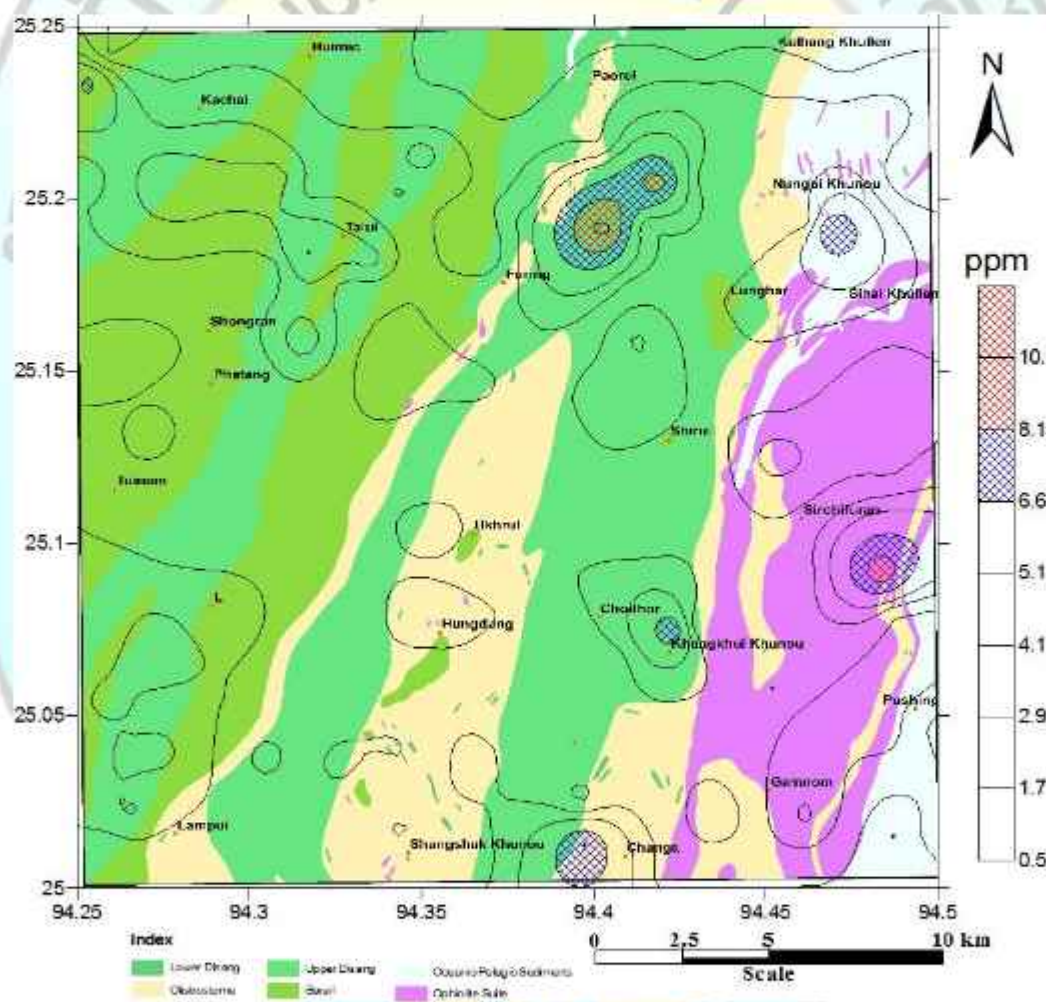


Fig.5.29b. Spatial distribution of Sn in the stream sediment/slope wash samples overlaid on geology of the study area.

Sn in stream sediment

The median value of Sn in stream sediments is 3.48 ppb with values varying from 0.48 to 11.13 ppb (Annexure-II). The distribution is positive skewness and kurtosis with values of 1.80 and 6.06 respectively. The higher values of Sn are observed with the OPS and Disang sediments, with maximum value in the northern part of the study area in Grid No. 138 of T.S. No. 83K/8 where Paleogene sedimentary rocks are exposed (Fig 5.29a &b). The high values in the study area may be due to the presence of Sn bearing heavy minerals like cassiterite within the sedimentary provenance.

5.4.20. Hafnium (Hf):

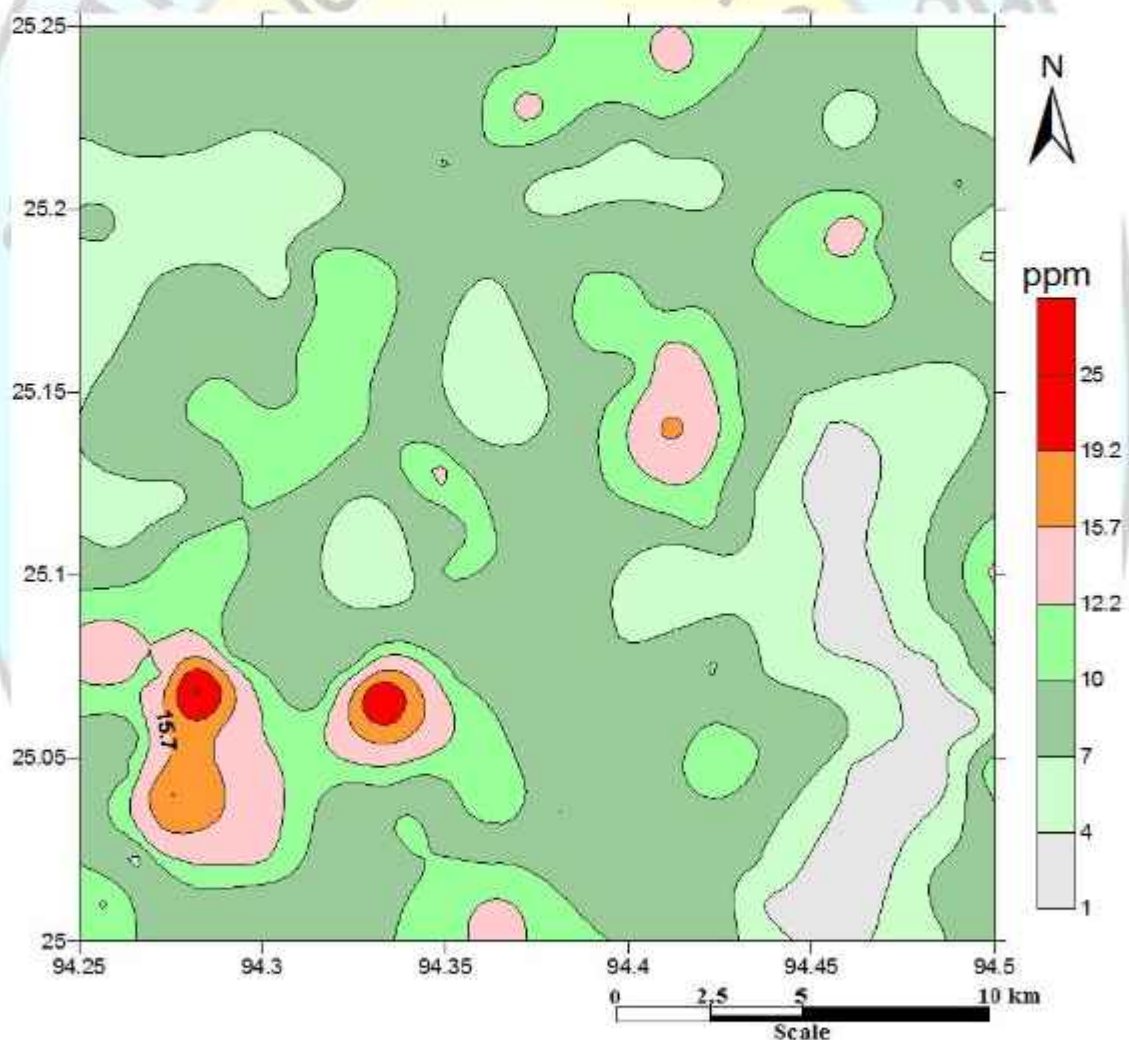


Fig.5.30a. Spatial distribution of Hf in the stream sediment/slope wash samples.

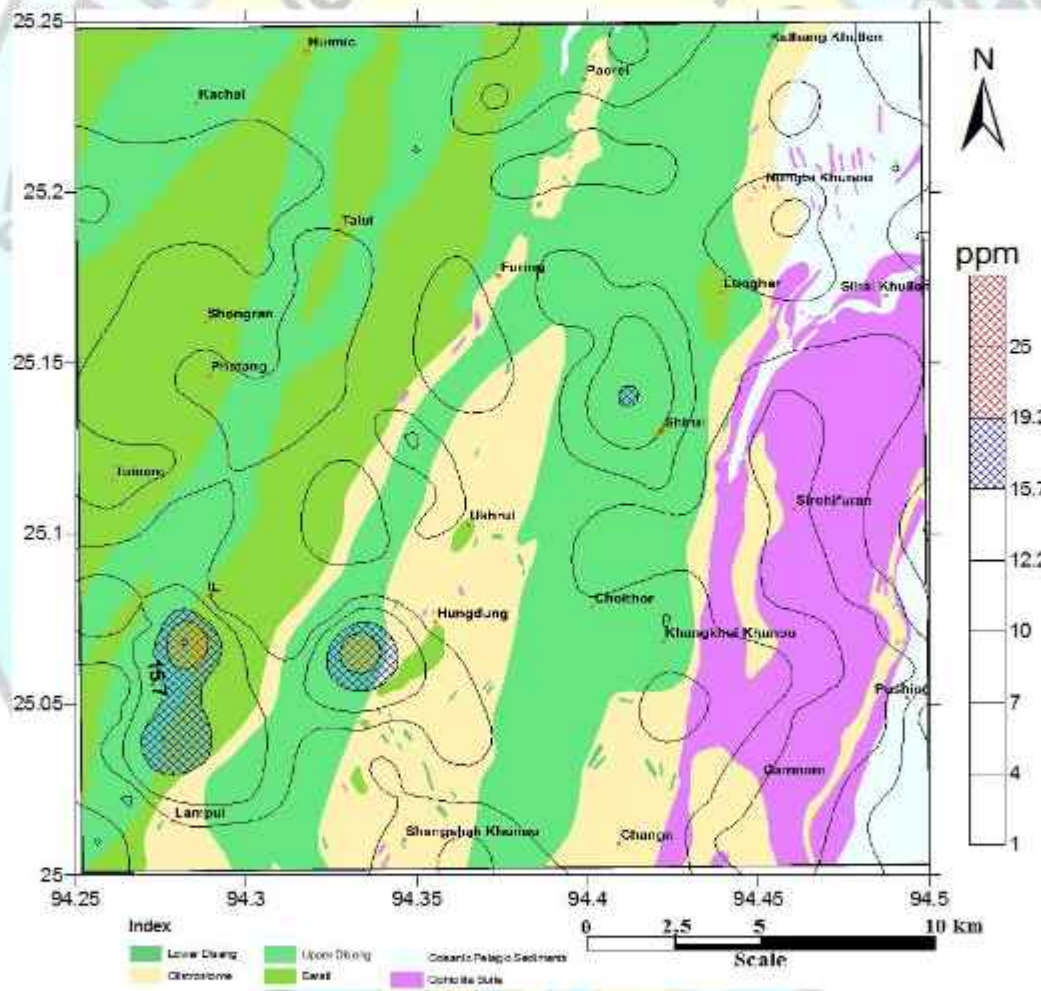
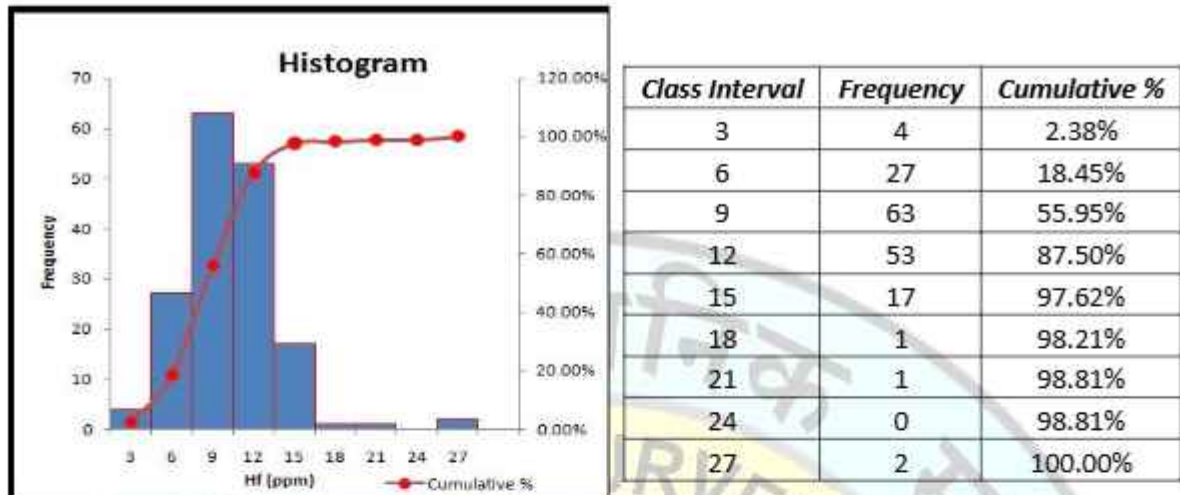


Fig.5.30b. Spatial distribution of Hf in the stream sediment/slope wash samples overlaid on geology of the study area.

Hf in stream sediment

The median value of Hf in stream sediments is 8.69 ppb with values varying from 1.80 to 26.93 ppb (Annexure-II). The high values of Hf are observed in the western part of

the study area where the Paleogene Disang and Barial sediments are exposed, with maximum value in Grid No. 41 of T.S. No. 83K/8 (Fig.5.30a & b). The distribution is positive skewness and kurtosis with values of 1.52 and 6.65 respectively. Hf shows a very strong positive correlation with Zr as well as shows positive correlation with Th and U, which suggest the presence of Hf within Zircon mineral within the Paleogene sediments, which are subsequently fractionated into streams sediments due to weathering.

5.4.21. Tantalum (Ta):

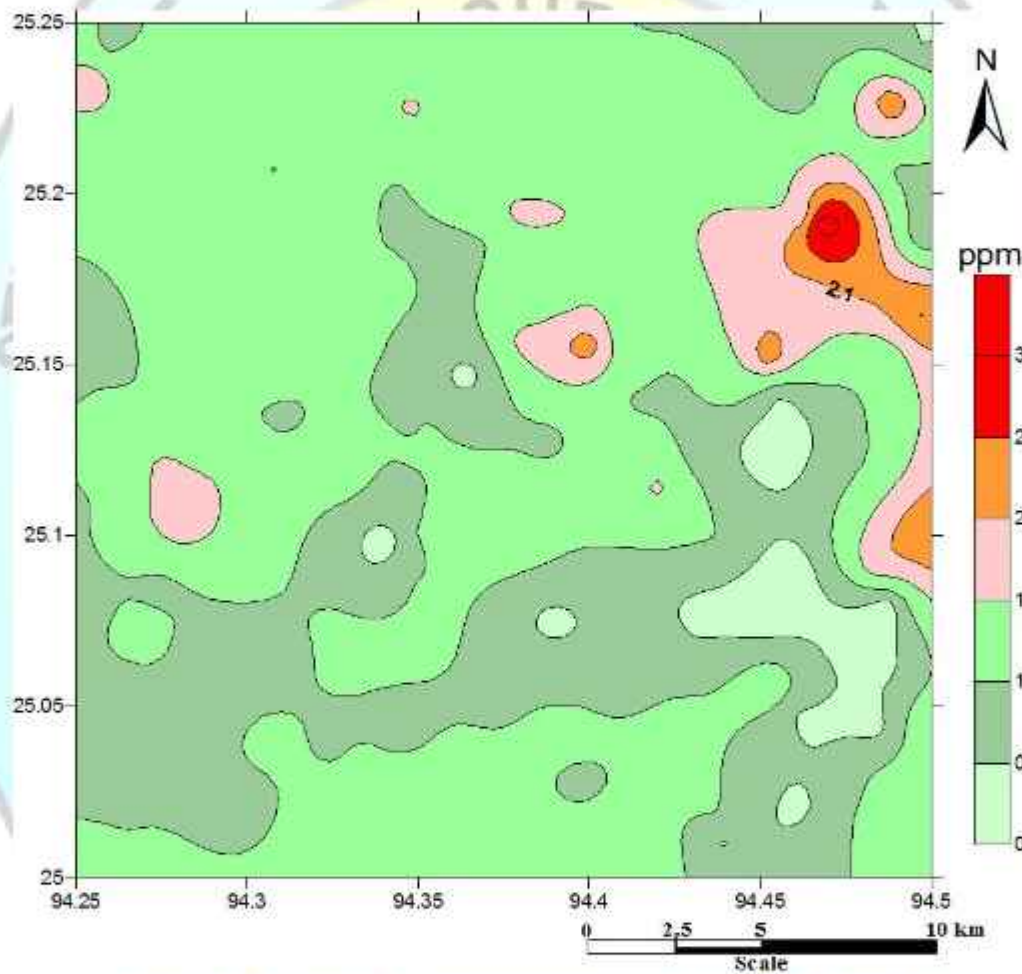
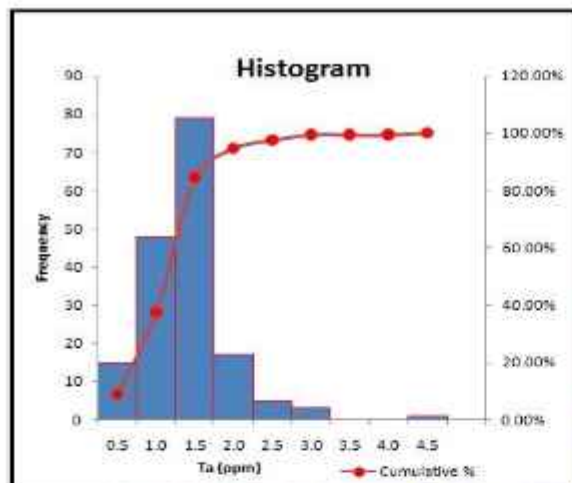


Fig.5.31a. Spatial distribution of Ta in the stream sediment/slope wash samples.



Class Interval	Frequency	Cumulative %
0.5	15	8.93%
1.0	48	37.50%
1.5	79	84.52%
2.0	17	94.64%
2.5	5	97.62%
3.0	3	99.40%
3.5	0	99.40%
4.0	0	99.40%
4.5	1	100.00%

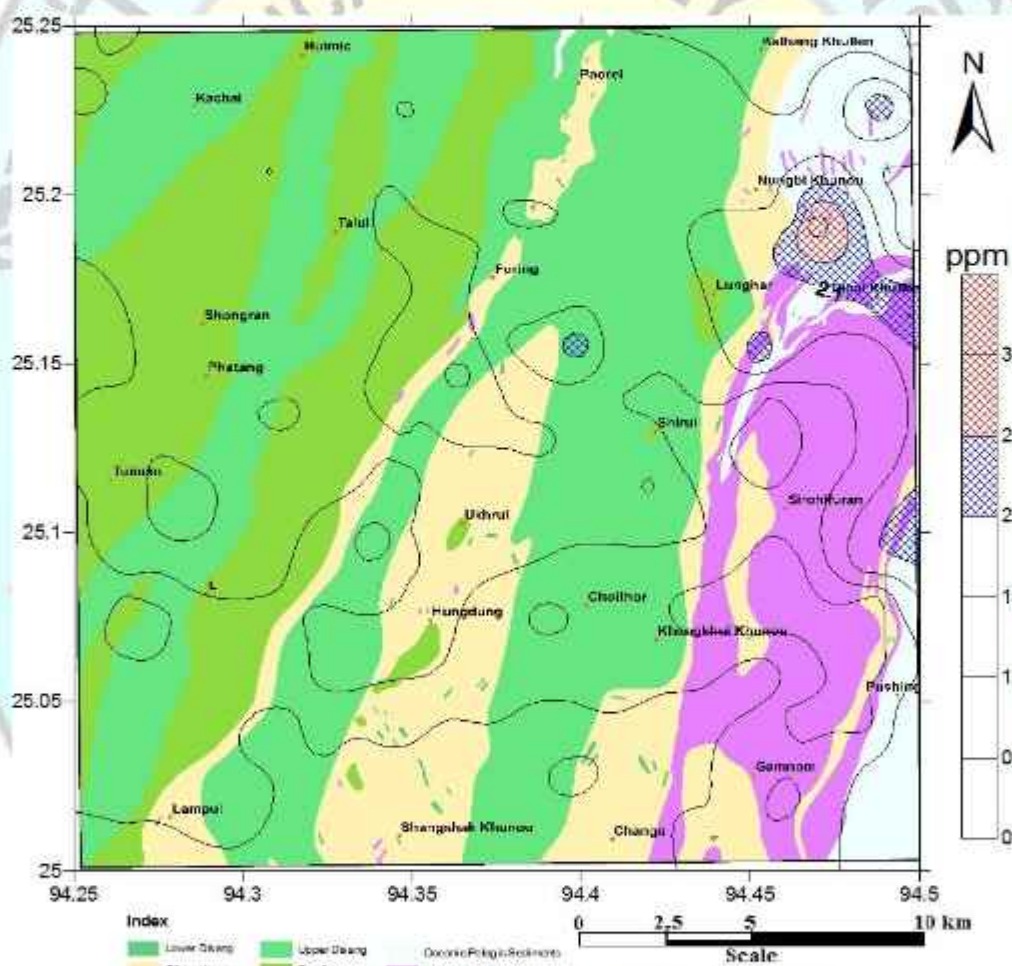


Fig.5.31b. Spatial distribution of Ta in the stream sediment/slope wash samples overlaid on geology of the study area.

Ta in stream sediment

The median value of Ta in stream sediments is 1.10 ppb with values varying from 1.13 to 4.16 ppb (Annexure-II). The higher values of Ta are observed within the OPS, with maximum value in the north eastern part of the study area in Grid No. 142 of T.S. No. 83K/8 (Fig.5.31a&b). The underlying lithology is represented by thinly interbedded marl with tuffaceous variegated shale. The distribution is positive skewness and kurtosis with values of 1.60 and 6.96 respectively. Ta shows very strong positive correlation with Nb.

5.4.22. Uranium (U):

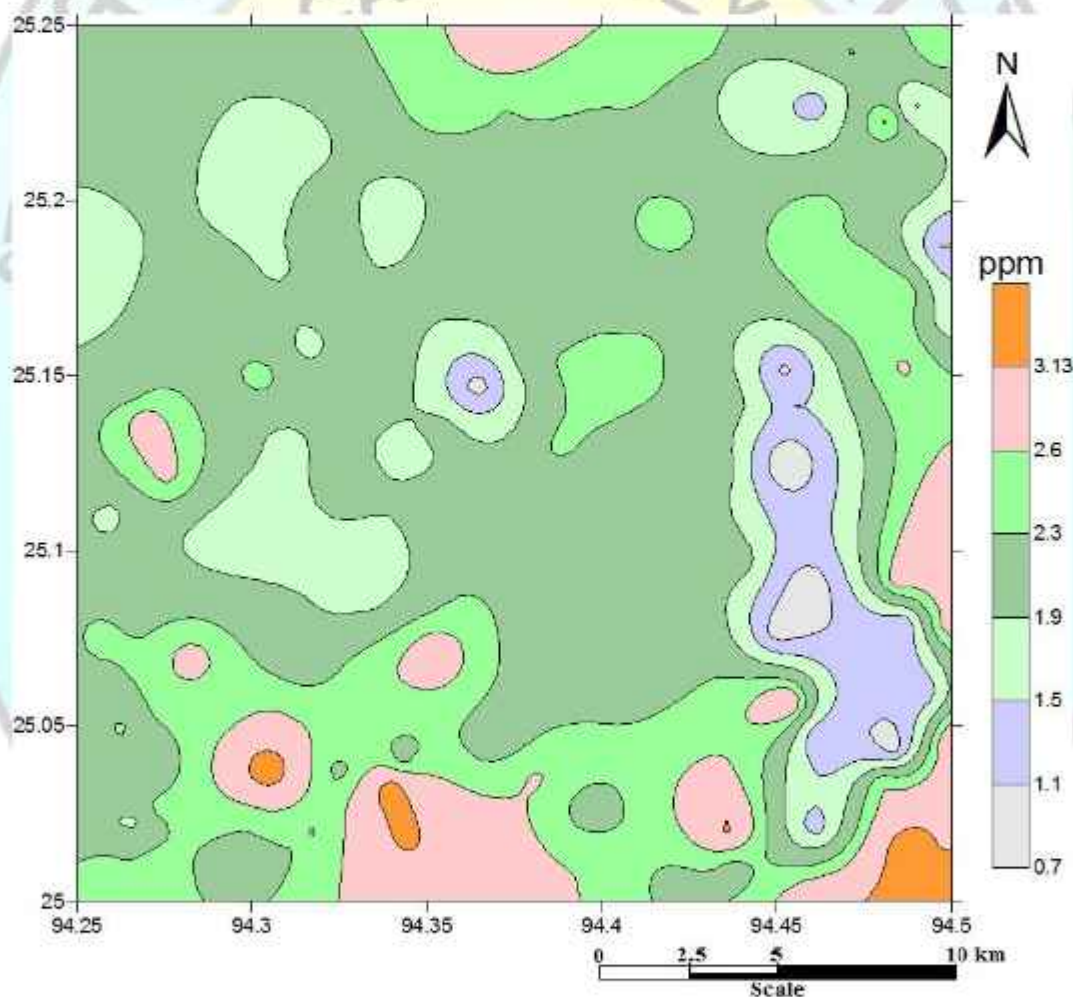


Fig. 5.32a Spatial distribution of U in the stream sediment/slope wash samples.

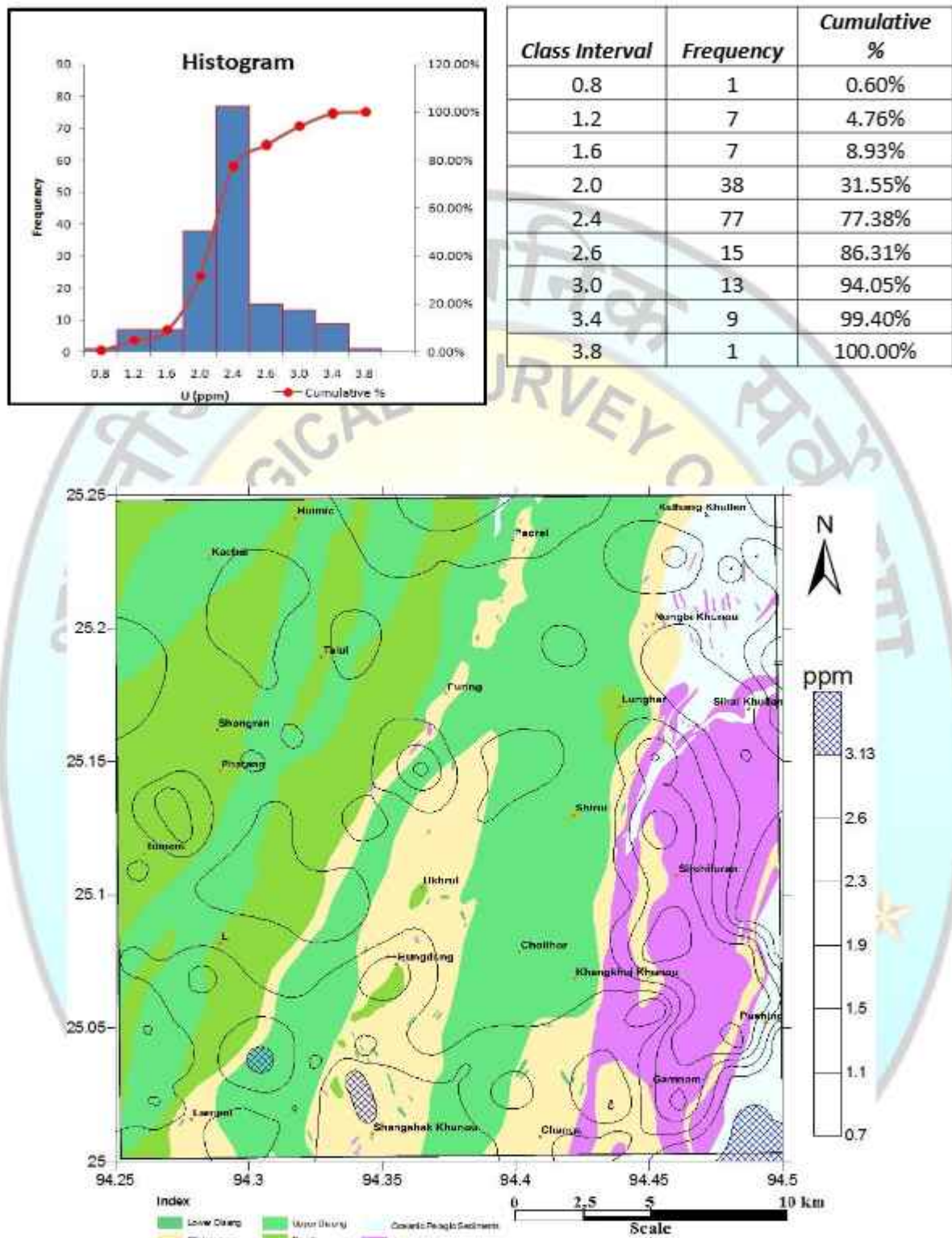


Fig.5.32b. Spatial distribution of U in the stream sediment/slope wash samples overlaid on geology of the study area.

U in stream sediment

The median value of U in stream sediments is 2.16 ppb with values varying from 0.67 ppm to 3.53 ppb (Annexure-II) showing maximum value in south western part of the study area, Grid No. 29 of T.S. No. 83K/8 where the Paleogene Disang, Olistostrome and OPS sediments are exposed (Fig. 5.32a&b). The distribution is negative skewness with values of -0.28 and positive kurtosis with values of 1.37 respectively. U shows strong positive correlation with radioactive elements like Rb and Th.

5.5. Distribution of Rare Earth Elements in the Stream Sediments:

The rare earth elements (REE) are the most useful of all trace elements and REE studies have important applications in igneous, sedimentary and metamorphic petrology. The REE comprise the series of metals with atomic numbers from 57-71 i.e. La to Lu. The REE are divided into three series as light rare earth elements (LREE: La, Ce, Pr, Nd, Pm and Sm), medium rare earth element (MREE: Eu, Gd, Tb and Dy) and heavy rare earth element (HREE: Ho, Er, Tm, Yb and Lu) depending upon the atomic numbers. All the REE form +3 ions of similar ionic radii and thus show similar physical and chemical properties. However the small but steady decrease in ionic radii with increasing atomic number is responsible for small differences in their behaviour which is exploited by a number of petrological processes causing the REE series to become fractionated relative to each other. It is this phenomenon which is used in geochemistry. The REE are regarded as amongst the least soluble trace elements and are relatively immobile during low-grade metamorphism, weathering and hydrothermal alteration. All the REEs show very strong positive correlation with other each other. The stream sediment samples show slight enrichment of LREE as compared with the MREE and HREE, with overall higher REE dispersion values confined within south eastern part of the study area. The lithofacies exposed is dominantly of thinly interbedded marl, variegated tuffaceous volcano sedimentary facies and shale.

5.5.1. Lanthanum (La):

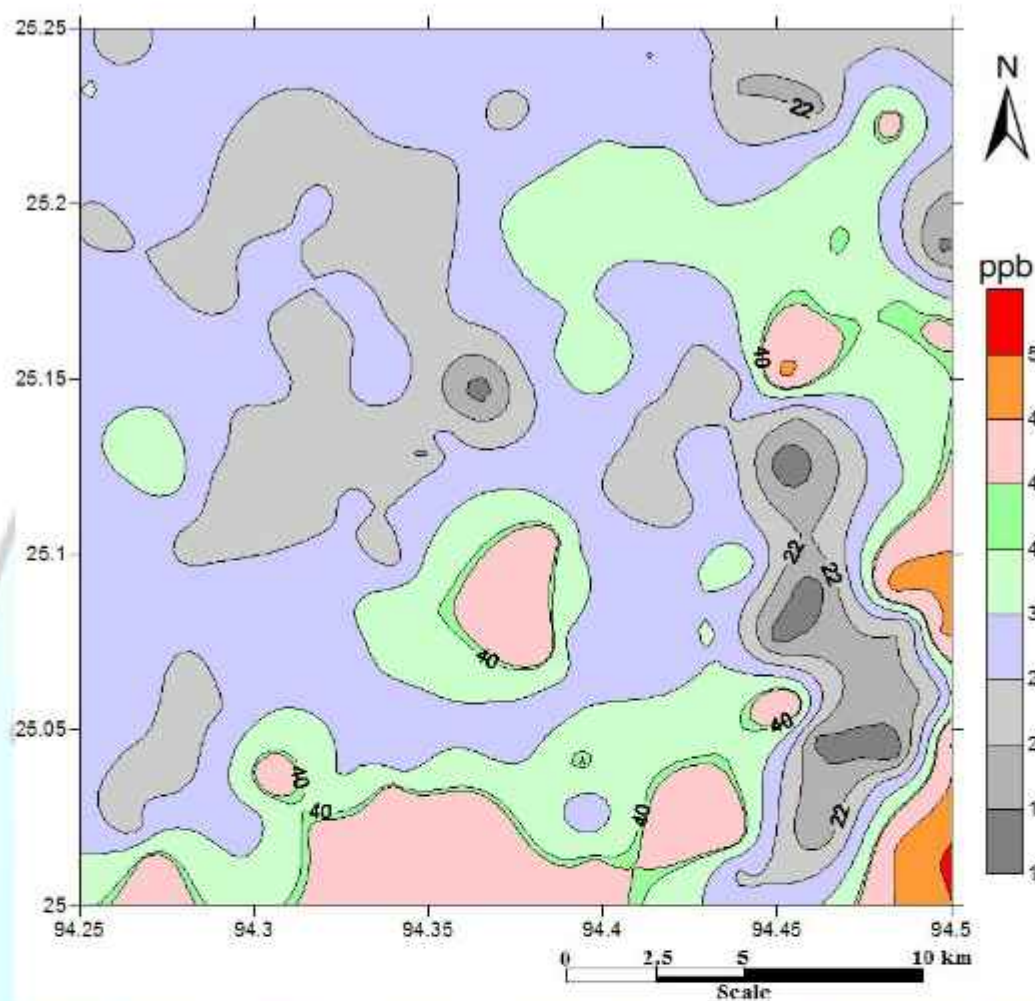


Fig.5.33a.Spatial distribution of La in the stream sediment/slope wash samples.



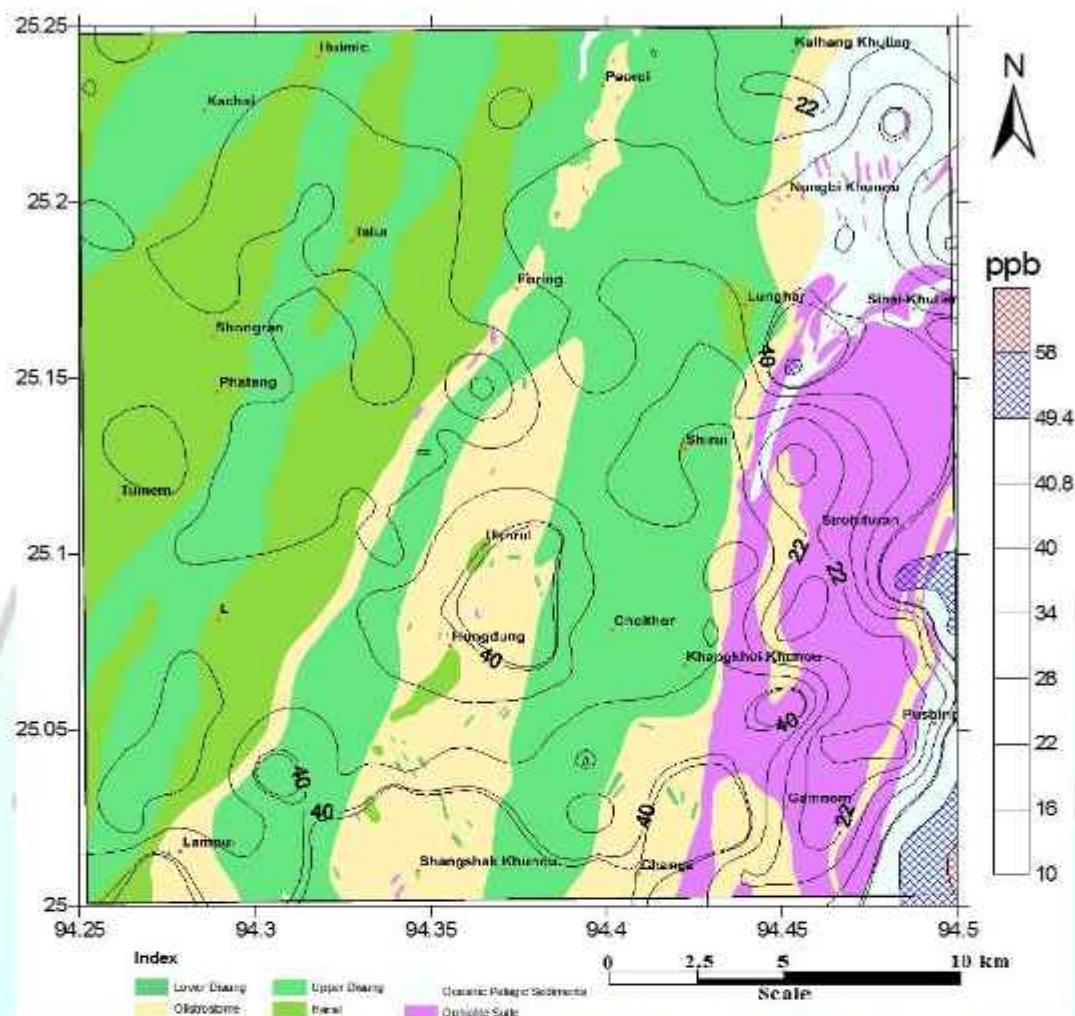


Fig.5.33b.Spatial distribution of La in the stream sediment /slope wash samples overlaid on geology of the study area.

La in stream sediment

The median value of La stream sediments is 31.01 ppb with values varying from 10.48 to 58.16 ppb (Annexure-III) showing maximum value in the south eastern corner of the study area, Grid No.13 of T.S. No. 83K/8 where rocks of ocean pelagic sediments are exposed (Fig.5.33a & b). The distribution is positive skewed with a value of 0.24 and positive kurtosis of 0.75.

5.5.2.Cerium (Ce):

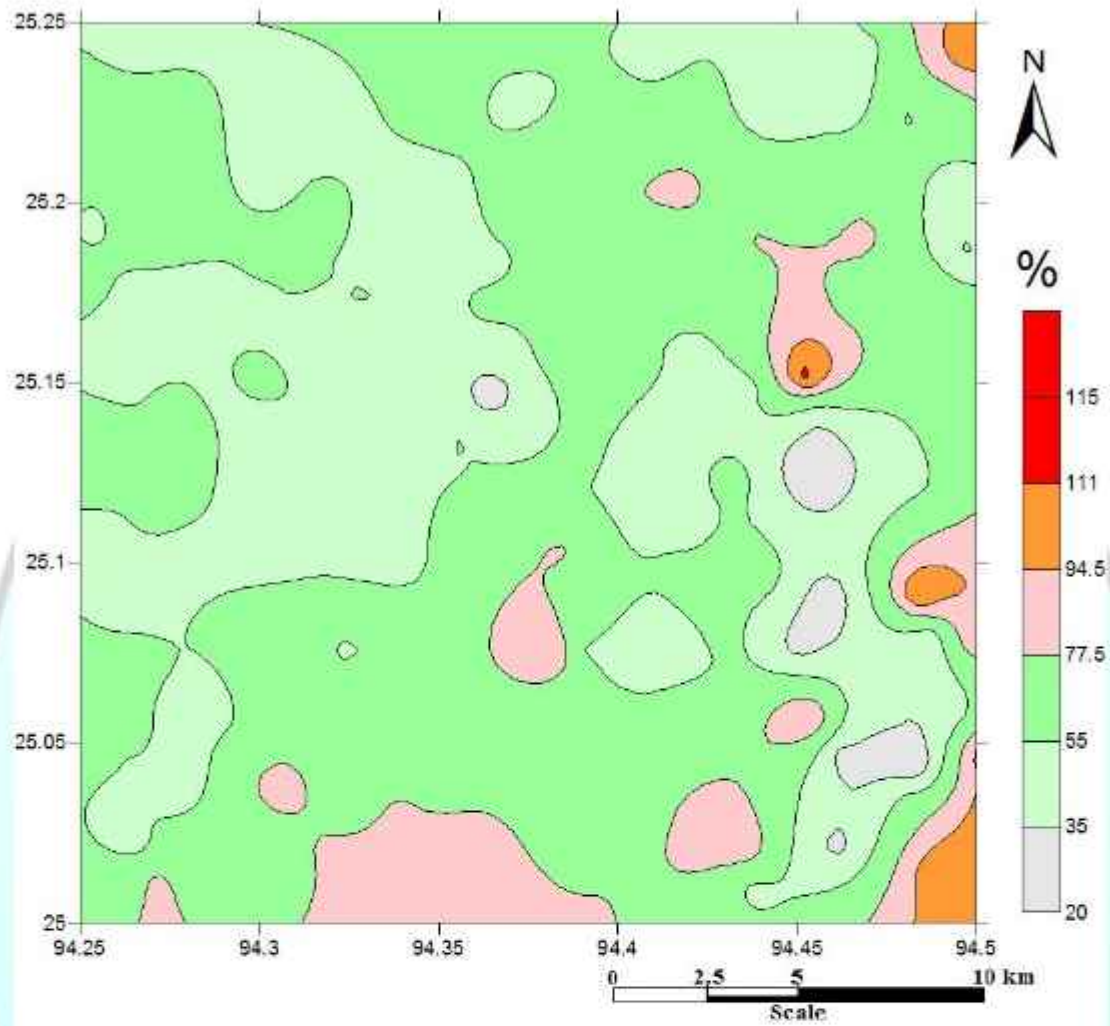
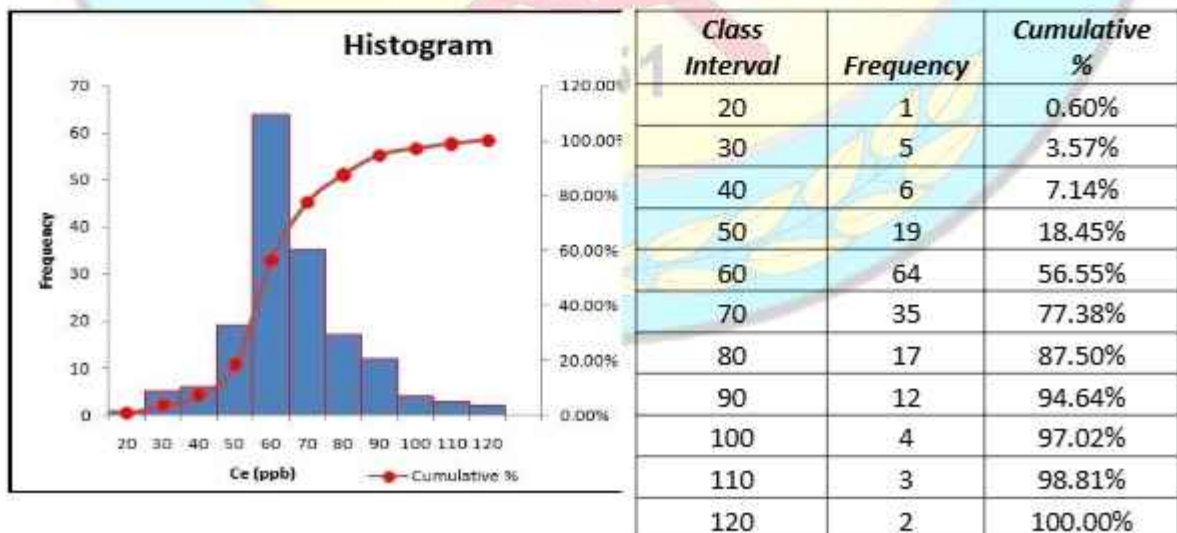


Fig.5.34a. Spatial distribution of Ce in the stream sediment /slope wash samples



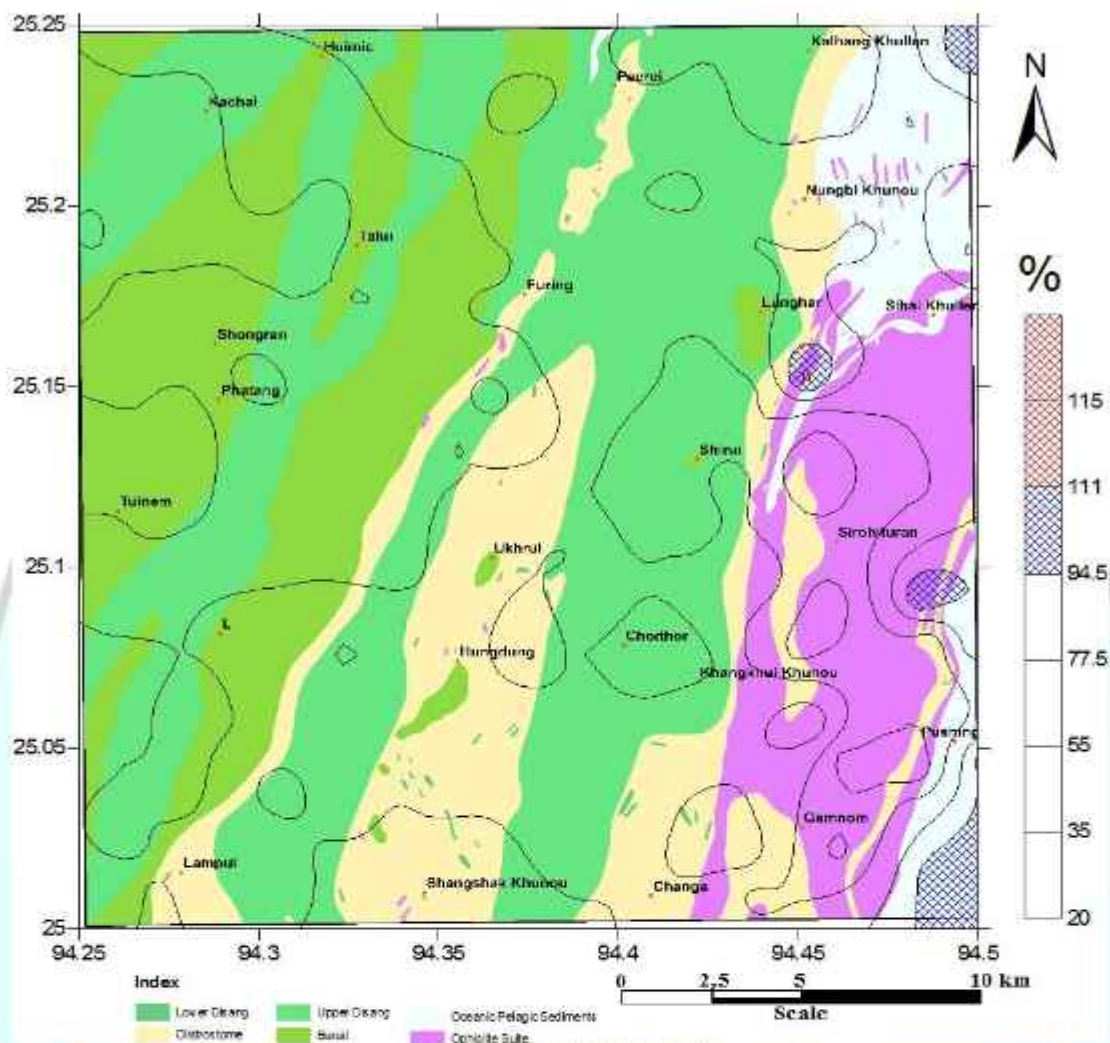


Fig.5.34b.Spatial distribution of Ce in the stream sediment /slope wash samples overlaid on geology of the study area.

Ce in stream sediment

The median value of Ce in stream sediments is 58.5 ppb with values varying from 19.02 to 119.17 ppb (Annexure-III) showing maximum value in the eastern part of the study area, Grid No. 114 of T.S. No. 83K/8 where ocean pelagic sediments and ophiolite are exposed (Fig.5.34a & b). The distribution is positive skewed with a value of 0.66 and positive kurtosis of 1.46. The concentration of Ce in finer sediments is more as the finer sediments has more surface area and adsorbed on the surface.

5.5.3. Praseodymium (Pr):

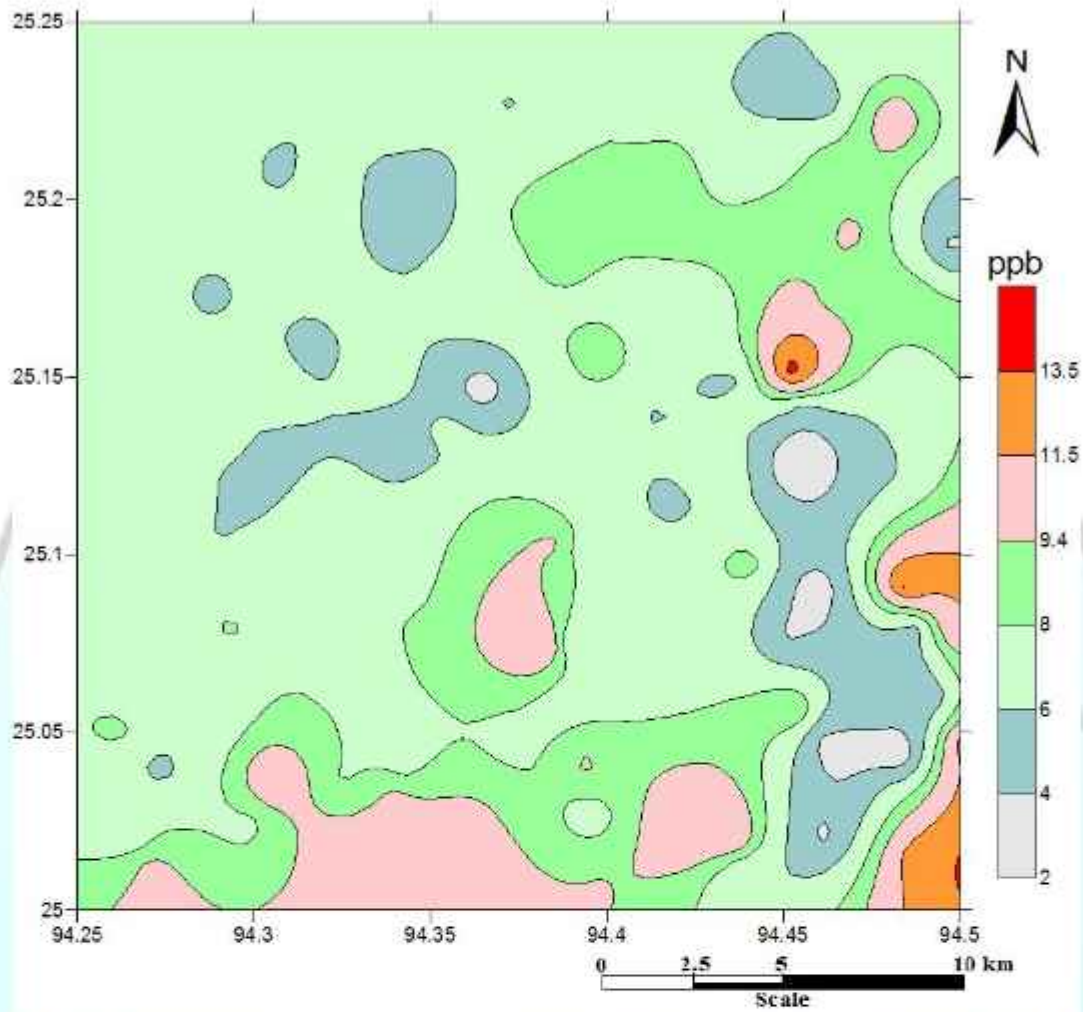
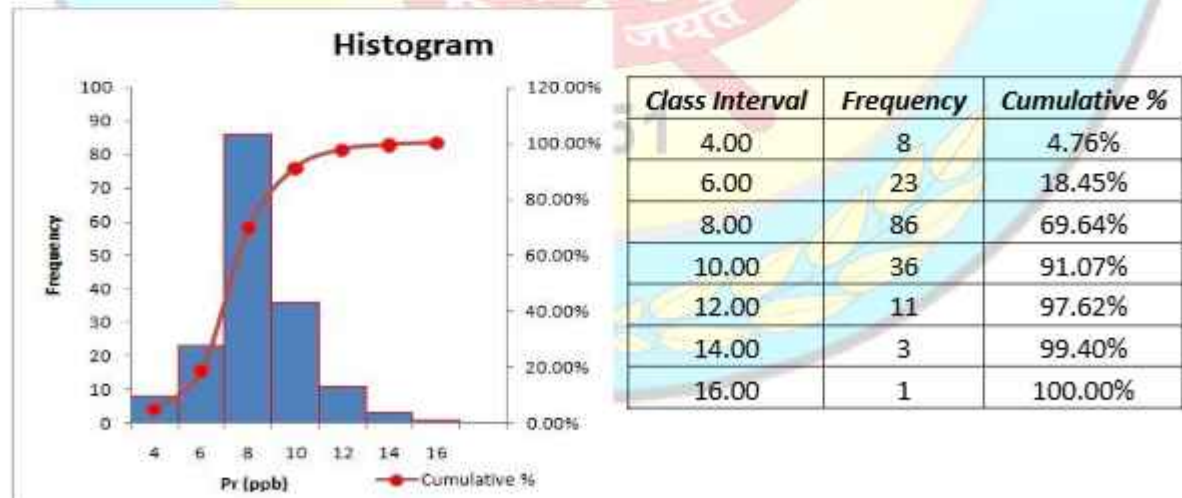


Fig.5.35a. Spatial distribution of Pr in the stream sediment/slope wash samples.



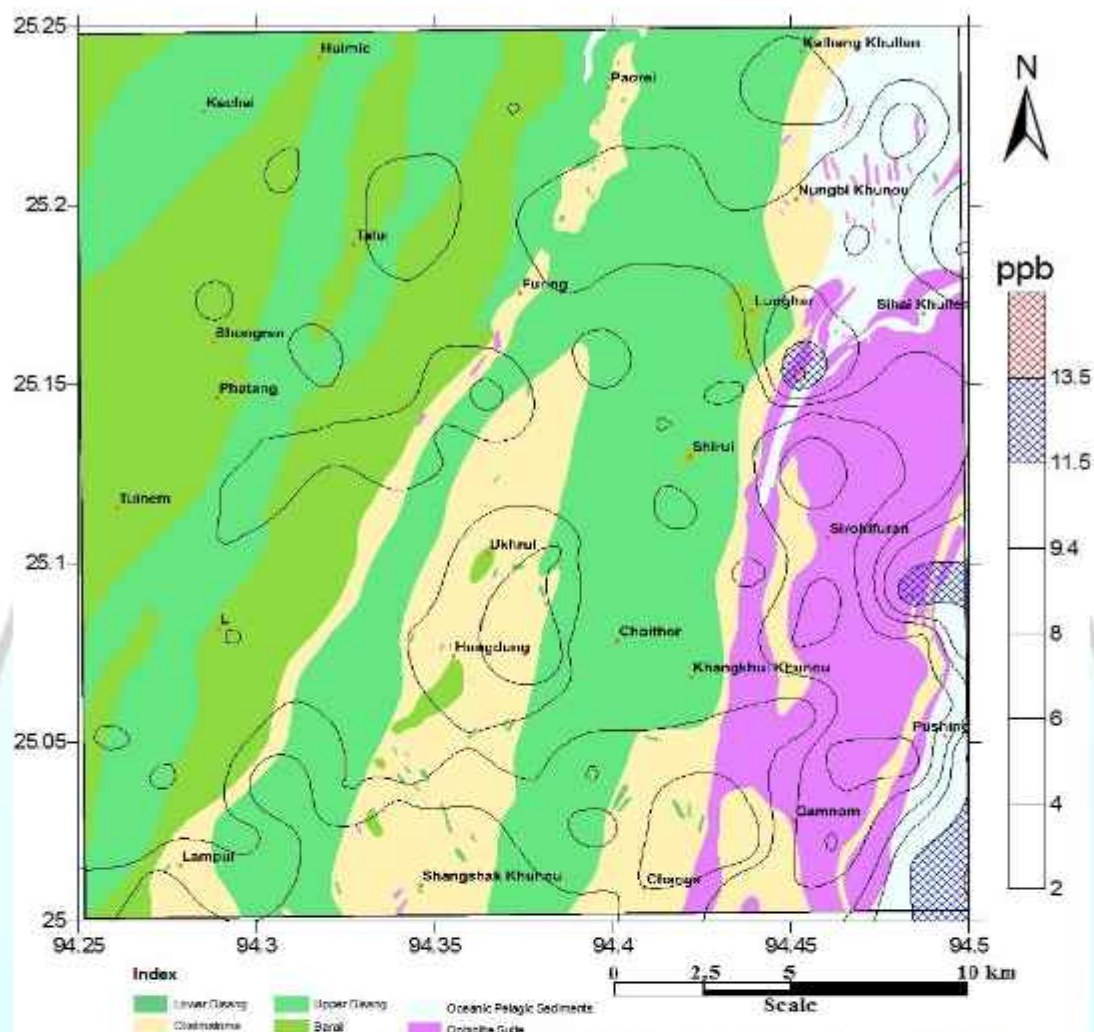


Fig.5.35b.Spatial distribution of Pr in the stream sediment/slope wash samples overlaid on geology of the study area.

Pr in stream sediment

The median value of Pr in stream sediments is 7.11 ppb with values varying from 2.07 to 14.65 ppb (Annexure-III) showing maximum value in eastern part of the study area, Grid No. 114 of T.S. No. 83K/8 where ocean pelagic sediments and ophiolite are exposed (Fig.5.35b). The distribution is positive skewed with a value of 0.53 and positive kurtosis of 1.56. The distribution map shows uniform and moderate distribution (Fig. 5.35a).

5.5.4. Neodymium (Nd):

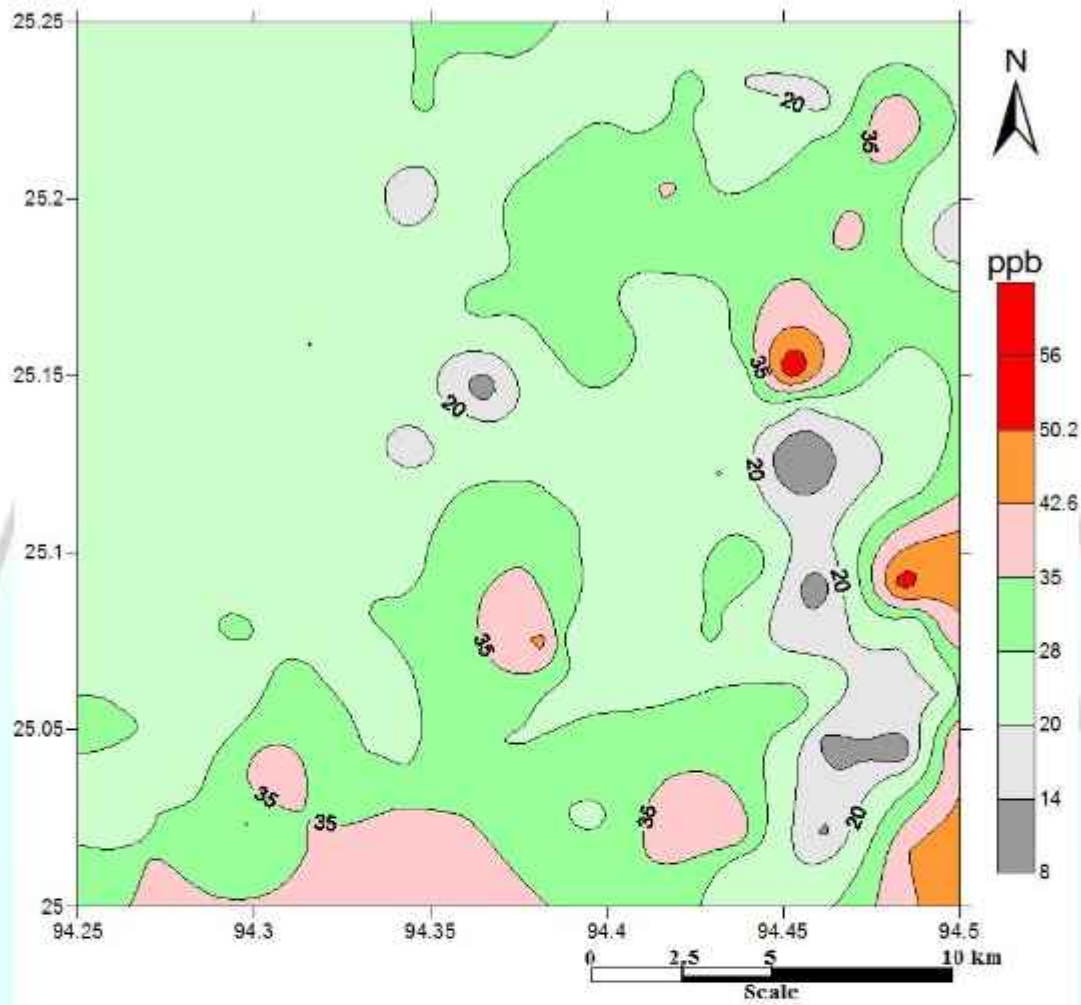
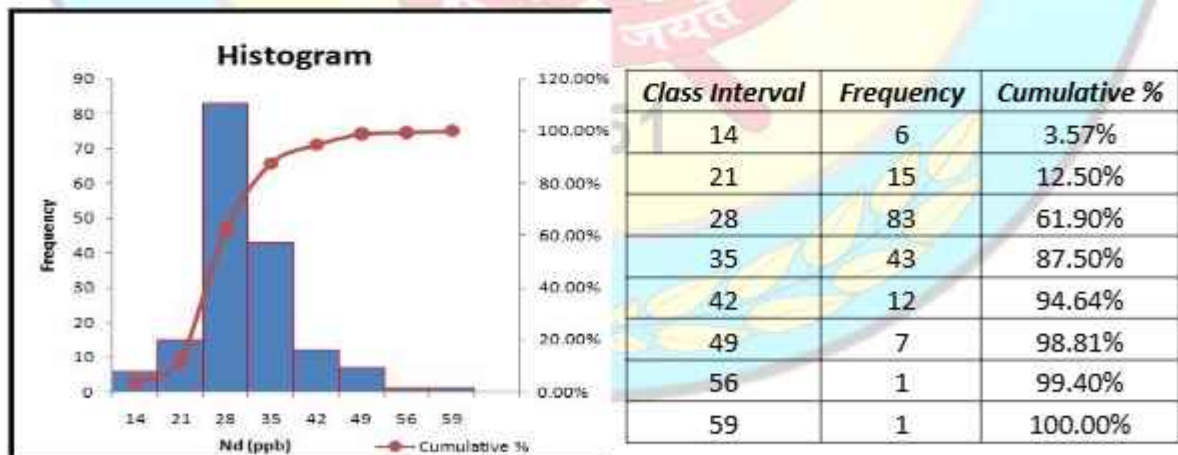


Fig 5.36a. Spatial distribution of Nd in the stream sediment/slope wash samples.



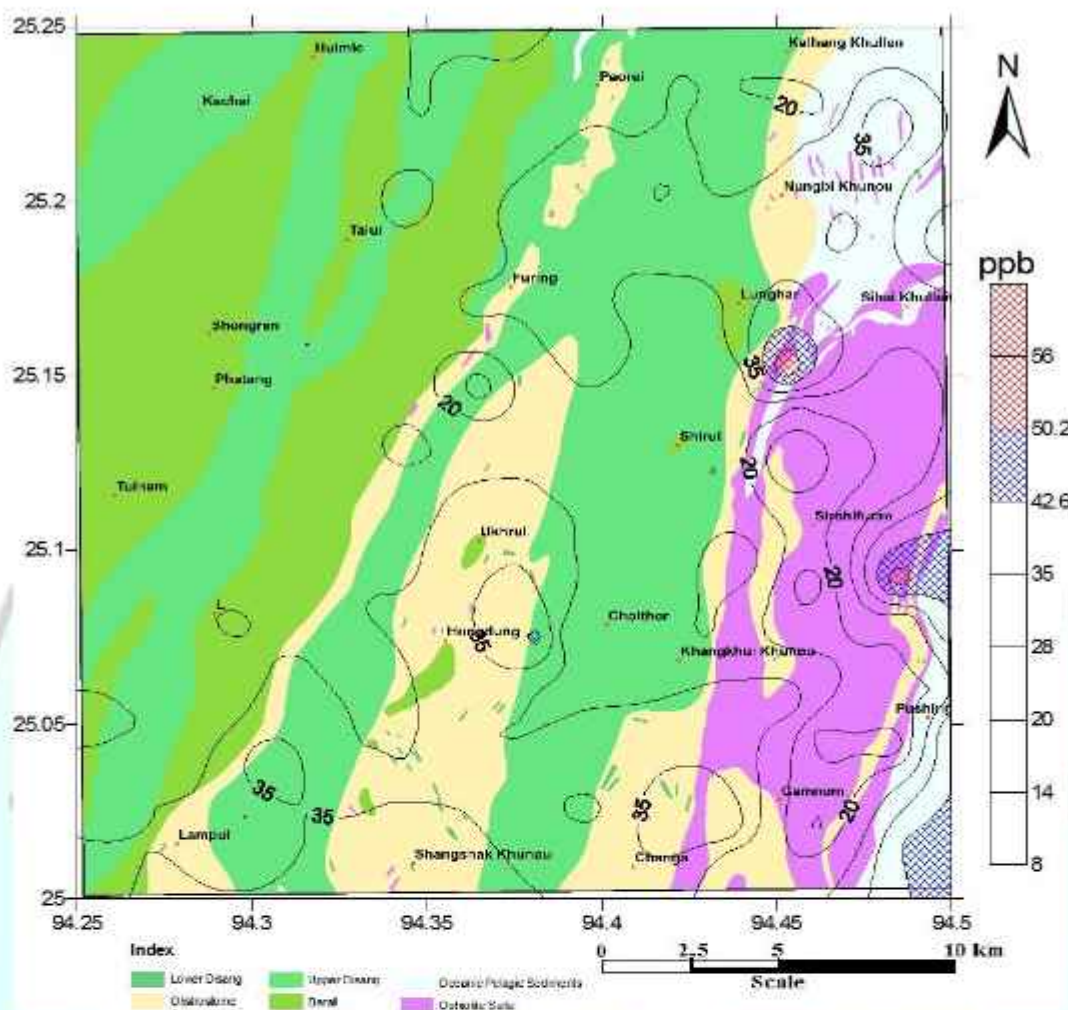


Fig.5.36b. Spatial distribution of Nd in the stream sediment /slope wash samples overlaid on geology of the study area.

Nd in stream sediment

The median value of Nd in stream sediments is 26.2 ppb with values varying from 7.54 to 58.80 ppb (Annexure-III) showing maximum value in the eastern part of the study area, Grid No. 114 of T.S. No. 83K/8 where ocean pelagic sediments and ophiolite are exposed (Fig.5.36b). The distribution is positive skewed with a value of 0.78 and positive kurtosis of 2.5. The Nd distribution map shows moderate values throughout the area as shown in Fig. 5.36a.

5.5.5. Samarium (Sm):

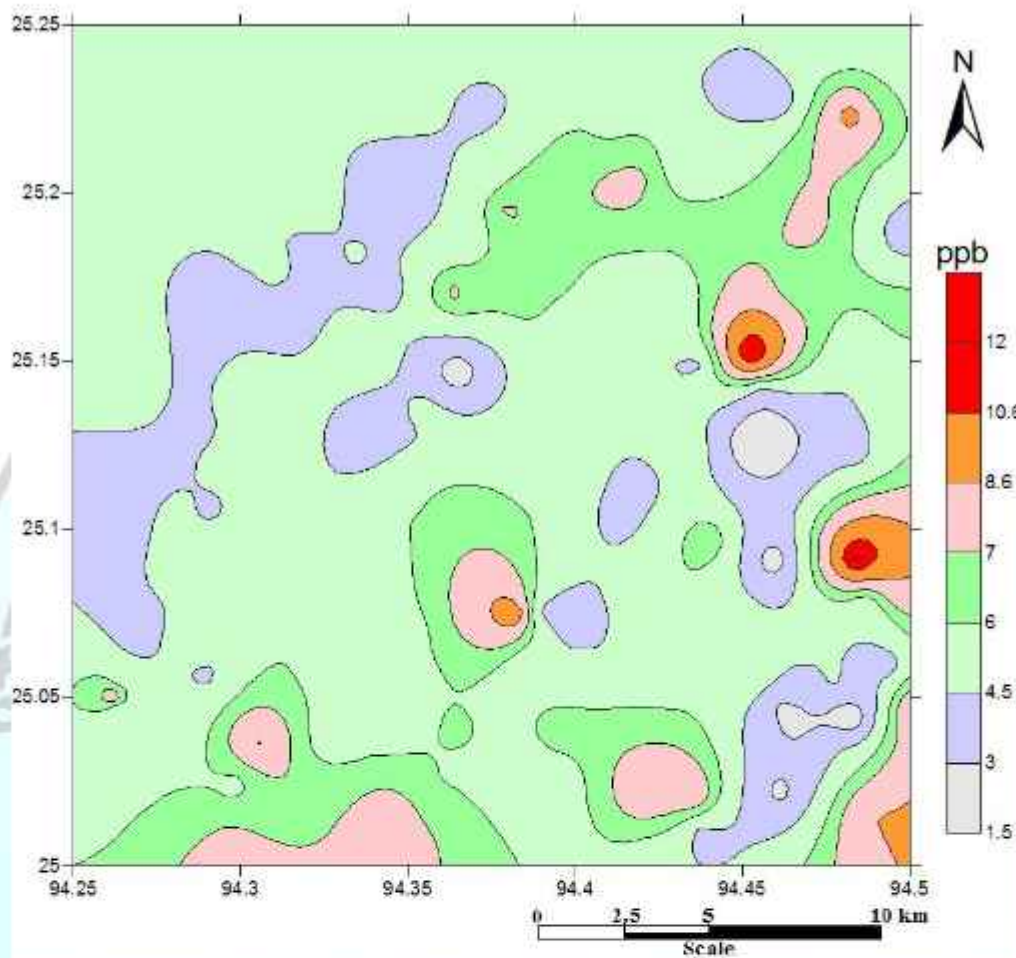
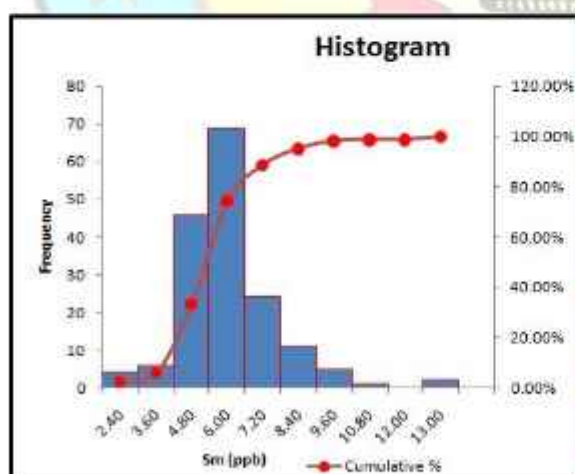


Fig.5.37a Spatial distribution of Sm in the stream sediment/slope wash samples.



Class Interval	Frequency	Cumulative %
2.40	4	2.38%
3.60	6	5.95%
4.80	46	33.33%
6.00	69	74.40%
7.20	24	88.69%
8.40	11	95.24%
9.60	5	98.21%
10.80	1	98.81%
12.00	0	98.81%
13.00	2	100.00%

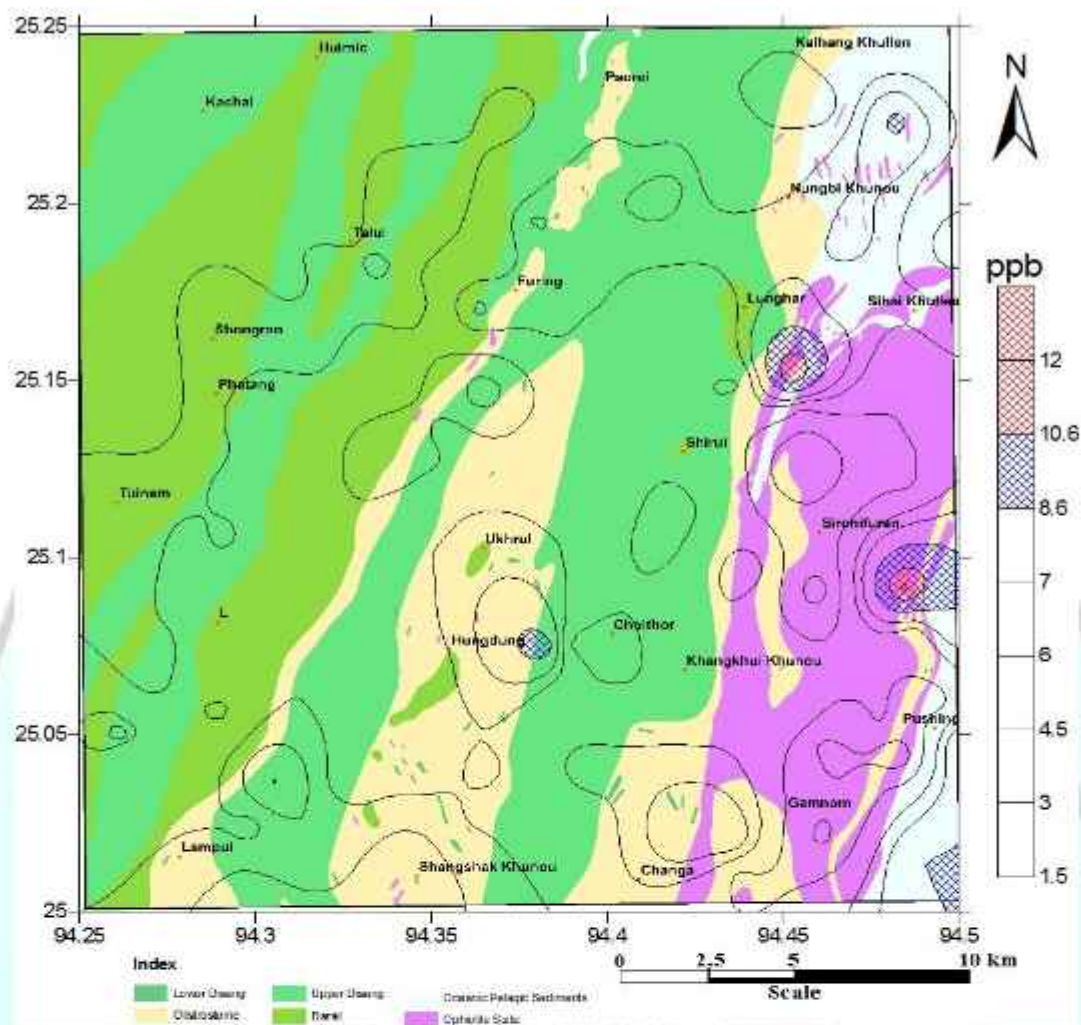


Fig.5.37b.Spatial distribution of Sm in the stream sediment/slope wash samples overlaid on geology of the study area.

Sm in stream sediment

The median value of Sm in stream sediments is 31.01 ppb with values varying from 1.50 to 12.73 ppb (Annexure-II) showing maximum value in the eastern part of the study area, Grid No. 115 of T.S. No. 83K/8 where rocks of OPS and Ophiolite are exposed (Fig. 5.37b). The distribution is positive skewed with a value of 1.25 and positive kurtosis of 4.41. The distribution map shows uniform and normal distribution throughout the study area (Fig. 5.37a).

5.5.6. Europium (Eu):

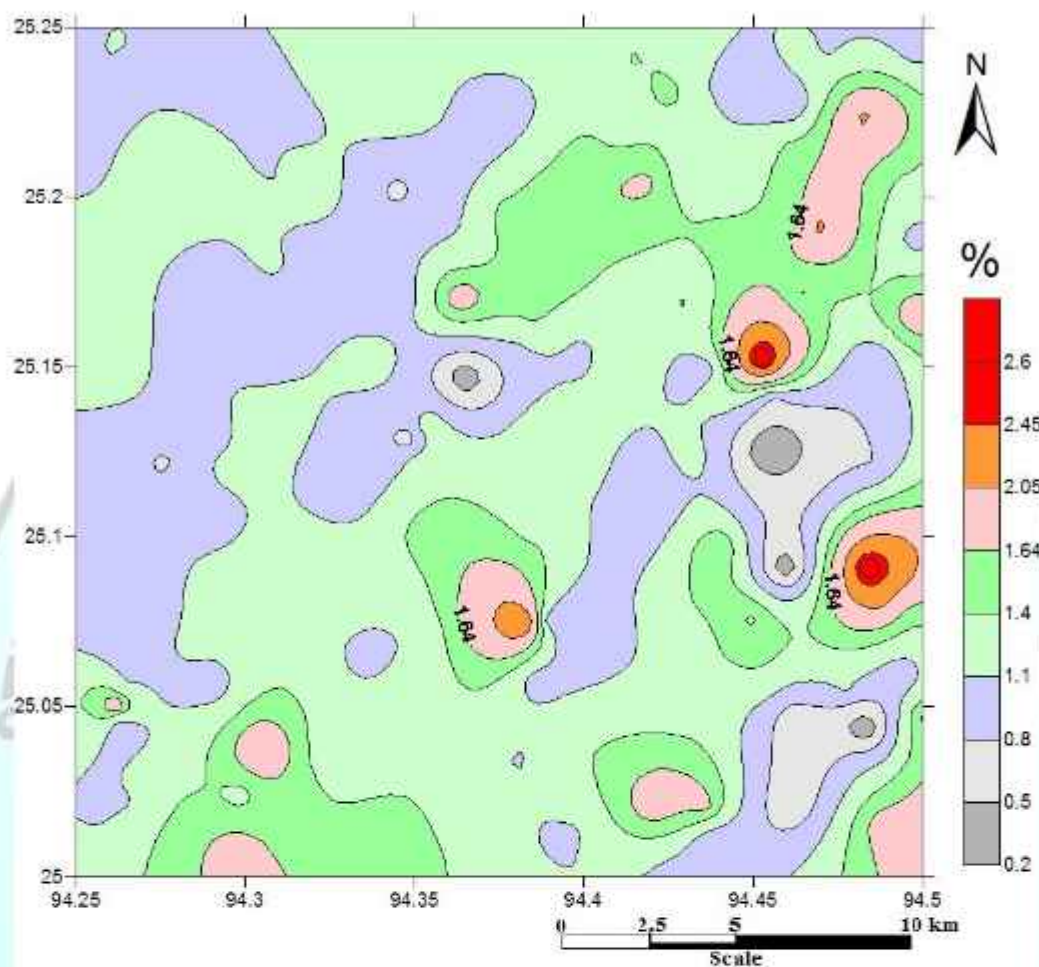
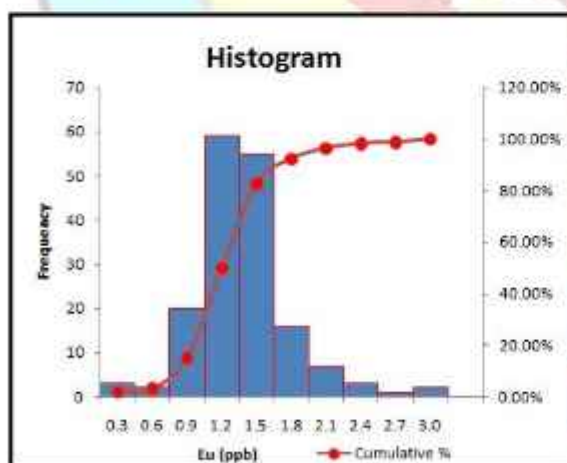


Fig.5.38a. Spatial distribution of Eu in the stream sediment/slope wash Samples.



Class Interval	Frequency	Cumulative %
0.3	3	1.79%
0.6	2	2.98%
0.9	20	14.88%
1.2	59	50.00%
1.5	55	82.74%
1.8	16	92.26%
2.1	7	96.43%
2.4	3	98.21%
2.7	1	98.81%
3.0	2	100.00%

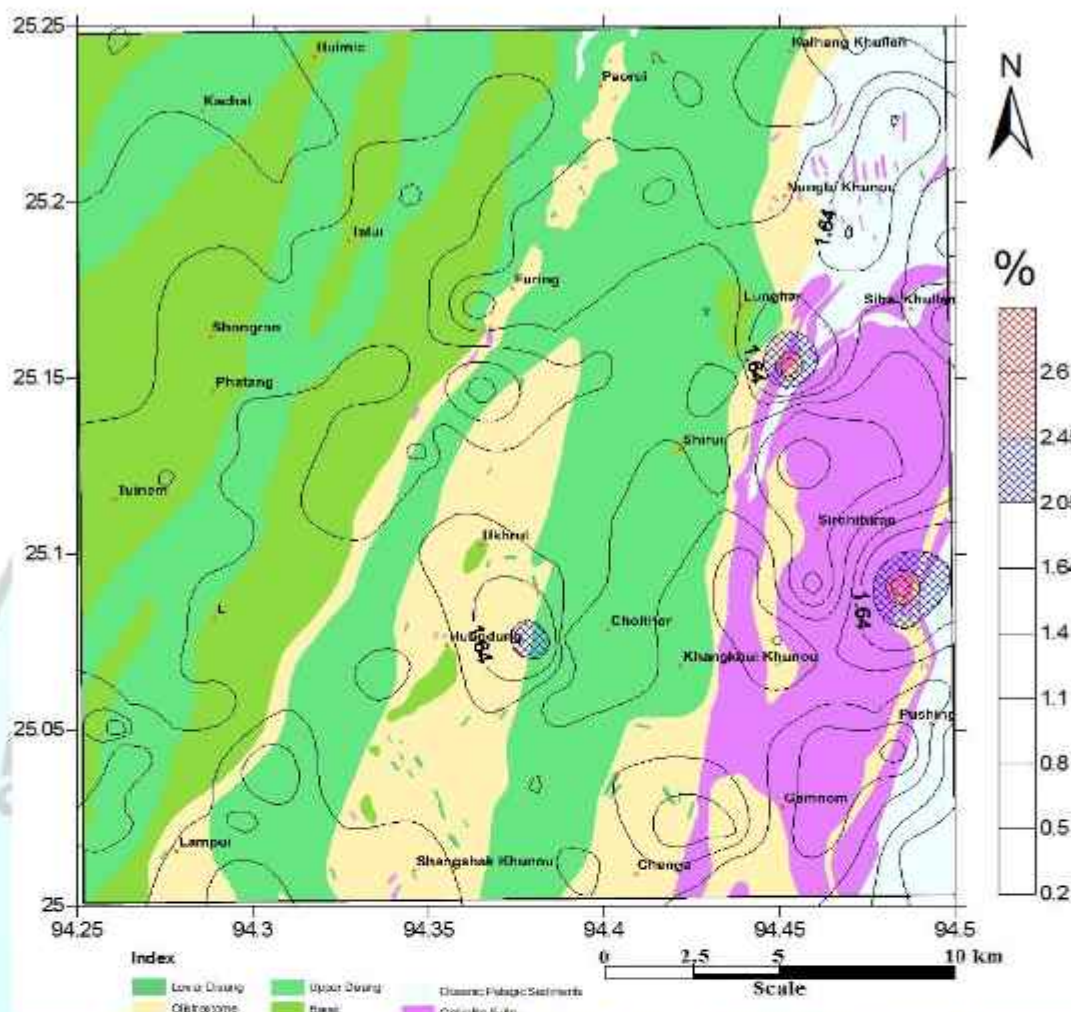


Fig.5.38b.Spatial distribution of Eu in the stream sediment/slope wash Samples overlaid on geology of the study area.

Eu in stream sediment

The median value of Eu in stream sediments is 1.20 ppb with values varying from 0.25 ppb to 2.97 ppb (Annexure-III) showing maximum value in the eastern part of the study area, Grid No. 114 of T.S. No. 83K/8 where Barail Group of rocks are exposed (Fig.5.38b). The distribution is positive skewed with a value of 1.004 and positive kurtosis of 3.23.

The distribution map shows relatively moderate values with uniform distribution in major part of the area (Fig. 5.39a). Eu is strongly fractionated into feldspar during fractional crystallisation of magma.

5.5.7. Gadolinium (Gd):

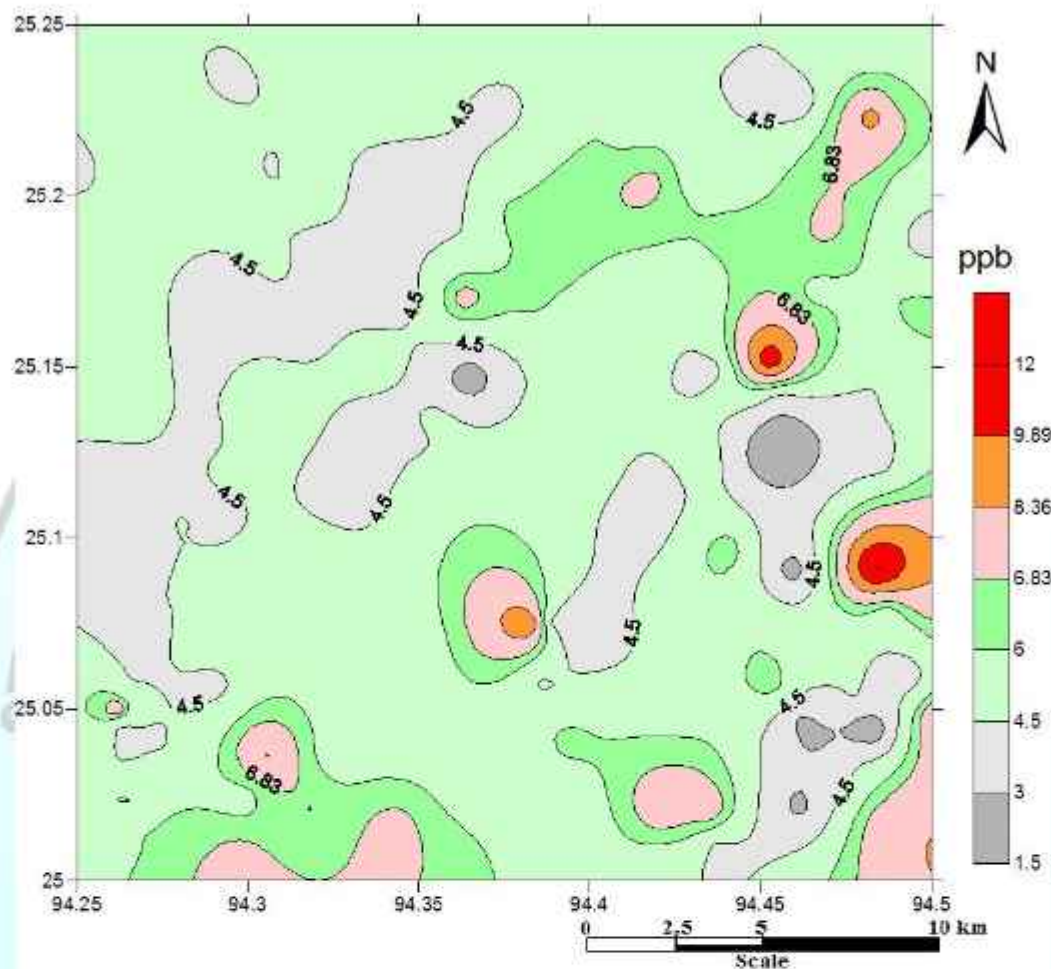
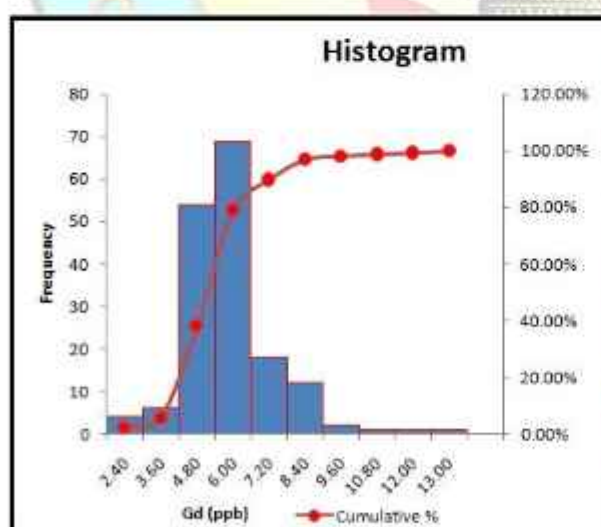


Fig.5.39a Spatial distribution of Gd in the stream sediment/slope wash Samples



Class Interval	Frequency	Cumulative %
2.40	4	2.38%
3.60	6	5.95%
4.80	54	38.10%
6.00	69	79.17%
7.20	18	89.88%
8.40	12	97.02%
9.60	2	98.21%
10.80	1	98.81%
12.00	1	99.40%
13.00	1	100.00%

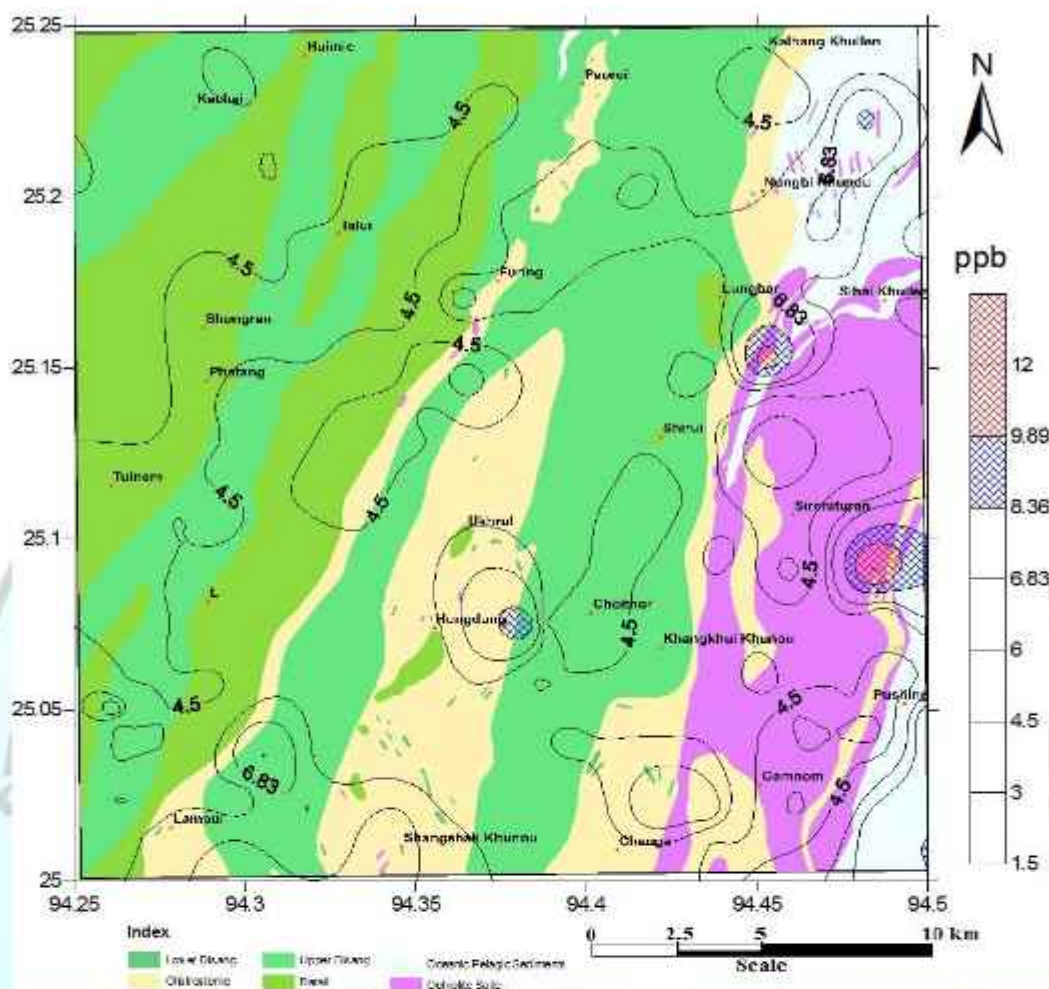


Fig.5.39b.Spatial distribution of Gd in the stream sediment/slope wash samples overlaid on geology of the study area.

Gd in stream sediment

The median value of Gd in stream sediments is 5.12ppb with values varying from 1.5 to 12.65ppm (Annexure-III) showing maximum value in the eastern part of the study area, Grid No. 114 of T.S. No. 83K/8 where rocks of ophiolite are exposed (Fig.5.39b). The distribution is positive skewed with a value of 1.26 and positive kurtosis of 4.30.

Gd shows uniform and relatively low distribution throughout the area (Fig. 5.39a).

5.5.8. Terbium (Tb):

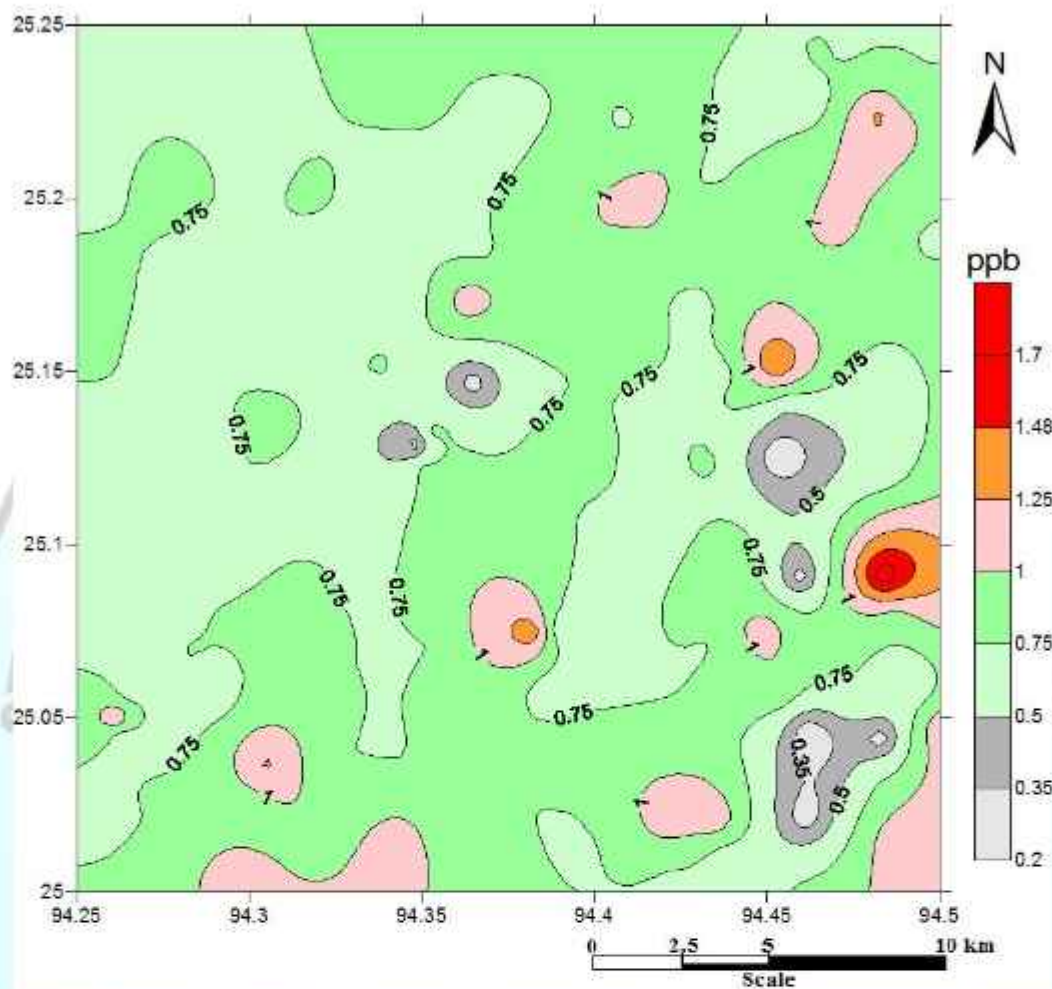
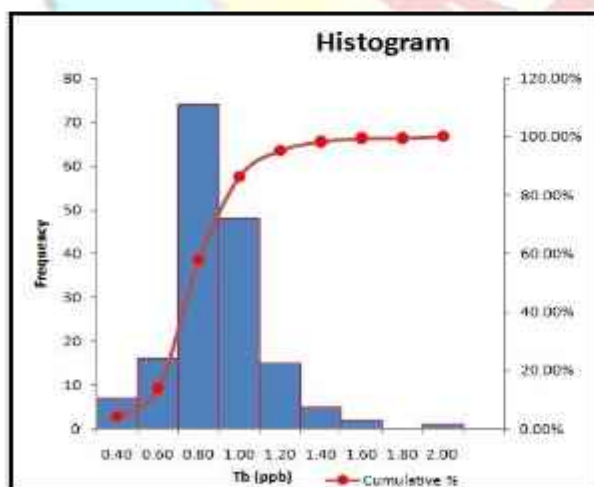


Fig.5.40a. Spatial distribution of Tb in the stream sediment/slope wash samples



Class Interval	Frequency	Cumulative %
0.40	7	4.17%
0.60	16	13.69%
0.80	74	57.74%
1.00	48	86.31%
1.20	15	95.24%
1.40	5	98.21%
1.60	2	99.40%
1.80	0	99.40%
2.00	1	100.00%

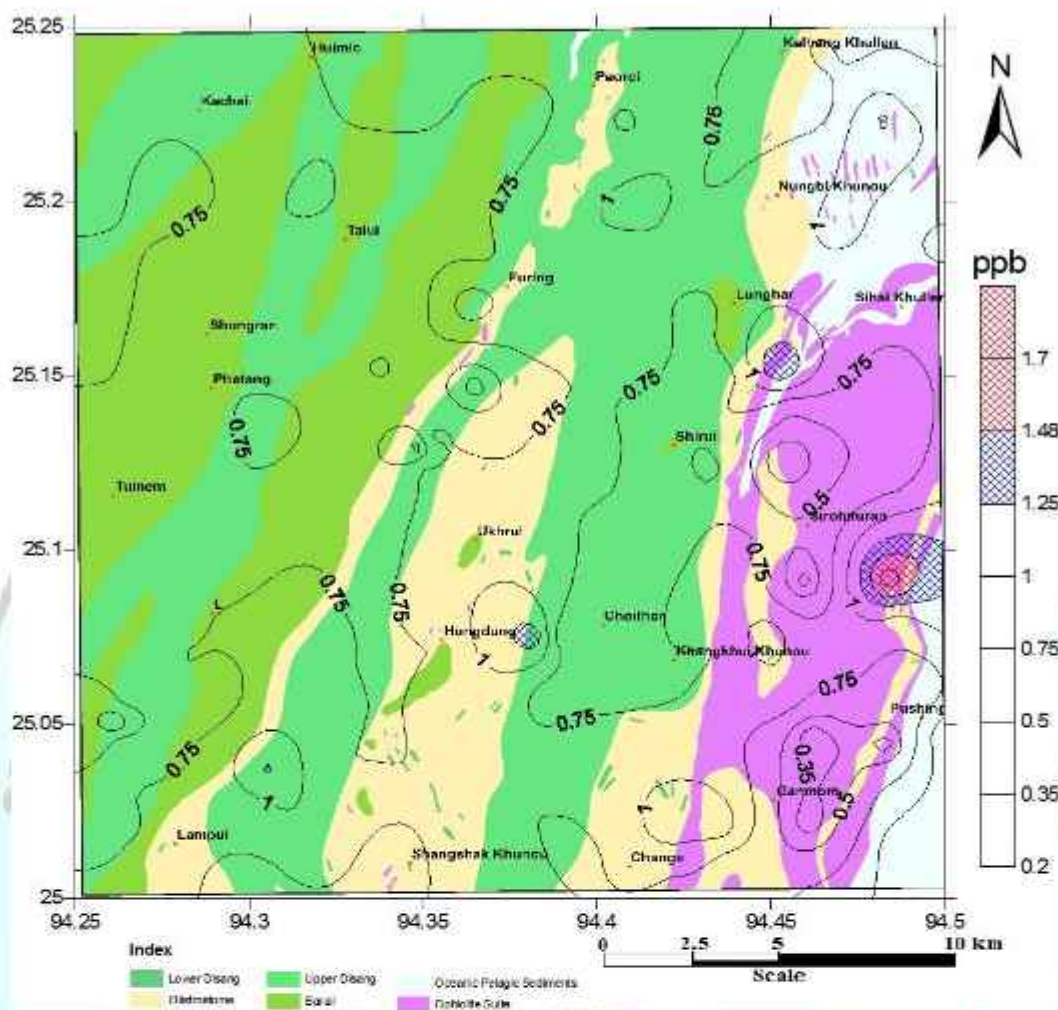


Fig 5.40b. Spatial distribution of Tb in the stream sediment/slope wash samples overlaid on geology of the study area.

Tb in stream sediment

The median value of Tb in stream sediments is 0.76 ppb with values varying from 0.22 to 1.90 ppb (Annexure-III) showing maximum value in eastern part of the study area, Grid No. 77 of T.S. No. 83K/8, where the ophiolite rocks are exposed (Fig.5.40b). The distribution is positive skewness and kurtosis with values of 0.88 and 3.69 respectively. Tb shows uniform and relatively low distribution throughout the area (Fig. 5.40a).

5.5.9. Dysprosium (Dy):

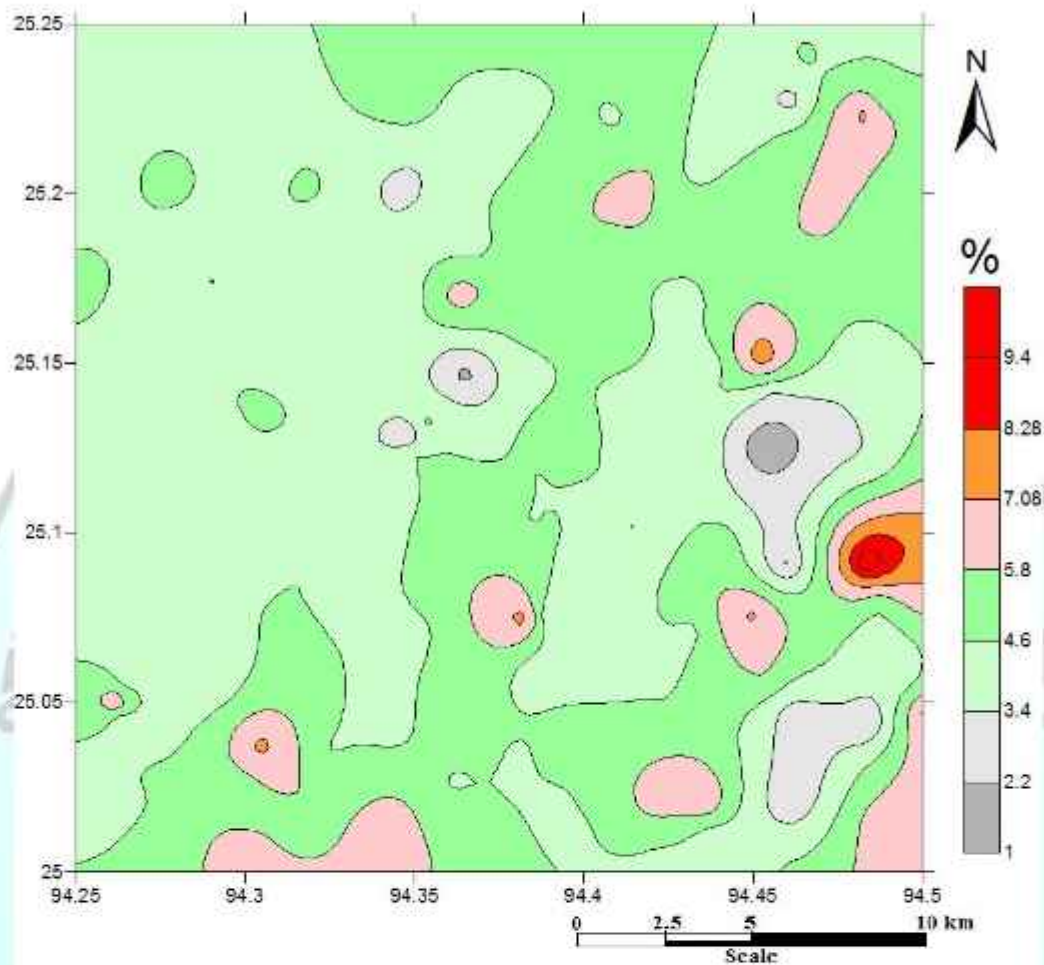
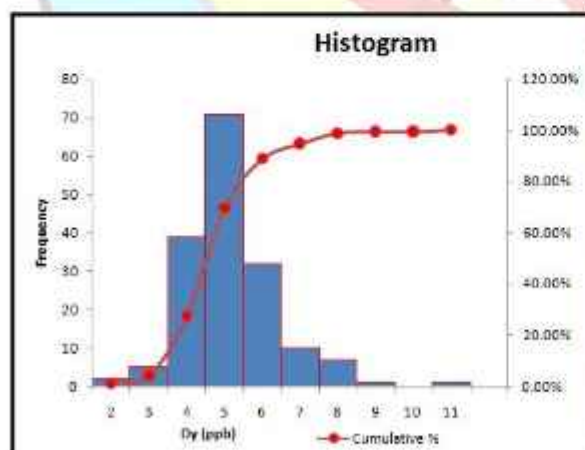


Fig.5.41a. Spatial distribution of Dy in the stream sediment/slope wash samples



Class Interval	Frequency	Cumulative %
2	2	1.19%
3	5	4.17%
4	39	27.38%
5	71	69.64%
6	32	88.69%
7	10	94.64%
8	7	98.81%
9	1	99.40%
10	0	99.40%
11	1	100.00%

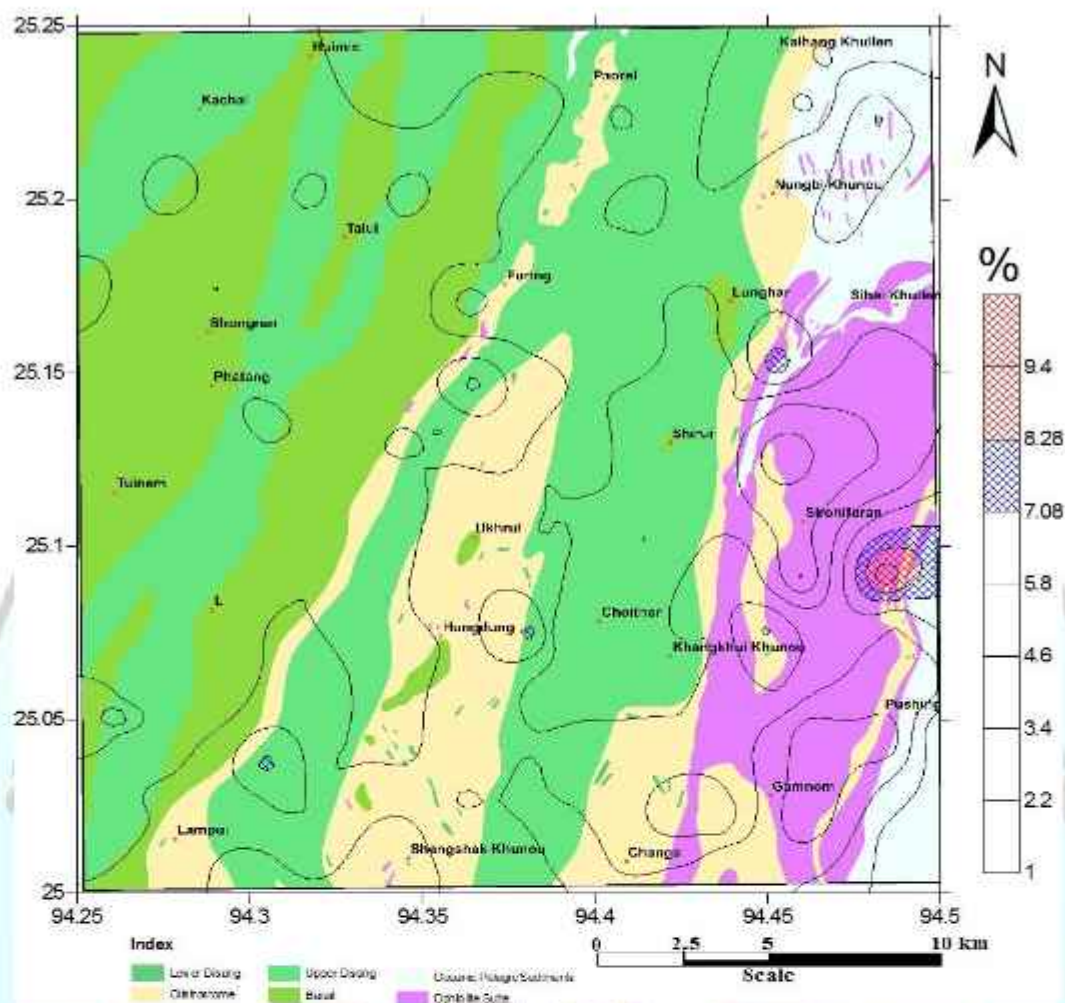


Fig.5.41b.Spatial distribution of Dy in the stream sediment/slope wash samples overlaid on geology of the study area.

Dy in stream sediment

The median value of Dy in stream sediments is 4.53 ppb with values varies from 1.30 to 10.56 ppb (Annexure-III) showing maximum value in the eastern part of the study area, Grid No. 77 of T.S. No. 83K/8, where the ophiolite rocks are exposed (Fig.5.41b). The distribution is positive skewness and kurtosis with values of 0.98 and 3.55 respectively. Tb shows uniform and relatively low distribution throughout the area (Fig. 5.41a).

5.5.10. Holmium (Ho):

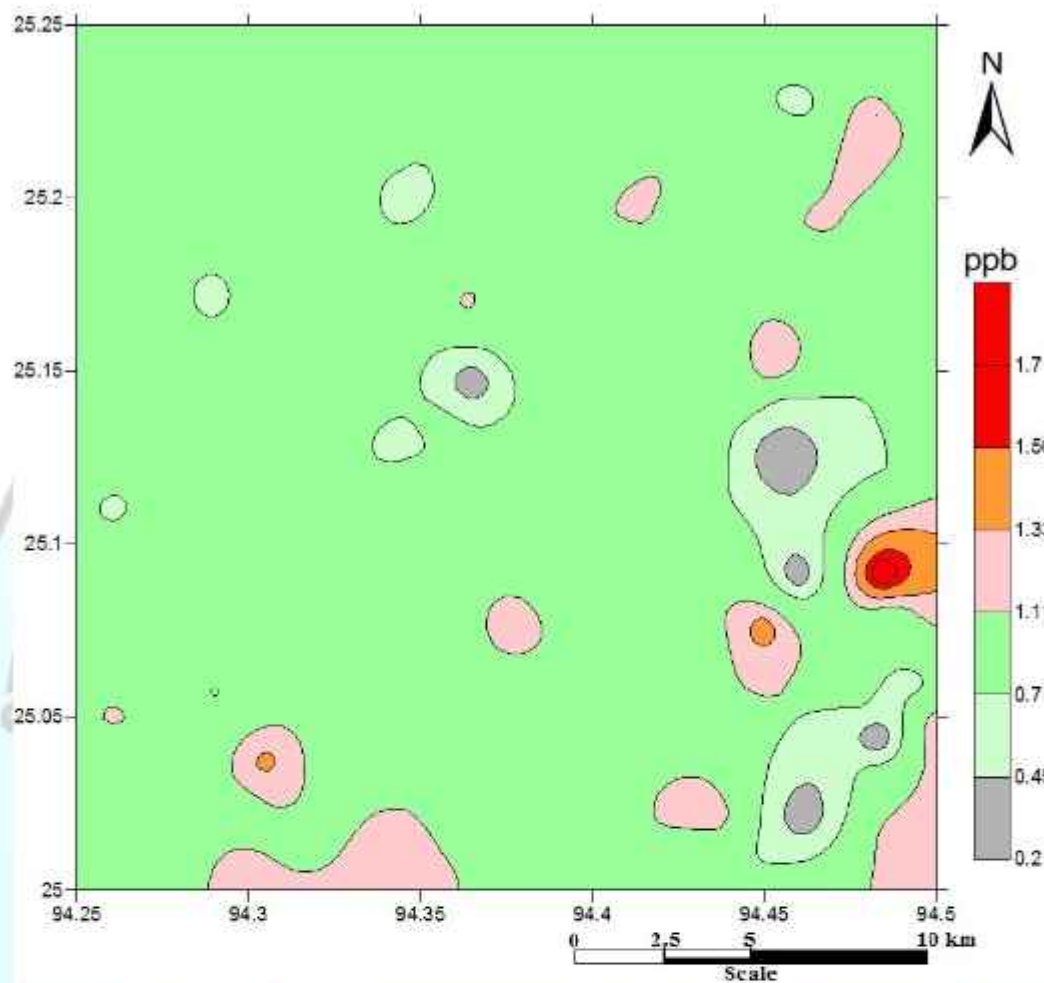
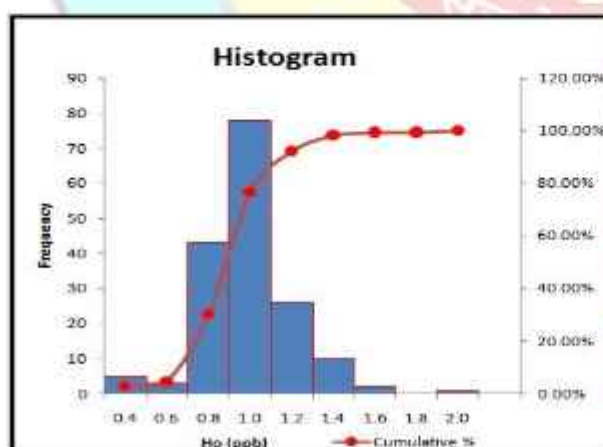


Fig.5.42a Spatial distribution of Ho in the stream sediment/slope wash samples



Class Interval	Frequency	Cumulative %
0.4	5	2.98%
0.6	3	4.76%
0.8	43	30.36%
1.0	78	76.79%
1.2	26	92.26%
1.4	10	98.21%
1.6	2	99.40%
1.8	0	99.40%
2.0	1	100.00%

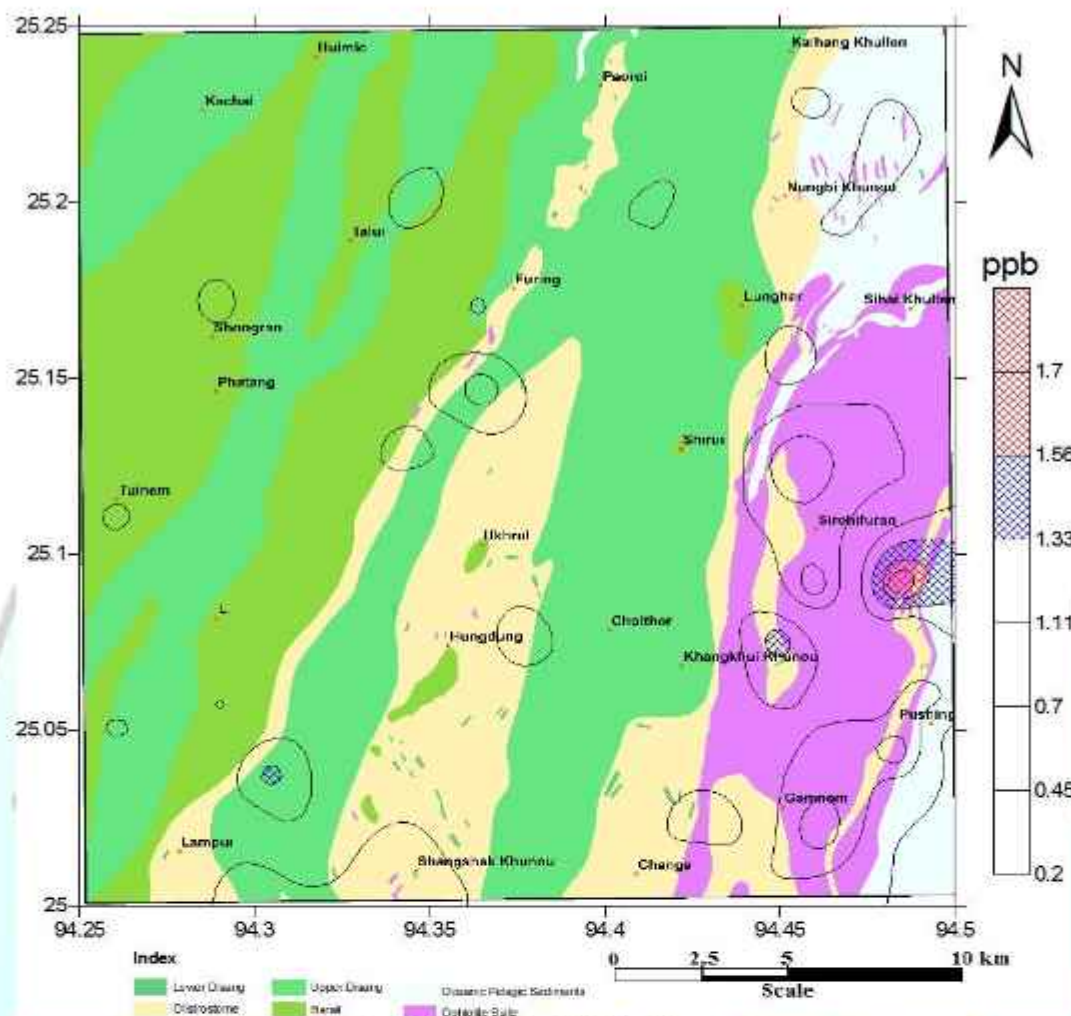


Fig.5.42b. Spatial distribution of Ho in the stream sediment/slope wash samples overlaid on geology of the study area.

Ho in stream sediment

The median value of Ho in stream sediments is 0.89 ppb with values varying from 0.25 to 1.94 ppb (Annexure-III) showing maximum value in the eastern part of the study area, Grid No. 77 of T.S. No. 83K/8 where rocks of ophiolite are exposed (Fig.5.42b). The distribution is positive skewness and kurtosis with values of 12.95 and 167.73 respectively. Ho shows uniform and relatively low distribution throughout the area (Fig.5.42a).

5.5.11. Erbium (Er):

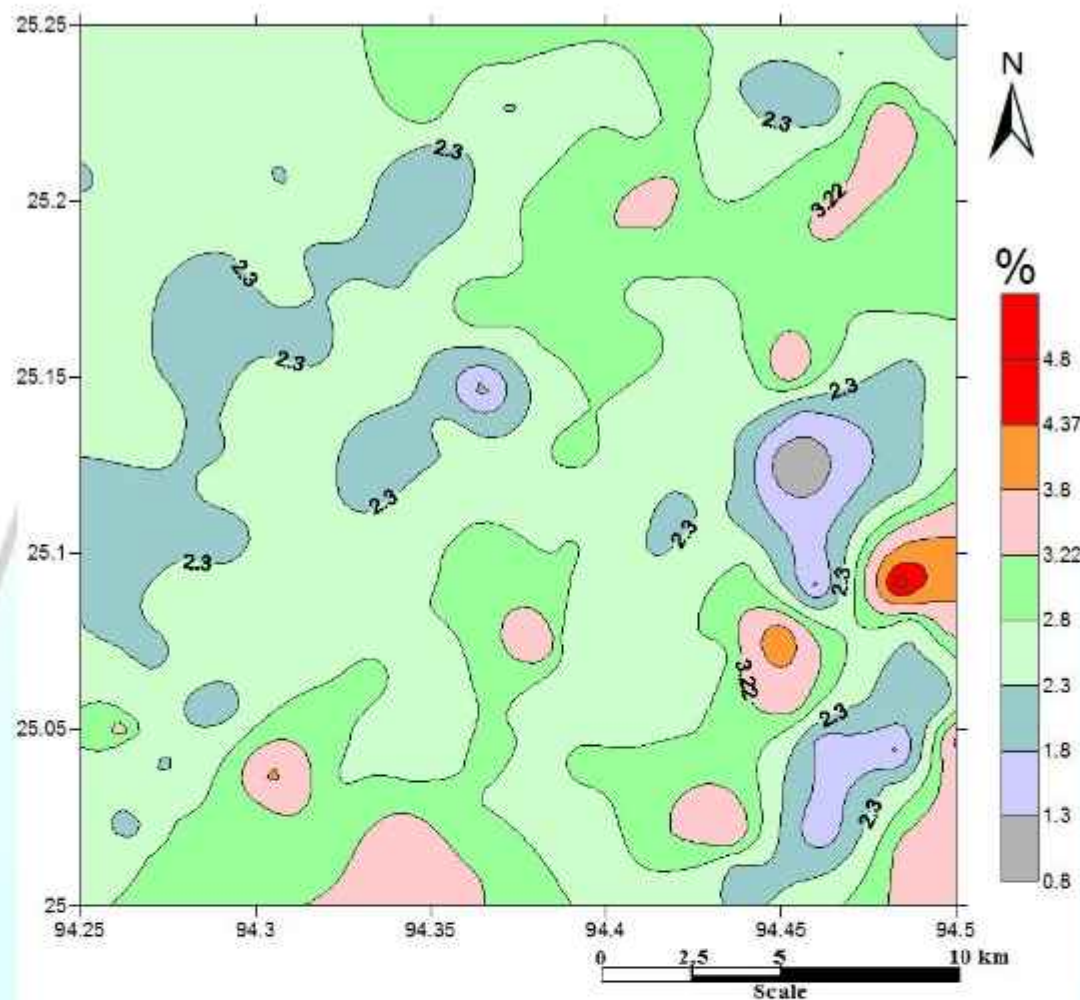
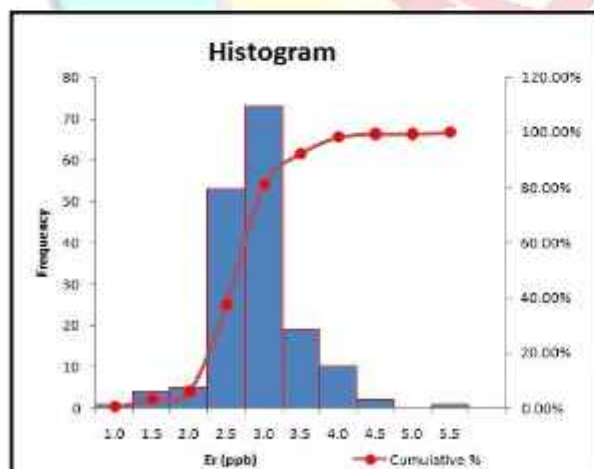


Fig 5.43a. Spatial distribution of Er in the stream sediment/slope wash samples



Class Interval	Frequency	Cumulative %
1.0	1	0.60%
1.5	4	2.98%
2.0	5	5.95%
2.5	53	37.50%
3.0	73	80.95%
3.5	19	92.26%
4.0	10	98.21%
4.5	2	99.40%
5.0	0	99.40%
5.5	1	100.00%

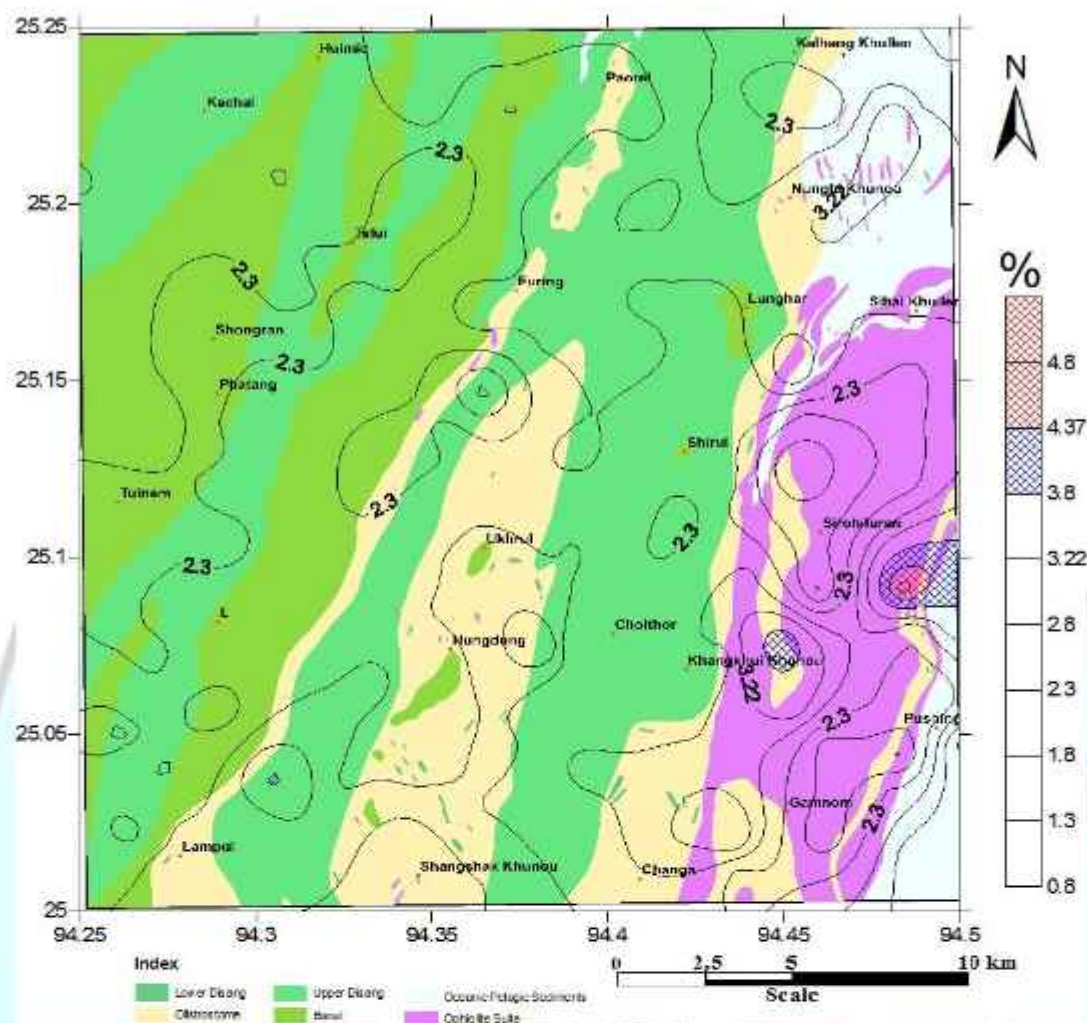


Fig.5.43b. Spatial distribution of Er in the stream sediment/slope wash Samples overlaid on geology of the study area.

Er in stream sediment

The median value of Er in stream sediments is 2.62 ppb with values varying from 0.75 to 5.14 ppb (Annexure-III) showing maximum value in the eastern part of the study area, Grid No.77 of T.S. No. 83K/8 where rocks of ophiolite rocks are exposed (Fig.5.43b). The distribution is positive skewness and kurtosis with values of 0.39 and 2.80 respectively. Er distributed uniformly with relatively low values throughout the area (Fig. 5.43a).

5.5.12. Thulium (Tm):

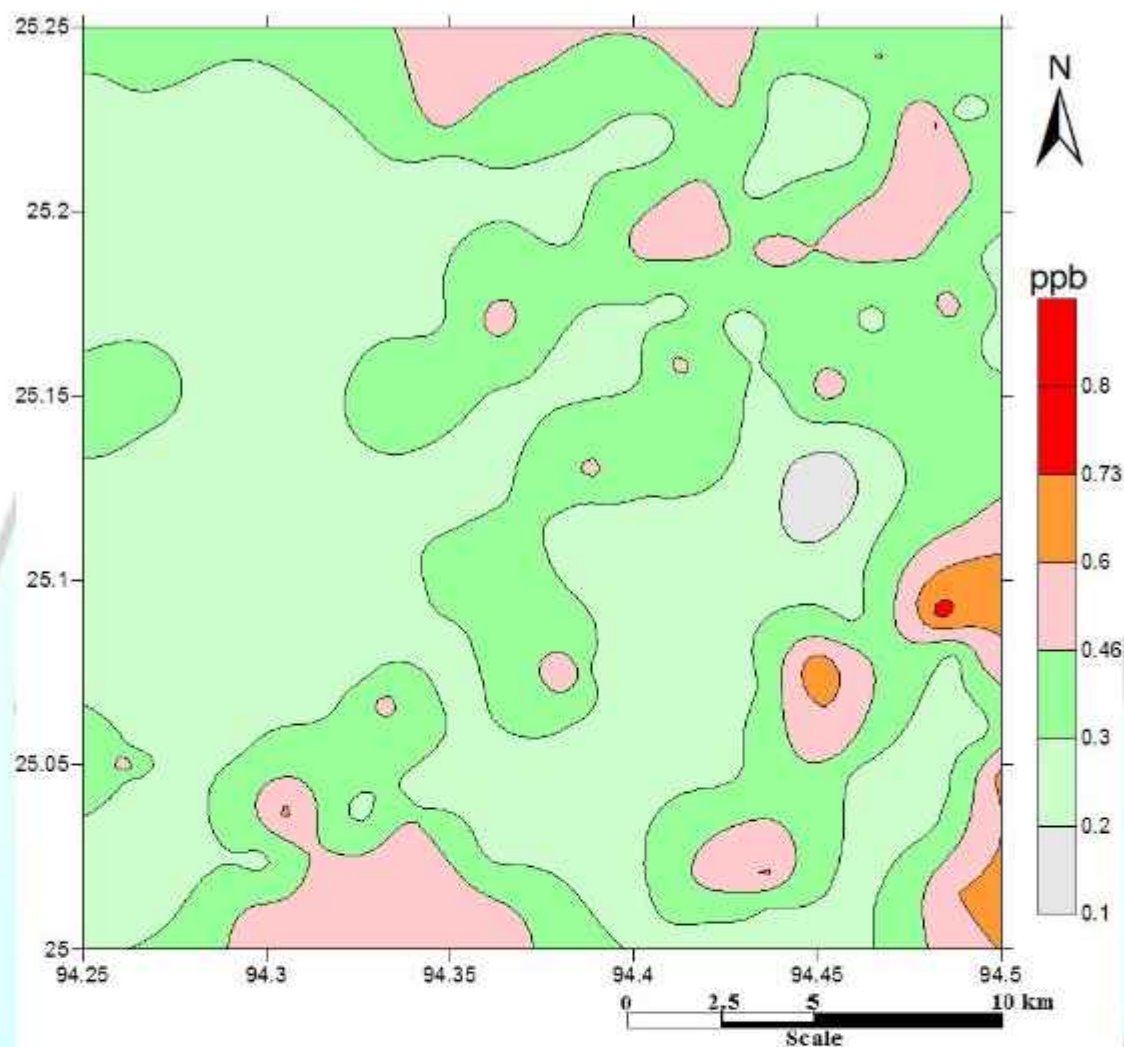
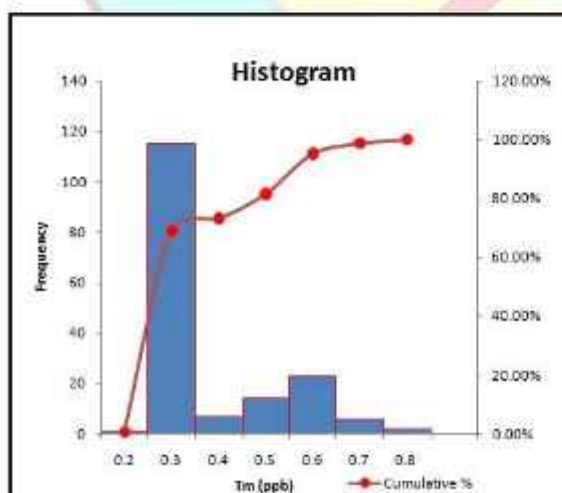


Fig.5.44a.Spatial distribution of Tm in the stream sediment/slope wash samples.



Class Interval	Frequency	Cumulative %
0.2	1	0.60%
0.3	115	69.05%
0.4	7	73.21%
0.5	14	81.55%
0.6	23	95.24%
0.7	6	98.81%
0.8	2	100.00%

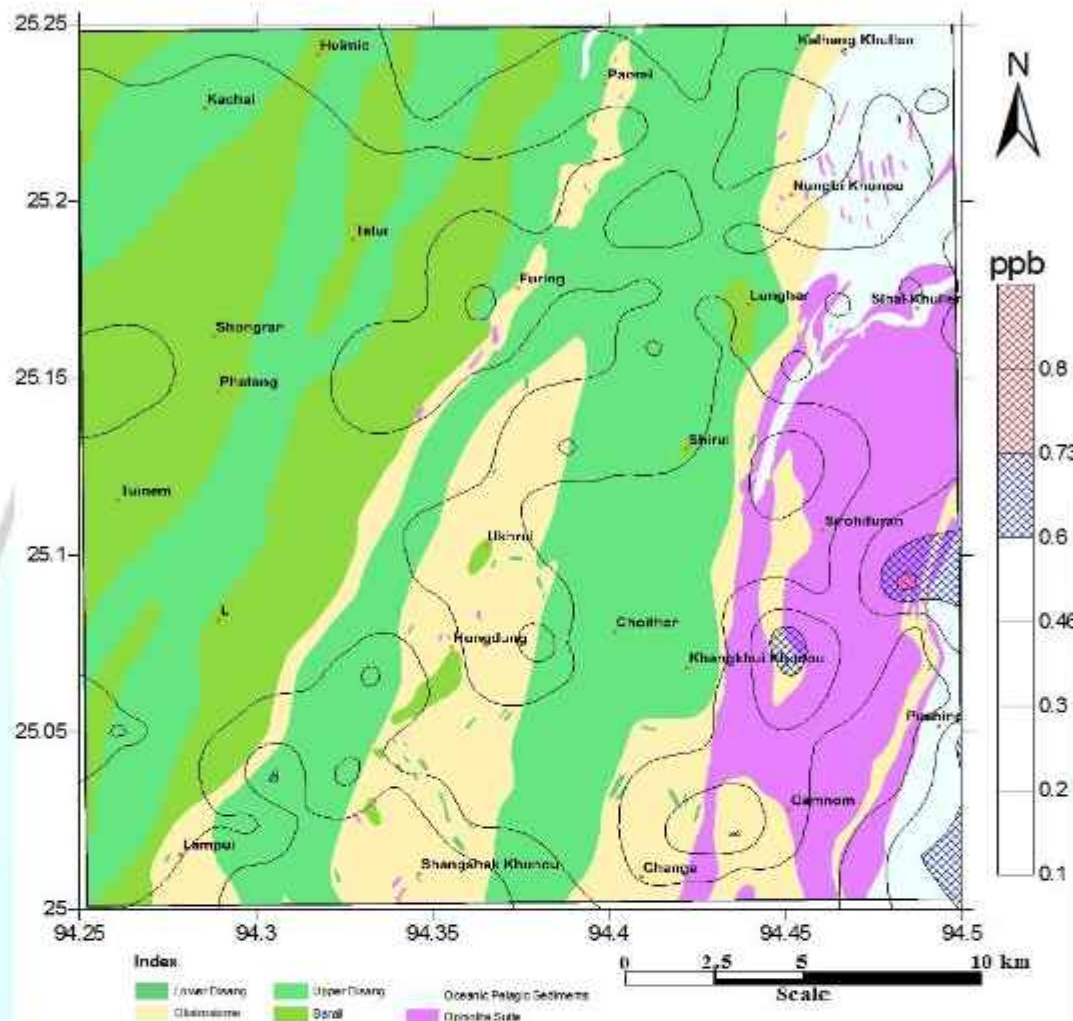


Fig.5.44b.Spatial distribution of Tm in the stream sediment/slope wash samples overlaid on geology of the study area.

Tm in stream sediment

The median value of Th is 0.25 ppb with varying from 0.13 to 0.79 ppb (Annexure-III) showing maximum value in the eastern part of the study area, Grid No.77 of T.S. No. 83K/8 where ophiolite rocks are exposed (Fig.5.44b). The distribution is positive skewed and kurtosis with values of 1.26 and 0.32. The distribution pattern shows uniform and low values throughout the area. (Fig. 5.44a).

5.5.13. Ytterbium (Yb):

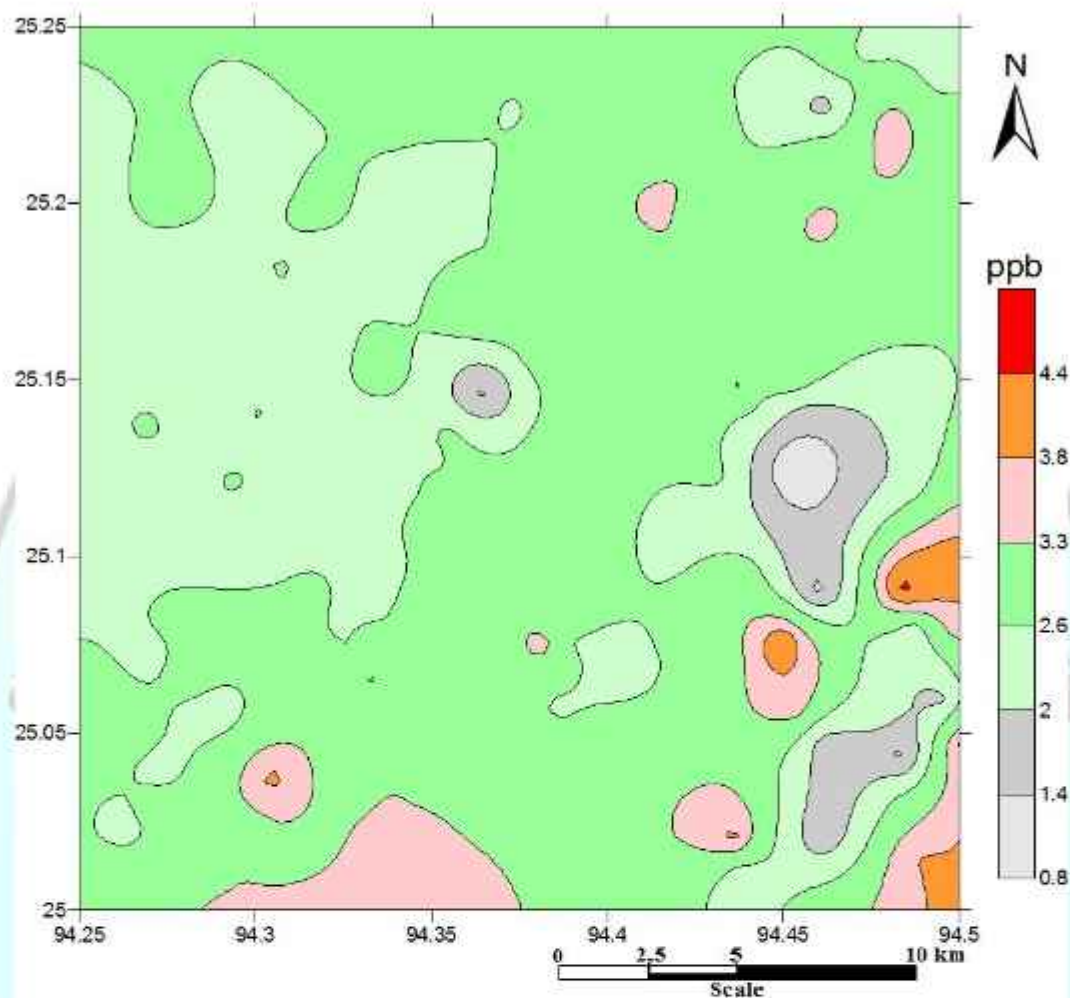
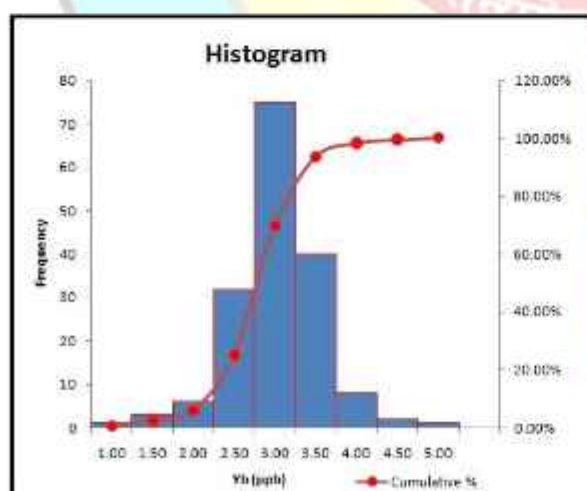


Fig.5.45a.Spatial distribution of Yb in the stream sediment/slope wash samples.



Class Interval	Frequency	Cumulative %
1.00	1	0.60%
1.50	3	2.38%
2.00	6	5.95%
2.50	32	25.00%
3.00	75	69.64%
3.50	40	93.45%
4.00	8	98.21%
4.50	2	99.40%
5.00	1	100.00%

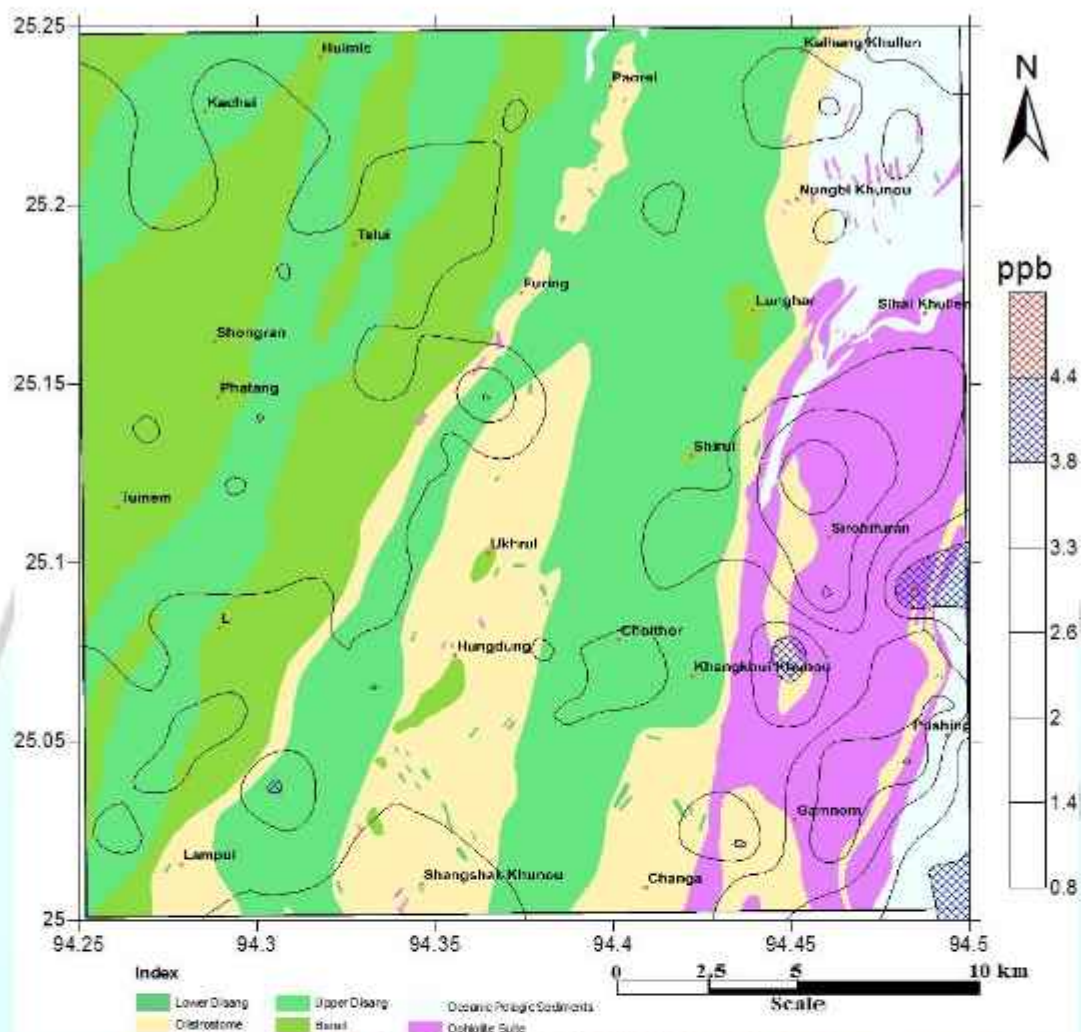


Fig.5.45b.Spatial distribution of Yb in the stream sediment/slope wash samples overlaid on geology of the study area.

Yb in stream sediment

The median value of Yb in stream sediments is 2.76 ppb with values varying from 0.80 to 4.62 ppb (Annexure-III) showing maximum value in the eastern part of the study area, Grid No.77 of T.S. No. 83K/8 where ophiolite rocks are exposed (Fig. 5.45b). The distribution is negative skewness with values of -0.16 and positive kurtosis with values of 2.13 respectively. The distribution of Yb in the study area is uniformly low (Fig. 5.45a).

5.5.14. Lutetium (Lu):

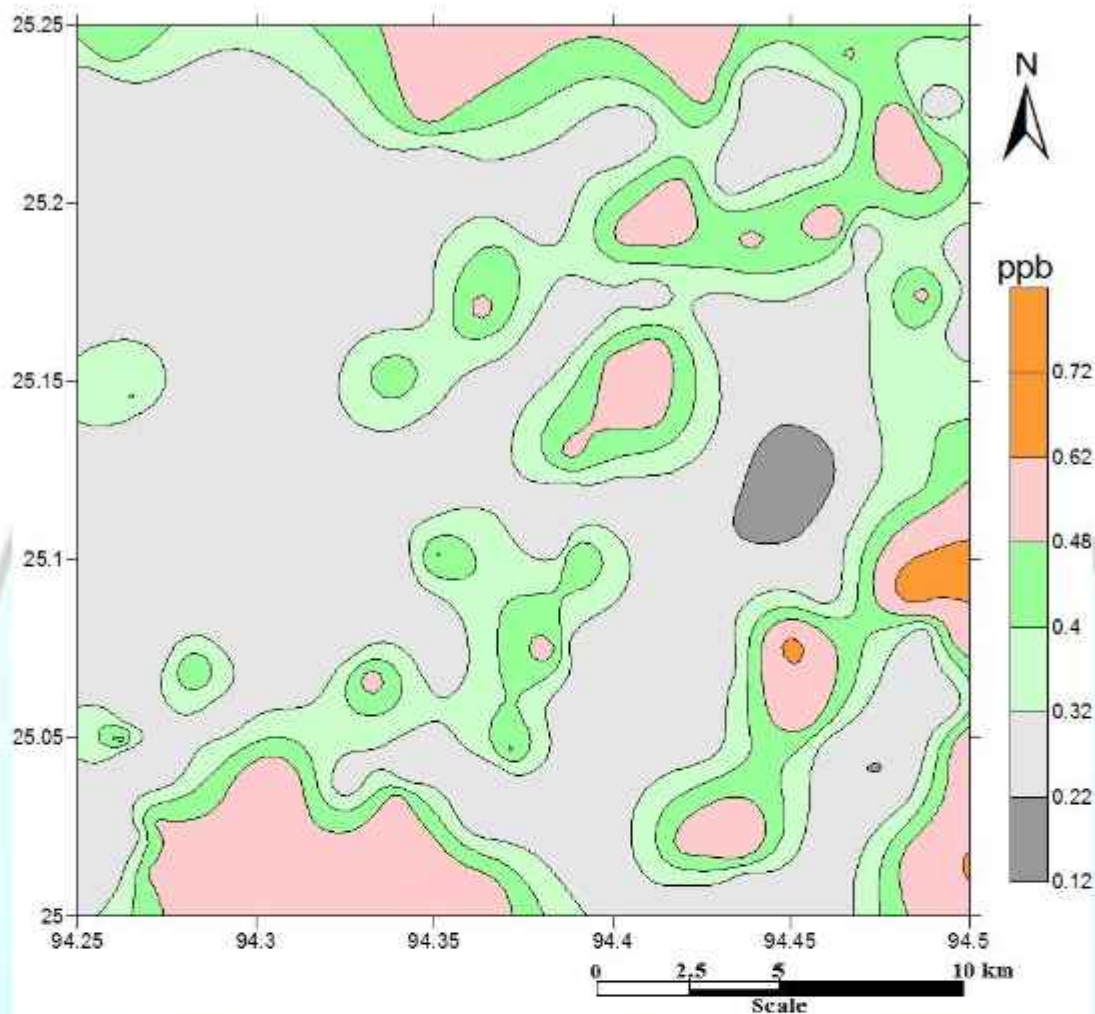
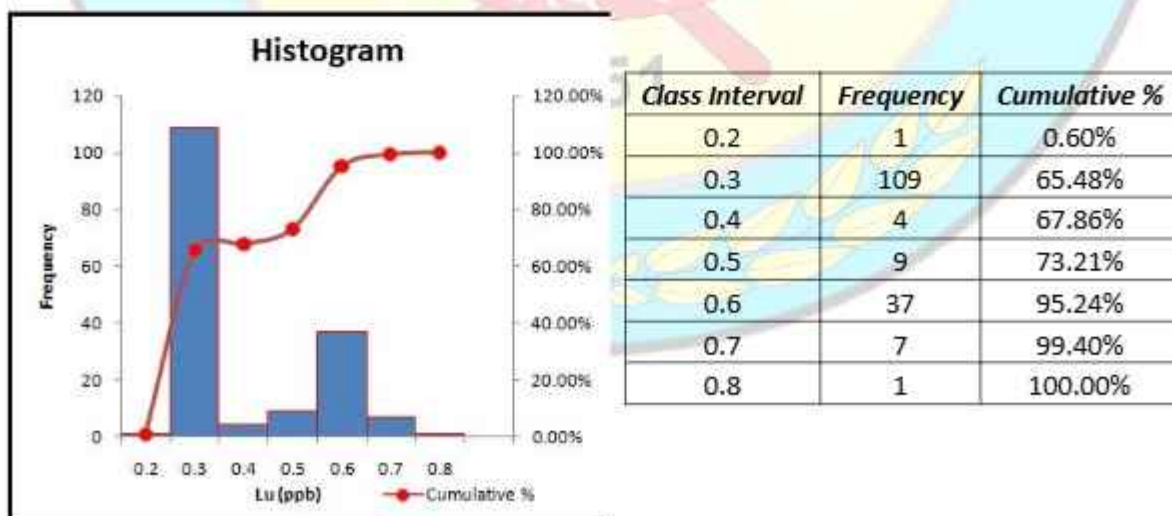


Fig.5.46a. Spatial distribution of Lu in the stream sediment/slope wash samples.



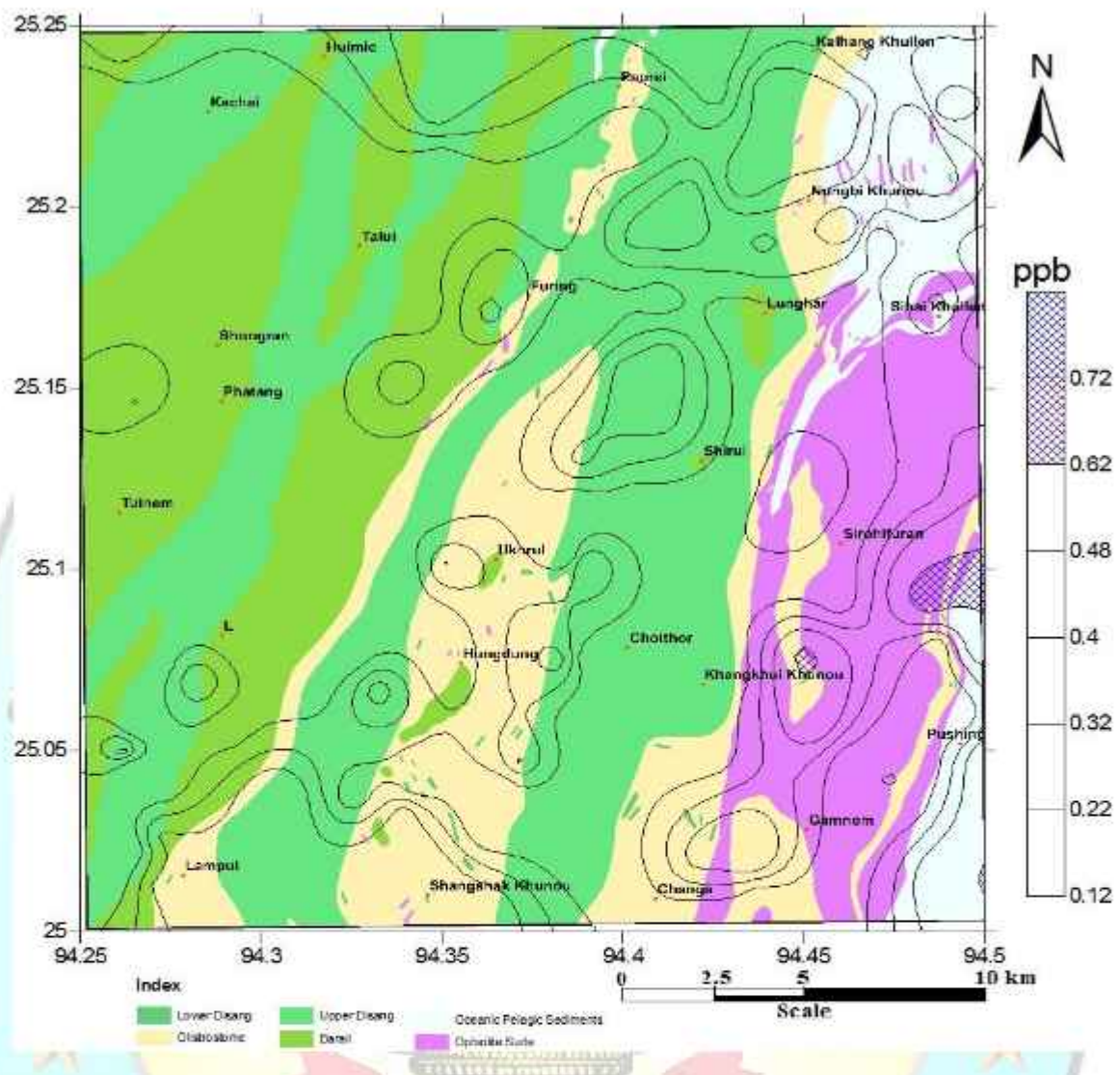


Fig.5.46b. Spatial distribution of Lu in the stream sediment/slope wash samples overlaid on geology of the study area.

Lu in stream sediment

The median value of Lu in stream sediments is 0.25 ppb values varying from 0.13 to 0.74 ppb (Annexure-III) showing maximum value in the eastern part of the study area, Grid No. 77 of T.S. No. 83K/8 where rocks of ophiolite are exposed (Fig.5.46b). The distribution is positive skewness with values of 0.92 and negative kurtosis of -0.71 respectively. The distribution pattern of Lu in the study area shows low to moderate uniform distribution throughout the entire area (Fig. 5.46a).

CHAPTER 6

6 Study of Water, Soil and Duplicate Samples

6.1. Water Sample Analysis

Total 9 nos. of water samples were collected from different locations each from 5'x5' grids of the Toposheet. In some cases artificial structures are erected across the channel for creating dam to store water for lean period and due to this interference, water gets contaminated beyond the limit where chemical analysis would reflect average geo-genic composition of a catchment basin. The stream water samples were collected in good quality plastic container (Torsen bottles) from the flowing stream. The stream water samples thus collected were stored in four different bottles from each of the sample location points and submitted to the Chemical Division, N.E.R., for analysis of elements recommended for GCM.

Analytical results of 9 stream water samples comprising the values of trace elements are received and tabulated in Annexure -VII. The result shows most of the elements are below detectable limit. Univariate statistical summary of some of trace elements and REEs from the water samples are given in the table below.

Table 6.1: Water Samples with location

Sl No.	Sample No.	Location			Elevation in Metre
		Grid Number	Latitude	Longitude	
1	83K8/A1/W/18	A1	25°10'1.219" N	94°18'41.511" E	1210
2	83K8/A2/W/18	A2	25°07'17.579" N	94°17'22.912" E	1170
3	83K8/A3/W/18	A3	25°02'14.835" N	94°18'40.471" E	1210
4	83K8/B1/W/18	B1	25°10'38.092" N	94°23'47.127" E	1260
5	83K8/B2/W/18	B1	25°09'48.891" N	94°24'5.597" E	1236
6	83K8/B3/W/18	B3	25°02'32.492" N	94°22'18.857" E	1373
7	83K8/C1/W/18	C1	25°14'21.814" N	94°29'27.106" E	1245
8	83K8/C2/W/18	C2	25°09'31.22" N	94°25'4.528" E	1312
9	83K8/C3/W/18	C3	25°03'24.266" N	94°25'4.105" E	1625

Table 6.2: Statistical summary of some of trace elements and REEs in water samples.

Elements	Mean	Med	Min.	Max.	Vari.	S. D	Skew.	Kurt.	M+SD	M-SD	M+2SD	M-2SD	M+3SD	M-3SD
Al	31.19	28.26	12.00	101.00	714.21	26.72	2.27	6.06	57.91	4.46	84.64	-22.26	111.36	-48.99
Ti	54.29	49.80	18.91	101.00	684.29	26.16	0.50	-0.69	80.45	28.14	106.61	1.98	132.77	-24.18
Cr	14.28	3.83	2.50	101.00	936.58	30.60	3.11	9.76	44.88	-16.32	75.49	-46.93	106.09	-77.53
Mn	30.27	9.83	3.30	101.00	1304.59	36.12	1.37	0.54	66.39	-5.85	102.51	-41.97	138.63	-78.09
Co	10.34	0.25	0.15	101.00	1014.84	31.86	3.16	10.00	42.19	-21.52	74.05	-53.38	105.90	-85.23
Ni	11.46	1.45	1.17	101.00	989.88	31.46	3.16	10.00	42.92	-20.00	74.38	-51.46	105.85	-82.93
Cu	12.68	2.76	1.79	101.00	963.38	31.04	3.16	9.99	43.72	-18.36	74.76	-49.40	105.80	-80.43
Zn	54.86	38.19	26.02	101.00	869.33	29.48	0.54	-1.79	84.34	25.37	113.83	-4.11	143.31	-33.59
Ga	10.23	0.14	0.12	101.00	1017.26	31.89	3.16	10.00	42.12	-21.67	74.02	-53.56	105.91	-85.46
Rb	10.72	0.69	0.38	101.00	1006.20	31.72	3.16	10.00	42.44	-21.00	74.16	-52.72	105.88	-84.44
Sr	146.85	139.13	53.21	249.76	5152.75	71.78	0.36	-1.37	218.64	75.07	290.42	3.29	362.20	-68.49
Y	10.16	0.08	0.04	101.00	1018.69	31.92	3.16	10.00	42.08	-21.75	74.00	-53.67	105.91	-85.59
Ag	10.19	0.11	0.05	101.00	1018.03	31.91	3.16	10.00	42.10	-21.71	74.01	-53.62	105.91	-85.53
Cd	10.22	0.13	0.10	101.00	1017.46	31.90	3.16	10.00	42.12	-21.68	74.01	-53.58	105.91	-85.48
Sn	10.48	0.44	0.15	101.00	1011.68	31.81	3.16	10.00	42.29	-21.33	74.09	-53.13	105.90	-84.94
Sb	10.40	0.19	0.11	101.00	1013.62	31.84	3.16	10.00	42.23	-21.44	74.07	-53.28	105.91	-85.12
Cs	10.11	0.01	0.01	101.00	1019.86	31.94	3.16	10.00	42.05	-21.82	73.98	-53.76	105.92	-85.70
Ba	25.03	12.26	8.50	101.00	803.08	28.34	2.58	7.02	53.37	-3.31	81.71	-31.65	110.04	-59.99
La	10.19	0.10	0.06	101.00	1018.17	31.91	3.16	10.00	42.09	-21.72	74.00	-53.63	105.91	-85.54
Ce	10.27	0.19	0.11	101.00	1016.28	31.88	3.16	10.00	42.15	-21.61	74.03	-53.49	105.91	-85.37
Pr	10.12	0.02	0.01	101.00	1019.73	31.93	3.16	10.00	42.05	-21.82	73.98	-53.75	105.92	-85.68
Nd	10.16	0.07	0.04	101.00	1018.73	31.92	3.16	10.00	42.08	-21.76	74.00	-53.67	105.91	-85.59
Gd	10.12	0.02	0.01	101.00	1019.73	31.93	3.16	10.00	42.05	-21.82	73.98	-53.75	105.92	-85.68
Hf	10.77	0.77	0.09	101.00	1005.43	31.71	3.16	9.99	42.48	-20.94	74.18	-52.65	105.89	-84.36
Ta	10.32	0.24	0.04	101.00	1015.30	31.86	3.16	10.00	42.18	-21.55	74.04	-53.41	105.91	-85.28
Pt	10.24	0.16	0.08	101.00	1017.07	31.89	3.16	10.00	42.13	-21.66	74.02	-53.55	105.91	-85.44
Au	10.11	0.01	0.00	101.00	1019.90	31.94	3.16	10.00	42.04	-21.83	73.98	-53.76	105.92	-85.70
Pb	11.10	1.05	0.70	101.00	997.90	31.59	3.16	9.99	42.69	-20.49	74.28	-52.08	105.87	-83.66

6.2. Soil Sample

Soil is one of the commonly available media for sampling and reflects variations in geogenic composition of the uppermost layers of the Earth's crust. Soil samples were collected from 5' x 5' grid. The purpose is to see the possibility of any deposits. From each soil sample collection site, two samples were collected by cutting a vertical section through the soil profile. One sample is collected from the upper horizon (Regolith) after removing the organic matter within top 0-25 cm depth and the other sample from within a depth of 50-200 cm.

A total of 18 soil samples of -80 mesh grain size (9 numbers of Regolith and 9 numbers of C-Horizon) have been collected one each from 5' x 5' grid. 02 C-horizon and 02 regolith samples each from soil developed from Ophiolite Belt, Olistostrome, Disang and Barial Group and one Ocean Pelagic Sediment (OPS) are collected. Analytical results of 46 elements (Major, Traces and REE) are available (Annexure IV, V & VI).

Table 6.3: Soil Samples with Location

Sl No.	Composite Sample No.	Location			Elevation In Metre
		Grid Number	Latitude (N)	Longitude (E)	
1	83K8/A1/R/19	A1	25°10'49.094"	94°18'15.78"	1359
2	83K8/A1/C/19	A1	25°10'49.094"	94°18'15.78"	1359
3	83K8/A2/R/19	A2	25°8'21.78"	94°16'40.06"	1575
4	83K8/A2/C/19	A2	25°8'21.78"	94°16'40.06"	1575
5	83K8/A3/R/19	A3	25°1'31.86"	94°19'2.61"	1224
6	83K8/A3/C/19	A3	25°1'31.86"	94°19'2.61"	1224
7	83K8/B1/R/19	B1	25°12'36.339"	94°22'2.307"	1830
8	83K8/B1/C/19	B1	25°12'36.339"	94°22'2.307"	1830
9	83K8/B2/R/19	B2	25°5'43.42"	94°22'40.94"	1684
10	83K8/B2/C/19	B2	25°5'43.42"	94°22'40.94"	1684
11	83K8/B3/R/19	B3	25°2'0.52"	94°19'42.14"	1334
12	83K8/B3/C/19	B3	25°2'0.52"	94°19'42.14"	1334
13	83K8/C1/R/19	C1	25°12'30.88"	94°27'9.45"	1673
14	83K8/C1/C/19	C1	25°12'30.88"	94°27'9.45"	1673
15	83K8/C2/R/19	C2	25°8'17.88"	94°27'41.45"	1915
16	83K8/C2/C/19	C2	25°8'17.88"	94°27'41.45"	1915
17	83K8/C3/R/19	C3	25°1'25.14"	94°26'45.63"	1972
18	83K8/C3/C/19	C3	25°1'25.14"	94°26'45.63"	1972

Table 6.4: Statistical summary of major oxides in soil samples (Regolith)

Oxides	Mean	Median	Minimum	Maximum	Variance	Std.Dev.	Skewness	Kurtosis
SiO ₂	59.828	63.140	31.170	72.550	148.826	12.199	-1.869	4.026
TiO ₂	0.933	1.010	0.410	1.080	0.042	0.206	-2.521	6.783
Al ₂ O ₃	13.710	14.730	8.710	16.370	5.577	2.362	-1.244	1.505
Fe ₂ O ₃	11.699	7.310	4.440	45.910	170.958	13.075	2.798	8.045
MnO	0.163	0.120	0.040	0.510	0.023	0.151	1.808	3.316
MgO	1.383	1.090	0.750	2.350	0.398	0.631	0.563	-1.456
CaO	0.137	0.100	0.050	0.410	0.012	0.111	2.253	5.639
Na ₂ O	0.139	0.140	0.010	0.230	0.004	0.060	-0.928	2.573
K ₂ O	1.184	1.290	0.320	1.640	0.138	0.372	-1.676	3.909
P ₂ O ₅	0.104	0.100	0.070	0.160	0.001	0.028	0.876	0.776

Table 6.5: Statistical summary of major oxides in soil samples (C-Horizon)

Oxides	Mean	Median	Minimum	Maximum	Variance	Std.Dev.	Skewness	Kurtosis
SiO ₂	59.41	63.32	33.78	67.97	108.26	10.40	-2.21	5.53
TiO ₂	0.90	0.94	0.40	1.07	0.04	0.21	-2.04	4.90
Al ₂ O ₃	15.24	15.49	7.21	18.74	10.58	3.25	-2.14	5.81
Fe ₂ O ₃	11.80	7.07	5.62	45.25	161.16	12.69	2.87	8.38
MnO	0.15	0.07	0.03	0.80	0.06	0.25	2.96	8.81
MgO	1.61	1.13	0.72	4.43	1.48	1.22	1.92	3.49
CaO	0.07	0.06	0.02	0.11	0.00	0.03	-0.25	-0.48
Na ₂ O	0.20	0.13	0.08	0.65	0.03	0.18	2.62	7.23
K ₂ O	1.53	1.50	0.55	2.18	0.25	0.50	-0.60	0.86
P ₂ O ₅	0.09	0.08	0.06	0.13	0.00	0.03	0.88	-0.75

Table 6.6: Statistical summary of Trace elements in soil samples (Regolith)

Elements	Mean	Median	Minimum	Maximum	Variance	Std.Dev.	Skewness	Kurtosis
Ba	232.00	244.00	98.00	371.00	8112.50	90.07	-0.31	-0.45
Co	52.22	21.00	15.00	233.00	5003.19	70.73	2.59	6.94
Cr	1098.11	267.00	142.00	6749.00	4612456.86	2147.66	2.86	8.31
Cu	37.22	26.00	14.00	136.00	1419.44	37.68	2.81	8.16
Ga	16.89	17.00	11.00	23.00	15.61	3.95	-0.03	-0.88
Nb	15.44	15.00	8.00	21.00	12.28	3.50	-0.84	2.67
Ni	688.00	81.00	51.00	4555.00	2154016.75	1467.66	2.87	8.39
Pb	17.44	17.00	9.00	24.00	18.03	4.25	-0.65	1.40
Sc	17.56	14.00	9.00	51.00	164.03	12.81	2.77	7.97
Sr	43.11	45.00	10.00	58.00	201.86	14.21	-1.72	3.86
V	147.33	124.00	89.00	326.00	5337.50	73.06	2.23	5.22
Y	21.44	21.00	13.00	28.00	16.78	4.10	-0.65	2.19
Zn	95.11	75.00	50.00	233.00	3118.36	55.84	2.24	5.60
Zr	210.44	242.00	26.00	277.00	6215.03	78.84	-1.84	3.80
Sn	2.35	2.20	1.52	3.14	0.28	0.53	-0.06	-1.00
Hf	8.35	9.07	0.86	11.07	10.76	3.28	-1.71	3.10
Ta	1.28	1.41	0.22	2.06	0.32	0.56	-0.83	0.43
Ge	1.82	1.46	1.06	4.70	1.29	1.14	2.52	6.66
Be	1.69	1.59	0.98	3.63	0.61	0.78	2.19	5.64
U	2.56	2.60	1.27	3.42	0.44	0.66	-0.69	0.70
As	10.24	10.35	7.51	12.72	2.99	1.73	-0.07	-0.63
Rb	78.70	83.53	36.15	94.69	324.78	18.02	-1.90	4.09
Th	12.58	12.59	5.59	16.76	10.95	3.31	-0.90	2.11

Table 6.7: Statistical summary of Trace elements in soil samples (C-horizon)

Elements	Mean	Median	Minimum	Maximum	Variance	Std.Dev.	Skewness	Kurtosis
Ba	240.11	243.00	137.00	361.00	6218.86	78.86	0.02	-1.15
Co	45.78	18.00	10.00	243.00	5690.94	75.44	2.80	8.00
Cr	1573.00	223.00	121.00	11383.00	13663110.00	3696.36	2.95	8.75
Cu	37.67	32.00	24.00	80.00	288.50	16.99	2.32	5.98
Ga	16.89	17.00	13.00	20.00	8.36	2.89	-0.42	-1.68
Nb	15.22	14.00	8.00	21.00	22.19	4.71	-0.23	-1.52
Ni	720.89	115.00	45.00	4888.00	2498829.86	1580.77	2.88	8.41
Pb	18.11	19.00	5.00	28.00	57.61	7.59	-0.39	-0.49
Sc	18.22	14.00	11.00	37.00	81.44	9.02	1.49	1.27
Sr	47.22	49.00	18.00	74.00	231.19	15.21	-0.27	1.77
V	145.00	136.00	104.00	261.00	2179.00	46.68	2.27	5.89
Y	23.89	24.00	14.00	29.00	23.61	4.86	-0.99	0.89
Zn	96.00	87.00	48.00	174.00	1212.00	34.81	1.36	3.22
Zr	217.00	227.00	66.00	285.00	4115.00	64.15	-1.77	4.18
Sn	3.31	2.83	1.90	8.35	3.88	1.97	2.56	7.02
Hf	9.47	10.09	4.57	12.20	5.64	2.38	-1.14	1.17
Ta	1.46	1.56	0.96	2.03	0.17	0.41	0.14	-1.50
Ge	1.95	1.42	1.15	5.26	1.66	1.29	2.60	7.03
Be	1.70	1.68	1.24	2.26	0.14	0.38	0.06	-1.59
U	2.84	2.97	1.23	3.97	0.76	0.87	-0.49	-0.04
As	12.55	12.49	10.68	15.16	2.07	1.44	0.69	-0.17
Rb	89.74	86.70	46.86	122.77	489.48	22.12	-0.54	0.80
Th	13.75	14.64	5.34	20.52	22.36	4.73	-0.31	-0.22

Table 6.8: Statistical summary of REE elements in soil samples (Regolith)

Elements	Mean	Median	Minimum	Maximum	Variance	Std.Dev.	Skewness	Kurtosis
La	37.11	38.85	15.67	45.11	74.28	8.62	-2.27	5.96
Ce	67.46	66.89	51.32	86.70	107.98	10.39	0.43	0.61
Pr	7.61	7.97	3.76	9.85	2.78	1.67	-1.57	4.01
Nd	26.92	28.17	13.86	34.90	33.07	5.75	-1.42	3.62
Eu	0.97	0.93	0.77	1.26	0.03	0.17	1.00	-0.20
Sm	4.98	4.90	3.42	6.62	0.83	0.91	0.31	1.02
Gd	4.70	4.48	3.43	6.20	0.87	0.93	0.75	-0.22
Tb	0.69	0.63	0.56	0.93	0.02	0.14	1.23	-0.02
Dy	4.22	3.88	3.39	5.57	0.56	0.75	1.17	0.14
Ho	0.97	0.93	0.72	1.27	0.03	0.17	0.57	0.07
Er	2.57	2.55	1.84	3.28	0.17	0.42	0.04	0.67
Tm	0.44	0.44	0.32	0.55	0.00	0.06	-0.03	0.70
Yb	2.78	2.86	2.14	3.44	0.14	0.37	0.02	0.65
Lu	0.46	0.48	0.34	0.57	0.00	0.06	-0.40	1.04

Table 6.9: Statistical summary of REE elements in soil samples (C-horizon)

Elements	Mean	Median	Minimum	Maximum	Variance	Std.Dev.	Skewness	Kurtosis
La	38.545	39.451	21.042	45.661	56.478	7.515	-1.794	3.763
Ce	73.310	80.071	33.915	99.219	414.893	20.369	-0.746	0.318
Pr	8.420	8.856	4.592	10.547	3.447	1.857	-1.033	1.281
Nd	30.573	30.832	21.678	37.627	27.674	5.261	-0.315	-0.416
Eu	1.125	1.114	0.724	1.492	0.058	0.242	-0.050	-0.549
Sm	5.615	5.396	3.392	7.324	1.364	1.168	-0.550	0.504
Gd	5.287	5.520	3.213	7.108	1.320	1.149	-0.289	0.365
Tb	0.772	0.771	0.503	1.010	0.026	0.160	-0.065	-0.393
Dy	4.665	4.576	3.290	5.746	0.705	0.840	-0.165	-1.105
Ho	1.055	1.064	0.589	1.280	0.049	0.220	-1.135	1.531
Er	2.784	2.892	1.488	3.456	0.348	0.590	-1.353	2.340
Tm	0.468	0.490	0.246	0.574	0.010	0.099	-1.477	2.683
Yb	2.977	3.135	1.540	3.632	0.413	0.643	-1.501	2.712
Lu	0.492	0.524	0.247	0.595	0.011	0.106	-1.723	3.481

6.2.1: Interpretation of soil samples

The soil samples shows enrichment of major elements like SiO_2 , K_2O and MgO and immobile elements (Al_2O_3 , Fe_2O_3) and depleted in TiO_2 , MnO , CaO and K_2O . The C-horizon soil sample shows slightly higher values as compared with the overlying regolith soil sample (Fig.6.1). The SiO_2 shows higher values in the central and western part of the study area as compared with the eastern part. The higher concentration of trace elements like Cr, Ni and Co is observed in the eastern part as compared with the central and western part of the study area. The soil samples from Ophiolite Belt exposed in the eastern part of the study area show anomalous values of Fe_2O_3 , Cr and Ni. The REE pattern for the soil pattern shows similar concentration, the soil sample from the exposed Barial rock soil profile shows lowest concentration and slight negative Eu anomaly is commonly observed in all the soil samples. (Fig.6.2)

The soil samples of the Paleogene sedimentary terrain (i.e, Disang, Barial and Olistostrome) and OPS show similar geochemical behavior. The SiO_2 shows high values of SiO_2 , Al_2O_3 and Fe_2O_3 , which is in coherent with the underlying lithology of sandstone, siltstone and shale. The slight high values of Cr (206 to 540ppm) and Ni (158 to 476ppm) is shown by the samples in the central part of the study area, which may indicate sediments partially having its provenance from the Ophiolite Belt exposed in the eastern part.

The lateritic soil capping developed above the protolith mafic/ultramafic rock varies in exposed outcrop thickness (0.5 to 3.5m) having boardly four soil horizons (i.e., ferric rich duricrust capping, plasmic limonitic soil horizon, oxidised goethite rich soil horizon, saprolitic soil horizon and saprock associated with saprolite soil).

The soil samples from Ophiolite Belt show anomalous values of Fe_2O_3 , Cr and Ni. Phangrai soil sample collected from regolith horizon characterised by the reddish limonitic soil (83K8/C2/R/19; Cr: 6749 ppm, Fe_2O_3 : 45.91% and Ni: 4555 ppm) and brownish yellow saprolitic soil horizon (83K8/C2/C/19; Cr: 1288 ppm, Fe_2O_3 : 12.33 % and Ni: 798 ppm) and Gamnom (83K8/C3/R/19 shows Cr: 12868 ppm, Fe_2O_3 : 13.23% and Ni: 687 ppm) and 83K8/C3/C/19; Cr: 11388 ppm, Fe_2O_3 : 45.29 % and Ni: 4888 ppm. The high values of Cr can be correlated with the chromite pod mineralisation exposed in the outcrop surface. The high values of Fe_2O_3 are supported by the presence of oxidised zone having goethite rich nodules within lateritic soil profile. The high values of Ni suggest some presence of Ni bearing mineral phases like garnierite and goethite.

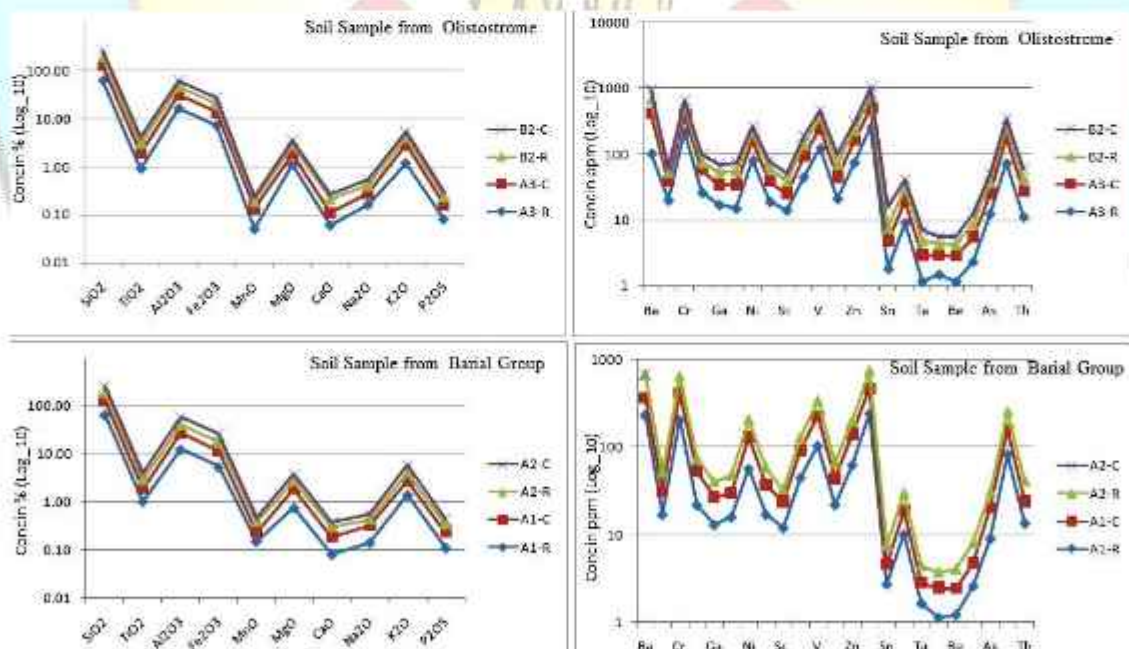


Fig.6.1 Major and trace element concentration spider diagram for soil (regolith and C-hoziron soil sample for Olistostrome and Barial Group)

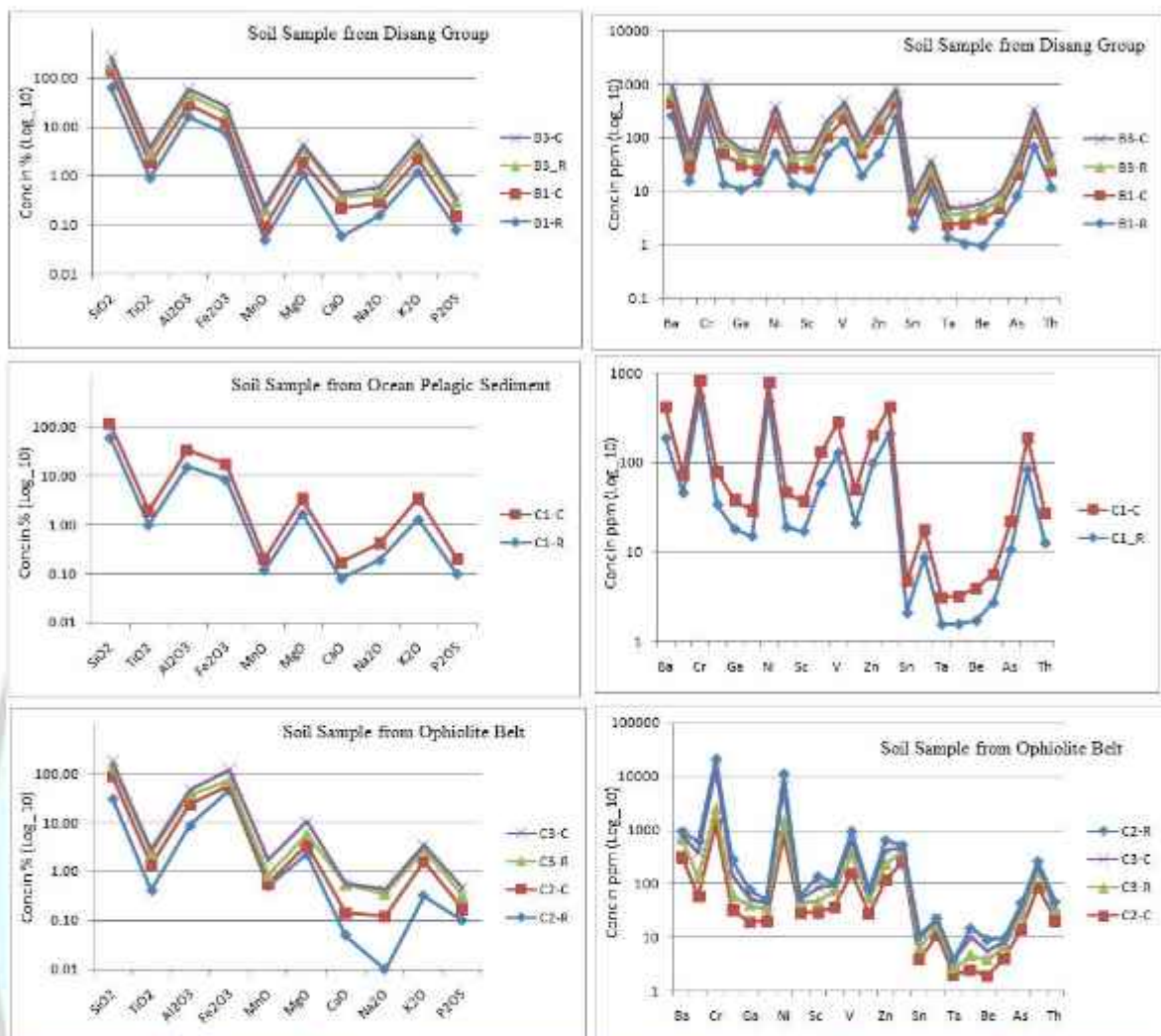


Fig.6.2 Major and trace element concentration spider diagram for soil (regolith and C-horizon soil sample from Ophiolite Belt, OPS and Disang Group)

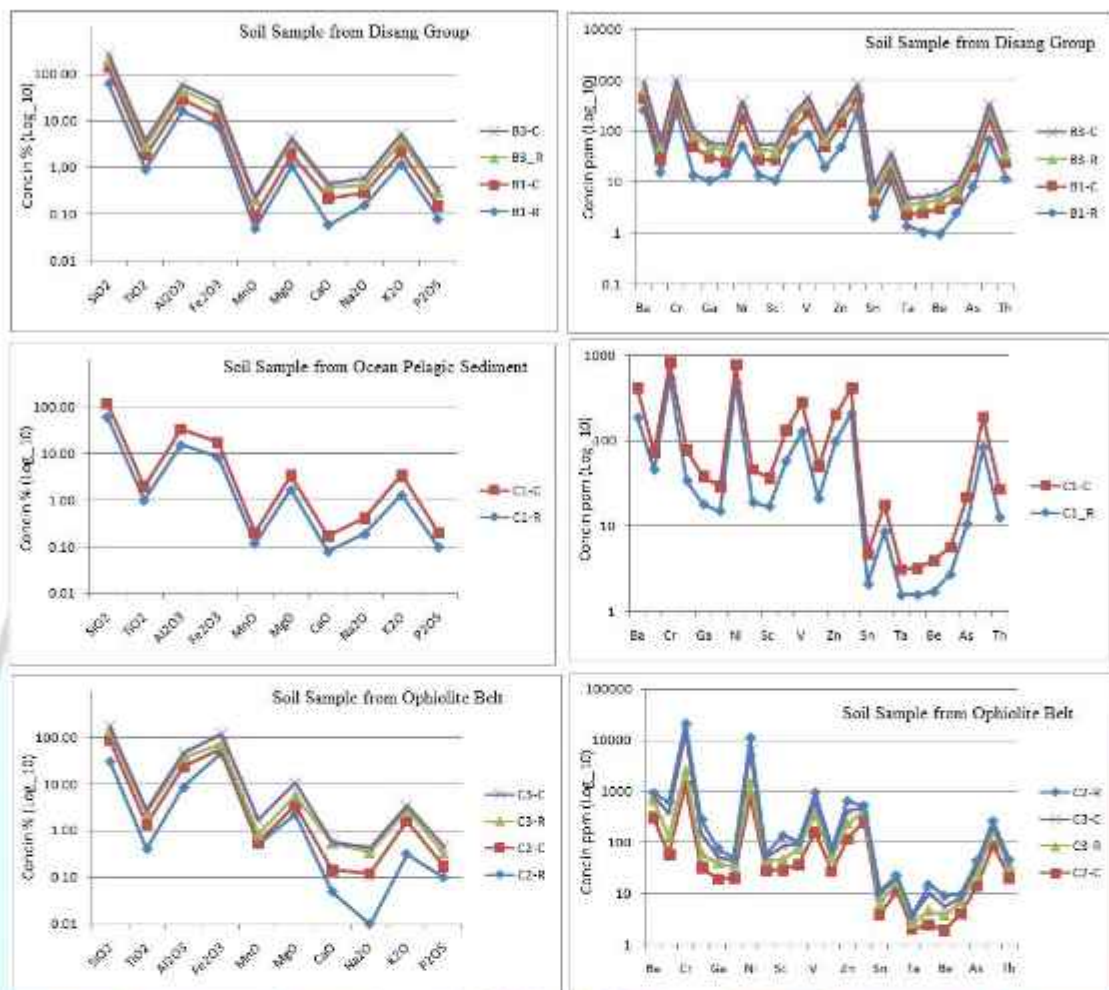


Fig.6.3 Major and trace element concentration spider diagram for soil (regolith and C-hoziron soil sample from Ophiolite Belt, OPS and Disang Group).

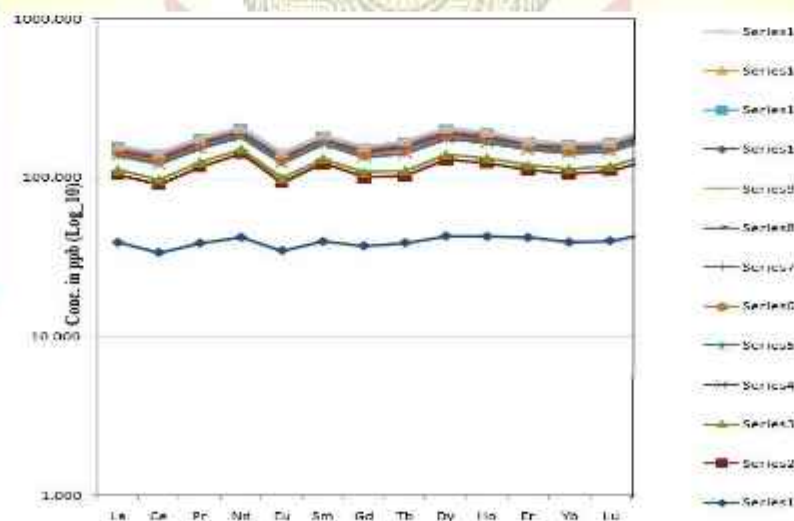


Fig.6.4 Rare earth element (REE) concentration spider diagram for soil (regolith and C-hoziron soil).

The potentially harmful elements (PHE's), known to have adverse physiological significance at relatively low levels, include As, Cd, Pb, Hg and some of the daughter products of U. These elemental concentration values of the soil have a diverse application in medical, health, environment and other societal issues. Many health problems have been found to be associated with the consumption of low or excess of micro, minor, REE and some other metals like Nb, Mo, Ta, Cs, Co, Cd, Hg, As and F etc. that directly or indirectly imparts an adverse effect.

The agricultural activities may be avoided as far as possible in such pockets where there is very high incidence of certain toxic elements. According to the U.S. Recommended Daily Allowances (USRDA) and biological roles of elements that the National Research Council (1989) lists as essential to health (Table.6.10) certain elements plays an important biological role.

Table :6.10 U.S. Recommended Daily Allowances (USRDA) and biological roles of elements that the National Research Council (1989) lists as essential to health

Element	USRDA	Biological role
Calcium (Ca)	800–1200 mg	Needed to build strong bones and teeth; for blood clotting, neural transmission, and muscle function.
Chlorine/Chloride (Cl)	750 –3600 mg	Needed to maintain water balance, osmotic pressure, and acid-base balance, for digestive acid
Chromium (Cr)	50 –200 µg	Needed for glucose metabolism
Copper (Cu)	1.5 –3 mg	Respiratory and red blood cell function; present in oxidative enzymes
Fluorine/Fluoride (F)	1.5 –4 mg	fluoride, prevents tooth decay or disease
Iodine (I)	150 µg	Needed for thyroid hormones, to control body temperature, metabolism, reproduction, and Growth
Iron (Fe)	10 –15 mg	Needed for hemoglobin in blood, energy production, and a healthy immune system
Magnesium (Mg)	280 –350 mg	Needed for healthy bones and blood vessels, muscle function, nerve transmission, and energy formation
Manganese (Mn)	2 –5 mg	Promotes growth, development, and cell function; cofactor in a number of enzymatic reactions
Molybdenum (Mo)	75 –250 µg	Promotes growth, development, and cell function; essential cofactor in certain enzymes
Phosphorous (P)	800–1200 mg	Essential for healthy bones and energy production; present in almost every chemical reaction within the body
Potassium (K)	2000–3500 mg	Regulates body fluid balance; aids muscle contraction and neural transmission
Selenium (Se)	55 –70 µg	Prevents cardiovascular disease and cancer; detoxifies several major
Sodium (Na)	500–2400 mg	Aids muscle contraction and neural transmission; maintains blood pressure
Zinc (Zn)	12 –15 mg	Maintains senses of taste and smell, and healthy immune system and growth; protects liver from chemical damage

Certain elements are toxic and are hazardous to plants and human health. Ranges for various levels of contamination for elements in soil and their toxicity impacts are provided in the Table 4.6 of WHO and others and Table 6.9 (CCME 1996).

Table:6.11 Micronutrient levels (ppm) in Soil (Compiled from WHO data and others)

Elements	Deficiency	Normal	Toxicity	Average range in soil	Concentration in the soil sample (Median value of C horizon of soil)
Fe	<20	20-1000	2000 & above	50-1000	47,394
Mn	<90	90-200	200 & above	260-840	309.8
Co	<25	25-60	60 & above	0.5-65	16.5
Ni	<100	100-N.A	N.A	2-750	51
Cu	<10	10-25	25 & above	14-29	22
Zn	<10	10-120	120 & above	34-84	43
B	<10	10-80	80 & above	2-130	Not analysed.
Mo	<0.1	0.1-90	90 & above	0.35-5.8	2.63

Table :6.12 Environmental and human health soil quality guidelines (CCME 1996, updated 2004) *All values in ppm*

Element	Crustal abundance	Soil abundance	Agricultural Soil		Toxic		China SS		
			Average	Range	Agri.	Industrial	Av.	Arid	Humid
Cu	70	30	13-24	1-205	63	100	21.6	12.8	21.4
Zn	80	90	64	17-125	200	360	69.6	52.6	74
Pb	16	35	32	3-189	70	600	24.9	20.7	30.8
As	5	6	5.8	<1-95	12	12			
Sb	0.2	1			20	40	0.76	0.53	0.74
Cd	0.2	0.35	0.06-1.1	0.01-2.5	1.4	27			
Cr	100	70	54	14-1300	64	87	56.4	33	53.4
Co	20	8	54	0.1-70	40	300	11.8	7	12
Ni	80	50	20	0.2-450	50	50	23.7	14.5	21.9
Mo	1.5	1.2	1.8	0.013-17	5	40	0.9	0.83	1.04
Hg	0.05	0.06	0.03	0.05-0.3	6.6	50	36 ppb	12 ppb	62 ppb
Se	0.05	0.4	0.33	0.005-3.5	1	3.9			
V	100	90	58	18-115	130	130			
F	950	200	329	10-1360	200	2000			
I	0.14	5	2.8	0.1-10					

Crustal average & soil abundance: from geochemical tables

Agr. Soil from book on Essentials of Medical Geology, Ed: Olle Selinus & others, 2005 Elsevier Pub.

Toxic: From Canadian Soil Quality guidelines (CCME 1996)

China Streams Sediments (SS): From Chinese Publication

6.3. Duplicate Samples

Total 09 nos. of duplicate stream sediment/slope wash samples were collected from different locations of the study area. Each of the duplicate samples was collected from 5' x 5' quadrant grids of the toposheet. All the duplicate stream sediment/slope wash samples were collected at the same time and same location of the original unit cell stream sediments collected. After processing the samples, a unique different number has been assigned and sent for analysis to check precision of the whole sampling process, including variability inherent at the field site, as well as variability from sample processing and analysis. Analytical result of the entire duplicate samples is available (Major, Traces & REE). Permissible variation in between the analytical results indicates the accurateness in the methodologies. Analytical result of duplicate samples and corresponding stream sediments/slope wash samples of elements (majors, traces and REEs) is given in Annexure-VIII, IX and X.



CHAPTER 7

7. SUMMARY, CONCLUSION AND RECOMMENDATION

7.1. Summary

During the field season 2018-19 Geochemical Mapping was taken up in Ukhrul district, Manipur covering parts of T.S. Nos. 83K/8 in 1:50,000 scale covering an area of 671 Sq.km. The study area can be broadly classified into two geological domains as Ophiolite suite of rocks overlain by the Ocean Pelagic Sediments (OPS) and Paleocene to Oligocene sedimentary succession. The main objective of the NGCM is to generate seamless geochemical baseline database for managing/developing natural resources and applications in agricultural, environmental, public health and other spheres of societal concern.

The analytical results of major oxides (package A), trace & REE's (package H) are available. Analytical result of the stream sediment/slope wash samples for 46 elements were received, of which analytical data of stream sediment/slope wash samples of 10 major oxides and 22 trace elements, 14 REEs were interpreted by univariate and bivariate statistical methods to understand the nature of distribution of the elements as well as interrelation between the elements. Geochemical maps depicting spatial distribution of the elements were prepared to interpret their distribution pattern in a secondary geochemical environment.

7.2 Conclusion

The elemental distribution pattern of major oxides / elements in stream sediment of the area is mainly controlled either by the underlying and surrounding lithology as well as physiography of the area.

(i). The high values of Cr (52 to 4810 ppm), Ni (917 to 5681 ppm) and Co (88 to 678 ppm) are observed in the stream sediments collected from eastern part of the study area i.e., NNE-SSW trending ridges of Phangrai, Shirui and Gamnom village, where mafic/ultramafic rocks of ophiolite is exposed. Cr shows strong positive correlation with Ni, Co, Cu and Fe_2O_3 ; good correlation with Ba, Zn, Ge, CaO, MgO, MnO and P_2O_5 . Cr shows negative correlation with all the REE except Ge, which shows strong positive

correlation. The strong positive correlation of Cr with Ni and Co indicates derivation of the sediments from the mafic/ultramafic mantle peridotite. The presence of podiform chromite in the field outcrop corroborates the geochemical anomalies.

(ii). The stream sediments samples collected from the ophiolite belt exposed in the eastern part of the study area i.e, NNE-SSW trending ridges of Phangrai, Shirui and Gamnom village shows high values of Fe_2O_3 (16.23 to 29.13%). Fe_2O_3 shows strong positive correlation with Cr, Ni, Co, Cu, V, Sc, MnO and moderate positive correlation with CaO, MgO, P_2O_5 and Ba. Fe_2O_3 shows negative correlation with all the REE expects Ge, which shows strong positive correlation. Field observation reveals the association of Fe with chromite as ferric chromite at Gamnom village as well as the presence of lateritic/limonitic soil capping above the mafic/ultramafic rocks is commonly observed in the outcrop, where ophiolite body is exposed. Petrographic studies shows high degree of serpentinisation of primary olivine and pyroxene, where of olivine releases fine magnetite mineral grains. Cr spinel is commonly associated with olivine minerals and orthopyroxene which is highly altered to serpentinite.

(iii). SiO_2 value in the samples derived from paleogene sediments shows high concentration ranging from 56 to 80.2%. The highest SiO_2 is reported from the Laisong Formation of Barial Group, where the rock exposures are mostly bluish grey, fine to medium grained sandstone. OPS show SiO_2 value between 50 to 56% and Ophiolite Belt derived stream sediments shows low SiO_2 concentration (36 to 50%). Silica (SiO_2) is the major constituent of nearly all rocks, higher concentration in felsic and intermediate igneous rocks as compared with mafic and ultramafic rocks.

(iv). Two soil and regolith samples each from soil developed from Ophiolite Belt, Olistostrome, Disang and Barial group and one Ocean Pelagic Sediment (OPS) are collected. The soil samples shows a general shows similar enrichment of major elements like SiO_2 , K_2O and MgO, Al_2O_3 , Fe_2O_3 and depleted in TiO_2 , MnO, CaO and K_2O . Trace elements like Ba, Cr, Ni and V shows relative enrichment as compared with other trace elements. The C-horizon soil sample shows slightly higher values as compared with the overlying regolith soil sample.

(v). The two soil samples from Ophiolite Belt show high values of Fe_2O_3 , Cr and Ni. Phangrai soil sample collected from regolith horizon characterised by the reddish limonitic

soil (83K8/C2/R/19; Cr: 6749 ppm, Fe₂O₃: 45.91% and Ni: 4555 ppm) and brownish yellow saprolitic soil horizon (83K8/C2/C/19; Cr: 1288 ppm, Fe₂O₃:12.33 % and Ni: 798 ppm) and Gamnom (83K8/C3/C/19 shows Cr: 12868 ppm, Fe₂O₃: 13.23% and Ni: 687 ppm) and 83K8/C3/C/19; Cr: 11388 ppm, Fe₂O₃:45.29 % and Ni: 4888 ppm. The REE pattern for the soil pattern shows similar concentration, the soil sample from the exposed Barial rock soil profile shows lowest concentration and slight negative Eu anomaly is commonly observed in all the soil samples.

7.3 Recommendation:

1. Detail subsurface study is required along the NNE-SSW trending ridges of Phangrai, Shirui and Gamnom village where preliminary findings of podiform chromite/ferric chromite hosted by mafic/ultramafic rocks of ophiolite occurred.
2. The stream sediments having its provenance from mafic/ultramafic rocks exposed along east of Kalhang Khullen, Phangrai, Shirui and Gamnom village give high values of Cr (4810 ppm), Ni (5681 ppm) and Co (678 ppm). The thick limonitic and saprolitic soil capping developed above the mafic/ultramafic rock shows supergene enrichment of Fe₂O₃, Cr, Ni and slightly Co. The mineral investigation of supergene enrichment deposits of Ni and Co by systematic detail sampling of different soil horizons of the laterite, limonitic and saprolite is required. Two blocks has been identified as prospect block for the mineral commodity Cr, Ni and Co and demarcated as block-A and B to take up for detailed mineral investigation (Fig. 7.1).
3. The detailed specialised thematic mapping is recommended for identification of the different facies of limestone (i.e., exotic limestone bocks within Paleogene sedimentary succession, insitu limestone/marl interbedded with volacano sedimentary facies and limestone containing volcanic bombs) which is exposed in and around Ukhrul town, Shangshak Khullen, Hundung, Choithor, Khangkhui, Mova villages, east of Phangrai village, Phangrai-Sihai village section and Kalhang Khunou-Huishu villages section. The detailed lithofacies mapping along with systematic sampling of limestone for paleontological studies and chemical analysis for preliminary limestone grade classification can be taken up.

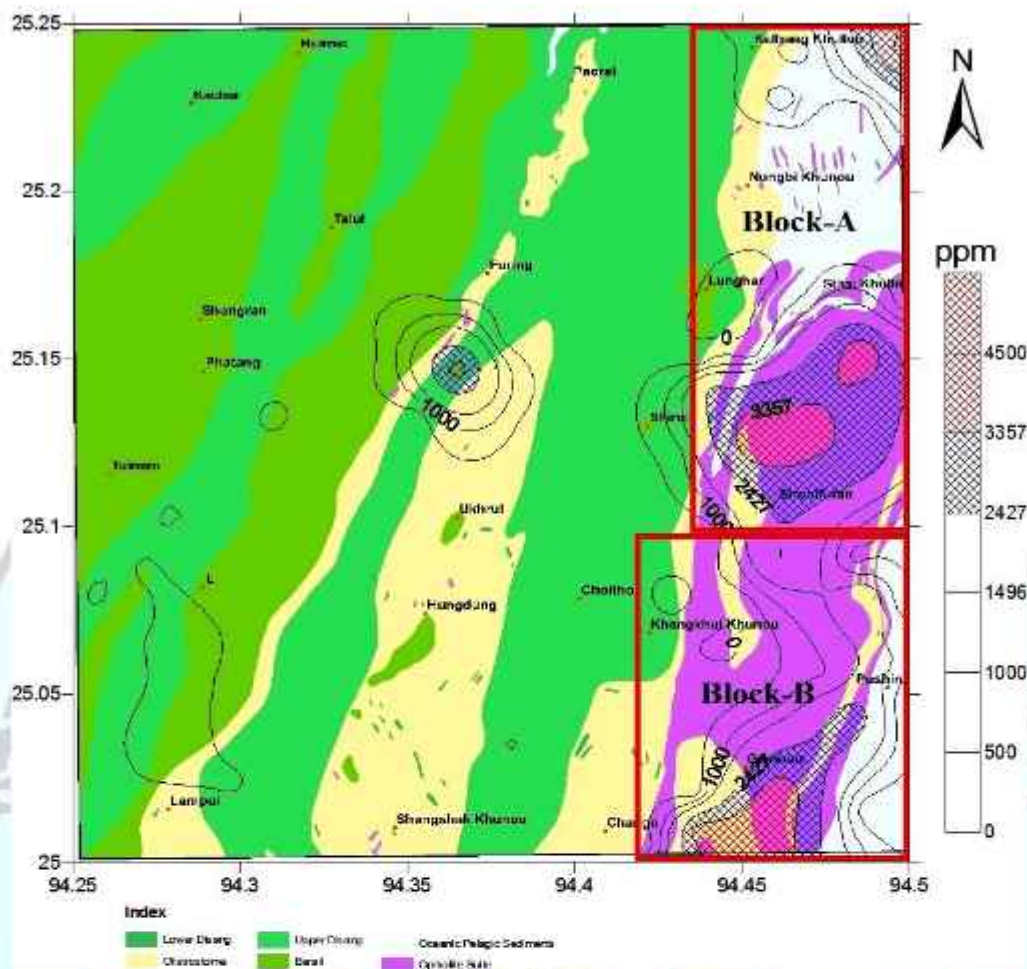


Fig.7.1 Mineral prospect block A and B for chromium, nickel and cobalt as a NGCM spin off project.

REFERENCE:

- Alan T. Baxter, Jonathan C. Aitchison, Sergey V. Zyabrev, Jason R. Ali., 2011. Upper Jurassic radiolarians from the Naga Ophiolite, Nagaland, northeast India
- Anand Alwar, M. A., Banerjee, B., and Dayal, B., 1961. Investigation of nickel and copper mineralization in Manipur. (Unpublished GSI report for FS: 1960-61)
- Brookins, D.G., 1988: Eh-pH diagrams for geochemistry. Springer-Verlag, Berlin-Heidelberg, p.176
- Cavalazzi, B., Agangia, A., Barbierib, R., Franchi, F., and Gasparotto, G., (2011). The formation of low temperature sedimentary pyrite and its relationship with biologically induced processes.
- CCME, (1996): Canadian Soil Quality guidelines
- Chakraborty, S.C., and Raina, V. K., 1985. A note on the reported occurrence of copper and nickel mineralization in Manipur. (Unpublished GSI report for FS: 1984-85)
- Chattopadhyay, B., and Roy, R. K., 1975. Systematic geological mapping and preliminary mineral investigation in parts of ultramafic belt in Manipur East District (Unpublished GSI report for FS:1974-75)
- Chattopadhyay, B.M., Venkataraman, P., Roy, D.K., Ghose, S., Bhattacharya, S.S., 1983. Geology of Naga Hills Ophiolites. Records Geological Survey of India 113 (2), 59-115.
- Chubala Shijoh., Vales Savio Peter., Priscilla Rinmuanpuui., Anushree Gogoi., Lakhi Patra., Abhinab Borah., Mohan Raj, E., Kritibas Das., Ramen Das., Abdurrahman., Tahir Mushtaq., Kowei Kapfo., Tushipokla., Santosh Kumar Patra., and Luangmei Limpou., 2015. Geochemical mapping in the Ophiolite Belt in parts of Manipur and Nagaland in parts of T.S. Nos. 83K/6, 7, 10, 11 & 12 (Unpublished GSI report for FS: 2014-15)
- Chattopadhyay, B.M., Venkataraman, P., Roy, D.K., Ghose, S., Bhattacharya, S.S., 1983. Geology of Naga Hills Ophiolites. Records Geological Survey of India 113 (2), 59-115.
- Das, J.N., Sukla, V. K., and Mishra, U. K., 1987. Report on interdisciplinary study in Manipur- Nagaland Ophiolite for evaluation of mineralization potential. (Unpublished GSI report for FS: 1986-87)
- Das, A. P. and Mishra, S., (2007): Hexavalent Chromium (vi): environment pollutant and health hazard, Journal of Environmental Research And Development, Vol. 2 No. 3, January-March 2008.

- Dutta, G.N., 1959. A preliminary note on the nickel mineralization at Kwatha and Nampesha- Humine area, Manipur State. (Unpublished GSI report for FS: 1958-59)
- Evans, P., 1964. The tectonic framework of Assam. *Journal Geological Society of India* 5, 80-96.
- Gaur, M. P., and Khan, I.K., 1984. Systematic Geological mapping around Paoyi-Paorei, Tolloi-Huimi area of Manipur East district, Manipur. (Unpublished GSI report for FS: 1983-84)
- Ghosh, S., Dutta, A., and Chandrashekhar, V., 1980. Intergrated sureveys in ultramafic belt of Manipur. (Unpublished GSI report for FS: 1979-80)
- Goshal, A. K., 1972. Detailed investigation of limestone around Ukhrul, Manipur East District, Manipur. (Unpublished GSI report for FS: 1971-72)
- Holland, H. D., (1978). *The Chemistry of the Atmosphere and Oceans*. Wiley, New York, 351 pp.
- Howarth, R.J., Thornton, I., (1983): Regional geochemical mapping and its application to environmental studies, In: Thornton, I. (Ed.), *Applied Environmental Geochemistry*, Academic Press, p. 41-73.
- Joshi, A., and Vidyadharan, K. T., 2008. Lithostratigraphy of the Naga-Manipur Hills (Indo-Burma Range) Ophiolite Belt from Ukhrul District, Manipur, India.
- Kevilhoutuo Theunuo., Guneshwar Singh T., and Angami J. K., 2015. Specialised Thematic Mapping Of Ophiolite Suite Of Rocks Of Manipur Between Ningthi To Nungbi Khullen, Ukhrul District, Manipur. (Unpublished GSI report for FS: 2013-14 and 2014-15)
- Mazumdar, M., and Rapa, D. A., 1973. Report on systematic geological mapping including mineral investigation in serpentinite belt, Manipur East District, Manipur. (Unpublished GSI report for FS: 1972-73)
- Marorie Wilson., (1989). *Igneous Petrogenesis*. Harper Collins Academic, 15-19pp
- Oldham, R.D., 1883. Report on the geology of parts of Manipur and Naga hills. *Geological Survey of India, Memoirs*, 19, 216-242.
- Pascoe, E. H., 1912. A traverse across the Naga hills of Assam from Dimapur to the neighbourhood of Saramati peak. *Rec. Geol. Surv. India.*, 42(4).
- Pascoe E. H., 1950. *A Manual of Geology of India and Burma*, Vol Nos. 1 to 3.
- Rudnick, R.L. and Gao, S. (2004): Composition of the Continental Crust. In: *Treatise on geochemistry*, Holland, H.D. and Turekian, K.K. (Editors), Elsevier, Amsterdam.

- Shukla, R., Shukla, V.K., and Vidyadharan, K.T., 1985. Report on systematic geological mapping around Haiyang Kuki, B.D. 30, Tusom Cisi, B.P. 129, Kongai Challao, B.P. 123, Chingai, B.P.127, 125, Huishu Walleli Chingsao, Manipur. (Unpublished GSI report for FS: 1984-85)
- Snyder, G.A., (1999): Vanadium. In: C.P. Marshall & R.W. Fairbridge (Eds.), Encyclopedia of Geochemistry. Kluwer Academic Publishers, Dordrecht, Germany, p. 656
- Ure, A.M. and Berrow, M.L.,(1982): The chemical constituents of soils. In: H.J.M. Bowen (Editor), Environmental Chemistry. R. Soc. Chem., Burlington House, London, pp. 94-202.
- Vidyadharan, K. T., and Anil Joshi, 1984. Report on systematic geological mapping around Lambui-Shangshak-Shingcha, Gamnom-Mapum, Ukhrul-Siroi, Nungbi-Khamasom sectors of Manipur Ophiolite belt, Ukhrul district, Manipur. (Unpublished GSI report for FS: 1983-84)
- Wedepohl, K. H., (1978): Handbook of Geochemistry, Vol. II/5. Springer.
- Zupančič, N. and Pirc, S., (1999): Calcium distribution in soil and stream sediments in Istria, Croatia and the Slovenian littoral. J. Geochem. Explor. 65, 205-218.



LOCALITY INDEX

Sl. No	Locality Name	Longitude	Latitude
1	Kachai Hokhorim	94° 16' 44.77"	25° 14' 16.77"
2	Huimi	94° 19' 7.307"	25° 14' 35.34"
3	Salchang	94° 22' 50.73"	25° 14' 46.65"
4	Paorei	94° 24' 1.18"	25° 14' 3.31"
5	Kalhang Khullen	94° 27' 20.16"	25° 14' 35.97"
6	Kachai Ngarei	94° 16' 53.72"	25° 13' 39.88"
7	Kachai Sinphungrim	94° 15' 33.50"	25° 13' 2.74"
8	Phungcgam	94° 23' 28.14"	25° 12' 34.02"
9	Nungbi Khunou	94° 27' 12.83"	25° 12' 6.97"
10	Tallui	94° 19' 38.33"	25° 11' 21.08"
11	Shangram (Samdal Khullen)	94° 17' 23.15"	25° 09' 55.09"
12	Furing	94° 22' 24.91"	25° 10' 27.77"
13	Phungrim	94° 25' 18.34"	25° 09' 53.57"
14	Lunghar	94° 26' 23.92"	25° 10' 13.77"
15	Sihai	94° 29' 27.89"	25° 10' 7.90"
16	Ngaiu	94° 19' 41.20"	25° 08' 34.98"
17	Siruhi (Sirui)	94° 25' 23.28"	25° 07' 46.83"
18	Langdang Khullen	94° 24' 10.28"	25° 6' 13.07"
19	Ukhrul	94° 21' 50.23"	25° 06' 31.22"
20	Salkhar	94° 18' 23.82"	25° 05' 28.77"
21	Lamlang Gate	94° 17' 19.46"	25° 04' 51.84"
22	Hungdung Upper	94° 21' 31.27"	25° 04' 46.77"
23	Choithar	94° 24' 3.98"	25° 04' 36.64"
24	Kangkhu Khullen	94° 25' 2.29"	25° 03' 40.98"
25	Hungdung Lower	94° 20' 53.88"	25° 03' 45.18"
26	Tushar	94° 18' 12.59"	25° 03' 24.95"
27	Chahi	94° 17' 29.11"	25° 04' 10.31"
28	Ringul	94° 15' 8.29"	25° 03' 3.69"
29	Simit	94° 17' 40.84"	25° 02' 15.99"
30	Nungshang khullen	94° 23' 47.22"	25° 02' 56.15"
31	Pushing	94° 29' 38.32"	25° 02' 56.34"
32	Nungshang Chinkha	94° 20' 44.08"	25° 01' 8.32"
33	Lambui	94° 16' 58.05"	25° 0' 59.75"
34	Shangshak Khullen	94° 20' 27.86"	25° 0' 33.24"
35	Sangjing	94° 21' 49.87"	25° 0' 55.84"
36	Changa	94° 24' 49.43"	25° 0' 27.45"
37	Singcha	94° 25' 49.35"	25° 0' 29.15"
38	Gamnong	94° 27' 18.23"	25° 1' 31.14"
39	Samsai	94° 23' 3.79"	25° 8' 54.49"
40	Phangrai	94° 28' 7.60"	25° 8' 13.55"
41	Phatang	94° 17' 28.08"	25° 9' 51.35"
42	Tuinem	94° 15' 30.86"	25° 7' 0.47"

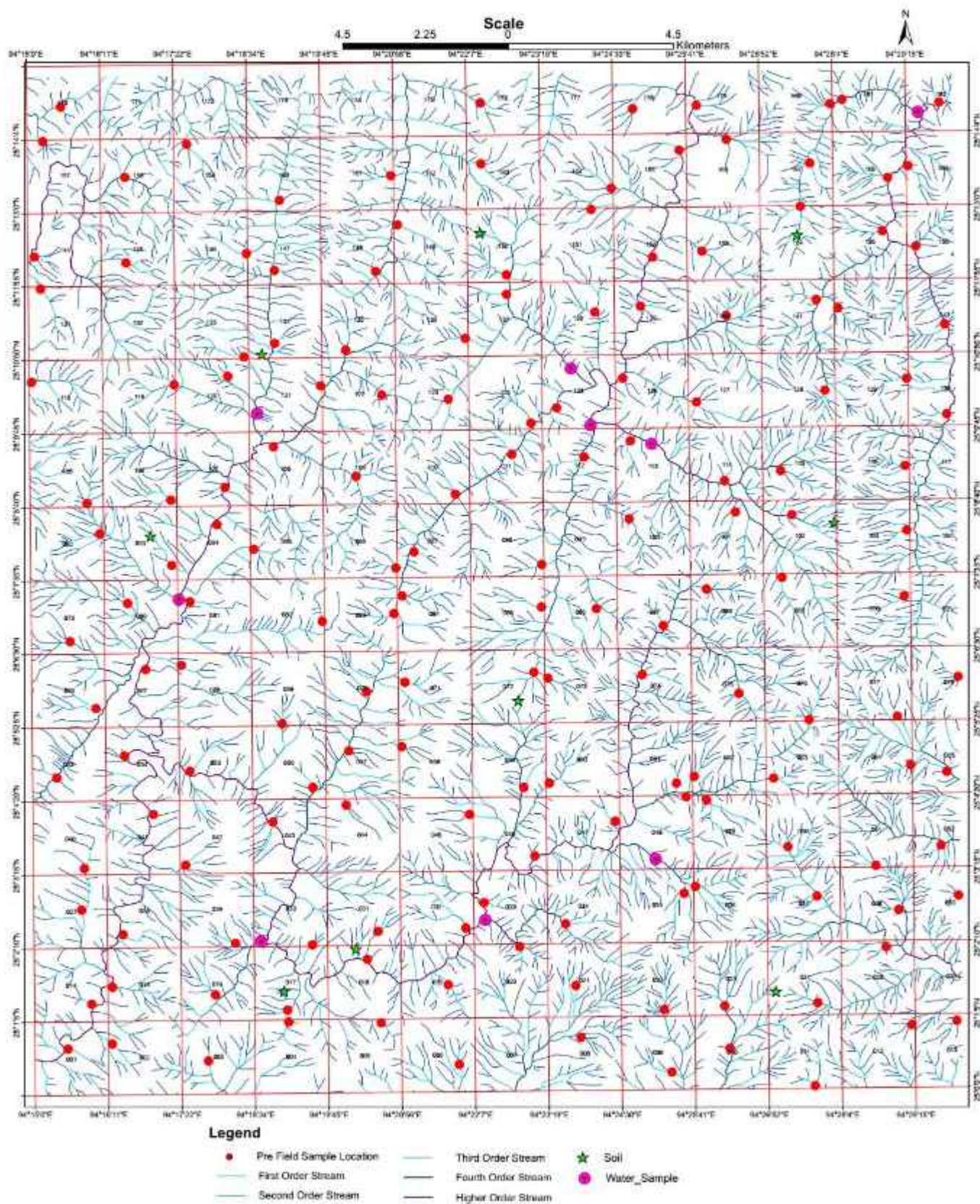


Plate No.2: Sample collection point superimposed on drainage map of
Toposheet No. 83K/8.

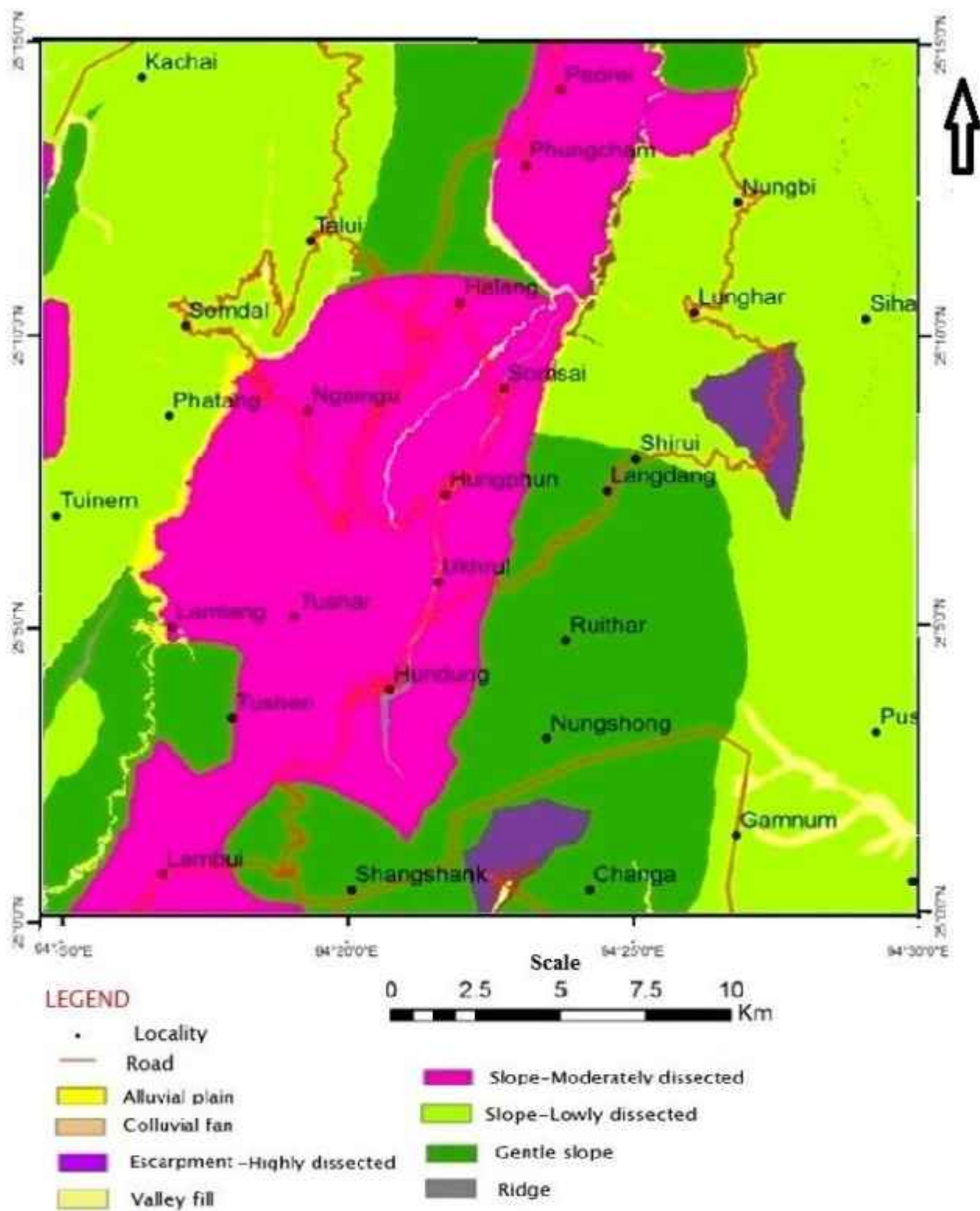


Plate No.3: Geomorphological map of Toposheet No. 83K/8.

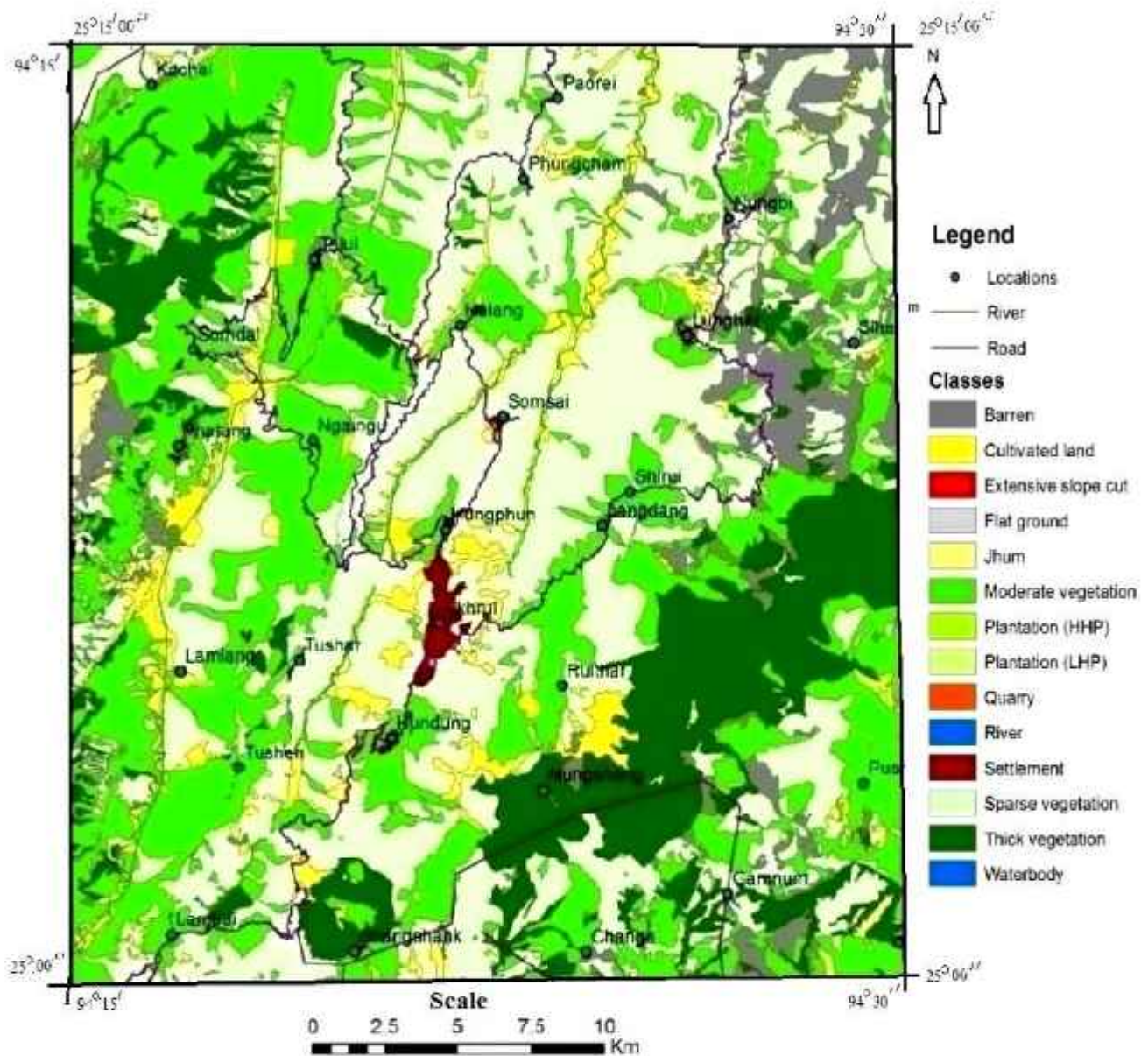


Plate No.4: Land Use and Land Cover map of Toposheet No. 83K/8.

**Analytical data of Major and Minor Oxides of Stream Sediment/Slope Wash Samples
(Values in %)**

Sample No.	SiO ₂	Al ₂ O ₃	Fe ₂ O ₃	TiO ₂	CaO	MgO	MnO	Na ₂ O	K ₂ O	P ₂ O ₅
83K8/001/S/18	66.14	14.14	5.59	1.00	0.40	1.26	0.09	0.48	1.53	0.09
83K8/002/S/18	61.38	13.52	6.16	1.25	0.56	1.12	0.15	0.23	1.96	0.34
83K8/003/S/18	58.75	18.88	6.63	0.99	0.42	1.38	0.14	0.47	2.05	0.11
83K8/004/S/18	60.37	16.52	8.66	1.00	0.64	1.10	0.11	0.43	1.87	0.15
83K8/005/S/18	58.62	19.29	6.03	0.98	0.32	1.20	0.10	0.27	2.43	0.18
83K8/006/S/18	67.33	13.72	5.94	1.25	0.26	1.01	0.13	0.19	1.48	0.11
83K8/008/S/18	62.98	13.61	5.67	1.13	0.66	1.07	0.19	0.21	1.78	0.20
83K8/009/S/18	64.65	14.14	5.98	1.08	0.64	0.97	0.12	0.28	1.76	0.16
83K8/010/S/18	39.20	12.01	29.13	0.47	0.43	3.61	0.53	0.15	0.77	0.17
83K8/011/S/18	40.53	15.35	24.92	0.80	0.23	1.46	0.45	0.16	1.18	0.21
83K8/012/S/18	57.10	16.65	7.19	1.08	0.15	1.29	0.17	0.35	2.41	0.14
83K8/013/S/18	57.56	17.18	6.18	1.37	0.22	0.74	0.29	0.49	2.27	0.18
83K8/014/S/18	59.92	13.67	5.44	0.70	1.37	1.51	0.08	0.71	1.76	0.20
83K8/015/S/18	66.11	14.18	4.95	0.85	0.12	1.13	0.07	0.57	1.84	0.09
83K8/016/S/18	63.83	15.95	5.31	0.86	0.23	1.06	0.05	0.44	2.14	0.11
83K8/017/S/18	61.38	16.09	7.25	1.09	0.55	1.20	0.16	0.49	1.86	0.12
83K8/018/S/18	61.51	15.25	6.32	1.09	0.23	0.78	0.24	0.17	1.45	0.14
83K8/019/S/18	61.81	14.91	6.01	1.22	0.18	0.82	0.16	0.23	1.61	0.25
83K8/020/S/18	56.20	15.37	7.97	1.00	0.48	3.19	0.17	0.20	1.28	0.30
83K8/021/S/18	60.65	16.49	5.80	0.92	0.53	1.58	0.11	0.53	2.01	0.18
83K8/022/S/18	56.66	17.16	6.58	1.03	0.77	1.68	0.13	0.60	2.33	0.18
83K8/023/S/18	52.23	18.45	6.52	0.86	0.85	1.46	0.19	0.31	3.37	0.26
83K8/024/S/18	36.61	9.62	25.41	0.46	2.09	9.17	0.51	0.13	0.47	0.14
83K8/025/S/18	42.89	13.77	18.94	0.65	0.70	2.59	0.42	0.17	1.12	0.25
83K8/027/S/18	71.07	12.46	4.70	0.98	0.17	0.96	0.07	0.25	1.27	0.08

Sample No.	SiO ₂	Al ₂ O ₃	Fe ₂ O ₃	TiO ₂	CaO	MgO	MnO	Na ₂ O	K ₂ O	P ₂ O ₅
83K8/028/S/18	65.66	14.18	4.98	0.70	0.30	1.08	0.08	0.66	1.86	0.10
83K8/029/S/18	57.86	20.02	5.31	0.90	0.61	1.16	0.08	1.17	3.26	0.11
83K8/030/S/18	63.14	15.96	6.45	0.96	0.36	1.44	0.13	0.40	1.67	0.12
83K8/031/S/18	59.06	18.55	6.66	0.97	0.48	1.23	0.14	0.72	1.87	0.12
83K8/032/S/18	61.68	16.17	6.97	0.93	0.44	1.41	0.11	0.49	1.83	0.12
83K8/033/S/18	62.92	15.42	5.66	0.96	0.39	1.21	0.11	0.68	1.86	0.17
83K8/034/S/18	61.86	16.12	6.81	0.98	0.29	1.42	0.19	0.21	2.16	0.16
83K8/035/S/18	58.61	15.95	6.83	0.98	0.70	1.50	0.17	0.39	1.75	0.18
83K8/036/S/18	54.42	18.47	8.80	0.94	0.29	1.82	0.22	0.54	2.02	0.16
83K8/037/S/18	41.01	8.68	10.13	0.65	1.16	14.01	0.22	0.35	0.95	0.23
83K8/038/S/18	40.81	6.87	16.94	0.26	1.48	16.86	0.32	0.17	0.27	0.12
83K8/039/S/18	56.70	16.66	8.02	1.17	0.12	1.12	0.14	0.30	1.37	0.16
83K8/040/S/18	63.29	16.20	6.79	0.92	0.21	1.30	0.07	0.33	1.83	0.09
83K8/041/S/18	68.62	13.66	4.04	0.74	0.32	0.93	0.07	0.61	1.76	0.09
83K8/042/S/18	67.07	14.84	4.06	0.67	0.30	0.77	0.09	0.15	1.91	0.15
83K8/043/S/18	60.10	17.12	6.91	0.91	0.53	1.53	0.11	0.76	1.93	0.12
83K8/044/S/18	61.41	13.66	3.96	1.00	1.00	1.21	0.04	0.30	1.50	0.16
83K8/045/S/18	57.06	15.89	6.48	0.87	0.13	1.11	0.15	0.16	1.61	0.16
83K8/046/S/18	55.03	15.09	6.20	0.93	0.49	1.27	0.21	0.21	1.84	0.25
83K8/047/S/18	55.55	17.55	8.04	0.85	0.41	2.16	0.06	0.47	1.81	0.1
83K8/048/S/18	58.99	17.82	6.92	0.91	0.43	2.37	0.12	0.71	2.15	0.10
83K8/049/S/18	50.39	17.34	7.07	0.92	0.77	1.22	0.19	0.36	1.91	0.24
83K8/050/S/18	61.23	17.51	5.47	0.84	0.2	1.28	0.07	0.41	2.69	0.1
83K8/051/S/18	40.96	12.42	10.52	0.54	1.16	12.20	0.27	0.31	1.03	0.24
83K8/052/S/18	51.02	8.10	12.72	0.52	0.87	7.01	0.36	0.45	0.75	0.33
83K8/053/S/18	71.62	11.99	3.44	0.85	0.46	1.10	0.11	0.28	1.52	0.13
83K8/054/S/18	69.35	12.83	4.95	0.82	0.15	1.12	0.07	0.34	1.63	0.11
83K8/055/S/18	63.28	15.99	6.31	1.03	0.30	1.27	0.14	0.35	1.70	0.08
83K8/056/S/18	65.16	14.81	4.48	0.75	0.41	1.26	0.11	0.68	2.08	0.12

Sample No.	SiO ₂	Al ₂ O ₃	Fe ₂ O ₃	TiO ₂	CaO	MgO	MnO	Na ₂ O	K ₂ O	P ₂ O ₅
83K8/057/S/18	58.41	15.77	7.35	1.07	0.39	1.34	0.1	0.58	1.86	0.13
83K8/058/S/18	62.93	14.16	5.94	0.91	0.3	1.64	0.11	0.48	1.76	0.12
83K8/059/S/18	54.55	18.97	9.21	1.11	0.61	1.32	0.29	0.48	2.34	0.12
83K8/060/S/18	55.27	17.55	7.75	0.87	0.11	1.73	0.11	0.33	1.9	0.13
83K8/061/S/18	59.52	15.6	6.48	0.83	0.4	1.49	0.11	0.44	1.78	0.12
83K8/062/S/18	54.68	14.94	8.91	0.88	0.33	2.3	0.16	0.57	1.63	0.16
83K8/063/S/18	38.84	16.26	14.37	1.97	0.54	1.89	0.3	0.66	0.82	0.46
83K8/064/S/18	48.78	11.66	17.05	0.61	0.41	4.13	1.68	0.36	1.04	0.17
83K8/065/S/18	58.09	13.56	8	0.8	0.51	5.27	0.18	0.34	2.06	0.15
83K8/066/S/18	57.11	17.04	7.68	0.86	0.11	1.28	0.06	0.1	1.43	0.09
83K8/067/S/18	67.67	13.36	4.94	0.74	0.22	1.12	0.05	0.54	1.54	0.09
83K8/068/S/18	66.02	15.15	5.31	0.77	0.34	1.16	0.12	0.42	1.57	0.1
83K8/069/S/18	61.33	15.6	6.52	0.84	0.37	1.89	0.12	0.59	1.91	0.1
83K8/070/S/18	59.42	16.34	8.09	0.8	0.37	1.65	0.09	0.62	1.78	0.07
83K8/071/S/18	55.38	16.45	4.65	0.84	0.23	1.27	0.05	0.7	3.12	0.09
83K8/072/S/18	61.66	14.79	6.44	1.15	0.45	1.08	0.12	0.24	1.84	0.16
83K8/073/S/18	58.47	18.49	6.09	0.93	0.37	1.31	0.2	0.46	2.25	0.07
83K8/074/S/18	62.48	14.59	5.01	0.95	0.31	1.04	0.12	0.27	1.55	0.14
83K8/075/S/18	51.28	14.93	6.39	0.79	1.37	1.61	0.3	0.28	2.21	0.29
83K8/076/S/18	43.02	5.09	16.23	0.41	1.16	15.94	0.34	0.21	0.56	0.13
83K8/077/S/18	53.02	16.71	6.76	0.87	0.86	2.65	0.51	0.81	2.89	0.31
83K8/078/S/18	54.32	18.41	6.33	0.87	0.6	1.92	0.2	0.79	2.97	0.19
83K8/079/S/18	59.53	15.51	6.14	0.84	0.68	1.71	0.15	0.26	1.68	0.2
83K8/080/S/18	62.37	15.91	6.6	0.91	0.06	1.11	0.09	0.13	1.51	0.07
83K8/081/S/18	62.76	15.57	5.11	0.73	0.41	1.55	0.1	0.73	1.96	0.12
83K8/082/S/18	62.12	13.79	4.94	0.88	0.52	1.04	0.14	0.41	1.68	0.16
83K8/083/S/18	57.86	15.7	7.06	0.84	0.26	1.98	0.09	0.54	1.78	0.09
83K8/084/S/18	62.41	16.12	6.12	0.83	0.38	1.41	0.08	0.64	1.94	0.13
83K8/085/S/18	61.21	15.28	6.36	0.9	0.42	1.69	0.09	0.75	1.79	0.1

Sample No.	SiO ₂	Al ₂ O ₃	Fe ₂ O ₃	TiO ₂	CaO	MgO	MnO	Na ₂ O	K ₂ O	P ₂ O ₅
83K8/086/S/18	62.56	14.81	5.17	0.89	0.36	1.14	0.1	0.67	1.82	0.16
83K8/087/S/18	67.07	12.94	4.91	0.85	0.19	0.98	0.06	0.34	1.24	0.1
83K8/088/S/18	51.78	15.22	9.16	0.66	0.96	6.21	0.21	0.58	2.02	0.12
83K8/089/S/18	38.74	5.38	13.97	0.29	1.17	20.1	0.29	0.15	0.38	0.09
83K8/090/S/18	48.86	9.28	13.16	0.7	1.02	2.34	0.57	0.26	1.23	0.28
83K8/092/S/18	57.59	15.27	6.85	0.93	0.39	1.33	0.14	0.18	1.78	0.13
83K8/093/S/18	62.1	13.18	5.78	0.86	0.27	1.62	0.14	0.22	1.56	0.14
83K8/094/S/18	64.29	14.93	4.6	0.76	0.14	1.09	0.09	0.34	1.38	0.15
83K8/095/S/18	67.07	13.22	3.27	0.67	0.25	0.88	0.1	0.35	1.49	0.21
83K8/096/S/18	68.39	12.63	4.81	0.97	0.13	0.92	0.12	0.19	1.46	0.12
83K8/097/S/18	59.92	17.43	6.75	0.91	0.31	1.7	0.07	0.74	1.97	0.08
83K8/098/S/18	58.12	16.39	8.04	0.9	0.47	1.45	0.12	0.6	1.73	0.07
83K8/100/S/18	63.57	15.8	5.56	0.82	0.3	1.41	0.09	0.34	1.57	0.12
83K8/101/S/18	44.35	3.08	11.97	0.22	1.03	24.92	0.21	0.12	0.18	0.06
83K8/102/S/18	45.49	9.31	21.2	0.48	0.58	7.98	0.32	0.07	0.58	0.09
83K8/103/S/18	50.32	10.12	14.4	0.72	0.69	2.83	0.72	0.21	1.05	0.22
83K8/105/S/18	57.67	14.87	6.5	0.75	0.86	2.27	0.15	0.38	1.74	0.24
83K8/106/S/18	62.75	13.18	5.15	0.86	0.77	2.15	0.15	0.44	1.04	0.23
83K8/107/S/18	62.82	13.42	5.89	0.88	0.36	1.66	0.13	0.22	1.88	0.17
83K8/108/S/18	64.79	15.44	4.77	0.74	0.31	1.52	0.05	0.77	1.85	0.09
83K8/109/S/18	64.73	14.75	5.94	0.8	0.48	1.65	0.11	0.4	1.65	0.14
83K8/110/S/18	45.76	6.98	17.46	0.49	1.31	8.07	0.4	0.17	0.44	0.06
83K8/111/S/18	69.17	11.13	3.83	1.03	0.31	0.86	0.12	0.31	1.26	0.12
83K8/112/S/18	70.55	10.63	4.64	1.24	0.08	0.59	0.21	0.18	1.26	0.13
83K8/113/S/18	63.58	14.58	5.82	0.86	0.25	1.27	0.08	0.38	1.7	0.11
83K8/114/S/18	67.5	13.47	4.94	0.89	0.15	1.07	0.06	0.4	1.62	0.1
83K8/115/S/18	59.88	13.18	10.26	1.15	0.36	1.89	0.13	0.52	3.19	0.11
83K8/116/S/18	48.9	10.68	16.24	0.73	0.4	3.47	0.65	0.18	1.14	0.26
83K8/118/S/18	56.66	15.15	7.48	0.82	0.6	2.56	0.23	0.46	1.98	0.33

Sample No.	SiO ₂	Al ₂ O ₃	Fe ₂ O ₃	TiO ₂	CaO	MgO	MnO	Na ₂ O	K ₂ O	P ₂ O ₅
83K8/119/S/18	63.65	14.33	5.9	0.83	0.27	1.96	0.12	0.42	1.35	0.12
83K8/120/S/18	59.99	13.87	6.36	0.87	0.37	1.63	0.14	0.22	2	0.13
83K8/121/S/18	71.82	12.44	3.99	0.78	0.23	0.93	0.04	0.24	1.56	0.09
83K8/122/S/18	66.42	13.39	4.19	0.86	0.35	1.22	0.08	0.57	1.82	0.1
83K8/123/S/18	55.85	16.89	7.79	0.83	0.22	1.77	0.13	0.32	2.07	0.1
83K8/124/S/18	60.06	16.98	6.77	0.88	0.76	1.61	0.11	0.82	1.97	0.13
83K8/125/S/18	61.48	16.62	6.81	0.86	0.75	1.63	0.14	0.79	1.94	0.13
83K8/126/S/18	60.3	15.87	6.03	0.88	0.42	1.29	0.09	0.61	1.89	0.13
83K8/127/S/18	58.48	15.79	6.49	0.91	0.38	1.62	0.14	0.57	1.58	0.14
83K8/128/S/18	61.93	14.13	4.86	0.82	1.09	1.23	0.15	0.5	1.82	0.22
83K8/129/S/18	61.42	13.27	7.96	1.23	0.25	1.68	0.34	0.33	1.47	0.15
83K8/130/S/18	50.85	14.83	8.41	1.61	1.78	2.5	0.18	0.72	1.6	0.27
83K8/131/S/18	60.25	15.95	7.17	0.83	0.45	2.08	0.08	0.72	2.02	0.11
83K8/133/S/18	59.68	15.33	7.08	0.78	0.42	2.52	0.07	0.79	1.79	0.09
83K8/134/S/18	66.85	14.53	4.71	0.78	0.18	0.96	0.05	0.14	1.66	0.1
83K8/135/S/18	61.58	14.53	5.38	0.78	0.65	1.71	0.16	0.55	1.97	0.15
83K8/136/S/18	66.14	13.67	4.93	0.85	0.26	1.03	0.08	0.53	1.57	0.12
83K8/137/S/18	57.97	15.87	6.82	1.03	0.76	1.18	0.17	0.43	2.01	0.12
83K8/138/S/18	60.12	16.51	7.1	0.95	0.43	1.35	0.11	0.72	2.08	0.12
83K8/139/S/18	63.77	15	6.09	0.84	0.3	1.25	0.11	0.79	1.74	0.1
83K8/140/S/18	62.24	15.47	7.49	0.98	0.24	1.17	0.17	0.49	1.98	0.12
83K8/141/S/18	60.14	16.5	5.93	0.85	0.42	1.42	0.15	0.59	2.17	0.13
83K8/142/S/18	52.29	14.81	8.47	1.93	1.3	3.18	0.16	1.06	2.16	0.2
83K8/143/S/18	54.55	14.01	11.1	1.61	0.74	1.88	0.23	1.42	0.32	0.1
83K8/144/S/18	59.13	13.88	6.12	0.83	0.4	1.88	0.1	0.55	1.56	0.14
83K8/145/S/18	57.85	16.8	6.8	0.81	0.42	2.09	0.15	0.59	1.88	0.13
83K8/146/S/18	60.28	16.51	6.81	0.77	0.5	2.33	0.1	0.73	1.81	0.1
83K8/147/S/18	60.66	16.77	7.58	0.84	0.21	1.82	0.08	0.67	1.9	0.09
83K8/148/S/18	66.64	12.89	3.61	0.68	0.6	1.03	0.19	0.34	1.42	0.24

Sample No.	SiO ₂	Al ₂ O ₃	Fe ₂ O ₃	TiO ₂	CaO	MgO	MnO	Na ₂ O	K ₂ O	P ₂ O ₅
83K8/149/S/18	69.92	13.12	2.92	0.65	0.35	0.84	0.16	0.18	1.65	0.15
83K8/150/S/18	58.18	16.65	7.35	1.02	0.54	1.33	0.12	0.46	1.86	0.12
83K8/151/S/18	59.55	15.8	6.89	0.9	0.7	1.51	0.12	0.78	1.99	0.15
83K8/152/S/18	61.03	16.58	6.84	1.03	0.42	1.31	0.17	0.62	2.08	0.12
83K8/153/S/18	62.09	15.79	6.75	0.84	0.35	1.44	0.13	0.29	1.71	0.12
83K8/154/S/18	54.81	15.22	6.77	1.03	1.1	1.33	0.38	0.28	2.25	0.3
83K8/155/S/18	57.21	16.05	6.61	1.05	0.73	1.28	0.12	0.71	2.65	0.18
83K8/156/S/18	60.47	15.03	5.84	1.22	0.58	1.18	0.3	0.45	2.02	0.22
83K8/157/S/18	67.73	11.58	4.21	0.91	0.49	1.34	0.08	0.47	1.64	0.14
83K8/158/S/18	57.84	15.85	7.65	0.88	0.38	1.98	0.2	0.31	1.77	0.16
83K8/159/S/18	65.33	13.21	5.09	0.94	0.3	1.36	0.09	0.52	1.69	0.16
83K8/160/S/18	62.47	14.81	5.27	0.81	0.25	1.43	0.03	0.58	1.63	0.12
83K8/161/S/18	80.02	8.81	2.36	0.71	0.13	0.65	0.09	0.24	1.01	0.11
83K8/163/S/18	64.75	14.36	5.15	0.81	0.2	1.15	0.03	0.69	1.65	0.1
83K8/164/S/18	63.31	15.17	5.91	0.93	0.31	1.14	0.1	0.37	1.7	0.12
83K8/165/S/18	58.41	19.09	6.67	0.89	0.37	1.5	0.1	0.71	2.61	0.09
83K8/166/S/18	64.71	14.09	6.6	0.81	0.24	1.68	0.07	0.84	1.5	0.09
83K8/167/S/18	52.73	9.09	8.15	0.63	0.78	10.5	0.16	0.47	0.9	0.12
83K8/168/S/18	60.53	15.48	6.01	0.91	0.52	1.84	0.16	0.45	2.55	0.12
83K8/169/S/18	54.97	11.9	8.51	1.48	0.92	4.66	0.17	1.16	1.36	0.18
83K8/170/S/18	65.3	14.75	5.85	0.8	0.29	1.87	0.07	0.47	1.74	0.1
83K8/176/S/18	61.88	16.35	6.02	0.84	0.26	1.36	0.05	0.64	2.01	0.1
83K8/178/S/18	65.63	15.75	6.76	0.97	0.2	1.23	0.05	0.59	1.86	0.09
83K8/179/S/18	65.83	13.84	5.97	0.88	0.4	1.67	0.1	0.68	1.49	0.11
83K8/180/S/18	61.72	16.14	5.73	0.78	0.53	2.19	0.08	0.66	1.93	0.12
83K8/181/S/18	64.28	13.12	6.33	0.72	0.51	2.93	0.11	0.64	1.55	0.11
83K8/182/S/18	47.82	9.81	24.7	0.65	0.21	1.9	1.41	0.07	0.65	0.07

Analytical Data of Trace Elements of Stream Sediment/Slope Wash Samples
(Values in ppm)

Sample No.	Ba	Co	Cr	Cu	Ga	Nb	Ni	Pb	Rb	Sc	Sr	Th	V	Y	Zn	Zr	Sn	Hf	Ta	Ge	Be	U
83K8/001/S/18	340	10	140	24	17	12	41	16	77.52	15	69	11.97	114	23	64	247	3.64	12.66	1.17	1.41	1.59	2.37
83K8/002/S/18	461	21	182	30	17	17	41	20	86.38	20	72	13.62	130	25	98	284	3.11	7.96	1.09	1.44	1.84	2.36
83K8/003/S/18	305	31	190	41	20	10	79	17	108.49	19	87	11.26	146	27	96	190	3.58	7.45	0.98	1.64	1.91	2.17
83K8/004/S/18	415	24	174	28	20	16	56	20	103.70	17	80	13.93	136	26	90	244	3.55	9.50	1.29	1.79	2.20	2.25
83K8/005/S/18	429	16	135	32	22	13	37	22	116.46	19	78	15.59	135	31	100	272	4.19	9.98	1.21	1.48	2.14	3.19
83K8/006/S/18	373	20	197	28	17	18	50	16	86.82	18	52	15.45	122	26	72	318	3.29	13.44	1.57	1.52	1.71	2.91
83K8/008/S/18	428	21	155	36	17	14	37	23	109.38	17	62	13.66	120	20	96	244	8.36	8.62	1.43	1.50	1.80	2.56
83K8/009/S/18	374	18	215	32	17	14	57	16	94.01	20	74	12.00	127	23	93	247	3.46	9.86	1.26	1.36	1.74	2.15
83K8/010/S/18	300	310	3922	15	14	12	2831	17	79.19	33	20	10.86	193	15	157	106	3.75	3.56	0.46	5.42	1.72	2.16
83K8/011/S/18	320	187	3829	71	18	14	1517	18	90.57	33	27	13.80	225	17	152	136	4.13	3.20	0.68	4.39	2.09	3.01
83K8/012/S/18	534	18	145	37	23	17	62	14	162.12	20	62	19.27	155	29	118	239	5.24	8.41	1.36	1.74	2.26	3.39
83K8/013/S/18	390	17	152	34	20	20	51	23	146.32	18	77	18.35	163	33	111	277	3.62	7.60	1.22	1.52	2.49	3.06
83K8/014/S/18	262	21	331	27	13	8	97	14	72.15	21	106	7.94	107	19	87	218	1.43	5.81	0.53	1.13	1.19	1.77
83K8/015/S/18	175	15	547	22	15	10	77	23	80.26	17	63	10.52	112	21	69	351	2.60	13.94	0.79	1.27	1.24	2.34
83K8/016/S/18	252	14	576	22	16	11	79	23	91.23	17	73	9.96	122	22	74	340	3.18	13.37	0.75	1.24	1.52	2.37
83K8/017/S/18	243	20	156	27	17	16	52	24	103.17	18	80	13.72	138	27	93	239	3.15	8.85	1.16	1.62	1.90	2.27
83K8/018/S/18	312	9	140	29	16	18	38	31	106.79	18	50	17.73	136	23	74	299	3.53	10.88	1.39	1.42	1.59	3.38
83K8/019/S/18	346	15	151	29	18	18	33	30	110.36	16	58	15.77	134	24	96	264	4.10	9.06	1.42	1.50	1.63	2.74
83K8/020/S/18	299	26	549	38	18	13	301	24	90.03	19	49	13.59	133	23	93	210	3.53	6.94	1.11	1.62	1.69	2.65
83K8/021/S/18	245	24	228	28	16	10	105	20	83.35	18	71	9.61	131	23	94	232	2.45	7.85	0.80	1.25	1.46	2.04
83K8/022/S/18	349	25	216	34	18	14	109	30	114.85	18	122	14.43	132	30	117	243	3.59	8.30	1.11	1.58	2.14	2.51
83K8/023/S/18	552	18	117	30	22	14	47	33	164.66	22	79	17.51	124	30	103	217	5.10	6.88	1.09	1.48	2.56	3.26
83K8/024/S/18	239	246	3981	53	10	7	3763	9	46.41	35	18	6.17	124	14	128	60	1.36	1.84	0.40	4.20	0.93	1.28
83K8/025/S/18	648	186	2539	56	16	10	1685	20	94.25	35	37	11.90	137	17	140	137	3.54	3.70	0.89	3.54	1.72	2.55
83K8/027/S/18	198	4	295	20	13	13	57	18	71.98	14	55	9.78	104	23	64	279	1.65	9.70	0.89	1.12	1.10	2.29
83K8/028/S/18	248	13	791	21	12	8	67	22	63.19	16	73	7.61	96	19	62	483	1.15	19.79	0.72	1.16	1.02	2.13

Sample No.	Ba	Co	Cr	Cu	Ga	Nb	Ni	Pb	Rb	Sc	Sr	Th	V	Y	Zn	Zr	Sn	Hf	Ta	Ge	Be	U
83K8/029/S/18	420	12	106	15	21	14	24	26	141.95	20	116	16.10	106	38	101	309	4.58	12.57	1.16	1.51	2.75	3.53
83K8/030/S/18	181	17	221	30	18	13	92	20	94.17	16	63	11.44	136	22	91	221	2.59	7.41	0.93	1.52	1.70	2.18
83K8/031/S/18	230	30	157	38	20	11	43	22	82.32	19	83	9.64	143	22	92	210	2.72	7.33	0.74	1.45	1.57	2.21
83K8/032/S/18	263	14	229	29	17	14	71	22	90.07	19	73	11.15	137	25	91	302	4.67	12.07	1.08	1.71	1.83	2.29
83K8/033/S/18	195	25	209	27	16	12	62	17	80.42	17	81	9.85	123	23	92	249	3.40	9.76	0.93	1.27	1.51	2.08
83K8/034/S/18	363	15	166	32	18	16	74	26	120.92	18	58	13.78	139	27	111	225	4.25	8.32	1.23	1.60	1.87	2.53
83K8/035/S/18	421	20	203	35	18	13	60	23	98.73	19	75	12.88	133	23	93	285	3.74	11.49	1.09	1.58	1.92	2.45
83K8/036/S/18	238	45	268	51	21	13	158	25	96.87	24	71	12.58	160	30	112	246	3.46	9.36	0.95	1.95	2.03	2.33
83K8/037/S/18	159	106	958	28	10	7	917	13	54.08	17	33	5.59	106	13	70	88	2.29	3.54	0.43	1.87	0.91	1.13
83K8/038/S/18	126	259	3081	40	9	0.25	2793	7	29.21	22	16	4.00	87	9	88	45	2.08	1.80	0.30	2.98	0.56	0.85
83K8/039/S/18	280	21	344	22	19	17	162	24	110.35	20	48	17.68	151	28	97	270	4.51	12.06	1.57	1.82	1.61	3.04
83K8/040/S/18	183	24	227	28	18	9	97	16	94.22	22	70	10.90	136	21	87	207	2.99	8.15	0.82	1.60	1.66	2.18
83K8/041/S/18	224	18	971	24	12	9	100	18	74.53	16	78	9.10	105	21	67	575	3.17	26.93	0.79	1.16	1.25	2.84
83K8/042/S/18	211	2	536	17	14	9	41	20	70.00	14	40	9.18	84	17	49	268	2.79	13.56	0.80	1.14	1.16	2.32
83K8/043/S/18	239	18	179	36	18	11	59	25	91.60	19	93	10.35	139	23	99	225	3.96	8.67	0.91	1.67	1.70	2.14
83K8/044/S/18	298	13	175	24	14	15	36	19	83.43	18	70	12.98	123	21	89	531	3.79	25.34	1.21	1.13	1.81	2.53
83K8/045/S/18	318	11	278	34	17	13	53	19	109.80	17	44	13.18	133	21	78	224	4.13	10.26	1.16	1.55	1.42	2.93
83K8/046/S/18	336	23	175	42	18	12	65	17	100.36	17	58	10.79	144	19	99	182	3.25	7.59	0.86	1.28	1.58	2.12
83K8/047/S/18	215	14	167	32	19	12	86	14	85.69	16	63	9.60	135	22	97	188	3.59	7.67	0.65	1.34	1.71	2.05
83K8/048/S/18	322	28	237	46	22	12	121	22	108.75	22	74	12.59	152	26	111	211	3.78	9.14	1.01	1.71	2.02	2.36
83K8/049/S/18	555	15	128	42	19	11	47	16	94.17	18	210	10.18	142	21	116	181	3.73	7.35	0.45	1.19	1.26	2.20
83K8/050/S/18	370	9	79	40	19	17	38	16	134.70	14	29	15.67	109	34	80	245	4.19	10.18	1.46	1.21	2.37	3.09
83K8/051/S/18	228	128	1007	49	13	6	1036	11	54.12	20	32	5.96	96	18	81	96	2.45	3.87	0.49	1.93	0.93	1.22
83K8/052/S/18	307	174	1566	39	10	7	1451	9	67.32	20	35	7.48	84	14	121	93	2.61	3.08	0.64	3.00	1.24	1.39
83K8/053/S/18	223	18	523	15	12	11	47	15	65.91	15	62	9.42	88	18	58	377	1.81	14.96	0.90	0.96	1.04	2.35
83K8/054/S/18	201	16	524	23	15	11	61	16	77.93	16	55	9.29	102	21	69	353	2.56	12.18	0.75	1.21	1.12	2.19
83K8/055/S/18	312	25	233	35	18	13	83	12	84.48	20	74	10.51	138	24	94	260	1.78	8.39	0.98	1.44	1.50	2.24
83K8/056/S/18	237	22	404	28	13	10	97	15	88.61	10	86	8.73	102	23	72	247	3.45	9.69	1.10	1.00	1.26	2.01

Sample No.	Ba	Co	Cr	Cu	Ga	Nb	Ni	Pb	Rb	Sc	Sr	Th	V	Y	Zn	Zr	Sn	Hf	Ta	Ge	Be	U
83K8/057/S/18	296	18	138	37	18	17	58	19	96.16	15	76	10.92	154	20	103	218	3.66	8.74	0.66	1.30	1.70	1.86
83K8/058/S/18	159	21	179	34	14	14	130	15	94.91	16	67	11.00	114	24	84	179	5.24	7.13	1.03	1.25	1.43	2.15
83K8/059/S/18	282	32	142	51	24	18	77	32	111.85	23	103	13.55	167	34	123	212	4.09	8.45	0.53	1.81	2.44	2.04
83K8/060/S/18	233	21	164	33	18	11	109	18	100.26	19	57	10.09	145	20	107	171	3.59	7.31	0.37	1.31	1.56	2.01
83K8/061/S/18	208	21	292	29	15	12	124	16	89.56	16	75	9.07	121	24	93	244	8.05	10.42	0.65	1.35	1.38	1.93
83K8/062/S/18	358	45	972	33	17	14	526	22	97.30	18	68	11.76	135	26	104	207	3.72	9.00	0.35	1.55	1.66	2.21
83K8/063/S/18	539	32	52	44	20	6	17	9	43.22	34	82	2.72	375	36	123	110	3.50	4.54	0.13	2.10	0.77	0.89
83K8/064/S/18	386	141	2111	55	14	8	2832	19	56.41	36	39	5.86	159	21	78	100	3.08	4.36	0.21	2.63	1.59	1.20
83K8/065/S/18	448	62	836	33	16	15	770	17	99.484	12	69	14.165	107	27	92	229	2.138	9.330	1.316	1.735	1.909	2.609
83K8/066/S/18	138	22	383	32	16	13	138	11	79.14	16	29	10.83	131	18	74	231	3.77	11.64	1.41	1.35	1.29	2.34
83K8/067/S/18	118	17	530	26	12	11	99	16	75.10	14	60	8.08	97	22	60	289	3.55	11.99	2.06	1.06	1.09	1.89
83K8/068/S/18	204	23	331	27	12	12	81	15	69.39	11	66	7.89	97	20	72	285	4.08	11.01	1.63	1.07	1.23	1.69
83K8/069/S/18	225	28	243	40	17	13	153	19	107.94	16	78	9.20	124	23	93	180	3.61	7.35	0.94	1.33	1.61	1.87
83K8/070/S/18	183	19	241	38	17	11	118	20	95.44	17	107	8.33	129	22	83	175	3.40	6.39	0.23	1.48	1.68	1.64
83K8/071/S/18	180	11	204	28	19	12	41	22	105.897	16	82	10.104	120	24	51	249	1.730	10.594	1.093	1.092	1.493	2.219
83K8/072/S/18	435	18	123	39	17	22	56	18	107.70	18	82	12.68	140	25	105	242	4.00	9.57	1.63	1.43	1.88	2.18
83K8/073/S/18	222	26	131	33	20	12	74	22	109.79	15	97	10.61	139	26	87	196	4.05	7.95	1.20	1.32	1.65	2.10
83K8/074/S/18	225	19	175	24	14	13	58	13	98.28	14	70	9.47	104	18	81	213	3.52	3.60	1.15	1.06	1.34	2.03
83K8/075/S/18	739	23	113	44	17	11	66	21	110.69	19	101	10.84	115	27	100	187	3.70	6.36	0.99	1.21	1.75	2.10
83K8/076/S/18	110	197	2534	34	10	7	3044	2	32.11	18	31	4.07	123	11	77	52	3.23	2.36	0.21	2.24	0.54	0.82
83K8/077/S/18	550	38	252	47	19	14	246	38	136.22	15	85	14.56	129	53	122	219	9.58	7.18	2.03	1.92	2.53	2.75
83K8/078/S/18	576	25	182	38	20	16	119	27	131.35	15	98	15.28	118	35	113	332	5.95	12.71	2.63	1.77	2.61	3.11
83K8/079/S/18	354	26	344	30	13	11	157	8	90.93	13	59	8.46	109	16	87	180	3.46	5.79	1.06	1.05	1.20	1.83
83K8/080/S/18	238	21	287	24	15	15	112	17	93.17	13	32	13.23	113	20	76	248	3.86	5.91	1.68	1.26	1.36	2.71
83K8/081/S/18	193	14	419	23	14	9	127	12	83.47	14	83	7.63	105	21	74	275	3.37	9.90	1.45	1.02	1.22	1.97
83K8/082/S/18	213	15	222	24	12	12	66	15	109.51	12	80	8.92	107	17	84	203	3.44	4.96	1.23	1.01	1.14	2.05
83K8/083/S/18	200	20	208	36	17	10	126	14	95.40	15	75	9.21	122	22	93	178	3.52	8.94	0.89	1.30	1.61	1.99
83K8/084/S/18	176	19	210	25	16	12	68	19	87.53	11	75	9.77	111	25	91	267	3.40	11.95	1.14	1.21	1.42	1.94

Sample No.	Ba	Co	Cr	Cu	Ga	Nb	Ni	Pb	Rb	Sc	Sr	Th	V	Y	Zn	Zr	Sn	Hf	Ta	Ge	Be	U
83K8/085/S/18	212	21	157	33	16	12	78	18	87.20	17	71	9.66	115	22	85	217	3.37	9.26	1.06	1.20	1.47	1.99
83K8/086/S/18	142	24	178	22	15	13	71	13	80.31	12	74	9.03	113	23	82	224	3.20	9.81	1.17	1.06	1.27	1.89
83K8/087/S/18	160	12	237	21	12	12	71	16	69.61	15	60	7.97	91	18	68	263	4.10	10.87	1.72	1.01	1.09	1.99
83K8/088/S/18	432	88	991	24	14	12	1208	20	102.98	13	67	11.62	100	23	85	170	3.74	7.48	0.73	1.50	1.64	2.26
83K8/089/S/18	25	179	3960	22	5	8	2610	12	21.129	18	16	3.301	87	6	85	41	0.922	2.706	0.230	1.936	0.444	0.666
83K8/090/S/18	528	142	3184	32	13	13	1108	24	92.138	14	43	11.171	139	15	132	157	2.687	7.187	1.165	2.052	1.433	2.425
83K8/092/S/18	293	25	204	37	18	15	112	18	100.64	16	53	12.92	119	23	93	229	4.98	9.88	1.42	1.25	1.58	2.79
83K8/093/S/18	248	24	225	33	14	13	113	14	95.68	15	45	10.59	113	19	72	182	3.55	8.83	1.01	1.04	1.32	2.25
83K8/094/S/18	159	18	382	17	12	11	91	9	71.09	16	53	7.72	96	25	67	275	4.24	11.95	1.04	0.89	0.98	1.95
83K8/095/S/18	215	11	575	12	10	10	49	11	72.14	13	40	7.87	72	12	46	284	3.09	12.04	0.93	0.89	0.99	1.87
83K8/096/S/18	243	23	238	29	12	13	87	12	73.02	11	58	6.03	96	20	75	219	3.27	13.06	0.99	0.67	0.85	1.62
83K8/097/S/18	289	23	230	33	19	12	99	12	94.94	18	82	9.92	140	26	96	235	3.44	8.72	1.02	1.27	1.51	2.27
83K8/098/S/18	313	23	133	41	18	13	65	23	95.75	18	69	10.40	149	24	93	184	3.44	9.13	0.90	1.26	1.46	2.40
83K8/100/S/18	188	16	250	23	14	10	75	14	67.615	17	63	8.848	108	22	85	368	1.874	16.880	0.972	1.087	1.310	2.280
83K8/101/S/18	25	141	2567	17	6	5	2474	1	93.39	9	14	10.18	63	5	58	31	3.41	8.35	1.25	1.38	1.72	1.96
83K8/102/S/18	190	206	2859	42	11	9	5681	9	48.41	27	18	7.33	151	15	114	76	3.30	3.58	0.47	2.88	1.08	1.53
83K8/103/S/18	514	155	2852	37	13	13	1651	16	89.556	20	37	11.458	148	16	127	141	1.944	5.912	1.218	2.319	1.444	2.400
83K8/105/S/18	360	24	356	30	15	10	153	16	86.052	15	62	10.236	117	19	89	178	1.708	8.287	0.932	1.161	1.523	2.119
83K8/106/S/18	339	22	385	15	12	13	138	16	59.66	8	64	9.60	88	17	64	212	3.24	11.07	1.29	0.89	1.08	2.13
83K8/107/S/18	295	25	184	31	17	14	122	15	98.15	17	56	11.64	105	22	81	197	3.49	8.71	1.27	1.03	1.44	2.48
83K8/108/S/18	159	20	423	30	12	11	106	11	66.48	12	81	7.14	106	21	72	313	5.96	11.19	1.07	1.05	1.05	1.77
83K8/109/S/18	254	31	294	33	16	11	154	17	86.490	10	72	10.041	112	22	97	214	1.847	8.668	1.015	1.153	1.529	2.194
83K8/110/S/18	120	190	3950	40	9	8	2584	8	27.23	21	26	3.82	147	10	74	87	2.70	3.94	0.31	2.55	0.58	0.86
83K8/111/S/18	175	12	132	19	11	17	43	17	67.84	11	58	10.69	88	26	84	278	3.17	7.95	1.79	0.97	1.17	2.30
83K8/112/S/18	189	21	113	19	12	23	28	16	76.31	19	52	12.89	90	26	51	281	3.19	8.85	2.41	1.09	1.13	2.46
83K8/113/S/18	149	27	210	33	14	11	83	21	76.203	15	66	10.123	113	24	77	312	1.435	13.738	1.013	1.126	1.415	2.353
83K8/114/S/18	167	19	218	25	13	14	69	14	63.24	15	66	8.15	96	24	74	284	3.90	7.47	1.10	1.06	1.06	1.95
83K8/115/S/18	269	53	128	50	23	27	113	15	123.27	15	39	9.60	128	37	142	250	3.89	7.41	2.39	2.19	2.59	0.95

Sample No.	Ba	Co	Cr	Cu	Ga	Nb	Ni	Pb	Rb	Sc	Sr	Th	V	Y	Zn	Zr	Sn	Hf	Ta	Ge	Be	U
83K8/116/S/18	468	182	4130	32	15	13	1453	19	92.278	20	37	12.849	159	15	140	160	2.340	5.499	1.143	2.507	1.531	2.678
83K8/118/S/18	389	33	201	45	17	11	165	17	97.79	17	71	9.30	130	26	103	150	3.61	5.22	0.93	1.34	1.61	1.74
83K8/119/S/18	194	22	311	29	14	13	148	13	70.26	13	44	9.39	98	20	75	224	3.31	8.97	1.18	1.13	1.26	2.09
83K8/120/S/18	236	28	261	37	15	14	128	19	94.63	12	57	9.29	113	22	82	188	3.27	6.61	1.29	1.24	1.42	1.93
83K8/121/S/18	171	16	367	23	12	13	75	12	70.78	10	55	9.75	80	19	59	278	3.38	11.75	1.36	1.03	1.23	2.29
83K8/122/S/18	203	24	366	19	12	12	108	13	65.97	10	69	8.15	94	19	65	265	2.93	7.94	1.08	0.91	1.03	2.00
83K8/123/S/18	194	43	195	55	18	10	164	19	98.10	20	62	10.13	143	30	103	153	3.91	6.10	0.93	1.51	1.77	2.04
83K8/124/S/18	197	16	175	33	18	13	80	16	91.78	19	94	10.85	132	25	98	224	4.38	9.61	1.50	1.38	1.79	2.12
83K8/125/S/18	211	22	188	34	18	13	90	24	86.62	16	89	10.89	123	25	95	256	4.57	11.79	1.45	1.47	1.70	2.11
83K8/126/S/18	187	19	170	25	16	13	67	17	79.69	14	83	9.11	117	23	83	233	3.78	9.26	1.36	1.20	1.45	1.94
83K8/127/S/18	225	24	145	36	16	11	66	12	70.32	16	63	9.43	119	23	107	218	4.01	9.09	1.41	1.22	1.42	2.16
83K8/128/S/18	844	14	108	22	15	14	50	19	98.23	13	115	12.59	96	27	94	255	4.70	10.64	1.81	1.11	1.65	2.54
83K8/129/S/18	501	49	724	41	14	20	568	16	69.63	18	58	11.08	118	26	120	247	4.35	9.83	2.21	1.60	1.51	2.57
83K8/130/S/18	441	28	313	39	18	34	100	11	55.15	18	115	7.56	155	25	93	256	3.78	8.42	2.83	1.57	1.51	1.71
83K8/131/S/18	193	25	182	39	17	12	133	16	81.45	13	79	9.42	132	23	93	170	4.10	7.81	1.19	1.26	1.48	1.85
83K8/133/S/18	148	30	266	39	15	9	168	15	98.07	16	78	10.22	132	21	96	167	3.99	6.82	1.38	1.47	1.74	1.84
83K8/134/S/18	157	14	350	15	13	12	74	18	66.58	13	48	9.45	89	20	70	256	6.82	11.66	1.21	1.21	1.21	2.03
83K8/135/S/18	252	27	350	27	13	10	131	13	78.91	15	90	8.59	113	18	92	235	5.52	10.17	1.04	1.12	1.32	1.85
83K8/136/S/18	190	17	239	17	13	11	92	12	80.512	15	68	9.565	103	18	72	191	1.645	7.291	0.917	0.953	1.219	2.240
83K8/137/S/18	345	28	135	40	20	15	69	20	98.41	19	80	12.03	143	28	94	223	4.42	10.22	1.77	1.50	1.89	1.99
83K8/138/S/18	218	24	142	29	18	15	75	23	99.97	15	91	11.90	136	27	97	223	11.13	9.24	1.58	1.48	1.83	2.09
83K8/139/S/18	138	23	177	25	16	10	78	21	99.639	15	76	13.813	117	24	86	244	3.973	9.917	1.337	1.908	1.880	2.498
83K8/140/S/18	241	31	185	31	18	15	94	26	102.99	17	70	13.15	134	28	99	240	3.73	10.41	1.77	1.63	2.00	2.19
83K8/141/S/18	304	26	173	31	16	14	84	20	91.95	15	84	12.60	119	29	88	300	3.74	13.86	1.72	1.30	1.91	2.62
83K8/142/S/18	294	32	213	42	19	39	135	11	65.84	19	128	8.37	184	26	97	240	8.40	9.03	4.16	1.82	1.64	2.28
83K8/143/S/18	117	33	56	43	17	8	24	7	18.30	21	73	4.59	303	23	79	137	3.64	3.40	0.56	1.71	0.93	1.01
83K8/144/S/18	189	22	299	35	13	13	142	15	74.85	16	65	9.84	109	18	79	186	3.21	6.01	1.11	1.21	1.37	1.92
83K8/145/S/18	172	28	207	35	17	11	134	16	89.23	14	78	9.85	124	24	88	190	6.14	5.39	1.32	1.44	1.54	1.96

Sample No.	Ba	Co	Cr	Cu	Ga	Nb	Ni	Pb	Rb	Sc	Sr	Th	V	Y	Zn	Zr	Sn	Hf	Ta	Ge	Be	U
83K8/146/S/18	201	26	242	37	17	10	166	20	67.55	16	81	8.80	122	24	95	183	5.57	4.35	0.97	1.18	1.28	1.65
83K8/147/S/18	151	23	190	30	18	12	129	22	91.07	16	74	10.08	130	24	96	187	3.82	5.95	1.27	1.51	1.62	2.04
83K8/148/S/18	465	11	373	23	9	11	67	12	59.63	5	64	7.39	72	16	82	238	2.68	7.06	0.95	0.80	0.97	1.76
83K8/149/S/18	359	7	508	18	12	12	42	12	77.66	7	49	9.35	59	18	61	280	4.91	10.37	1.46	1.04	0.91	2.19
83K8/150/S/18	270	21	153	31	18	15	82	16	95.72	19	71	12.37	150	24	104	203	3.19	4.30	1.46	1.54	1.75	2.24
83K8/151/S/18	213	22	148	34	17	13	69	13	95.77	15	84	12.12	125	24	95	232	2.76	5.75	1.43	1.44	1.79	2.09
83K8/152/S/18	233	29	138	37	19	16	77	22	105.68	17	98	13.52	135	29	97	231	9.20	5.11	1.61	1.50	1.84	2.24
83K8/153/S/18	184	38	234	36	15	12	165	25	77.48	16	55	10.84	127	23	77	214	3.36	8.19	1.24	1.29	1.52	2.13
83K8/154/S/18	811	31	187	59	16	14	103	15	79.96	16	114	8.86	114	26	114	189	3.42	6.88	1.29	1.28	1.54	1.80
83K8/155/S/18	288	23	106	48	17	15	46	12	84.42	21	72	9.94	141	33	91	190	3.49	7.99	1.38	1.38	1.77	1.97
83K8/156/S/18	388	25	116	30	16	23	64	20	80.056	15	59	9.891	115	26	94	239	1.794	10.457	0.911	1.177	1.529	2.271
83K8/157/S/18	263	21	253	21	12	15	108	8	81.75	14	90	10.04	80	22	66	214	7.14	8.12	1.87	1.12	1.21	2.17
83K8/158/S/18	237	28	210	37	18	14	148	21	80.64	19	64	10.31	137	25	123	227	3.40	8.94	1.36	1.38	1.53	2.04
83K8/159/S/18	181	23	204	30	13	13	107	14	76.33	9	67	9.33	104	24	79	200	3.26	8.13	1.26	1.08	1.27	1.94
83K8/160/S/18	169	18	234	26	15	12	98	19	68.39	10	70	8.18	102	22	83	221	3.17	8.56	1.15	1.03	1.28	1.84
83K8/161/S/18	188	7	412	9	7	12	32	13	74.339	13	34	10.408	54	19	36	308	1.904	7.041	1.650	1.121	1.574	2.367
83K8/163/S/18	209	13	265	25	13	10	121	15	48.289	12	74	9.251	106	20	97	211	1.272	13.468	0.999	0.664	0.778	2.308
83K8/164/S/18	218	19	221	34	16	14	84	16	77.06	15	69	10.15	103	23	79	231	3.82	9.58	1.52	1.29	1.37	2.26
83K8/165/S/18	234	17	173	31	22	12	96	16	113.68	18	107	10.88	139	27	99	213	3.54	9.25	1.32	1.42	1.76	2.13
83K8/166/S/18	137	17	238	25	13	12	152	18	59.73	12	68	7.70	106	22	91	227	3.09	9.42	1.12	1.17	1.23	1.69
83K8/167/S/18	175	57	1349	23	12	9	1114	8	40.34	9	53	6.50	94	17	71	140	3.10	5.62	0.83	1.59	0.97	1.27
83K8/168/S/18	414	29	163	35	19	16	116	25	106.34	18	80	15.19	115	36	91	230	3.66	9.89	1.83	1.32	1.81	2.77
83K8/169/S/18	210	42	569	42	13	26	576	7	45.38	17	94	6.86	125	26	87	185	3.25	6.53	2.59	1.52	1.15	1.34
83K8/170/S/18	224	30	271	28	14	12	143	18	86.330	12	67	9.715	113	22	74	200	1.402	8.352	0.882	1.012	1.398	2.237
83K8/176/S/18	227	28	371	33	15	12	129	14	87.695	15	75	12.468	121	23	88	267	1.655	9.124	1.229	1.240	1.571	2.818
83K8/178/S/18	171	19	161	26	16	18	76	22	90.122	12	80	10.451	122	28	92	266	1.983	12.956	1.055	1.173	1.518	2.452
83K8/179/S/18	135	21	280	28	13	14	137	23	73.421	10	73	11.034	112	22	79	236	1.356	9.988	1.039	1.163	1.403	2.349
83K8/180/S/18	169	16	280	38	14	11	126	11	83.259	13	78	11.982	113	25	82	239	1.350	9.153	0.871	1.097	1.500	2.371

83K8/181/S/18	211	34	510	29	12	11	361	19	71.440	16	70	8.727	111	21	69	216	256.392	7.799	0.813	1.888	1.415	1.844
83K8/182/S/18	644	678	4810	62	11	11	3500	29	55.702	22	18	10.511	227	14	91	112	1.772	4.780	0.514	4.055	1.935	2.549



**Analytical Data of Rare Earth Elements of Stream Sediment/Slope Wash Samples
(Values in ppm)**

Sample No.	La	Ce	Pr	Nd	Eu	Sm	Gd	Tb	Dy	Ho	Er	Tm	Yb	Lu
83K8/001/S/18	36.65	66.96	8.49	30.54	1.13	5.59	5.10	0.73	4.36	0.86	2.59	0.25	2.83	0.25
83K8/002/S/18	44.03	79.95	9.88	35.99	1.34	6.39	6.12	0.86	4.98	0.98	2.90	0.25	3.16	0.50
83K8/003/S/18	34.99	67.68	8.75	33.57	1.80	7.37	7.26	1.08	6.15	1.15	3.20	0.52	3.30	0.54
83K8/004/S/18	41.79	76.50	9.63	35.41	1.41	6.44	6.09	0.90	5.32	1.03	3.01	0.50	3.17	0.51
83K8/005/S/18	45.09	84.09	10.79	39.68	1.65	7.62	7.26	1.08	6.28	1.21	3.56	0.59	3.81	0.60
83K8/006/S/18	46.24	86.36	10.47	37.45	1.32	6.79	6.33	0.92	5.50	1.09	3.23	0.54	3.46	0.55
83K8/008/S/18	41.22	76.24	9.29	33.33	1.07	5.48	5.04	0.71	4.36	0.88	2.65	0.25	3.00	0.25
83K8/009/S/18	37.57	67.96	8.53	30.52	1.11	5.44	5.00	0.72	4.33	0.87	2.58	0.25	2.74	0.25
83K8/010/S/18	27.23	51.16	5.99	21.17	0.81	4.15	4.16	0.60	3.72	0.70	2.09	0.25	2.25	0.25
83K8/011/S/18	32.44	68.95	7.37	26.19	1.08	5.34	5.29	0.79	4.76	0.90	2.67	0.25	2.96	0.25
83K8/012/S/18	53.72	102.27	12.51	43.68	1.75	8.51	8.16	1.16	6.50	1.24	3.55	0.59	3.79	0.59
83K8/013/S/18	58.16	107.88	13.40	47.20	1.80	8.67	8.21	1.15	6.71	1.28	3.59	0.64	3.81	0.62
83K8/014/S/18	24.43	45.59	6.00	22.45	1.07	4.64	4.42	0.65	3.79	0.73	2.12	0.25	2.37	0.25
83K8/015/S/18	30.92	57.68	7.52	27.70	1.32	5.67	5.69	0.84	4.92	0.95	2.77	0.25	2.98	0.50
83K8/016/S/18	30.76	58.34	7.51	27.47	1.30	5.58	5.37	0.82	5.01	1.00	2.87	0.25	3.08	0.50
83K8/017/S/18	41.84	79.55	9.81	35.75	1.52	7.00	6.88	0.98	5.80	1.07	3.08	0.51	3.14	0.51
83K8/018/S/18	42.63	81.86	9.66	32.88	1.08	5.99	5.77	0.81	4.94	0.99	3.04	0.52	3.34	0.53
83K8/019/S/18	45.20	82.92	10.04	34.52	1.10	5.86	5.37	0.75	4.46	0.91	2.82	0.25	3.09	0.25
83K8/020/S/18	36.14	69.34	8.07	27.96	1.07	5.14	5.13	0.74	4.42	0.86	2.58	0.25	2.81	0.25
83K8/021/S/18	28.27	52.66	6.92	25.24	1.24	5.19	5.12	0.77	4.65	0.90	2.63	0.25	2.90	0.25
83K8/022/S/18	45.13	84.08	10.92	39.90	1.83	8.17	7.77	1.12	6.23	1.13	3.26	0.53	3.30	0.52
83K8/023/S/18	49.16	89.70	11.54	41.28	1.74	8.19	7.68	1.16	6.90	1.27	3.76	0.63	3.94	0.63
83K8/024/S/18	15.93	29.51	3.54	12.71	0.56	2.61	2.62	0.25	2.43	0.25	1.42	0.25	1.55	0.25
83K8/025/S/18	29.94	59.42	6.45	23.36	0.94	4.56	4.56	0.67	4.04	0.78	2.32	0.25	2.42	0.25
83K8/027/S/18	28.67	55.23	6.84	25.14	0.95	4.71	4.19	0.65	4.11	0.86	2.58	0.25	2.74	0.25
83K8/028/S/18	22.32	42.36	5.58	23.38	1.15	4.53	4.37	0.66	4.13	0.77	2.24	0.25	2.42	0.25

Sample No.	La	Ce	Pr	Nd	Eu	Sm	Gd	Tb	Dy	Ho	Er	Tm	Yb	Lu
83K8/029/S/18	46.07	89.40	11.35	42.19	2.05	8.93	8.68	1.31	7.52	1.43	3.97	0.65	3.96	0.64
83K8/030/S/18	33.32	62.38	7.83	28.56	1.13	5.26	5.11	0.75	4.52	0.90	2.72	0.25	2.91	0.25
83K8/031/S/18	31.23	58.75	7.46	27.63	1.27	5.27	5.02	0.74	4.36	0.87	2.52	0.25	2.56	0.25
83K8/032/S/18	35.74	67.25	8.46	31.51	1.39	6.27	5.87	0.89	5.30	1.01	2.87	0.25	3.05	0.25
83K8/033/S/18	29.54	57.20	7.35	27.80	1.33	5.78	5.57	0.86	5.13	1.00	2.88	0.25	2.98	0.50
83K8/034/S/18	42.00	78.17	9.77	35.13	1.39	6.79	6.49	0.94	5.40	1.03	2.98	0.25	3.01	0.25
83K8/035/S/18	37.51	71.61	8.70	31.21	1.26	5.84	5.38	0.79	4.68	0.95	2.81	0.25	2.93	0.25
83K8/036/S/18	34.49	70.31	8.86	34.73	2.01	8.13	8.25	1.28	7.06	1.28	3.53	0.57	3.46	0.56
83K8/037/S/18	14.32	30.92	3.32	12.51	0.63	2.70	2.76	0.25	2.82	0.56	1.64	0.25	1.73	0.25
83K8/038/S/18	10.92	20.48	2.46	9.17	0.25	1.96	1.94	0.25	2.02	0.25	1.17	0.25	1.24	0.25
83K8/039/S/18	49.93	97.65	11.94	43.37	1.67	8.39	8.08	1.20	7.13	1.34	3.90	0.64	3.85	0.61
83K8/040/S/18	31.00	58.62	7.37	26.83	1.15	5.16	4.72	0.71	4.33	0.89	2.63	0.25	2.77	0.25
83K8/041/S/18	26.60	50.56	6.70	24.76	1.22	5.29	5.12	0.77	4.34	0.83	2.54	0.25	2.99	0.51
83K8/042/S/18	27.73	53.11	6.46	22.73	0.92	4.25	4.06	0.61	3.51	0.67	2.04	0.25	2.29	0.25
83K8/043/S/18	31.76	60.37	7.79	28.40	1.38	5.97	5.54	0.84	4.85	0.91	2.71	0.25	2.82	0.25
83K8/044/S/18	33.37	61.98	7.60	26.60	1.02	4.92	4.73	0.74	4.50	0.92	2.94	0.51	3.38	0.55
83K8/045/S/18	36.49	69.61	8.44	29.35	1.15	5.58	5.26	0.75	4.36	0.84	2.52	0.25	2.73	0.25
83K8/046/S/18	31.06	58.61	7.17	25.09	0.96	4.52	4.25	0.61	3.67	0.73	2.28	0.25	2.52	0.25
83K8/047/S/18	31.92	53.07	6.64	24.23	1.01	4.44	4.32	0.63	3.80	0.77	2.37	0.25	2.50	0.25
83K8/048/S/18	36.42	69.45	8.96	33.21	1.67	7.10	6.89	1.02	5.93	1.09	3.16	0.25	3.39	0.55
83K8/049/S/18	34.04	56.59	7.12	26.44	1.21	5.13	4.85	0.71	4.24	0.83	2.51	0.25	2.65	0.25
83K8/050/S/18	50.09	99.59	9.70	33.18	1.31	5.83	6.47	0.94	5.75	1.15	3.48	0.58	3.57	0.58
83K8/051/S/18	18.30	35.75	4.83	19.39	1.11	4.70	4.67	0.73	4.27	0.78	2.20	0.25	2.29	0.25
83K8/052/S/18	23.89	44.70	5.53	20.11	0.90	4.03	3.90	0.57	3.43	0.64	1.82	0.25	1.90	0.25
83K8/053/S/18	30.14	55.69	6.84	24.52	0.90	4.31	4.20	0.60	3.76	0.74	2.26	0.25	2.57	0.25
83K8/054/S/18	28.97	53.05	6.89	24.67	1.01	4.68	4.45	0.67	3.99	0.80	2.45	0.25	2.73	0.25
83K8/055/S/18	33.94	64.51	8.19	28.95	1.26	5.63	5.18	0.76	4.52	0.85	2.53	0.25	2.81	0.25
83K8/056/S/18	30.79	53.05	6.76	25.53	1.27	5.34	5.11	0.78	4.49	0.86	2.55	0.25	2.59	0.25

Sample No.	La	Ce	Pr	Nd	Eu	Sm	Gd	Tb	Dy	Ho	Er	Tm	Yb	Lu
83K8/057/S/18	38.14	65.45	7.98	28.97	1.20	5.31	4.98	0.71	4.21	0.82	2.47	0.25	2.53	0.25
83K8/058/S/18	39.61	63.88	8.12	30.03	1.30	5.84	5.55	0.82	4.80	0.94	2.82	0.25	2.87	0.25
83K8/059/S/18	48.27	96.15	11.71	45.30	2.52	9.96	9.91	1.43	7.60	1.34	3.73	0.57	3.45	0.54
83K8/060/S/18	32.00	54.78	6.62	23.52	0.93	4.22	3.89	0.58	3.53	0.74	2.38	0.25	2.59	0.25
83K8/061/S/18	29.29	50.35	6.49	24.99	1.25	5.34	5.22	0.79	4.69	0.89	2.65	0.25	2.76	0.25
83K8/062/S/18	35.81	61.77	7.86	29.30	1.35	5.99	5.81	0.88	5.19	0.98	2.87	0.25	2.89	0.25
83K8/063/S/18	13.18	27.80	3.83	17.00	1.70	5.03	5.80	1.11	7.37	1.47	4.32	0.71	4.27	0.68
83K8/064/S/18	21.82	42.50	5.16	20.98	2.10	5.32	5.43	0.85	4.73	0.86	2.34	0.25	2.26	0.25
83K8/065/S/18	50.021	82.627	10.480	38.493	1.485	7.409	6.844	1.010	5.865	1.111	3.239	0.530	3.272	0.538
83K8/066/S/18	29.43	57.84	6.08	20.92	0.78	3.65	3.81	0.56	3.41	0.70	2.19	0.25	2.43	0.25
83K8/067/S/18	26.89	48.67	6.28	23.10	1.09	4.82	4.57	0.69	3.99	0.76	2.29	0.25	2.42	0.25
83K8/068/S/18	26.47	48.15	5.94	21.54	0.96	4.30	4.13	0.61	3.63	0.71	2.14	0.25	2.27	0.25
83K8/069/S/18	30.73	57.05	7.19	26.19	1.29	5.48	5.26	0.79	4.61	0.88	2.59	0.25	2.66	0.25
83K8/070/S/18	25.85	48.70	6.16	23.16	1.19	4.92	4.68	0.71	4.18	0.81	2.39	0.25	2.46	0.25
83K8/071/S/18	35.265	59.333	7.704	28.937	1.509	6.053	5.526	0.825	4.724	0.922	2.758	0.464	2.991	0.498
83K8/072/S/18	45.46	80.13	9.70	34.12	1.25	6.09	5.53	0.77	4.53	0.88	2.69	0.25	2.80	0.25
83K8/073/S/18	35.65	63.28	7.91	28.91	1.38	5.79	5.45	0.81	4.83	0.95	2.89	0.25	3.08	0.51
83K8/074/S/18	31.36	55.67	6.67	23.16	0.87	4.11	3.68	0.54	3.33	0.70	2.23	0.25	2.45	0.25
83K8/075/S/18	38.04	66.98	8.69	33.26	1.63	6.84	6.65	0.98	5.40	0.99	2.83	0.25	2.74	0.25
83K8/076/S/18	12.25	24.63	2.62	9.85	0.25	2.06	2.13	0.25	2.00	0.25	1.19	0.25	1.21	0.25
83K8/077/S/18	54.06	112.63	13.73	54.53	2.85	12.71	12.65	1.90	10.56	1.94	5.14	0.79	4.62	0.74
83K8/078/S/18	49.49	90.05	11.47	46.04	1.92	8.62	8.30	1.26	7.65	1.37	4.01	0.66	4.06	0.66
83K8/079/S/18	30.55	52.59	6.18	21.54	0.85	3.69	3.75	0.56	3.41	0.69	2.08	0.25	2.14	0.25
83K8/080/S/18	36.81	73.47	7.53	25.45	0.77	4.21	4.34	0.59	3.53	0.72	2.28	0.25	2.54	0.25
83K8/081/S/18	23.84	47.74	5.65	21.69	1.19	4.83	4.75	0.75	4.40	0.84	2.52	0.25	2.65	0.25
83K8/082/S/18	28.81	52.23	6.53	23.74	0.93	4.51	3.87	0.55	3.50	0.73	2.26	0.25	2.47	0.25
83K8/083/S/18	29.56	53.69	6.81	25.25	1.18	5.14	4.91	0.73	4.34	0.84	2.49	0.25	2.66	0.25
83K8/084/S/18	29.05	53.76	6.81	25.40	1.24	5.35	5.22	0.80	4.68	0.90	2.66	0.25	2.80	0.25

Sample No.	La	Ce	Pr	Nd	Eu	Sm	Gd	Tb	Dy	Ho	Er	Tm	Yb	Lu
83K8/085/S/18	30.33	55.81	7.03	26.11	1.18	5.35	5.08	0.78	4.59	0.88	2.63	0.25	2.76	0.25
83K8/086/S/18	27.08	50.75	6.49	24.10	1.19	5.18	5.12	0.79	4.72	0.90	2.67	0.25	2.79	0.25
83K8/087/S/18	23.57	46.26	5.38	20.10	0.81	3.87	3.57	0.55	3.45	0.70	2.17	0.25	2.40	0.25
83K8/088/S/18	34.72	63.08	8.05	28.82	1.22	5.85	5.51	0.81	4.66	0.89	2.65	0.25	2.68	0.25
83K8/089/S/18	10.485	19.023	2.073	7.538	0.311	1.496	1.500	0.223	1.301	0.254	0.753	0.129	0.799	0.134
83K8/090/S/18	33.532	54.115	6.370	22.758	0.813	4.289	4.163	0.618	3.637	0.707	2.132	0.362	2.253	0.379
83K8/092/S/18	35.83	68.46	7.62	26.53	1.02	4.93	4.96	0.72	4.28	0.85	2.54	0.25	2.67	0.25
83K8/093/S/18	30.76	55.33	6.74	23.69	0.84	4.14	4.13	0.60	3.59	0.71	2.19	0.25	2.41	0.25
83K8/094/S/18	25.43	48.57	6.11	23.49	1.24	5.15	5.22	0.83	4.85	0.91	2.63	0.25	2.62	0.25
83K8/095/S/18	24.98	48.77	5.92	22.55	1.22	4.95	5.12	0.80	4.69	0.87	2.48	0.25	2.48	0.25
83K8/096/S/18	20.11	37.30	4.15	14.39	0.64	2.79	2.83	0.25	2.62	0.52	1.63	0.25	1.84	0.25
83K8/097/S/18	30.86	58.33	7.41	27.66	1.33	5.70	5.53	0.82	4.82	0.93	2.78	0.25	2.92	0.25
83K8/098/S/18	31.93	59.16	7.53	28.24	1.38	5.89	5.69	0.84	5.08	0.97	2.94	0.50	3.11	0.51
83K8/100/S/18	27.298	45.839	5.930	22.398	1.136	4.724	4.646	0.725	4.375	0.868	2.620	0.458	2.975	0.511
83K8/101/S/18	30.03	55.94	7.05	25.75	1.33	5.53	5.32	0.81	4.69	0.89	2.61	0.25	2.70	0.25
83K8/102/S/18	23.42	38.81	5.10	18.80	0.76	3.84	3.71	0.56	3.19	0.61	1.80	0.25	1.80	0.25
83K8/103/S/18	37.114	58.409	6.900	24.622	0.913	4.692	4.585	0.672	3.874	0.754	2.226	0.376	2.357	0.392
83K8/105/S/18	32.618	52.219	6.779	25.030	1.202	5.030	4.949	0.738	4.217	0.810	2.367	0.395	2.508	0.410
83K8/106/S/18	29.45	53.10	6.10	21.71	0.93	4.26	4.19	0.63	3.79	0.73	2.18	0.25	2.34	0.25
83K8/107/S/18	33.55	60.76	7.33	26.22	0.96	4.67	4.67	0.68	4.03	0.81	2.44	0.25	2.58	0.25
83K8/108/S/18	22.22	45.07	5.31	19.80	1.02	4.18	4.13	0.63	3.77	0.74	2.18	0.25	2.38	0.25
83K8/109/S/18	32.262	53.014	6.863	25.916	1.254	5.356	5.182	0.785	4.630	0.892	2.632	0.442	2.799	0.469
83K8/110/S/18	11.93	25.11	2.70	9.99	0.25	1.93	1.90	0.25	1.77	0.25	1.09	0.25	1.21	0.25
83K8/111/S/18	32.12	59.37	7.33	26.91	1.08	5.31	5.10	0.77	4.66	0.92	2.76	0.25	2.92	0.25
83K8/112/S/18	40.01	73.49	8.94	31.36	1.03	5.55	5.13	0.76	4.71	0.95	2.92	0.25	3.05	0.51
83K8/113/S/18	31.991	54.995	7.059	26.951	1.418	5.838	5.640	0.881	5.197	1.003	2.926	0.495	3.170	0.537
83K8/114/S/18	24.25	50.18	5.80	21.45	0.99	4.33	4.07	0.63	3.83	0.77	2.34	0.25	2.56	0.25
83K8/115/S/18	53.35	119.17	14.65	58.80	2.97	12.73	11.45	1.55	8.06	1.38	3.72	0.54	3.16	0.25

Sample No.	La	Ce	Pr	Nd	Eu	Sm	Gd	Tb	Dy	Ho	Er	Tm	Yb	Lu
83K8/116/S/18	35.646	61.701	6.793	23.981	0.842	4.463	4.426	0.644	3.741	0.725	2.192	0.364	2.325	0.383
83K8/118/S/18	29.10	55.97	6.85	25.92	1.37	5.65	5.55	0.86	4.94	0.91	2.59	0.25	2.56	0.25
83K8/119/S/18	26.89	53.05	5.77	20.63	0.86	3.91	3.87	0.57	3.34	0.66	2.00	0.25	2.21	0.25
83K8/120/S/18	29.34	54.19	6.58	23.96	1.01	4.51	4.43	0.67	4.04	0.79	2.39	0.25	2.51	0.25
83K8/121/S/18	30.26	55.76	6.89	24.50	0.92	4.43	4.13	0.61	3.79	0.75	2.37	0.25	2.58	0.25
83K8/122/S/18	25.99	52.97	6.04	22.04	0.87	4.02	3.76	0.59	3.70	0.76	2.33	0.25	2.55	0.25
83K8/123/S/18	30.56	58.06	7.87	30.42	1.88	7.39	7.53	1.17	6.52	1.18	3.26	0.52	3.23	0.52
83K8/124/S/18	33.19	61.93	7.83	29.07	1.42	6.16	5.92	0.89	5.10	0.99	2.87	0.25	3.00	0.25
83K8/125/S/18	34.25	61.96	7.80	28.80	1.40	6.01	5.80	0.87	5.11	0.96	2.87	0.25	3.04	0.25
83K8/126/S/18	30.30	60.31	6.87	26.10	1.30	5.45	5.28	0.82	4.77	0.91	2.69	0.25	2.80	0.25
83K8/127/S/18	28.84	59.04	6.81	24.73	1.07	4.83	4.45	0.67	4.10	0.83	2.55	0.25	2.75	0.25
83K8/128/S/18	38.87	69.96	8.79	31.98	1.37	6.24	5.65	0.82	4.84	0.94	2.82	0.25	2.97	0.25
83K8/129/S/18	39.68	71.60	9.02	32.24	1.39	6.14	5.92	0.88	5.18	1.02	2.98	0.50	3.19	0.52
83K8/130/S/18	42.45	72.73	9.28	34.44	1.92	6.86	6.60	0.94	5.23	0.97	2.78	0.25	2.71	0.25
83K8/131/S/18	27.33	54.15	6.48	23.99	1.15	4.87	4.64	0.69	4.06	0.78	2.34	0.25	2.48	0.25
83K8/133/S/18	29.76	60.21	7.00	26.18	1.25	5.41	5.11	0.76	4.49	0.87	2.58	0.25	2.65	0.25
83K8/134/S/18	27.31	55.38	6.17	22.39	0.84	4.06	3.85	0.55	3.43	0.69	2.16	0.25	2.35	0.25
83K8/135/S/18	25.64	51.10	5.92	21.96	1.06	4.62	4.30	0.64	3.73	0.74	2.22	0.25	2.33	0.25
83K8/136/S/18	31.019	51.683	6.690	25.080	1.141	5.006	4.582	0.679	4.045	0.805	2.435	0.413	2.627	0.444
83K8/137/S/18	39.99	76.66	9.25	34.60	1.66	7.17	6.91	0.99	5.51	1.02	3.00	0.25	2.99	0.25
83K8/138/S/18	35.59	74.32	8.51	31.79	1.59	6.81	6.59	0.99	5.77	1.10	3.21	0.53	3.21	0.52
83K8/139/S/18	38.121	69.917	9.191	34.043	1.534	6.856	6.621	1.010	5.945	1.109	3.224	0.531	3.323	0.540
83K8/140/S/18	38.12	78.45	8.83	32.21	1.46	6.59	6.32	0.93	5.39	1.04	3.03	0.50	3.18	0.51
83K8/141/S/18	38.06	76.23	8.92	33.48	1.50	6.81	6.61	0.99	5.77	1.12	3.33	0.54	3.44	0.57
83K8/142/S/18	41.27	82.32	9.84	37.29	2.17	7.78	7.33	1.08	6.08	1.12	3.20	0.50	3.03	0.25
83K8/143/S/18	14.12	31.97	3.58	14.37	0.98	3.54	3.75	0.68	4.58	0.93	2.87	0.25	3.10	0.25
83K8/144/S/18	29.46	59.45	6.61	24.06	0.99	4.53	4.29	0.61	3.67	0.74	2.27	0.25	2.42	0.25
83K8/145/S/18	29.33	60.39	7.09	26.84	1.37	5.75	5.73	0.85	4.98	0.94	2.73	0.25	2.81	0.25

Sample No.	La	Ce	Pr	Nd	Eu	Sm	Gd	Tb	Dy	Ho	Er	Tm	Yb	Lu
83K8/146/S/18	24.18	48.90	5.68	21.39	1.08	4.55	4.39	0.66	3.92	0.75	2.26	0.25	2.35	0.25
83K8/147/S/18	29.75	61.54	7.29	27.78	1.43	6.01	5.70	0.88	5.07	0.97	2.88	0.25	2.99	0.25
83K8/148/S/18	22.72	43.49	4.92	17.54	0.75	3.32	3.26	0.50	3.15	0.64	2.02	0.25	2.19	0.25
83K8/149/S/18	26.93	54.07	5.80	21.13	0.89	4.05	4.01	0.59	3.57	0.72	2.07	0.25	2.26	0.25
83K8/150/S/18	35.96	74.08	8.45	31.08	1.40	6.20	5.79	0.83	4.89	0.95	2.88	0.25	2.96	0.25
83K8/151/S/18	35.10	70.96	8.06	30.56	1.49	6.36	6.06	0.92	5.25	1.00	2.97	0.25	3.12	0.25
83K8/152/S/18	40.29	84.26	9.46	35.68	1.71	7.42	7.18	1.06	6.03	1.14	3.31	0.53	3.35	0.53
83K8/153/S/18	30.22	63.57	7.00	25.60	1.12	5.08	4.94	0.71	4.29	0.84	2.57	0.25	2.63	0.25
83K8/154/S/18	32.28	60.98	7.76	28.42	1.38	5.40	5.39	0.81	4.79	0.92	2.72	0.25	2.77	0.25
83K8/155/S/18	37.46	65.19	9.06	35.11	1.76	7.51	7.28	1.10	6.43	1.19	3.42	0.56	3.37	0.55
83K8/156/S/18	26.397	50.019	6.818	26.232	1.448	5.878	5.907	0.936	5.357	0.997	2.895	0.485	3.071	0.515
83K8/157/S/18	34.72	62.29	7.73	27.26	0.96	4.77	4.64	0.64	3.93	0.80	2.38	0.25	2.52	0.25
83K8/158/S/18	30.91	59.35	7.25	26.16	1.10	5.04	4.91	0.72	4.26	0.84	2.50	0.25	2.63	0.25
83K8/159/S/18	29.46	53.85	6.82	24.95	1.00	4.64	4.38	0.64	3.91	0.77	2.34	0.25	2.51	0.25
83K8/160/S/18	24.90	46.53	6.00	22.09	1.05	4.55	4.57	0.72	4.25	0.81	2.44	0.25	2.56	0.25
83K8/161/S/18	33.123	63.706	7.779	28.737	1.402	5.627	5.709	0.879	5.240	1.025	3.041	0.513	3.269	0.540
83K8/163/S/18	25.776	48.486	5.790	20.617	0.778	3.795	3.841	0.596	3.728	0.745	2.246	0.384	2.523	0.428
83K8/164/S/18	30.47	58.38	7.23	25.94	1.09	5.11	4.82	0.70	4.40	0.88	2.61	0.25	2.83	0.25
83K8/165/S/18	31.73	61.16	7.72	28.95	1.47	5.99	5.90	0.87	5.15	1.00	2.98	0.50	3.18	0.53
83K8/166/S/18	21.20	40.44	5.25	19.55	1.03	4.27	4.34	0.67	4.01	0.78	2.21	0.25	2.40	0.25
83K8/167/S/18	19.70	35.93	4.69	17.36	0.82	3.53	3.45	0.51	3.03	0.58	1.72	0.25	1.76	0.25
83K8/168/S/18	44.40	82.64	11.22	42.79	2.13	9.38	9.10	1.32	7.40	1.36	3.80	0.63	3.74	0.61
83K8/169/S/18	37.43	58.29	8.86	33.74	1.92	7.12	6.97	1.02	5.60	1.03	2.87	0.25	2.74	0.25
83K8/170/S/18	25.674	47.641	6.371	23.563	1.110	4.827	4.511	0.708	4.338	0.847	2.567	0.434	2.758	0.462
83K8/176/S/18	32.878	59.928	7.862	29.498	1.323	5.822	5.691	0.872	5.151	0.999	2.953	0.493	3.111	0.512
83K8/178/S/18	27.817	51.604	7.002	26.789	1.410	5.725	5.721	0.876	5.103	0.972	2.831	0.474	3.047	0.508
83K8/179/S/18	28.633	53.215	7.081	26.884	1.258	5.474	5.288	0.836	4.970	0.949	2.806	0.472	3.002	0.502
83K8/180/S/18	28.697	51.946	7.100	26.934	1.319	5.542	5.464	0.837	5.007	0.975	2.877	0.478	3.087	0.511

Sample No.	La	Ce	Pr	Nd	Eu	Sm	Gd	Tb	Dy	Ho	Er	Tm	Yb	Lu
83K8/181/S/18	26.450	50.121	6.279	23.320	1.036	4.620	4.424	0.667	3.928	0.776	2.330	0.390	2.505	0.407
83K8/182/S/18	25.374	108.260	6.384	23.049	1.017	4.737	5.071	0.715	4.214	0.800	2.257	0.386	2.441	0.393



Analytical Data of Oxides of Soil Samples
(values in %)

Sample No.	SiO ₂	TiO ₂	Al ₂ O ₃	Fe ₂ O ₃	MnO	MgO	CaO	Na ₂ O	K ₂ O	P ₂ O ₅
83K8/A1/R/19	66.04	1.02	12.42	5.42	0.15	0.75	0.08	0.14	1.40	0.11
83K8/A1/C/19	64.27	0.90	15.11	6.52	0.09	1.13	0.11	0.19	1.33	0.13
83K8/A2/R/19	65.97	1.01	13.64	5.96	0.15	0.91	0.12	0.11	1.39	0.11
83K8/A2/C/19	63.32	1.05	16.76	7.54	0.07	0.98	0.06	0.10	1.71	0.08
83K8/A3/R/19	63.14	0.91	16.37	7.31	0.05	1.09	0.06	0.16	1.19	0.08
83K8/A3/C/19	64.84	1.07	15.46	6.79	0.09	0.79	0.05	0.12	1.76	0.08
83K8/B1/R/19	72.55	0.89	11.96	4.44	0.04	0.76	0.16	0.13	0.99	0.07
83K8/B1/C/19	58.69	0.81	17.52	7.07	0.04	2.66	0.09	0.65	2.18	0.06
83K8/B2/R/19	67.14	1.08	14.86	6.53	0.05	0.93	0.10	0.13	1.14	0.08
83K8/B2/C/19	67.04	1.06	15.74	6.49	0.05	0.85	0.06	0.13	1.32	0.06
83K8/B3/R/19	60.17	1.04	15.53	8.12	0.11	1.73	0.17	0.15	1.64	0.13
83K8/B3/C/19	67.97	0.90	15.49	5.62	0.03	0.72	0.05	0.16	1.50	0.06
83K8/C1/R/19	60.57	1.00	15.17	8.37	0.12	1.69	0.08	0.19	1.29	0.10
83K8/C1/C/19	56.80	0.94	18.74	8.61	0.08	1.68	0.09	0.23	2.12	0.10
83K8/C2/R/19	31.17	0.41	8.71	45.91	0.51	2.24	0.05	0.01	0.32	0.10
83K8/C2/C/19	58.00	0.95	15.11	12.33	0.06	1.23	0.09	0.11	1.27	0.07
83K8/C3/R/19	51.70	1.04	14.73	13.23	0.29	2.35	0.41	0.23	1.30	0.16
83K8/C3/C/19	33.78	0.40	7.21	45.25	0.80	4.43	0.02	0.08	0.55	0.13

**Analytical data of Trace Elements of Soil Samples
(Values in ppm)**

Sample No.	Ba	Co	Cr	Cu	Ga	Nb	Ni	Pb	Sc	Sr	V	Y	Zn	Zr	Sn	Hf	Ta	Ge	Be	U	As	Rb	Th
83K8/A1/R/19	234	17	206	22	13	16	57	17	12	45	104	22	63	242	2.729	10.113	1.647	1.135	1.217	2.598	9.092	82.863	13.553
83K8/A1/C/19	139	14	213	31	14	14	75	20	12	47	125	22	80	227	1.902	8.817	1.168	1.342	1.235	2.171	11.336	75.150	10.473
83K8/A2/R/19	304	21	225	22	13	18	74	21	9	38	111	23	58	276	3.140	10.868	1.607	1.266	1.593	3.332	10.196	94.691	16.760
83K8/A2/C/19	361	19	223	37	19	21	115	23	14	41	136	24	85	285	2.983	12.204	1.560	1.626	2.070	3.853	15.162	122.774	18.927
83K8/A3/R/19	103	20	218	26	17	15	81	19	14	45	124	21	75	258	1.805	9.067	1.158	1.486	1.151	2.307	12.429	73.053	11.080
83K8/A3/C/19	308	18	178	31	17	19	83	19	11	49	122	23	87	237	2.977	10.620	1.707	1.404	1.681	3.130	12.493	106.192	15.538
83K8/B1/R/19	264	16	268	14	11	15	53	14	11	50	89	20	50	248	2.141	10.892	1.409	1.062	0.977	2.577	8.346	69.394	12.025
83K8/B1/C/19	176	11	160	35	20	10	129	14	16	57	136	29	95	198	2.108	7.222	0.958	1.417	2.027	2.285	12.510	97.783	11.637
83K8/B2/R/19	283	15	142	18	19	21	51	24	14	48	115	28	69	277	2.830	11.066	2.061	1.413	1.364	3.422	12.724	88.108	16.703
83K8/B2/C/19	259	10	121	24	17	19	53	17	12	49	113	27	76	273	8.350	10.090	2.009	1.333	1.333	3.354	13.196	83.947	16.187
83K8/B3/R/19	244	25	267	35	17	17	158	17	13	56	136	20	95	190	2.203	7.766	1.263	1.456	1.723	1.978	10.350	93.165	11.868
83K8/B3/C/19	243	12	312	25	13	12	45	10	13	53	104	20	48	208	2.198	11.502	1.191	1.146	1.252	2.593	11.904	80.774	10.528
83K8/C1/R/19	187	46	540	34	18	15	476	19	17	58	128	21	98	210	2.080	8.562	1.549	1.562	1.701	2.717	10.562	83.533	12.585
83K8/C1/C/19	227	27	279	44	20	14	302	27	20	74	151	29	103	206	2.697	9.228	1.583	1.649	2.258	2.972	11.438	107.460	14.642
83K8/C2/R/19	98	233	6749	136	23	8	4555	9	51	10	326	13	233	26	1.524	0.863	0.220	4.704	3.625	1.272	7.509	36.148	5.588
83K8/C2/C/19	311	58	1288	32	19	20	798	28	29	37	157	27	116	253	3.745	10.981	2.029	2.406	1.885	3.967	14.184	86.695	20.516
83K8/C3/R/19	371	77	1268	28	21	14	687	17	17	38	193	25	115	167	2.690	5.929	0.603	2.273	1.868	2.855	10.918	87.356	13.083
83K8/C3/C/19	137	243	11383	80	13	8	4888	5	37	18	261	14	174	66	2.833	4.570	0.970	5.256	1.567	1.233	10.682	46.855	5.339

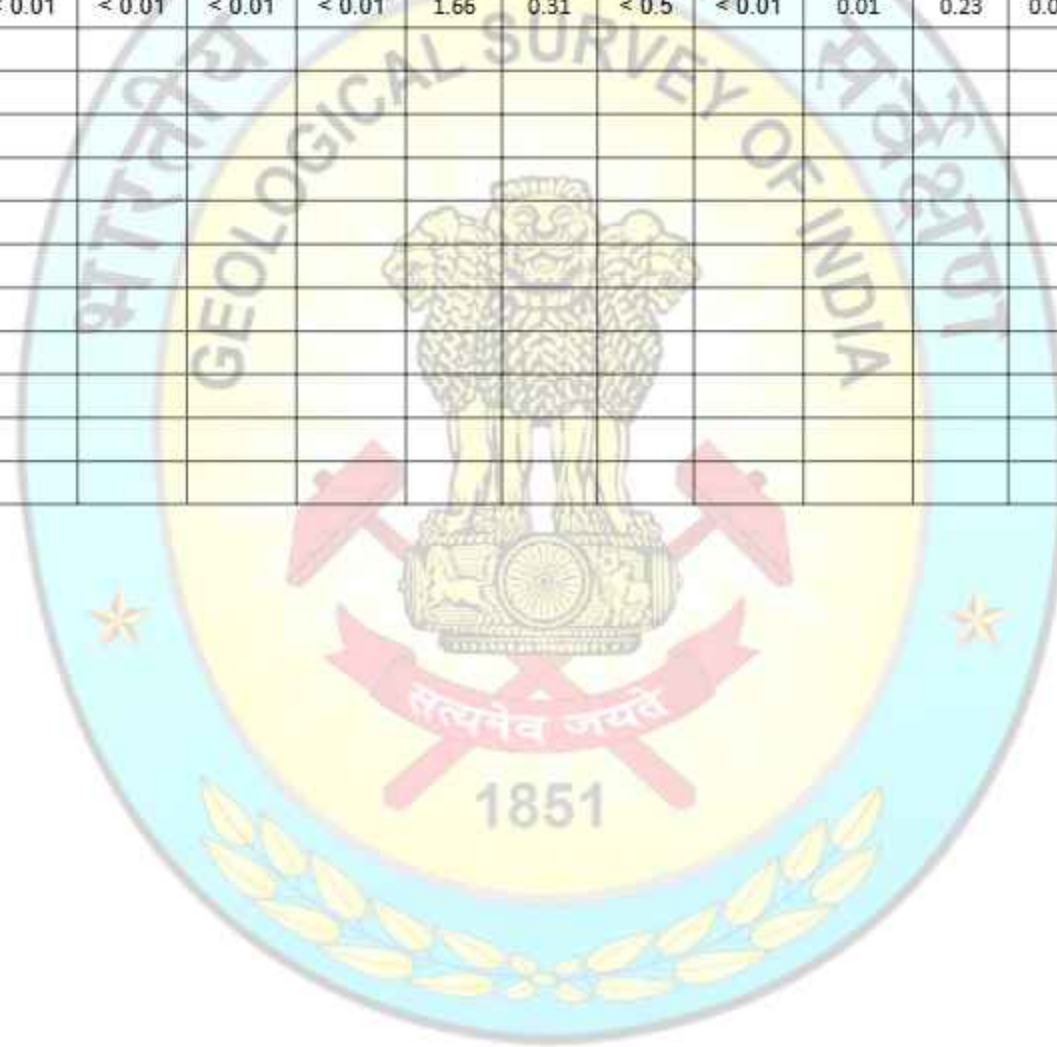
Analytical data of Rare Earth Elements of Soil Samples
(Values in ppm)

Sample No.	La	Ce	Pr	Nd	Eu	Sm	Gd	Tb	Dy	Ho	Er	Tm	Yb	Lu
83K8/A1/R/19	38.850	65.025	7.552	26.473	0.849	4.664	4.296	0.611	3.735	0.876	2.367	0.409	2.609	0.439
83K8/A1/C/19	33.638	56.426	6.838	24.570	0.925	4.629	4.255	0.634	3.991	0.948	2.541	0.433	2.757	0.461
83K8/A2/R/19	38.504	77.739	8.225	28.304	0.882	4.901	4.993	0.726	4.352	1.010	2.673	0.459	2.948	0.497
83K8/A2/C/19	41.874	99.219	8.947	30.599	0.994	5.336	5.520	0.771	4.576	1.064	2.892	0.490	3.135	0.530
83K8/A3/R/19	34.658	57.667	6.866	24.121	0.863	4.368	3.981	0.597	3.874	0.931	2.554	0.440	2.860	0.485
83K8/A3/C/19	39.451	82.564	8.856	30.832	1.015	5.396	4.966	0.703	4.272	1.010	2.742	0.470	3.025	0.502
83K8/B1/R/19	36.976	63.193	7.473	26.564	0.935	4.929	4.476	0.648	3.877	0.878	2.326	0.388	2.516	0.423
83K8/B1/C/19	38.623	63.415	8.307	30.988	1.492	6.461	6.360	0.964	5.586	1.227	3.107	0.512	3.201	0.524
83K8/B2/R/19	42.613	86.696	9.846	34.899	1.252	6.620	6.197	0.926	5.565	1.266	3.281	0.548	3.442	0.566
83K8/B2/C/19	42.429	80.071	9.404	33.599	1.166	6.138	5.573	0.813	5.009	1.167	3.098	0.523	3.361	0.560
83K8/B3/R/19	41.816	68.985	8.376	29.506	1.016	5.023	4.481	0.624	3.792	0.891	2.397	0.404	2.573	0.426
83K8/B3/C/19	39.050	66.213	7.844	28.236	1.114	5.310	4.801	0.691	4.056	0.933	2.437	0.406	2.561	0.431
83K8/C1/R/19	39.806	69.663	7.969	28.172	0.930	4.877	4.307	0.627	4.004	0.991	2.698	0.462	2.958	0.497
83K8/C1/C/19	45.141	84.522	10.449	37.024	1.338	6.547	5.785	0.859	5.457	1.280	3.456	0.574	3.632	0.595
83K8/C2/R/19	15.672	51.317	3.758	13.855	0.770	3.424	3.428	0.560	3.385	0.717	1.837	0.321	2.139	0.341
83K8/C2/C/19	45.661	93.447	10.547	37.627	1.359	7.324	7.108	1.010	5.746	1.278	3.293	0.558	3.579	0.580
83K8/C3/R/19	45.108	66.886	8.452	30.364	1.255	5.987	6.134	0.932	5.353	1.200	2.995	0.486	3.001	0.481
83K8/C3/C/19	21.042	33.915	4.592	21.678	0.724	3.392	3.213	0.503	3.290	0.589	1.488	0.246	1.540	0.247

Analytical data of Stream Water Samples: Trace Elements (All Values in ppb)

Sample No.	Li	Be	Al	Sc	Ti	V	Cr	Mn	Co	Ni	Cu	Zn	Ga	As	Rb	Sr	Y
83K8A1//W/18	< 10	< 0.1	26.53	< 25	48.40	< 5	< 5	87.95	0.35	1.36	2.80	27.66	0.16	< 1	0.88	157.20	0.06
83K8/A2/W/18	< 10	< 0.1	< 25	< 25	34.87	< 5	< 5	34.97	0.26	1.17	2.72	41.46	0.14	< 1	0.62	134.17	0.06
83K8/A3/W/18	< 10	< 0.1	34.43	< 25	74.60	< 5	< 5	12.65	0.35	1.57	3.28	89.10	0.15	< 1	0.98	225.95	0.09
83K8/B1/W/18	< 10	< 0.1	< 25	< 25	64.64	< 5	< 5	6.11	0.24	1.34	2.64	31.74	0.14	< 1	0.85	249.76	0.04
83K8/B2/W/18	< 10	< 0.1	< 25	< 25	51.20	< 5	< 5	37.59	0.24	1.37	2.43	26.02	0.14	< 1	0.71	144.09	0.10
83K8/B3/W/18	< 10	< 0.1	34.92	< 25	35.52	< 5	5.41	7.00	0.22	1.32	3.55	78.82	0.14	< 1	0.57	84.01	0.09
83K8/C1/W/18	< 10	< 0.1	29.99	< 25	83.53	< 5	5.16	6.19	0.33	1.76	4.02	34.10	0.14	< 1	0.66	243.57	0.09
83K8/C2/W/18	< 10	< 0.1	< 25	< 25	18.91	< 5	10.92	3.30	0.15	2.18	1.79	34.93	0.12	< 1	0.38	53.21	0.04
83K8/C3/W/18	< 10	< 0.1	37.01	< 25	30.28	< 5	7.80	5.92	0.22	1.52	2.56	83.75	0.13	< 1	0.57	75.59	0.07
Sample No.	Mo	Ru	Rh	Ag	Cd	Sn	Sb	Cs	Ba	La	Ce	Pr	Nd	Sm	Eu	Gd	Tb
83K8A1//W/18	< 0.5	< 0.02	< 0.01	0.13	0.13	0.33	0.20	0.01	8.50	0.07	0.13	0.01	0.05	< 0.03	< 0.03	0.02	< 0.01
83K8/A2/W/18	< 0.5	< 0.02	< 0.01	0.08	0.11	0.50	1.48	0.01	11.95	0.08	0.15	0.02	0.06	< 0.03	< 0.03	0.02	< 0.01
83K8/A3/W/18	< 0.5	< 0.02	< 0.01	0.11	0.16	0.72	0.29	0.01	33.39	0.14	0.29	0.03	0.10	< 0.03	< 0.03	0.02	< 0.01
83K8/B1/W/18	< 0.5	< 0.02	< 0.01	0.05	0.12	< 0.3	0.15	0.02	12.56	0.07	0.12	0.01	0.04	< 0.03	< 0.03	< 0.02	< 0.01
83K8/B2/W/18	< 0.5	< 0.02	< 0.01	0.11	0.13	0.37	0.16	0.01	11.30	0.12	0.27	0.02	0.08	< 0.03	< 0.03	0.02	< 0.01
83K8/B3/W/18	0.50	< 0.02	< 0.01	0.14	0.12	0.89	0.17	0.01	11.71	0.13	0.27	0.03	0.09	< 0.03	< 0.03	0.03	< 0.01
83K8/C1/W/18	0.68	< 0.02	< 0.01	0.05	0.15	< 0.3	0.24	0.01	35.02	0.08	0.15	0.02	0.07	< 0.03	< 0.03	0.02	< 0.01
83K8/C2/W/18	< 0.5	< 0.02	< 0.01	0.07	0.10	< 0.3	0.11	0.01	11.17	0.06	0.11	0.01	0.04	< 0.03	< 0.03	< 0.02	< 0.01
83K8/C3/W/18	< 0.5	< 0.02	< 0.01	0.19	0.15	0.53	0.16	0.01	13.68	0.11	0.22	0.02	0.08	< 0.03	< 0.03	0.02	< 0.01
Sample No.	Dy	Ho	Er	Tm	Yb	Lu	Hf	Ta	W	Re	Ir	Pt	Au	Tl	Pb	Bi	U
83K8A1//W/18	< 0.01	< 0.01	< 0.01	< 0.01	< 0.01	< 0.01	1.32	0.75	< 0.5	< 0.01	0.01	0.18	0.02	< 0.01	0.72	< 0.02	< 0.02
83K8/A2/W/18	< 0.01	< 0.01	< 0.01	< 0.01	< 0.01	< 0.01	0.53	0.17	< 0.5	< 0.01	< 0.01	0.10	0.01	< 0.01	1.00	< 0.02	< 0.02
83K8/A3/W/18	< 0.01	< 0.01	< 0.01	< 0.01	< 0.01	< 0.01	0.82	0.27	< 0.5	< 0.01	< 0.01	0.14	0.01	< 0.01	2.10	< 0.02	< 0.02
83K8/B1/W/18	< 0.01	< 0.01	< 0.01	< 0.01	< 0.01	< 0.01	0.09	0.07	< 0.5	< 0.01	< 0.01	0.08	0.01	< 0.01	1.10	< 0.02	< 0.02

83K8/B2/W/18	< 0.01	< 0.01	< 0.01	< 0.01	< 0.01	< 0.01	0.71	0.23	< 0.5	< 0.01	< 0.01	0.19	0.01	< 0.01	0.70	<0.02	<0.02
83K8/B3/W/18	< 0.01	< 0.01	< 0.01	< 0.01	< 0.01	< 0.01	0.95	0.25	< 0.5	< 0.01	< 0.01	0.21	0.01	< 0.01	0.83	<0.02	<0.02
83K8/C1/W/18	< 0.01	< 0.01	< 0.01	< 0.01	< 0.01	< 0.01	0.28	0.08	< 0.5	< 0.01	< 0.01	0.12	0.01	< 0.01	1.66	<0.02	<0.02
83K8/C2/W/18	< 0.01	< 0.01	< 0.01	< 0.01	< 0.01	< 0.01	0.29	0.04	< 0.5	< 0.01	< 0.01	0.11	0.00	< 0.01	0.76	<0.02	<0.02
83K8/C3/W/18	< 0.01	< 0.01	< 0.01	< 0.01	< 0.01	< 0.01	1.66	0.31	< 0.5	< 0.01	0.01	0.23	0.01	< 0.01	1.16	<0.02	<0.02
Sample No.	Hg																
83K8A1//W/18	< 3																
83K8/A2/W/18	< 3																
83K8/A3/W/18	< 3																
83K8/B1/W/18	< 3																
83K8/B2/W/18	< 3																
83K8/B3/W/18	< 3																
83K8/C1/W/18	< 3																
83K8/C2/W/18	< 3																
83K8/C3/W/18	< 3																



**Analytical data of Oxides of Duplicate Stream Sediment/Slope wash Samples
with Original Samples (Values in %)**

Sample No.		SiO ₂	TiO ₂	Al ₂ O ₃	Fe ₂ O ₃	MnO	MgO	CaO	Na ₂ O	K ₂ O	P ₂ O ₅
83K8/006/S/18	Original	67.33	1.25	13.72	5.94	0.13	1.01	0.26	0.19	1.48	0.11
83K8/201/S/18	Duplicate	68.97	1.16	12.85	5.93	0.12	0.99	0.24	0.15	1.41	0.11
83K8/011/S/18	Original	40.53	0.80	15.35	24.92	0.45	1.46	0.23	0.16	1.18	0.21
83K8/202/S/18	Duplicate	48.19	0.84	15.12	25.04	0.49	1.53	0.19	0.11	1.24	0.23
83K8/015/S/18	Original	66.11	0.85	14.18	4.95	0.07	1.13	0.12	0.57	1.84	0.09
83K8/203/S/18	Duplicate	66.31	0.80	13.92	4.86	0.06	1.09	0.10	0.54	1.77	0.09
83K8/080/S/18	Original	62.37	0.91	15.91	6.60	0.09	1.11	0.06	0.13	1.51	0.07
83K8/204/S/18	Duplicate	62.25	0.91	15.94	6.59	0.09	1.03	0.05	0.13	1.49	0.07
83K8/097/S/18	Original	59.92	0.91	17.43	6.75	0.07	1.70	0.31	0.74	1.97	0.08
83K8/205/S/18	Duplicate	60.46	0.91	16.93	6.73	0.07	1.64	0.30	0.75	1.92	0.07
83K8/143/S/18	Original	45.49	0.48	9.31	21.20	0.32	7.98	0.58	0.07	0.58	0.09
83K8/206/S/18	Duplicate	37.57	0.23	3.25	13.31	0.29	23.11	1.45	0.13	0.23	0.12
83K8/097/S/18	Original	54.55	1.61	14.01	11.1	0.23	1.88	0.74	1.42	0.32	0.1
83K8/207/S/18	Duplicate	61.08	1.60	13.53	11.11	0.23	1.99	0.73	1.82	0.31	0.10
83K8/146/S/18	Original	60.28	0.77	16.51	6.81	0.1	2.33	0.5	0.73	1.81	0.1
83K8/208/S/18	Duplicate	61.18	0.77	15.34	6.82	0.10	2.59	0.47	0.70	1.70	0.09
83K8/164/S/18	Original	63.31	0.93	15.17	5.91	0.1	1.14	0.31	0.37	1.7	0.12
83K8/209/S/18	Duplicate	63.77	0.90	14.67	5.88	0.10	1.30	0.29	0.37	1.59	0.11

**Analytical data of REEs of Duplicate Stream Sediment/Slope wash Samples
with Original Samples (Values in ppb)**

Sample No.		La	Ce	Pr	Nd	Sm	Eu	Gd	Tb	Dy	Ho	Er	Tm	Yb	Lu
83K8/006/S/18	Original	46.24	86.36	10.47	37.45	6.79	1.32	6.33	0.92	5.50	1.09	3.23	0.54	3.46	0.55
83K8/201/S/18	Duplicate	46.454	78.658	9.426	33.399	1.219	6.114	5.839	0.839	4.981	1.160	2.929	0.489	3.129	0.520
83K8/011/S/18	Original	32.44	68.95	7.37	26.19	5.34	1.08	5.29	0.79	4.76	0.90	2.67	<0.5	2.96	<0.5
83K8/202/S/18	Duplicate	36.819	70.156	7.450	26.785	1.089	5.497	5.469	0.820	4.760	1.065	2.726	0.459	2.935	0.474
83K8/015/S/18	Original	30.92	57.68	7.52	27.70	5.67	1.32	5.69	0.84	4.92	0.95	2.77	<0.5	2.98	0.50
83K8/203/S/18	Duplicate	30.862	51.750	6.810	25.575	1.309	5.418	5.285	0.795	4.641	1.031	2.616	0.437	2.820	0.474
83K8/080/S/18	Original	36.81	73.47	7.53	25.45	4.21	0.77	4.34	0.59	3.53	0.72	2.28	<0.5	2.54	<0.5
83K8/204/S/18	Duplicate	38.049	69.997	7.171	24.410	0.800	4.093	4.189	0.591	3.659	0.867	2.343	0.411	2.721	0.458
83K8/097/S/18	Original	30.86	58.33	7.41	27.66	5.70	1.33	5.53	0.82	4.82	0.93	2.78	<0.5	2.92	<0.5
83K8/205/S/18	Duplicate	35.766	59.705	7.817	29.106	1.429	6.048	5.824	0.889	5.233	1.191	3.039	0.511	3.266	0.545
83K8/143/S/18	Original	23.42	38.81	5.10	18.80	3.84	0.76	3.71	0.56	3.19	0.61	1.80	<0.5	1.80	<0.5
83K8/206/S/18	Duplicate	6.291	11.134	1.261	4.465	0.191	0.934	0.940	0.144	0.846	0.195	0.507	0.087	0.552	0.094
83K8/097/S/18	Original	14.12	31.97	3.58	14.37	3.54	0.98	3.75	0.68	4.58	0.93	2.87	<0.5	3.10	<0.5
83K8/207/S/18	Duplicate	16.634	33.628	3.839	15.303	1.045	3.751	4.112	0.745	4.959	1.181	3.090	0.523	3.362	0.547
83K8/146/S/18	Original	24.18	48.90	5.68	21.39	4.55	1.08	4.39	0.66	3.92	0.75	2.26	<0.5	2.35	<0.5
83K8/208/S/18	Duplicate	30.889	50.580	6.576	24.597	1.210	5.107	4.945	0.746	4.316	0.961	2.441	0.404	2.586	0.426
83K8/164/S/18	Original	30.47	58.38	7.23	25.94	5.11	1.09	4.82	0.70	4.40	0.88	2.61	<0.5	2.83	<0.5
83K8/209/S/18	Duplicate	35.419	59.668	7.395	27.195	1.152	5.336	4.958	0.755	4.631	1.054	2.754	0.469	2.992	0.495

**Analytical data of Trace Elements of Duplicate Stream Sediment/Slope wash Samples
with Original Samples (Values in ppm)**

Sample No.		Ba	Co	Cr	Cu	Ga	Nb	Ni	Pb	Sc	Sr	V	Y	Zn	Zr	Sn	Hf	Ta	U	Be	Ge	As	Rb	Th
83K8/008/S/18	Original	373	20	197	28	17	18	50	16	18	52	122	26	72	318	3.29	13.44	1.57	2.91	1.71	1.52	7.47	86.82	15.45
83K8/201/S/18	Duplicate	231	21	157	32	15	19	61	12	12	52	115	24	68	295	6.527	11.127	1.874	2.662	1.669	1.457	8.775	83.114	14.044
83K8/011/S/18	Original	320	187	3829	71	18	14	1517	18	33	27	225	17	152	136	4.13	3.20	0.68	3.01	2.09	4.39	14.00	90.57	13.80
83K8/202/S/18	Duplicate	346	204	3889	83	21	16	1671	22	35	29	222	22	161	151	2.558	5.874	1.174	3.077	2.086	4.186	14.07 6	85.559	13.882
83K8/015/S/18	Original	175	15	547	22	15	10	77	23	17	63	112	21	69	351	2.60	13.94	0.79	2.34	1.24	1.27	6.59	80.26	10.52
83K8/203/S/18	Duplicate	145	23	486	23	14	11	89	12	12	58	95	21	63	321	2.340	19.668	1.414	2.195	1.206	1.137	6.868	77.585	8.973
83K8/080/S/18	Original	238	21	287	24	15	15	112	17	13	32	113	20	76	248	3.86	5.91	1.68	2.71	1.36	1.26	10.73	93.17	13.23
83K8/204/S/18	Duplicate	239	24	262	26	16	14	109	20	11	32	114	18	78	247	2.695	12.079	1.705	2.856	1.535	1.344	9.583	90.537	13.736
83K8/097/S/18	Original	289	23	230	33	19	12	99	12	18	82	140	26	96	235	3.44	8.72	1.02	2.27	1.51	1.27	9.28	94.94	9.92
83K8/205/S/18	Duplicate	266	22	206	35	18	12	95	16	14	81	131	26	90	231	2.709	9.446	1.386	2.438	1.702	1.412	9.274	93.241	10.770
83K8/143/S/18	Original	190	206	2859	42	11	9	5681	9	27	18	151	15	114	76	3.30	3.58	0.47	1.53	1.08	2.88	7.36	48.41	7.33
83K8/206/S/18	Duplicate	<50	202	2796	13	6	6	2198	10	10	18	71	6	53	26	1.197	0.733	0.354	0.414	0.296	1.706	1.727	19.243	1.980
83K8/097/S/18	Original	117	33	56	43	17	8	24	7	21	73	303	23	79	137	3.64	3.40	0.56	1.01	0.93	1.71	3.81	18.30	4.59
83K8/207/S/18	Duplicate	171	33	56	41	16	8	30	2	29	73	304	24	82	136	1.699	5.153	0.859	1.106	0.963	1.813	2.835	19.561	4.897
83K8/146/S/18	Original	201	26	242	37	17	10	166	20	16	81	122	24	95	183	5.57	4.35	0.97	1.65	1.28	1.18	8.07	67.55	8.80
83K8/208/S/18	Duplicate	180	25	262	36	17	11	160	11	16	82	120	22	95	186	1.841	7.947	1.108	1.857	1.567	1.338	7.301	87.354	9.338
83K8/164/S/18	Original	218	19	221	34	16	14	84	16	15	69	103	23	79	231	3.82	9.58	1.52	2.26	1.37	1.29	9.94	77.06	10.15
83K8/209/S/18	Duplicate	230	23	226	35	14	15	89	20	14	69	107	23	83	235	1.676	8.100	1.118	2.428	1.502	1.229	9.284	82.714	11.087

1851

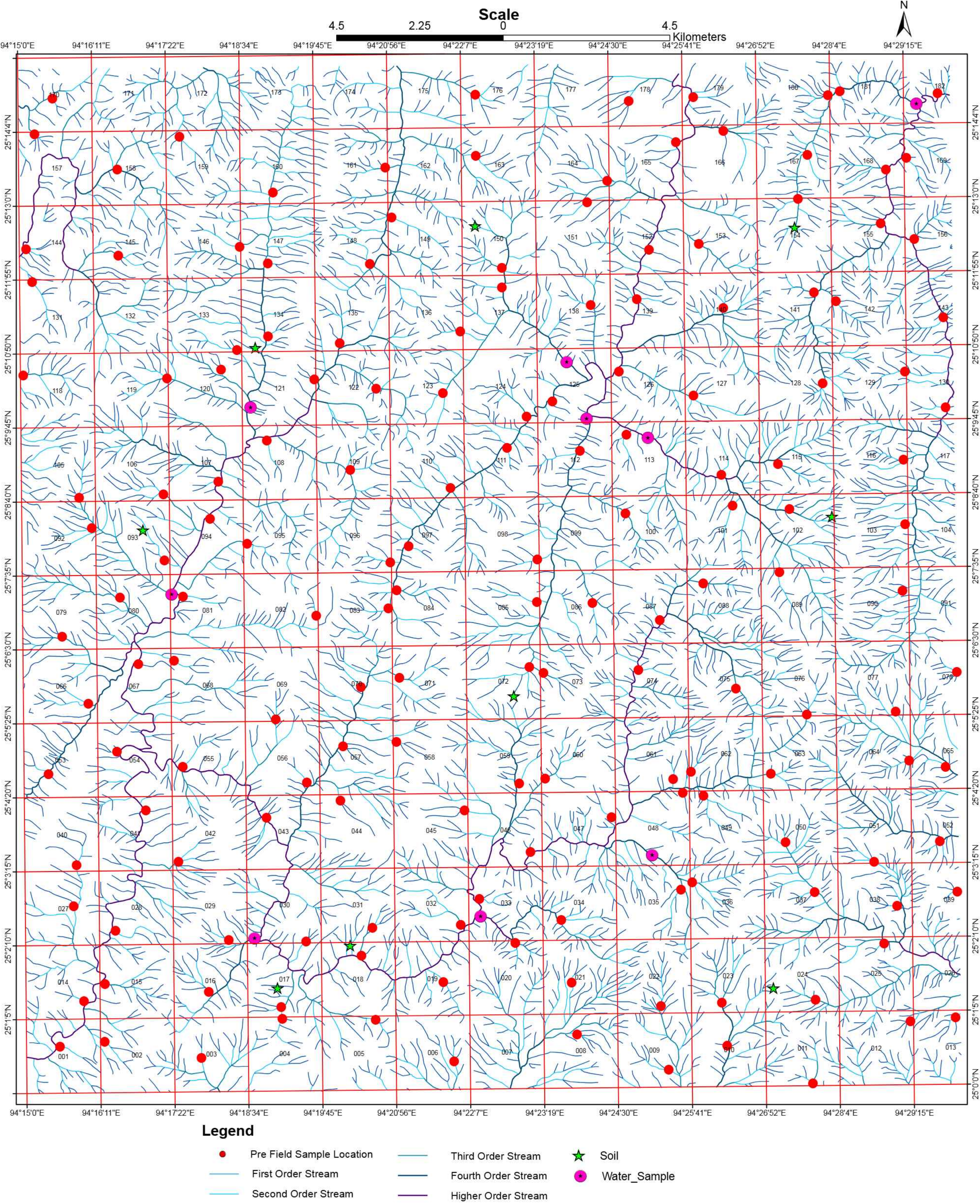
Status of Analytical chemical data Received

Lab No.	Media of Samples	Packages Received
3249 (50 samples)	Stream Sediment Samples	A, B, D, E, F, G, H, J
3406 (96 samples)	Stream Sediment Samples	A, F, G, H
3477 (9 samples)	Water samples	B, C
3478 (27 samples)	Soil samples and Duplicate samples	A, H
3493 (22 samples)	Stream Sediment Samples	A, H

Chemical Analysis Packages Index:

Sample packages	Analytical Techniques	Oxides & Elements Analysed
A.	XRF	SiO ₂ , Al ₂ O ₃ , Fe ₂ O ₃ , TiO ₂ , CaO, MgO, MnO, Na ₂ O, K ₂ O, P ₂ O ₅ , Ba, Co, Cr, Cu, Ga, Nb, Ni, Pb, Rb, Sc, Sr, Th, U, V, Y, Zn, Zr
B.	GF-AAS	Au
C.	F-AAS	Li
D.	HG-AAS	As, Sb, Bi, Se, Te
E.	ISE	F
F.	GF-AAS	Cd, Ag
G.	CV-AAS	Hg
H.	ICP-MS	La, Ce, Pr, Nd, Eu, Sm, Gd, Tb, Dy, Ho, Er, Tm, Yb, Lu, U, Hf, Ta, Ge, Be
I.	FA-GFAAS	Pt, Pd
J.	ICP-MS	Mo, In, Cs, Tl, W, Sn
Water Samples	W (A)	pH, EC, HCO ₃ ⁻ , Cl ⁻ , SO ₄ ²⁻ , NO ₃ ⁻ , Ca ²⁺ , Na ⁺ , K ⁺ , PO ₄ ³⁻ , SiO ₂
	W (B)	La, Ce, Pr, Nd, Eu, Sm, Gd, Tb, Dy, Ho, Er, Tm, Yb, Lu, U, Hf, Ta, Ge, Be
	W (C)	As, F, B
	W (D)	Hg

DRAINAGE MAP WITH POSTFIELD SAMPLE LOCATIONS IN AND AROUND UKHRUL, UKHRUL DISTRICT, MANIPUR, T.S. NO. 83K/08





भारत सरकार
Government of India
भारतीय भूवैज्ञानिक सर्वेक्षण
Geological Survey of India

**मणिपुर के उखरूल जिले के ओफियोलइट बेल्ट में गंनोम-
येनटीमक्षेत्र में क्रोमियम, निकेल और बेस मेटल खनिज के लिए
टोही सर्वेक्षण (जी-४)**

**Reconnaissance survey for chromium, nickel and base metal
mineralization in Gamnom-Yentem area in part of Ophiolite
belt, Ukhrul District, Manipur (G-4)**

टोपोशीट्स: 83 K/8 & 83 L/5/ Toposheet No.: 83K/8& 83 L/5
मदसंख्या: M2AFGBM-MEP/NC/NER/SU-MAN/2019/24286
Item no.: M2AFGBM-MEP/NC/NER/SU-MAN/2019/24286

कार्यसत्र 2019-20 का अंतिम प्रतिवेदन
Final Report for Field Season 2019-20

इमोमेरेन आओ, वरिष्ठ भूवैज्ञानिक
वालेस सावियो पीटर, वरिष्ठ भूवैज्ञानिक

Imomeren Ao, Senior Geologist
Vales Savio Peter, Senior Geologist

मिशन-II
MISSION-II

राज्य इकाई: मणिपुर – नागालैंड/State Unit: Manipur – Nagaland
उत्तरपूर्व क्षेत्र/North Eastern Region
दीमापुर/Dimapur

जून, 2021
June, 2021

**Reconnaissance survey for chromium, nickel and base metal mineralization in
Gamnom-Yentem area in part of Ophiolite belt, Ukhrul District, Manipur (G4)**

Item Code: M2AFGBM-MEP/NC/NER/SU-MAN/2019/24286

Field Season: FS 2019-20

CONTENTS

CHAPTER-1	सारांश SUMMARY	1-3 4-5
CHAPTER-2	INTRODUCTION	6-8
	2.1 Present work	7
	2.2 Objective	7
	2.3 Personnel	7
	2.4 Nature and quantum of work	7
	2.5 Acknowledgement	8
CHAPTER-3	PROPERTY DESCRIPTION	9-15
	3.1 Title of ownership	9
	3.2 Details of the area	9-14
	3.2.1 Name of village/district/state	9
	3.2.2. Survey of India toposheets Nos.	9
	3.2.3. Geo-coordinates of the mapped block	9
	3.2.4. Cadastral details of the area with land use	10
	3.2.5. Free hold/lease hold	11
	3.2.6. Location and accessibility	11
	3.2.7 Physiography	11
	3.2.8 Drainage	11
	3.2.9 Climate	12
	3.2.10 Rainfall	13
	3.2.11 Flora and Fauna	13
	3.3 Infrastructure & environment	14-15
	3.3.1 Local infrastructure	14
	3.3.2 Local inhabitants and culture	15
CHAPTER-4	PREVIOUS EXPLORATION	16-21
	4.1 Details of previous exploration/investigation carried by other agencies/parties.	16-19
	4.2 Details of aero-geophysical and geophysical mapping	19-21
CHAPTER-5	GEOSCIENCE INVESTIGATION	22-62
	5.1 Regional Geology	22-29
	5.1.1 Aerial reconnaissance	22
	5.1.2 Brief regional geology	22
	5.1.3 Regional stratigraphy	29
	5.2 Detailed Geological Exploration	30-46
	5.2.1 Outcrop map on 1:12,500 scale	30
	5.2.2 Large scale mapping on 1:12,500 scale	30
	5.2.3 Description of rock types	31
	5.2.4 Petrological Studies	37
	5.2.5 Structure	41

	5.2.6 Metamorphism	43
	5.2.7 Mineralogy of the ore zones and ore textures	43
	5.2.8 Sampling	44
	5.2.9 Discussion of results of chemical analysis samples	46
	5.3 Geophysical exploration	61
	5.4 Geochemical exploration	61
CHAPTER-6	INTEGRATION OF GEOLOGICAL, GEOCHEMICAL AND GEOPHYSICAL EXPLORATION DATA AND INTERPRETATION THEREOFF Overlay studies in GIS (Geological, Geochemical and Geophysical maps)	62
CHAPTER-7	MINERAL PROSPECT	63-68
	7.1 Surface indication of mineralization	63
	7.2 Mode of occurrence	65
	7.3 Nature and control of mineralization	65
	7.4 Details of mineralized zones	66
	7.5 Alterations zones and its relevance with mineralization	67
	7.6 Genesis of mineralization/Genetic model for mineralization	68
CHAPTER-8	RECOMMENDATION	69-71
CHAPTER-9	CONCLUSION	72-73
	LOCALITY INDEX	74
	REFERENCES	75
LIST OF FIGURES		
Fig.1	Location of the study area	9
Fig.2	Land use/land cover map of parts TS 83K/8 and 83L/5 covering the study area	10
Fig.3	Drainage map superimposed on the Digital Elevation Model (DEM) map of the area prepared using ASTER DEM	12
Fig.4	The Magnetic (TF) contour map superimposed on detailed geological map around Gamnom-Harbui Khayui. Magnetic Surveyed by Kumar, et al, 2016	21
Fig.5	Field photograph showing harzburgite of transitional peridotite northeast of Gamnom (25°01'40.9" / 94°26'52.1")	34
Fig.6	Field photograph showing serpentized harzburgite of transitional peridotite northwest of Pushing (25°03'09.1" / 94°28'10.1")	34
Fig.7	Field photograph showing hob-nail texture on the surface of Harzburgite of transitional peridotite at Gamnom (25°00'41.1" / 94°27'10.1")	35
Fig.8	Field photograph showing chromitite pods south of Khankui-khullen. (25°00'47.9" / 94°25'47.9")	35
Fig.9	Field photograph showing mafic cumulate body of gabbro at	36

	Gamnorn (25°01'28" / 94°27'8")	
Fig.10	Field photograph showing exposure of argillaceous unit in olistoliths northwest of Pushing (25°02'40.8" / 94°28'45.6")	36
Fig.11	Field photograph showing exposure of chert unit in olistoliths west of Gamnorn (25°01'30.0" / 94°25'29.3")	36
Fig.12	Photomicrograph showing exsolution lamellae of Clinopyroxene (CPX) within orthopyroxene (OPX) surrounded by olivine (OL) Partially serpentinised Harzburgite (transitional peridotite) under crosspolarized light at 4x magnification. West of Gamnorn (25°01'53.8" / 94°26'32.0")	38
Fig.13	Photomicrograph showing break down of Orthopyroxene (OPX) surrounded by serpentinized olivine (OL) in Harzburgite (transitional peridotite) under crosspolarized light at 2.5x magnification. East of Changa (25°00'50.6" / 94°25'3.9")	38
Fig.14	Photomicrograph showing neoblastic olivine (NbOL) surrounded by serpentinized Olivine in Harzburgite (transitional peridotite) under cross polarized light at 4x magnification. East of Gamnorn (25°01'28.7" / 94°27'12.9")	39
Fig.15	Photomicrograph showing chrome spinel (CrSp) surrounded by orthopyroxene (OPX) in Harzburgite (transitional peridotite) under cross polarized light at 4x magnification. West of Gamnorn (25°01'53.8" / 94°26'32.0")	39
Fig.16	Photomicrograph showing chrome spinel (CrSp) surrounded by orthopyroxene in Harzburgite (transitional peridotite) under plane polarized light at 2.5x magnification. south of Khangkui Khullen (25°00'39.5" / 94°25'42.8")	39
Fig.17	Photomicrograph showing relict magnetite (Mag) surrounded by olivine in Harzburgite (transitional peridotite) under cross polarized light at 4x magnification. East of Gamnorn (25°01'28.7" / 94°27'12.9")	39
Fig.18	Photomicrograph showing sub-ophitic texture in gabbro with large plagioclase laths (Pg) surrounded by chlorite (Cl) and hornblende (Hb) also showing breaking down of smaller weaker grains (cataclastic texture) due to exerted pressure of thrusting. cross polarized light at 2.5x magnification. Gamnorn (25°01'28.0" / 94°27'8")	40
Fig.19	Photomicrograph of Xenomorphic Clinopyroxene(Cpx) showing intergrowth with laths of plagioclase (Pl) in gabbro.	40
Fig.20	Photomicrograph of Skeletal magnetite (Mag) grains within plagioclase (Pl) laths in gabbro.	40
Fig.21	Photomicrograph of fine laths of plagioclase occurring as inclusion within Clinopyroxene (Cpx). Plagioclase and Clinopyroxene laths often show intergranular texture.	41

Fig.22	Photomicrograph of Clinopyroxene (Cpx), plagioclase (Pl) and skeletal magnetite (Mag) within an altered plagioclase groundmass.	41
Fig.23	Brecciated peridotite in a sandy matrix, South of Gamnom (25°00'37.7" / 94°27'54.9")	42
Fig.24	Photomicrograph showing cataclastic texture of chromite grains (Cr) in chromitite reflected light at 2.5x magnification. Gamnom (25°00'58.7" / 94°27'14.7")	44
Fig.25	Photomicrograph showing corroded grains of chromite (Cr) in chromitite reflected light at 2.5x magnification. Gamnom (25°00'58.7" / 94°27'14.7")	44
Fig.26	MgO vs other major oxides scatter plot of ultramafic rocks (oxide in %)	47
Fig.27	ACM and AFM plots of ultramafic rocks with fields of ultramafic cumulates and metamorphic peridotites after Coleman (1977)	48
Fig.28	Variation plot of Cr vs Ti vs Al vs Mn vs Ni in red soil samples	49
Fig.29	Field photographs showing section of trench-1 at Gamnom (25°00'58.1" / 94°27'12.7").	50
Fig.30	Schematic sketch of Trench-1	50
Fig.31	Variation plot of Cr vs Ni in trench-1	51
Fig.32	Field photographs showing section of trench-2 at Gamnom (25°00'58.3" / 94°26'59.9").	52
Fig.33	Schematic sketch of Trench-2	52
Fig.34	Variation plot of Cr vs Ni in trench-2	53
Fig.35	Field photographs showing section of trench-3 south of Khangkui Khullen (25°00'48.0" / 94°26'47.8").	54
Fig.36	Schematic sketch of Trench-3	54
Fig.37	Variation plot of Cr vs Ni in trench-3	55
Fig.38	Field photographs showing section of trench-4 south of Yentem (24°58'56.2" / 94°26'01.8").	56
Fig.39	Schematic sketch of Trench-4	56
Fig.40	Variation plot of Cr vs Ni in trench-4	57
Fig.41	Field photographs showing section of trench-5 west of Pushing	58
Fig.42	Schematic sketch of Trench-5	58
Fig.43	Variation plot of Cr vs Ni in trench-5	59
Fig.44	Major oxide composition in Gabbros	59
Fig.45	REE plot in Gabbro's	60
Fig.46	Variation plot of Fe vs Al vs Cr vs Ni in red soil samples	61
Fig.47	Field photograph showing chromitite pods at Gamnom. (25°00'58.7" / 94°27'14.7")	63
Fig.48	Field photograph showing chromitite pods west of Pushing.	64

	(25°02'49.3" / 94°28'30.3")	
Fig.49	Field photograph showing chromitite pods south of Khankui. (25°00'48 " / 94°25'47.8")	64
Fig.50	Recommended blocks for further exploration	71

LIST OF TABLES

Table-1	Nature and Quantum of work	8
Table-2	Generalised stratigraphic succession of Manipur	29
Table-3	Lithostratigraphy of the study area	31
Table-4	Details of chemical composition of Chromite along with locations	66
Table-5	Details of chemical composition of Chromite along with locations in trenching samples	67
Table-6	Details of chemical composition of red soil samples	68
Table-7	Details of recommended blocks for further exploration	70

LIST OF ANNEXURES

Annexure-I	Chemical analysis results of bed rock samples (BRS)
Annexure-II	Chemical analysis results of petrochemical samples (PCS)
Annexure-III	Chemical analysis results of pitting-trenching samples (PTS)

LIST OF PLATES

Plate-I	Large scale geological map of Gamnom-Yentem area, Ukhrul district, Manipur in parts of toposheet No. 83K/8, 83L/5 (1:12,500)
Plate-II	Location of sampling points on large scale geological map of Gamnom-Yentem area, Ukhrul district, Manipur in parts of toposheet No. 83K/8, 83L/5 (1:12,500)

LIST OF APPENDIX

Appendix-I	Data sheet report movement in connection with its scrutiny
Appendix-II	Certificate of the quality of the report
Appendix-III	Information Sheet for Bibliography Database in Unpublished reports
Appendix-IV	Five Point Performa
Appendix-V	UNFC Compliance Format
Appendix-VI	Geological inputs

अध्याय 1

सारांश

ओफियोलाइट बेल्ट, उखरूल जिला, मणिपुर (G4) के हिस्से में ग्नोम-रेंटेम क्षेत्र में क्रोमियम, निकल और बेस मेटल खनिज के लिए टोही सर्वेक्षण

आइटम कोड: M2AFGBM-MEP / NC / NER / SU-MAN / 2019/24286

फील्ड सीज़न: FS 2019-20

द्वारा

इमरोमेन एओ, वरिष्ठ भूवैज्ञानिक

वैलेस सवियो पीटर, वरिष्ठ भूवैज्ञानिक

FS 2019-20 के दौरान, मणिपुर केफिओलाइट बेल्ट में ग्नोम-रेंटेम क्षेत्र के अल्ट्रामैफिक और माफिक चट्टानों में क्रोमियम, निकल और आधार धातुओं के खनिज क्षेत्रों का पता लगाने के उद्देश्य से टोही सर्वेक्षण किया गया था। प्रस्तावित क्षेत्र निर्देशांक से घिरा है। a) $25^{\circ}03'20''$ / $94^{\circ}25'35''$, (b) $25^{\circ}03'20''$ / $94^{\circ}29'30''$, (c) $24^{\circ}58'53''$ / $94^{\circ}27'44''$, (d) $24^{\circ}58'00''$ / $94^{\circ}24'54''$, (e) $25^{\circ}00'00''$ / $94^{\circ}24'54''$, टोपोशीट सं. के भीतर आते हैं। 83K/8 और 83L/5। बड़े पैमाने पर भूवैज्ञानिक मानचित्रण (1:12,500 स्केल) में बेड रॉक नमूनों, पेट्रोलॉजिकल नमूने, थैली / खाइयों के नमूनों का व्यवस्थित संग्रह 60कि.मी. क्षेत्र शामिल है।

अध्ययन क्षेत्र बर्मीज़ प्लेट के नीचे भारतीय प्लेट के उप-क्षेत्र क्षेत्र के साथ नागालैंड हिल ओफियोलाइट परिसर के थ्रस्टेड अनुक्रम का प्रतिनिधित्व करता है। अध्ययन क्षेत्र में माफिक-अल्ट्रामैफिक्स और ऑलेस्टिथिथिक इकाई को उजागर किया गया है। अल्ट्रामैफिक्स में नागिनकरण के विभिन्न डिग्री के साथ पेरिडोटाइट का प्रभुत्व है। आंशिक रूप से सर्पिनाइज्ड पेरिडोटाइट अक्सर सतह पर अच्छी तरह से विकसित हॉब नाखून बनावट का प्रदर्शन करते हैं जहां पाइरॉक्सिन खनिज सर्पिनिज्ड ग्राउंड मास से प्रतिरोधी इकाई के रूप में बाहर निकलते हैं। स्लिकेनसाइड्स का विकास सामान्यतः देखा जाता है। माफिक का प्रतिनिधित्व बड़े पैमाने पर गैब्रो द्वारा किया जाता है जो अध्ययन क्षेत्र में 2 स्थानों पर होता है, जो ग्नोम में एक और पुशिंग के एक पश्चिम में होता है। ओलेस्टिथिथिक इकाई को एक अर्गिलैसियस मैट्रिक्स के

भीतर शेल, चर्ट, चेरी लिमस्टोन और सर्पिनाइज्ड अल्ट्रामाफ़िक्स जैसी चट्टानों के अराजक वितरण की विशेषता है। अल्ट्रामैफ़िक अनुक्रम का ओलेस्टिथिक इकाई के साथ एक जोरदार संपर्क है। लिथोलॉजिकल संपर्कों को शायद ही कभी उजागर किया जाता है क्योंकि उनमें से अधिकांश खड़ी पहाड़ियों, मोटी वनस्पतियों और अपक्षय वाली मिट्टी से मलबे के प्रवाह से ढंके होते हैं, जो संपर्क के विलंब को बाधित करते हैं।

पेरिडोटाइट शरीर 0.5 सेमी से 1 सेमी तक अलग-अलग आयामों के संचयी दिखाता है। पेरिडोटाइट संक्रमणकालीन पेरिडोटाइट जोन से संबंधित होता है जिसकी पुष्टि पतले खंड के अध्ययन और नेओब्लास्टिक ओलिविन और कोरोड क्रोम स्पिनल का पता लगाने से होती है। संक्रमणकालीन पेरिडोटाइट के इस मेजबान चट्टान के भीतर, यह देखा गया है कि 1-2 मीटर आयाम के क्रोमाइट पॉइस गमनोम के पश्चिम में, खंगखुई खुल्लेन के दक्षिण पूर्व और पुशिंग के पश्चिम में होते हैं। इन क्रोमाइट पॉइस के विस्तार में देरी करने के लिए, ग्नोम में 20 c.m.m और खंगखुई खुल्लेन में 10 c.m.m, रेंटेम में 10 cu.m और पुशिंग में 10 cu.m हैं जहाँ पॉडफॉर्म क्रोमाइट के सबूत सामने आए थे। हालांकि, क्रोमाइट पॉइस का विस्तार स्थापित नहीं किया जा सका। उन स्थानों पर जहाँ गहरे लाल रंग की मिट्टी देखी गई थी, निकेल की एकाग्रता का पता लगाने के लिए मिट्टी के नमूने एकत्र किए गए थे।

नमूनाकरण मुख्य रूप से संक्रमणकालीन पेरिडोटाइट्स से किया गया था, उनके भीतर क्रोमाइट की घटनाओं को देखते हुए। ग्नोम के पास, खंगखुई खुल्लेन के दक्षिण और पुशिंग गांवों के पश्चिम में क्रोमाइट घटनाएँ दर्ज की गईं। बड़े पैमाने पर मानचित्रण के दौरान, 150 नग। रॉक रॉक नमूने (बीआरएस), 25 नग पेट्रोकेमिकल नमूने (पीसीएस), 10 नग तत्वों के नमूने के प्लैटिनम समूह (PGE), 25 नग पेटोलोजिकल नमूने, 10 नग। अयस्क माइक्रोस्कोपी नमूने और क्षेत्र के खनिजकरण का मूल्यांकन करने के लिए 50 घन मीटर ट्रेचिंग नमूने लिए गए।

पेरिडोटाइट के पेटोलॉजिकल अध्ययन से पता चलता है कि पेरिडोटाइट्स मुख्य रूप से संरचना में लैज़ॉलिटिक होते हैं जिनमें क्लिनोपॉक्सीन और ऑर्थोपॉक्सीन का जैतून, क्रोम-स्पिनल और मैग्नेटाइट के साथ समान-खनिज प्रतिशत होता है जो गौण खनिज चरण को पूरा करता है। क्रोम-स्पिनल (कोरोडेड सीमा दिखाते हुए) को राहत दें और लेरज़ोलाइट में कंकाल मैग्नेटाइट का अवलोकन करें। कॉस्ट क्लिनोपॉक्सीन और ऑर्थोपॉक्सीन पर नियोब्लास्टिकोलिविन का विकास

मनाया जाता है, जो कि मैटल-सेगमेंट में पाइरोक्सीन के विघटन और ओलिविन के क्रिस्टलीकरण से युक्त मेल-रॉक इंटरैक्शन के कारण होता है। राहत क्लिनिकोप्रोक्सेन की अनाज की सीमाओं को मंजूरी दी जाती है। ओलिविन और ऑर्थोपाक्सीन आंशिक रूप से नागिनयुक्त होते हैं। इन सभी साक्ष्यों से साबित होता है कि यह पेरिडोटाइट (लेज़ोलाइट) ओपियोलाइट अनुक्रम की संक्रमणकालीन पेरिडोटाइट परत से संबंधित है। पतले खंड में गब्रो ने उप-ऑपिटिक को बदल दिया और पायरोक्सीन और हॉर्नब्लेन्ड की ऑपिटिक बनावट को बदल दिया। क्लिनोपाइरोक्सीन को ज्यादातर क्लोराइट में बदल दिया जाता है। एम्फिबोल का गठन पाइरोक्सीन के टूटने से होता है। प्लेगियोक्लेज़ का सरलीकरण आमतौर पर मनाया जाता है।

संक्रमणकालीन पेरिडोटाइट (हर्जबर्गाइट) का विश्लेषणात्मक परिणाम Fe_2O_3 (7%-13.7%), MgO (29% - 40.72%), Al_2O_3 (0-17.62%), TiO_2 (<0.01-1.9%), Cr_2O_3 (37-6879ppm), Cr (37ppm-9254ppm), Ni (30-8606ppm), Va (0-611ppm), Co (5-436ppm), Cu (<5-99ppm), Pb (2-14ppm), Zn (3-14ppm) 5-274ppm); नमूनों में जो क्रोमाइट असर वाले संक्रमणकालीन पेरिडोटाइट्स (हर्जबर्गाइट) हैं, सीआर मान 31.11% से 53.5% तक दिखाते हैं। गनम में खाई के दौरान एकत्र किए गए नमूनों में निकेल के उच्च मूल्यों को देखा गया है जो 1.07% -1.79% से लेकर येंटेम में एक नमूना निकेल का 1.41% है। 21 नग लाल मिट्टी के नमूने एकत्र किए गए थे और परिणामों में Fe_2O_3 प्रतिशत 10% से 43.75% और Al_2O_3 0.2-14.66% से लेकर दिखाया गया था।

CHAPTER 1 SUMMARY

Reconnaissance survey for chromium, nickel and base metal mineralization in Gamnom-Yentem area in part of Ophiolite belt, Ukhrul District, Manipur (G4)

Item Code: M2AFGBM-MEP/NC/NER/SU-MAN/2019/24286

Field Season: FS 2019-20

By

Imomeren Ao, Sr. Geologist

Vales Savio Peter, Sr. Geologist

During FS 2019-20, reconnaissance survey was carried out with an objective to locate mineralised zones of chromium, nickel, and base metals in ultramafic and mafic rocks of Gamnom-Yentem area in the Manipur Ophiolite belt. The proposed area is bounded by coordinates (a) 25°03'20" / 94°25'35", (b) 25°03'20" / 94°29'30", (c) 24°58'53" / 94°27'44", (d) 24°58'00" / 94°24'54", (e) 25°00'00" / 94°24'54", fall within toposheet no. 83K/8 and 83L/5. Large scale geological mapping (1:12,500 scale) involves systematic collection of bed rock samples, petrochemical samples, petrological samples, pitting/trenching samples for an area of 60sq.km.

The study area represents the thrust sequence of the Nagaland Hill Ophiolite complex along the subduction zone of the Indian plate below the Burmese plate. The study area exposes mafic-ultramafics, and olistolithic unit. The ultramafics are dominated by peridotite with different degrees of serpentinization. Partially serpentinized peridotite often exhibit well developed hob nail texture on the surface where pyroxene minerals protrudes out as resistant unit from serpentinized ground mass. Development of slickensides is a commonly observed. The mafic is represented by massive gabbro which occurs as intrusive within the ultramafics which occur in 2 locations in the study area, one at Gamnom and another west of Pushing. The olistolithic unit is characterized by chaotic distribution of rocks such as shale, chert, cherty limestone and serpentinized ultramafics, within an argillaceous matrix. The ultramafic sequence has a thrust contact with the olistolithic unit. The lithological contacts are rarely exposed as most of them are covered by debris flow from steep hills, thick vegetation and weathered soil, impeding delineation of contact.

The peridotite body shows cumulates of varying dimensions from 0.5cm to 1cm. The peridotite belongs to the transitional peridotite zone which is confirmed by thin section studies and detection of neoblastic olivine and corroded chrome spinel. Within this host rock of transitional peridotite, it is observed that chromitite pods of dimension 1-2m occurs in patches west of Gamnom, south east of Khangkhui Khullen and west of Pushing. To delineate the extension of these chromitite pods, 20 cu.m of trenching was carried out at Gamnom and 10 cu.m in Khangkhui Khullen, 10 cu.m in Yentem and 10 cu.m in Pushing where evidences of podiform chromite were encountered. However, the extension of the chromitite pods could not

be established. At places where deep red soil was observed soil samples were collected to ascertain the concentration of Nickel.

Sampling was carried out mainly from the transitional peridotites, considering the reported occurrences of chromitite within them. Chromite occurrences were reported near Gamnom, South of Khangkui Khullen and west of Pushing villages. During the course of large scale mapping, 150 nos. of bed rock samples (BRS), 25 nos. of petrochemical samples (PCS), 10 nos. of platinum group of elements samples (PGE), 25 nos. petrological samples, 10 nos. of ore microscopy samples and 50 cu m trenching samplings were carried out, to evaluate the mineralization of the area.

Petrological study of peridotite reveals that the peridotites are mainly harzburgitic in composition having equi-modal percentage of clinopyroxene and orthopyroxene with olivine, chrome-spinel and magnetite completes the accessory mineral phase. Relict chrome-spinel (showing corroded boundary) and relict skeletal magnetite is observed in harzburgite. Development of neoblastic olivines at the cost clinopyroxene and orthopyroxene is observed which is due to melt-rock interaction involving dissolution of pyroxenes and crystallization of olivine in the mantle segment. Grain boundaries of relict clinopyroxenes are corroded. Olivine and orthopyroxene are partially serpentinised. All these evidences prove that this peridotite (harzburgite) belongs to the transitional peridotite layer of the ophiolite sequence. Gabbro in thin section exhibit sub-ophitic to ophitic texture of pyroxene and hornblende within altered plagioclase laths. Clinopyroxenes are mostly altered to chlorite. Amphibole is formed by the breakdown of pyroxene. Sericitization of plagioclase is commonly observed.

The analytical result of the transitional peridotite(Harzburgite) is characterised by Fe_2O_3 (7%-13.7%), MgO (29% - 40.72%), Al_2O_3 (0-17.62%), TiO_2 (<0.01-1.9%), Cr (37ppm-9254ppm), Ni (30-8606ppm), Va (0-611ppm), Co (5-436ppm), Cu (<5-99ppm), Pb (2-14ppm), Zn (5-274ppm); in samples which are chromitite bearing transitional peridotites (harzburgite) show Cr_2O_3 values ranging from 31.11% to 53.53%. High values of nickel have been observed in samples collected during trenching at Gamnom which ranges from 1.07% -1.79% and in Yentem one sample yields 1.41% of nickel. 21 nos. of red soil samples were collected and the results showed Fe_2O_3 percentages ranging from 10% to 43.75% and Al_2O_3 ranging from 0.2-14.66%.

CHAPTER 2

INTRODUCTION

In the eastern extremities of Nagaland and Manipur State, chromium and other mafic-ultramafic rock hosted metal deposits, including those rich in nickel, copper, platinum-group elements (PGEs), or vanadium, are generally found in layered mafic-ultramafic igneous complexes. Mafic-ultramafic bodies belonging to the Naga-Manipur Hills ophiolite belt of rocks are exposed bearing NNE-SSW trend, they are tectonically sandwiched between the Disang flysch in the west and low grade metamorphic rocks in the east. The linear belt bearing dismembered slices of ophiolite rocks runs from Mon district in northern Nagaland and extends to the southern parts of Manipur. The aerial width of these rocks varies from 5 to 15 km in and comprises a wide variety of litho-members derived from oceanic, volcano-clastic and volcano-plutonic origins that have been subject to a wide range of deformation, subduction and exhumation. The litho-units belonging to the Naga-Manipur Hills ophiolite belt of rocks include serpentinite, peridotite (mainly harzburgite with minor lherzolite), pyroxenite, dunite, gabbro, amphibolite, basalt, spilite, basaltic andesite, trachyte, diorite, plagiogranite, tuffaceous volcanics, chert, limestone, inter-layered chert-volcanics, agglomerate tuff, greywacke, tuffaceous shale/phyllite, schist, granulite etc. In the proposed study area, the peridotite bodies are thrust over the sedimentaries (variegated shale, grey shale, slate, siltstone intercalated with sandstone) and podiform chromite has been reported in these. Several investigations have shown high contents of Cr, Ni and associated metals at Gamnom, Khangkui Khullen and Pushing.

In Ukhrul area of Manipur state, occurrences of chromitite were accounted for close to Phangrai, Shirui, Gamnom, Shingcha and Pushing villages (Ghosh et al., 1980, Vidyadharan, K. T. et al., 1985, Ramprasad, Y. et al., 1982, 1984, Gupta, K.S. et al., 1992, Theunuo, K. et al., 2015). Chromites were additionally revealed in the lower reaches of the Harbui Khayui ridge in the South and Southwest augmentation of Gamnom. Large podiform disseminated chromite; occurrences related with serpentinized harzburgite were accounted for near Gamnom (K. S. Gupta et al., 1992). In Gamnom, Ukhrul, Manipur, magnetic survey separated three sorts of anomalies, i.e. (1) high and sharp magnetic anomalies of short frequencies conceivably relating to chromite bodies and associated rocks, (2) Moderate to high magnetic anomalies indicates the ultramafic bodies and (3) Flat magnetic anomalies having minor variations relates to the presence of tertiary sediments/soil cover or change in formation (R. Kumar et al., 2016). Ramprasad, Y et al., (1982, 1984) reported enrichment of Ni (up to 9000ppm) in the soil developed over the ultramafic, near Gamnom area, although Ni sulphides mineralization was not reported.

2.1 PRESENT WORK

In pursuance of the Field Season Program of the Geological Survey of India, State Unit: Manipur-Nagaland, Dimapur for the Field Season 2019-20, reconnaissance survey for chromium, nickel and base metal mineralization was carried out in Gamnom-Yentem area, Ukhrul District of Manipur vide item No. M2AFGBM-MEP/NC/NER/SU-MAN/2019/24286. Large Scale Mapping (LSM) of 60 sq. km. area in 1:12500 scale was covered around Gamnom-Yentem, in Ukhrul district, Manipur. The mapping includes bed rock sampling along with pitting/trenching and laboratory petrology studies and analysis of samples. The Nature and Quantum of work during the field season is given in Table. 1.

2.2 OBJECTIVE

To delineate potential zones of chromium, nickel and base metal mineralization in ultramafic and mafic rocks of Gamnom-Yentem area in Manipur ophiolite belt.

2.3 PERSONNEL

The personnel involved in the project with number of field days are tabulated below:

Sl. No.	Name of personnel	Field days
1	Imomeren Ao, Senior Geologist	120
2	Vales Savio Peter, Senior Geologist	115
3	J. K. Angami, Director	8

2.4 NATURE AND QUANTUM OF WORK

The nature and quantum of work carried out during F.S 2019-20 is summarized in the table. 1.

Table. 1: Nature and Quantum of work

Nature of Work	Total Workload envisaged	Work proposed for FS 2019-20	Total Achievement (April,19 to Mar, 20)
Aerial Rec. Survey	300 sq. km	300 sq. km	300 sq.km
1. Geological Survey LSM (1:12,500)	60 sq.km	60 sq.km	60 sq.km
2. Technological survey A. Surface Exploration – Pitting and Trenching	50 cu.m	50 cu.m	50 cu.m
3. SMPL:-			
a) BRS (Groove, Channel)	150 nos.	150 nos.	150
b) PTS	50 nos.	50 nos.	50
c) PS	25 nos.	25 nos.	25
d) OM	10 nos.	10 nos.	10
e) EPMA	10 nos.	10 nos.	10
f) PCS	25 nos.	25 nos.	25
4. Chemical analyses (SMPL)	225 nos.	225 nos.	225

*Modified because Drilling and geophysical components were cancelled by competent authorities

2.5 ACKNOWLEDGEMENT

The authors acknowledge the administrative and financial support and technical guidance of Shri P. V. Ramanamurthy, Dy. Director General, State Unit: Manipur-Nagaland. The authors express sincere gratitude and thanks to Shri J. K. Angami, Director, State Unit: Manipur - Nagaland, under whose supervision the work has been successfully carried out. The ADG & HOD and Dy. Director General & RMH-II, NER, Shillong, is also gratefully acknowledged for monitoring the project. The Chemical division and Petrology division, GSI, NER, Shillong is acknowledged for providing chemical data and thin sections. The authors also acknowledge the colleagues and other office staffs of State Unit: Manipur - Nagaland, GSI Dimapur, for their support in various occasions during the work. The authors also express sincere thanks to the village head of Singcha, Khangkhui Khullen, Pushing, Changa and Yentem villages and local people in particular for their help and cooperation throughout the work.

CHAPTER 3

PROPERTY DESCRIPTION

3.1. Title of ownership: The area is under private ownership of local people.

3.2.Details of the area:

3.2.1. Name of village/district/state: The area under investigation consists of Khangkhui Khullen Village under Ukhrul District Manipur and Singcha Village, Changa village, Yentem Village and Pushing village under the newly reconstituted Kamjong district, Manipur

3.2.2. Survey of India toposheets No.: 83K/8, 83L/5

3.2.3. Geo-coordinates of the mapped block: The area is bounded by coordinates (a) $25^{\circ}03'20''$ / $94^{\circ}25'35''$, (b) $25^{\circ}03'20''$ / $94^{\circ}29'30''$, (c) $24^{\circ}58'53''$ / $94^{\circ}27'44''$, (d) $24^{\circ}58'00''$ / $94^{\circ}24'54''$, (e) $25^{\circ}00'00''$ / $94^{\circ}24'54''$. (Fig.1)

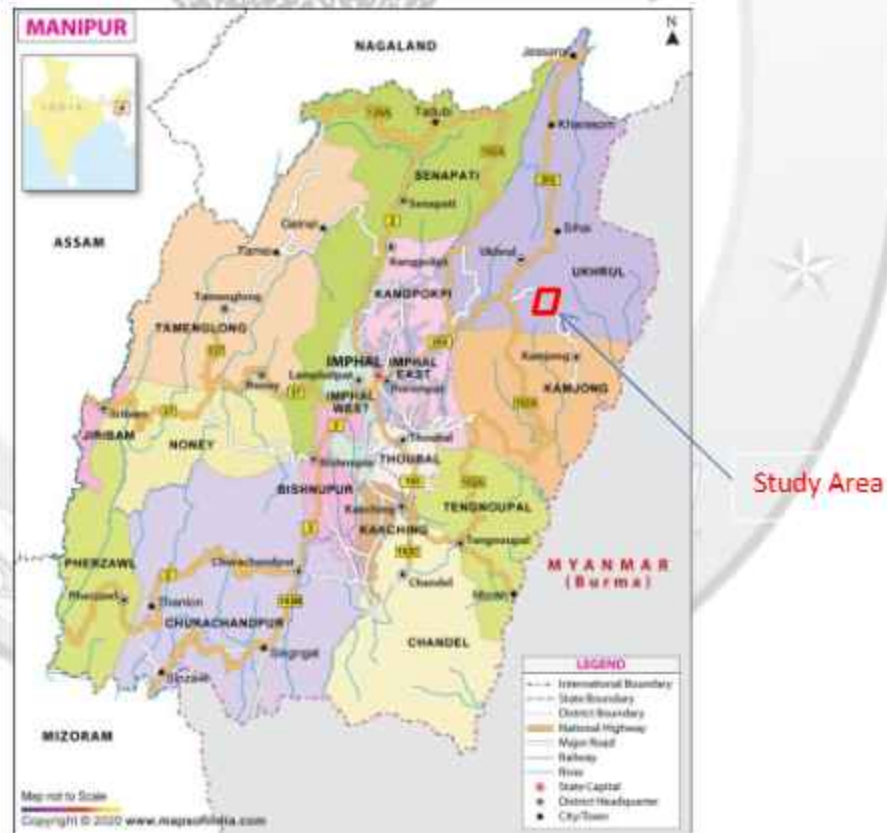


Fig.1. Location of the study area

3.2.4. Cadastral details of the area with land use: Most part of the study area is under thick vegetation cover. However at places of gentler slopes, cattle grazing and pond fish culture are practiced by the local people. The land use/land cover map is given in Fig.2.

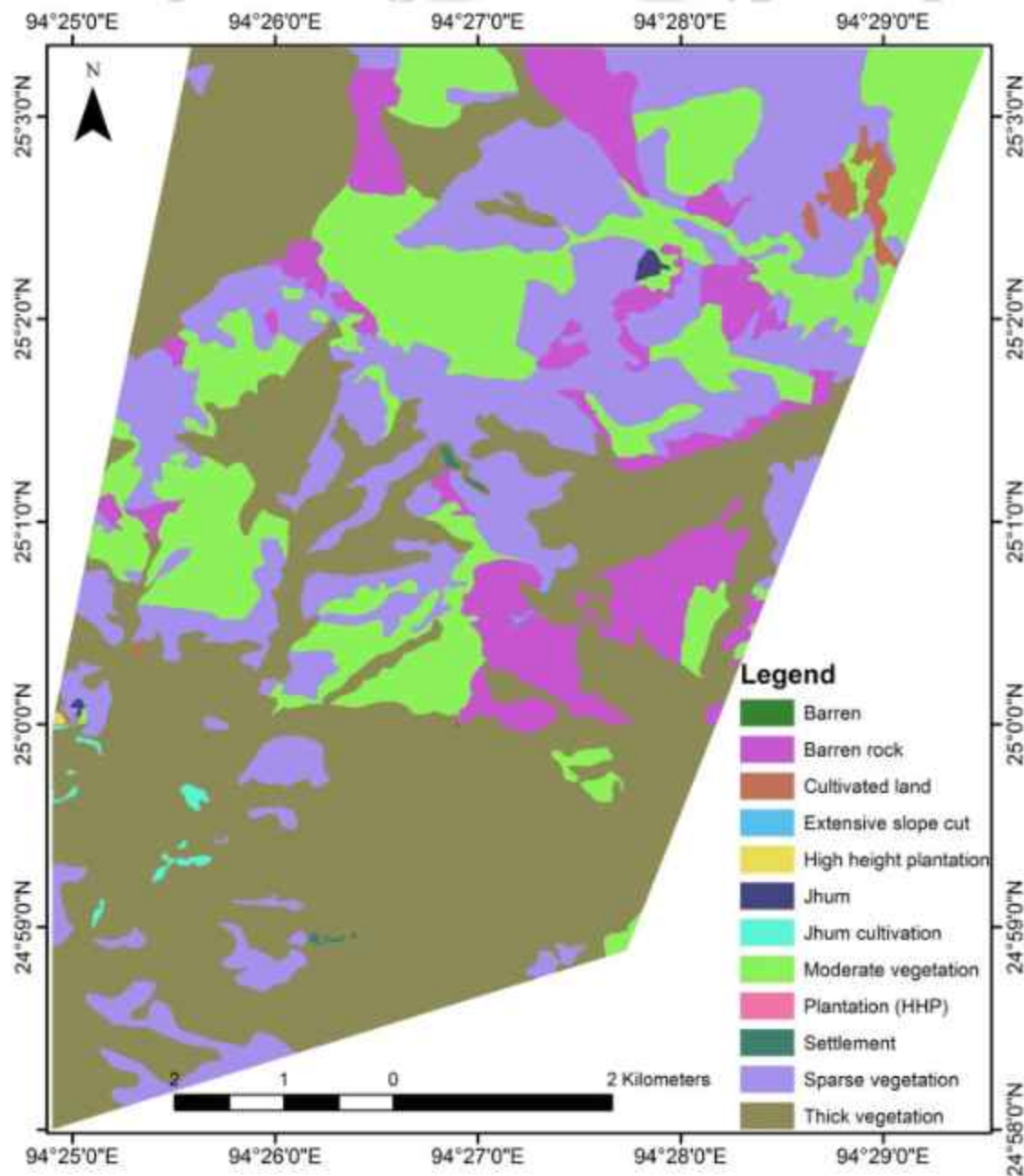


Fig.2. Land use/land cover map of parts TS 83K/8 and 83L/5 covering the study area.

(Map prepared Landslide Division, GSI, Nagaland and Manipur, Dimapur during 2017)

3.2.5. Free hold/lease hold: The land belongs to the local people and the land is not leased.

3.2.6. Location and accessibility: The study area is connected with Imphal by the Imphal-Gamnom-Kamjong state highways. Interior villages are connected with this state highway by non-metalled road. The nearest railhead is Dimapur railway station of the North East Frontier Railways (NEFR). The nearest airport to the study area is Imphal international airport.

3.2.7. Physiography

Physiographically the area is characterized by a rugged hilly terrain with N-S to NNE-SSW trending parallel ridges with deep and wide gorges. The minimum elevation in the study area is 365 m above mean sea level and the maximum elevation is 2547 m above mean sea level (Fig.3). The ridge tops of the area are usually occupied by ultramafic rocks with sparse vegetation and pine tree cover whereas the slopes and gorges are cover with dense forest with thick undergrowth which are impenetrable. Pine forests dominate in the higher elevation.

3.2.8. Drainage

There are no major rivers flowing through the study area but 1st order, 2nd order and 3rd order streams showing a dendritic pattern are present. The drainage density is high with a wide network of streams. The highest elevation of the area is 2547m above msl lying in the north western part, south of Khankui Khullen village. Comparatively gentler slopes and the low-lying valley areas along streams are usually cultivated. The drainage map of the area is shown in Fig.3.

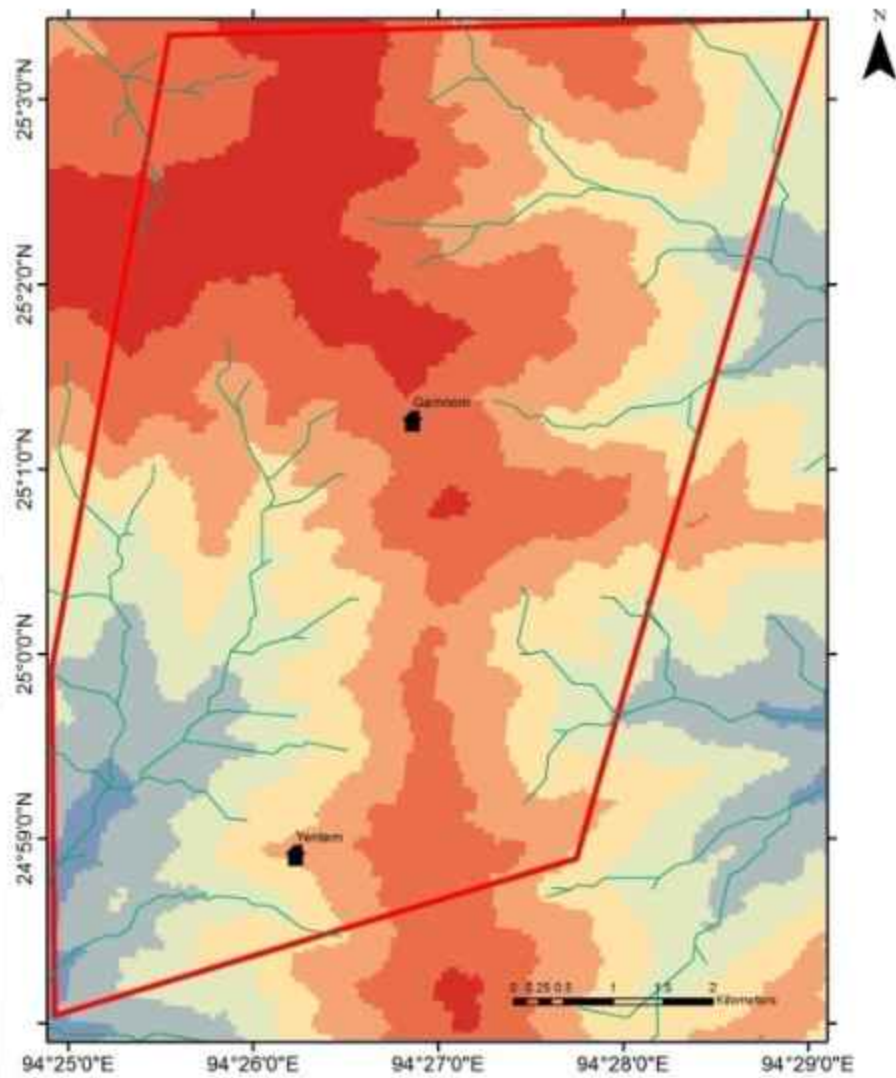


Fig.3. Drainage map superimposed on the Digital Elevation Model (DEM) map of the area prepared using ASTER DEM.

3.2.9. Climate

The region experiences tropical to sub-tropical climate and the humidity ranges from sweltering and sticky in peak summer and cold and dry in winter season. Winter begins from October and extends to February and the temperature step by step ascends from April to September. The normal minimum temperature shifts from 0° to 5° C, during winter, sometimes it dips under zero in the period of December to February. Very light snowfall and ground icing

are normal in the higher elevations during the mid-winter. The normal extreme temperature fluctuates from 25 to 30°C.

3.2.10. Rainfall

The monsoon season begins toward the end of April and the area gets substantial precipitation from southwest monsoon rains between May to September. The normal precipitation of the zone is of around 2000-2300mm per annum.

3.2.11. Flora and Fauna

The region is the home of a diverse assortment of plants and animals, some of which are found in this district and are proclaimed endangered species by the Government of Manipur. Considering the bio-variety and to guarantee persistent protection of the verdure, a large portion of the pieces of south-east Asia including Manipur and its bordering area of the Indo-Myanmar Hill Range have been proclaimed as a bio-diversity hot spot by World Wildlife Fund. Natural life populace in the region is exceptionally sparse in light of hunting and deforestations for development and logging of wood.

The area harbours a large number of plant taxa, more than 1000 species of angiosperms. Diversity of Algae, Fungi, Bryophytes, Pteridophytes and Gymnosperms are still required to explore, however, diversity of angiosperms are mostly explored. Dominant angiosperm families are Orchidaceae, Asteraceae, Poaceae, Liliaceae (*Lilium*), Ericaceae (mostly *Rhododendron*), Zingiberaceae, Leguminosae, Fagaceae (*Quercus* & *Castanopsis*). Some Endangered and endemic plants are *Lilium mackliniae* Sealy, *L. davidii* Duch., *Vaccinium lamellatum* P.F.Stevens, *Vaccinium manipurens* (Watt ex Brandis) Sleumer, *Agapetes mannii* Hemsl., *A. borii* Airy Shaw, *Rhododendron johnstoneanum* Watt ex Hutch. and so many other species of angiosperms and other plant groups which need to be explored for further documentation purpose. (S. Panda, 2013)

Shiroy Lily, an endemic Lily, is declared as the State flower of Manipur since 21-3-1989 but has unfortunately become a rare and threatened species due to intensive tourist activities which are especially organized during the blossoming period of the lily. The dumping of waste, plastic,

plucking of flowers and uprooting etc. have threatened the sustenance of the species, and therefore the State Forest Department has been taking up several projects involving local Tangkhul Nagas as volunteers with financial assistance from Forest Department to save Shiroy Lily.

Like flora, faunal diversity is also more unique, much varied and not explored completely yet. Mammals and birds are explored mostly while reptiles (recently seen Burmese subspecies of Python, *Python molurus vittatus*), amphibians, insects and other animals are less explored. The following mammals and birds are observed: Leopard (*Panthera tigris* L), Gaur (*Bos frontalis* Lamb), Wild dog (*Cuon alpinus* Dhole), Hoolock Gibbon (*Hylobates hoolock* Harlan), stump-tailed Macaque (*Macaca arctoides* Geoffroy), Slow Loris (*Nycticebus coucang* Boddaert), Golden Cat (*Catopuma temminckii* Vigors & Horsfield) and birds like Blyth's Tragopan (*Tragopan blythii* Jerdon), Mrs. Hume's Pheasant (*Syrnaticus humie* Hume *humie*), Green Pea Fowl (*Pavo muticus* L), Greater Spotted Eagle (*Aquila clanga* Pallas), Spot-billed Pelican (*Pelecanus philippensis* Gmelin), Rufous-necked Hornbill (*Aceros nipalensis* Hodgson), Eye-browed Thrush (*Turdus obscurus* L), Grey Sibia (*Heterophasia gracilis* McClelland), Tickell's Brown Hornbill (*Annorrhinus tickelli* Blyth *tickelli*). (S. Panda, 2013)

3.3. INFRASTRUCTURES AND ENVIRONMENT

3.3.1. LOCAL INFRASTRUCTURE: All the villages (Khangkhui Khullen, Singcha, Yentem, Changa and Pushing), within the present investigation are connected by unmetalled road which are motorable only during dry season. All these villages are small villages with an average of 50 partially occupied houses as the owners have relocated to areas with better infrastructure like Ukhrul town and Imphal city. Khangkhui Khullen and Changa are electrified and receive regular electricity. Singcha, Yentem and Pushing although electrified had complete blackouts for the entire period we have worked there. Mobile network and internet connectivity is very poor in the area where you get good signal only on the peaks of the hills and that too the connectivity is very weak.

3.3.2. LOCAL INHABITANTS AND CULTURE:

The major inhabitants of area belong to Tangkhul Nagas, a Sino-Tibetan and Tibeto-Burman origin. Linguistically, the Tangkhuls belong to a large language family called SinoTibetan, within that family to the sub-family Tibeto-Burman. The earliest home of the Tangkhuls was the upper reaches of Huang heo and Yangtze Rivers which lies in the Zinjiang province of China. One group moved towards east and southeast to be become known as Chinese, another group moved southward to become the tribes of Tibeto-Burman which includes the Tangkhuls and other Naga sub tribes. That was between about 10,000 B.C. to 8000 B.C. Thus, the Tangkhuls as also other Naga tribes have travelled from China to Myanmar and from there finally they came into their present land (Manipur) traversing through innumerable snow covered landscapes, mountains and wild forests confronting wild beasts and wild tribes. The Tangkhuls came together with the Maos, Poumeis, Marams and Thangals because all of them have references to their dispersal from Makhel, a Mao village in Senapati district. They had also erected megaliths at Makhel in memory of their having dispersed from there to various directions. (S. Panda, 2013)

CHAPTER 4

PREVIOUS EXPLORATION

4.1. DETAILS OF PREVIOUS EXPLORATION/INVESTIGATION CARRIED OUT BY OTHER AGENCIES/ PARTIES

The first geological survey of the ultramafic belt in Manipur-Nagaland belt was carried out by Oldham (1883) in course of endeavor to Manipur Naga slopes; he gave a wide picture of geology of Manipur. Later on Pascoe (1912) gave a classical account of the different mafic and ultramafic suites, after which then termed the lithounits as ophiolite, amid his traverse to Saramati peak. There after again Pascoe, (1950) detailed intrusive event of serpentinite along the contacts of Disang and Makware beds of Burma (with more prominent degree of metamorphism, foliation and intense textures) and estimated a plausible Upper Cretaceous age for the serpentinite intrusion.

From the late 1950's Geological Survey of India have carried out mineral investigation and systematic geographical mapping programs in several parts of Manipur. Preliminary studies for copper and nickel mineralization around Nungou, Ningthi, Konkan-Thana were carried out by Chakraborty et al., (1958). Copper-Nickel mineralisation is hosted within the suite of altered basic and ultrabasic rocks. The mineralized vein varies in width from 2 inches to 1 ft and has been exposed for a strike coherence of almost 4'-5' and found to proceed along plunge for around 5 ft. The most mineralized zone show regional trends of S20°E/N20°W direction near the base and swivelling to N10°E/S10°W. Copper sulphide and ferrous/ferric sulphides are found as fracture intrusions. The sulphide mineralization is controlled by large N/S trending joints in spite of the fact that the individual pockets or lenses within the mineralized zone are orchestrated in an en-echelon design. Tests of mineralized rocks analysed 3.55% Cu and 0.07% Ni.

Prasad and Sharma (1977) amid their integrated survey including systematic geological mapping for the appraisal of Nickel mineralization in soil along the Sangsai-Gamnon road and systematic collection of integrated samples in select regions of ultramafic belt close to Gamnom, Manipur East Dist., Manipur has established few chromitite pockets. Analytical results revealed that Nickel value ranging from 120 to 8500 ppm, and Co from 120 to 760 ppm from 126 nos. of soil tests.

Sharma, et al., (1982, 1984) carried out integrated survey for Nickel and related metal within the region around Gamnom region, Manipur. Chromite stash of 10m x 2.5 m was detailed within the hill top, northwest of Gamnom. Geochemical data of serpentinised peridotite shown Nickel content within the range of 0.6-1.2% and revealed relatively high values of Nickel (up to 9000ppm) within the soil developed over the ultramafic. In spite of this fact that, no sulfide bearing zone could be found in this range. The thickness of the soil ranges from 0.5m to 4m as observed in auger borehole drilling. They reported that the A horizon is generally brown to grayish and is upto 0.5 m and the B horizon upto 2.5m is characteristically brown to deep brown and destitute of any ferruginous concretion, clayey in nature whereas the C horizon is developed over pulverized serpentinite.

Geological mapping in parts of Ukhrul area Ophiolite Belt was carried out by Vidyadharan et al (1984) and he further separated sedimentary rocks occurring on both sides of the ophiolite belts and assigned the sedimentary unit occurring within the western part of ophiolite as "wild flysh" and sediments towards east of the ophiolite belt as epimetamorphic sediments identical to Nimi Formation of Nagaland. Within the course of mapping they have found a number of pockets of limestones in both the sedimentary unit east as west of the ophiolites. Chromite lenses, streaks and dissemination inside olivine and orthopyroxene bearing peridotite were detailed.

Upon request from the Directorate of Commerce and Businesses, Manipur for investigation of chromitite occurrences within the lower reaches of Harbui Khayui hill in the south and southwest extension of Gamnom, GSI has conducted detailed geophysical survey in Hangkau area and Phangrai area, Ukhrul district, Manipur amid FS: 1988-89 and FS: 1991-92 respectively. Das et al., (1989) detailed pod/pocket of chromite uncovered from the serpentinised harzburgites. These pods/pockets are of measurement 10mX4m, profoundly elongate and occur generally close or at the contact with coarse grained harzburgite around Hangkau area, Ukhrul dist., Manipur. The investigation of chromitite yielded Fe (10.30-9.05%), Cr (30.30-24.60%), Ni (0.12-0.12%) and Mn (upto 0.14%). Bed rock sampling of harzburgite and sheared harzburgite indicated Cr (0.10- 0.16%, average 0.13) and Ni (0.12-0.54%, average 0.32).

Venkataramana et al., (1989) concluded that from the order of magnitudes of magnetic and resistivity values, the anomalies can be inferable to the sources at shallow depth. Further, N. Venkataramana et al (1993) have concluded that a gravity rise of around 0.1-0.15 mgal was

noticed over zones encompassing harzburgites having hob-nail texture. Shallow depth persistence of 5-7 m was evaluated for anomalous zones containing known chromite mineralization. Most of the known chromitite events are found to occur inside magnetic high zones differentiated on the premise of magnetic properties of soil, rocks and chromite. The minimum is confined to the ultramafics consisting of serpentinites, dunite and harzburgites. They concluded that chromitite of Phangrai region are generally massive and uneven type and is of metallurgical and refractory grade.

Gupta et al., (1991, 1992) detailed events of massive chromitite related with serpentinized harzburgites as podiform lenses and boulders, nodular chromitite with nodules extending from few millimetres to 0.5cm, which laterally grade to massive type and dispersed chromitite ore in affiliation with magnetite. These chromitites were detailed around Phangrai slope, Siruhi furor, between Siruhi-Lungha road related with serpentinized harzburgite. Limited analysis of pit/trench samples indicate maximum value of Cr₂O₃ (53.29%), Fe₂O₃ (14.77%), Al₂O₃ (16.19%), MgO (18.24%) and Ni (0.23%) from 29 nos. of samples. They reported that the chromite falls under grade-I and II categories.

Yanthan, et al. during FS 2009-10 & 2010-12 for investigation for Platinum group of element in ophiolite belt of Manipur, although encouraging PGE values were not detailed, they have detailed metallurgical grade chromitite and high values of Nickel (up to 7910ppm) and Chromium (upto 2852ppm) in Manipur ophiolite. The contents of Platinum (2.5-20ppb), Palladium (2.5-5ppb), Iridium (5-330ppb), Ruthenium (35-840ppb) and Rhodium (5-35ppb) were detailed in chromitite. The peridotites have lower concentration of PGE as compared to chromitites (Pt=2.5-30ppb; Pd=2.5-55ppb; Ir=1.5-15ppb; Ru=1.5-35ppb; Rh=1.5-10ppb).

Theunuo, et al., (2015) documented that the ophiolite sequences are influenced by prominent high angle northeast-southwest anatomizing fault framework which not only controls the outcrop pattern but also exhibits repetitions of members of ophiolite sequence including oceanic pelagic sediment. The faulted contacts are characterized by abundant silicification, brecciation and gouges. The transitional peridotite of ultramafic ophiolite is additionally traversed by several N-S shear zones. They have detailed the biggest clusters of podiform chromitite from Gamnom area, with a measurement of almost 100x50m. The massive chromitite body occurs as pods and lenses inside coarse grained harzburgite. Events of chromitite pods were also detailed from Nungbi, Phangrai-Shirui, Gamnon, Pushing and East of Apong town. The

examination of bed rock sample of peridotite demonstrated Nickel(1988-3996 ppm) and Chromium (1086-4772ppm).Occurrences of chromite have been reported from the adjoining areas of Gamnom, Shingcha and Harbui Khayui hill ranges in Khangkhui hamlet, Ukhrul, Manipur. GSI has located clusters of chromitite pods towards SE of Gamnom, and subsequently, the Directorate of Commerce and Industries; Govt. of Manipur has further assessed these resources in detail. In Manipur ophiolite, chromitite occurrences are associated with ultramafics as nodular and podiform bodies while few occur as massive bodies.

In view of the favourable and encouraging result of Chromium, Nickel and associated base metal mineralization reported by the earlier workers in the adjacent block and other part of ophiolite of Nagaland and Manipur, the present reconnaissance survey work was carried out.

4.2. DETAILS OF AERO-GEOPHYSICAL AND GEOPHYSICAL MAPPING

The present study area around Gamnom was surveyed by magnetic methods (Kumar et al., 2016). They have reported overall magnetic variation of 2912 nT (46003 to 48915 nT) (Fig. 4). On the premise of qualitative analysis of the Magnetic (T.F.) outline, and magnetic profiles, three sorts of magnetic anomalies were distinguished within the study area by them; i.e. high and sharp magnetic anomalies of short wavelengths, moderate to high magnetic anomalies of varying wavelengths and flat magnetic profiles. The noteworthy sharp high magnetic anomalies of brief wavelengths, bipolar in nature having variations from 450 nT to 2900 nT, were traced at few places within the study area. They reported that these high and sharp magnetic anomalies of short wavelengths conceivably correspond to chromite bodies and related rocks and the sharp gradient of the magnetic anomaly show the shallow nature of the source rock. Further they stated moderate to high magnetic anomalies wide in nature, of the order of 1000 nT may represent the ultramafics bodies whereas flat magnetic profiles having very small variations may reveal the presence of tertiary sediments/soil cover or change in formation. According to them these classification of magnetic anomalies has significantly contributed in distinguishing different geological formations and locating possible zones of chromite mineralization.

Their magnetic Reduced to Pole (RTP) map has shown that prominent high and low zones within the ultramafics where the prominent magnetic highs are reflected as zones of highly

serpentinized ultramafic rocks while magnetic lows correspond to harzburgites under soil cover with less deformation. Their studies revealed that shallower interface corresponds to the average depth of smaller magnetic bodies at 53 m, while deeper interface represents the average depth of basement at 100 m in the study area. They estimated average depths to the top of the causative bodies producing the magnetic anomalies vary from 18 m to 46 m and having average width of the bodies are varying from 70 m to 109 m and dip lying between 07° and 75° . They suggested that nature of magnetic anomalies indicates the possibility of small sized and discontinuous chromite bodies in the study area.



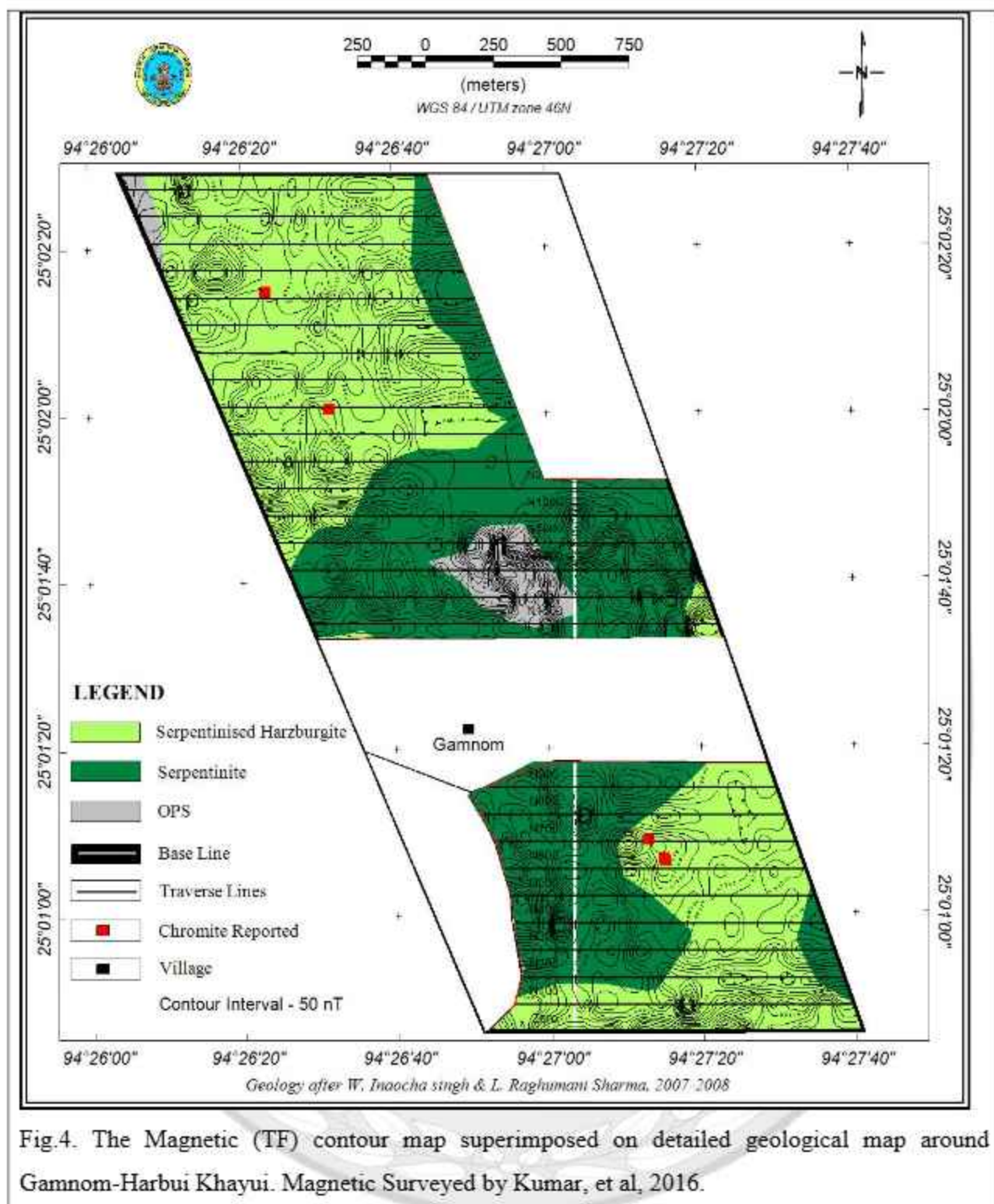


Fig.4. The Magnetic (TF) contour map superimposed on detailed geological map around Gamnom-Harbui Khayui. Magnetic Surveyed by Kumar, et al, 2016.

CHAPTER 5

GEOSCIENCE INVESTIGATION

5.1. REGIONAL GEOLOGY

5.1.1. Aerial reconnaissance

There is no earlier report available on aerial photographs. Aerial reconnaissance using ASTER imagery was tried but due to the thick vegetative foliage and dense forests covering the study area it was not possible to generate any distinguishable geological features nor could any geographical features be identified prominently. The lineament could not be delineated from the Google earth satellite imagery on the scale of the present mapping as the resolution of Google earth imagery is not that high and the thick vegetation proved to be a hindrance. (Fig.5)

5.1.2. Brief regional geology

5.1.2. A. Ophiolite zone

Ophiolite zone is linearly aligned in north-south direction from Nagaland in the north and nearly parallel to the eastern margin in the southern part of the Manipur. This belt extends to southwest of Moreh. It occurs as a series of lensoid bodies of ophiolite rocks of variable dimensions. The bodies are steeply dipping and striking in NNE-SSW directions. They occur as fault-contacted slices within pelagic shale-sandstone association. The ophiolites and enclosing sedimentary rocks have been thrust over by metamorphics in the northeastern part, which comprise quartzite, phyllite and marble. The thrust contact is characterised by intense fracturing, brecciation, mylonitisation and silicification (Venkataramana, 1985). Ophiolite zone contains a group of oceanic pelagic rocks which occur mainly in the east and include chert, thin limestone, quartzite and phyllite. The rocks exhibit feeble metamorphic characters but occurrences of radiolaria and diatoms in the cherts bear a positive indication of their origin in deep oceanic sector. Vidhyadharan et al., (1984) have correlated this epimetamorphic rock group, especially occurring in northeastern part of Manipur, to the Nimi Formation of Nagaland. The major litho units of the ophiolite suite are described below starting from the bottom most to the top most:

5.1.2. A.i. Transitional peridotite

Theunuo et al (2015), have stated that transitional peridotite consists mainly of harzburgite with minor lherzolite occurs as detached blocks and lenses which are sometimes strongly deformed and serpentinized and the degree of serpentinization ranges from 60 – 90 vol%. They have observed notable pervasive shear foliation marked by serpentine that has been developed throughout the bodies of the transitional peridotite which tends to overpower the original igneous texture. They observed that the original lithounits in the shear zone could be discernible only in shear lenses and extensive soil and forest cover impeded in delineation of larger individual bodies.

Chromitite pods of varying dimensions were reported by Theunuo et al. (2015) to occur within transitional peridotite unit as minor lithounits. They stated that the chromitites were dark grey to black, massive, hard and resistant unit with high specific gravity and occurs as pods and lenses of varying dimensions (1m X 2m upto 70 m X 40 m), as massive podiform type or as stringers and disseminated type. The notable observation was that these pods of chromitite bodies were mainly associated with harzburgite of the transitional peridotite.

5.1.2. A.ii. Cumulate

Theunuo et al (2015) have observed that the layered mafic-ultramafic cumulate consists of peridotite and gabbro as major unit and occurs mostly at the hill top and/or higher topographic level invariably overlying the transitional peridotite unit. Cumulate rocks are medium to very coarse grained, melanocratic, hard and massive, which exhibit crude layering. Harzburgite is the predominant cumulate peridotite mostly occurring as bouldery outcrop. Lherzolite variety is rare and the isolated bouldery out crop is dark green to black in colour and are hard, massive, and compact and the relict prism of orthopyroxene grains are sparsely distributed in dark crystalline serpentine matrix and characterized by conchoidal fractures. Dunite is mostly altered to serpentinite and often eroded showing light dull matty green color and occurring as minor patches and lenticular bodies; sometimes they host pods and lenses of chromite or as disseminated euhedral specks of chromite. Cumulate gabbros are mesocratic medium to coarse grained, massive and hard composing of feldspar along with pyroxene minerals. Crude layering

is observed at the outcrop, sometimes they occur as intrusives within the lowermost transitional peridotite unit.

5.1.2. A.iii. Gabbro

Theunuo et al (2015) observed that the isotropic gabbro dykes are characterized by green pyroxene and dirty white feldspar minerals which can be seen in hand specimen. Gabbro body of 2 m width and about 30 m length were intruded in ocean pelagic sediments.

5.1.2. A.iv. Volcanics

In the regional observations made by Theunuo et al (2015), volcanic rocks are represented by a) vesicular flow basalt b) pillow basalt and c) volcanic agglomerate. These rocks occur at north of Phangrai interleaved with chert and cherty limestone. However, smaller outcrops without any extension were observed at Ningthi and north-west of Phangrai (30 m X 20 m). Vesicular/amygdular basalts are characterized by vug-filled amygdules of zeolites and calcite, showing spheroidal weathering. Pillow basalts were observed to be characterized by stackings of round to elliptical pillows of various sizes (8-85 cm in diameter). In many sections pillows are marked with chilled margin, radial cracks and highly altered spilitic groundmass as matrix. According to them agglomerate units consists of angular to sub-rounded volcanic clasts of different sizes ranging from 4 to 50 cm. Larger clasts have vesicles and amygdules filled by secondary quartz, calcite and zeolites, the sub-rounded clasts could be identified as lapillis and bombs and exhibit a typical weathering pattern with dark reddish grey to maroon soil color.

5.1.2. A.v. Ocean Pelagic Sediments:

The ocean pelagic sediments non-conformably occur over mafic-ultramafic sequence of ophiolite and consist of slaty-shale and phyllite, chert bands and minor meta-arenite and graywackes. Lensoidal outcrop of serpentinised peridotite and volcanics were also observed within the phyllites which are the predominant argillaceous rock of ocean pelagic sediment unit and are dark to greenish grey in colour and thinly foliated with moderate to steep dip. Variegated cryptocrystalline radiolarian chert occurs as isolated bodies in different lithounits. Grey chert interbedded with khaki green shale is also observed at north-east of Nungbi that sometimes occurring olistostrome. Sandstones with mudclasts are poorly sorted and dirty brown in color

occurs as lenticular bodies of varying sizes. No primary sedimentary structures are usually preserved in the rock.

5.1.2. A.vi. Olistostrome

According to earlier workers the major olistostrome unit occurs between Disang Group of rocks and ophiolite and non-conformably overlies the mafic-ultramafic sequence of ophiolite along the eastern and southern margin of ophiolite and oceanic pelagic sediments. They are characterized by chaotic distribution of olistoliths such as limestone, quartzite, chert, cherty limestone, silicified carbonate rocks, serpentinised ultramafics and gabbros, within an argillaceous matrix. Sometimes deformed chert bodies are observed within the olistostromal unit as exotic blocks without any structural relation with the surrounding carbonaceous shale.

5.1.2. B. Disang group

The Disang rocks are essentially monotonous alteration of argillaceous and arenaceous facies. The arenaceous material gradually increases from the bottom towards the top. They are mainly composed of dark gray splintery and somewhere slaty with numerous thin rainifying quartz veins. Few serpentinised intrusions are also marked here and there. Shales are dark-gray in colour, friable with fine laminations and show gradual decrease towards the top where sandstones predominate. Concentric flankings and curved faces are also seen in some of the shale surfaces.

5.1.2. C. Barail group

5.1.2. C.i. Laisong Formation

The oldest Formation, Laisong Formation is represented by grey coloured medium to fine grained, hard, micaceous sandstones with frequent intercalations of dark grey sandy shale and slate. The thickness of individual sandstone beds varies from 30cm to 2.5 m in the area. Dark grey siltstones at the base of the Laisong Formation have yielded a rich assemblage of invertebrate fossils. Fragmentary plant remains and ichnofossils are quite common. Evidently, shallow marine conditions of deposition are suggested for the Laisong Formation. (Ranga Rao, 1983).

5.1.2. C.ii. Jenam Formation

Jenam Formation gradationally overlies Laisong Formation. Evans (1932) described that the Jenam beds in the Schuppen Belt are argillaceous in the lower part and arenaceous in the upper part and forms a transitional zone with the overlying Renji Stage. This Formation is represented by a predominantly argillaceous sequence of dark grey siltstones, shales, thin sandstone bands, carbonaceous bands, and a number of coal seams. Sedimentary structures in siltstones include small scale cross laminations and parallel bedding shales contain molluscs and carbonised plant matter at places.

5.1.2. C.ii. Renji Formation

The top of Barail Group in Schuppen Belt is designated as Renji Formation which has a great thickness of ferruginous sandstone and gradationally overlies jenam Formation. Due to changes in depositional environment and unconformable overlap of Surma rocks, the thickness of Renji rocks varies widely in the different tectonic slices of Schuppen Belt. Evans (1932) described this unit as "a great thickness of hard, ferruginous, usually massive sandstones occurring above the soft Jenam beds". It is made up of very thick multistoried sandstone units with a number of grit beds (2000 metres).

5.1.2. D. Surma group

5.1.2. D.i. Bhuban Formation

The rock types comprise arenaceous units of Lower Bhuban, argillaceous facies of Middle Bhuban and coarse grained sandstone of Upper Bhuban. Interbands of gray bluish clay and clay partings are conspicuous of the group which distinguishes it from the underlying Barail Group and overlying Tipam Group. At places Surma sedimentation commenced with the deposition of Middle Bhuban Formation and is followed by Upper Bhuban and Bokabil Formations. Surma Group shows a distinctive pattern of progressive transgression of Surma Sea in the Naga Hills Schuppen Belt, Prasad and Sarma (1981)

5.1.2. D.ii. Bokabil Formation

Bokabil Formation, the topmost unit of Surma Group, displays characteristic lithological attributes, with alternation of ripple drift, cross laminated sandstone and shales (200 metres). The unit has a predominantly argillaceous lithology dominated by khaki coloured, finely cross

laminated siltstones, sandstones with thin sandstone lenses. A fine alternation of laminated sandstones and shales is the distinguishing feature of the Bokabil Formation (Yedekar and Ray, 1984). Bokabil Formation is dominantly argillaceous consisting of finely cross laminated, wavy laminated and occasionally flaggy siltstone with alternating parallel laminated fine to medium grained sandstones.

5.1.2. E. Tipam group

Tipam Group is developed in Schuppen Belt and Assam Shelf. In Schuppen Belt it is having a thickness of 1800-2200 metres in Zubza area and consists of the Tipam Sandstone and Girujan Clay Formation.

5.1.2. E.i. Tipam Sandstone Formation

Tipam Sandstone Formation overlies Surma Group with gradational contact indicating that Tipam-Surma contact may be a facies boundary and time transgressive. It is subdivided into the lower Tipam Sandstone Formation and the upper Girujan Clay Formation. Tipam Sandstone Formation, exhibits very little variation in lithological characters, and comprises thickly bedded bluish grey to light grey ferruginous sandstones with thin interbands of siltstones and shales, which become light brown on weathering. Fairly coarse current bedded sandstones and megacross beddings make up the bulk of this rock. Evans (1932) recorded that in outcrops of Tipam Group southwest of Naga Hills the clay beds within Tipam Sandstone are generally rare and appear to be lenticular. Tipam Sandstone in Naga Hills has yielded some bivalve fossils only, which are not age specific. The microflora suggests a Middle- Upper Miocene age. Multistoreyed sandstone is common with streaks of lignitised material, petrified logs of wood and clay pellets.

5.1.2. E.ii. Girujan Clay Formation

Girujan Clays rests over Tipam Sandstone Formation gradationally and comprises argillaceous sequence of reddish, buff, grey mottled clays, sandy clays and channel sandstones. Chakradhar and Gaur (1985) reported escape traces of worm burrows. Joshi and Yedekar, 1983 reported the best exposure of Girujan Clays in Schuppen Belt is seen in Merapani-Wokha road section around Baghty where mottled clay-channel sandstone association bears the distinct environmental signature of flood plain deposits with network of meandering stream channels. Petrographic studies reveal that quartz is the dominant mineral with a few plagioclase and rock

fragments. Quartz grains are subrounded to subangular, moderately sorted and with fewer matrixes (Prasad, 1981). The heavies show a high proportion of opaques and less epidote than found in Tipam Sandstone (Jena and Devdas, 1984).

5.1.2. F. Namsang Formation

The youngest Neogene sequence of Schuppen Belt is Namsang Formation. It is well exposed in Lakhuni and Changki Tectonic blocks, where locally it attains a thickness of 600 metres (Yedekar and Ray, 1984). It overlies Girujan Clays with an erosional unconformity, marked by thick beds of conglomerate with subrounded clasts of sandstone and channel grits. Namsang Beds are poorly consolidated and consists of mottled clays, sandstones, conglomerates, grits and some lenticular lignite variety of coal. Pebbles are mainly of Barail and Surma Sandstone, siltstone, and clay (Prasad, 1981 & Devdas and Gandhi, 1985). Pebble length varies from a few cm to 20 cms.

5.1.2. G. Dihing Formation

Dihing Formation unconformably overlies the Namsang Formation and Girujan Clays (Chakradhar and Gaur, 1985) which comprises of Pebble beds. It comprises thick beds of gravel with subordinate clay and has a thickness of 150 to 250 metres. The gravel beds exhibit poor sorting. Nature and attitude of beds are in conformity with the regional trend and help in differentiating this formation from the overlying Quaternary gravels which shares angular unconformity. Dihing Formation from Tuli area was described by Sarma and Bhartiya (1978). Boulders are uncommon. Pebbles are derived from older formations and cementing material is a mixture of silica and clay.

5.1.2. H. Alluvium

The majority of the Quaternary deposits in the state are located in Imphal valley, covering an area of about 2250 sq km. The older units viz., Motbung and Kangla-Tongbi surface are best developed in northern and western periphery of the valley. They abut against Tertiary hills having distinct fan characters. Sekmai surface is a flat to gently sloping alluvial terrain bearing both escarpments and overlapping relation with Kangla-Tongbi and Lamsang surfaces. Lamsang surface shows relict flood plain features like levees and back-swamps. Lilong surface is

lacustrine fluvial in nature and comprises the present day natural levees of Imphal, Iril, Thoubal and other tributaries. Evidences of neotectonism have been recorded in the northern part of the Imphal valley, and can be traced along the Limakong River, a tributary of the Imphal River. The river sections expose a sequence of folded and tilted peat beds of probable Pleistocene age overlain by a blanket of undisturbed Upper Pleistocene and Holocene fluvial sediments.

5.1.3. Regional Stratigraphy

Table.2: Generalized stratigraphic succession of Manipur

(After GSI, Misc. Publ.30, part IV, vol. - I (part-2), 2012)

Age	Group	Formation	Member	Lithology
Recent and Pleistocene		Alluvium		Alluvium and Terrace deposit
-----Unconformity-----				
Plio-Pleistocene		Dihing		Conglomerate, grits, sandstone and clay beds
-----Unconformity-----				
Pliocene		Namsang		Thick beds of grits and conglomerates with occasional sandstone and claystone
-----Unconformity-----				
Miocene	Tipam	Girujan clay		Clay, mottled sandy clay, mudstone with subordinate ferruginous sandstone
		Tipam sandstone		Thickly bedded, medium to coarse ferruginous sandstones with interbands of siltstones and clay
Miocene	Surma	Bokabil		Shale siltstone alteration with minor sandstone
		Bhuban		
-----Disconformable boundary-----				
Oligocene	Barail	Renji		Coarse, gritty, massive and well bedded sandstone with current bedding and ripple marks, with plant remains and coal streaks and conglomerate
		Jenam		
		Laisong		
-----Unconformity-----				
Middle to Upper Eocene	Disang	Upper Disang		Shale, Siltstone, Greywacke with rhythmite, minor sandstone bands with fossils and slices of ophiolite
Upper Cretaceous to Lr. Eocene		Lower Disang		Shale, Greywacke with rhythmite, minor sandstone bands, Slate and phyllite
-----Tectonic / Unconformity-----				
Cretaceous to Lr. Eocene	Ophiolite Belt	Lushat Formation		Shale and siltstone with interbands of radiolarian chert and limestone
		Ophiolite (Igneous)		Dismembered tectonic slices of serpentinites, cumulates and volcanic

5.2. DETAILED GEOLOGICAL EXPLORATION

5.2.1. Outcrop map on 1:12,500 scale

The outcrop map on 1:12,500 scale is provided as Plate-I.

5.2.2. Large scale mapping on 1:12,500 scale

Large scale mapping covering an area of 60 sq km on 1:12500 scale was carried out around Gamnom, Singcha, Yentem, Pushing, Changa and Khangkui Khullen villages.

The rock types of the study area include (i) Transitional Peridotite (Harzburgite), (ii) Gabbro, and (iii) Olistoliths.

The Ophiolite occurs as dismembered tectonic slices and the sequences are affected by prominent high angle NE-SW thrust system manifested by repetitions of members of transitional peridotite, Gabbro and olistolith. The contacts between different lithologies are mostly concealed under thick vegetation and scree and are mostly inferred. The thrusts are discerned only by the break in stratigraphical order and by repetition of units. There is no surface indication of these thrusts which are generally concealed by the thick vegetative foliage. Due to complex nature of deformation and alteration, the ophiolites are highly dismembered. However, volcanic rocks and pelagic sediments associated with peridotite/ultramafics are considered as the topmost litho-member of the Ophiolite sequence; this criteria has been used to delineate and differentiate various tectonic slices. The various lithounits show a preferred N-S orientation with the general strike of the thrust. Lithostratigraphic succession of the study area is given in Table 3.

Table 3: Lithostratigraphy of the study area

Group	Member	Lithology	Description
-	-	Olistoliths	Chaotic mixture of units such as chert and serpentized ultramafics within an argillaceous to arenaceous matrix.
-----Nonconformity-----			
Ophiolite Suite	Mafic cumulates	Gabbro	Dark grey, Plutonic, large crystals of pyroxenes visible.
	Transitional Peridotites	Harzburgite	Green to dark grey, crystals of pyroxenes visible clearly visible. This unit is the host rock for podiform chromite.
Base not exposed			

5.2.3. Description of rock types

The study area exposes predominantly the Ophiolite suite comprising the dismembered 1) transitional peridotite, 2) mafic cumulates consisting of gabbro and 3) olistoliths. The complete ideal ophiolite sequence is not preserved in this study area and only two member units of the ophiolite sequence are present here which are repeatedly thrust over each other along with a unconformable olistolithic unit (Plate-I).

5.2.3.1. Ophiolite suite

The major lithounits includes: i) Transitional Peridotite and ii) Mafic cumulate sequence (gabbro). The contact between the ophiolite suite and the Olistoliths is unconformable trending NE-SW direction. The dismembered ophiolite slices are lensoidal, curvilinear, cusped-lobate shape and their disposition are the product of multi-episodes of thrusting. The transitional peridotites are partially serpentised and often exhibit well developed cumulate texture. Typical hobnail textures are common weathering features as ortho-pyroxene protrudes as resistant mineral over the groundmass. Sporadic occurrences of gabbro cumulate show bouldery outcrop and are noted in Gamnom and northwest of Pushing.

5.2.3.1.a. Transitional peridotite

The occurrences of transitional peridotite are generally blocky and discontinuous and blocks (Fig.5) are sometimes embedded within a strongly deformed and serpentized matrix (Fig.6). At places, thick limonitic soil developed over the peridotite. Only the Harzburgite variation of the transitional peridotite is observed in the study area which is confirmed by thin section studies and detection of neoblastic olivine and corroded chrome spinel.

5.2.3.1.a.i. Harzburgite

In field, the harzburgites show cumulate texture which upon weathering produces hobnail texture. It is difficult to identify the nomenclature of these rocks directly in field (thin section studies is a must) based on individual grains but some mineral grains like bronzite (ortho-pyroxene) can be easily picked up due to its bronze color. (Fig.7) The rock as a whole is light to dark green in colour. The harzburgite unit here represents the fertile part of the transitional zone of the mantle. This unit has undergone serpentinisation to a varying degree and show an olive green colour with amorphous groundmass with shiny prism of pyroxene attributed for hobnail structure upon weathering. Serpentine and talc is developed along the fracture planes due to shearing and are characterized by presence of fibrous or bladed variety of serpentines giving a scaly appearance to the rock with slickensides in all possible orientation which in turn results in total deformation of the primary igneous texture.

Chromitite

During the course of mapping isolated chromitite pods occur within host rock of transitional peridotite (harzburgite) in Gamnom, west of Gamnom, south of Khankui Khullen and northwest of Pushing village (Fig.8). Clusters of chromitite pods have been delineated and plotted on the map (Plate-I). They are black to dark grey in colour elliptical in nature and their size varies from 0.25m to 2m in diameter. These chromitite pods have no evident structural or geological control and relationship and occur as sporadic pods within the transitional peridotite (harzburgite).

5.2.3.2. Mafic Cumulate

Gabbro

Only gabbro belonging to the mafic cumulates is exposed in the area. Two discontinuous lenses of gabbro are exposed one at Gamnom about 100m x 150m in dimension and another west of

Pushing 80mx 120m in dimension. They occur as oval-shaped bodies showing concordant relationship with the transitional peridotite directly overlying it and the nature of this contact appears to be gradational with the cumulate peridotites omitted as per the ideal ophiolitic sequence. Hand specimens are marked by appearance of feldspar along with pyroxene minerals and are light grey to dark grey in colour depending upon the degree of weathering. They occur as thin slivers which die out after a short distance either gradationally into the transitional peridotite. Mild pervasive shear foliation is observed (Fig. 9).

5.2.3.3. Olistolith

Olistolithic unit occurs mainly as an unconformable layer lying over the ophiolite suite of rocks and is observed in the study area as repetitive units due to multiple thrusts (Fig. 10). The olistolith observed juxtaposed with ophiolite suite contain solely sedimentary olistoliths viz. sandstones bearing few limestone clasts/chert (Fig.11) of varying dimensions ranging from 1cm to 20cm. The association of olistoliths in these olistolithic units indicate the origin or development prior to emplacement of ophiolite suite (wherein only sedimentary units that was available on the prevailing continental margin to the east of the basin). The continued subduction during the Eocene Period would have destabilized the continental margin slope causing submarine mass movements which have given rise to these olistolithic units. Field observation indicates that these olistolithic units are of tectono-sedimentary origin.



Fig.5. Field photograph showing harzburgite of transitional peridotite northeast of Gamnom (25°01'40.9" / 94°26'52.1")

Fig.6. Field photograph showing serpentized harzburgite of transitional peridotite northwest of Pushing (25°03'09.1" / 94°28'10.1")





Fig.7. Field photograph showing hob-nail texture on the surface of Harzburgite of transitional peridotite at Gamnom ($25^{\circ}00'41.1''$ / $94^{\circ}27'10.1''$)



Fig.8. Field photograph showing chromitite pods south of Khankui-khullen. ($25^{\circ}00'47.9''$ / $94^{\circ}25'47.9''$)



Fig.9. Field photograph showing mafic cumulate body of gabbro at Gamnom (25°01'28" / 94°27'8")



Fig. 10. Field photograph showing exposure of argillaceous unit in olistoliths northwest of Pushing (25°02'40.8" / 94°28'45.6")



Fig.11. Field photograph showing exposure of chert unit in olistoliths west of Gamnom (25°01'30.0" / 94°25'29.3")

5.2.4. PETROLOGICAL STUDIES

5.2.4.i. Transitional peridotite

The transitional peridotites commonly occur in between tectonite and cumulate peridotite and are mainly harzburgitic. Both ortho as well as clino pyroxenes and relict olivine (now serpentinitised) porphyroclasts are having corroded grain boundary. Olivine occurs in two distinct modes: (a) protogranular olivine and (b) small neoblasts and fine-grained olivine often brecciated. As a whole, transitional peridotite show porphyroclastic granular texture and contain spinel grains of lensoid and equidimensional or skeletal shape. Plastic strain in the form of strain shadow in olivine porphyroclasts and kink bands in pyroxenes represent post-igneous features. Chrome-spinel that notably occurs could be part of relict chromite (Kamenetsky et al., 2001). Serpentinized peridotite comprises of partially serpentinitized olivine, orthopyroxene and clinopyroxene with profuse development of exsolution lamellae (Fig. 12).

5.2.4.i.a. Harzburgite

It shows protogranular texture defined by large hypidiomorphic to xenomorphic orthopyroxenes, highly serpentinitised olivine and minor clinopyroxenes (Fig. 13). The presence of neoblastic olivine (Fig. 14) and corroded chrome spinel (Fig. 15) (Fig. 16) are evident that this Harzburgite belongs to the transitional zone of peridotites. Segmental foliation, granulation and brecciation are common. Large orthopyroxene grains show zoning at the grain margin and alteration (i.e. orthopyroxene to clinopyroxene) at fracture zone are also observed.

The orthopyroxenes under plane light are pale colored with greenish to pinkish pleochroism. Pure enstatites can be colorless, where as those with higher Fe contents correspond to darker colors. They show high positive relief and euhedral crystals will be stubby prisms. Anhedral grains may fill the space between other grains.

The clinopyroxenes under plane light show colorless, grey, pale green, pale brown, or brownish green and darker colours corresponding to higher Fe content. They can be weakly pleochroic and have a high positive relief with a typical pyroxene cleavage. Under crossed polars they show lower to middle second order colours. Basal sections will show symmetrical extinction, longitudinal sections will have inclined extinction and be length slow. They are distinguished from orthopyroxenes by inclined extinction and higher birefringence.

Apart from olivine grains are also present which show weak, pale green pleochroism in thin section. Olivine is commonly recognized by its high retardation, distinctive fracturing, lack of cleavage, and alteration to serpentine. Due to intensive shear foliation, granulation and brecciation, most of the grains are broken down into smaller grains and serpentinised but core remains unaltered. During the process of serpentinisation, opaque (magnetite) (Fig.17) get accumulated at the networking veins of serpentine.

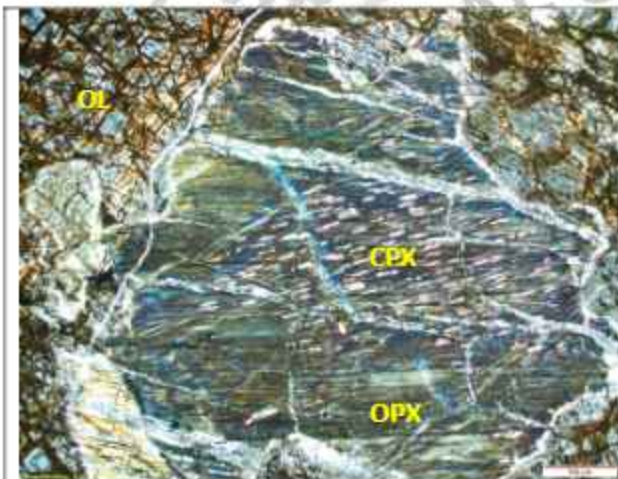


Fig.12. Photomicrograph showing exsolution lamellae of Clinopyroxene (CPX) within orthopyroxene (OPX) surrounded by olivine (OL) Partially serpentinised Harzburgite (transitional peridotite) under crosspolarized light at 4x magnification. West of Gamnom (25°01'53.8" / 94°26'32.0")

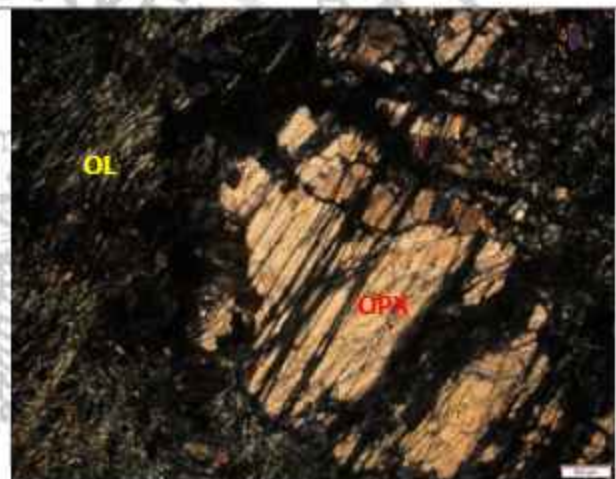


Fig. 13. Photomicrograph showing break down of Orthopyroxene (OPX) surrounded by serpentinized olivine (OL) in Harzburgite (transitional peridotite) under crosspolarized light at 2.5x magnification. East of Changa (25°00'50.6" / 94°25'3.9")

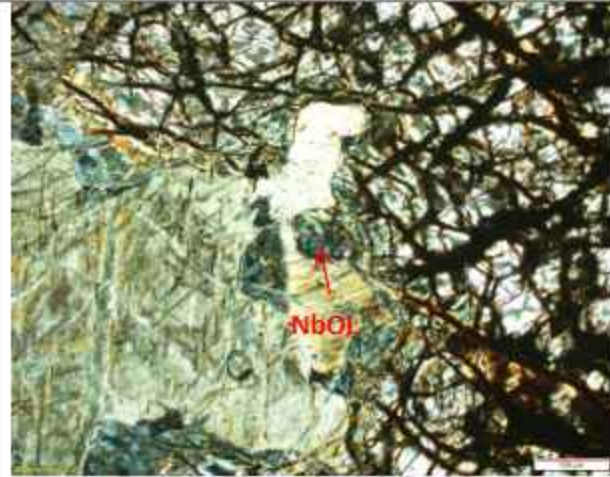


Fig.14. Photomicrograph showing neoblastic olivine (NbOL) surrounded by serpentinized Olivine in Harzburgite (transitional peridotite) under cross polarized light at 4x magnification. East of Gamnom ($25^{\circ}01'28.7''$ / $94^{\circ}27'12.9''$)

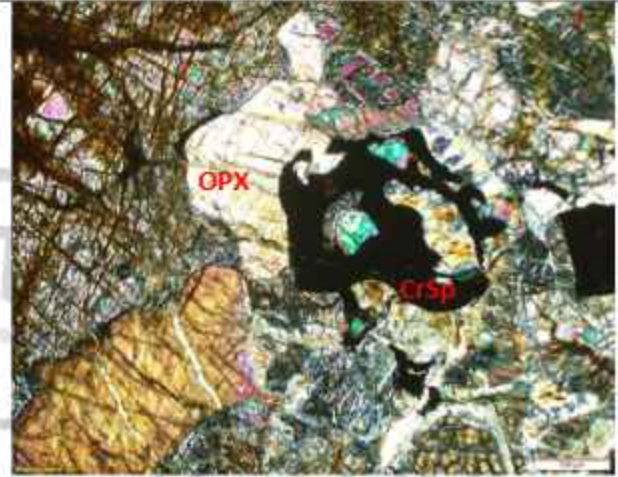


Fig.15. Photomicrograph showing chrome spinel (CrSp) surrounded by orthopyroxene (OPX) in Harzburgite (transitional peridotite) under cross polarized light at 4x magnification. West of Gamnom ($25^{\circ}01'53.8''$ / $94^{\circ}26'32.0''$)

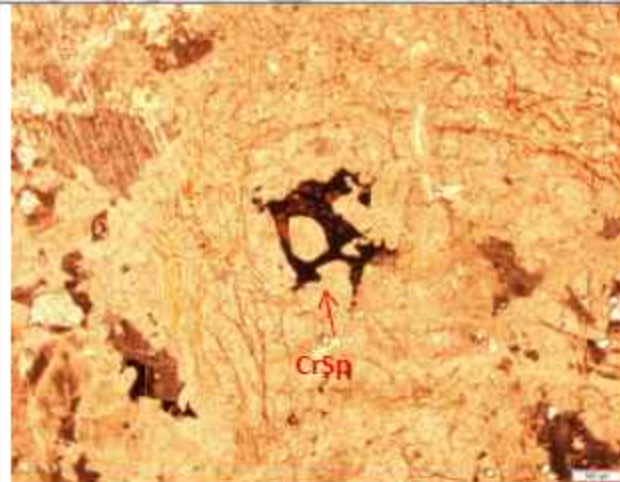


Fig.16. Photomicrograph showing chrome spinel (CrSp) surrounded by orthopyroxene in Harzburgite (transitional peridotite) under plane polarized light at 2.5x magnification. south of Khangkui Khullen ($25^{\circ}00'39.5''$ / $94^{\circ}25'42.8''$)

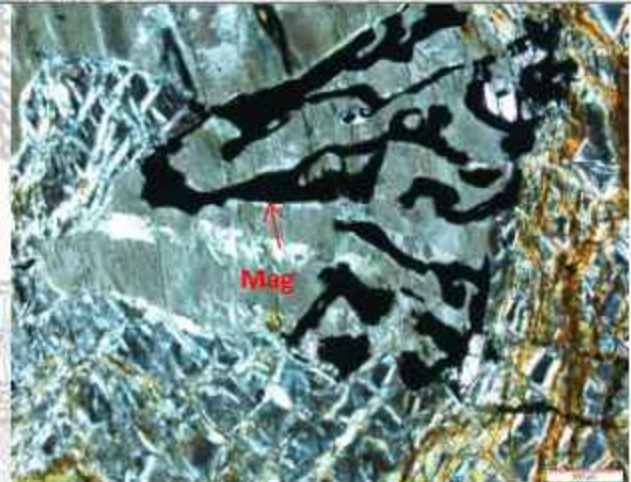


Fig.17. Photomicrograph showing relict magnetite (Mag) surrounded by olivine in Harzburgite (transitional peridotite) under cross polarized light at 4x magnification. East of Gamnom ($25^{\circ}01'28.7''$ / $94^{\circ}27'12.9''$)

5.2.4.ii. Mafic cumulates

Gabbro

Thin section studies have revealed that the gabbro shows cumulate (ophitic to sub-ophitic) texture in which the plagioclase laths (Fig.21) are surrounded by hornblende, chlorite (Fig.18) clinopyroxenes (Fig.19) and minor skeletal magnetite grains (Fig.20) (Fig.22) Pressure exerted due to thrusting has given rise to cataclastic texture in the weaker grains which have broken down into finer grains.

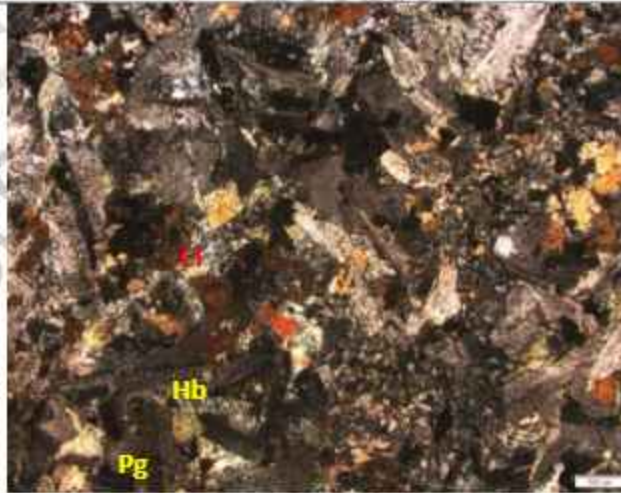


Fig.18. Photomicrograph showing sub-ophitic texture in gabbro with large plagioclase laths (Pg) surrounded by chlorite (Cl) and hornblende (Hb) also showing breaking down of smaller weaker grains (cataclastic texture) due to exerted pressure of thrusting, cross polarized light at 2.5x magnification. Gamnom (25°01'28.0"/ 94°27'8")

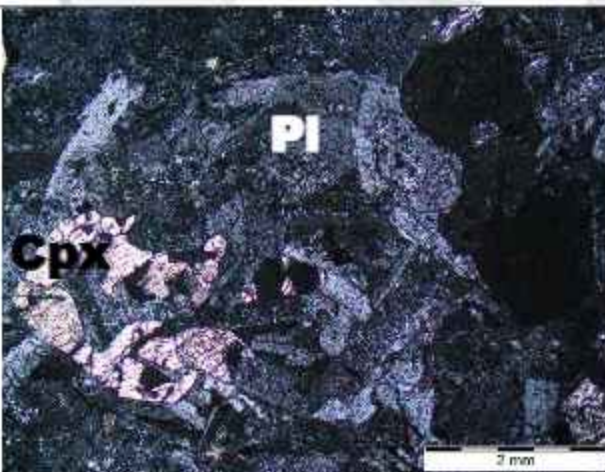


Fig.19. Photomicrograph of Xenomorphic Clinopyroxene(Cpx) showing intergrowth with laths of plagioclase (Pl) in gabbro.

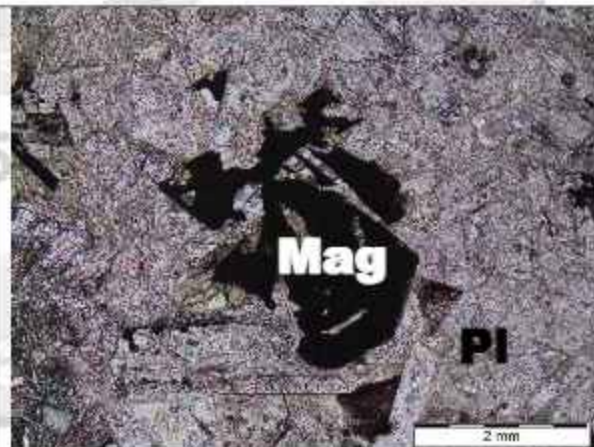
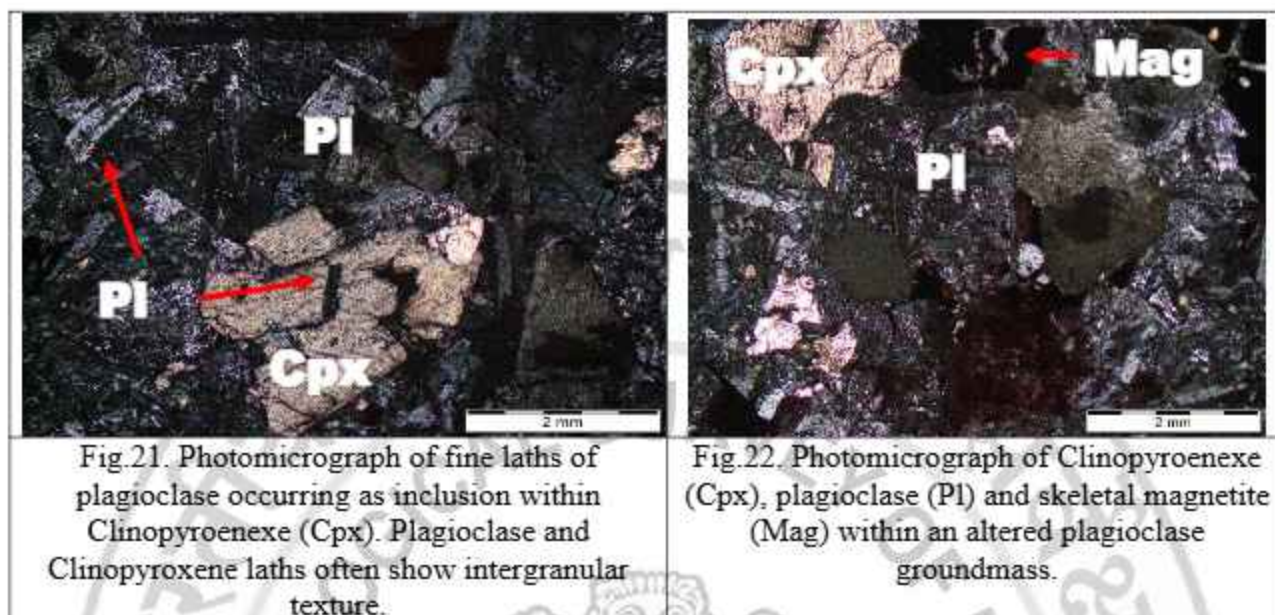


Fig.20. Photomicrograph of Skeletal magnetite (Mag) grains within plagioclase (Pl) laths in gabbro.



5.2.5. STRUCTURE

The mafic-ultramafic sequence of ophiolite belt the study area is bounded in west by ocean pelagic sediments. The present outcrop pattern and occurrence of various mafic-ultramafic bodies, the overall shape of the ophiolite belt and its contact relation with the olistoliths is mainly controlled by later deformation events.

5.2.5.a. Primary structures

Magmatic layering observed in gabbro and transitional peridotite are the primary structure in the mafic-ultramafic bodies of ophiolite. These magmatic layering are defined in transitional peridotite by grain size variations of pyroxenes whereas in gabbro it is marked by colour banding of mafic and felsic rich bands. Sedimentary rocks of olistoliths are marked by layered debris flows; although the layering is not prominent.

5.2.5.b. Secondary structures.

Foliation

Weak foliations are developed in the transitional peridotite part of ophiolite at certain locations and are marked by development of serpentines and shear lenses.

Thrust

Zone of intense brecciation, silicification, gouge and development of profuse slickensides were observed at many places which are indications of a zone of thrusting rather than a sharp thrust contact. Occurrences of prominent brecciated zones were observed south of Khangkui at the contacts of transitional peridotite and olistoliths. Brecciated zones were also observed around the olistoliths surrounded by transitional peridotites. These zones are generally having north-south trend and are marked by angular clast of chert, greywacke, limestone and fragments of ultramafics. Brecciated boulders, and/or discrete occurrences of gouge were seen many a place at the contacts of transitional peridotite and olistoliths, however, their continuation could not be traced due to inaccessibility, thick vegetations and soil cover (Fig.23).



Fig.23. Brecciated peridotite in a sandy matrix,
South of Gamnom (25°00'37.7"/ 94°27'54.9")

The geological cross sections of the area also reveal process of reverse movement of transitional peridotite blocks against olistoliths against sub-parallel longitudinal NE-SW fault. The thrusts are sinusoidal in nature and therefore some units like that of the mafic-cumulates consisting of Gabbro die off after short distances. Repetitive stacking of these units due to thrust dynamics are observed in the study area.

5.2.6. METAMORPHISM

Features bearing evidences of metamorphism is absent in the study area although high pressure metamorphic rocks like garnet granulite, garnet amphibolites have been reported north east of the study area around Tusom C.V (V.S.Peter et al, 2019). The study area does not exhibit any metamorphic rocks as the peridotite here falls in the transitional peridotite zone and has not been subducted to greater depths for the effect of metamorphism to be evident. The chromitites are basically derived from the primary melt itself and do not appear to be products of metasomatism. At places, the original character of igneous rocks is altered because of deformation and serpentinization but there are no major indicators to suggest that this zone has undergone a considerable degree of metamorphism as no metamorphic rocks are observed to occur.

5.2.7. MINERALOGY OF THE ORE ZONES AND ORE TEXTURES

The occurrence of cluster of podiform chromite was delineated in Gamnom, south of Khangkui Khullen, Yentem and northwest of Pushing village during the course of mapping. The chromitite occurs in cluster of different dimension (0.5 to 1.5m) within this area as isolated bodies within the host rock of Harzburgite (transitional peridotite). They occur as podiform type. Chromitites are dark grey to black, massive, hard and resistant unit with high specific gravity.

Chromitite

Chromitite occurs as isolated pods within the host rock of harzburgite (transitional peridotite). Ore microscopy studies reveal a cataclastic texture (Fig.24) in which the chromite grains (grey to reddish grey) are highly fractured and brecciated. The cores of these fractured grains are well preserved where as its boundaries have been granulated and amalgamated into the surrounding

minerals. Some samples show corroded grain boundaries in the chromite grains (Fig.25) within the minerals of the host harzburgite.

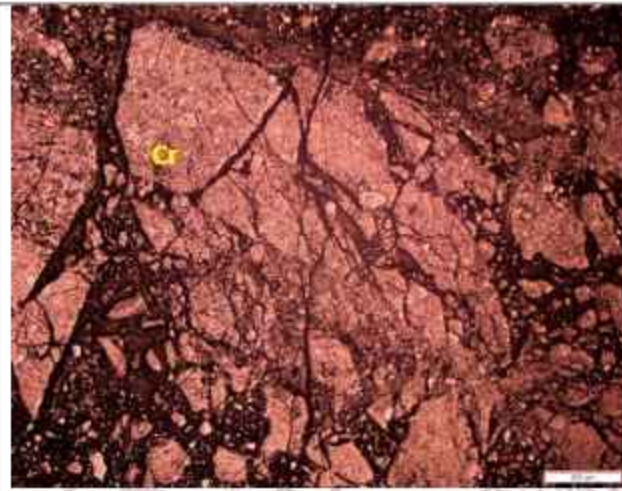


Fig. 24. Photomicrograph showing cataclastic texture of chromite grains (Cr) in chromitite reflected light at 2.5x magnification. Gamnom (25°00'58.7" / 94°27'14.7")

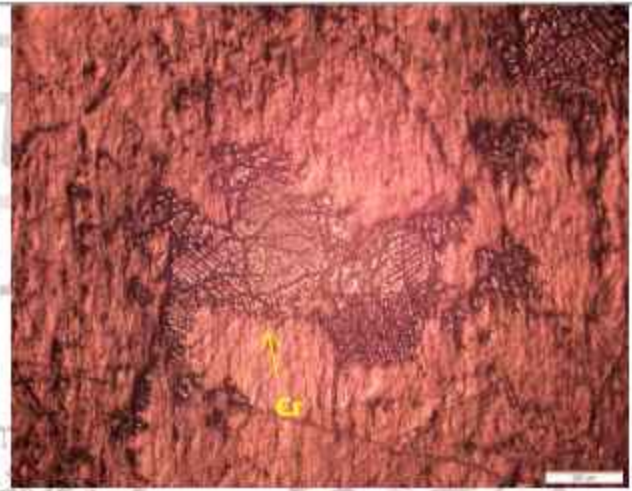


Fig.25. Photomicrograph showing corroded grains of chromite (Cr) in chromitite reflected light at 2.5x magnification. Gamnom (25°00'58.7" / 94°27'14.7")

Nickel

High values of nickel have been observed in samples collected during trenching at Gamnom (trench 2). The values of chromium are notably lower in these samples. The details are mentioned in the following part on discussion about pitting and trenching. And the nickel values at Gamnom (trench 2) range from 1.07% -1.79% and in Yentem(trench 4) the values of nickel from one sample yields 1.41%.

5.2.8. SAMPLING

BED ROCK SAMPLING

150 Nos. of bed rock samples (BRS) in the form of grab samples, weighing approximately 2-2.5kg were collected by chipping the exposed rocks. These samples were cleaned, dried, powdered and sieved through -120 mesh. The sieved sample weighing about 500gm each were collected. These samples are made into two halves of 250 gm each by coning

and quartering. One half of 250gm of each samples was sent for laboratory analysis as recommended, while the other half is kept as duplicate samples for future reference. Due care has been taken to avoid any type of contamination during processing of the samples. A total of 150 BRS were thus, collected, processed and analysed for, Cu, Pb, Zn, Ni, Co, Sb, Ba, Bi, As, Ag, Au, Cr, V, Ti, Trace and major oxides. (Refer Plate-II)

PETRO CHEMICAL SAMPLING

25 Nos. of Petro Chemical Samples (PCS) in the form of fresh grab samples, weighing approximately 2-2.5kg were collected by chipping the exposed rocks. These samples were cleaned, dried, powdered and sieved through -120 mesh. The sieved sample weighing about 500gm each were collected. These samples are made into two halves of 250gm each by coning and quartering. One half of 250gm of each samples was sent for laboratory analysis as recommended, while the other half is kept as duplicate samples for future reference. Due care has been taken to avoid any type of contamination during processing of the samples. A total of 150 BRS were thus, collected, processed and analysed for, Cu, Pb, Zn, Ni, Co, Sb, Ba, Bi, As, Ag, Au, Cr, V, Ti, Trace and major oxides and also REE.

PITTING/TRENCHING SAMPLING

A total of 5 trenches, three having dimension 10mx1mx1m each were carried out near the vicinity of chromitite occurrence to delineate the continuity of chromitite body. However only in two trenches boulders of chromitite was intersected within 1m length of the trench. In all other trenches peridotite and red soils were encountered. Sampling was carried at 1m interval within the trench and in all 50 nos. rock samples were collected. The samples were collected by chiselling, after cleaning the trench. The processing of pitting trenching samples follows the same methodology for preparation of bed rock samples (BRS).

5.2.9. DISCUSSION OF RESULTS OF CHEMICAL ANALYSIS SAMPLES

5.2.9.1. BED ROCK SAMPLES:

TRANSITIONAL PERIDOTITE (HARZBURGITE)

The analytical result of bed rock samples is given in annexure-I. The peridotite in the area is characterised by the content of Fe_2O_3 (7%-13.7%), MgO (29% - 40.72%), Al_2O_3 (0-17.62%), TiO_2 (<0.01-1.9%), Cr_2O_3 (37-6879ppm), Cr (37ppm-9254ppm), Ni (30-8606ppm), Va (0-611ppm), Co (5-436ppm), Cu (<5-99ppm), Pb (2-14ppm), Zn (5-274ppm).

Scatter plots of whole rock analysis for MgO vs other major oxides (Fig.26) suggest that the peridotites in the study area belong to the same peridotite type, which is the transitional peridotite variant as confirmed by thin section studies. This is supported by the fact that mostly all the plots do not show much scattering from the normal and plots are clustered together.

The plots for whole rock major oxide in ACF and AFM ternary diagrams (Fig.27) suggest that the peridotites plotted belong to the metamorphic peridotite type and cumulate peridotite type according to the plots suggested by Coleman (1977).

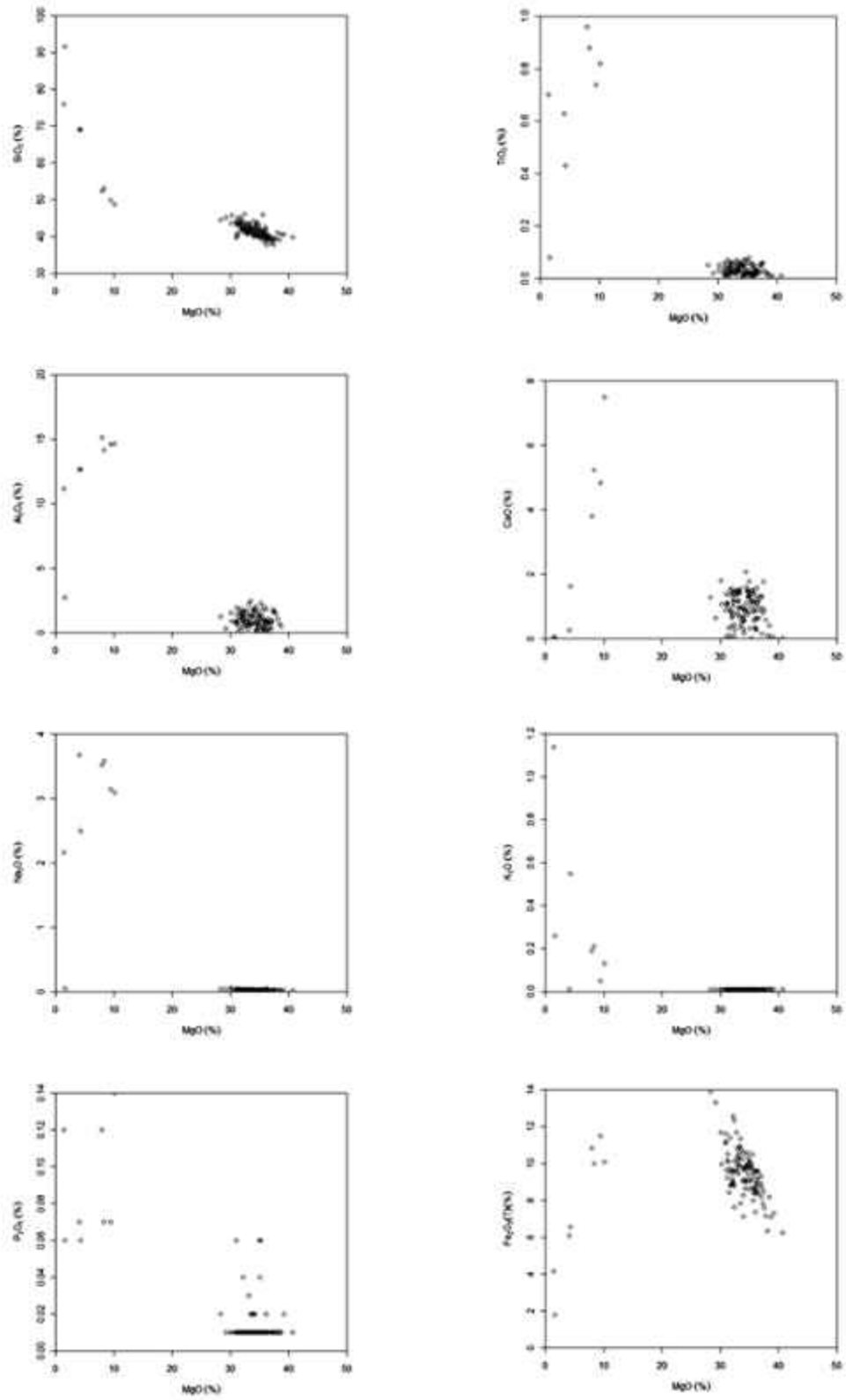


Fig.26. MgO vs other major oxides scatter plot of ultramafic rocks (oxide in %)

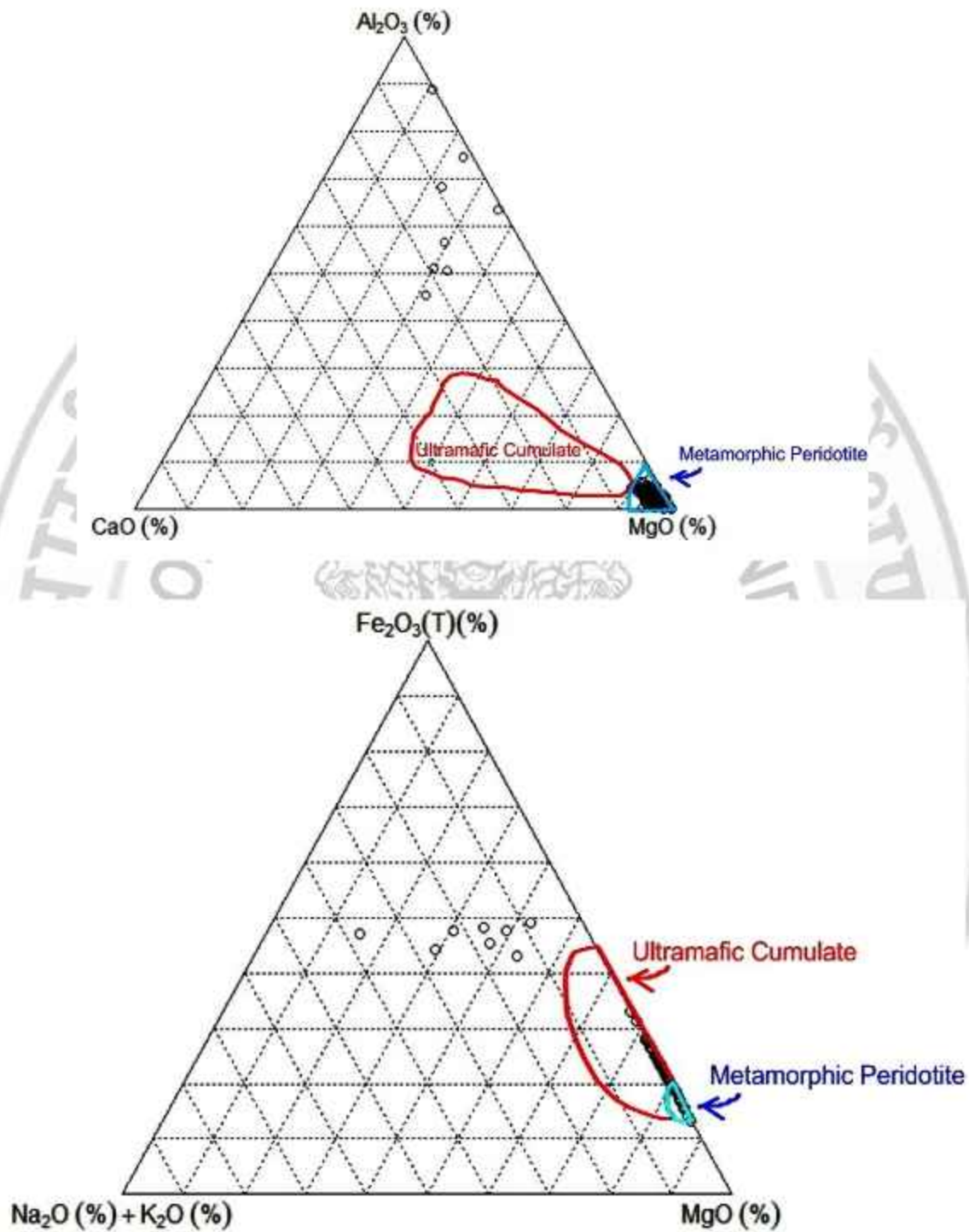


Fig.27. ACM and AFM plots of ultramafic rocks with fields of ultramafic cumulates and metamorphic peridotites after Coleman (1977)

CHROMITITE

The analytical result of bed rock samples is given in annexure-I. In samples which are chromitite bearing transitional peridotites (harzburgite) the Cr values range from 31.11% to 53.53% (Fig.28).

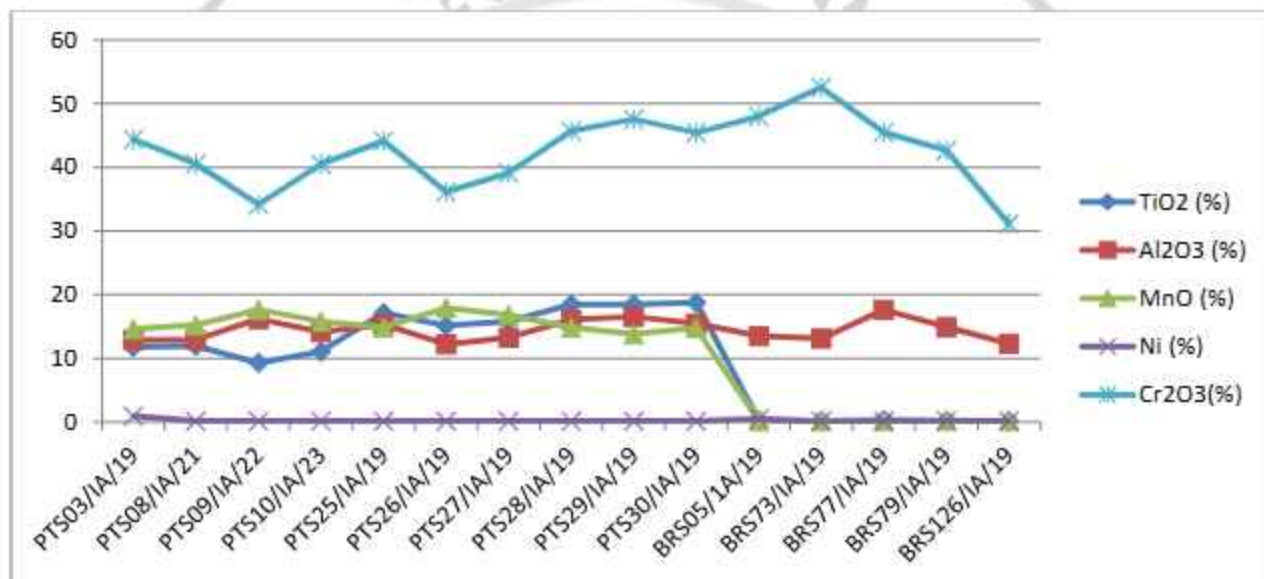


Fig.28. Variation plot of Cr vs Ti vs Al vs Mn vs Ni in red soil samples

5.2.9.2. PITTING/TRENCHING :

Trench-1

This trench with a dimension of 10m x 1m x 1m was carried out at Gamnom at (25°00'58.1" / 94°27'12.7"). R.L top is 1922m. R.L bottom 1921m. The trench was laid in E-W across the general trend of the chromite occurrences in Harzburgite groundmass with a lateritic soil. The details of the trench section and the corresponding sketch are given in Fig.29 and 30. In this trench almost 40% of the samples are chromitite pods with chromite percentage ranging from 34.1% to 44.37% (Fig.31) (refer Annexure-III).



Fig. 29. Field photographs showing section of trench-1 at Gamnom in transitional peridotite ($25^{\circ}00'58.1''$ / $94^{\circ}27'12.7''$).

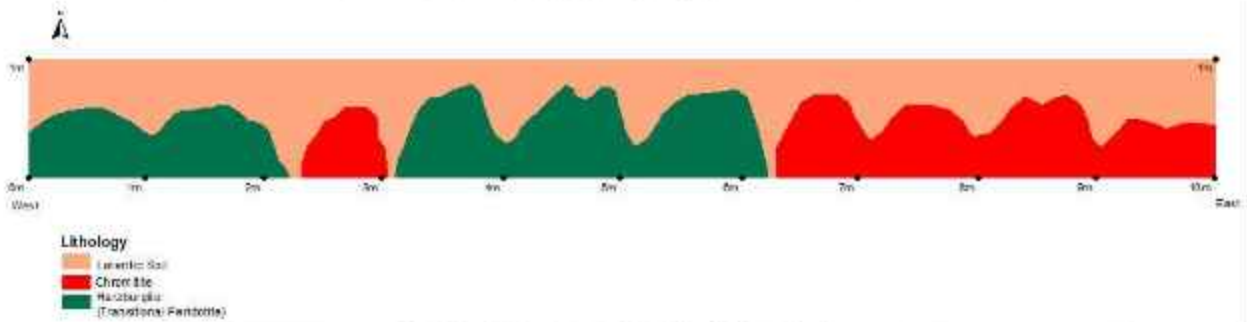


Fig.30. Schematic sketch of Trench-1

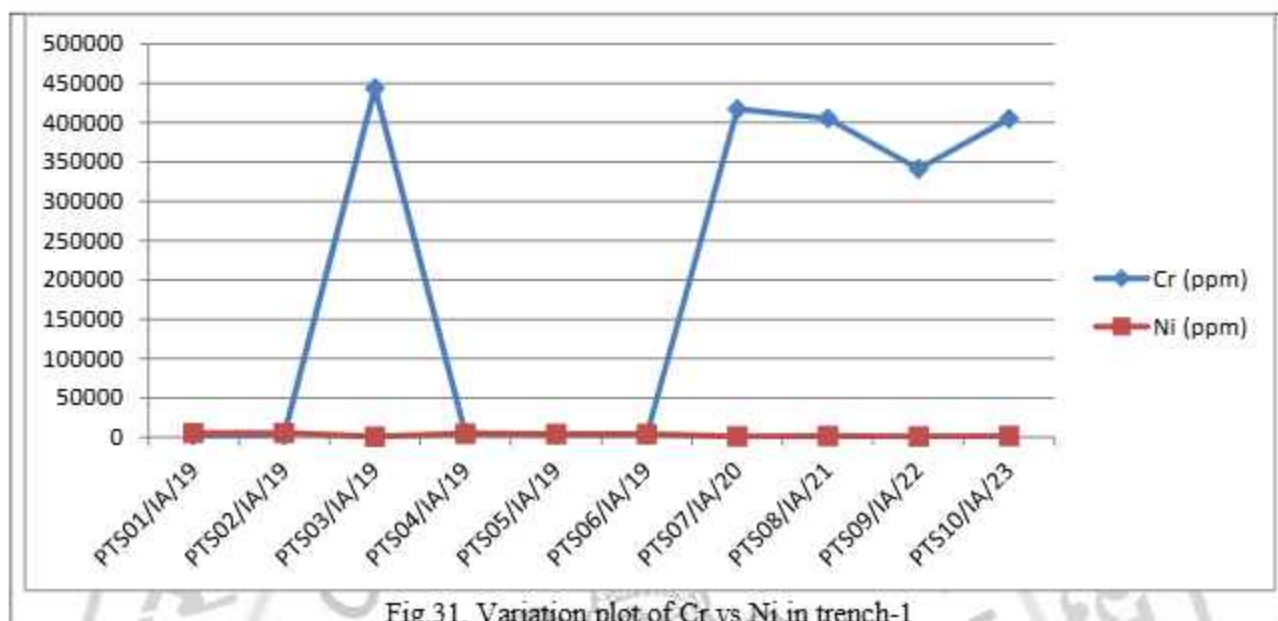


Fig.31. Variation plot of Cr vs Ni in trench-1

Trench-2

This trench with a dimension of 10m x 1m x 1m was carried out at Gamnom at (25°00'58.3" / 94°26'59.9"). The trench was laid in E-W across the general trend of the chromite occurrences. R.L top is 1919m. R.L bottom 1918m. The trench was laid in E-W across the general trend of the chromite occurrences in Harzburgite groundmass with a lateritic soil. The details of the trench section and the corresponding sketch are given in Fig.32 and 33. In this trench almost all of the samples are show high nickel percentage ranging from 0.54% to 1.67% i.e. 0.54% to 1.67%. The chromium values range from 2433ppm to 3519ppm (Fig.34)(refer Annexure-III).



Fig.32. Field photographs showing section of trench-2 at Gamnom in transitional peridotite ($25^{\circ}00'58.3''$ / $94^{\circ}26'59.9''$).

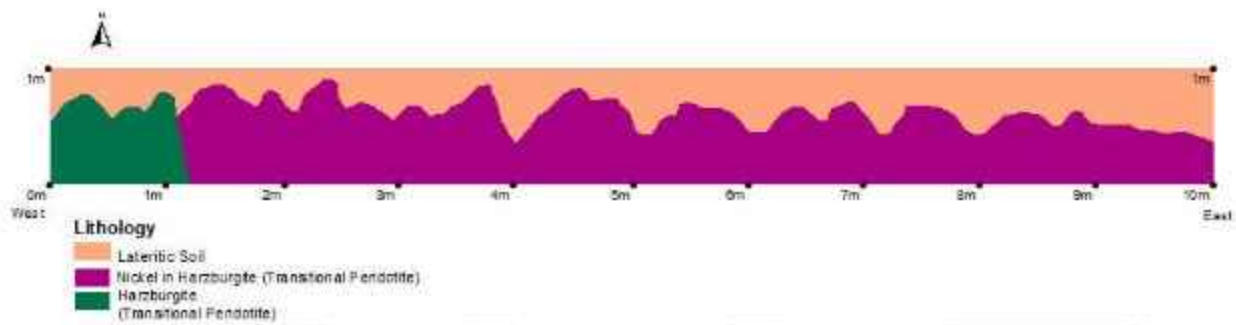


Fig.33. Schematic sketch of Trench-2

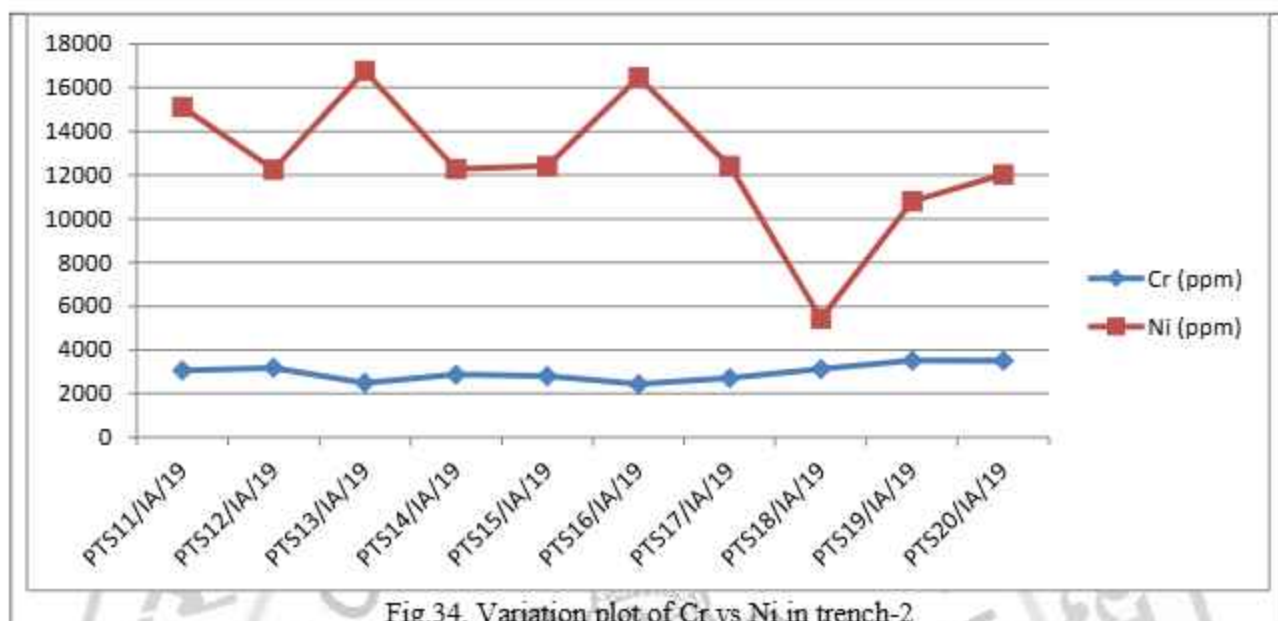


Fig.34. Variation plot of Cr vs Ni in trench-2

Trench-3

This trench with a dimension of 10m x 1m x 1m was carried out south of Khangkui Khullen (25°00'48.0" / 94°25'47.8"). The trench was laid in E-W across the general trend of the chromite occurrences. R.L top is 1651m. R.L bottom 1650m. The trench was laid in E-W across the general trend of the chromite occurrences in Harzburgite groundmass with a lateritic soil. The details of the trench section and the corresponding sketch are given in Fig.35 and 36. In this trench almost 60% of the samples are chromitite pods with chromite percentage ranging from 36.11% to 47.51%. Also some of the samples show high nickel percentage ranging from 1225ppm to 18580ppm i.e. 0.23% to 1.85% (Fig.37). (refer Annexure-III)



Fig.35. Field photographs showing section of trench-3 south of Khangkui Khullen in transitional peridotite ($25^{\circ}00'48.0''$ / $94^{\circ}26'47.8''$).

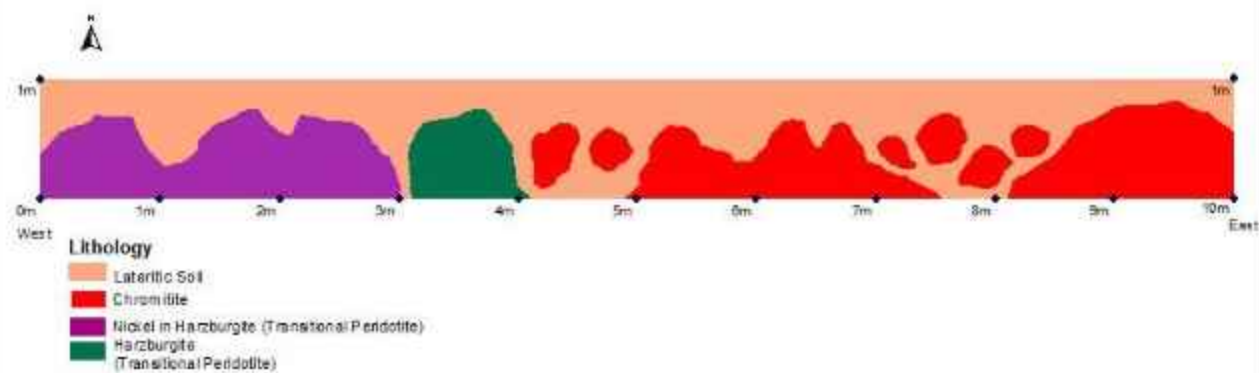


Fig.36. Schematic sketch of Trench-3

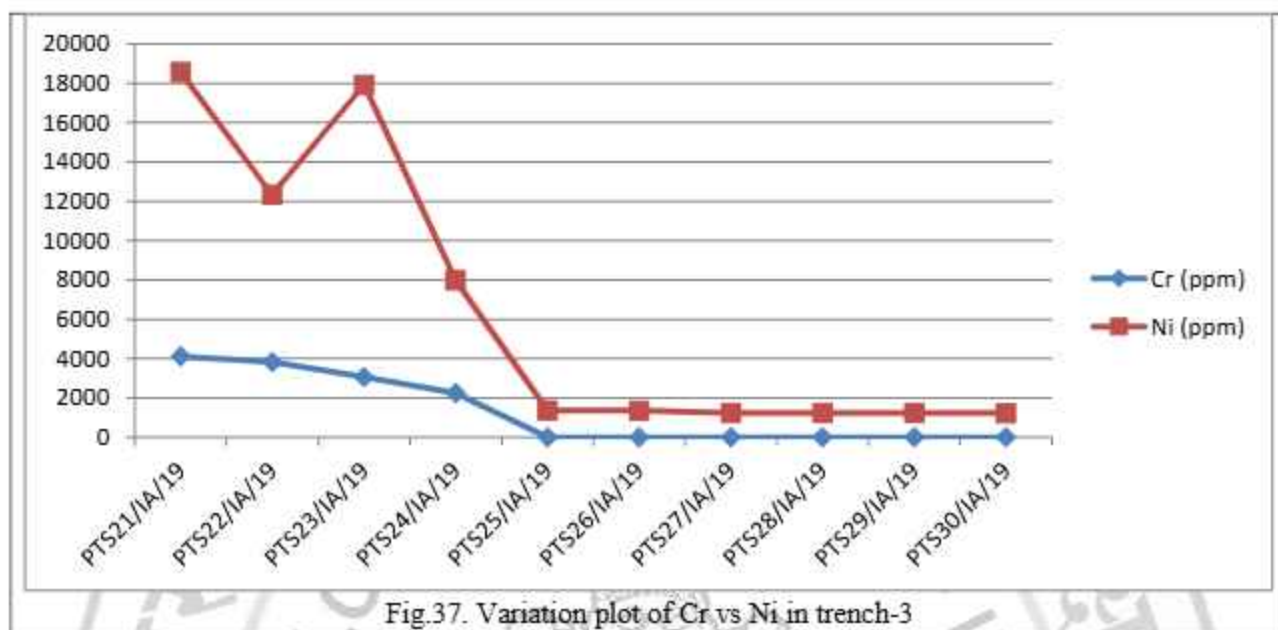


Fig.37. Variation plot of Cr vs Ni in trench-3

Trench-4

This trench with a dimension of 10m x 1m x 1m was carried out at Yentem ($24^{\circ}58'56.2''$ / $94^{\circ}26'01.8''$). R.L top is 1515m. R.L bottom 1514m. The trench was laid in E-W across the general trend of the chromite occurrences in Harzburgite groundmass with a lateritic soil. The details of the trench section and the corresponding sketch are given in Fig.38 and 39. The trench was laid in E-W across the general trend of the chromite occurrences (Fig.40). (refer Annexure-III)



Fig.38. Field photographs showing section of trench-4 south of Yentem in transitional peridotite ($24^{\circ}58'56.2''$ / $94^{\circ}26'01.8''$).



Fig.39. Schematic sketch of Trench-4

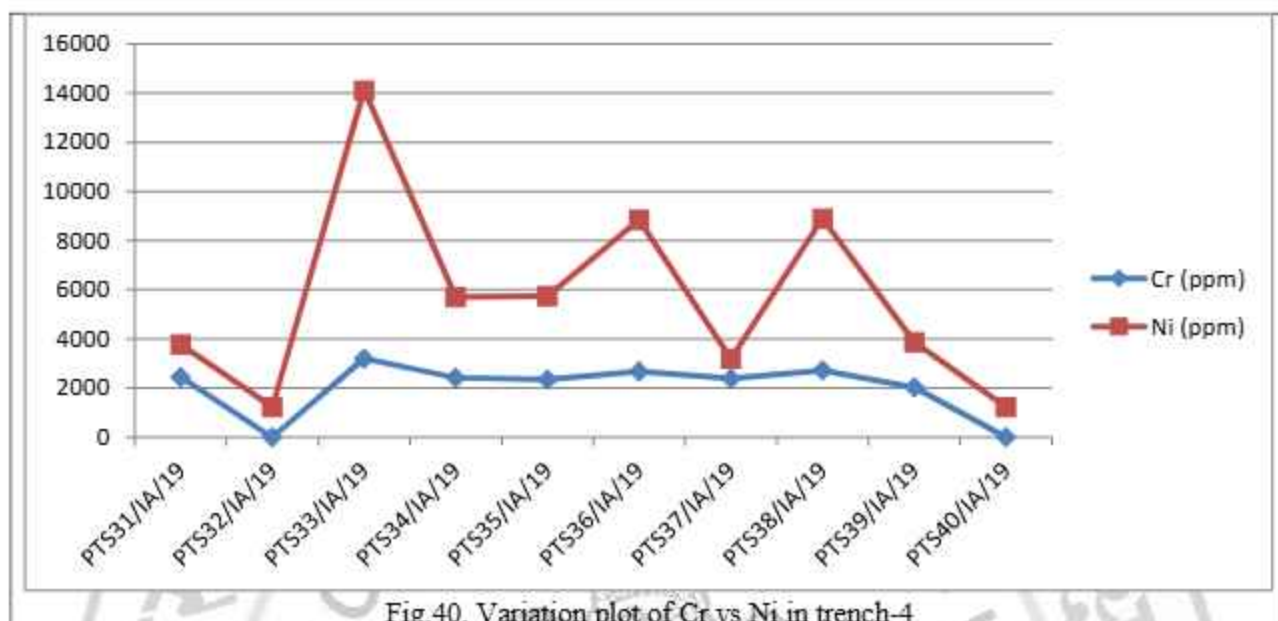


Fig.40. Variation plot of Cr vs Ni in trench-4

Trench-5

This trench with a dimension of 10m x 1m x 1m was carried out west of Pushing (25°02'53.1" / 94°28'30.3"). R.L top is 1441m. R.L bottom 1440m. The trench was laid in E-W across the general trend of the chromite occurrences in Harzburgite groundmass with a lateritic soil. The details of the trench section and the corresponding sketch are given in Fig.41 and 42. Chromium and nickel content is low in this trench (Fig.43). (refer Annexure-III)



Fig.41. Field photographs showing section of trench-5 west of Pushing in transitional peridotite ($25^{\circ}02'53.1''$ / $94^{\circ}28'30.3''$).

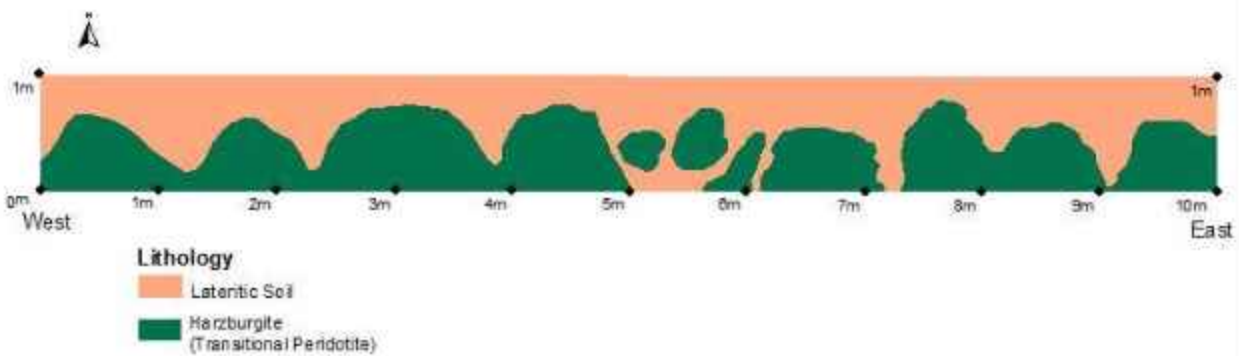


Fig.42. Schematic sketch of Trench-5

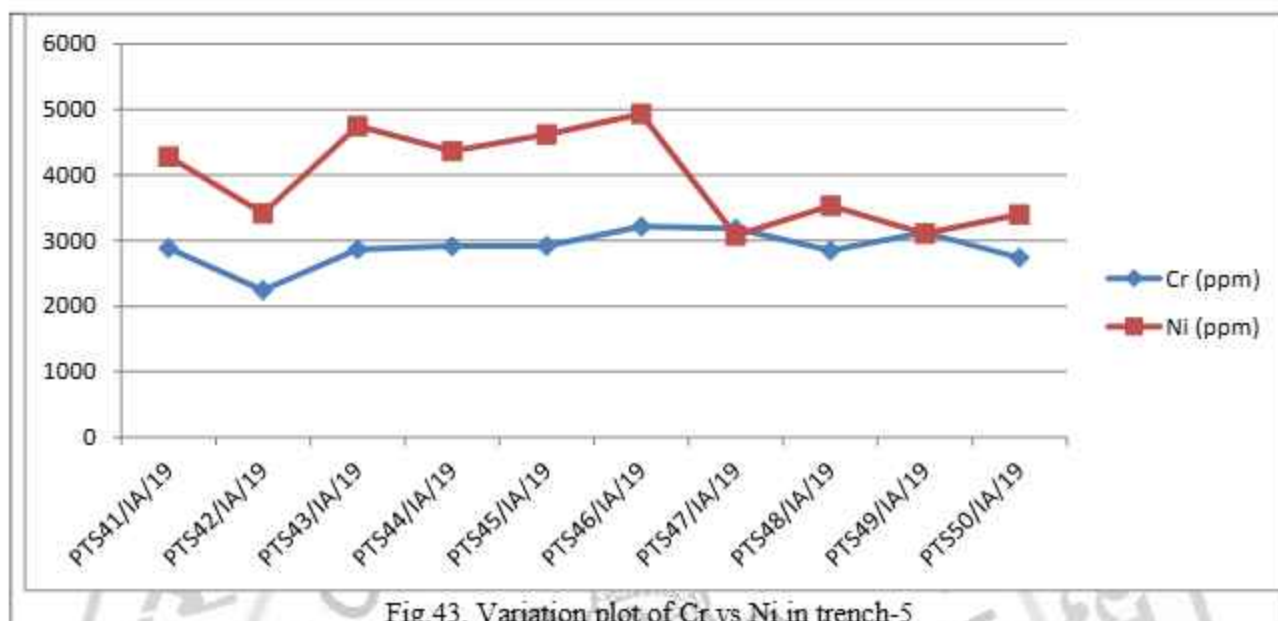


Fig.43. Variation plot of Cr vs Ni in trench-5

5.2.9.3. PETROCHEMICAL SAMPLES

GABBRO

Gabbro was sampled at Gamnom and west of Pushing; in one sample from the gabbro (PCS01) body at Gamnom the Ti was about 54.52% the rest of them had uniform composition. The sample from the Gabbro body in west of Pushing (PCS25) showed higher Al_2O_3 and lower Fe_2O_3 compared to the gabbro body at Gamnom (Fig.44) (refer Annexure-II)

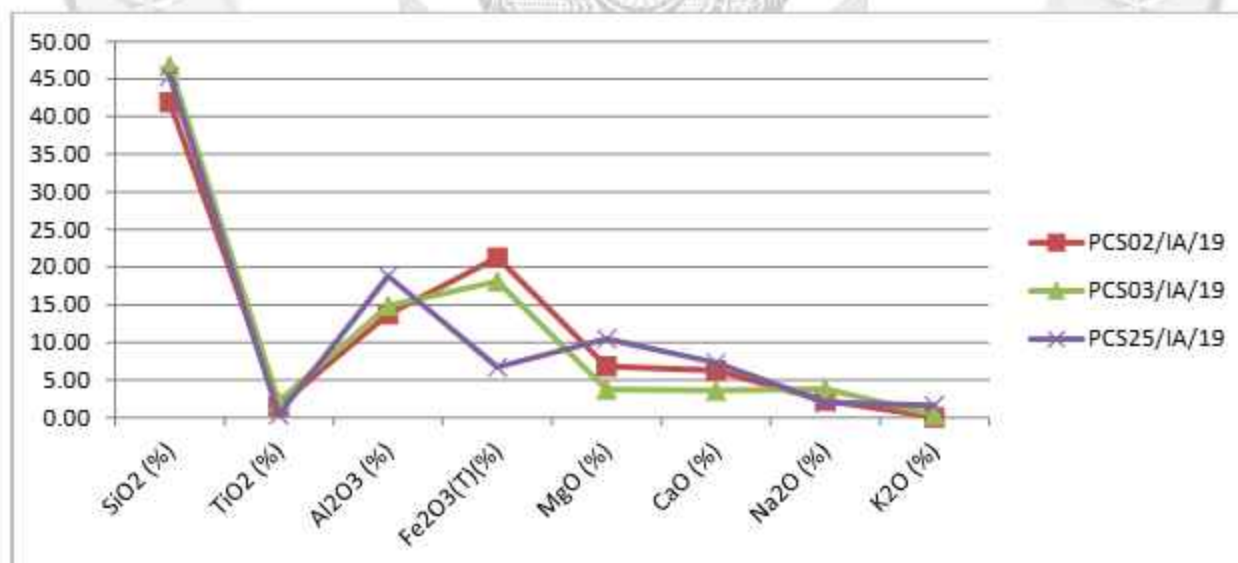


Fig.44. Major oxide composition in Gabbros

The REE plot of the gabbro samples show an almost uniform scatter plot Sample PCS25 shows slightly lower amounts of REE(Fig.45).

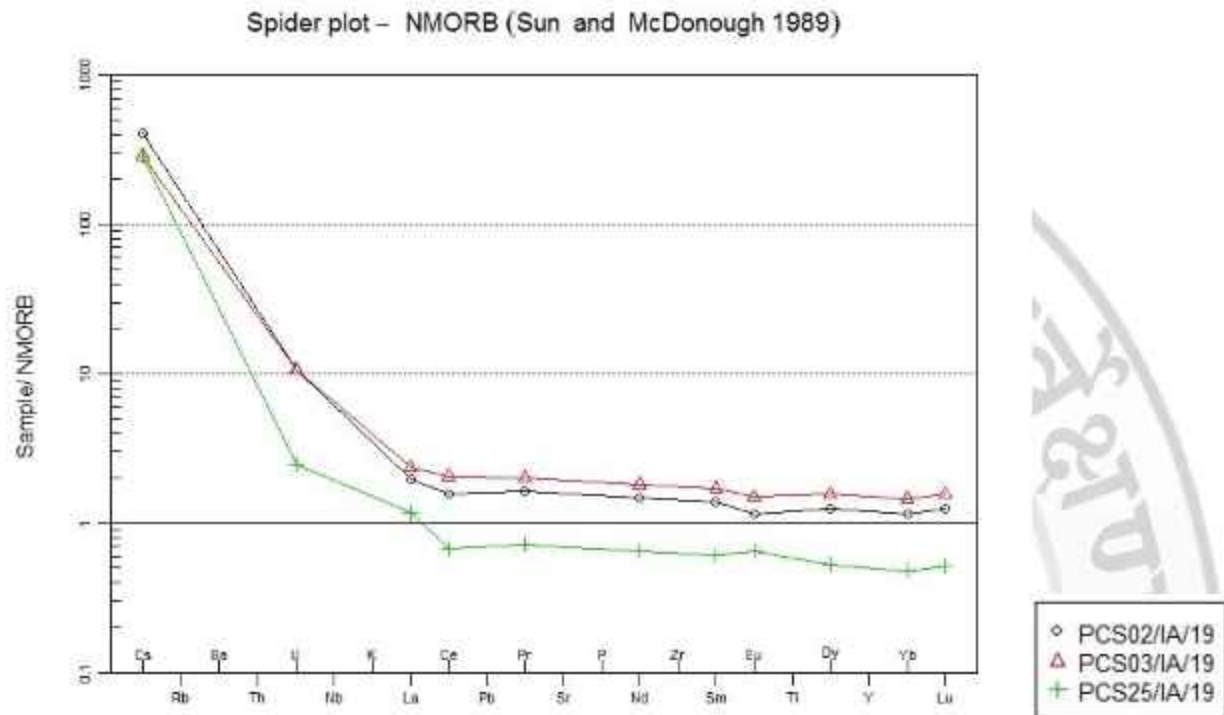


Fig.45. REE plot in Gabbro

RED SOIL

Red soil samples were collected at locations where they were present and the results show Fe_2O_3 percentages ranging from 10% to 43.75% (Fig.46). (refer Annexure-II)

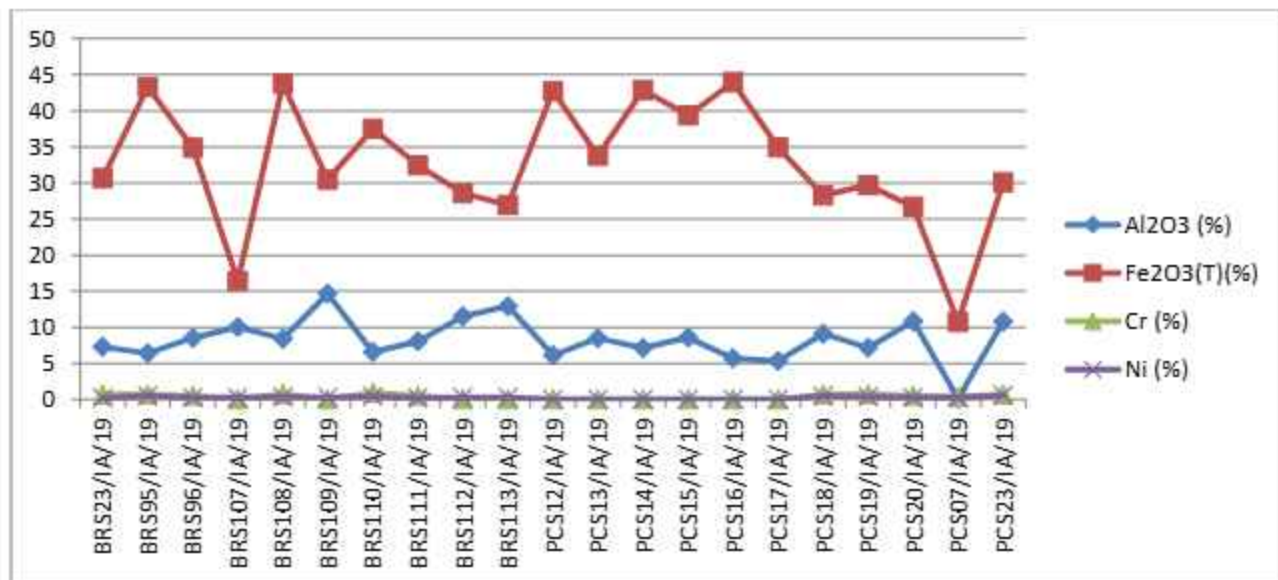


Fig.46. Variation plot of Fe vs Al vs Cr vs Ni in red soil samples

5.3. GEOPHYSICAL EXPLORATION

Geophysical survey was cancelled by the competent authorities.

5.4. GEOCHEMICAL EXPLORATION

No Geochemical data is available for the study area.

CHAPTER 6

INTEGRATION OF GEOLOGICAL, GEOCHEMICAL AND GEOPHYSICAL EXPLORATION DATA AND INTERPRETATION THEREOFF

OVERLAY STUDIES IN GIS (GEOLOGICAL, GEOCHEMICAL AND GEOPHYSICAL MAPS)

Geochemical and Geophysical mapping was not included as part of the present study.



CHAPTER 7

MINERAL PROSPECT

7.1. SURFACE INDICATION OF MINERALIZATION

Surface indications of chromite mineralization have been recorded in the study area at Gamnom, south of Khangkui Khullen and west of Pushing) during the course of mapping.

At Gamnom the podiform chromites are banded with strike direction north-south dipping easterly. The chromitite pods are embedded in harzburgitic host rock and they are surrounded by lateritic soil (Fig.47) and occupy the top of the hills. This area measures around 80m x 150m. West of Pushing the podiform chromitite is embedded in harzburgitic host rock and is surrounded by soil along the hill slope (Fig.48). At south of Khankui Khullen the podiform chromitite is embedded in harzburgitic rock and surrounded by lateritic soil (Fig.49).



Fig.47. Field photograph showing chromitite pods at Gamnom. (25°00'58.7" / 94°27'14.7")



Fig.48. Field photograph showing chromitite pods west of Pushing. ($25^{\circ}02'49.3''$ / $94^{\circ}28'30.3''$)



Fig.49. Field photograph showing chromitite pods south of Khankui. ($25^{\circ}00'48''$ / $94^{\circ}25'47.8''$)

7.2. MODE OF OCCURRENCE

In the study area, the chromitites occur in clusters as pods of dimensions ranging from 0.5m to 1.5m . They occur as isolated bodies at Gamnom, South of Khangkui Khullen and Pushing within a harzburgitic host rock surrounded by lateritic soil. The colour of the chromitites ranges from grey to black and appear as massive, hard units that are resistant to weathering with a high specific gravity. The chemical analysis of chromitite bearing transitional peridotites (harzburgite) shows Cr values ranging from 31.11% to 53.53% which is of metallurgical grade. The lateral extension of the chromitite bodies could not be established by pitting/trenching. (Plate-I)

7.3. NATURE AND CONTROL OF MINERALIZATION

The chromitite in this area has been observed to occur within harzburgitic host rock occurring in the transitional peridotite zone of the ophiolitic sequence. This has been ascertained by the presence of neoblastic olivine and relict chrome spinel/magnetite specs in the groundmass. The ACM and AFM plots (Fig.27) suggest that the peridotite falls in the ultramafic/metamorphic peridotites zone. Chrome-spinel (or chromite) is well established alteration-resistant petrogenetic and tectonic setting indicator for mafic-ultramafic rocks (e.g. Barnes and Roeder, 2001; Lee, 1999; Kamenetsky et al., 2001; Arai et al., 2006). There seems to be no evidence as to why these clusters occur as isolated clusters with no general control. They appear to be parts of dislocated tectonic slivers that have been thrust over each other and occupy random positions in the ophiolites of Manipur.

7.4. DETAILS OF MINERALIZED ZONES

The details of chromitites with their chemical composition from and their location are given below:

Table.4. Details of chemical composition of Chromitite along with locations:

SAMPLE NO.	BRS05/1A/19	BRS73/1A/19	BRS77/1A/19	BRS79/1A/19	BRS126/1A/19
location	Gamnorn	West of Gamnorn	South of Khangkui Khullen	South of Khangkui Khullen	West of Pushing
LATITUDE	25.0163	25.0111	25.0133	25.0086	25.0470
LONGITUDE	94.4541	94.4389	94.4300	94.4294	94.4751
LAB.NO.	3592/5	3732/60	3732/64	3732/66	3954/08
SiO ₂ (%)	9.33	6.28	3.24	8.16	21.72
TiO ₂ (%)	0.22	0.2	0.33	0.2	0.14
Al ₂ O ₃ (%)	13.51	13.11	17.62	14.93	12.27
Fe ₂ O ₃ (T)(%)	13.78	14.2	16.11	16.29	12.15
MnO (%)	0.17	0.19	0.19	0.22	0.17
MgO (%)	14.41	11.79	14.81	14.21	18.71
CaO (%)	0.29	0.71	0.06	0.96	0.08
Na ₂ O (%)	0.04	0.03	0.03	0.03	0.04
K ₂ O (%)	0.01	0.02	0.01	0.03	0.01
P ₂ O ₅ (%)	<0.01	<0.01	<0.01	0.03	<0.01
Ni (ppm)	500	1034	1061	1662	1533
Cr (%)	48%	52.53%	45.48%	42.67%	31.11%

Table.5. Details of chemical composition of Chromitite along with locations in trenching samples:

SAMPLE NO.	LOCATION	LATITUDE	LONGITUDE	LAB.NO.	TiO ₂ (%)	Al ₂ O ₃ (%)	MnO (%)	Ni (%)	Cr ₂ O ₃ (%)
PTS03/IA/19	Gamnom	25.0161	94.4535	3731/03	11.81	12.88	14.58	0.924	44.37
PTS08/IA/21	Gamnom	25.0161	94.4535	3731/08	11.96	12.88	15.22	0.151	40.53
PTS09/IA/22	Gamnom	25.0161	94.4535	3731/09	9.26	16.14	17.62	0.13	34.1
PTS10/IA/23	Gamnom	25.0161	94.4535	3731/10	11.04	14.11	15.78	0.148	40.5
PTS25/IA/19	S.of Khangkui Khullen	25.0133	94.4299	3731/25	17.13	15.3	14.85	0.137	44.11
PTS26/IA/19	S.of Khangkui Khullen	25.0133	94.4299	3731/26	15.13	12.19	17.9	0.134	36.11
PTS27/IA/19	S.of Khangkui Khullen	25.0133	94.4299	3731/27	15.74	13.24	16.81	0.124	39.09
PTS28/IA/19	S.of Khangkui Khullen	25.0133	94.4299	3731/28	18.48	16.06	14.84	0.124	45.66
PTS29/IA/19	S.of Khangkui Khullen	25.0133	94.4299	3731/29	18.5	16.53	13.82	0.125	47.51
PTS30/IA/19	S.of Khangkui Khullen	25.0133	94.4299	3731/30	18.75	15.46	14.77	0.123	45.43

No significant mineralized zones could be delineated except for clusters of chromitite pods of dimensions ranging from 0.5m-1.5m at Gamnom, south of Khangkui Khullen and Pushing and the details of their chemical composition are stated above.

7.5. ALTERATION ZONES AND ITS RELEVANCE WITH MINERALIZATION

Red soil samples were collected at zones near the chromitite occurrences and they yielded iron oxide and alumina rich compositions. The details of the soil composition are mentioned below.

Table.6. Details of chemical composition of red soil samples:

SAMPLE NO.	LATITUDE	LONGITUDE	Al ₂ O ₃ (%)	Fe ₂ O ₃ (T)(%)	Cr (%)	Ni (%)
BRS23/IA/19	25.0134	94.4514	7.31	30.67	0.6879	0.1937
BRS95/IA/19	24.9818	94.4322	6.42	43.32	0.6914	0.5114
BRS96/IA/19	24.9833	94.4337	8.55	34.87	0.4988	0.2207
BRS107/IA/19	25.0138	94.4292	10.06	16.39	0.NA	0.2348
BRS108/IA/19	25.0123	94.4286	8.39	43.75	0.7094	0.3089
BRS109/IA/19	25.0103	94.4286	14.66	30.46	0	0.2615
BRS110/IA/19	25.0080	94.4294	6.59	37.50	0.9254	0.3953
BRS111/IA/19	25.0093	94.4304	8.03	32.44	0.497	0.1865
BRS112/IA/19	25.0105	94.4304	11.49	28.58	0	0.2811
BRS113/IA/19	25.0141	94.4308	12.91	26.93	0	0.2806
PCS12/IA/19	24.9818	94.4322	6.14	42.74	0	0
PCS13/IA/19	24.9833	94.4337	8.50	33.76	0	0
PCS14/IA/19	24.9823	94.4338	7.12	42.90	0	0
PCS15/IA/19	24.9825	94.4338	8.59	39.38	0	0
PCS16/IA/19	24.9747	94.4265	5.70	43.97	0	0
PCS17/IA/19	24.9745	94.4271	5.33	34.95	0	0
PCS18/IA/19	25.0119	94.4308	9.1	28.28	0.6849	0.4466
PCS19/IA/19	25.0165	94.4299	7.16	29.71	0.7353	0.354
PCS20/IA/19	25.0374	94.4374	10.86	26.73	0.5068	0.2283
PCS07/IA/19	25.0134	94.4514	0.15	10.75	0.3251	0.2516
PCS23/IA/19	25.0445	94.4722	10.78	30.08	0.678	0.5724

7.6. GENESIS OF MINERALIZATION/GENETIC MODEL OF MINERALIZATION

The mineralization of chromitite pods occurs in harzburgitic host rock. This harzburgite is part of the transitional peridotite zone of the ophiolitic sequence and is confirmed by traces of relict chrome- spinel and relict magnetite in petrographic studies along with the occurrence of neoblastic olivines. The podiform chromites are slightly deformed but show no evidences of subsequent major tectonic events in the form of foliation and other metamorphic textures after emplacement. Therefore, any tectonic setup of dissemination of these chromitites can be ruled out and they are part of the primary emplacement processes during the formation of the ophiolitic units.

CHAPTER 8

RECOMMENDATION

Based on the analytical results, chromitite bearing transitional peridotites (harzburgite) show Cr_2O_3 values ranging from 31.11% to 53.53%, and also high values of nickel have been observed at Gamnom which ranges from 1.07% -1.79% and in Yentem yielding 1.41% of nickel. Scout drilling can be undertaken to check for the extent of depth of the chromitite and nickel occurrences in between, south of Khangkui Khullen (Block A), Gamnon (Block B and C) and Yentem (Block D) as demarcated on the map (Fig.50).

Red soil samples collected at Gamnom and south of Khangkui Khullen showed Fe_2O_3 percentages ranging from 10% to 43.75% and Al_2O_3 ranging from 0.2-14.66%. Further detailed studies can be undertaken.

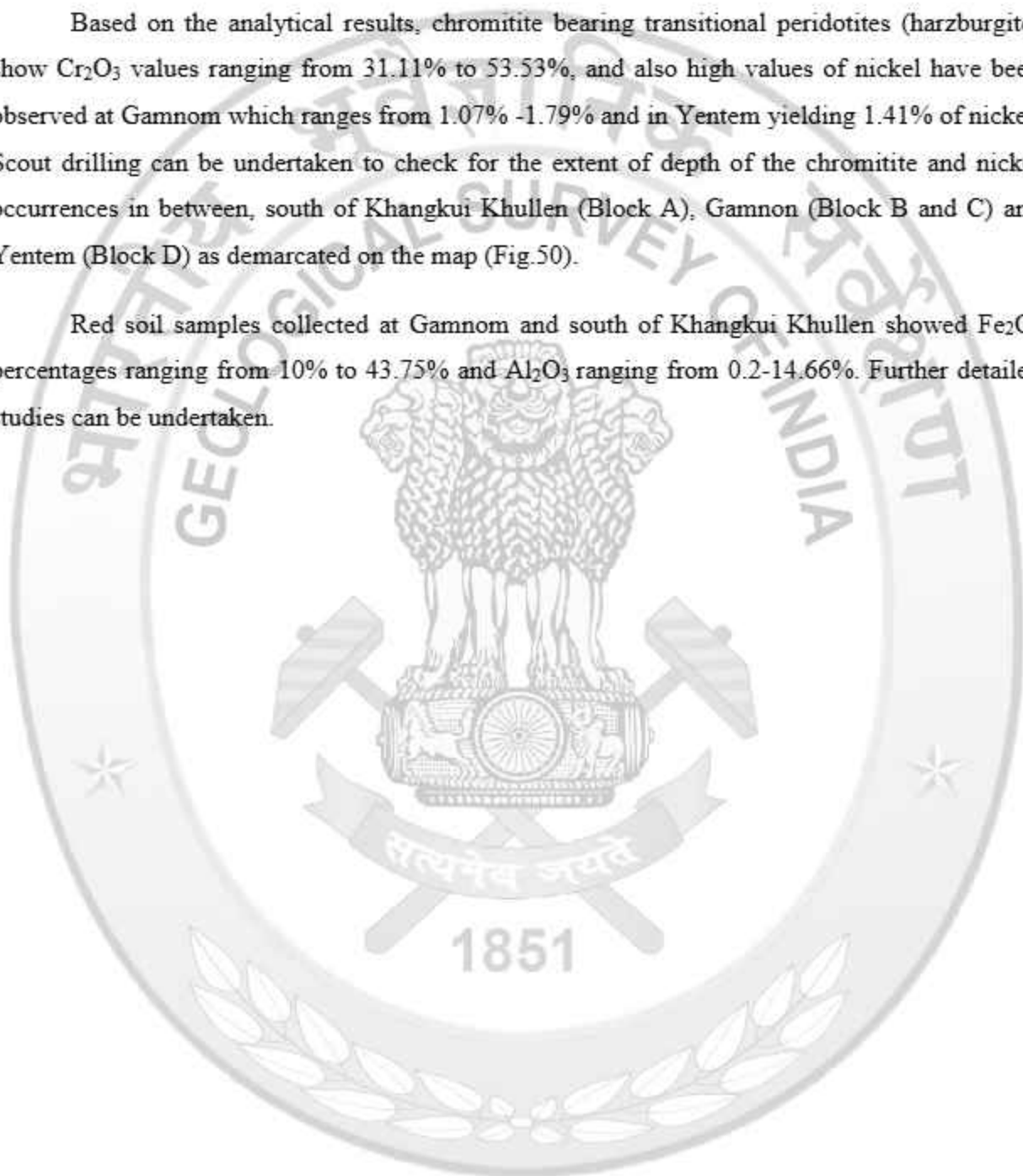


Table.7. Details of recommended blocks for further exploration:

Block	Location of the blocks		Significant values with sample no.
	Latitude	Longitude	
A	25° 1' 3.1"	94° 25' 41.1"	BRS77/IA/19 - 45.48% of Cr ₂ O ₃ ,
	25° 1' 3.8"	94° 26' 00.0"	BRS79/IA/19 - 42.67% of Cr ₂ O ₃
	25° 0' 20.3"	94° 25' 51.8"	PTS25/IA/19 - 44.11% of Cr ₂ O ₃
	25° 0' 23.8"	94° 25' 31.7"	PTS26/IA/19 - 36.11% of Cr ₂ O ₃ ,
			PTS27/IA/19 - 39.09% of Cr ₂ O ₃ ,
			PTS28/IA/19 - 45.66% of Cr ₂ O ₃
			PTS29/IA/19 - 47.51% of Cr ₂ O ₃ , PTS30/IA/19 - 45.23% of Cr ₂ O ₃
B	25° 1' 1"	94° 26' 19.4"	BRS73/IA/19 - 52.53% of Cr ₂ O ₃
	25° 1' 0.3"	94° 26' 34.5"	
	25° 1' 24.5"	94° 26' 24.2"	
	25° 0' 27.9"	94° 26' 9.0"	
C	25° 1' 27.9"	94° 26' 57.3"	PTS03/IA/19 - 44.37% of Cr ₂ O ₃
	25° 1' 23.1"	94° 27' 26.5"	PTS08/IA/19 - 40.53% of Cr ₂ O ₃ ,
	25° 0' 32.7"	94° 27' 11.8"	PTS09/IA/19 - 34.1% of Cr ₂ O ₃ ,
	25° 0' 27.6"	94° 26' 47.7"	PTS10/IA/19 - 40.5% of Cr ₂ O ₃ PTS11/IA/19- PTS20/IA/19 showing Ni ranging from 0.54 to 1.676% from transitional peridotite
D	24° 59' 10.6"	94° 25' 59.3"	PTS33/IA/19 – 1.41% of Ni
	24° 59' 9.2"	94° 26' 13.1"	PTS36/IA/19 – 0.88% of Ni,
	24° 58' 41.6"	94° 26' 5.6"	PTS38/IA/19 – 0.88% of Ni,
	25° 58' 43.7"	94° 25' 50.4"	

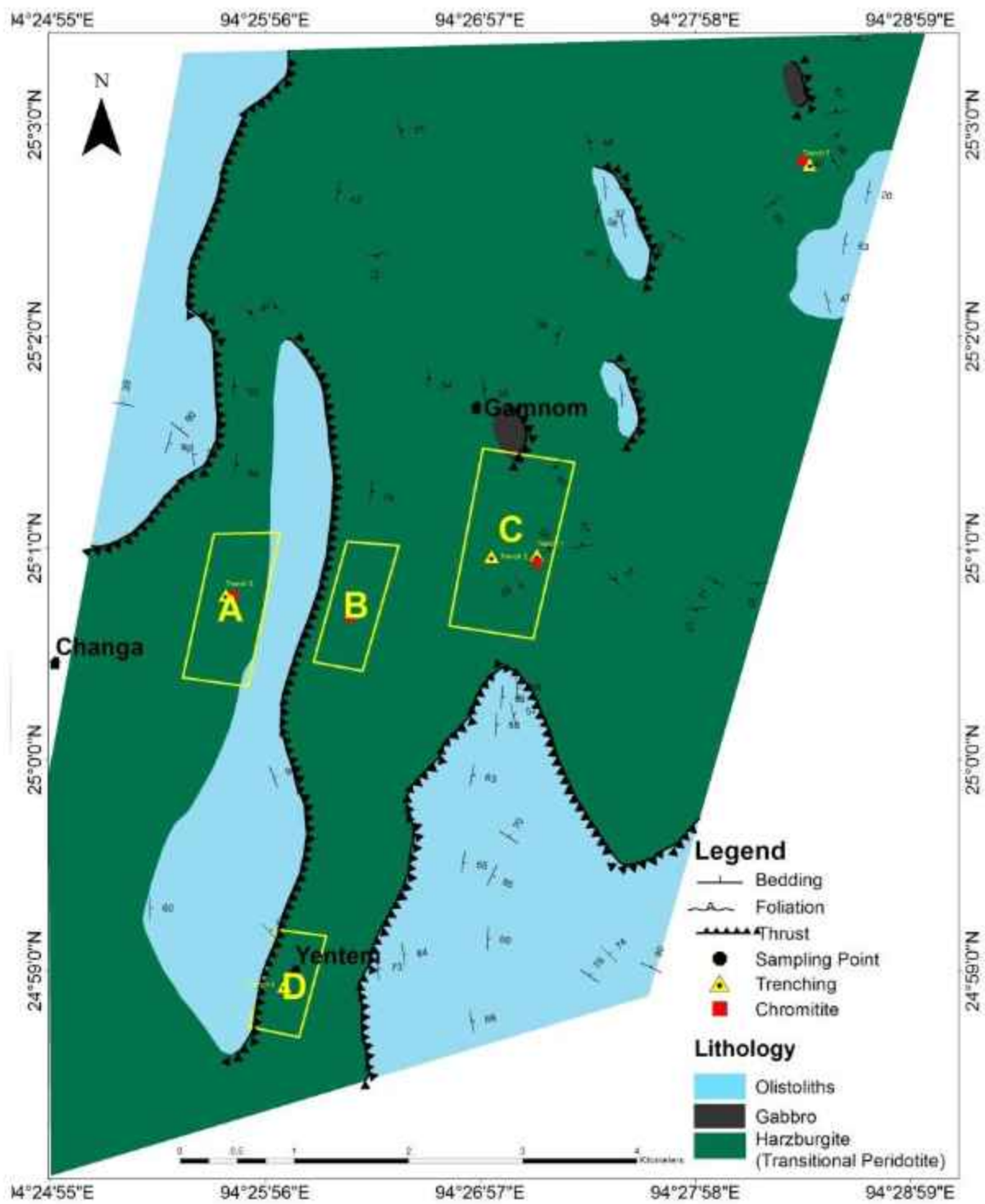


Fig.50. Recommended blocks for further exploration

CHAPTER 9

CONCLUSION

In the Gamnom-Yentem area, exploration for possible chromium, nickel and base metal mineralization was carried out during the course of Large Scale Mapping of 1:12,500 scale. It is part of the Manipur ophiolite belt which belongs to the Arakhan-Yoma fold belt.

The mapped area exposes a part of the ophiolite suite comprising of ophiolite units forming tectonic slivers which is thrust along with olistolithic units around Gamnom, Yentem, south of Khangkui Khullen and Pushing villages. The ophiolite is dominated by transitional peridotite along with thin slivers of Gabbro occurring at Gamnom and west of Pushing. This ophiolitic unit is juxtaposed along with the later deposited unit of olistoliths comprising of shales, sandstones and ophiolitic fragments. All the units occur as detached tectonic slivers which bear an N-S trend dipping easterly. The ophiolitic rock do not exhibit any traces of metamorphism and are thus confirmed to be part of the primary melt that was emplaced during the layering of the ophiolite sequence. Due to this the original igneous fabric has been maintained in fresh rocks belonging to the ophiolite sequence. But most of the surficial locations expose only highly weathered parts of the peridotitic rocks (harzburgite) that have undergone serpentinization. Hobnail texture which is a prominent feature of these weathered rocks is noticed everywhere within the peridotites which exhibits the protruding large crystals of orthopyroxenes within a ground mass of serpentinized peridotite. The gabbros form small tectonic slivers that are wedged between the harzburgites and show sub-ophitic texture where the amphiboles and laths of plagioclase are visible. The olistoliths comprise of thick sequence of flysch sediments with rhythmites of shale/slate, siltstone, and minor fine grained sandstone. It occurs with intercalation of siltstone and sandstone beds along with fragments of ophiolitic rocks. The lithological contacts are rarely exposed as most of them are covered by slides from steep hills, thick vegetation and weathered soil, impeding delineation of contact.

Petrological study of peridotite reveals that the peridotites are mainly harburgitic in composition having equi-modal percentage of clinopyroxene and orthopyroxene with olivine, chrome-spinel and magnetite completes the accessory mineral phase. Relict chrome-spinel (showing corroded boundary) and relict skeletal magnetite is observed in harzburgite. Development of neoblastic olivines at the cost clinopyroxene and orthopyroxene is observed

which is due to melt-rock interaction involving dissolution of pyroxenes and crystallization of olivine in the mantle segment. Grain boundaries of relict clinopyroxenes are corroded. Olivine and orthopyroxene are partially serpentinised. All these evidences prove that this peridotite (harzburgite) belongs to the transitional peridotite layer of the ophiolite sequence. Gabbro in thin section exhibit sub-ophitic to ophitic texture of pyroxene and hornblende within altered plagioclase laths. Clinopyroxenes are mostly altered to chlorite. Amphibole is formed by the breakdown of pyroxene. Sericitization of plagioclase is commonly observed.

The analytical result of the transitional peridotite(Harzburgite) is characterised by Fe_2O_3 (7%-13.7%), MgO (29% - 40.72%), Al_2O_3 (0-17.62%), TiO_2 (<0.01-1.9%), Cr (37ppm-9254ppm), Ni (30-8606ppm), Va (0-611ppm), Co (5-436ppm), Cu (<5-99ppm), Pb (2-14ppm), Zn (5-274ppm); in samples which are chromitite bearing transitional peridotites (harzburgite) show Cr_2O_3 values ranging from 31.11% to 53.53%. High values of nickel have been observed in samples collected during trenching at Gamnom which ranges from 1.07% -1.79% and in Yentem one sample yields 1.41% of nickel. 21 nos. of red soil samples were collected and the results showed Fe_2O_3 percentages ranging from 10% to 43.75% and Al_2O_3 ranging from 0.2-14.66%.

LOCALITY INDEX

Location	Latitude	Longitude	Toposheet No.
Gamnom	25°01'28"	94°27'8"	83 K/8
Khankhui Khullen	25°03'30"	94°25'10"	83 K/8
Pushing	25°02'30"	94°29'45"	83 K/8
Singcha	25°00'30"	94°29'45"	83 K/8
Yentem	24°59'10"	94°26'00"	83 L/5



REFERENCES

1. **Chakradhar, M and Gaur, M.P., (1985):** Systematic Geological Mapping around Jaluke, Kohima district, Nagaland. (F.S. 1984-85.)
2. **Chakravarty S. C. et al (1958):** A note on the reported occurrence of copper and nickel mineralisation in Manipur.
3. **Coleman R.G., (1977):** Ophiolites: Ancient oceanic lithosphere? (Minerals and rocks, Vol. 12, Springer)
4. **Das J. N. et al (1989):** Report on preliminary investigation of chromite occurrences in Hangkai area, Ukhrul dist., Manipur state. (F.S.1988-89.)
5. **Devdas, V and Gandhi, P (1985-86):** Systematic geological mapping in Maromi-Akaluto-Suruhuto areas Zunheboto district, Nagaland. (F.S.1985-86)
6. **Evans, P. (1932):** Explanatory notes to accompany a table showing the Tertiary succession in Assam. (Trans. Min. Geol. Met. Inst. Ind. Vol. 27. pp. 168 – 248)
7. **Geological Survey of India, (2011):** Geology and Mineral resources of Manipur, Mizoram, Nagaland and Tripura. (Geological Survey of India, Miscellaneous Publication, No.30, Part IV, Vol. 1, Part- 2)
8. **Ghosh, S. Dutta, A. and Chandrashekhar, V. (1980):** Integrated surveys in ultramafic belt of Manipur. (F.S.1979-80).
9. **Gupta, K.S et al (1992):** Report on preliminary investigation for chromite in Phangrai and Mantunching blocks of Ukhrul and Chandel districts, Manipur. (F.S.1989-90).
10. **Jena S.K. and Devdas V. (1984):** Systematic Geological mapping in (I) Didiua-New Yachang area, Wokha district, Nagaland. Geol. Surv. of India. (F.S.1983).
11. **Joshi A. And Yedekar, (1983):** Report on Bhandari- Lakhuti-Lotsu area, district Wokha, Nagaland. Geol. Surv. of India. Progress Report (F.S. 1981-82).
12. **Kamenetsky et al. 2001:** Factors controlling chemistry of magmatic spinel: an empirical study of associated olivine, Cr-spinel and melt inclusions from primitive rocks. (*Journal of Petrology* 42, 655-671.)
13. **Kumar, R. et al (2016):** Magnetic Survey for Chromite and associated mineral zones in Harbui Khayui-Gamnon Ophiolite Belt, Ukhrul District, Manipur. Unpublished GSI Report (F.S.2015-16).

14. **Oldham, R.D. (1883):** Report on the geology of parts of Manipur and Naga hills. (Geological Survey of India, Memoirs, 19, 216-242)
15. **Panda S. (2013):** An Overview of effective and promising role of Tangkhul Nagas in Shirui Village of Manipur-Ukhrul district in India to protect Shirui-Lily at Shirui Hills facilitating effective conservation of other threatened wildlives and their habitats in and around Shirui Hills. (Seventh Biennial Conference Indian Society for Ecological Economics (INSEE) Global Change, Ecosystems, Sustainability)
16. **Pascoe E.H., (1912):** Traverse across Naga Hills of Assam from Dimapur to the neighbourhood of Saramati peak. (Records. Geological Survey of India Vol XLII, pt.4.)
17. **Pascoe E. H., (1950):** A Manual of Geology of India and Burma. (Vol. Nos. 1 to 3.)
18. **Prasad, L.M, (1980-81):** A note on the reconnaissance stage geological investigation of Muhari. (F.S.1980-81)
19. **Prasad and Sharma (1977):** Integrated survey involving systematic geological mapping for the assessment of Ni content in soil along the Sangsai-Gamnon road. (F.S.1976-77)
20. **Ramprasad Y. et al (1984):** Integrated Survey in the serpentinite belt in Manipur east district, Manipur. (F.S.1983-84)
21. **Ramprasad Y. et al (1982):** Integrated survey for Ni-Co-V and pt. Group of metals and reported occurrences of asbestos and soapstone in the serpentinite belt in Manipur east, dist., (part of toposheet no. 83k/sw). (GSI progress report for F.S.1976-77)
22. **Ranga Rao, A.(1983):** Geology and hydrocarbon potentials of a part of Assam-Arakan basin and its adjoining region. Symp. Petroliferous basins of India. Pp. 127-158.
23. **Sarma, H. And Bhartiya, S.P. (1978):** Systematic Geological mapping around Tuli-Marangkong, Changtongya area of Mokokchung district. Nagaland, Geol. Surv. of India. (F.S. 1977-78)
24. **Spray J.G. (1984):** Possible causes and consequences of upper mantle decoupling and ophiolite displacement. (Geological Society (London) Special Publication 13, 255-268)
25. **S. Sun, W.F. Mc Donough (1989):** Chemical and Isotope Systematics of Ocean Basalts: Implications for Mantle Composition and Processes (vol. 42, Geological Society, London (1989), pp. 313-345)

26. **Theunuo K., et al. (FS 2013-15):** Specialised Thematic Mapping Of Ophiolite Suite Of Rocks Of Manipur Between Ningthi To Nungbi Khullen, Ukhrul District, Manipur (F.S.2013-15)
27. **Venkatramana, N. et al (1992):** Report on preliminary geophysical investigation for Chromite occurrences in Hangkau area, Ukhrul district, Manipur. Unpub. GSI Report (F.S.1988-89).
28. **Venkatramana, P. (1985):** Geology and Petrology of Manipur-Nagaland ophiolite Belt. (Rec. GSI Vol. 115 pt.2, pp 98-104)
29. **Venkatramana, N. et al (1993):** Report on preliminary geophysical investigation for Chromite occurrences in Phangrai area, Ukhrul district, Manipur. Unpub. GSI Report (F.S.1992-93).
30. **Vidyadharan. K.T. et al (1984):** Report on systematic geological mapping around Lambui-Shangshak-Shingcha, Gamnom-Mapum, Ukhrul-Siroi, Nungbi-Khamasom sectors of Manipur Ophiolite belt, Ukhrul district, Manipur. (F. S.1983-84).
31. **Vidyadharan K. T. et al (1985):** Report on the interdisciplinary studies in Manipur – Nagaland Ophiolites (Parts of Toposheet Nos. 83 K/7, 8, 11 and 12) (F. S.1983-84)
32. **Peter V.S et al, (2019):** Specialised thematic mapping in and around New Tusom – Chingai to elucidate the tecto-metomorphitic history in Naga hills ophiolite belt of Nagaland-Manipur and to delineate the associate mineralization (F.S.2017-18 and 2018-19)
33. **Yanthan, N. et al (2012):** Investigation for Platinum Group of elements in ophiolite belt of Manipur (G-4, Stage). Unpublished G.S.I. final report, (F.S.2009-10 & 2010-12)
34. **Yedekar, D.B. and Ray, B. (1984):** Systematic Geological mapping in Changpang Mirinokpo area, Wokha and Mokokchung districts, Nagaland. Geol. Surv. of India (F.S. 1983-84.)

Plate I
LARGE SCALE GEOLOGICAL MAP
OF GAMNOM-YENTEM AREA,
UKHRUL DISTRICT, MANIPUR
IN PARTS OF T.S. NOS.83K/8 & 83L/5
(1:12,500)

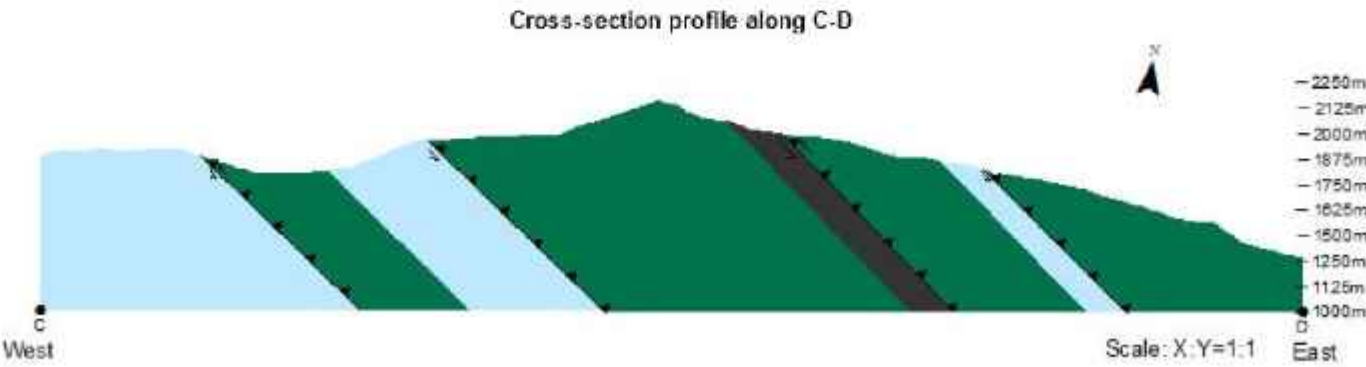
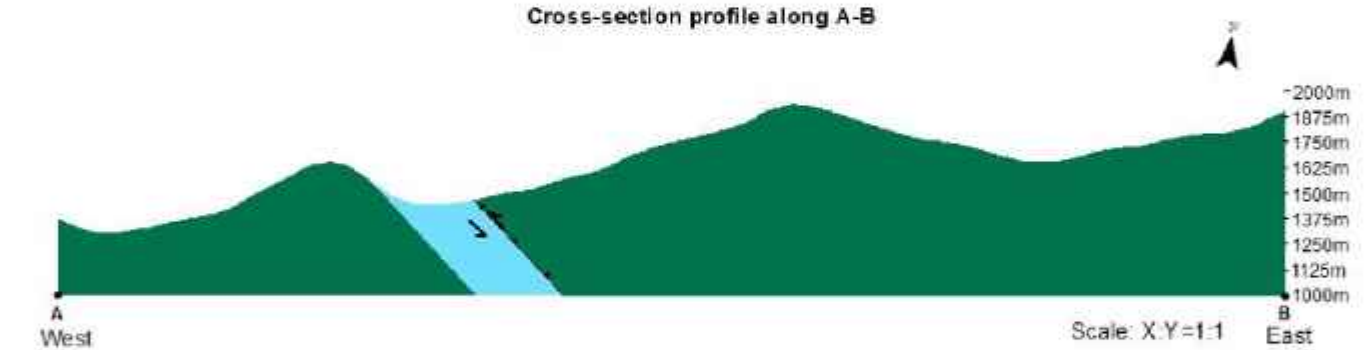
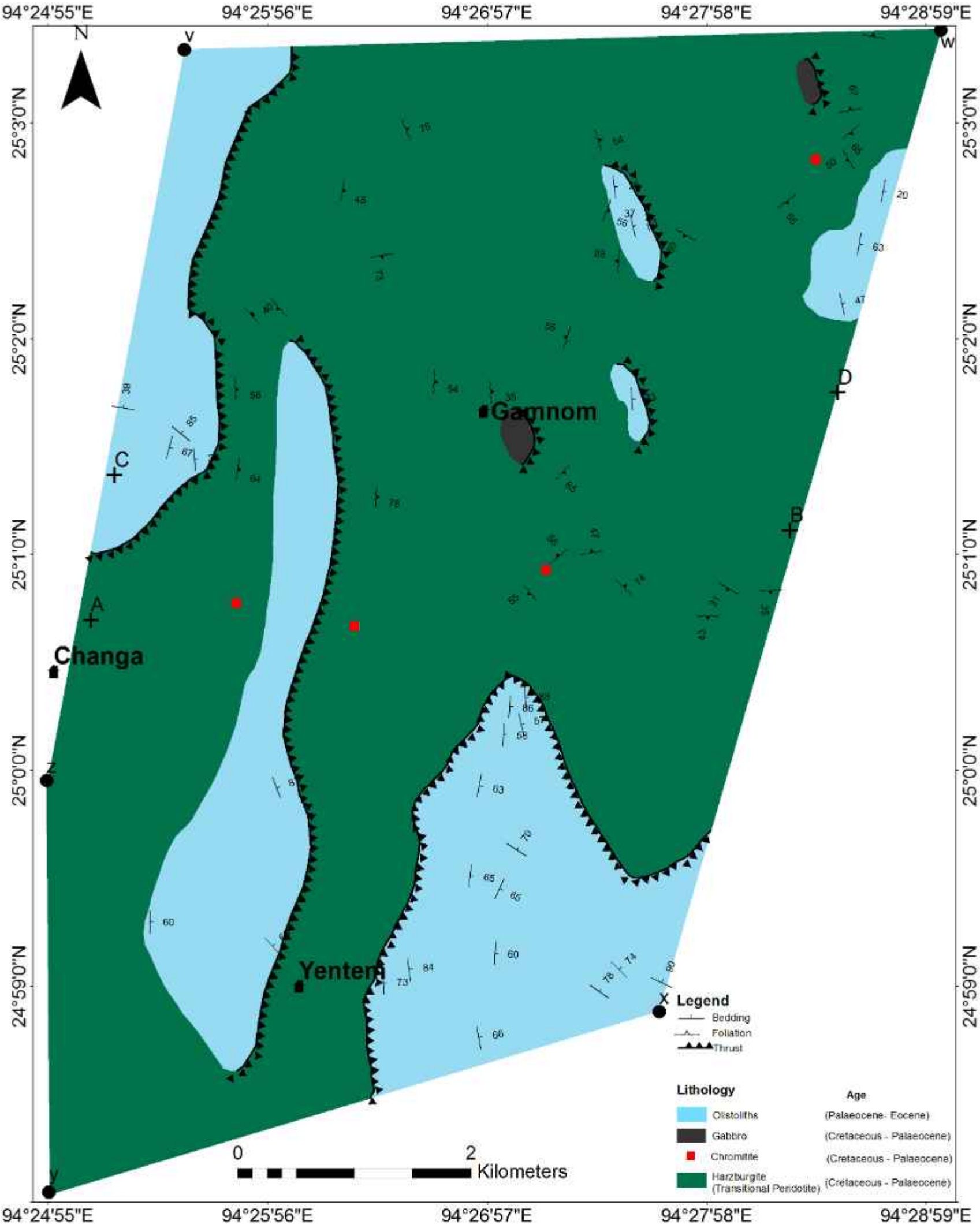
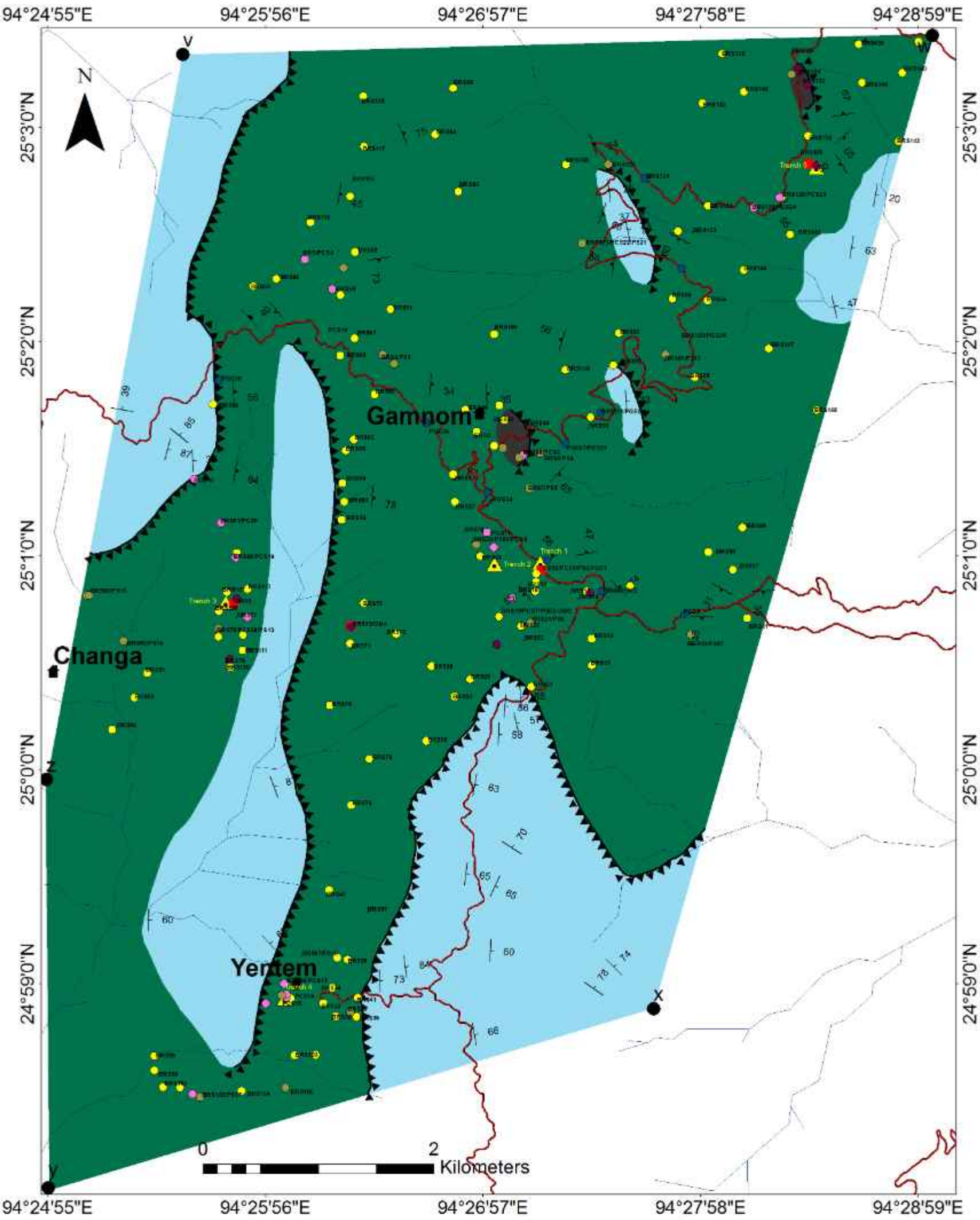












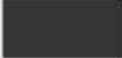




Plate II

LOCATION OF SAMPLING POINTS ON LARGE SCALE GEOLOGICAL MAP OF GAMNOM-YENTEM AREA, UKHRUL DISTRICT, MANIPUR IN PARTS OF T.S. NOS.83K/8 & 83L/5 (1:12,500)



Legend

	Drainage	Sample type
	Road	 BRS
	Bedding	 OM
	Foliation	 PCS
	Thrust	 PGE
	Trenching	 PS
Lithology		Age
	Olistoliths	(Palaeocene- Eocene)
	Gabbro	(Cretaceous - Palaeocene)
	Chromitite	(Cretaceous - Palaeocene)
	Harzburgite (Transitional Peridotite)	(Cretaceous - Palaeocene)

GEOLOGICAL SURVEY OF INDIA

APPENDIX-I

Data sheet on report movement in connection with its scrutiny



Project/Division: Mineral Exploration, SU: Manipur-Nagaland
 PSP No: M2AFGBM-MEP/NC/NER/SU-MAN/2019/24286, Mission: IIA
 Title of the report: Reconnaissance survey for chromium, nickel and base
 metal mineralization in Gamnom-Yentem area in part of Manipur
 ophiolite belt, Ukhrul District, Manipur.

Name of author (s): Imomeren Ao, Sr. Geologist (PI) Y. S. Peter, Geologist	Date of submission of report to the Supervisory Officer: 20-06-2020 Signature of the senior most author:
Name of Supervisory Officer: J. K. Angami, Director	Date of receipt of report: 30-06-2020 Date of completion of scrutiny: 15-07-2020 Date of handing over report to the author after scrutiny: 15-07-2020 Signature:
Name of author (s) To whom the report has been handed over by the Supervisory Officer: Imomeren Ao, Sr. Geologist	Date of receipt after scrutiny: 15-07-2020 Signature: Date of resubmission: 28-07-2020 Signature:
Supervisory Officer: J. K. Angami, Director	Date of receipt after modification: 29-07-2020 Date of handing over report to the Regional Mission Head: 31-07-2020 Signature:
Name of Regional Mission Head: RANJIT RANJAN RAUL	Date of receipt of report: Date of handing over the report after peer review to the Project Director: Signature:
Name of Supervisory Officer: J. K. Angami, Director	Date of receipt from the Regional Mission Head after peer review: 06-10-2020 Date of handing over to author(s): 07-10-2020 Signature:
Name of author(s): Imomeren Ao, Sr. Geologist (PI) Y. S. Peter, Geologist	Date of receipt of report from Supervisory Officer: 07-10-2020 Date of handing over report after modification to Supervisory Officer: 25-03-2021 Signature:
Name of Supervisory Officer: J. K. Angami, Director	Date of receipt of report after modification from the author(s): 25-04-2021 Date of handing over report to Regional Mission Head: 28-04-2021 Signature:
Name of Regional Mission Head: RANJIT RANJAN RAUL	Date of receipt after modification from the Project Director: 03/06/2021 Date of handing over the report to the HoD of the Region for approval: 08.06.2021 Signature:
Name of the HoD of the Region: DR. RAJESHWAR DDG & HOD	Date of receipt of report for approval: 08.06.2021 Date of approval: 08.06.2021 Date of sending back report to Project Director: Signature of the HoD:
Name of the Project Director: J. K. Angami, Director	Date of receipt of report after approval of HoD: 25/6/21 Date of circulation of report: Signature:



GEOLOGICAL SURVEY OF INDIA

Certificate of Quality of the Report

Project/Division: SU: Manipur-Nagaland

FSP No. M2AFGBM-MEP/NC/NER/SU-MAN/2019/24286

Mission: II

Title of the report: Reconnaissance survey for chromium, nickel and base metal mineralization in Gannam-Yentem area in part of Ophiolite belt, Ukhrul District, Manipur (G4)

Part-A

This is to certify that the following officer(s) have carried out the above mentioned FSP and are responsible for collection of field data, carrying out the required laboratory analysis, compilation and synthesis of field data, coalition of the data and writing of the report as per the approved guidelines. The duration of field stay of each officer(s) is as against his/her name.

Name(s)/Designation of the Field Officer	Total field stay during the FSP (No. of days)	Signature with date
Imomeren Ao, Sr. Geologist	120	
Vales Savio Peter, Sr. Geologist	115	

Part-B

This is to certify that drilling has been carried out and completed as per the table given below: NA

Drilling Unit No.	Date of commencement of drilling	Date of completion of drilling	Name and Signature of the Director Drilling

Part-C

This is to certify that geophysical component of the item has been carried out as per the table given below: NA

Name(s)/Designation of Geophysicist	Date of commencement of work	Date of completion of work	Signature with date of the Geophysicist
Name and signature with date of the Director (Geophysics)			

Part-D

This is to certify that the chemical analysis of the geological samples has been carried out as per the table given below:

Name of Director in charge of the Chemical Lab.	Dates of receipt of samples from the field officer party				Date of providing complete analytical results to the field officer.	Signature with date of the Director Chemistry
Director Chemical Division NER, Shillong	NLS	28 Nov	NER 3754(1)	31 Nov (15.10.2018)	12.02.2021	Jayaude K. Naik
			NER 3754(2)	02 Dec (11.12.18)		
			NER 3755(1)	05 Dec (14.02.19)		
			NER 3755(2)	05 Dec (14.02.19)		
	NRY	14 Dec	NER 3755(3)	11 Dec (15.10.2018)		
			NER 3755(4)	12 Dec (11.12.18)		
			NER 3755(5)	13 Dec (14.02.19)		
			NER 3755(6)	13 Dec (14.02.19)		
	NTR	30 Dec	NER 3755(7)	30 Dec (21.12.19)		
			NER 3755(8)	30 Dec (21.12.19)		
Shr J.K. Naik, Director	NLS	10 Dec	NER 3755(9)	02 Dec (11.10.2018)		
			NER 3755(10)	02 Dec (11.10.2018)		

Part-E

This is to certify that the below mentioned Supervisory Officer(s) have supervised the above item and have provided guidance to the field Officer(s). The number of inspection visits and total duration of field visits is as per the below table. It is also certified that the work carried out under the project is of high standards, the norms of field work, lab work etc. have been followed. It is also certified that thorough scrutiny of the report for maintaining the scientific contents and its Quality has been overseen.

Name(s) Designation of the Supervisory Officer	No. of inspection visits made to the field area	Total No. of days spent on inspection visit	Signature with date
Shr J.K. Angami, Director	3	8	J.K. Angami

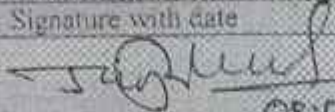
Part-F

This is to certify that the report has been thoroughly scrutinized at the Regional Mission/Head level. The scientific contents and the Quality of the report are certified. The report has been peer reviewed and the needed corrections have been attended to.

Name(s) Designation of the Regional Mission	Signature with date
Head RANJIT RANJAN RAUL	R. Raul

Part-G

This is to certify that the above report has been scrutinized at various levels and has also been peer reviewed. On being satisfied regarding the scientific contents and the Quality of the report, the undersigned has accorded approval for its circulation.

Names/ Designation of the Regional HoD	Signature with date
Dr. J. Rajeshwar Deputy Director General & HOD, GSI, NER, Shillong	 08.06.2024

Appendix-III

INFORMATION SHEET FOR BIBLIOGRAPHY DATABASE IN UNPUBLISHED REPORTS

TITLE OF FIELD	REQUIRED INFORMATION
TITLE	Title of the report: Reconnaissance survey for chromium, nickel and base metal mineralization in Gamnom-Yentem area in part of Ophiolite belt, Ukhrul District, Manipur (G4) <i>{As it appears in the report}</i>
AUTH	Name of author (s): Ao Imomeren, Vales Savio Peter. <i>{Surnames first, with first letter in capitals}</i>
TDOC	Type of documents: Finale report for the FS 2019-2020. <i>Fill in any one of the following-</i> Final report / Interim report / General report / Preliminary report / Pre-construction report / Post-construction report / Construction report.
CONF	Identification of the confidentiality of the report: Open <i>Fill in any one of the following-</i> Secret / Confidential / Classified / Restricted / Open / General / Unclassified
CORP	Corporate body (ies): <i>Fill in name of the following from where report is being issued.</i> Region : North Eastern State Unit : Manipur- Nagaland Division / Project : Mission-IIA
BENE	Name of the beneficiary of the study when GSI has worked for some external organisation or ministries: Not Applicable <i>{e.g. Dept. of Irrigation, Govt. of Rajasthan; Ministry of Defence}</i>
DCNU	Document number: FSP No. M2AFGBM-MEP/NC/NER/SU-MAN/2019/24286, vide item no: Mission: II-A <i>{The item no. as it appears in the Annual Programme - FSP}</i>
FSPR	Field Season Programme Year: 2019-2020
DPUB	Date of publication of the document: March, 2021 <i>{Year and month only}</i>
ABST	Concise abstract of the document restricted to 2000 characters (inclusive of blank spaces) Included in the report
MPRF	Mapping reference: Toposheet (s) No. : 83K/8 and 83L/5 Landsat Scene (s) No. if any: none

PROFORMA

- Title of the Report : Reconnaissance survey for chromium, nickel and base metal mineralization in Gamnom-Yentem area in part of Ophiolite belt, Ukhrul District, Manipur (G4).
- Name of the authors : Imomeren Ao , Vales Savio Peter
1. Background of the investigation at whose instance or with what particular objective in view the investigation was undertaken : In Ukhrul district of Manipur state, Occurrences of chromitite were reported near Phangrai, Shirui, Gamnom, Shingcha and Pushing villages (Ghosh et al., 1980, Vidyadharan, K. T. et al., 1985, Ramprasad, Y. et al., 1982, 1984, Gupta, K.S. et al., 1992, Theunuo, K. et al., 2015). New occurrences of chromites were also reported in the lower elevation of the HarbuiKhayui hilltop in the South and Southwest extension of Gamnom. Occurrences of massive chromite nodular chromite disseminated chromite ore associated with seipentinisedharzburgite were reported(K. S. Gupta et al., 1992).
- GSI has conducted geophysical survey in Hangkau and Phangrai area in Ukhrul district, Manipur (N.Venkataramana et al., (1989,1993). Significant and sharp magnetic responses have been recorded over ultramafics and over known chromite occurrences in the area. From the order of magnitudes of magnetic and resistivity values, the anomalies can be attributable to the sources at shallow depth. Shallow depth persistence of 5 to 7 meters was estimated for anomalous zones containing known chromitemineralization.
- K. Sharma, et al., (1982, 1984) reported enrichment of Ni (up to 9000ppm) in the soil developed over the ultramafic, near Gamnom area, although Ni sulphides mineralization was not reported.
- Occurrences of chromite have beenreported from the adjoining areas of Gamnom, Shingcha and HarbuiKhayui hill ranges in Khangkhui hamlet, Ukhrul, Manipur. GSI has located clusters of chromitite pods towards SEof Gamnom, and subsequently, the Directorate of Commerce and Industries, Govt. of Manipur has

further assessed these resources in detail. In Manipur ophiolite, chromitite occurrences are associated with ultramafics as nodular and podiform bodies while few occur as massive bodies.

Prasad and Sharma (1977) during their integrated survey involving systematic geological mapping for the assessment of Ni content in soil along the Sangsai-Gamnom road and systematic collection of integrated samples in select areas of ultramafic belt near Gamnom, Manipur East Dist., Manipur has located few chromitite pockets. Analytical results indicate that Ni value range from 120 to 8500 ppm, and Co from 120 to 760 ppm from 126 nos. of soil samples.

Gupta and Purushothaman (1991) carried out preliminary investigation for chromite in Phangrai and Mantumching blocks of Ukhrul and Chandel districts, Manipur. They have reported occurrences of chromitite in the form of pods, pocket and lenses within the serpentinized harzburgite with varying degrees of serpentinization. The large size of the chromite pieces and the scale of the chromite segregations that are randomly distributed certainly suggest that the first stage of chromite formation was related to a deep mantle magmatic segregation of chromite. Limited analysis of pit/trench samples indicate maximum value of Cr₂O₃ (53.29%), Fe₂O₃ (14.77%), Al₂O₃ (16.19%), MgO (18.24%) and Ni (0.23%) from 29 nos. of samples. They reported that the chromite falls under grade-I and II categories.

Yanthan et al. (2012) carried out PGE investigation in HarbuiKhayui-Gamnom area; however, no encouraging values are indicated. Higher values of Ni (1946 to 4101 ppm), Cr (1697 to 2852 ppm) in peridotite and Ni (2159 to 2344 ppm) Cr (1511 to 2222 ppm) in harzburgite were reported from 60 nos. of samples.

Theunuo et al. (2015) carried out Specialised Thematic Mapping (1:25,000) of ophiolite suite of rocks of Manipur between Ningthi to NungbiKhullen, Ukhrul District, Manipur and has reported large clusters of chromitite pods from Gamnom area, with a dimension of about 100mx50m. Ni values range from 1988 to 3996 ppm, and Cr from 1086 to 4772 ppm. The chromitite body occurs only as

Pods and lenses within coarse grained harzburgite.

Taking into consideration all the above aspects, preliminary investigation has been carried out during FS 2019-2020 with an objective to delineate potential zones of chromium, nickel and base metal mineralization in mafic-ultramafic rocks of Gamnom-Yentem area in the Manipur ophiolite belt.

2. Whether the item of investigation was included in the approved programme for the year concerned. If so, particulars, such as item No., page reference etc. may be given. : Yes, Item No. M2AFGBM-MEP/NC/NER/SU-MAN/2019/24286.
3. Date of commencement of the investigation with month and year, and exact number of days spent by the officers(s) in the field in connection with the investigation : 10th June 2019
Imomeren Ao, Senior Geologist 120 days,
Vales Savio Peter, Senior Geologist, 115 days.
4. Brief comments by Director/Supervisory officer on the conclusion and recommendation by the author(s) with suggestion for implementing the same. : I agree with the interpretation, conclusions and recommendations drawn by the authors in accordance with the field and available analytical data and recommend follow up of the investigation. Chromitite bearing transitional peridotites (harzburgite) show Cr₂O₃ values ranging from 31.11% to 53.53%, and also high values of nickel have been observed at Gamnom which ranges from 1.07% -1.79% and in Yentem yielding 1.41%. Scout drilling as suggested by the authors can be undertaken to check for the extent of depth of the chromitite and nickel. Red soil samples collected at Gamnom and south of Khangkui Khullen showed Fe₂O₃ percentages ranging from 10% to 43.75% and Al₂O₃ ranging from 0.2-14.66%.
5. Please state specifically how the results of the investigation were achieved compared with the objective for which it was undertaken. : The investigation fulfilled its objective successfully and has achieved the target in stipulated time though the work was executed in adverse ground reality.



Place: Dimapur
Date: 30.03.2021

Signature:
Name: J. K. Angami
Designation: Director

FORMAT OF REPORT ON MINERAL EXPLORATION IN TERMS OF UNFC COMPLIANCE			
Title of the report	Reconnaissance survey for chromium, nickel and base metal mineralization in Gamnom-Yentem area in part of Ophiolite belt, Ukhrul District, Manipur (G4)		
Authors	Imomeren Ao, Senior Geologist Vales Savio Peter, Senior Geologist		Year: 2019-20
Stage: G-4	Nature of compliance required	Complied (Page No.) / Not complied	Remarks
I) Summary	(1) Factual Data	Complied (Summary)	
	(2) Recommendations	Complied (Page No. 72)	
	(3) Cost estimation	Not complied	
II) Introduction	(4) Scope & Purpose	Complied (Page No. 7)	
	(5) Authority	Complied (Page No. 7)	
	(6) Current/Post Property Examination (BGI)	Not complied	
	(7) Principal Sources of Information	Complied (Page No. 7)	
	(8) Acknowledgement	Complied (Page No. 8)	
III) Property Description	(9) Size, Continuity, Shape, surface rights	Complied (Page No. 9)	
	(10) Third party issue	Not complied	
	(11) Climate/rights with dates	Complied (Page No. 13)	
	(12) Land Title Officer	Not complied	
	(13) Lat/Long/Village/town/district/mine site	Complied (Page No. 75)	
	(14) Accessibility/infrastructure	Complied (Page No. 11)	
	(15) Land nature/water/timber/power/gas/agriculture/manpower	Complied (Page No. 11)	
	(16) Environmental issues/plan act/park/preservation	Complied (Page No. 13)	
	(17) Climate/topography	Complied (Page No. 13)	
	(18) Impact on landscape on mining	Not complied	
	(19) Map of area/Block with roads/accessibility	Complied (Fig.1, Page-11 and Plate-1)	
IV) History	(20) Previous work highlights	Complied (Page No.17-20)	
	(21) Attachment of previous maps/sections/tables	Complied (Fig. 4, Page 22 and plate-I)	
	(22) Previous Mining History	Not complied	
	(23) Reasons for closure	Not complied	
	(24) Earlier production data	Not complied	
	(25) Data on nearby mines	Not complied	
(V) Geoscience investigation			
(1) Geology	(26) Stratigraphy	Complied (Page No. 33)	
	(27) Lithology	Complied (Page No. 17-20)	
	(28) Structure (with maps/profiles)	Complied (Page No. 45)	
	(29) Alteration Zones	Complied (Page No.70)	
	(30) Geotechnical	Not complied	
	(31) Adequacy of data density	Complied (Plate-I)	
	(32) Reliability (quality & quantity)	Complied (Page No. 72-73)	
	(33) Geological model	Not complied	
(II) Investigation methods	(34) Instrument & Technique	Complied (Page No. 49)	
	(35) Geology (Map with scale)	Complied (Plate-1)	

	(36) Geophysical (with maps & scale)	Not Complied	
	(37) Geochemical (with map & scale)	Not complied	
	(38) Data density of above	Complied (Plate-1,2,3)	
	(39) Size & style of mineralised zone	Complied (Page No. 66-70)	
	(40) Diagrams	Complied (Page No. 53-63)	
	(41) Metallurgical tests	Not complied	
	(42) Deleterious contamination source	Not complied	
(VI) Mineral Deposits			
(I) Features of deposit	(43) Type of mineralisation	Complied (Page No66)	
	(44) Mode of occurrence	Complied (Page No. 68)	
	(45) Nature of mineralisation (gosaan/alteration/structure)	Complied (Page No. 68)	
	(46) Reflectance of Mineralisation on geology/gp/gc	Not complied	
	(47) Map given	Complied (Plate-1)	
(II) Sampling details	(48) Quality & Quantity of sample information	Complied (Annexure-I-III)	
	(49) Reliability on resource estimation	Not complied	
	(50) Nature of sampling Bed rock/grab/channel)	Complied (Page No. 49)	
	(51) Sampling method	Complied (Page No. 49)	
	(52) Introduction of duplicates in analysis	Not complied	
(III) Analysis details	(53) Laboratory		
	(54) Analytical methods		
	(55) Precision & accuracy		
	(56) Cross check analysis details	Not complied	
(IV) Quality/Grade	(57) Statistical data processing	Not complied	
	(58) Cut off grade	Not complied	
	(59) Assumptions	Not complied	
(V) Resource estimation	(60) Geological interpretation	Complied (Page No. 72-73)	
	(61) Statement of tonnage & grade	Not complied	
	(62) Geometry of mineralisation assumed	Not complied	
	(63) Method adopted to arrive estimation	Not complied	
	(64) Estimation	Not complied	
(VI) Economic viability	(65) Rough estimation of economic viability	Not complied	
	(66) Intrinsic economic interest	Not complied	
	(67) Eventual economic exploration	Not complied	

CERTIFICATE: Certified that this report is in compliance with UNFC G-4 stage of Mineral investigation

Place:

Date:

Scrutinizer & Designation:

Signature:

Appendix-VI

GEOLOGICAL INPUTS **Information for Mineral Search and Exploration**

A. Number of field days spent by Geologist and Surveyor:

S. No.	Name and designation	Number of days
1.	Imomeren Ao, Senior Geologist	120
2.	Vales Savio Peter, Senior Geologist	115

B. Pitting and trenching: 50 cu.m

C. Drilling : Nil

D. Laboratory analysis:

SL.	Nature of analysis	No.	Method	Radicals
i.	Mineralogical	Nil		
ii.	Chemical analysis of core samples	Nil		
iii.	Soil samples	Nil		
iv.	Rock samples (BRS, PCS, PTS, PGE)	235	XRF, ICP-MS	Major oxides, REE, Traces, Base metal
v.	Gold	Nil		
vi.	Hydrological	Nil		
vii.	Geotechnical study	Nil		
viii.	Petrological study	35		



भारत का राजपत्र The Gazette of India

सी.जी.-डी.एल.-अ.-07042022-234959
CG-DL-E-07042022-234959

असाधारण
EXTRAORDINARY

भाग II—खण्ड 3—उप-खण्ड (i)
PART II—Section 3—Sub-section (i)

प्राधिकार से प्रकाशित
PUBLISHED BY AUTHORITY

सं. 270]
No. 270]

नई दिल्ली, बृहस्पतिवार, अप्रैल 7, 2022/चैत्र 17, 1944
NEW DELHI, THURSDAY, APRIL 7, 2022/CHAITRA 17, 1944

खान मंत्रालय

अधिसूचना

नई दिल्ली, 7 अप्रैल, 2022

सा.का.नि. 284(अ).—केंद्रीय सरकार, खान और खनिज (विकास और विनियमन) अधिनियम, 1957 (1957 का 67) की धारा 4 की उपधारा (1) के दूसरे परंतुक द्वारा प्रदत्त शक्तियों का प्रयोग करते हुए और भारतीय गुणवत्ता परिषद् के राष्ट्रीय शिक्षा और प्रशिक्षण प्रत्यायन बोर्ड (क्यूसीआई-एनएवीईटी) द्वारा प्रदत्त प्रत्यायन के परिणामस्वरूप, उक्त अधिनियम की धारा 4 की उपधारा (1) के उक्त दूसरे परंतुक के प्रयोजनों के लिए भारत सरकार के खान मंत्रालय के आदेश संख्या एम. VI-16/15/2021-खान VI, तारीख 12 अगस्त, 2021 (जिसे इसमें इसके पश्चात् प्रत्यायित प्राइवेट खोज अभिकरणों की अधिसूचना के लिए उक्त मार्गदर्शक सिद्धांत कहा गया है) द्वारा जारी किए गए प्रत्यायित प्राइवेट खोज अभिकरणों की अधिसूचना के लिए मार्गदर्शक सिद्धांतों में यथा विनिर्दिष्ट "प्रवर्ग 'क' खोज अभिकरण" के अधीन मैसर्स यूनाईटेड एक्सप्लोरेशन इंडिया प्राइवेट लिमिटेड को अधिसूचित करती है।

2. अभिकरण, प्रत्यायित प्राइवेट खोज अभिकरणों की अधिसूचनाओं के लिए उक्त मार्गदर्शक सिद्धांतों में विनिर्दिष्ट शर्तों की अनुपालना के साथ भावी संक्रियाएं करेगा।

3. यह अधिसूचना राजपत्र में इसके प्रकाशन की तारीख को प्रवृत्त होगी और अधिसूचना की तारीख से तीन वर्ष की अवधि के लिए या उसकी समाप्ति तक या प्रदत्त प्रत्यायन की समाप्ति तक, जो भी पहले हो विधिमाम्य होगी।

[फा. सं. एम-VI-16/22/2022-खान VI]

डॉ. वीणा कुमारी डरमल, संयुक्त सचिव

MINISTRY OF MINES**NOTIFICATION**

New Delhi, the 7th April, 2022

G.S.R. 284(E).—In exercise of the powers conferred under the second proviso to sub-section (1) of section 4 of the Mines and Minerals (Development and Regulation) Act, 1957 (67 of 1957) and consequent upon accreditation provided by the National Accreditation Board for Education and Training of the Quality Council of India (QCI-NABET), the Central Government hereby notifies the M/s. United Exploration India Private Limited under 'Category A Exploration Agencies' as specified in the guidelines for notification of accredited private exploration agencies issued by the Government of India in the Ministry of Mines vide order No. MVI-16/15/2021-Mines VI, dated the 12th August, 2021 (hereafter referred to as the said guidelines for notification of accredited private exploration agencies) for the purposes of the said second proviso to sub-section (1) of section 4 of the said Act.

2. The agency shall carry out prospecting operations in compliance with the conditions specified in the said guidelines for notifications of accredited private exploration agencies.

3. This notification shall come into force on the date of its publication in the Official Gazette and shall remain valid for a period of three years from the date of notification or till expiry or termination of the accreditation granted, whichever is earlier.

[F. No. M-VI-16/22/2022-Mines VI]

Dr. VEENA KUMARI DERMAL, Jt. Secy.

Annexure-3
Details of Project Members and Associates

❖ **ABOUT UNITED EXPLORATION INDIA PRIVATE LIMITED:**

United Exploration India Private Limited (UEIPL) is an emerging consulting firm managed by professionals and performed by a perfect mixture of technical experience and energy, in field of mining, geology & survey wherein end-to-end solutions is being offered to client.

UEIPL is an ISO 9001:2015 company and has also been accredited under the scheme of QCI NABET as an Exploration (APA) and Mine Planning Preparation Agency (MPPA). A detail of the company can be sought out in the company's website www.unitedexploration.co.in.

UEIPL has been engaged in several nos. of exploration projects in India which involves around 4.00 lakhs meter of drilling supervision. Besides Exploration and Drilling Projects in both Coal and Non-Coal, UEIPL has also been engaged by several esteemed clients for carrying out different reports like:

- Geological Report of Coal & Non Coal,
- Mining Plan & Mine Closure Plan (for both Major and Minor Minerals),
- Environmental Impact Assessment & Environmental Management Plan Study,
- Technical Assessment reports during auctioning of both coal and mineral blocks,
- Due-diligence Reports for both Coal & Minerals,
- Forest and Environment Clearances (through our associate M/s CEMC Limited, Bhubaneswar, also a NABET accredited company),
- Hydro-geological Study,
- Geophysical Survey for Groundwater survey and mineral exploration
- GIS and Remote Sensing for Land Information System,
- Topographic and Stack (Volume) Survey work with DGPS and/or ETS.
- Detailed Project Report and Feasibility Reports
- District Survey reports

Besides the knowledge base report preparation, UEIPL also entered to cater the drilling needs of various clients.

❖ **STRENGTHS:**

The strength of the organization is skilled human resources with an enriched versatility with senior renowned professionals. The team is well composed of:

- 16 Geologists.
- 5 Mining engineers.
- 1 Geophysicist.
- 3 Surveyors.
- 2 drilling operators & other supporting staffs.
- 2 Civil Engineers.
- 1 Electrical Engineer.
- 5 Other Administrative officers and Staffs.

❖ **ASSETS:**

Beside our well-trained human resources UEIPL has a huge support of modern software's & equipment's.

➤ **SOFTWARE'S:**

- GEOVIA Minex 6.3.
- GEOVIA SURPAC 2022
- ARES Commander 2020 for survey data analysis, volumecalculation.
- AutoCAD 2020 for survey data analysis, volume calculation.
- Arc-GIS Software.

➤ **SURVEY EQUIPMENTS:**

- Three number of Total Stations: SOKKIA CX 65, SOKKIA CX 101, SOKKIA 107.
- One Scanner: TRIMBLE STS 730

➤ **DRILLING EQUIPMENTS:**

- 1 number KDR-500 and 1 umber KDR 750- 500 to 700m drilling capacity.
- 2 number of Voltas 180 drill rig driven by P4 Engine. Capacity- 300

meters.

- 1 number Joy-12B of 250m drilling capacity.

❖ TEAM PROFILE:

Name	Qualification	Technical Experience
Mr. Joydeep Banerjee	M.sc. Geology, RQP- IBM. MAusIMM., Project Coordinator under NABET Scheme of Prospecting/ Exploration Agency (APA) & Mining Plan Preparing Agency (MPPA).	Having more than 20 years of experience in the field of mineral industry and has obtained vast experiences in the field of coal exploration, Iron Ore exploration, Bauxite exploration, Chromite Exploration, Graphite Exploration etc. Throughout his career he has worked in both the domestic and overseas environment for exploration and mining project implementations. His strength lies in a thorough understanding of resource modeling and effective utilization of modeling software's. He is also an expert in the field of Remote sensing & GIS.
Mr. Indrajit Mukherjee	M.Sc in Geology	More than 23 years of Experience in Geological field, more than 12 years of experience in Forest Clearance.
Dr. Sukhen Majumder,	M. Tech (2005) in Applied Geology, IIT, Kharagpur. Ph.D. (2009) in Structural Geology, IIT-Kharagpur. MAusIMM. Technical Area Expert (Geo/HG) under NABET Scheme of Prospecting/ Exploration Agency (APA) & Mining Plan Preparing Agency (MPPA).	14 years of experience. Specialized in mineral exploration and project management, particularly in metals. His skills include exploration project management, detailed structural mapping, geological-geotechnical logging and sampling, geochemical surveys, profile mapping, litho-stratigraphic correlation, database management, quality analysis and quality check in compliance with international standards, preparing geological reports. He has worked in various exploration projects, mostly in different parts of India and Africa.
Mr. Debnath Adhikary	M.Sc (Tech) from Banaras Hindu University.	More than 5+ years of experience. Mr. Adhikary is being engaged in exploration job since joining in this organisation. Assisted in different Geological Report Preparation works.

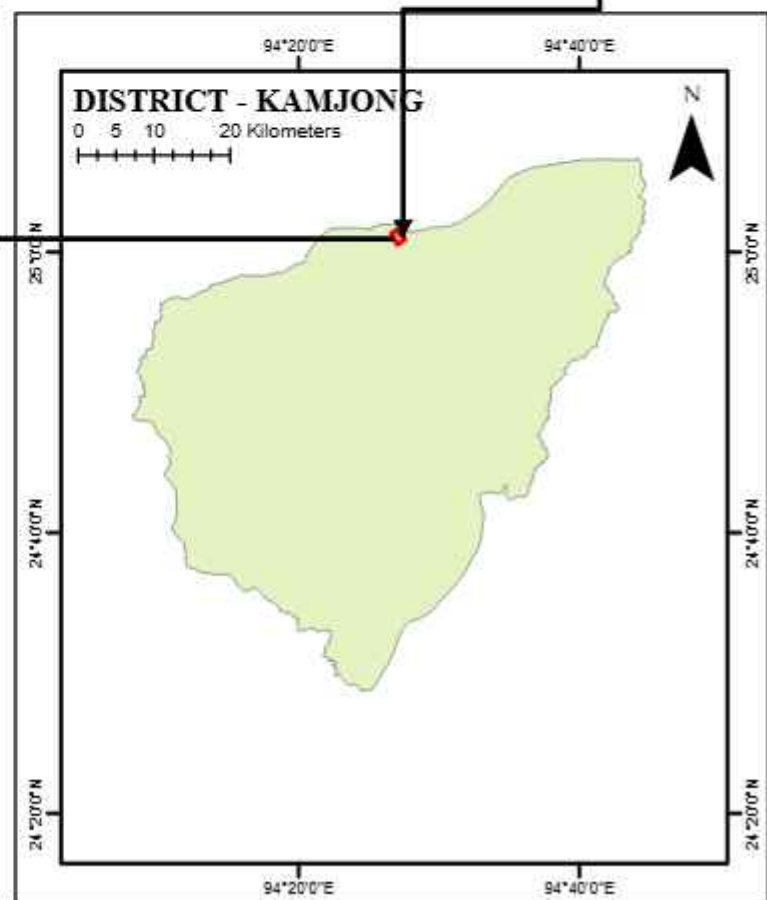
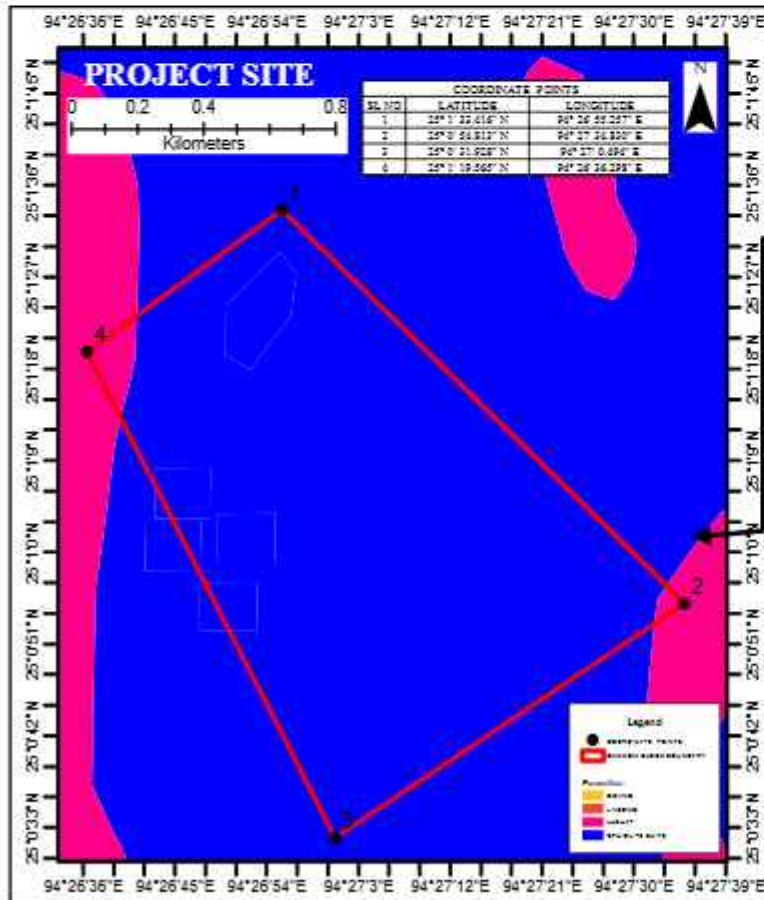
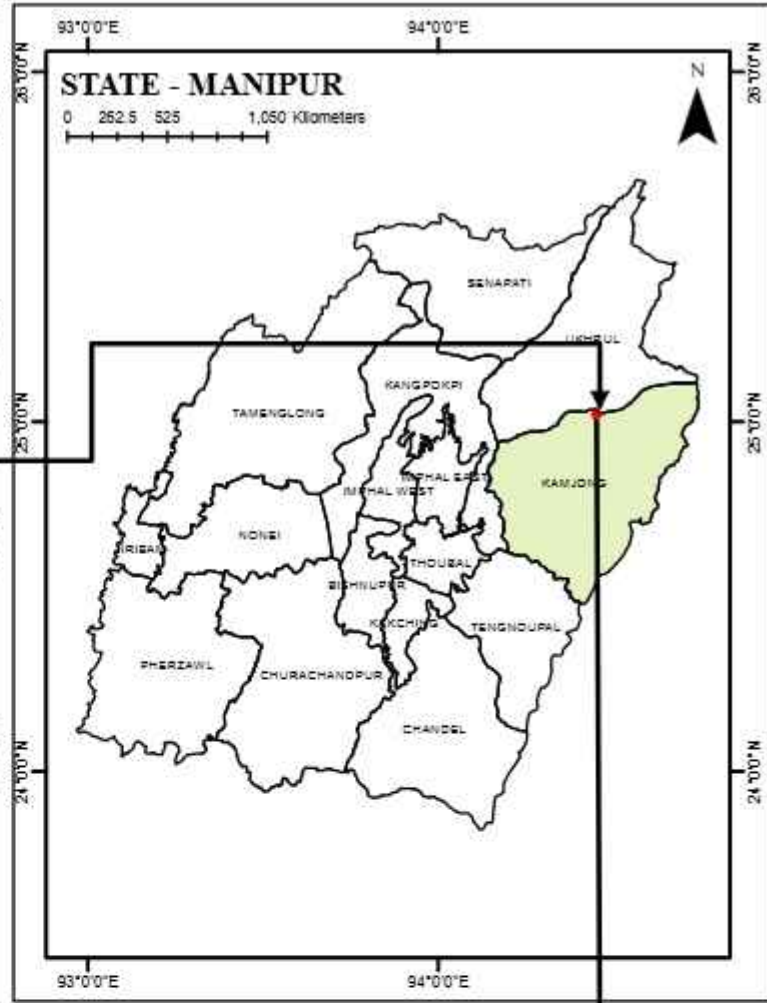
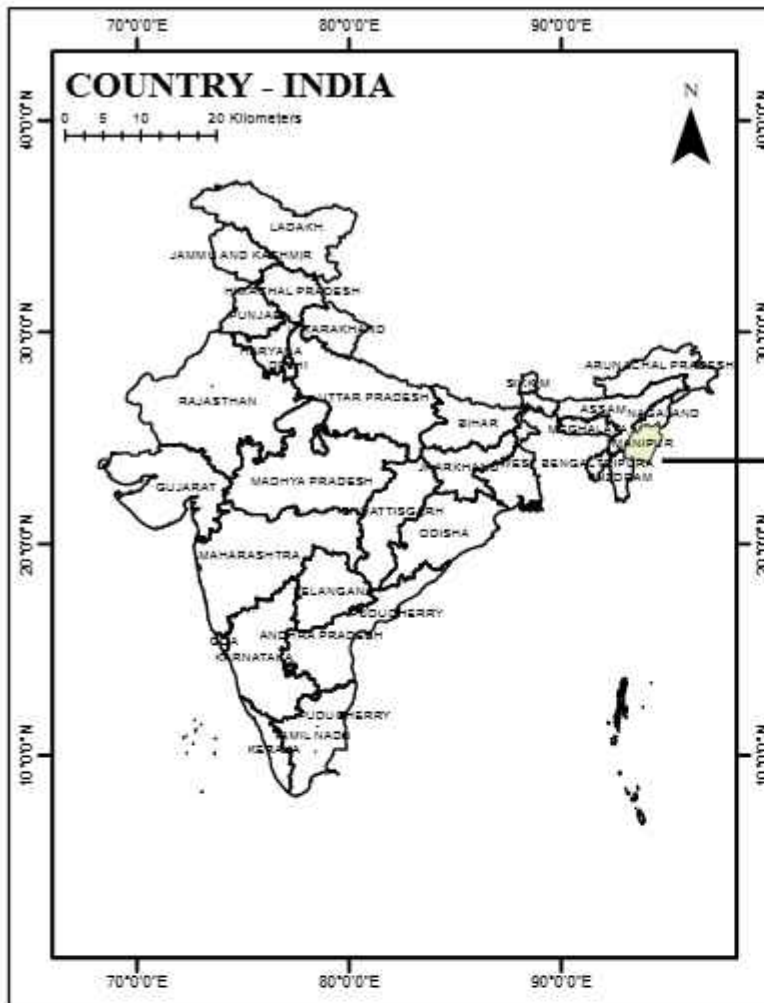
**NMET Proposal
Chhattisgarh**

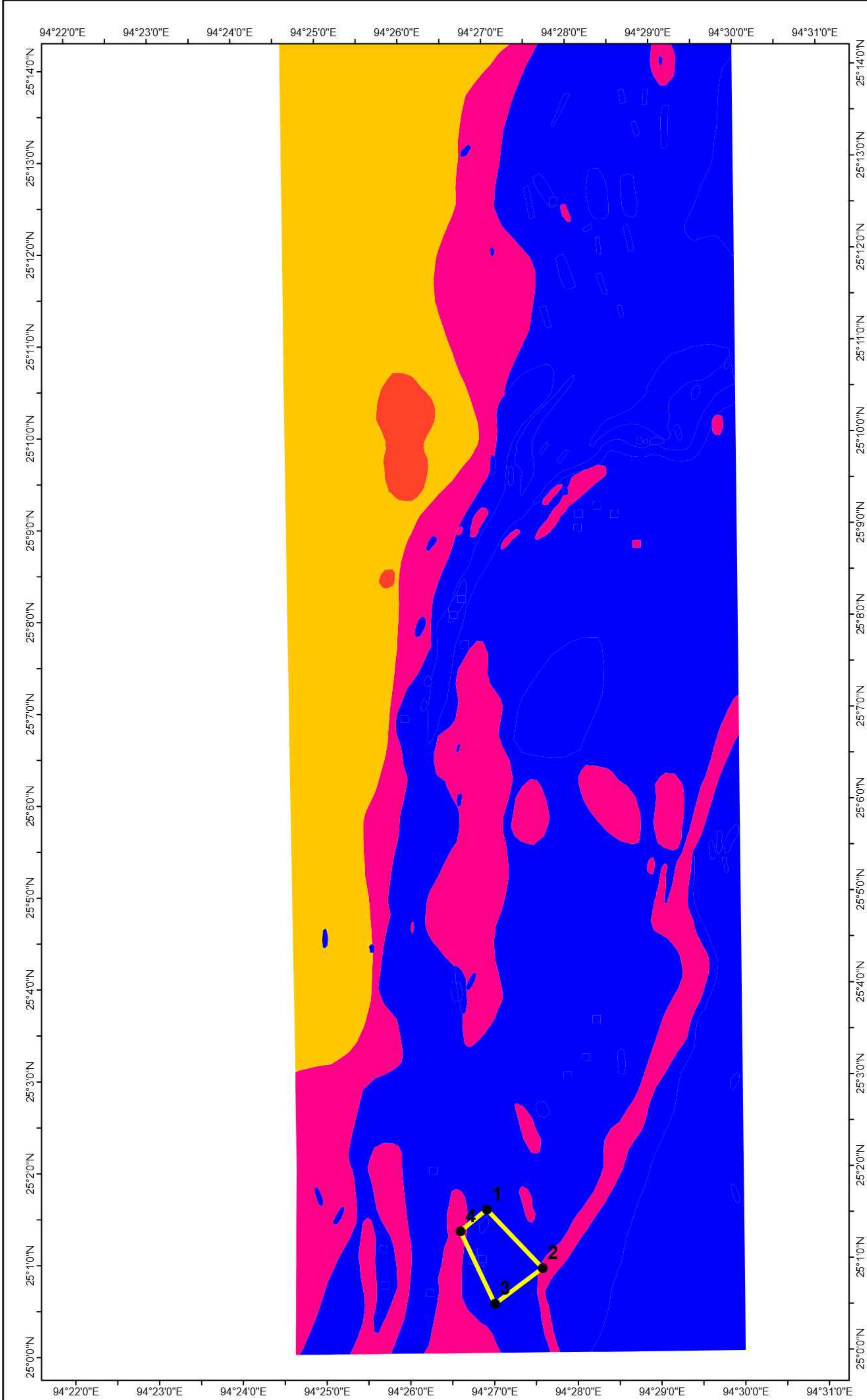
Name	Qualification	Technical Experience
Mr. Deep Konar	M.Sc. in Geology from IIT Bhubaneswar.	5.0 years of experience in managing exploration project. Prepared geological report. Software modeling through Surpac.
Mr. Shouvik Sen	M. Sc Applied Geology from Calcutta University	1 year experience in project management, geological mapping, sampling, database preparation, geological report preparation.
Sk. Rabiul Islam	B.Sc. Hons. Surveyors Competency Certificate from DGMS. Technical Area Expert (SUR) under NABET Scheme of Prospecting/Exploration Agency (APA) & Mining Plan Preparing Agency (MPPA).	More than 15 years of experiences. Surveying & leveling, assist to prepare Mining Plan/Review of Mining, Forest Diversion proposal, liaison work with Indian Bureau of Mines, Forest department, Pollution Control Board.
Ms. Jinia Rahaman	M. Sc in Geography from Vidyasagar University; P.G. Diploma in Applied Geoinformatics (Remote Sensing & GIS)	Ms. Rahaman is having 2 years of experience and has been engaged in various GIS related job.

❖ ASSOCIATES FOR OUT SOURCE JOBS:

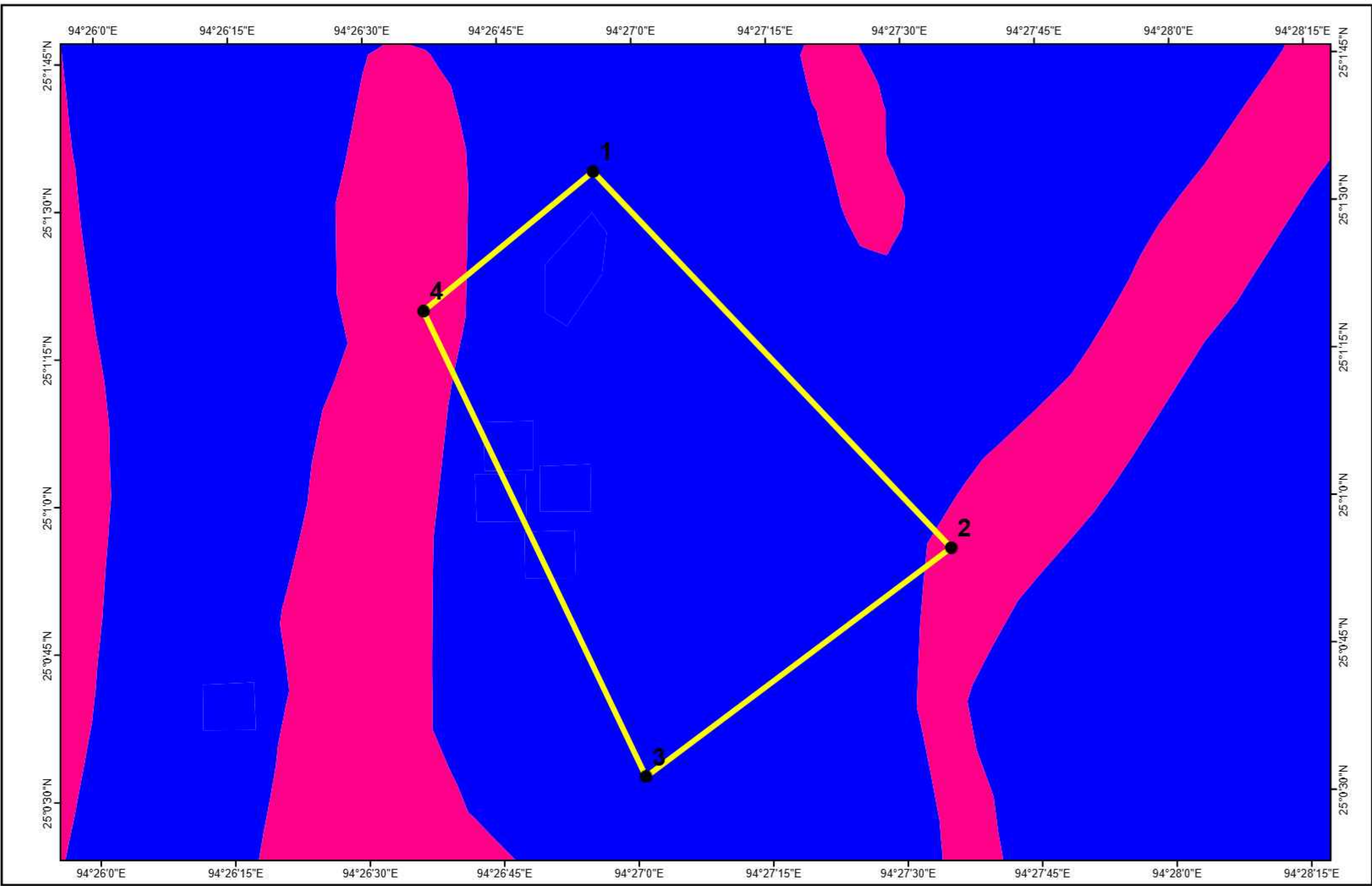
Job Type	Organization	Expertise
Chemical analysis	SHIVA Lab, Bangalore	The laboratory is accredited by NABL, APEDA, FASSAI, ISO 9001:2015 Certified and recognized by other governmental departments.

LOCATION MAP





GEOLOGICAL MAP OF PROPOSED GAMNOM BLOCK



COORDINATE POINTS		
SL NO	LATITUDE	LONGITUDE
1	25° 1' 33.416" N	94° 26' 55.257" E
2	25° 0' 54.813" N	94° 27' 34.830" E
3	25° 0' 31.928" N	94° 27' 0.494" E
4	25° 1' 19.565" N	94° 26' 36.298" E

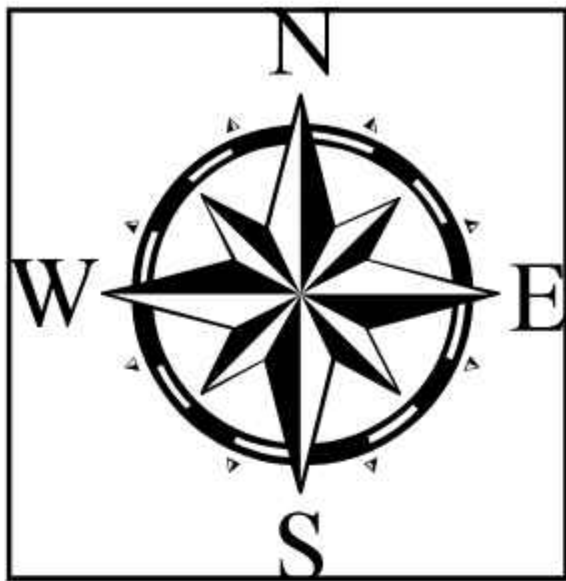
LEGEND

- COORDINATE POINTS
- GAMNOM BLOCK BOUNDARY

Formation

- DISANG
- LIASONG
- LUSHAT
- OPHIOLITE SUITE

GEOLOGICAL MAP OF GAMNOM BLOCK



COORDINATE POINTS		
SL NO	LATITUDE	LONGITUDE
1	25° 1' 33.416" N	94° 26' 55.257" E
2	25° 0' 54.813" N	94° 27' 34.830" E
3	25° 0' 31.928" N	94° 27' 0.494" E
4	25° 1' 19.565" N	94° 26' 36.298" E

LEGEND

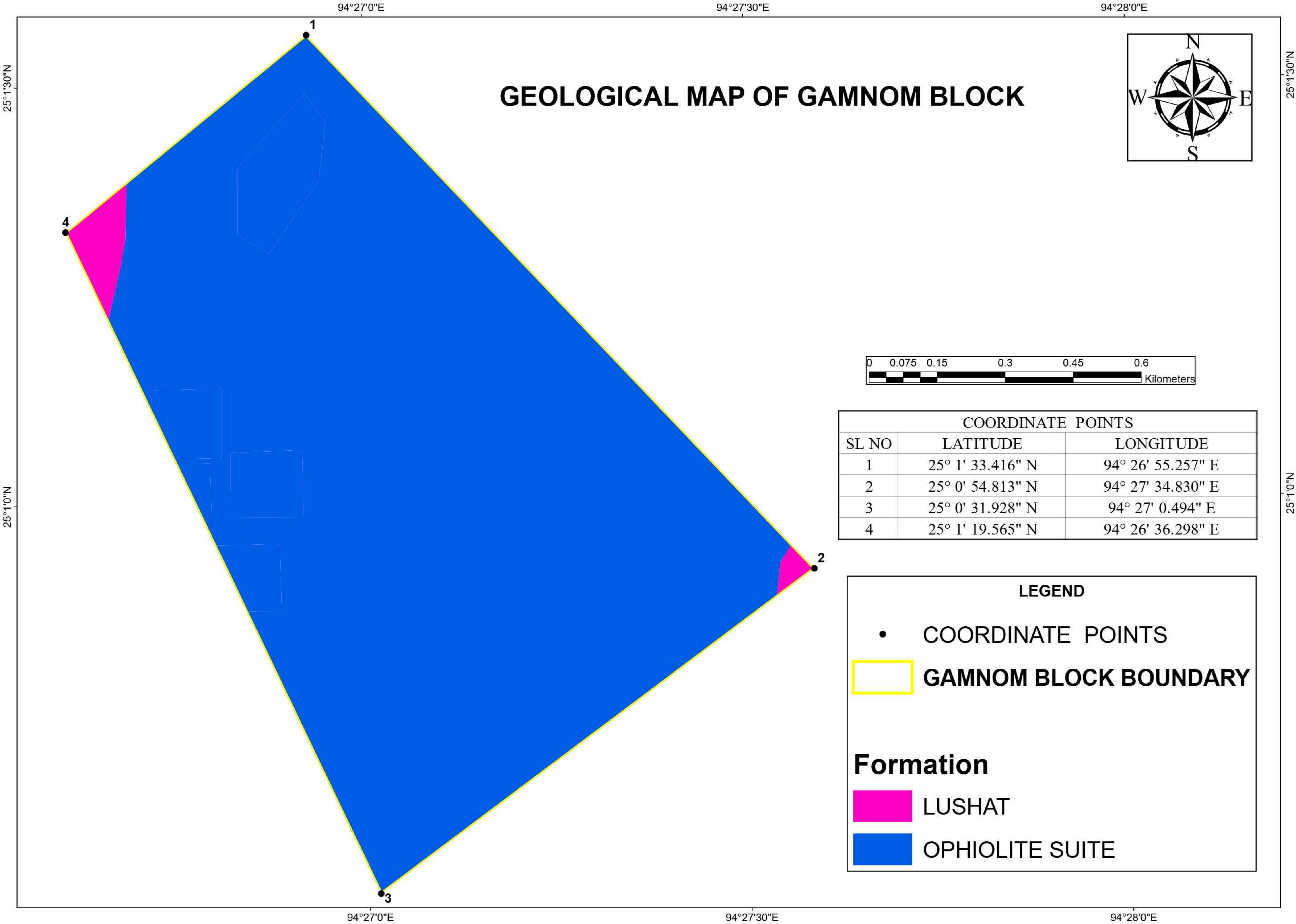
• COORDINATE POINTS

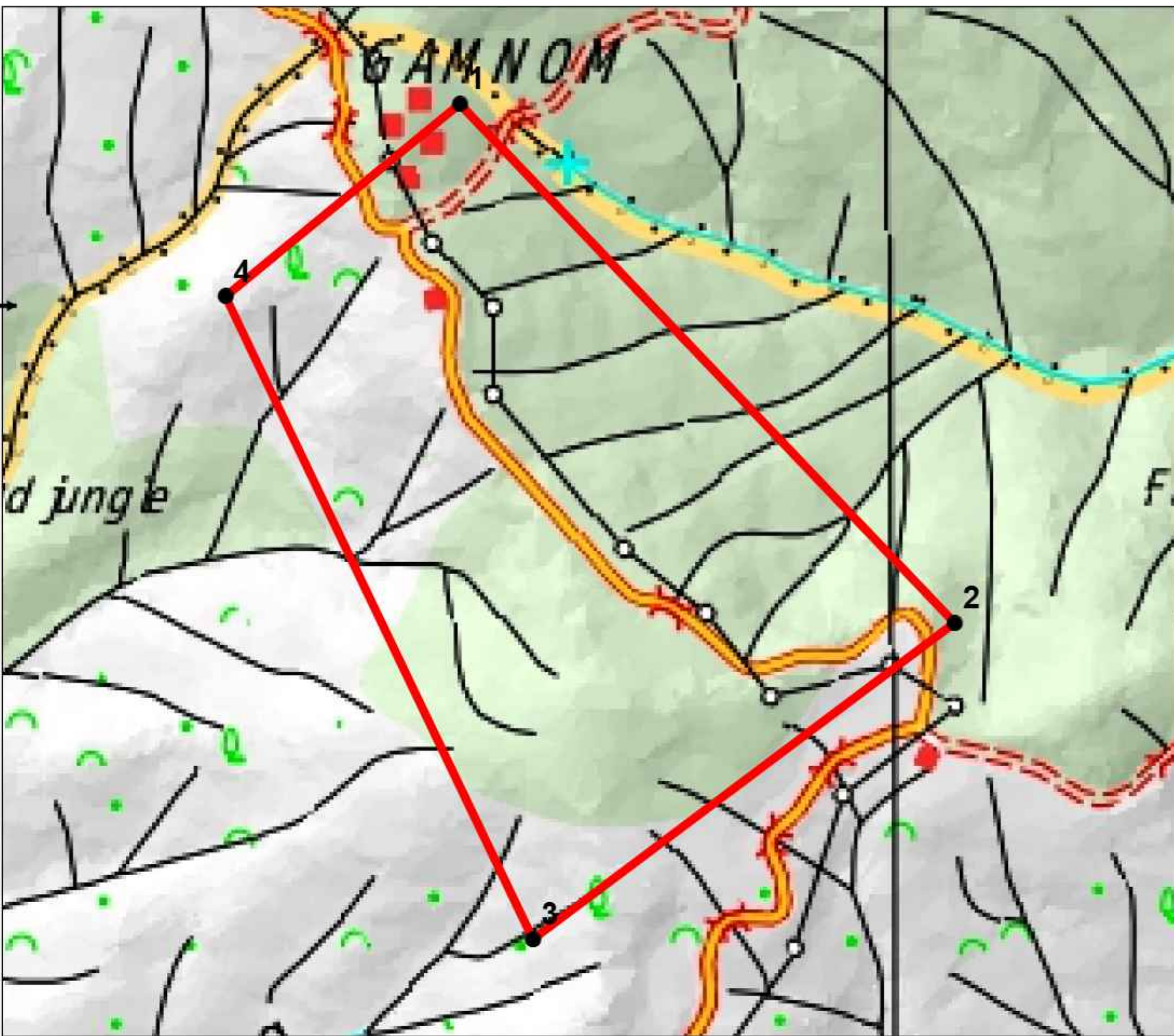
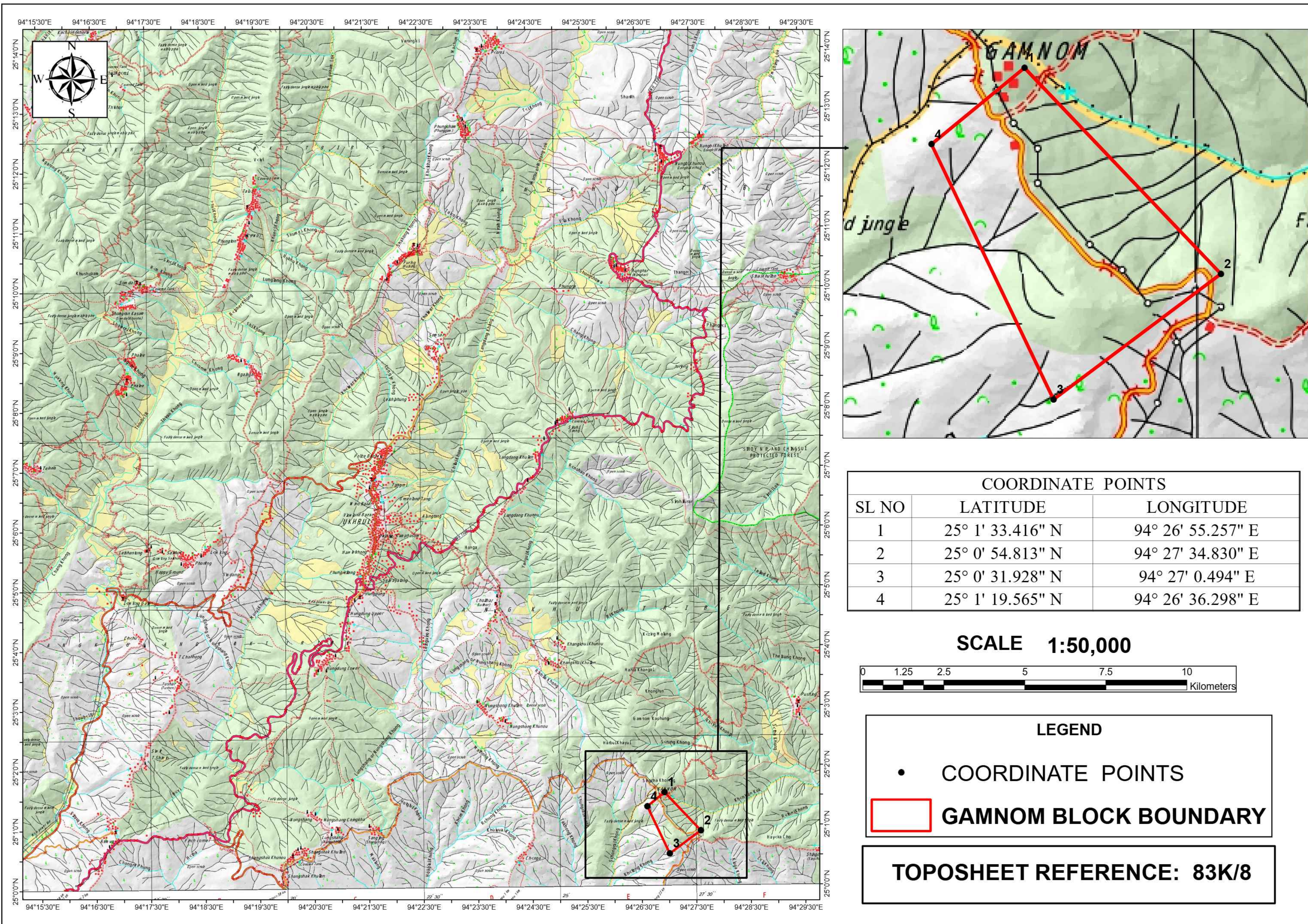
 GAMNOM BLOCK BOUNDARY

Formation

 LUSHAT

 OPHIOLITE SUITE





COORDINATE POINTS		
SL NO	LATITUDE	LONGITUDE
1	25° 1' 33.416" N	94° 26' 55.257" E
2	25° 0' 54.813" N	94° 27' 34.830" E
3	25° 0' 31.928" N	94° 27' 0.494" E
4	25° 1' 19.565" N	94° 26' 36.298" E

SCALE 1:50,000



LEGEND

•

COORDINATE POINTS

GAMNOM BLOCK BOUNDARY

TOPOSHEET REFERENCE: 83K/8